UNIVERSITE DE LIÈGE

Faculté des Sciences – Département des Sciences de la Vie

GIGA-Molecular Biology of Diseases

Laboratory of Gene Expression and Cancer

CONTRIBUTION OF mRNA DEGRADATION TO THE ONCOGENIC FUNCTIONS OF A FUSION TRANSCRIPTION FACTOR

Bartimée GALVAN

Doctoral dissertation to obtain the grade of « Doctorat en Sciences », in

« Biochimie, Biologie moléculaire et cellulaire, Bioinformatique et modélisation »

Promoteur: Pr. Franck DEQUIEDT

Academic year 2022-2023

EXAMINATION COMMITTEE

Dr. Ingrid Struman (Committee chair)
Université de Liège, GIGA, Molecular Angiogenesis Laboratory

Pr. Franck Dequiedt (Promotor)
Université de Liège, GIGA, Laboratory of Gene Expression and Cancer

Dr. Yvette Habraken (Secretary)
Université de Liège, GIGA, Laboratory of Gene Expression and Cancer

Dr. Marc Muller
Université de Liège, GIGA, Laboratory for Organogenesis and Regeneration

Dr. Pierre Close
Université de Liège, GIGA, Cancer Signaling

Pr. Cyril Geydan
Université Libre de Bruxelles, Laboratoire de Biologie moléculaire du gène

Dr. Martin Dutertre
INSERM, Institut Curie, Biologie de l'ARN, signalisation et cancer

Pr. Thomas Grünewald
Hopp Children's Cancer Center Heidelberg, Division of Translational Pediatric Sarcoma Research

ABSTRACT

Gene fusions are an important class of somatic alterations in cancer. In many well-known cases, they encode aberrant fusion transcription factors (TFs) with neomorphic DNA-binding preferences. FET::ETS fusions represent a notable family of TFs. They result from the juxtaposition of a member of the FET (FUS/EWSR1/TAF15) family of RNA-binding proteins to a member of the ETS superfamily of TFs (*e.g.*, FLI1 and ERG). These fusions are oncogenic drivers in many sarcomas and leukemias but challenging drug targets. An important limiting factor in developing therapies for them relies in our partial understanding of their underlying pathogenic molecular mechanisms. To date, the oncogenic functions of FET::ETS fusion proteins are almost exclusively confined to the control of mRNA synthesis. Based on a growing number of studies that identified non-canonical roles in the control of mRNA decay for various non-fusion (wild-type) DNA-binding TFs in human, we investigated whether FET::ETS fusion TFs might also be involved in mRNA decay. To test this possibility, we reasoned that Ewing sarcoma might represent an attractive model for a proof-of-concept study. Ewing sarcoma is an aggressive bone and soft-tissue childhood cancer as well as a paradigm for solid tumor development after a single genetic event. In ~85% of patients, this disease is driven by the fusion protein EWSR1::FLI1 (EF). Structurally, EF is a well-defined TF containing a potent amino-terminal transactivation domain that is intrinsically-disordered and a carboxy-terminal ETS DNA-binding domain. Molecularly, EF is known to orchestrate oncogenic gene expression programs by reprogramming enhancers and promoters via phase transition and hijacking of chromatin regulators; as well as by remodeling the 3D genome architecture. In this work, we report that EF also reprograms gene expression by affecting mRNA stability and decipher the molecular mechanisms underlying this function. We show that EF is recruited to mRNAs via interaction with the RNA-binding protein HuR (also known as ELAVL1), and promotes mRNA decay by binding to CNOT2, a component of the CCR4-NOT deadenylation complex. Interestingly, we evidence that EF antagonizes the normal mRNA protective function of HuR through its association with CCR4-NOT. Importantly, we show that EF-mediated mRNA decay supports Ewing sarcoma biology and yields a new vulnerability towards HuR inhibition. Finally, our data indicate that the control of gene expression by fusion TFs might represent a more complex scheme than anticipated, integrating mRNA synthesis and degradation, and thereby providing novel actionable molecular targets.

RÉSUMÉ

Les fusions géniques constituent une classe importante d'altérations somatiques dans les cancers. Dans de nombreux cas bien connus, elles codent pour des facteurs de transcription aberrants dits de fusion présentant des propriétés néomorphes de liaison à l'ADN. Les fusions FET::ETS représentent une famille notoire de facteurs de transcription de fusion. Elles résultent de la juxtaposition d'un membre de la famille FET (FUS/EWSR1/TAF15) des protéines liant l'ARN à un membre de la superfamille des facteurs de transcription ETS, tels que FLI1 et ERG. Ces fusions sont des drivers oncogéniques qui sont responsables de plusieurs sarcomes et leucémies mais des cibles thérapeutiques complexes. Un obstacle important dans le développement de thérapies pour ces fusions réside dans notre compréhension partielle des mécanismes moléculaires pathogéniques sous-jacents. A ce jour, les fonctions oncogéniques des fusions FET::ETS sont presque exclusivement confinées au contrôle de la synthèse de l'ARNm. Sur base d'un nombre grandissant d'études qui ont identifié des fonctions non-canoniques dans le contrôle de la dégradation de l'ARNm pour différents facteurs de transcription chez l'homme, nous avons entrepris d'examiner si les facteurs de transcription de fusion FET::ETS pourraient également être impliqués dans la dégradation de l'ARNm. Pour tester cette possibilité, nous avons pensé que le sarcome d'Ewing pourrait représenter un contexte attractif pour une étude de preuve-de-concept. Le sarcome d'Ewing est un cancer pédiatrique aggressif des os et des tissus mous, et un paradigme pour le développement d'une tumeur solide après une seule aberration génétique. Chez ~85% des patients, cette maladie est dirigée par la fusion protéique EWSR1::FLI1 (EF). Sur le plan structurel, EF est un facteur de transcription bien défini contenant un puissant domaine de transactivation intrinsèquement désordonné en position amino-terminale et un domaine de liaison à l'ADN ETS en position carboxy-terminale. Sur le plan moléculaire, EF orchestre des programmes oncogéniques d'expression des gènes en reprogrammant divers éléments activateurs et promoteurs par ses propriétés de transition de phase et la perturbation de régulateurs chromatiniens, ainsi qu'en refaçonnant l'organisation 3D de l'architecture du génome. Dans ce travail, nous rapportons que EF reprogramme aussi l'expression génique en influençant la stabilité de l'ARNm et déchiffrons le mécanisme moléculaire impliqué. Nous montrons que EF est recruté sur l'ARNm en interagissant avec la protéine de liaison à l'ARN nommée HuR (aussi connue sous le nom de ELAVL1) et déclenche leurs dégradation en liant la sous-unité CNOT2 du complexe de déadénylation CCR4-NOT. Aussi, nous mettons en évidence que, de par son association avec le complexe CCR4-NOT, EF est capable de contrecarrer le rôle normal de stabilisation de l'ARNm de HuR. Mais surtout, nous montrons que la dégradation de l'ARNm par EF contribue à la biologie du sarcome d'Ewing et crée une nouvelle vulnérabilité envers l'inhibition de HuR. Finalement, nos données indiquent que le contrôle de l'expression des gènes par les facteurs de transcription de fusion pourrait représenter un schéma plus compliqué

qu'anticipé, intégrant à la fois la synthèse et la dégradation de l'ARNm, et offrant par là de nouvelles cibles thérapeutiques.

ACKNOWLEDGEMENTS

été très précieuse ! Merci à Charlotte, nos discussions musicales et spirituelles me manquent toujours ! Merci à Despoina, notre déesse grecque ! Je suis très heureux de te connaître ! Merci à Marco ! Tes cheesecakes sont une tuerie ! Merci à Mégane la sanguinaire ! Je garde un excellent souvenir de nos conversations spirituelles ! J'espère que toi aussi ! Merci à Marco Gianfrancesco, le bodybuilder du labo et un sacré coco ! Merci à Judit, notre petite hispanique nationale ! Ta bonne humeur était comme un vent de fraicheur ! Merci à Margaud ! Merci à Julien même si on ne se connait pas si bien ! Merci à Marielle, notre doyenne à tous (elle va me tuer). Ton énergie est tout à la fois fascinante et terrifiante ! Merci à Cédric ! Nos conversations sport/voitures autour d'un petit café avec Johnny vont me manquer. Merci aussi pour ton assistance dans le labyrinthe des produits chimiques ! Merci à Giugiu ! C'était génial de pouvoir tous se retrouver chez toi même quand c'était Tanguy qui m'avait invité haha ! Plus sérieusement, merci pour toutes les fois où tu nous as accueilli Axel et toi ! Je n'oublierai jamais ces moments ! Merci à toi Céline pour toutes ces conversations en culture ! C'étaient de très bons moments ! Merci aussi à Sarah et Amandine ! C'était tellement triste de vous voir partir en bas ! Merci à François, le dictateur du L2 au grand cœur (il est catho le petit). Merci à Manu pour ton hospitalité ! J'ai passé d'excellents moments chez toi ! Merci à toi aussi Alex pour ta grande gentillesse. Merci à vous trois pour votre grande aide et votre diligence dans le design des constructions et lignées ! Un coucou spécial à Vincianne (qui l'a exigé) et à Audrey. C'est chouette de vous revoir régulièrement !

Il est temps maintenant de remercier les petits nouveaux. Je suis très heureux de vous connaître tous. Zarah, notre fleur élevée, ce fut un réel de bonheur de travailler avec toi ! Toujours à courir partout mais d'une gentillesse légendaire, tu vas beaucoup me manquer. Merci encore pour tous les petits cadeaux du Liban ! Je suis heureux de savoir que je suis enfin parvenu à te faire rire à mes blagues à la fin de ma thèse ! ;D Merci à mes deux étudiants adorés : Margaux et Loic ! Ce fut un pur plaisir de t'encadrer Margaux même si l'ORFeome nous a réservé quelques surprises… Je te souhaite que les difficultés des manips s'en aillent bien vite car tu le mérites !! Merci à toi aussi Loic ! Bon je sais que ton mémoire a été fort chamboulé avec ce foutu covid, mais j'espère que tu ne m'en voudras pas éternellement haha :p En tout cas, tu t'en es super bien sorti ! Merci pour ton intérêt pour le projet dès le départ et ton envie débordante à vouloir le faire avancer ! Ton aide a été précieuse quand j'étais au labo mais aussi pendant la rédaction ! Merci pour tes nombreuses relectures ! J'espère que notre belle collaboration continuera encore longtemps ! Merci à toi Mimi ! Je sais que ton déménagement chez nous n'a pas été des plus faciles mais j'espère avoir modestement contribué à soulager cet inconfort. En tout cas, j'ai beaucoup apprécié nos diverses conversations au petit matin ! Merci à Florence, notre Kate Middleton belge ! Votre passage à la maison était vraiment un très très bon moment ! Merci à Benedetta ! Viva Italia ! Ma connaissance de l'italien s'arrête malheureusement là :p Merci aussi à Olivia qu'on oublie pas ! Merci à Jérémy ! Quoi qu'ils en disent, tu t'es très bien débrouillé sur ton snow mais

x

TABLE OF CONTENTS

LIST OF FIGURES

LIST OF TABLES

ABBREVIATIONS

aa: amino acid

ActD: actinomycin D

AMD: ARE-mediated mRNA decay

APA: alternative polyadenylation

APL: acute promyelocytic leukemia

ARE: AU-rich element

AREBP: ARE-binding protein

ATAD: amino-terminal activation domain

AYA: adolescent and young adult

CCR4-NOT: Complex Catabolite Repression 4 (CCR4)-Negative On TATA-less (NOT)

cDNA: complementary DNA

CDS: coding sequence

ChIP-seq: chromatin immunoprecipitation-sequencing

CR: chromatin regulator

CT: computed tomography

CTAD: carboxy-terminal activation domain

CTD: carboxy-terminal domain

DBD: DNA-binding domain

DHTS: dihydrotanshinone-I

DMSO: dimethylsulfoxide

DNA: deoxyribonucleic acid

EBS: ETS-binding site

EF: EWSR1::FLI1

EISA: exon-intron split analysis

ELAVL1 (HuR): Embryonic Lethal Abnormal Vision-Like protein 1

EMT: epithelial-to-mesenchymal transition

ER: endoplasmic reticulum

ERG: ETS-Related Gene

ESFT: Ewing sarcoma family of tumors

ETS: E-twenty-six-specific sequence, E26 transforming sequence

EV: extracellular vesicle

EwS: Ewing sarcoma

EWSR1 (EWS): Ewing sarcoma breakpoint region 1

EXOSC: essential exosome core component

FACS: fluorescence-activated cell sorting

FDA: Food and Drug Administration

FET: FUS/EWSR1/TAF15

FEV: Fifth Ets Variant

FISH: fluorescence *in situ* hybridization

FLI1: Friend Leukemia virus Integration 1

FUS: Fused in Sarcoma

F-Luc: *Firefly* luciferase

GMD: glucocorticoid-mediated mRNA decay

GO: gene ontology

GLuc: *Gaussian* luciferase

gPCA: *Gaussian* luciferase protein complementation assay

GRO-seq: global run-on sequencing

GTF: general transcription factor

GWAS: genome-wide association study

HGNC: HUGO Gene Nomenclature Committee

HL: half-life

HNS: nucleocytoplasmic shuttling sequence

hMSC: human mesenchymal stem cell

IHC: immunohistochemistry

IDP: intrinsically-disordered protein

IDR: intrinsically-disordered region

IP: immunoprecipitation

iPPI: protein-protein interaction inhibitor

KD: knockdown

LC: low complexity

LLPS: liquid-liquid phase transition

PB: processing body (P-body)

PPI: protein-protein interaction

lncRNA: long non-coding RNA

miRISC: miRNA-induced silencing complex

miRNA: microRNA

MLLE: mademoiselle

MoRF: molecular recognition feature

MRI: magnetic resonance imaging

mRNA: messenger RNA

mRNP: messenger ribonucleoprotein

MS: mass spectrometry

ncRNA: non-coding RNA

NAR: Not1 anchor region

NGD: no-go decay

NLS: nuclear localization signal

NMD: nonsense-mediated mRNA decay

NSCS: neural-crest derived cell

NSD: non-stop decay

nt: nucleotide

NTD: amino-terminal domain

N&B: Number and Brightness

ODE: ordinary differential equation

ORF: open reading frame

PABPC: cytoplasmic poly(A)-binding protein

PABPN: nuclear poly(A)-binding protein

PAR-CLIP: photoactivable-ribonucleoside-enhanced CLIP

PCA: principal component analysis

PD-L1: Programmed Death-Ligand 1

PET: positron emission tomography

PLA: proximity-ligation assay

PNT: Pointed domain

PPI: protein-protein interaction

pre-mRNA: precursor mRNA

PrLD: prion-like domain

PROTAC: proteolysis targeting chimaeras

PRO-seq: precision run-on sequencing

PTC: premature termination codon

PTM: post-translational modification

RBP: RNA-binding protein

RGG: arginine-glycine-glycine

RIP: RNA immunoprecipitation

RNA: ribonucleic acid

RNAPII: RNA polymerase II

RNA-seq: RNA-sequencing

RRM: RNA recognition motif

RT: reverse transcription

RT-qPCR: real-time quantitative polymerase chain reaction

R-Luc: *Renilla* luciferase

scRNA-seq: single-cell RNA-sequencing

SG: stress granule

siRNA: small interfering RNA

SLiM: short linear motif

SMD: Staufen-mediated mRNA decay

TAD: topologically-associating domain

TAF15: TATA-binding associated factor 15

TF: DNA-binding transcription factor

TFMD: transcription factor-mediated mRNA decay

TSS: transcription start site

uORF: upstream ORF

UPR: unfolded protein response

UTR: untranslated region

WB: western blotting

PREAMBLE

In the laboratory of "Gene Expression and Cancer" (University of Liege, GIGA), Franck Dequiedt's team investigates non-canonical functions of TFs (*i.e.*, sequence-specific DNA-binding factors, see definition below) in co-/post-transcriptional processes including pre-mRNA splicing, mRNA degradation and translation. These functions are studied in important developmental contexts and in cancer. The prototypical models of the laboratory are the *FET*::*ETS*[1] gene fusions, which juxtapose a member of the FET (FUS/EWSR1/TAF15) family of RNA-binding proteins to a member of the E-twenty-six transformation specific (ETS) superfamily of TFs. These gene fusions encode oncogenic drivers in a number of sarcomas and leukemias. Strikingly, FET::ETS fusions invariably fuse the FET-derived low complexity N-terminal region upstream of the ETS-derived DNA-binding domain. Consequently, their oncogenic functions are, to date, almost exclusively attributed to their role as aberrant TFs. However, our recent work on EWSR1::FLI1 (EF), which is pathognomonic of Ewing sarcoma, has challenged this view as we identified novel co-/post-transcriptional functions for this fusion TF in alternative splicing. In the context of this work, we also identified an unsuspected function in the active control of mRNA decay by combining wet-lab techniques and bioinformatic approaches (article in preparation for submission to 'Molecular Cell' journal). Interestingly, these findings come in the wake of multiple studies establishing the implication of several non-fusion TFs in the regulation of alternative splicing and mRNA stability. We believe that a comprehensive understanding of how aberrant TFs like EF contribute to oncogenic gene expression programs can only arise from integrating their transcriptional and post-transcriptional functions.

In this work, the term of 'transcription factors' refers to as proteins that regulate RNAPII-dependent transcription by binding to a specific DNA sequence within promoters or enhancers/silencers. A defining feature of TFs is thus that they harbor at least one DNA-binding domain. In addition to their DNA-binding domain(s), TFs may contain a regulatory domain (*e.g.*, transactivation domain). However, the only presence of a DNA-binding domain is often taken as an indicator of ability to regulate transcription because TFs can act by simply masking the DNA-binding site of other proteins [1]. Also, general transcription factors (GTFs), which are part of the basal transcriptional machinery and represent, *per se*, an important class of TFs, are not considered here because many of them do not actually bind to DNA. Likewise, transcriptional cofactors that do not bind to DNA but control mRNA synthesis via the recruitment of other factors or via chromatin-based events (*e.g.*, the deposition of epigenetic marks) are also not considered here, unless otherwise clearly stated.

---

[1] To avoid confusing syntax in the designation of gene fusions, and in line with HUGO Gene Nomenclature Committee (HGNC) recommendations [699]; gene fusions are denoted in this work using a double colon (::) as a separator instead of a hyphen (-) or a forward slash (/). Moreover, genes involved in gene fusions – *i.e.*, parent genes – are denoted by their italicized HGNC approved gene symbols, whereas proteins are not written in italics. For example, *A*::*B* denotes a fusion of the *A* and *B* genes, whereas A::B denotes the corresponding protein product.

SECTION I   INTRODUCTION

1. Ewing sarcoma

Ewing sarcoma (EwS) is an aggressive bone and soft-tissue pediatric tumor, and a paradigm for solid tumor development after a single genetic event. Genetically, this disease is characterized by pathognomonic *FET::ETS* gene fusions, which juxtapose a member of the FET family of RNA-binding proteins to a member of the ETS superfamily of TFs. Arising in 85% of cases, *EWSR1*::*FLI1* (EF) represents the most frequent gene fusion in EwS and the figurehead of *FET*::*ETS* gene fusions. It encodes a dominant oncoprotein with neomorphic DNA-binding preferences that drives sarcomagenesis by completely rewiring gene expression programs. So far, the oncogenic function of EF has mainly been attributed to its aberrant control of transcription and epigenetic mechanisms. However, recent insights have revealed that the control of post-transcriptional processes, such as alternative splicing, also contributes to the oncogenic functions of EF. Besides suggesting that the molecular functions of the fusion TF EF might be more complex than previously anticipated, these findings might also offer unique therapeutic opportunities for this difficult-to-target chimera.

In this chapter, I will discuss several aspects of EwS biology with a focus on its driver fusion TF EF. First, I will cover the clinical features, cell of origin and genetics of EwS. Second, I will describe the aberrant molecular functions of EF. On this basis, I will next briefly discuss EwS cell plasticity and metastasis. Finally, I will review the main therapeutic options in targeting the fusion protein EF and highlight why a comprehensive understanding of the mechanisms employed by oncogenic fusion proteins like EF represents an important premise for developing novel targeted therapies.

1.1. Clinical features

1.1.1.   Seminal observation and classification

EwS was first reported by James Ewing in 1921 as a new bone tumor entity named "diffuse endothelioma of bone" in several young patients aged from 14 to 19 years old [2]. During the last century, several neoplasms with immunohistomorphologically similar features and harboring chromosomal translocations were subsequently described; comprising extraosseous EwS, peripheral primitive neuroectodermal tumors and Askin tumors. Historically, they were regrouped in the EwS family of tumors (ESFTs) [3]. In 2013, the World Health Organization (WHO) classification of sarcomas redefined ESFTs as one uniform entity named 'Ewing sarcoma', with the presence of *FET*::*ETS* gene fusions as unifying genetic hallmark [4]. Also part of this WHO classification, Ewing-like sarcomas constitute a group of small round cell sarcomas with similar phenotypic and clinical features than EwS [5]. They comprise CIC-fused sarcomas [6], [7], BCOR-rearranged sarcomas [8], and NFATC2 sarcomas [9]. Previously, these tumors were considered as EwS but, since around 2010, they are recognized as a distinct entity because they lack the disease-defining *FET*::*ETS* gene fusions [5]. Ewing-like sarcomas are not discussed further in the rest of this manuscript but are extensively reviewed in [10].

More broadly, EwS belongs to the group of sarcomas. With more than 100 histological subtypes, sarcomas represent heterogeneous and clinically challenging bone and soft-tissue tumors, which are not necessarily characterized by gene fusions [11]. Altogether, sarcomas account for >10% of all pediatric cancers, thereby constituting the second most common type of solid tumor in children and adolescents [12].

1.1.2. Tissue localization

EwS primary tumors can virtually originate from any anatomical sites, but most commonly involve the skeleton (~80%). The pelvis, ribs and proximal long bones (femur or tibia) are recurrent occurring sites. Less frequently (~20%), EwS also arise in extraosseous sites; predominantly involving the thoracic wall, gluteal muscle, pleural cavities and cervical muscles. In metastatic EwS, the lungs, bone and bone marrow represent the main niches [13], [14]. The most frequent primary and metastatic sites of EwS are summarized in **Figure 1**.

Primary sites

Bone (~80%)

Axial skeleton (45%)
• Pelvis (20%)
• Ribs (10%)
• Other axial bones (15%)

Distal skeleton (35%)
• Femur (12%)
• Humerus (4%)
• Other distal bones (19%)

Extraosseous location (~20%)

Bone

Metastatic sites

Lungs

Bone marrow
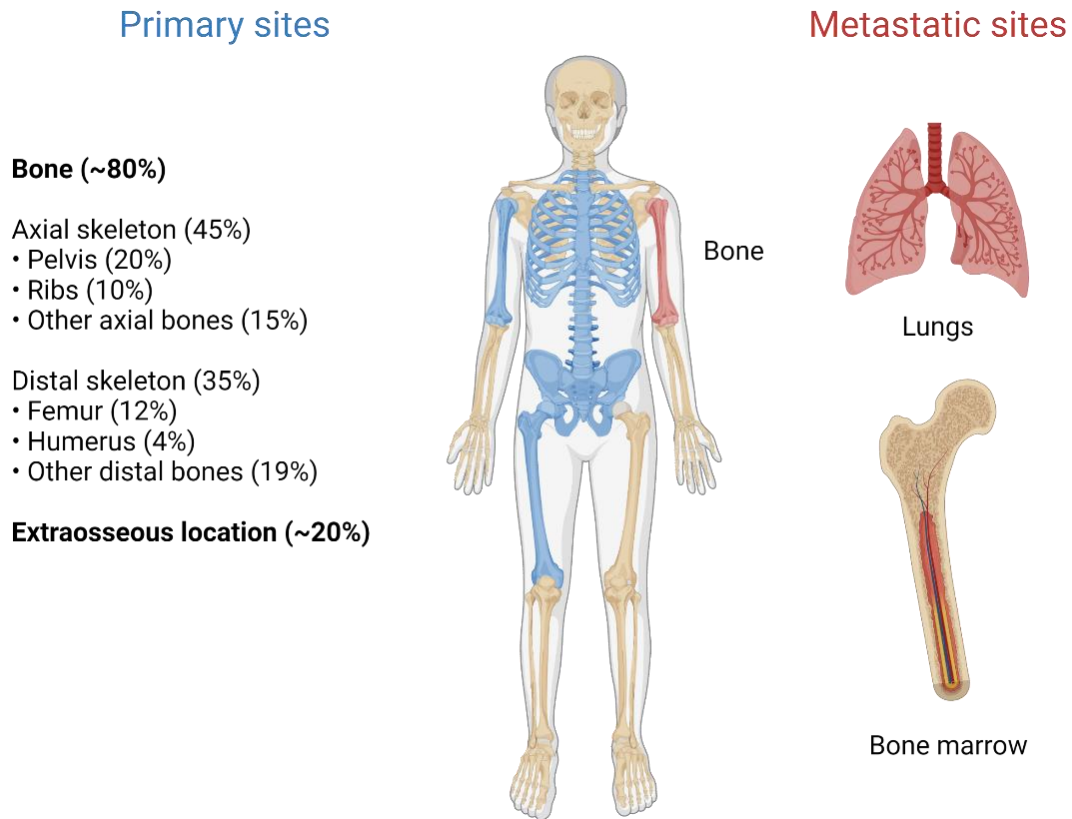
Figure 1. Main occurring sites in primary and metastatic EwS. Primary and metastatic sites are indicated in blue and red, respectively. Modified from [13], [14]. Created with BioRender.com.

1.1.3. Histology

Histologically, EwS is composed of undifferentiated small round blue cells with scanty cytoplasm; and expressing high levels of the transmembrane glycoprotein CD99 (also known as MIC2) [15] (**Figure 2**). Although strong CD99 expression is also detected in other sarcomas or in leukemias [16], this feature represents a routine diagnostic biomarker of EwS [15].
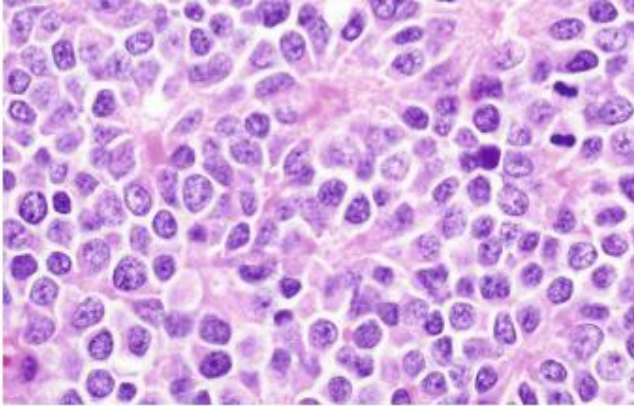
a   **b**
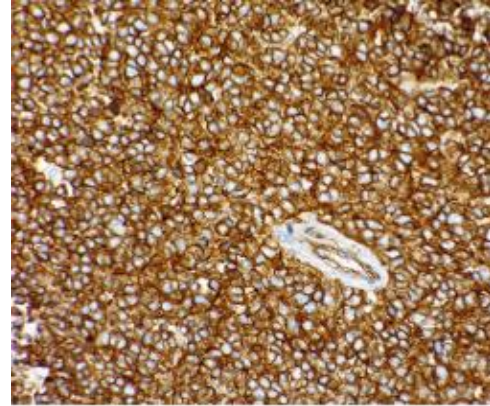
Figure 2. Histomorphology of EwS biopsy specimen. (a) Classical haemotoxylin and eosin staining showing small round cells with prominent nuclei and minimal cytoplasm, which reflect impaired differentiation. (**b**) Immunohistochemical staining of CD99 showing diffuse and intense plasma membrane expression. Modified from [5].

1.1.4. Epidemiology, demography and etiology

Epidemiologically, EwS mainly affects children, adolescents and young adults (AYAs), with a median age of 15 years old at diagnosis. It accounts for about 2% of childhood cancers; thus representing, after osteosarcoma, the second most common bone tumor in young patients. Males are also slightly more affected than females (sex ratio of 3:2) [17]. Interestingly, the location sites of EwS are age-dependent, with skeletal origin being more frequent in younger patients. In older patients, EwS tend to arise more predominantly in soft-tissue and is associated with worse outcome [5].

Demographically, EwS has a relatively constant incidence of ~1.5 cases per million children and AYAs per year in Europeans. By contrast, annual rates are of ~0.8 and ~0.2 in Africans and Asians [17], thus indicating that Europeans are much more at risk of developing EwS compared to other populations. Interestingly, EwS incidence is lower in Americans of African ancestry than in those of European ancestry [17]. Together, these epidemiologic biases suggest that genetic germline variants rather than environmental or lifestyle factors might predispose to this disease [5]. Accordingly, except an Australian study which related farm exposure to EwS risk [18], no environmental factors have so far been implicated, further supporting a genetic component in

EwS etiology. Although some anecdotal familial cases have been reported [19], this disease is however not associated with strong hereditary disorders. Nevertheless, genome-wide association study (GWAS) described genetic variants within six loci (EGR2, TARDBP, RRE1, KIZ and NKX2-2) that contribute to EwS susceptibility [20]. Interestingly, they found that these risk haplotypes were more prevalent in people of European ancestry, thus providing a possible explanation to the geographic bias observed in EwS incidence [20]. Additionally, germline polymorphisms within the DNA-binding sites of EF and the *CD99* locus have also been associated with EwS etiology [21], [22].

1.1.5. Diagnosis

1.1.5.1.   Symptoms

Symptoms of EwS are largely non-specific leading to delayed diagnosis with median time of 3-9 months [23]. Nevertheless, time to diagnosis does not correlate with overall survival [24]. Symptoms vary depending on the occurring tumor site, and can comprise localized pain, swelling, and in advanced cases, fever, nights sweats, fatigue and weight loss [23]. Understandably, pain is often mistaken for 'bone growth' or injuries resulting from sports or daily life activities. Therefore, and since pathological fracture is reported in only 10-15% of cases, unexplained pain lasting >1 month should prompt further investigation [5].

1.1.5.2.   Diagnostic work-up

Diagnosis starts with a physical examination, sometimes leading to the detection of a palpable soft-tissue mass depending on the occurring site. Radiologic analysis is usually more strongly suggestive (**Figure 3**). It allows to identify primary tumor sites and to evaluate the presence of metastasis. Magnetic resonance imaging (MRI) is used in cases of extraosseous EwS. Moreover, bone scintigraphy, positron emission tomography (PET) alone or in combination with computed tomography (CT) can also be used to further evaluate the metastatic status as well as for monitoring response to treatment in newly diagnosed patients. Finally, a definitive diagnosis is provided after molecular analysis of surgically resected tumor specimens. This relies on immunohistochemistry (IHC) for biomarkers like CD99, FLI1, CAV1, NKX2-2, BCL-11B and GLG1 [5]; fluorescence *in situ* hybridization (FISH) using either EWSR1 break-apart probe (**Figure 4**) or dual color EWSR1 and FLI1 probes; and RT-qPCR with primers spanning the breakpoint region [25].

1.1.5.3.   Emerging diagnostic tools

Liquid biopsy represents a highly relevant approach for the management of difficult-to-approach tumors [25] like EwS [5]. However, to date, no blood or urine biomarkers are available for EwS. The only exception is serum lactate dehydrogenase for which elevated levels have been reported to correlate with tumor burden and to have diagnostic and prognostic value. Recent advents in bioinformatics is now offering new possibilities in exploiting blood biomarkers like circulating tumor cells, cell-free circulating tumor DNA, and tumor-derived extracellular vesicles, and their cargo (nucleic acids, proteins, lipids and metabolites). For example, copy numbers of cell-free EWSR1::ETS fusion sequences has been reported to correlate with EwS risk factors like disease stage, tumor volume and response to treatment [26] (reviewed in [27]). Alternatively, flow cytometry-based detection of CD99-positive cells in peripheral blood might also represent an interesting approach [28]. Recently, an innovative study has reported a machine learning approach to classify sarcomas based on DNA methylation profiling data. In the future, the specificity of the sarcoma methylome might also be exploited for diagnostic applications [29]–[31].
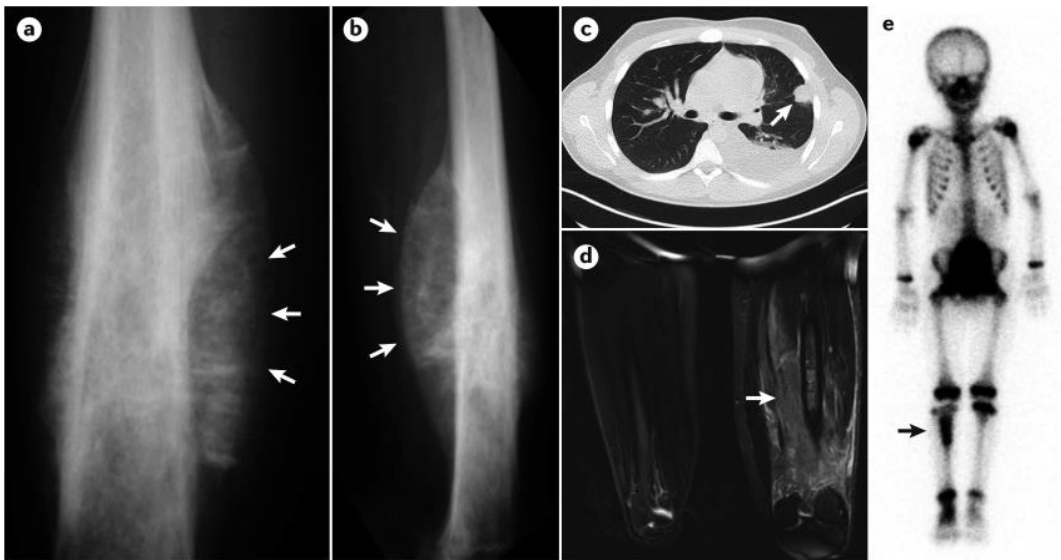
Figure 3. Radiological presentation of EwS. Anteroposterior (**a**) and lateral (**b**) X-ray images showing an osteolytic lesion of EwS (arrows) in a femur. (**c**) CT scan of the lungs showing a pulmonary metastasis (arrow). (**d**) MRI scan showing the primary tumor in the femur shown in (**a**) and soft-tissue oedema (arrow). (**e**) Bone scintigraphy evidencing an EwS tumor mass in the right tibia (arrow). From [5].
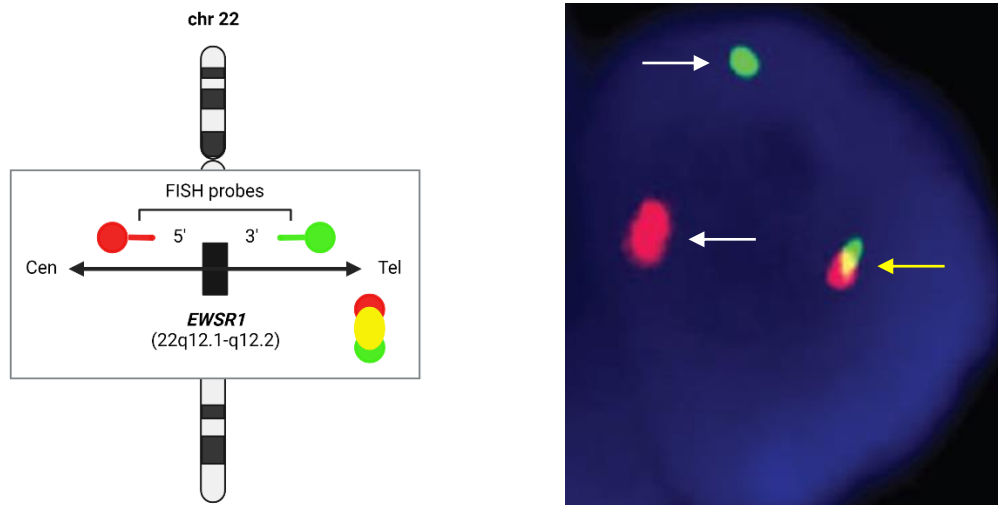
Figure 4. Fluorescence *in situ* hybridization in EwS. Right panel illustrates the approach based on *EWSR1* break-apart probes**.** Right panel shows an interphase nucleus with one normal fusion signal (yellow arrow) and one split signal pattern (white arrows) indicating rearrangement of one copy of EWSR1 region. Cen = centromere, Tel = telomere. Modified from [25], [32]. Created with BioRender.com.

1.1.6. Prognosis factors and treatment

1.1.6.1. Overall survival

EwS is an aggressive malignant neoplasm and ~25% of patients already present metastases at diagnosis that are often resistant to intensive therapy. Disease stage represents the main prognosis factor. Relapsed EwS displays the worse outcome with <10% of 5-year overall survival. Then, comes metastatic disease which is unsurprisingly associated with lower survival rates (<30%) than localized disease (~70%) [33], [34].

The tumor occurring site and volume are the next most important prognostic factor. In particular, patients with distal primary tumors generally exhibit better outcome than patients with proximal tumors, where local treatment may be challenging owing to the proximity to vital organs [5]. Moreover, extraosseous locations are generally associated with a more favorable outcome than bone locations [35]. Large tumor volumes (>200 mL) at diagnosis is another unfavorable prognostic factor [36].

1.1.6.2. Management

Typically, the care of newly diagnosed patients combines intensive (poly)chemotherapy, local surgery and/or radiotherapy. Patients with metastatic disease can alternatively be involved on randomized clinical trials. Chemotherapy is administered before surgery to reduce the size of the primary tumor and to target micrometastases that are expected to occur in all patients [5]. In the clinics, the exact chemotherapy regimens might slightly differ in Europe and North America but, generally, they rely on well-known anticancer drugs such as vincristine, ifosfamide, cyclophosphamide, etoposide, cisplatin, doxorubicin and methotrexate [37], [38]. Surgery and/or

radiotherapy ensure local control of the disease. Surgery consists in resection of tumor tissues. When post-surgical reconstruction is required but not feasible, EwS can sometimes lead to amputation [5].

1.1.6.3.   Emerging therapies

Although the introduction of chemotherapy improved survival in patients with localized disease from 10% to 70%, it is associated with acute and chronic adverse effects that affect the quality of life in survivors [5]. These adverse effects range from reduced fertility, cardiomyopathy, renal insufficiency to therapy-induced secondary cancers [5]. Therefore, dismal prognosis of metastatic and relapsed EwS, compromised quality of life in survivors, mutilating surgeries as well as resistance to therapy have long motivated the development of novel therapeutic approaches.

Like other cancers, immunotherapy (*e.g.*, immune checkpoint inhibitors, adoptive T-cell therapies, cancer vaccines) represents an attractive approach [39] that is currently investigated in sarcomas [27]. However, fusion-positive sarcomas, like EwS, are often referred to as 'immune deserts' or 'cold tumors' owing to weak immune infiltration [5], [27]. Importantly, EwS displays very low expression levels of programmed death ligand 1 (PD-L1), indicating that immune checkpoint inhibitors are probably irrelevant in this context [40], [41]. The implication of the insulin-like growth factor (IGF) pathway in EwS biology prompted the development of anti-IGFR1 antibodies but with limited success in clinical trials owing to resistance development [42]. Despite modest results so far, immunotherapy remains a clinically feasible approach for the management of EwS [43]–[45]. In particular, EF-specific neoantigens (derived from the breakpoint region) might represent attractive immune targets to induce EwS-specific T-cell responses [46], [47]. Readers interested about neoantigens-based immunotherapy can refer to [48], [49] for extensive review.

1.2. Cell of origin

More than a century after the groundbreaking discovery of EwS, the cell of origin of this disease remains an enigma owing to its undifferentiated phenotype [5], [50]. Since no genetic subtypes have been described, EwS is thought to derive from a single cellular lineage. Importantly, ectopic expression of EF induces senescence or apoptosis in most untransformed cells [51], suggesting that a permissive cellular context is required to recapitulate EwS biology. As EwS predominantly arises in bone, its cell of origin may reside in developing bone mesenchyme [52], [53]. Historically, several candidate cells have been proposed such as bone marrow-derived mesenchymal stem cells (MSCs), neural-crest-derived cells (NSCSs), bone progenitors and osteochondrogenic progenitors [51], [52]. In particular, NSCSs have been reported as candidate cells because EwS cells expressed NSCS-specific markers. However, expression of EF has been described to impose neuronal and endothelial features on non-EwS permissive cellular contexts [54], [55]. This feature has probably mistaken James Ewing himself in its original phenotypic classification [53]. These observations indicate that the expression of NSCS-specific markers most probably result from the

transcriptional reprogramming function of EF rather than reflecting the phenotype of the supposed cell of origin.

MSCs are pluripotent cells that have self-renewal capacity and the ability to differentiate along the adipogenic and osteogenic lineages [56]. To date, they represent the best candidate cell of origin of EwS for two main reasons [5]. First, expression of EF in MSCs impairs differentiation, leads to cell transformation and tumor growth that phenocopy Ewing tumors (*e.g.*, CD99 expression) [57]–[59]. Second, the knockdown of EF in EwS cells shapes a transcriptome that resemble the one of MSCs and results in the gain of pluripotency [60]. For these reasons, EwS is classified among mesenchymal tumors [11].

1.3. Genetics

Genetically, EwS is mainly characterized by *FET*::*ETS* gene fusions, which associate a member of the FET RNA-binding protein family and an ETS TF. Here, I will start with a brief presentation of the landscape of *FET::ETS* gene fusions in EwS. Next, I will highlight important insights of their respective parent gene families. Finally, I will cover other genetic abnormalities that, to a lower extent, also contribute to EwS biology.

1.3.1.   FET::ETS gene fusions

FET::*ETS* gene fusions are the genetic hallmark of EwS. They encode neomorphic fusion proteins which constantly associate the N-terminal transactivation low complexity region of FET proteins to the C-terminal DNA-binding domain of ETS TFs [5]. Historically, they were considered to primarily arise from balanced reciprocal chromosomal translocations [5], a common cause of gene fusions during which DNA segments are rearranged by transfer between chromosomes without the loss of genetic material [61]. The first translocation, t(11;22)(q24;q12) responsible for EwS was identified in 1983 [62] and molecularly elucidated as being *EWSR1*::*FLI1* in 1992 [63]. Recently, *EWSR1*-derived gene fusions have been described to frequently arise from chromoplexy, complex loop-like rearrangements, rather than by simple translocations [64].

Found in 85% of cases, EF represents the most recurrent genetic event in EwS [5], [14]. In the remaining 15% of cases, *EWSR1 or FUS* are fused to other ETS members such as *ERG*, *FEV*, *ETV1* and *ETV4* [65]–[72]. Interestingly, these different but related gene fusions drive EwS tumors with similar phenotypic and clinical features [73]. Recently, a genetic variant implicating TAF15, the third member of the FET family, has been discovered in EwS [74]. The landscape of *FET*::*ETS* gene fusions in EwS is depicted in **Figure 5**.
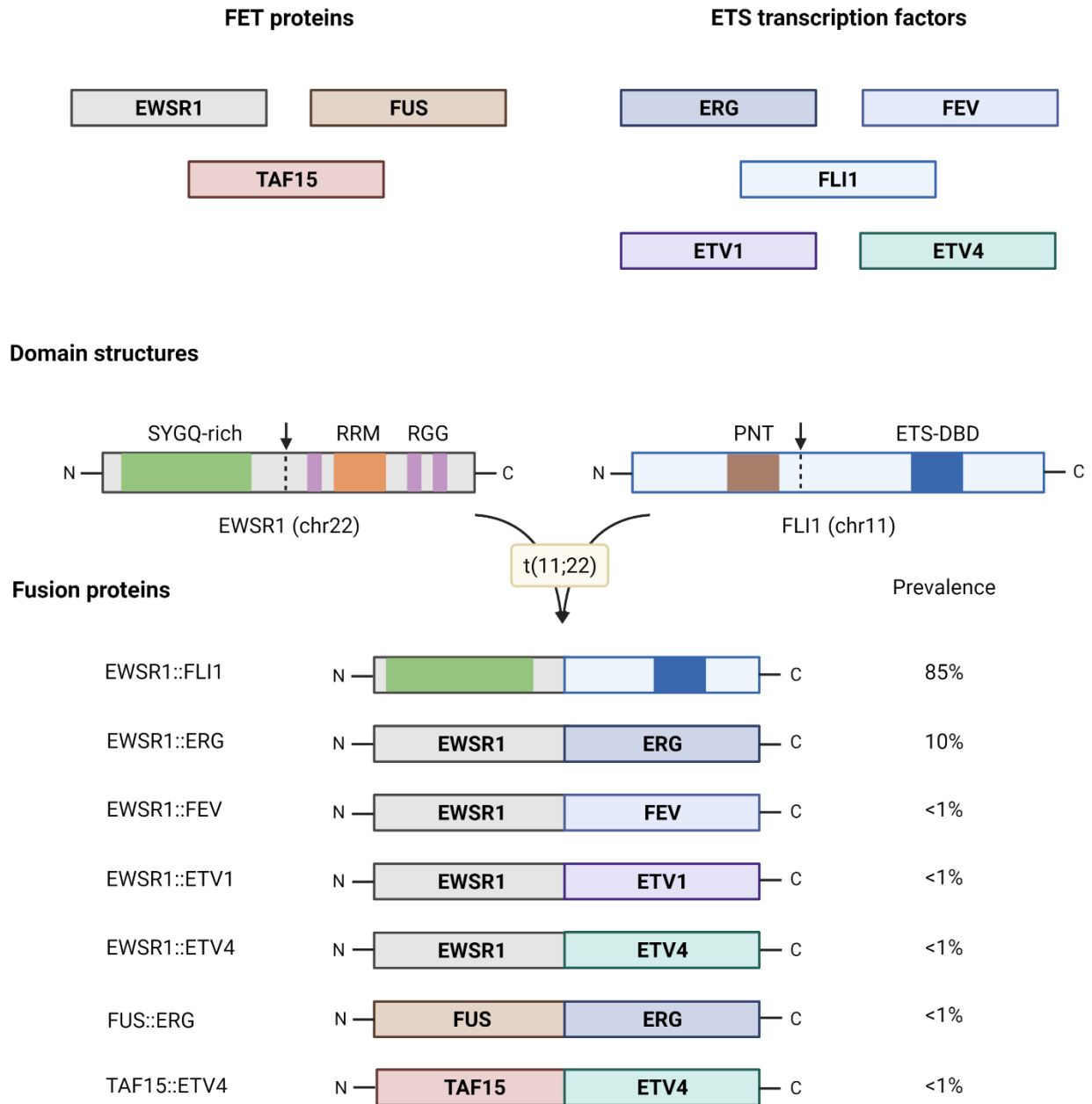
Figure 5. Main *FET*::*ETS* gene fusions observed in EwS. Arrows indicate breakpoint regions. Modified from [14]. Created with BioRender.com.

Gene fusion breakpoints designates the chromosomic regions where the aberrant rejoining occurs [61]. Depending on their precise locations within parent loci, different variants have been described for *FET*::*ETS* gene fusions. Of note, variants can also result from alternative splicing of the fusion pre-mRNA. In the context of the EF transcript, a dozen variants have been reported (**Figure 6**) [25]. The two most frequent variants contain EWSR1 exon 7 and either FLI1 exon 6 (also known as fusion type I) or FLI1 exon 5 (also known as type II) [65]. Although this remains unclear, the different variants of EF seem to have similar prognostic values.
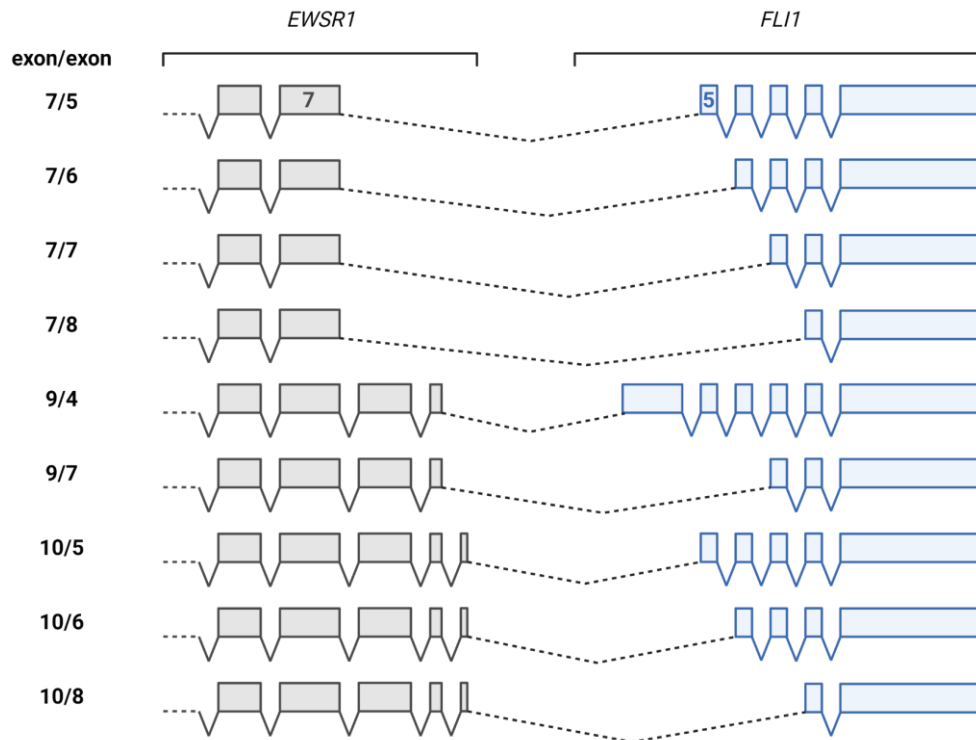
Figure 6. Schematic representation of several EF variants. EF variants can arise from different breakpoint choices in *EWSR1* and *FLI1* loci, as well as from alternative splicing of *EF* pre-mRNA. EF 7/6 = type I, EF 7/5 = type II, EF 10/6 = type III, EF 7/7 = type IV. Modified from [25]. Created with BioRender.com.

1.3.2.   The FET family of RNA-binding proteins
1.3.2.1.   General presentation

The FET gene family comprises three members: *FUS* (*Fused in sarcoma*), *EWSR1* (*Ewing sarcoma breakpoint region 1*, or also *EWS*) and *TAF15* (*TATA-binding associated factor 15*). They encode ubiquitous RNA-binding proteins (RBPs) that belong to the superfamily of heterogeneous nuclear ribonucleoprotein particle (hnRNP) proteins [75]. Structurally, FET proteins share high sequence homology and display a common domain organization, including a low-complexity (LC) N-terminal transactivation domain, several arginine-glycine-glycine-rich (RGG) boxes, a RNA recognition motif (RRM), a zinc finger domain (ZnF), and a C-terminal nuclear localization signal (NLS) [75], [76]. FET proteins are evolutionary-conserved in vertebrates, suggesting that they play important functions [75].

In eukaryotic cells, FET members are nucleocytoplasmic shuttling proteins that are mainly located in the nucleus [76]. They are described as multifunctional RBPs with ability to bind both DNA and RNA. They have been implicated in many aspects of gene expression regulation as well as in DNA damage repair. In the nucleus, FET proteins can serve as positive or negative transcription coregulators via interactions with TFs, the RNA polymerase II (RNAPII), the TFIID complex and chromatin regulators [75]. Importantly, wild-type FET proteins are generally considered as weak

transcriptional activator owing notably to in-*cis* repression of the NTD by RGG boxes in the C-terminal domain (CTD) [77]. In addition to transcription, FET proteins have described regulatory functions in pre-mRNA splicing [78], [79], mRNA export and miRNA processing [80], [81]. They can bind to GU-rich motifs within untranslated regions (UTRs) of many transcripts via their RNA-binding domain [75], [82]. In the cytoplasm, and under specific conditions, FET proteins can regulate translation [83] and mRNA stability [84], and are involved in the formation of membrane-less RNA granules via their LC NTD and RGG boxes [75], [76]. The domain organization and above-described molecular functions of FET proteins are summarized in **Figure 7**. Although FET proteins have also been suggested to play non-redundant functions, their specificity remains unclear.
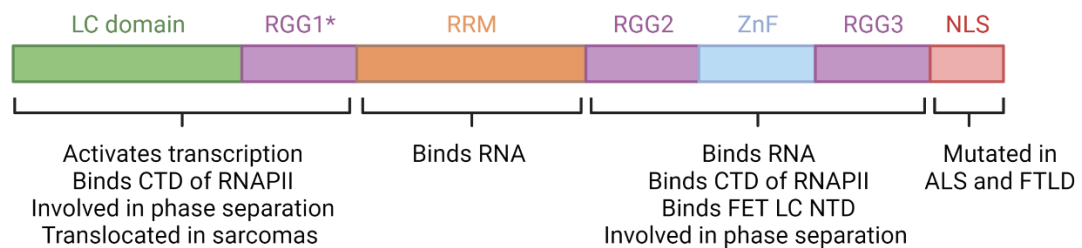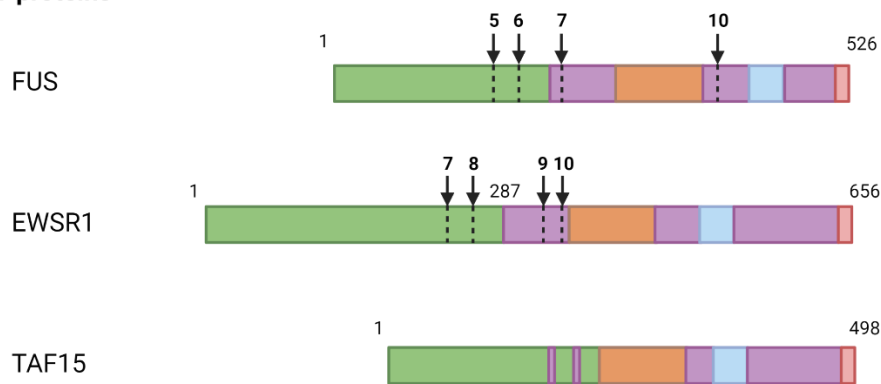
Figure 7. Domain organization and brief overview of the molecular functions of the FET proteins. Asterisk indicates that the first RGG domain is not very apparent in TAF15. Arrows indicate breakpoint regions. Numbers in bold indicate exons. Modified from [75]. Created with BioRender.com.

1.3.2.2. Structural disorder and phase transition

Like many other RBPs and TFs, FET proteins are intrinsically-disordered proteins (IDPs). IDPs represent a growing fraction of the human proteome (~30%) [85]. They contain intrinsically disordered regions (IDRs). IDRs are "protein sequences that lack a defined 3D structure under naive or physiological conditions" [86], [87]. IDRs are characterized by a low overall hydrophobicity that prevents protein folding into typical protein structures such as α-helices and

β-sheets[2] [87]. They are further classified between molecular recognition features (MoRFs) [88], short linear motifs (SLiMs) [89], and low complexity (LC) sequences [90]. FET RGG boxes represent a typical example of SLiMs. This class of IDRs mediates protein-protein interactions and is often the site of post-translational modifications (PTMs) [87]. By contrast, the FET NTD belongs to the LC class. LC sequences are defined as amino acid sequences >100 residues with repeats of one to a few residues [90]. In particular, the FET NTD is composed of 30 degenerated hexapeptide repeats (DHRs), defined by the prion-like[3] SYGQQS consensus motif (**Figure 8**). In DHRs, the aromatic amino acid tyrosine in second position is absolutely conserved. Importantly, aromaticity of the LC NTD is critical for transcription and transforming activity of EF [91], [92]. Within the first 64 amino acids, the FET domain has been reported to mediate homotypic and heterotypic protein-protein interactions [93].
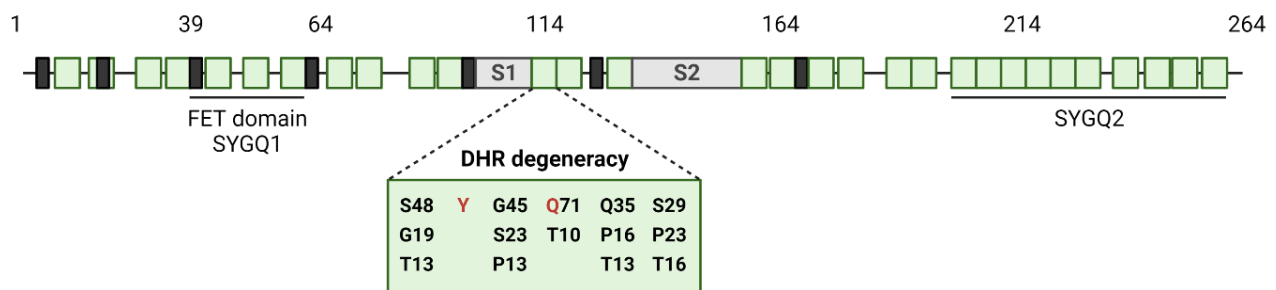
Figure 8. Composition of the EWSR1 low-complexity N-terminal domain. DHRs are represented by the green boxes. They are defined by the SYGQQS consensus motif. DHR degeneracy is shown. For each amino acid position, the percentages of prevalence of alternative amino acids are indicated by numbers. The tyrosine (Y, red) in second position is absolutely conserved. The glutamine in fourth position (Q, red) is largely conserved. Tyrosines outside of DHRs are indicated by black boxes. Spacers between DHRs are generally of only a few residues except for S1 and S2 (shown in light grey), which are 12 and 25 residues, respectively. Modified from [91]. Specific subregions (*i.e.*, FET domain [93], SYGQ1 and SYGQ2 [92]) described in the literature are shown. Created with BioRender.com.

Despite lacking 3D structure, IDPs are fully-functional proteins and have key biological functions [94]. Notably, IDPs often occupy central positions within protein interactome, suggesting that IDRs participate in numerous protein-protein interactions [95]. Moreover, IDRs confer liquid-liquid phase transition properties to IDPs[4] [85]. In the context of FET proteins, the LC NTD and RGG boxes promote the formation of membrane-less liquid-like condensates via multivalent cation-π interactions between tyrosine and arginine residues [96], [97]. FET phase separation is

---

[2] IDRs can however gain a more ordered state of folding into specific conditions, such as upon interaction.

[3] The FET LC NTD is also referred to as prion-like domain (PrLD) in the literature because its amino acid composition is reminiscent of prions [700]. First discovered in the 1960's, prions can cause neurodegenerative disorders in humans, such as Creutzfeldt-Jacob or Kuru [701].

[4] LLPS is a physicochemical process during which a homogeneous solution spontaneously demixes into two or more distinct phases owing to changes in the environment, such as temperature, pH, salt or protein concentrations. LLPS regulates the formation of biomolecular condensates, which are emerging as a widespread mechanism of spatiotemporal coordination in eukaryotic cells [199].

dynamically regulated by several PTMs, including tyrosine phosphorylation [98], O-GlcNAcylation [99], arginine methylation [100], [101] and arginine citrullination [102] (**Figure 9**). Under physiological conditions, phase separation is a reversible process that underlines FET molecular functions [75]. For example, in the nucleus, FUS has been proposed to function in transcription by clustering with RNAPII via phase transition [97]. RNAPII clustering is thought to regulate the transition from the initiation to the elongation phase by controlling the accessibility of the RNAPII CTD for phosphorylation [103]. In stress conditions, phase transition of FET proteins is a key determinant in the formation of cytosolic membrane-less RNA granules [75]. As discussed later, these granules are involved in the regulation of mRNA translation, storage and degradation.
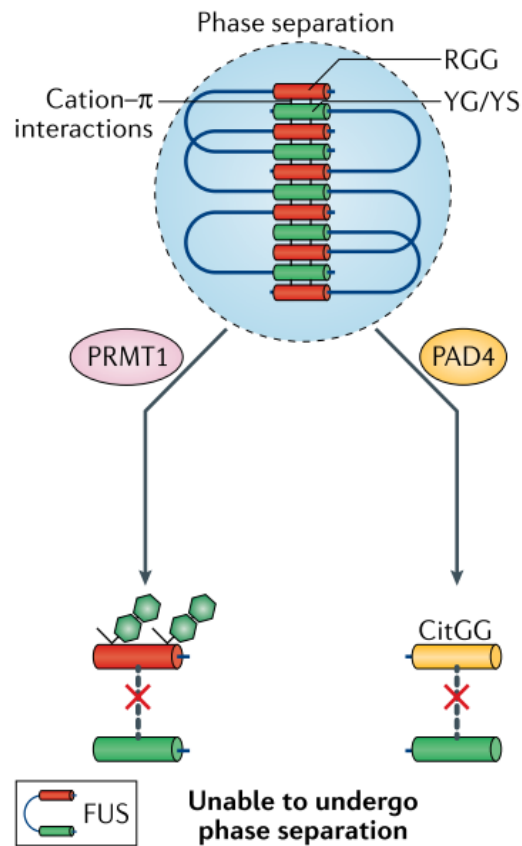
Figure 9. Regulation of FUS phase separation by PTMs in arginine residues. FUS phase separation is mediated via cation-π interactions between its tyrosine-rich low complexity domain (YS/YS, green) and its arginine-glycine-glycine-rich domain (RGG, red). Methylation of arginine residues within RGG domains by PRMT1 or their citrullination (CitGG) by PAD4 disrupt cation-π interactions, and thus prevent FUS phase separation. Modified from [104].

1.3.2.3.   Medical significance

FET proteins are of great medical interest because their dysfunction has been related to many disorders. They are involved in the pathogenesis of a number of sarcomas and leukemias via fusions [105], and neurodegenerative diseases via point mutations or aberrant PTMs [75], [76]. Overexpression of EWSR1 has also been linked to multiple myeloma progression [106].

a) Cancers

EWSR1 and *FUS* (previously known as TET) were initially discovered because of their implication in chromosomal rearrangements in sarcomas [107]. Interestingly, ~50% of sarcomagenic fusions contain a member of the FET family [108]. Strikingly, the LC NTD is invariably present and fused in 5'position of either an ETS factor (FET::ETS fusions) or another TF (FET::non-ETS fusions). In both cases, FET-derived rearrangements lead to fusion TFs. Importantly, the NTD confers two main aberrant features to FET-derived fusions. First, it provides a potent transactivation domain because inhibition by the CTD in wild-type FET proteins is lost via fusion. For this reason, EF has been described as a stronger transcriptional activator that non-fusion FLI1 [109]. Second, it provides neomorphic properties to EF via phase transition [92]. This topic will be further discussed later. Importantly, FET-derived fusions give rise to well-defined entities, including for example EwS (EWSR1::FLI1), desmoplastic small round cell tumors (EWSR1::WT1), myxoid liposarcoma (FUS::DDIT3), clear-cell sarcoma and angiosarcoma (EWSR1::ATF1), extraskeletal myxoid chondrosarcoma (EWSR1/TAF15::NR4A3) and acute myeloid and/or lymphoblastic leukemia (FUS::ERG) [110]. This suggests that FET-derived fusions act as dominant oncoproteins. They are summarized in **Figure 10.**
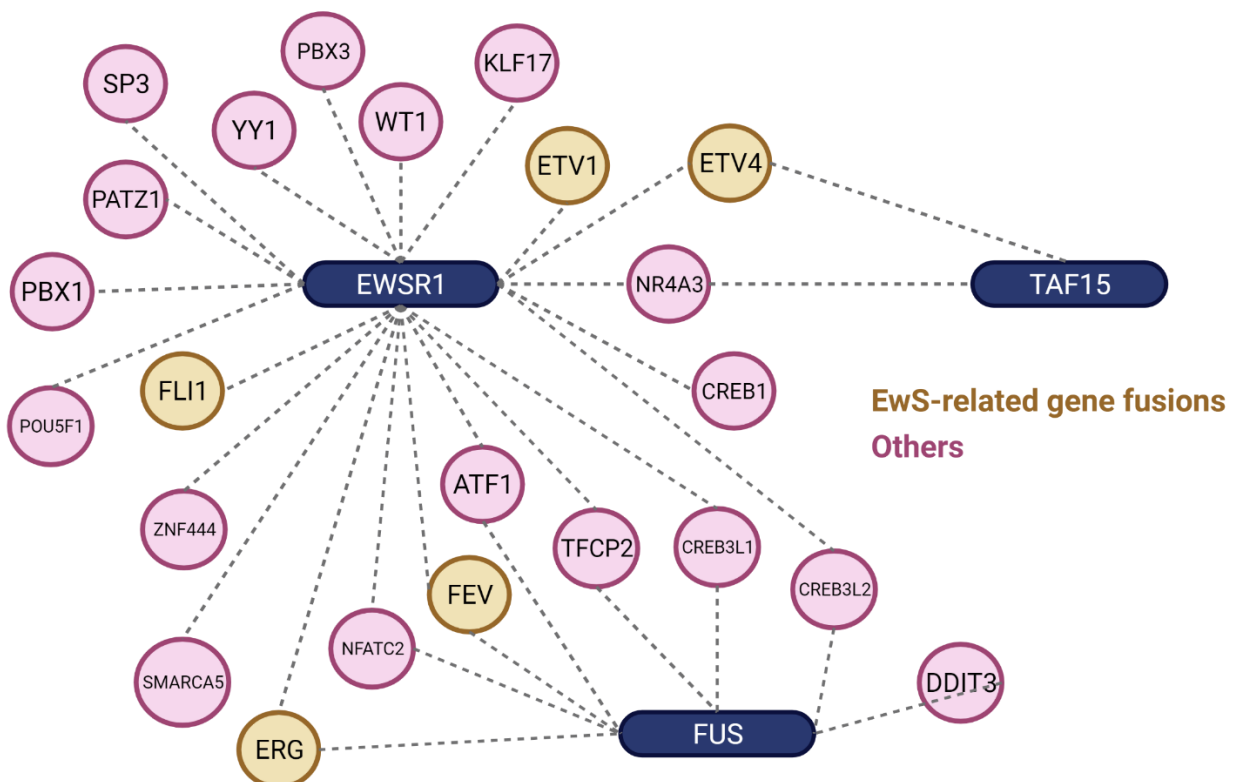
Figure 10. Network of recurrent pathognomonic FET-derived gene fusions in sarcomas and leukemias. EwS-related gene fusions are in brown. Non-EwS-related gene fusions are in red. From [108]. Created with BioRender.com.

b) Neurodegenerative diseases

FET proteins, and mainly FUS, are responsible for neurodegenerative diseases such as amyotrophic lateral sclerosis and frontotemporal dementia [111]. In this context, point mutations or aberrant PTMs in the NLS or IDRs deregulate their nucleocytoplasmic shuttling and phase transition properties [100]–[102]. This leads to unphysiological and irreversible solid-like aggregations of FET proteins in the cell cytoplasm (**Figure 11**). How FET protein aggregation drives neurodegeneration is unclear. It has been proposed to contribute in a dual manner. On the one hand, it may act by toxic gain-of-function by sequestering essential regulators and/or triggering aberrant signaling pathways that ultimately result in cell death [112]. On the other hand, it may also act by depleting the normal functions of FET proteins.
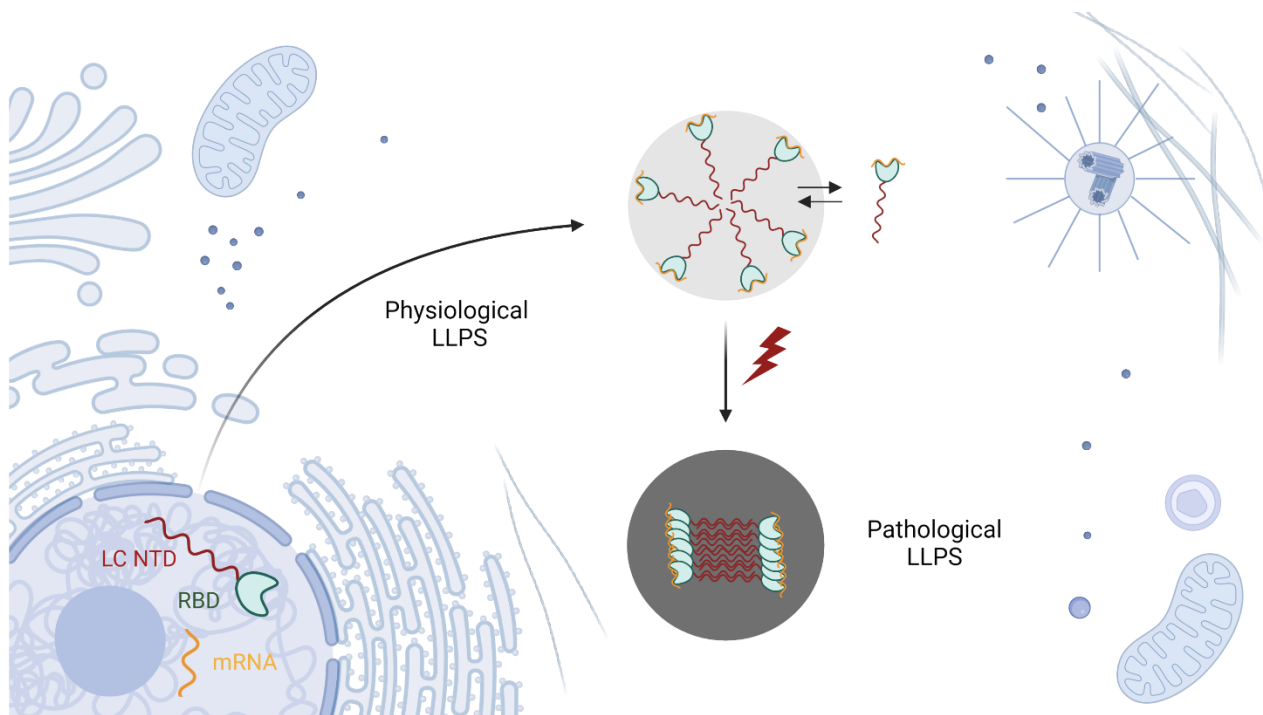
Figure 11. LLPS of FET proteins in physiology and neurodegeneration. See main text for details. LC NTD = low-complexity N-terminal domain, RBD = RNA-binding domain, LLPS = liquid-liquid phase separation. Modified from [113]. Created with BioRender.com.

1.3.3.   The ETS transcription factor superfamily

1.3.3.1.   General presentation

The E-twenty-six-specific sequence (or also E26 transforming sequence, ETS) family represents a large family of TFs, comprising 28 proteins distributed within 12 subgroups/subfamilies with 1 to 3 members (**Figure 12**) [114]. ETS proteins are implicated in various biological processes, but they typically control gene expression during embryonic development and differentiation. Structurally, this metazoan-specific family is defined by its evolutionary-conserved DNA-binding domain (ETS domain) [114]–[116]. All ETS factors can bind to the core GGAA/T motif [117]. Below I focus my description on the Erg subfamily.
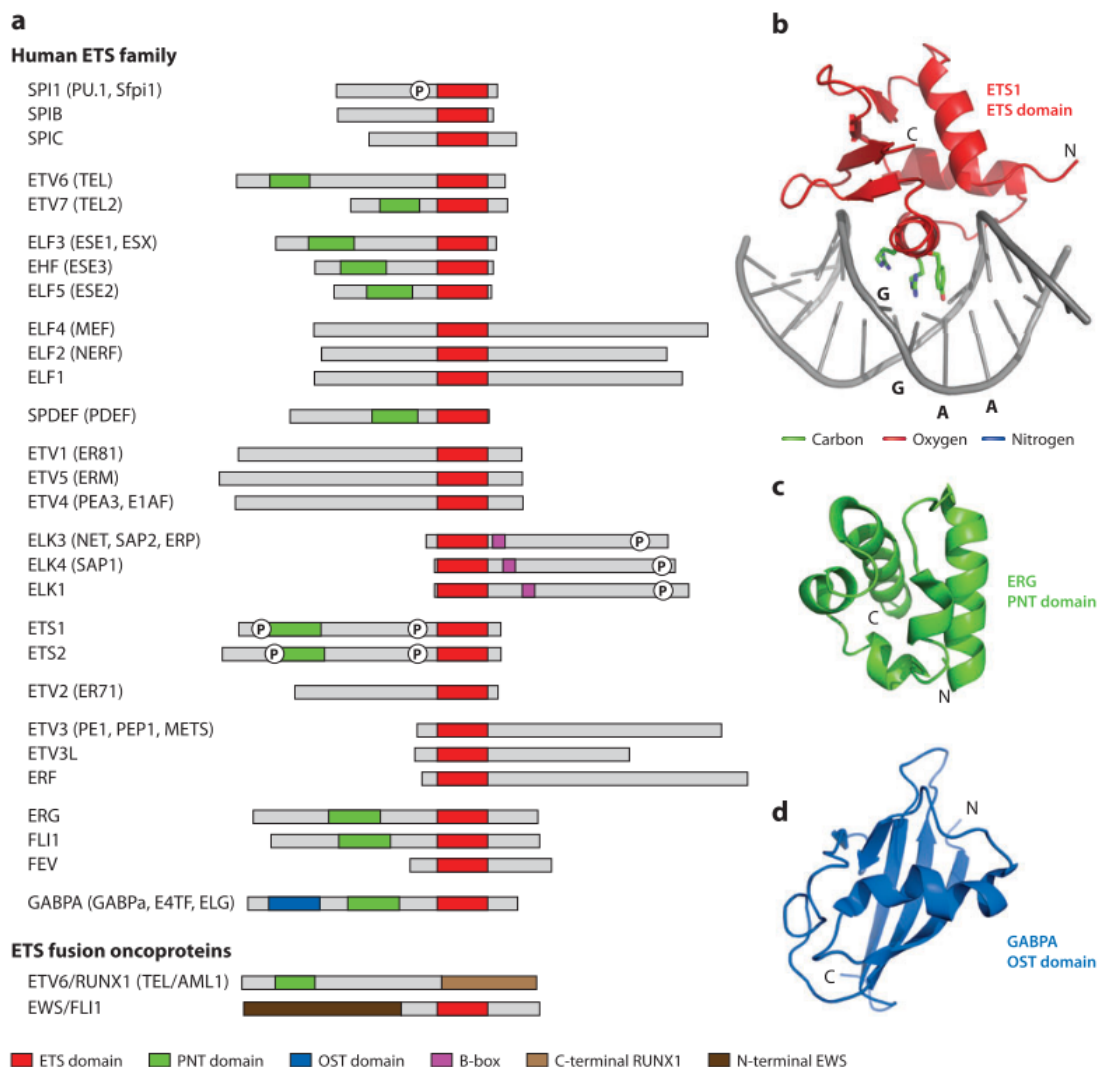
Figure 12. The ETS superfamily of transcription factors. (**a**) Nomenclature and domain composition of human ETS proteins. Two examples of ETS-derived gene fusions are given. (**b-d**) Ribbon diagrams of ETS1 ETS domain (**b**), ERG PNT domain (**c**) and GABPA OST domain (**d**). From [114].

The Erg subfamily of ETS factors is composed of three members: *ERG* (*ETS-Related Gene*), *FLI1* (*Friend Leukemia virus Integration 1*) and *FEV* (*Fifth Ets Variant*). They encode tissue-restricted developmental TFs. In adults, ERG expression is mainly found in endothelial cells, FLI1 in hematopoietic cells and FEV in neurons. During embryogenesis, ERG and FLI1 are key regulators of hematopoiesis. Interestingly, they have also been linked to differentiation of cartilage and bone formation owing to their localization in precartilaginous region. In contrast, FEV is thought to be involved in brain development [114]–[116].

Structurally, ERG and FLI1 are very homologous. They contain a central ETS domain flanked by two transcriptional activation domains – namely ATAD in amino-terminal position and CTAD in carboxy-terminal position (**Figure 13**). Both are able to activate or repress gene expression. The ATAD contains an ~85-aa long pointed (PNT) domain that is related to the Sterile Alpha Motif superfamily. Together with the ETS domain, it is involved in DNA-binding but can also mediate interactions with proteins, RNA and lipids. ERG and FLI1 also contain several nuclear localization signal (NLS), in N-terminal of the PNT domain and within the ETS domain. In constrast, FEV is more divergent. It does not contain an ATAD domain and its CTAD is less homologous compared to the one of ERG and FLI1 [115], [118].

Erg factors
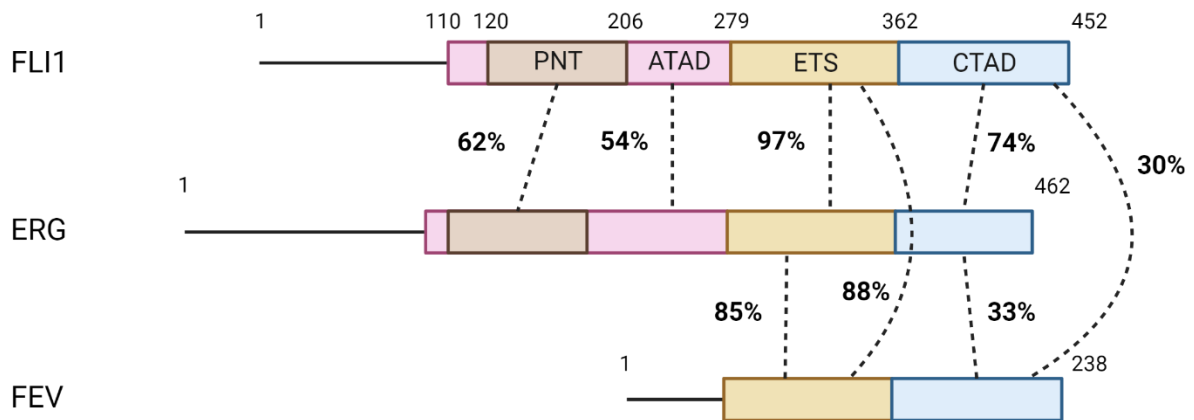
Figure 13. Domain composition of the Erg subfamily of ETS transcription factors. Percentages of homology between Erg proteins are indicated for each domain. Modified from [118]. Created with BioRender.com.

Erg proteins have been largely described for their role in transcription, which has been related to the regulation of the cell cycle, proliferation, differentiation, apoptosis, adhesion, angiogenesis, migration and inflammation. Interestingly, some ETS factors, and in particular ERG, have been implicated in post-transcriptional processes, such as pre-mRNA splicing [119], and mRNA degradation (see later) [120]. Together, these data indicate that ETS factors control gene expression in a diversified manner and should not thus be regarded solely as TFs.

17

1.3.3.2.   ETS DNA-binding domain

The ETS DNA-binding domain belongs to the superfamily of winged helix-turn-helix DNA-binding domains (DBD) [115], [121]. It is 85-aa long and is composed of three α-helices and four anti-parallel stranded β-sheets organized as follows: α1-β1-β2-α2-α3-β3-β4 [122], [123]. Two conserved arginine residues in the third helix enables binding to the core consensus ETS-binding site (EBS) GGA[A/T]. Most ETS factors bind DNA over a 12-15-bp long region centered on the EBS [117]. In the human genome, ChIP-seq experiments revealed that the EBS is enriched near the transcription start site (TSS) in promoters, in enhancers as well as in intronic regions of a myriad of genes [114]. Importantly, ETS factors are known to control gene expression in a combinatorial manner via PPIs that often implicate other TFs [115]. Beyond this, DNA-binding preferences are further determined by the DNA flanking regions of the EBS, the relative expression pattern of ETS factors (competition for EBS in promoters/enhancers) and autoinhibition/autoactivation events via intramolecular interactions. Interestingly, the ATAD has been described to stabilize the ETS DBD. Finally, alternative splicing and PTMs can also impact the DNA-binding capacity of ETS factors [114], [115].

1.3.3.3.   Medical significance

ETS factors, and in particular the Erg subfamily, are implicated in several cancers via overexpression or gene fusions. Their dysregulation has mainly been related to their well-described role in the control of transcription [124], [125]. ETS overexpression can cause leukemias while ETS-derived fusions are responsible for several sarcomas, leukemias, breast, gastric, head and neck, prostate and thyroid cancers [124]. In ETS-derived fusions, the ETS DBD is often conserved and fused in 3'position of a ubiquitous RBP, such as in FET::ETS fusions. In this context, the otherwise tissue-restricted DBD becomes often highly active owing to the association with an active promoter[5], as exemplified in *EWSR1*::*FLI1*. In some cases, such as in ETV6-derived fusions, the PNT domain instead of the DBD is conserved via fusion and associated in 5'position of either another TF (ETV6::RUNX1) or the tyrosine kinase domain of diverse oncogenes [124].

1.3.4.   Other genetic alterations

As for most childhood cancers, EwS (dark blue in **Figure 14**) is characterized by a relatively silent/quiet genome compared to adulthood cancers and presents one of the lowest mutation rate across all cancer types [126]. For this reason, EwS is generally considered as a prototypic model to study oncogenic processes in a simplified genetic context [14].

---

[5] As a result of the reciprocal translocation, FLI1::EWSR1 is also produced but rarely observed in EwS because this fusion is controlled by the tissue-restricted promoter of FLI1 [5]. This variant has been reported to be necessary for EwS growth and to collaborate with EF in MSCs to promote proliferation [702].
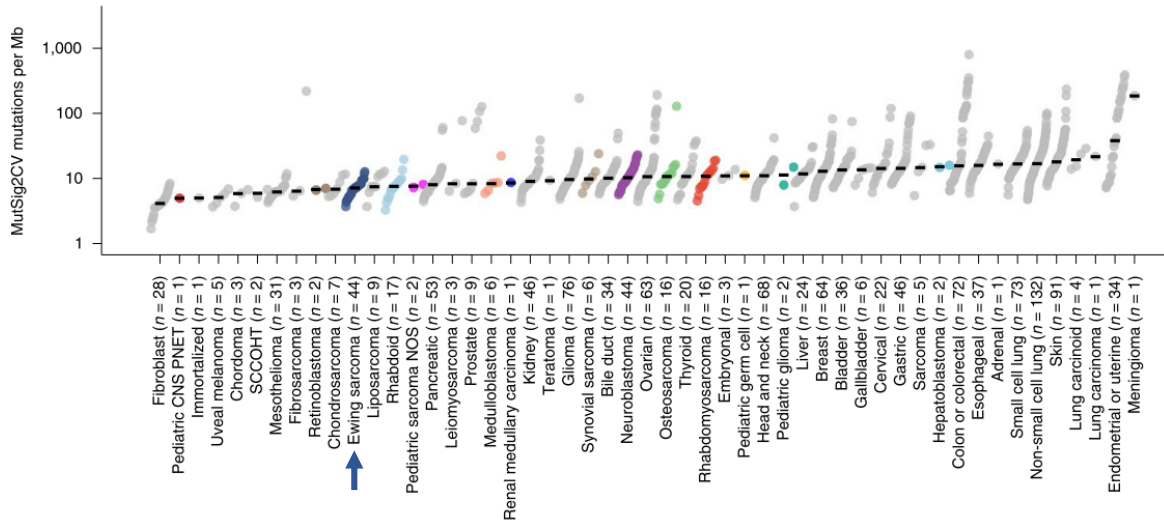
Figure 14. Mutational rates as mutations per Mb in whole-exome sequencing as calculated using MutSig2CV (y axis), grouped by solid tumor type (x axis), with diseases ordered by median burden. Each circle represents an individual cell line with pediatric tumors colored by type; the black line represents the median mutation rate per tumor type. EwS is indicated by the arrow. Modified from [126].

Typically, the natural history of EwS is thought to start with the emergence of a first oncogenic hit (*i.e.*, *FET*::*ETS* gene fusions), which are sufficient for the initiation and maintenance of sarcomagenesis in a permissive microenvironment [56]. Recently, whole-genome sequencing studies of EwS have identified additional recurrent mutations that can accelerate disease progression and are associated with poor patient outcome, including STAG2 (cohesin subunit SA-2, 15-21%), CDKN2A (cyclin-dependent kinase inhibitor 2A, 10-22%), TP53 (tumor protein 53, 5-7%), EZH2 (methyltransferase, ~3%), ZMYM3 (cell morphology and cytoskeletal organization, ~3%) and BCOR (transcriptional co-repressor, ~3%) [127]–[129]. Notably, STAG2 mutations have been shown to cause aneuploidy in human neoplasms [130]. Interestingly, ~13% of EwS patients have been reported to display inactivating germline mutations in DNA repair genes, such as BRCA1 [131]. The pathological role of this 'BRCAness signature' remains however unclear [5]. Recently, genome-wide association studies (GWAS) have identified six additional EwS susceptibility loci, comprising TARDBP (a RBP that is structurally similar to EWSR1), known EF target-genes (EGR2 and NKX2-2), members of core EF regulatory circuitries (RREB1) and genes involved in centrosome stabilization (KIZ) and apoptosis (BMF) [5], [20], [132]. Interestingly, frequencies of most risk loci show disparities between Europeans and Africans, thus contributing to the demographic bias in EwS incidence [20]. Finally, cytogenetic analyses have also revealed recurrent copy number variations in EwS, including chromosome (chr) 8 gain (50%), chr2 and 1q gain (25%), chr20 gain (10-20%) and chr16q loss [133]–[135]. Some of these chromosomal abnormalities are sometimes used for routine diagnosis by FISH [5]. The mutational landscape of several EwS cell lines is summarized in **Figure 15**.
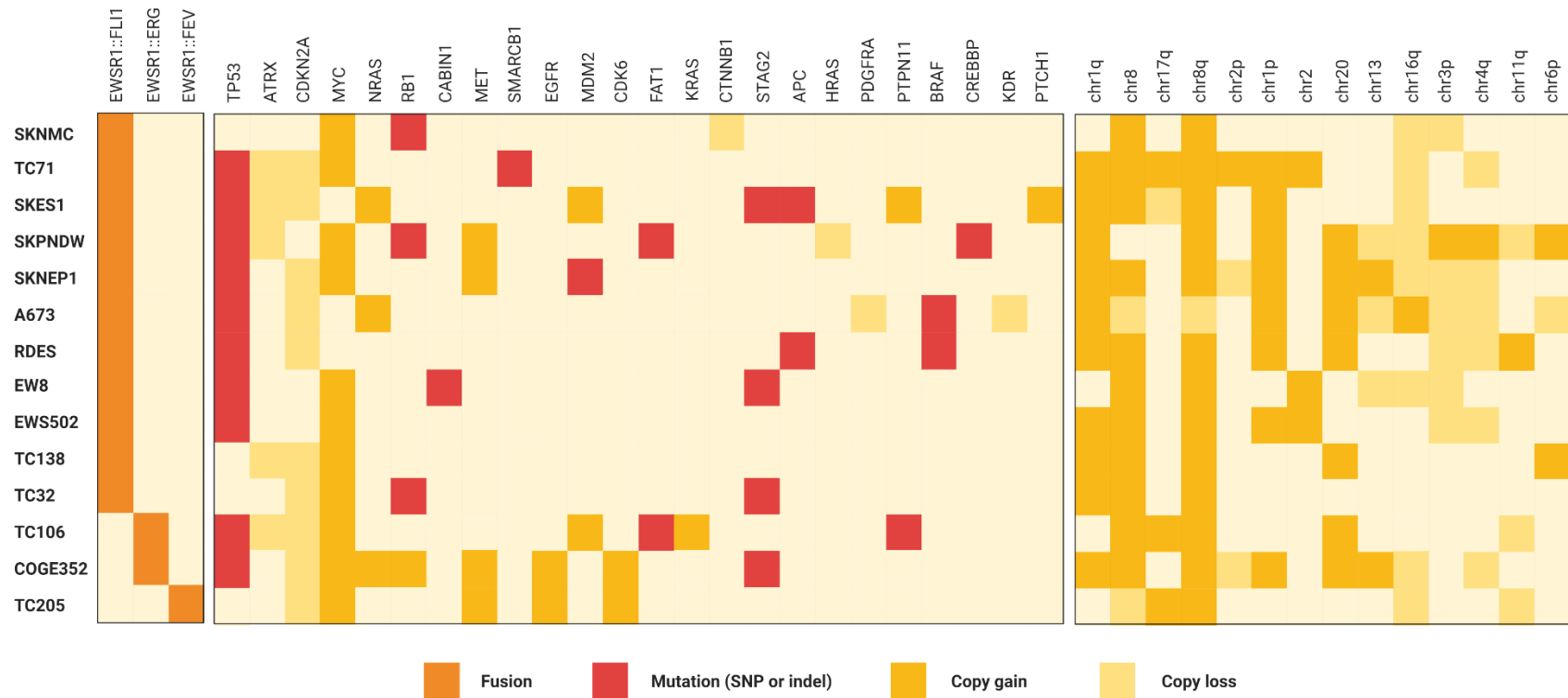
Figure 15. Mutational landscape of several EwS cell lines determined by whole-exome sequencing. Modified from [126]. Created with BioRender.com.

1.4. Oncogenic molecular properties of EF

EF is the main driver of EwS because it is critical for cell transformation and proliferation [57], [136], [137]. Despite this well-established importance, the precise molecular functions of EF are still under intense investigations, leading to several dozens of high-profile publications each year. Novel findings are constantly illustrating how diverse and complex are the roles of EF. To date, EF has mainly been studied as an aberrant TF owing to its inherited domain composition. According to the current model, EF drives tumorigenesis by actively deregulating transcriptional and epigenetic processes. Previously, post-transcriptional processes were considered to contribute indirectly to EwS, notably as a result of the loss of wild-type EWSR1 functions[6] [79]. Interestingly, a number of recent studies have now revealed that EF can also play an active role in alternative splicing, indicating that post-transcriptional dysregulation might also directly contribute to Ewing sarcomagenesis. Here, I successively review the aberrant control of transcription, chromatin organization and epigenetic marks, and post-transcriptional processes by EF.

1.4.1. Transcription regulation

Structurally, EF encodes a well-defined TF containing a potent amino-terminal transactivation domain (ATAD) and a C-terminal DBD, respectively derived from the NTD of EWSR1 and the CTD of FLI1 (**Figure 16**). Initially, this domain composition led to the idea that EF serves as an aberrant TF in EwS [63], [138]. Below I discuss early and more recent observations supporting a role for EF in the control of transcription, and briefly cover the relationship between this function and EwS biology and susceptibility.
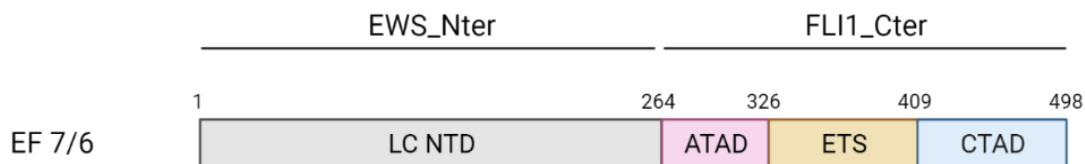
Figure 16. Domain composition of the EF 7/6 fusion protein. Created with BioRender.com.

1.4.1.1. Early observations

EF was first described as a potent transcriptional activator [109], [138], [139]. Both EWSR1 ATAD and FLI1 DBD were evidenced to be critical for EF-mediated transformation [109], [140], [141], suggesting that transcriptional activation is key in EwS biology. Importantly, EF also appears to act as a transcriptional repressor [142], [143] in a way that has been related with the FLI1 CTAD domain [144]. This domain was proposed to confer regulatory functions to the transcriptional activity of EF and to be critical for EF-mediated transformation [144]. The importance of the CTAD has been further supported recently [145]. Consistently with a role in transcription, many transcriptional targets were identified using either ectopic expression of EF in heterologous

---

[6] In EwS, EWSR1-derived gene fusions can lead to EWSR1 haploinsufficiency [79].

systems, mainly NIH3T3 mouse fibroblasts at first [146]–[149] and later MSCs [150], [151]; or silencing of EF in patient-derived EwS cell lines [143], [152]–[154].

1.4.1.2.   Transcriptome profiling

More recently, microarray and deep-sequencing-based profiling analyses revealed that EF completely reprograms the expression of thousands of genes to support sarcomagenic transformation. Surprisingly, more genes were found to be repressed than activated by EF with a ratio of ~3:1. Gene ontology analysis of activated genes revealed enrichment in genes related to cell-cycle regulation and cell proliferation. By contrast, repressed genes are enriched in genes related to epithelial-to-mesenchymal transition (EMT), cell adhesion, cell migration, cell morphology and differentiation [155].

1.4.1.3.   DNA-binding motifs

In the cell nucleus, EF binds to DNA via the DBD of FLI1. Interestingly, ChIP-seq studies revealed that EF binds to two types of motifs in the genome [156], [157] (**Figure 17**). As initially evidenced [138], EF binds to canonical EBS composed of a single GGAA element like wild-type FLI1. Additionally, EF binds to GGAA microsatellites – *i.e.*, repetition of GGAA elements [156], [158], [159]. Since parent proteins are unable to bind to GGAA repeats, this DNA-binding preference represents a neomorphic property of the fusion protein. Importantly, several transcriptional targets of EF were demonstrated to be physically regulated by GGAA repeats identified within promoters, distant regulatory enhancers or introns. This includes for example NR0B1 (also known as DAX1), CAV1, FCGRT, FEZF1, SOX2 and SOX6 [158], [160], [161]. Although exceptions exist, EF has been reported to display distinct transcriptional regulatory activities depending on the binding site: activated genes are often associated with GGAA repeats while repressed genes tend to be associated with canonical EBS [157]. Molecular dissection of GGAA repeats revealed that EF-target genes exhibit maximal responsiveness for 18 to 26 repetitions. Outside this range, EF-responsiveness is reduced [21], [162]. I further discuss the importance of GGAA repeats in EwS biology later.

Figure 17. ChIP-seq-identified DNA-binding motifs of EF, canonical ETS factors and FLI1. Modified from [163].

1.4.1.4.   GGAA repeats

In the human genome, GGAA repeats are widespread and are found both within intergenic and intragenic regions. In particular, >2,500 genes have been related to such elements [158]. Historically, GGAA repeats were considered to be 'junk DNA' – *i.e.*, DNA regions without apparent importance. EwS represents one of the first example of the utilization of such regions as DNA response elements by a TF [164].

Another interesting feature of GGAA repeats is that they are poorly conserved throughout evolution. This explains the discrepancies between transcriptional targets identified in murine NIH3T3 cells and human EwS cells [51], [165], [166]. Furthermore, germline polymorphisms[7] in GGAA repeats regulating critical EF transcriptional targets, including notably NR0B1 [21], [167], CAV1 [167], EGR2 [168], and MYBL2 [169] have been linked to patient outcome and/or EwS susceptibility (**Figure 18**).
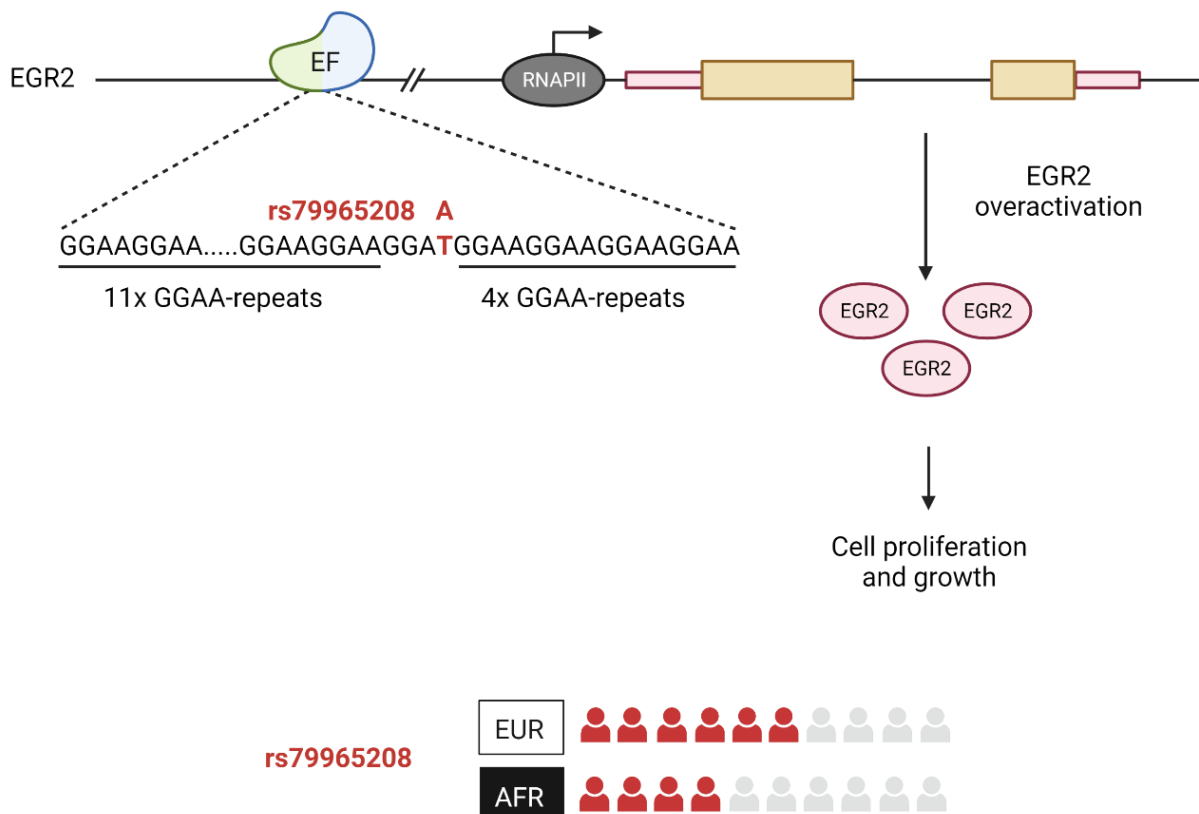
Figure 18. GGAA polymorphisms in EGR2 loci and EwS susceptibility in European and African populations. Modified from [113]. Created with BioRender.com.

---

[7] Including variations in size, length or genomic location

1.4.1.5.   Indirect regulation of transcription

Surprisingly, the comparison of the modulated targets after EF knockdown and EF-bound ChIP-seq targets revealed an overlap of only ~10%, suggesting that most of the transcriptional effects of EF are actually indirect. Several mechanisms have been proposed to account for this observation. First, as for ETS factors, sequence specificity can be dictated through cooperation with other TFs. Cooperation between EF and other TFs, such as AP.1, E2F, NRF1 and NFY, has indeed been reported [170]. Second, part of EF transcriptional signature can be orchestrated via other transcriptional regulators whose expression is altered by EF [171]. In this context, activation of NKX2-2 by EF was described to partly mediate EF-dependent repression of mesenchymal features [172], [173]. Another interesting example is provided by FEZF1, a TF and a direct target of EF, that has recently been described to regulate the expression of neural-specific genes in EwS, which might contribute to the imposition of a neural phenotype on EwS cells [174]. Third, interference with the activities of transcriptional regulators can also play a role. Notably, EF has been described to perturb MRTFB/YAP-1/TEAD target gene regulation, thereby participating in the cytoskeletal reprogramming of EwS cells [175]. Finally, by regulating DNA accessibility, epigenetic mechanisms play a fundamental role in transcription regulation. Therefore, their deregulation by EF are also susceptive to contribute both directly and indirectly to Ewing sarcomagenesis. These mechanisms are discussed below.

1.4.2.   Chromatin organization and epigenetic marks

Ectopic expression of EF in MSCs leads to important morphological changes and impair differentiation. Given the importance of epigenetic mechanisms in cell identity and the remarkably low level of genetic alterations in EwS, aberrant rewiring of the epigenome by EF was invoked to play a critical part in this tumor.

The epigenetic mechanisms are well-known to regulate gene expression by making DNA more or less accessible to the transcription machinery without changing the DNA sequence[8]. In eukaryotic cells, this epigenetic control can occur at multiple levels that range from DNA modification (*e.g.*, methylation), histone modification, nucleosome repositioning, to remodeling of the 3D chromatin architecture. In EwS, EF has been described to affect all these levels to create a unique chromatin landscape that functionally supports oncogenic transformation [176] (**Figure 19**). Importantly, analysis of EwS epigenomics have further supported MSCs as putative cells of origin for two main reasons. First, stem cells chromatin appears to offer a permissive environment that is exploited by EF. Second, silencing of EF in EwS leads to an epigenetic signature resembling the one in MSCs [177]. Below I describe how EF remodels the chromatin organization and the epigenetic marks in EwS.

---

[8] The epigenetic mechanisms are commonly defined as the "chromatin-based events that regulate DNA-templated processes" [703].
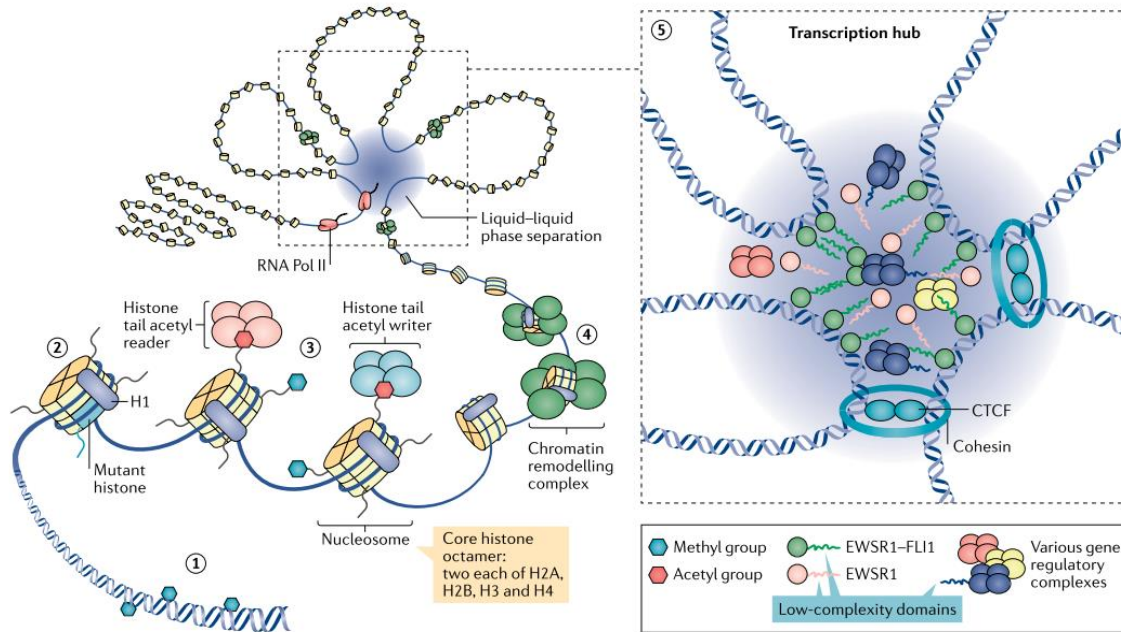
Figure 19. Epigenomic deregulation by EF in EwS. (**1**) DNA modification, such as methylation. (**2-3**) Histone modification, such as methylation and acetylation. (**4**) Nucleosome repositioning by chromatin remodelling complexes. (**5**) Remodeling of the 3D chromatin architecture (*e.g.*, chromatin looping). From [176].

1.4.2.1.   Enhancers reprogramming

In EwS, epigenetic changes within enhancers are so profound that it has been defined as an 'enhancer disease' [178], [179]. EF can either activate *de novo* enhancers[9] (EwS-specific enhancers) or repress enhancers that are usually active in MSCs (MSC-specific enhancers). Enhancers reprogramming occurs via either DNA-binding-dependent or DNA-binding independent mechanisms. When bound to DNA, EF has been demonstrated to utilize divergent mechanisms to activate or repress enhancers depending on the underlying DNA sequence (**Figure 20**) [157]. At GGAA repeats, EF multimers promote chromatin opening and induces *de novo* enhancers that physically interact with target promoters, which ultimately leads to gene activation [157]. Interestingly, EF multimers are able to recruit the BRG1/BRM (BAF)[10] (also known as SWI/SNF complex) chromatin-remodeling complex via phase separation of its prion-like LC NTD [92], [180]. Importantly, tyrosines within this region appear to be essential in this process because their mutation abrogate the interaction with the BAF complex. In addition to BAF, EF multimers recruit the MLL methyltransferase complex and the histone acetyltransferase p300. By methylating or acetylating specific lysine residues on histones, these enzymes induce further chromatin relaxation [178]. By contrast, at single GGAA elements, EF monomers inactivate

---

[9] Enhancers are cell type-specific and dynamically used regulatory elements that control the temporal and spatial activation of gene expression [704].

[10] The BAF complex is a well-known regulator of chromatin accessibility at enhancer and promoter regions.

conserved enhancers by acting as dominant negative factors, leading to gene repression. More specifically, they displace physiologically-bound ETS factors along with their associated chromatin regulators, resulting in the silencing of genes activated by wild-type ETS factors [157]. EF might also recruit the corepressor nucleosome remodeling NuRD complex and the LSD1 deacetylase to further reduce chromatin accessibility, as evidenced for the *LOX* gene target [181]. Interestingly, enhancers reprogramming has been reported to activate oncogenes as well as potential therapeutic targets, and to repress tumor-suppressors and mesenchymal lineage regulators [157]. Like for enhancers, EF also establishes divergent chromatin remodeling inside promoters [178].

By hijacking chromatin regulators, EF acts as a pioneer factor, converting silent chromatin regions into fully active enhancer to drive aberrant transcriptional programs. Very interestingly, several other sarcomagenic gene fusions, including FUS::DDIT3 in liposarcoma [182], [183], PAX3::FOXO1 in alveolar rhabdomyosarcoma [184], [185], and SS18::SSX in synovial sarcoma [186]; have also been reported to deregulate epigenetic programs. Among them, FUS::DDIT3 and SS18::SSX have notably been reported to hijack normal BAF function [182], [183], [187], [188], suggesting that this feature might represent a common theme among dominant fusion TFs. Another interesting point is that all these fusions harbor tyrosine-rich IDRs.
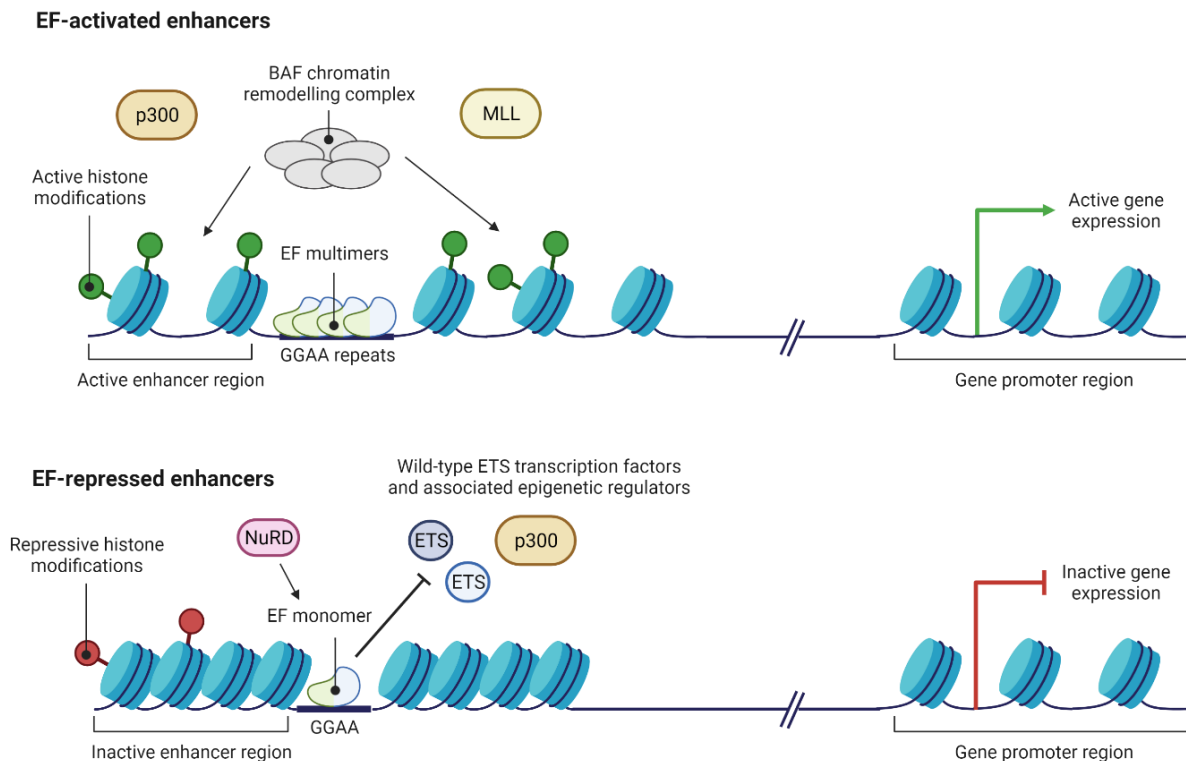
Figure 20. EF-mediated enhancer reprogramming in EwS. See main text for details. Modified from [110]. Created with BioRender.com.

Intriguingly, most deregulated/repressed enhancers in EwS are not bound by EF, suggesting the implication of indirect epigenetic mechanisms. Several mechanisms have been proposed, including notably the activation of negative chromatin regulators like EZH2[11] [189] or core regulatory circuitry TFs like KLF15, TCF4 and NKX2.2 [190], and the recruitment of HDACs [191], co-repressor NurD complex and histone demethylases like LSD1 [181]. Noteworthy, genome-wide DNA methylation sequencing studies revealed EwS-specific hypomethylation in enhancers targeted by EF [179]. This epigenetic change has been proposed to synergize with EF-mediated enhancers reprogramming.

1.4.2.2.   3D chromatin architecture remodeling

In the eukaryotic cell nucleus, DNA is not linear but rather exhibits a complex multiscale 3D organization, that hierarchically comprises chromosome territories, compartments and topologically-associating domains (TADs) (**Figure 21**). At the level of TADs, chromatin loops mediate important transcriptional regulatory functions by shaping promoter-enhancer interactions. Their formation is regulated by two main architectural proteins, namely cohesin and CTCF (**Figure 22**) [192], [193]. Interestingly, 3D genome architecture appears to drive stem cell differentiation decisions [192].

In EwS, EF is now emerging to actively remodel 3D chromatin architecture, leading to the creation of oncogenic transcription hubs within super-enhancer regions[12]. In these hubs, EF establishes novel interactions between promoters and distant enhancers via aberrant chromatin looping [176]. Chromatin looping in EwS is mediated in a cohesin/CTCF-independent manner via phase separation of EF at GGAA repeats [176] (**Figure 19**), further highlighting the importance of the EWSR1-derived LC NTD. On this basis, EF has also been described to redefine TAD boundaries in order to support EwS development [194]. Amazingly, two other oncogenic fusion TFs have recently been reported to also mediate aberrant chromatin looping via phase separation, including ESWR1::ATF1 in clear cell sarcoma [195], and NUP98::HOXA9 in leukemia [196]–[198]. Together, these findings illustrate that phase separation is becoming an increasingly-recognized driving force of oncogenesis, and that fusion TFs like EF support neoplastic transformation by acting as master chromatin regulators [199][110].

---

[11] EZH2 is involved in the repression of differentiation and the maintenance of stemness.
[12] Super-enhancers are large genomic regions enriched in active enhancers. They have been identified as critical regulators of cellular identity [705].
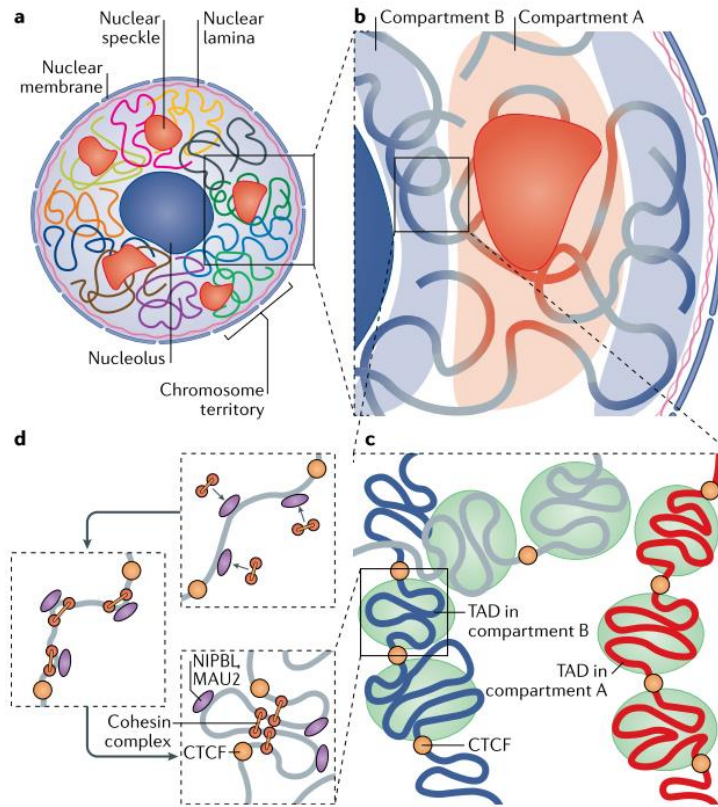
Figure 21. 3D genome structural organization in eukaryotes. (**a**) Chromosome territories. (**b**) Compartments. (**c**) Topologically-associating domain (TAD). (**d**) Chromatin loops and associated architectural proteins. From [192].
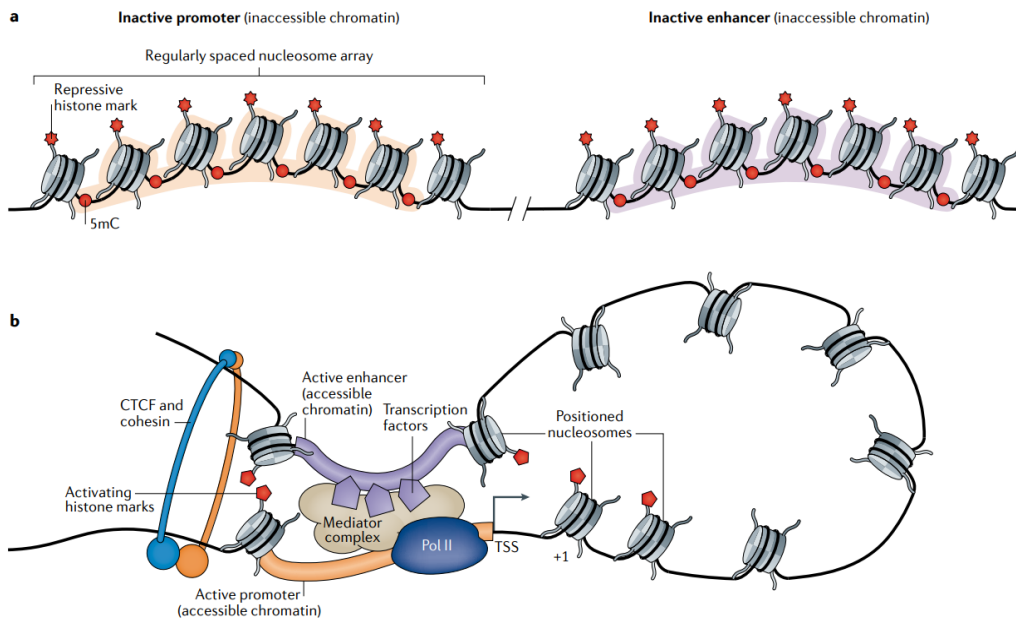
Figure 22. Chromatin looping mediated by CTCF and cohesin shapes promoter-enhancer interactions. After chromatin looping, distant promoter (orange) and enhancer (purple) can become close. From [200].

1.4.3.   Post-transcriptional processes

Because the RBD of EWSR1 is lost via fusion, post-transcriptional processes were originally assumed to contribute indirectly to EwS pathogenesis, notably via disruption of wild-type EWSR1 splicing-related functions. Nevertheless, some studies very early hypothesized that EF might also actively reprogram gene expression via post-transcriptional processes, notably pre-mRNA alternative splicing based on two main observations. First, DNA-binding mutants of EF conserve a transforming potential, suggesting that EF also induces DBD-independent oncogenic pathways [201], [202]. Second, EF is able to bind to splicing factors and can alter splice site selection, for example by interfering with splicing factors [203]–[205]. Until recently, these aspects have however remained largely overlooked compared to the transcriptional function of EF.

1.4.3.1.   Modulation of alternative splicing

In 2008, EF has been reported to influence splicing of cyclin D1 gene (CCND1). Upon interaction with RNAPII within CCND1 locus, EF slows down elongation rate and promotes the production of a more oncogenic isoform named cyclin D1b [206], [207]. These results support a role for EF in alternative splicing by modulating RNAPII elongation rate.

More recently, EF has been shown to modulate alternative splicing via more direct mechanisms. In 2014, EF is shown to compromise alternative splicing of FAS death receptor via direct interaction with wild-type EWSR1 [79]. In 2015, EF is reported to bind directly to RNA [208], which is a striking observation given that the RBD of EWSR1 is lost via fusion and that FLI1 lacks any canonical RBD. The same year, another study from the same research group identified a consensus RNA-binding motif for EF using CLIP-seq. They found that this motif is enriched in 5'exon-intron boundaries [209]. In this study, an interactome of EF based on liquid chromatography and mass spectrometry (MS) is also reported for the first time. To date, it represents the only publicly-available interactome for EF. Interestingly, KEGG-pathway analysis of MS-identified binding partners revealed a strong enrichment (~30%) for spliceosome-related factors, suggesting that EF is a network hub involved in alternative splicing regulation. Accordingly, exon array and RT-qPCR analyses led to the identification of >70 targets with either retained or skipped exons, including *ARID1A*, *RUNX2*, *EZH2*, *TERT*, *CUL4A*, *CAV3*, *CALD1*, *HDAC8*, *USP2*, and *IGFBP3* [209]. Mechanistically, EF-mediated alternative splicing appears to occur in a DHX9[13]/DDX5-dependent manner because treatment of EwS cells with YK-4-279 – a small molecule inhibitor previously reported to disrupt interactions between EF and RNA helicases [208], [210] – reverts EF-mediated alternative splicing events without affecting its transcriptional activity [209]. Previously, YK-4-279 had been shown to impair tumor growth in EwS orthotopic xenografts [210]. Taken together, these findings indicate that the aberrant regulation of alternative splicing by EF might also directly contribute to EwS development. Although the specificity and the efficacy of this drug remains disputable in light of more recent studies [211],

---

[13] Also known as RNA helicase A (RHA)

this illustrates that protein-protein interaction inhibitors (iPPIs) might represent an interesting class of drugs to target oncogenic partnerships implicating LC fusion TFs.

The interactomic study of EF is the first demonstration that EF actively reprograms alternative splicing in EwS. In addition, this study supports the old idea that the splicing activity of EWSR1 is perturbed via fusion, which would contribute indirectly to EwS development. Indeed, EWSR1 and EF appeared to belong to distinct spliceosome-related network, with EWSR1 network implicating YB-1 and DHX9 and EF network implicating PRPF6, hnRNPK, DDX5 and DHX9 [79], [204], [209], [212]. Therefore, the gained copy of EF cannot compensate for the lost copy of EWSR1.

Recently, several studies have reinforced the idea that EF actively deregulates alternative splicing in EwS [119], [213], [214]. In particular, in the lab of "Gene Expression and Cancer", we identified that EF alters the RBFOX2-mediated splicing regulatory function of wild-type ERG proteins in a way that supports EwS cell phenotype [119].

1.4.3.2.   Deregulation of non-coding RNAs

Non-coding RNAs (ncRNAs), including notably microRNAs (miRNAs) and long non-coding RNAs (lncRNAs) are well-known post-transcriptional regulators with documented roles in diseases [215], [216]. In EwS, several studies have reported altered expression of miRNAs (*e.g.*, hsa-miR-145, miR-30a-5p and miR-214-3p) [217]–[224], as well as lncRNAs (*e.g.*, EWSAT1, SOX2OT, TUG1 and FOXP4-AS1) [225]–[228]. Perturbation of ncRNAs might arise from transcriptional deregulation or defects during their processing, and has been linked to important aspects of EwS biology, including for example cell proliferation, cell plasticity, metastasis [219], and transcriptional repression [225]. Given the well-characterized role of ncRNAs in processes like mRNA translation and degradation, these findings suggest that EF might also indirectly deregulate cytoplasmic post-transcriptional processes.

1.4.3.3.   Other processes

Although it has not been formally demonstrated yet, EF might also control late post-transcriptional processes in a direct manner (*i.e.*, not via the modulation of the expression of direct post-transcriptional factors). Supporting this, prior to this work, we found numerous RBPs in the published interactome of EF [209]. In particular, by comparing the list of EF potential binding partners with literature-curated lists of RBPs and TFs [1], [229], we found ~22% of RBPs (123 out of 548 EF interactors) and only 2% of TFs (11 out of 548 EF interactors) (**Figure 23a**). In particular, RRM-containing RBPs appeared to be highly enriched (**Figure 23b**). Interestingly, KEGG-pathway analysis of EF interactors strikingly revealed that ~30% of them are related to metabolism, ~11% to RNA transport, and ~10% to mRNA degradation and surveillance while cell cycle regulators, the most investigated class, represent ~9% of this interactome (**Figure 23c**) (data from [209]). In this interactome, we also identified 15 mRNA-decay[14] associated factors (**Figure**

---

[14] Several of these factors will be further described in the next chapter.

23d), which led us to hypothesize that EF might be involved in the control of mRNA stability in addition to its functions in the control of transcription and alternative splicing. Of note, one cannot exclude that the identification of post-transcriptional factors among EF interactors also indicate that these factors might work as transcriptional cofactors of EF (*i.e.*, involved in EF-mediated transcription regulation). Recently, a growing number of exciting studies have reported direct roles in the control of mRNA stability for many canonical non-fusion DNA-binding TFs in humans, thus providing a rationale for investigating such post-transcriptional roles for other TFs. These studies will be further discussed at the end of the next chapter. Interestingly, although anecdotic, EF has been described to decrease, via an uncharacterized mechanism, the mRNA stability of IGFBP3 (insulin-like growth factor binding protein 3) [230], previously reported as a direct repressed transcriptional targets of EF [143]. Taken together, these observations might point towards novel post-transcriptional function of EF, and thereby unanticipated actionable molecular targets.

a

b

c
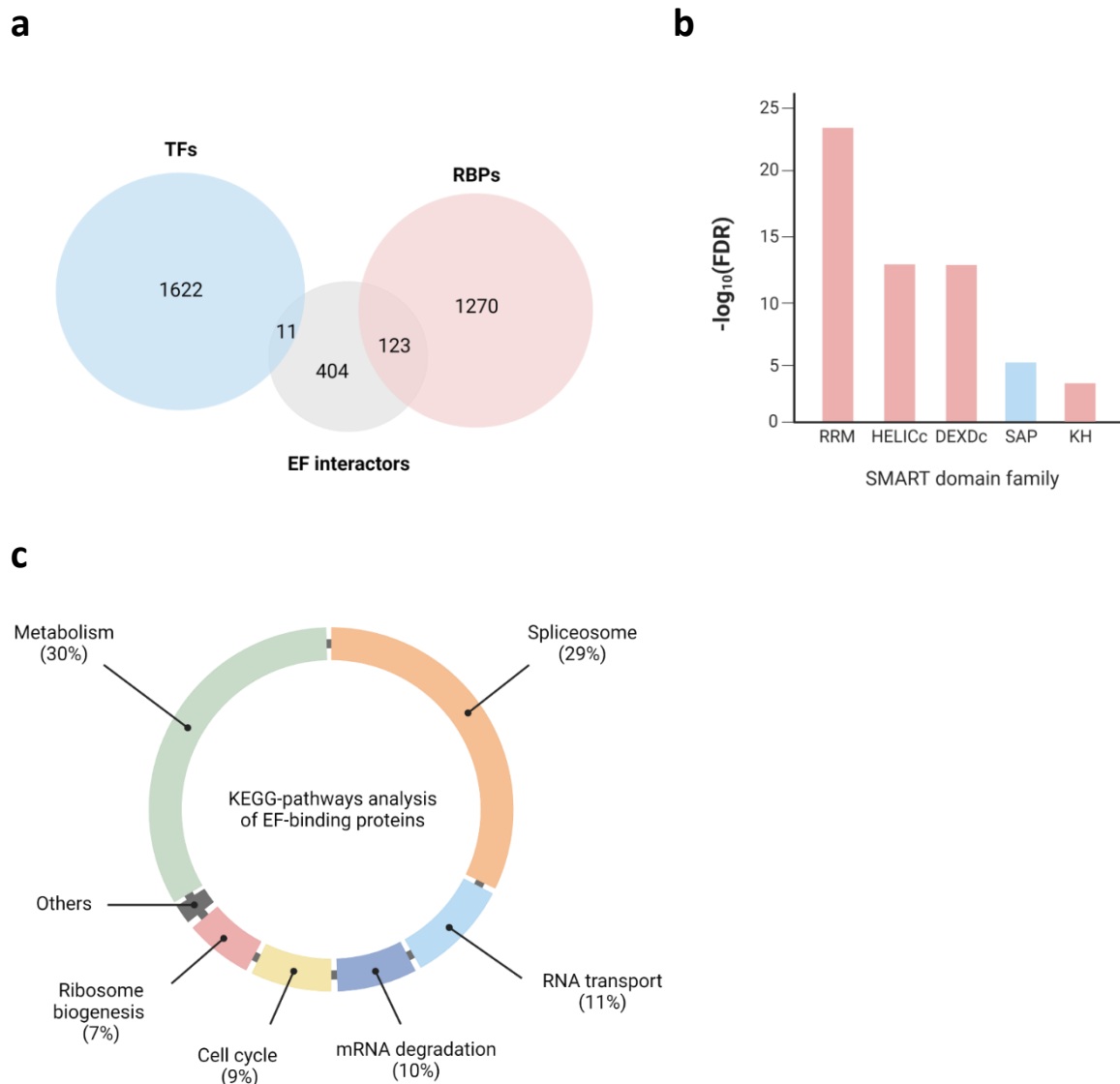
d
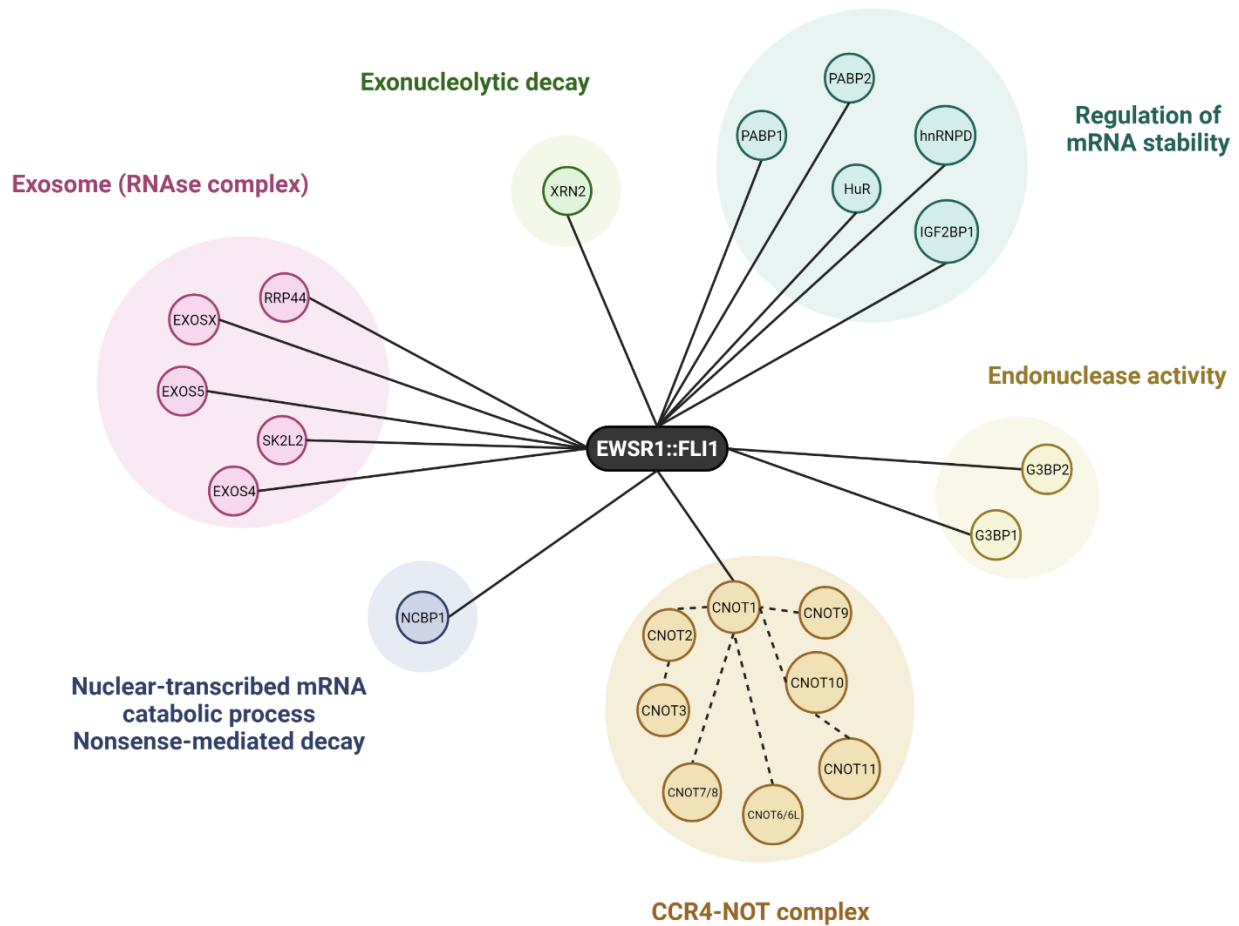
Figure 23. Characterization of the EF interactome. (**a**) Overlap between EF interactors and literature-curated lists of RNA-binding proteins (RBPs) and transcription factors (TFs) from [228], [229]. (**b**) SMART domain analysis with DAVID. (**c**) KEGG-pathway analysis. (**d**) mRNA-decay associated factors found in the interactome. Data from [209]. Created with BioRender.com.

1.5. Cell plasticity, tumor heterogeneity and metastasis

Cell plasticity, tumor heterogeneity and metastasis are important aspects of cancer biology that, unsurprisingly, also resonate in the context of EwS.

1.5.1. Cell plasticity

Phenotypic plasticity is an emerging dimension of the hallmarks of cancer [231]. This trait has been related to aggressiveness because plastic tumors can more easily adapt to their microenvironment. Partial epithelial-to-mesenchymal transition (EMT) is generally considered to be an important driver of phenotypic plasticity [231]. EMT is a reversible cellular program during which an epithelial cell transdifferentiates into a mesenchymal cell. During EMT, epithelial cells lose their junction as well as apical-basal polarity and reorganize their cytoskeleton to increase motility of individual cells. This in turn enables the development of an invasive phenotype. In normal cell physiology, EMT is part of morphogenesis in embryos and tissue homeostasis (*e.g.*, wound healing and stemness) in adults. Rather than a binary process, EMT represents a continuum between two end point states that can be executed partially. In cancer, partial EMT provides the plasticity that is necessary for tumor progression, metastasis and resistance to therapy [232]–[234]. Interestingly, EwS has also been reported to display phenotypic plasticity, with features from both epithelial and mesenchymal states, through a process resembling partial EMT [235]. Three main models, not mutually exclusive, have been proposed to account for phenotypic plasticity in EwS.

1.5.1.1. Fluctuations in EF expression levels

A first model relates EwS cell plasticity to passive fluctuations in EF expression levels that lead to two main cell subpopulations, largely contributing to EwS intra-tumoral heterogeneity[15] (**Figure 24**) [236], [237]. Cells with high expression of EF (EF^{high} cells) represent the most important part of the tumor. They display an epithelial-like phenotype characterized by impaired differentiation, high proliferation rate and cell-cell interactions [5], [236]. This is in part explained by the fact that EF represses the transcription of mesenchymal-specific genes [238] via both direct [157] and indirect mechanisms [175]. By contrast, cells with low expression of EF (EF^{low} cells) represent a rare fraction of the tumor. They display a mesenchymal-like phenotype characterized by a spindle-shaped cell morphology, metastatic/invasive-prone and cell-matrix interactions [5], [236]. Different factors have been proposed to affect EF levels, including for example stochastic events, diffusible factors from the microenvironment (*e.g.*, growth factors), cell stress and hypoxia [239].

---

[15] Tumor heterogeneity in EwS has now started to be explored through single-cell RNA-sequencing studies [237], [706].
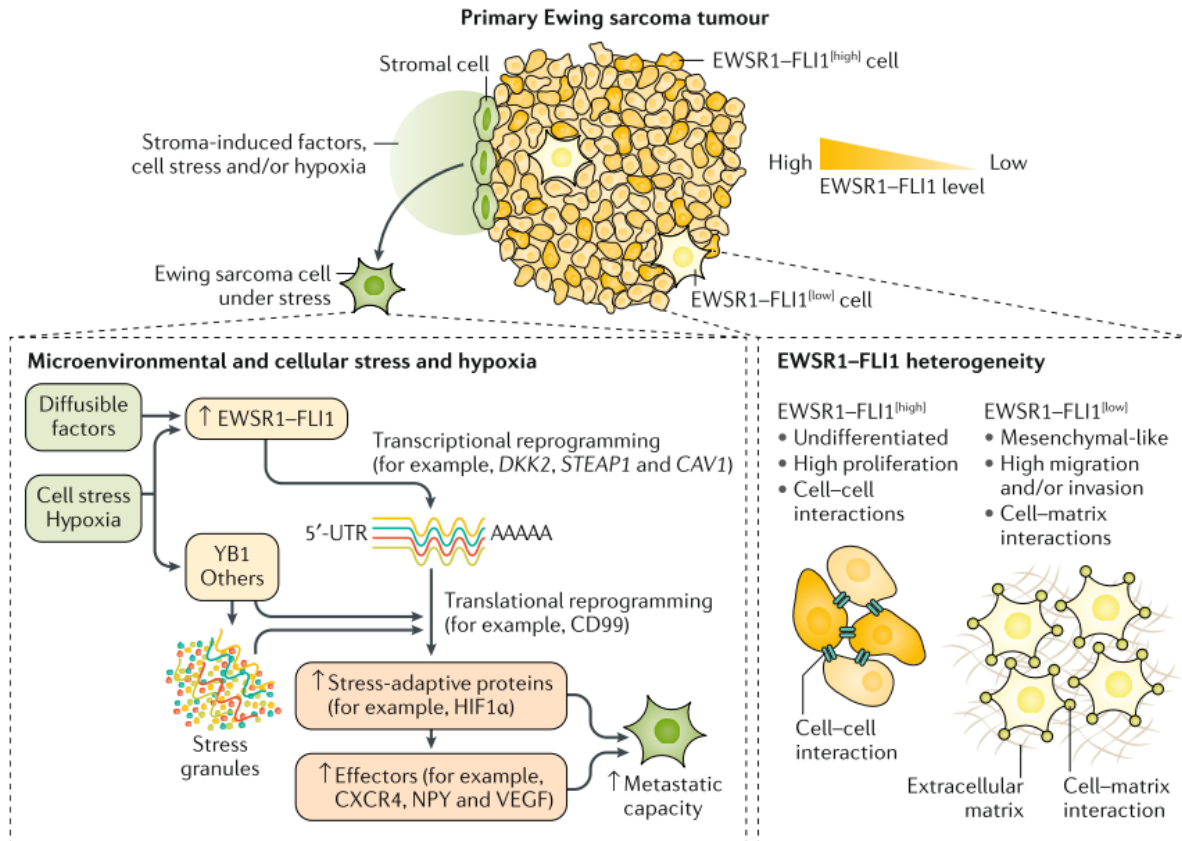
Figure 24. Fluctuations in EF expression levels drives EwS cell plasticity. See main text for details. From [5].

1.5.1.2. Transcriptional antagonisms

A second model relates EwS cell plasticity to competing transcriptional activities between EF and other TFs or epigenetic regulators (**Figure 25**). Three examples are described below. The first one is ZEB2, a key regulator of EMT, that is known to repress the epithelial phenotype. In conjunction with EF which represses the mesenchymal phenotype, ZEB2 and EF would act as opposite forces, keeping EwS in a metastable state, ideally positioned along the mesenchymal axis for successful growth and metastasis [240]. A second example is KDM5A and PHF2, two epigenetic regulators that have been shown to activate pro-metastatic genes repressed by EF in order to support EwS metastasis [241]. The last example is HOXD13, a developmental TF that is induced by EF via reprogramming of a GGAA repeats enhancer. HOXD13 mitigates EF-mediated repression of the mesenchymal phenotype by binding and activating specific EF-repressed genes [242].
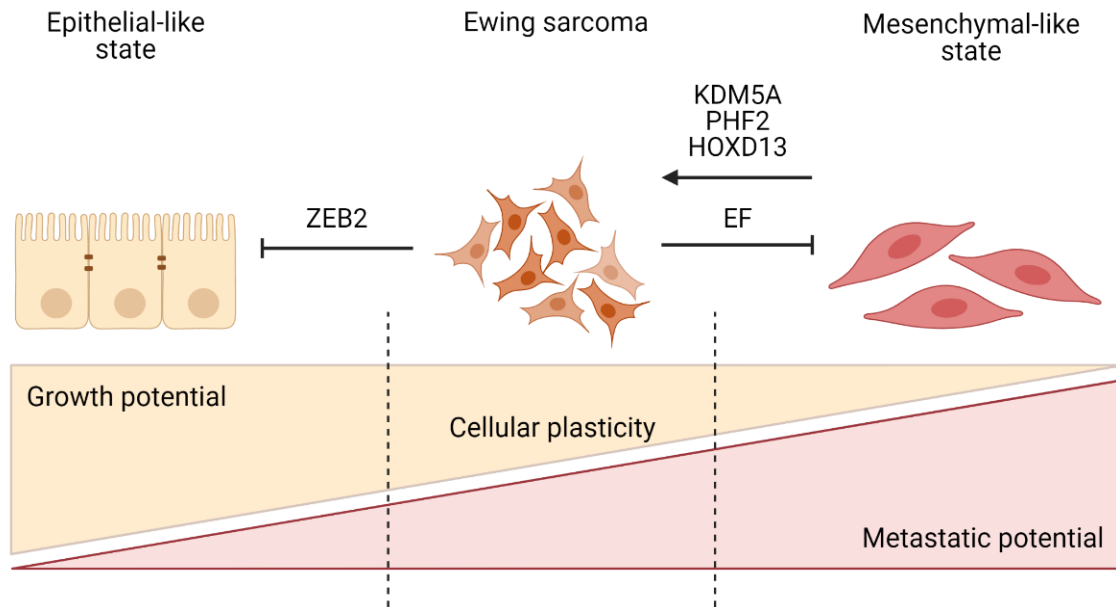
Figure 25. Transcriptional antagonisms drive EwS cell plasticity. See main text for details. Created with BioRender.com.

1.5.1.3.   Post-transcriptional effects

Although hypothetical, a third model might relate EwS cell plasticity to indirect post-transcriptional effects via EF-mediated deregulation of ncRNAs.

1.5.2. Metastasis

Metastasis is one of the main adverse prognostic factor in EwS, notably by increasing the risk of relapse. Over time, a number of key metastatic regulators have been identified in EwS but no clear unifying model currently exists [5]. EwS invasive and migratory features are collectively determined by transient reduction in EF expression levels [236], *STAG2* loss-of-function mutations [243], [244], polymorphisms in *CD99* locus [22], EF-dependent transcriptional modulation of specific genes including notably; IL1RAP [245], tyrosine kinase ERBB4 (suppression of detachment-induced cell death or anoikis)[16] [246], thyroid receptor TRIP6 [247], transmembrane protein STEAP1 [248], [249], DKK2 [250], G-protein coupled receptor GPR64 [251], CAV1 (MAPK/ERK signaling pathway) [252], EZH2 [189], HOXD13 [242], TCF7L1 [253], HEY1, SIRT1 (NOTCH-p53 signaling axis) [254], [255], and SPRY1 [256]. Other metastatic determinants are EF-mediated deregulation of miRNAs [219], [223], [224], adaptation to cellular stress during the course of tumor growth; like hypoxia (HIF1α [239], NPY [257], YB1 [258]) or growth factors deprivation (Src [259], CXCR4 and Rho-GTPases [260]), or during therapy, and finally factors from the tumor microenvironment (*e.g.*, growth factors and cytokines) [261]–[263].

---

[16] ERRB4-mediated suppression of anoikis relies on PI3K-AKT and FAK pathways. It explains why EwS cells can survive as spheroids in suspension cultures.

1.6. Targeting EF

As unique hallmarks of fusion-harboring cancer cells, driver gene fusions are, in essence, terrific drug targets. Therefore, fusion-harboring malignancies[17] might represent a subset uniquely susceptive to precision oncology. However, attempts at targeting fusions have so far yield contrasted results, depending on the class involved [108], [110]. On the one hand, targeting fusion protein kinases with kinase inhibitors revealed to be a success story. Since 2001, the approval of imatinib for BCR::ABL in chronic myeloid leukemia by the Food and Drug Administration (FDA) has provided a framework for many other kinase oncoproteins; such as EML4::ALK (lung cancer) [264], RET- (thyroid and lung cancers) [265], and NTRK-derived fusions (various cancers) [266]. Today, kinase inhibitors represent the largest class of targeted therapies with 68 FDA-approved drugs [267]. On the other hand, drugging fusion TFs remains challenging for three main reasons. First, they lack any enzymatic activity. Second, they frequently involve IDRs, which are considered undruggable [268]. Third, the pathogenic mechanisms employed by this class of gene fusions are complex and remain poorly understood at the molecular level, although progress is being made [108], [110].

Here, I briefly review the arsenal of options that exists to target EF and illustrate how a better molecular understanding of this fusion TF is now offering promising therapeutic avenues for EwS and a roadmap for other fusion TFs-driven cancers like sarcomas and leukemias. Additionally, these considerations provide a rationale for targeting non-fusion TFs, which represent common determinants in diseases and challenging drug targets [269]–[271]. For didactic purposes, the therapeutic options of EF are classified between strategies acting at either the DNA-level, RNA-level or protein-level. At each level, these strategies are further classified between direct and indirect approaches. Main options are summarized in **Figure 26**. Important EwS-related targetable molecules (proteins or lncRNAs) are presented in **Figure 27**. A more extensive review of available therapeutic options and targets for EwS can be found in [45], [272], [273].

---

[17] Gene fusions are estimated to account for about 20% of human cancer morbidity [707] and have been identified in a number of haematological malignancies and solid tumors like sarcomas [708].
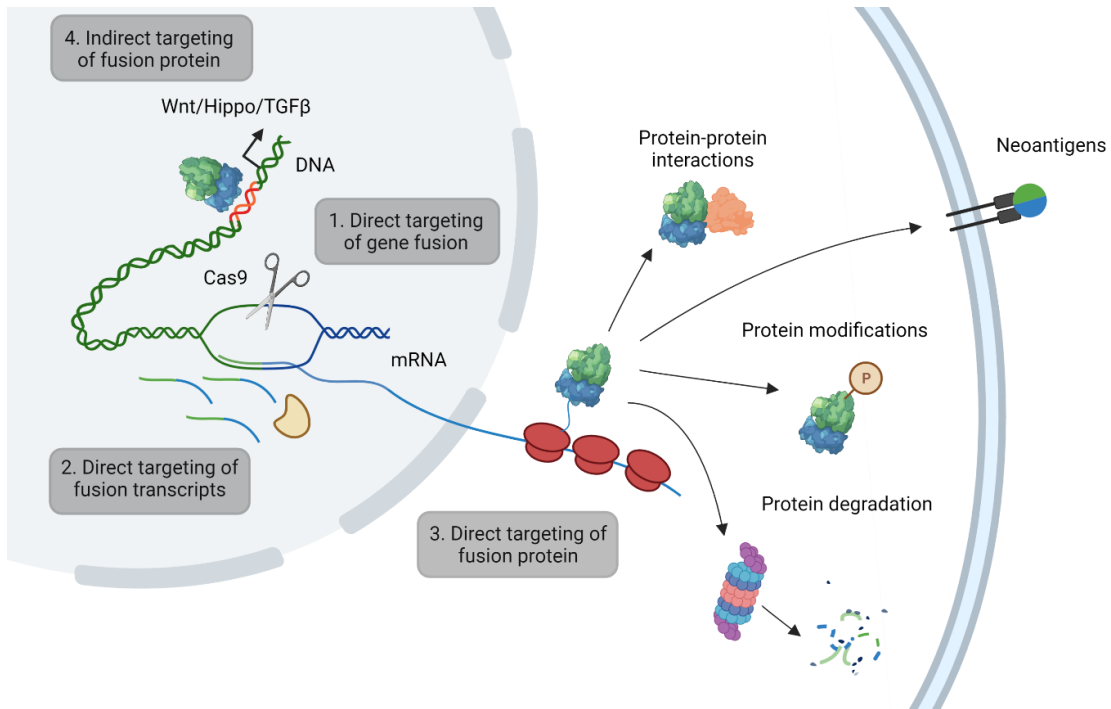
Figure 26. Overview of the potential opportunities in targeting EF. See main text for details. Modified from [270]. Created with BioRender.com.
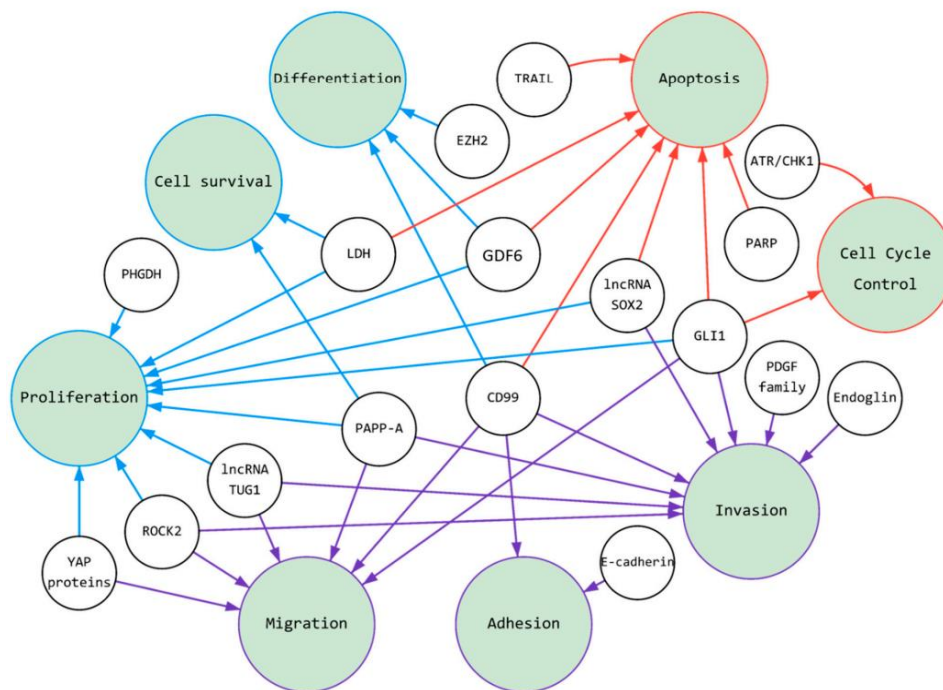
Figure 27. Overview of EwS-related targetable molecules (proteins or lncRNAs) and their associated cancer hallmarks. Cancer hallmarks are grouped into three different categories (colored in blue, red and purple). From [273].

1.6.1. Targeting EF at the DNA level

This strategy aims at hijacking the oncogenic activity of EF by targeting either the gene fusion itself (direct approaches) or the DNA-binding motif recognized by EF (indirect approaches).

1.6.1.1.   Direct approaches

Direct approaches attempt at interfering with the biogenesis of EF fusion mRNA. Two main options have been described: (1) CRISPR-Cas9-based inactivation of the EF rearranged gene[18] [274] which might be combine with CD99-targeting nanoparticles as a delivery strategy [275] and (2) the use of pharmacologic inhibitors (such as BET bromodomain inhibitors) or RNA interference (RNAi) to target the epigenetic regulation of EF expression [276].

1.6.1.2.   Indirect approaches

Indirect approaches attempt at interfering with the functionality of EF by altering its DNA-binding motif within regulatory enhancers that are critical for tumor growth[19]. To date, CRISPR-Cas9-based epigenome editing has been successfully applied to silence NR0B1 [162] and SOX2 genes [277]. Rather than erasing, exploiting neomorphic DNA-binding preferences of EF in order to express therapeutic genes, such as a suicide gene, represent an alternative and highly attractive approach [278].

1.6.2. Targeting EF at the RNA level

This strategy aims at hijacking the oncogenic activity of EF by targeting either the chimeric mRNA transcript itself (direct approaches) or the mRNA transcripts encoding targets of EF that are essential for EwS development (indirect approaches).

1.6.2.1.   Direct approaches

Direct approaches attempt at interfering with the synthesis of EF fusion protein. Two main approaches have been described whether the target is either EF mRNA or EF pre-mRNA. First, RNAi targets EF mRNA using small-interfering RNAs (siRNAs). Initially, it was used to investigate the biological importance of EF for EwS biology [136], [137], [279]. Later, it was proposed in the treatment of EwS. Despite recent progress, RNAi-based therapies remain however challenging owing to difficulties in delivering siRNAs to tissues and the inherent instability of siRNAs following cellular delivery. In the context of EwS, this type of therapies is further hampered by the fact that EF^{low} cells are more metastatic and more chemoresistant than EF^{high} cells, which thus compromises therapeutic efficacy. Alternatively, targeting the splicing machinery involved in the

---

[18] This option might imply a genomic cleavage [274] or the insertion of a suicide gene, as envisioned with prostate cancer [709].

[19] Not all enhancers are expected to contribute to EwS development. A major challenge is thus to identify actionable enhancer elements.

production of mature EF mRNA transcripts represent another attractive approach. It has been reported for EF as well as other gene fusions [280]–[282].

1.6.2.2.   Indirect approaches

Indirect approaches attempt at interfering with the protein synthesis of important transcriptional targets of EF via RNAi. In the future, this strategy might also be applied to important splicing targets of EF.

1.6.3.   Targeting EF at the protein level

This strategy aims at hijacking oncogene activity of EF by targeting either the fusion protein itself (direct approaches) or downstream effectors/pathways (indirect approaches). Collectively, these approaches aim to impede either protein fusion viability or functionality.

1.6.3.1.   Direct approaches

Direct approaches include four main options: targeting EF fusion protein stability, targeting functional PTMs of EF, targeting EF-protein/DNA interactions and targeting EF structural disorder. I briefly cover these approaches successively.

Fusion proteins that implicate pro-oncogenes often display aberrant increased protein stability due to the loss of ubiquitination sites from parent proteins [283], as illustrated for EF in **Figure 28.** Targeted protein degradation aims thus to exploit the inherent protein homeostatic mechanisms of cancer cells to induce fusion protein degradation. In acute promyelocytic leukemia (APL), all-trans retinoic acid and arsenic trioxide were serendipitously found to induce degradation of PML::RARα, the oncogenic driver of APL. Their use turned APL into a largely curable disease. This demonstration of efficacy fostered the development of bifunctional small molecule protein degraders (also known as proteolysis targeting chimaeras, or PROTACs). These compounds are designed to induce degradation of a target protein by coupling it to the proteasome. This is achieved using a bivalent small molecule with affinity for both the target protein and an E3 ligase complex. Treatment of cells with these compounds induces dimerization of the target and an E3 ligase complex, leading to target ubiquitylation and degradation (**Figure 29**) [110], [284]. This approach has been successfully used to create specific degraders of several clinically relevant drug targets, including for example BCR::ABL in chronic myelocytic leukemia. Interestingly, an adapted version of PROTACs has been recently described to specifically target TF, namely TRAFTACs [285]. Although these generalizable approaches have never been applied to EF, they might represent promising therapeutic options for EwS in the future [286]. Finally, increasing rather than decreasing EF protein stability in order to create 'oncogene overdose' might also be a promising avenue in EwS [287].
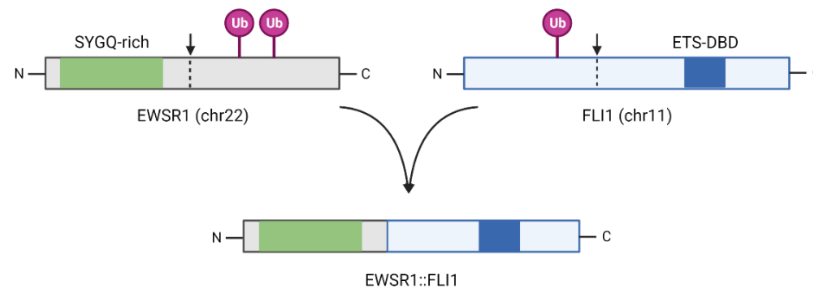
Figure 28. Loss of ubiquitination sites via fusion in EF. Modified from [283]. Created with BioRender.com.
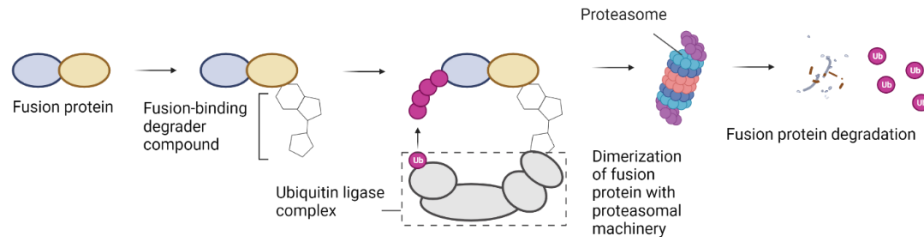
Figure 29. Targeted protein degradation using PROTACs. Modified from [110]. Created with BioRender.com.

PTMs represent important determinants of protein functionality and viability [288]. In the context of EF, PTMs of specific residues have been described to affect its transcriptional activity, including notably phosphorylation [289], acetylation, arginine methylation and O-GlcNAcylation [290]. Additionally, deubiquitination of EF by USP19 has been described to increase its protein stability [291]. Inhibiting enzymes responsible for EF PTMs using pharmacological inhibitors or RNAi might thus constitute another option.

Protein-protein interactions (PPIs) and protein-DNA interactions are underlying TF functionality. Disruptors of these interactions represent thus an attractive drug class. Previously, I described YK-4-279, a small molecule inhibitor that targets interactions between EF and RNA helicases [208], [210]. To date, it is the only known example of iPPI in the context of EwS. In the future, it might however be exploited to target other important PPIs, such as the ones with the BAF complex. Unfortunately, the low specificity of PPIs might represent an obstacle for future clinical trials. Targeting EF-DNA interactions is another option. Interestingly, lurbinectedin and tarbectedin have been reported to mediate the nucleolar redistribution of EF, thereby compromising its access to DNA [292], [293].

Structural disorder is an important feature of fusion proteins. Beyond driving aberrant phase transition, it enables fusion proteins to escape cellular surveillance that eliminates misfolded proteins. Accordingly, breakpoints have been reported to avoid ordered domains, which would otherwise result in the production of structurally aberrant chimeras [283], [294], [295]. Furthermore, structural disorder enables the interplay of remote elements within fusion proteins. For example, in fusion protein kinases, disorder enables constitutive kinase activity through either autophosphorylation (*e.g.*, BCR::ABL) or dimerization (*e.g.*, EML4::ALK). In fusion TFs, disorder

enables the communication between the DNA-binding and transactivator elements [295]. In the future, the better understanding of these mechanisms should undoubtedly provide innovative therapeutic opportunities in diseases [296], which should benefit EwS.

1.6.3.2.   Indirect approaches

Indirect approaches attempt at targeting molecular effectors, cooperating signaling pathways, or downstream effects of EF.

Oncogenic drivers depend on many proteins to mediate their aberrant functions even if they do not necessarily interact together. Identifying these dependencies (also known as vulnerabilities) through genomic or pharmacological screens has yield exciting therapeutic targets, especially in high mutational-burden adult cancers. Interestingly, a systematic study has recently reported that pediatric cancers display a similar complexity of genetic vulnerabilities [126]. Several targets have been described to evoke vulnerability in EwS, including notably chromatin regulators (*e.g.*, HDACs, DNA methyltransferases, LSD1) [191], [297], [298], CDK7/12/13 [299], CD99 [300], STAG1 (in STAG2-mutated EwS) [301], *etc*.

In EwS, many signaling pathways have been reported to cooperate with EF function in order to support tumor development, such as IGF-1R pathway [302]–[305], mitogen-activated protein kinase pathway [252], [306], sonic hedgehog pathway [307], [308], and Wnt/β-catenin pathway [309], [310]. Each of them provides unique opportunities to indirectly target EF [270].

Downstream effects of EF can also be exploited for therapy. One interesting case is the accumulation of R-loops in the genome of EwS cells owing to EF transcriptional activity. R-loops are three-stranded nucleic acid structures including a RNA-DNA hybrid and a single-stranded DNA. Although their precise function is unclear, they have been linked to genome instability [311]. In EwS, BRCA1 is partially inactivated owing to its sequestration within these structures, leading to impaired homologous recombination. Similar to BRCA-deficient tumors, EwS is thus highly sensitive to PARP inhibitors (*e.g.*, olaparib) [312]. In EwS, EF also causes replication stress by accelerating entry into S phase. In ~50% of patients, chr8 gain (trisomy 8) mitigates this stress via single gene copy gain of RAD21 [313]. In this context, targeting RAD21 might thus be exploited to dampen EwS tumor fitness. Finally, targeting important transcriptional targets of EF or their downstream effects represents another option, as illustrated with EZH2 [314], PLK1 [315], and SOX6-mediated sensitivity to oxidative stress [161].

2. mRNA degradation

Historically, mRNA degradation has remained largely overlooked compared to mRNA production. Being not less complex, this molecular process is, however, a quintessential aspect of gene expression regulation and an exciting area of research, notably because it is increasingly recognized as an important driving force in malignancies.

In this chapter, I will first situate mRNA degradation[20] in the molecular journey of a typical eukaryotic protein-coding mRNA (*i.e.*, transcribed by RNAPII). Next, I will describe the different pathways, its associated machineries and subcellular locations. Then, I will discuss the multilayered importance of mRNA degradation and review several mechanisms of regulation. Finally, I will cover different cases of coupling that exist between mRNA decay and the other steps of gene expression and present why canonical DNA-binding TFs are today emerging as key coordinators of the mRNA lifecycle.

2.1. Molecular steps of gene expression

Gene expression is defined as "the production of an observable phenotype by a gene – usually by directing the synthesis of a protein" [316]. This is a multistep process that, in eukaryotes, implicates the two main cellular compartments: the nucleus and the cytoplasm (**Figure 30**).

2.1.1.   Nuclear steps

The journey of a typical mRNA starts in the nucleus from transcription of a specific DNA region (*i.e.*, making an RNA copy of a DNA segment). This process is mainly controlled by the transcription machinery, epigenetic marks and chromatin topology. The transcription machinery mainly consists of general transcription factors (GTFs, including TFII-B, -D, -E, -F and -H), RNAPII, the Mediator complex and DNA-binding TFs [317]. It involves many distinct steps, including, briefly, the selection of the DNA region to copy by one or several TFs, the remodeling of the chromatin landscape to increase DNA accessibility, the assembly of the preinitiation complex, and the transcription cycle of RNAPII (further divided into initiation, elongation and termination phases) [318]. During transcription, the nascent precursor mRNA (pre-mRNA) is processed into mature mRNA [319]. This includes capping (or the addition of a protective m^7G cap at the 5'end by specific enzymes) [320], splicing (or the excision of introns and ligations of exons by the spliceosome) [321]; as well as cleavage by CPSF and polyadenylation (or the addition of a protective tail of adenosines at the 3'end). Poly(A) tail addition is controlled by the nuclear poly(A)-binding protein (PABPN) [322]. During splicing, the pre-mRNA transcript can be alternatively spliced through exon skipping (the removal of specific exons), intron retention, or a selection between mutually exclusive exons or alternative splice sites. This process generates mRNA species that can vary in their coding sequence or untranslated regions [323]. In addition, the mRNA can be edited and

---

[20] Degradation of RNAPI- and RNAPIII-derived transcripts is not covered here. Also, degradation of pre-mRNAs is not the main focus of this chapter, although this aspect is briefly mentioned in several places.

modified by specific class of enzymes (further described later in this chapter) [324]. Of note, pre-mRNA processing is mainly achieved during transcription in higher eukaryotes. After release from RNAPII, the fully mature RNA is thus swiftly exported to the cell cytoplasm.

2.1.2. Cytoplasmic steps

In the perspective of the central dogma of molecular biology, mRNA is an intermediary that largely exists to produce proteins. After its arrival in the cytoplasm, cytoplasmic poly(A)-binding protein (PABPC) binds mRNA poly(A) tail and promotes translation by the 80S ribosome. When necessary, deadenylation (or the shortening and removal of mRNA poly(A) tail) allows mRNA to quit translation and initiates degradation [322]. Finally, degradation trims mRNA sequence, thereby allowing the recycling of mRNA constituents for another journey of expression.
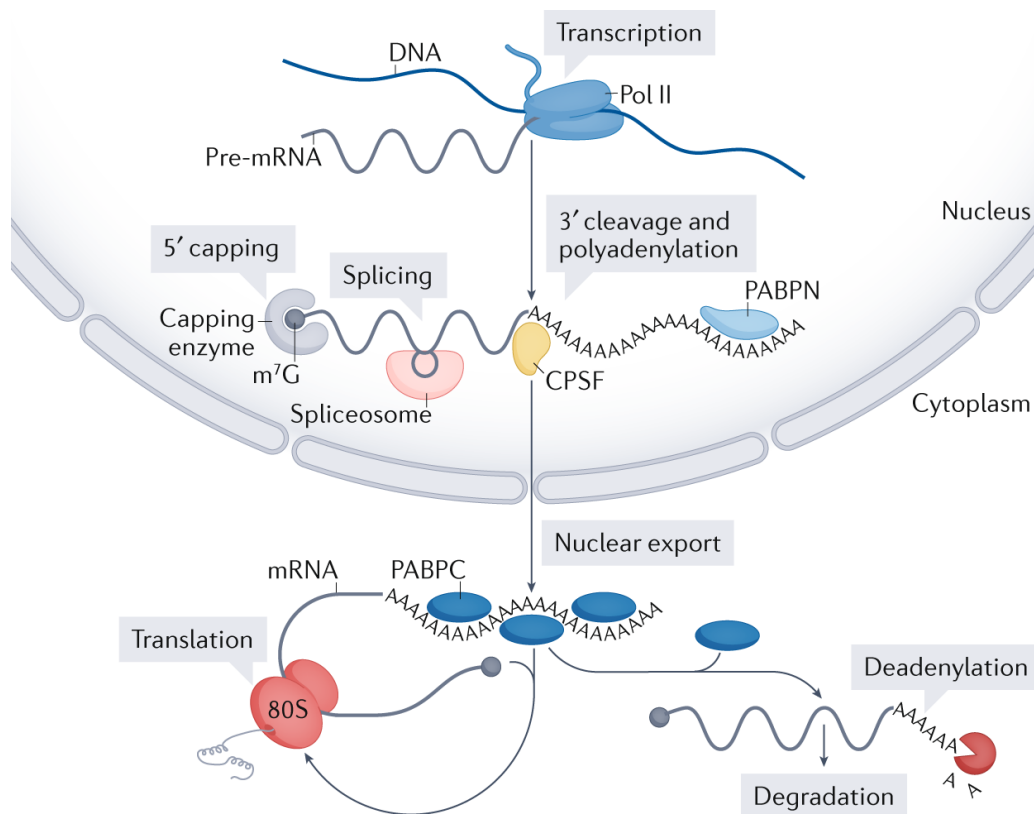
Figure 30. Molecular steps of gene expression. See main text for details. Alternative splicing, mRNA editing and modification are not represented. From [322].

For a number of reasons briefly introduced below and further discussed in the rest of this chapter, the above description corresponds to an over-simplistic view of gene expression and, more specifically, of mRNA degradation. First, mRNA degradation is much more than a waste-disposal system that takes place at the end of a productive life. Instead, by controlling mRNA levels at all steps, it represents a crucial regulatory system of gene expression [325], [326]. Additionally, it provides an efficient surveillance mechanism that eliminates error-containing transcripts encoding potentially toxic proteins [325], [326]. Second, mRNA degradation is a complex process

with different underlying pathways that implicate functionally elaborated and massively regulated machineries [327], [328]. mRNA degradation is not restricted to the cytoplasm but can also occur in the nucleus [329]. Third, the cytoplasmic fate of mRNAs is not necessarily to enter translation, and then to be degraded. Rather, mRNAs can undergo either translation, degradation or storage in specific subcellular compartments, such as processing-bodies and stress granules [330]. As we will see, changes in the length of mRNA poly(A) tail is an important determinant of mRNA fate in the cytoplasm [322]. Finally, the existence of functional coupling between mRNA degradation and the other steps of gene expression adds another layer of complexity to this molecular process [331]–[333].

2.2. Pathways of mRNA degradation

mRNA degradation is a complex process that consists of four main types of ribonucleolytic activities, including deadenylation, decapping, exonucleolytic decay and endonucleolytic cleavage [322]. Deadenylation delineates two main routes whether it is implicated or not [325], [326], the choice of which depending on both the cellular context and the mRNA substrate [334].

2.2.1.   Deadenylation-dependent decay

Deadenylation-dependent mRNA decay (also known as canonical/bulk mRNA decay) is the 'superhighway to destruction' because the bulk of mRNAs undergoes decay via this route [325]. It is initiated by deadenylation, a reversible and often rate-limiting step, and followed by irreversible exonucleolytic decay [325], [326] (**Figure 31**).
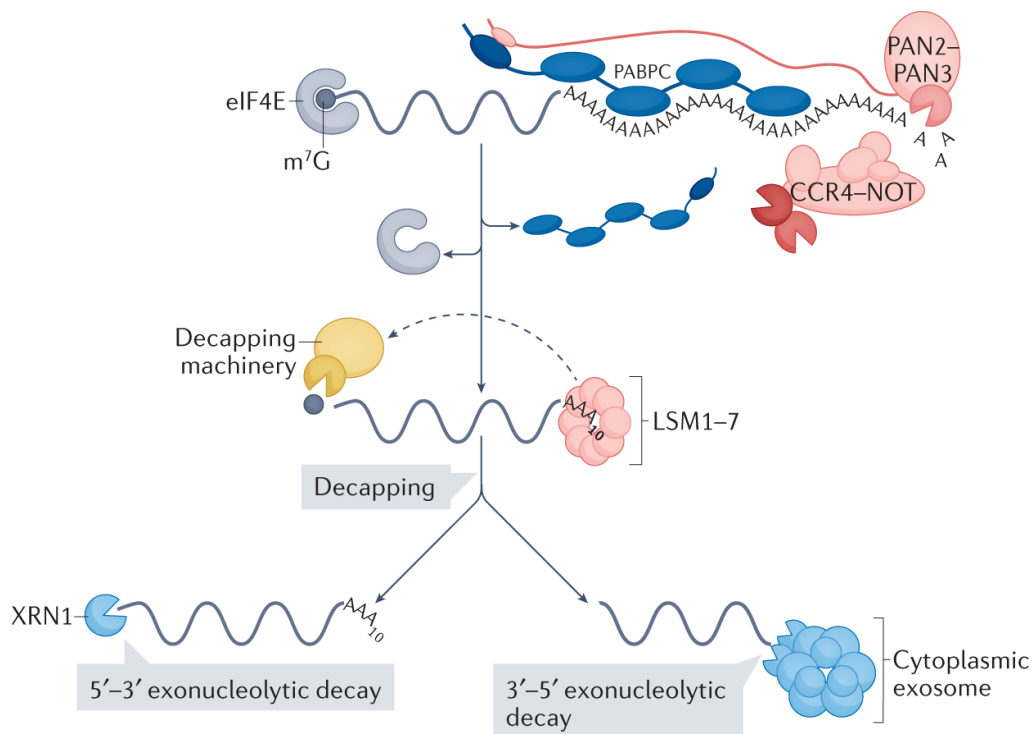
Figure 31. Pathways of deadenylation-dependent decay. See main text for details. From [322].

2.2.1.1.   Deadenylation

Deadenylation consists in the shortening of the protective poly(A) tail at the mRNA 3'end. This process is catalyzed by multisubunit machineries, including the CCR4-NOT and PAN2-PAN3 deadenylation complex. Most of our current understanding of this process comes from early studies in yeast [322].

a) Poly(A) tail

mRNA poly(A) tails are protective structures that, along with the cap at the 5'end, regulate important post-transcriptional aspects of RNA biology. Poly(A) tail are found on almost every transcript, the only known exception being some mammalian histone transcripts. They are added cotranscriptionally within 10-30 nucleotides (nt) downstream of a polyadenylation signal[21] (PAS) by a poly(A) polymerase after mRNA cleavage [335]. In metazoans, full-length poly(A) tails are thought to be ~200-250 nt in length, which is significantly longer than in yeasts (~70 nt in *Saccharomyces cerevisia*e) [322]. Poly(A) tails function as master regulators of gene expression. They are necessary for proper mRNA export from the nucleus to the cytoplasm; and contribute positively to the translation status and the stability of mRNAs [322], [336]. The connection between tail length and translation or mRNA stability is not always straightforward. Although mRNAs with longer tails tend to be translated more efficiently, specific subsets of highly translated mRNAs have much shorter poly(A) tails than expected [337]. Nevertheless, this case seems to represent an exception rather than the rule. Furthermore, shortened poly(A) tails does not necessarily correlate with decreased mRNA stability, notably because shortened poly(A)-mRNAs can also be stored in specific cytoplasmic RNA granules without being further degraded [330]. Interestingly, poly(A) tail can also contain non-A nucleotides and are thus not as uniform as once hypothesized [338], [339]. In particular, the incorporation of guanosines instead of adenosines has been reported to increase mRNA stability by slowing down deadenylation [340]. This process is sometimes exploited by viruses to protect their transcripts from the host deadenylation machinery [341]. By contrast, uridylation has been described to promote mRNA decay [338].

b) Poly(A)-binding proteins

Poly(A) tails are coated by poly(A)-binding proteins (PABP). Several PABP have been described. In the nucleus, PABPN initially bind poly(A) tails but is next replaced by PABPC in the cytoplasm, supposedly after the first round of translation. The significance of this transition remains elusive [322]. Here, I only discuss the role of PABPC.

PABPC binds poly(A) tails with a footprint of ~20-30 nt via several RRM domains [342], [343], implying that longer tails can bind more PABPC molecules [344]. Structurally, PABPC also contains a proline-rich linker and a C-terminal mademoiselle (MLLE) domain. The MLLE domain is recognized by PAM2-containing proteins and thus drive heterotypic protein-protein interactions

---

[21] Polyadenylation signals are elements with the canonical sequence AAUAAA or a close variant.

[345] (**Figure 32a, b**). By contrast with yeasts that encode only one isoform (Pab1), mammals encode multiple isoforms, PABPC1 being the major and most abundant one [336].

A minimum tail length of ~30 nt is generally required to confer stability and to allow translation [346], [347]. Because this corresponds to the footprint of an individual PABPC monomer, PABPC itself has been proposed to underline the positive effects of poly(A) tails on stability and translation. PABPC is thought to confer mRNA stability by shielding the 3' end from deadenylases [348], [349]. Although this holds true, the reality is more complex because PABPC can also stimulate the catalytic activity of the deadenylation complexes [350], as discussed later. In addition, PABPC is thought to stimulate translation by participating in the circularization of mRNA via interactions with eukaryotic translation initiation factors 4G (eIF4G) and eIF4E which bound the 5'cap structure [351]. These interactions make mRNAs to adopt a 'closed loop' form that is thought to help the recruitment of the small (40S) ribosomal subunit [352] (**Figure 32c, d**). By enabling direct physical communication between the 5'cap and the 3'poly(A) tail, mRNA circularization would facilitate ribosome recycling, as well as to act as a quality control mechanism that ensures that translation does not initiate on a partially degraded mRNA [322].
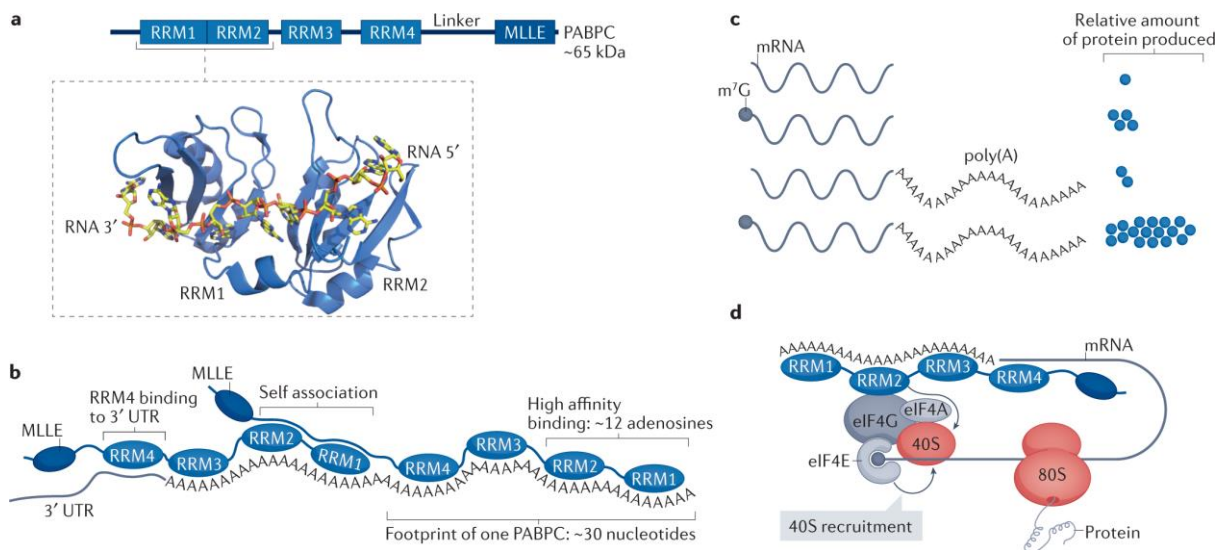
Figure 32. Overview of PABPC. (**a**) Domain composition of human PABPC protein. A crystal structure of the RRM1-RRM2 region bound to poly(A) RNA is shown (PDB 1CVJ). RRM = RNA recognition motif, MLLE = mademoiselle domain. (**b**) Disposition of PABPC molecules on the poly(A) tail. (**c**) Synergy of mRNA protective structures in translation efficiency. (**d**) The 'close loop' translation initiation model. From [322].

c) Deadenylase complexes

Deadenylases are exonucleases that act specifically on adenosines to shorten or remove poly(A) tails. Typically, they function as multisubunit protein complex. In eukaryotes, PAN2-PAN3 and CCR4-NOT represent the two main deadenylases [322]. Their different subunits are summarized in **Table 1**. A third deadenylase, named poly(A)-specific exoribonuclease (PARN) has also been identified. However, PARN is not found in all eukaryotes and has been described to play more specific functions, for example, in the maturation of some ncRNAs [322].

Table 1. Major deadenylases in eukaryotes. From [322].

Complex	Subunit name			Function
	Homo sapiens	**Saccharomyces cerevisiae**	**Schizosaccharo-myces pombe**	
PAN2-PAN3	PAN2	Pan2	-	DEDD exonuclease
	PAN3	Pan3	-	RNA binding, scaffold
CCR4-NOT	CNOT1	Not1	Not1	Scaffold
	CNOT2	Not2	Not2	NOT box scaffold
	CNOT3	Not3, Not5	Not3	NOT box scaffold
	(CNOT4)	Not4	Mot2	RING E3 ligase
	CNOT6, CNOT6L	Ccr4	Ccr4	EEP exonuclease
	CNOT7, CNOT8	Pop2	Caf1	DEDD exonuclease
	CNOT9	Caf40	Rcd1	Protein-protein interaction
	CNOT10	-	-	-
	CNOT11	-	-	RNA binding
	-	Caf130	-	-

PAN2-PAN3 complex is composed of three subunits: two copies of PAN3 forms an asymmetric homodimer that serves as a scaffold for one copy of PAN2 [353]–[355]. PAN2 is the catalytic subunit of the complex and is a DEDD-type exonuclease [334]. PAN2-PAN3 is recruited to mRNA via several interactions, that notably occur between the PAM2 motif (identified within an IDR) of PAN3 and the MLLE domain of PABPC [356] (**Figure 33**). In yeast, PAN2 and PAN3 genes are not essential [357], [358]. Deletion of either gene does not appear to substantially affect mRNA half-life because PAN2-PAN3 and CCR4-NOT have partially overlapping functions. PAN2-PAN3 may be more important in specific cellular circumstances [359].
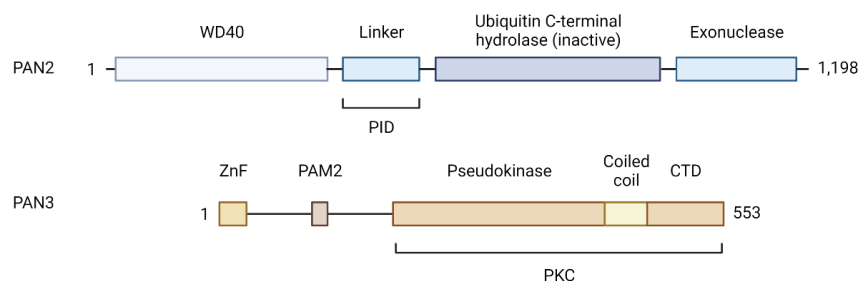
Figure 33. Domain composition of PAN2 and PAN3 proteins. WD40 = short structural motif composed of ~40 amino acids that often terminates with a tryptophan (W) – aspartic acid (D) dipeptide, PID = phosphotyrosine interaction domain, PKC = domain homologous to protein kinase C, ZnF = zinc finger, PKC = CTD = C-terminal domain. Modified from [354]. Created with BioRender.com.

CCR4-NOT[22] is a megadalton and highly conserved multisubunit complex. It is composed of nine core subunits, including two exonucleases: CCR4-associated factor 1 (Caf1; also known as CNOT7 or CNOT8 in mammals) and Ccr4 (also known as CNOT6 or CNOT6L in mammals) [322]. Caf1 and Ccr4 are DEDD-type and EEP-type exonucleases, respectively [360]. In mammals, CCR4-NOT complex incorporates either CNOT7 or CNOT8 and either CNOT6 or CNOT6L, leading to four different versions of the complex [361], [362]. Lack of Caf1 or Ccr4 in yeast results in slowed and incomplete deadenylation [360]. The significance of multiple deadenylases within the CCR4-NOT complex has been a subject of debate and is discussed below.

CNOT1 is the largest subunit (>200 kDa) and serves as a scaffold for the assembly of the complex (**Figure 34**). It contacts most of the other subunits [363], [364] and is the only essential subunit for viability in yeast [365]. CNOT2 and CNOT3 associate with the C-terminal region of CNOT1, forming the 'NOT module' [366]. They have been linked with decapping in yeast [367], and function as a platform for RBPs [364]. CNOT4 is an E3 ubiquitin ligase that promote protein degradation, notably of ribosomal proteins [322], and that has been related with cotranslational control [368]. CNOT9 mediates interaction with RNA and several RBPs [364]. Finally, CNOT10 and CNOT11 are less well-characterized but appear to also mediate interactions with RNA [364]. Although some subunits might function independently of the full complex, knockdown of specific subunits leads to smaller and less stable forms of the CCR4-NOT complex [369].
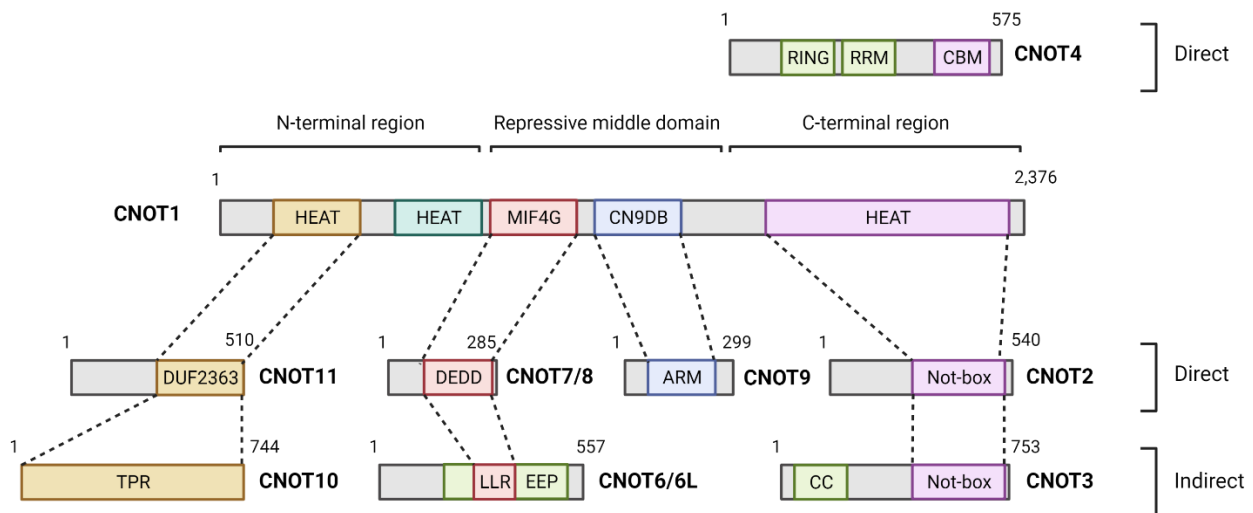
Figure 34. Domain composition and interactions within the CCR4-NOT complex. Modified from [360]. Created with BioRender.com.

In cells, PAN2-PAN3 and CCR4-NOT can specifically be recruited to mRNA transcripts by PABPs, RBPs or miRNAs [322], [359]. As mentioned earlier, some subunits of the deadenylation complexes are also able to bind mRNA directly and might further help in the recruitment onto mRNA.

---

[22] Or also, complex catabolite repression 4 (CCR4)-negative on TATA-less (NOT)

Beyond its cytoplasmic function in mRNA deadenylation, CCR4-NOT has been reported to act as a master regulator of gene expression in the cell nucleus as well as in the cell cytoplasm. In the nucleus, it is implicated in transcriptional regulation, chromatin modification, RNA export, nuclear RNA surveillance and DNA damage repair. In the cytoplasm, it is also implicated in the control of translation fidelity [360], [361].

d) Models of deadenylation

The relevance of multiple deadenylase complexes as well as deadenylase subunits within CCR4-NOT is a major question in the field of RNA degradation. Several models have been proposed to account for this intriguing diversity (**Figure 35**). One of them is that the deadenylation complexes function in a biphasic (or sequential) manner. According to this model, deadenylation, mechanistically, starts with a phase of rapid shortening to ~150 nt by PAN2-PAN3 (initiation phase). As the tail is shortened, its affinity for PAN2-PAN3 is decreased. This first phase is followed by a second phase of slow shortening to ~10 nt by CCR4-NOT (completion phase). In this model, PAN2-PAN3 and CCR4-NOT preferentially remove the distal and the proximal parts of the poly(A) tail, respectively [322]. Another model, that is complementary to the one presented above, is that the CCR4 and CAF1 deadenylases of CCR4-NOT have separated roles and function in a cyclic manner [359], [370]. CCR4 is a general deadenylase that can degrade mRNA poly(A) tail when it is bound by PABPC while CAF1 is a specialized deadenylase that can only degrade naked poly(A) tail [350]. In this model, deadenylation by CCR4-NOT is mediated by cycles of CCR4/CAF1 activity [322]. In addition, the existence of multiple deadenylases allows cells to diversify mRNA control and is exploited for the coupled control of translation and mRNA stability [334].
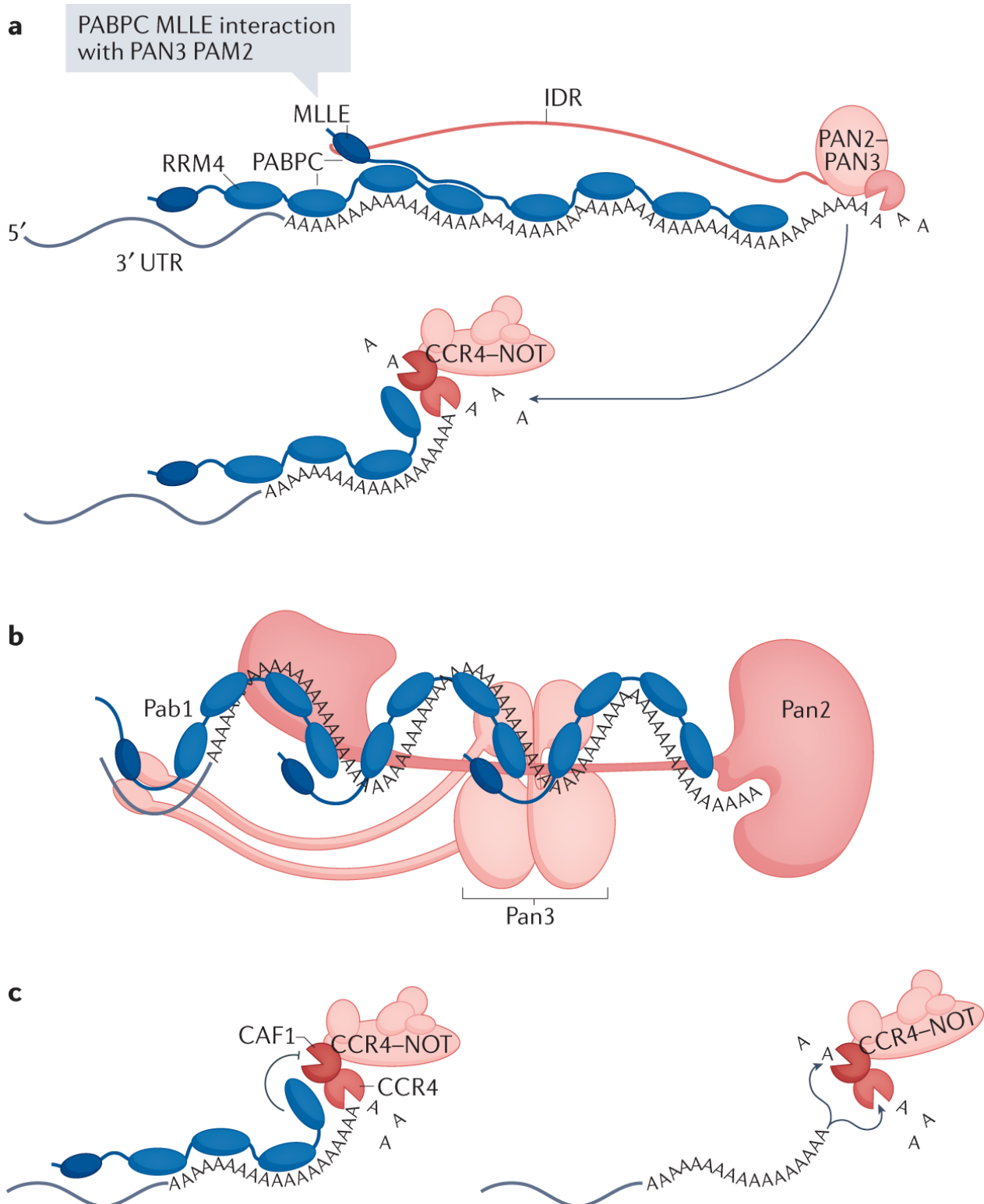
Figure 35. Deadenylation by PAN2-PAN3 and CCR4-NOT. (**a**) Biphasic model of deadenylation. (**b**) Model of the budding yeast Pan2-Pan3-Pab1-poly(A) tail complex based on cryoEM data. (**c**) Cyclic deadenylation mediated by the CCR4-NOT complex. See main text for details. From [322].

e) Fates of poly(A)-shortened mRNAs

Deadenylation disrupts the mRNA 'close loop' form and thus represses translation. Interestingly, poly(A)-shortened mRNAs do not necessarily undergo exonucleolytic decay. Instead, they can be stored with their translation apparatus within cytosolic biomolecular condensates like processing bodies (P-bodies or PBs) and stress granules (SGs), waiting to be later either degraded or, after lengthening of their poly(A) tail (also known as readenylation) redirected to polysomes. They can also be exchanged between PBs and SGs. In the cytoplasm, the fate of mRNAs is dynamic and can thus oscillate between polysomes, RNA granules and mRNA-degradation machineries [330] (**Figure 36**).
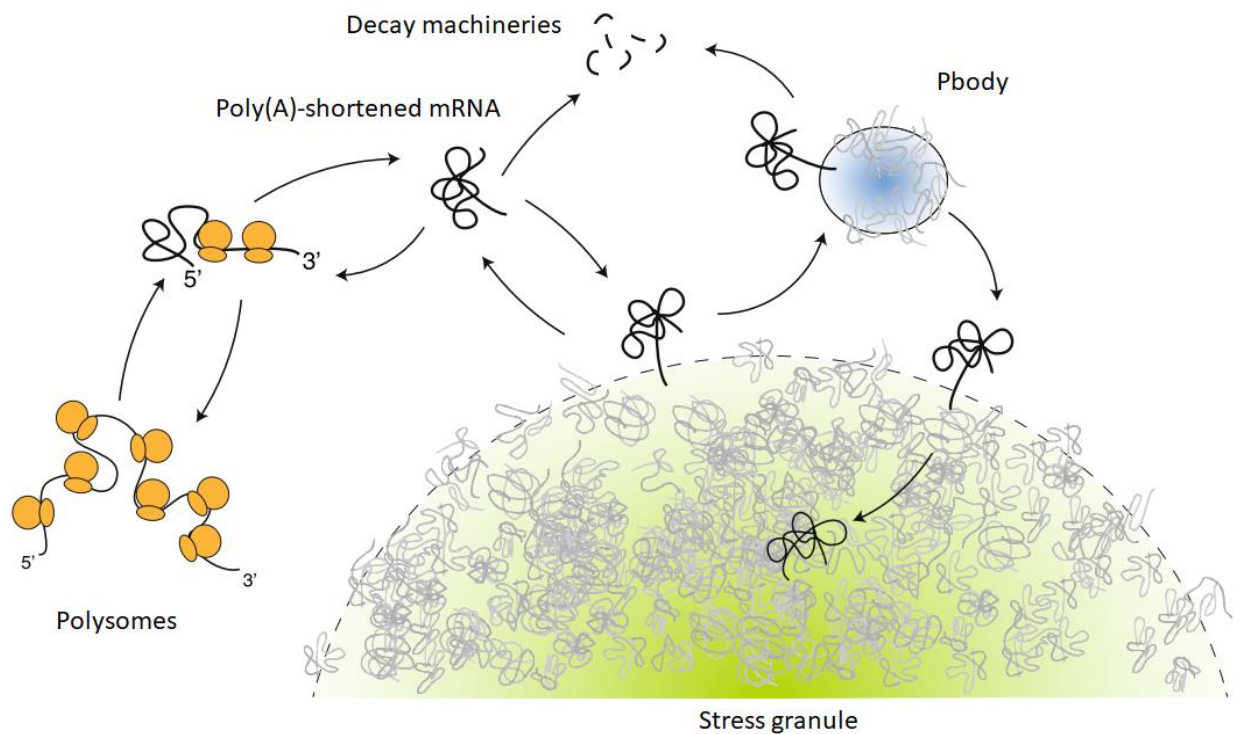
Figure 36. The cytosolic fate of poly(A)-shortened mRNAs. Poly(A)-shortened can either be redirected to polysomes, stored within RNA granules (such as P-bodies and stress granules) or degraded by decay machineries. Modified from [371].

2.2.1.2.   Exonucleolytic decay

Following deadenylation, exonucleolytic decay leads to irreversible destruction by targeting the body of the mRNA. Two types of directionality have been described whether mRNAs are degraded from their 5'end (5'–3' mRNA decay) or their 3'end (3'–5' mRNA decay). Knockout experiments in yeast revealed that neither of these two pathways appears to be indispensable but rather works redundantly, favored pathway seems to be determined in a context-dependent manner [325], [326]. For example, transcripts that are restricted to the nucleus because of a defect in export undergo decay through both routes. By contrast, unspliced pre-mRNAs and mRNAs with defective polyadenylation are subject to more rapid decay via mainly the 3'–5' route [329].

a) Decapping and 5'–3' mRNA decay

Exonucleases have access to mRNA body when at least one of the mRNA protective structures (*i.e.*, the 5'cap and the 3'poly(A) tail) is compromised. Therefore, to proceed with 5'–3' mRNA decay, the cap needs first to be removed. Decapping is achieved by the DCP1/2 complex. Several accessory factors are required for efficient decapping such as the LSM1-7 complex, the DDX6 RNA helicase and enhancer of decapping cofactors such as EDC3 and EDC4. After decapping, the mRNA is degraded by the exoribonuclease XRN1 [325], [326]. Interestingly, IDRs and LLPS have also been implicated in the formation of the decapping complexes [372].

b) 3'–5' mRNA decay

Alternatively, poly(A)-shortened mRNAs can be degraded from their unprotected 3'end by the RNA exosome complex. In humans, the RNA exosome complex is composed of nine core subunits (EXOSC1-9, namely essential exosome core component) and many cofactors, including DIS3, MPHOSPH6, EXOSC10, C1D, the Trf4-Air2-Mtr4 polyadenylation (TRAMP) complex, the nuclear exosome targeting (NEXT) complex, the CBCA complex, and the poly(A) RNA exosome targeting (PAXT) connection [329] (**Figure 37**). A comprehensive description of the RNA exosome complex is beyond the scope of this work. Only some important features are highlighted below.
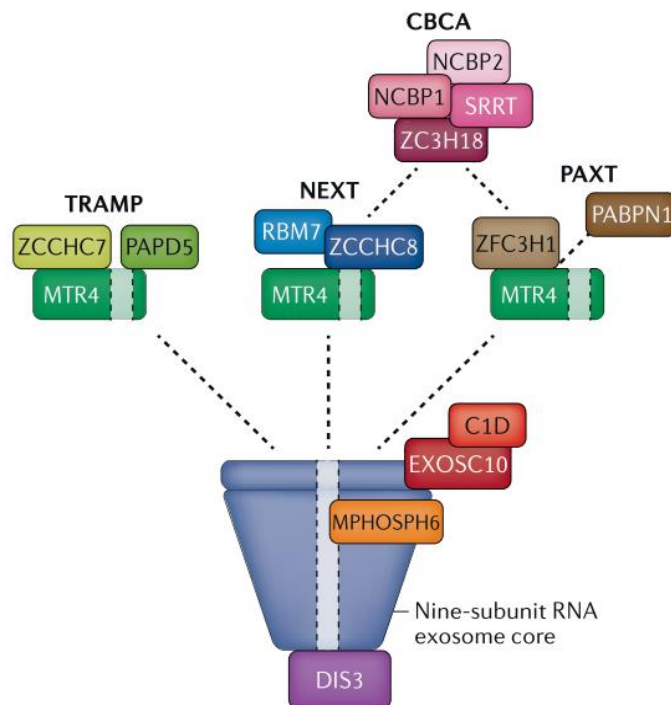
Figure 37. The human RNA exosome and its cofactors. See main text for details. From [329].

First, the basic structure of the RNA exosome is conserved among eukaryotes, although important differences exist (see below) [329]. Second, the RNA exosome can be found in both cellular compartments. Third, contrary to yeast, the human genome encodes three functionnaly distinct DIS3 homologues (DIS3, DIS3L, and DIS3L2) [329]. Moreover, the composition of the RNA

exosome throughout the cell differs between yeast and human. For example, in yeast, RNA exosomes with the homologue of EXOSC10 (known as Rrp6) are only found in the nucleus. Also, RNA exosomes with DIS3 can be found in both the nucleus (nucleolus included) and the cytoplasm. Instead, RNA exosomes with DIS3 are excluded from the nucleolus in human. Of note, RNA exosomes with DIS3L are restricted to the cytoplasm [373]. Finally, the RNA exosome complex is involved in several aspects of RNA biology, including RNA surveillance, pre-mRNA processing, control of mRNA levels, and, more strikingly, transcription regulation (see later) [329], [373].

2.2.2. Deadenylation-independent mRNA decay

Two other unusual routes to decay that are not initiated by deadenylation have also been described – deadenylation-independent decapping and endoribonucleolytic cleavage. Deadenylation-independent decapping might be used when deadenylation is prevented, for example by intramolecular pairing that block access to deadenylases. During endoribonucleolytic cleavage, mRNAs are cleaved within their body by an endonuclease (*e.g.*, IRE1, PMR1, RNAse MRP), producing two fragments that are subsequently degraded by the XRN1 and the RNA exosome exonucleases. Transcripts targeted by this pathway notably include those targeted by perfectly matching miRNAs, small interfering RNAs (siRNAs) and specific mRNA surveillance pathways [325].

2.3. Subcellular localization of mRNA decay

mRNA degradation can occur both in the nuclear and cytoplasmic compartments in order to either regulate gene expression levels or to eliminate faulty transcripts.

2.3.1. Nuclear decay

Cytoplasmic mRNA decay is often the focus of study but nuclear pre-mRNA/mRNA decay is also essential in cells for several reasons[23]. First, it is an important "caretaker of nuclear hygiene" by eliminating faulty transcripts that frequently arise during mRNA synthesis and processing. Second, it participates in the overall control of mRNA levels, and is thus also part of gene expression regulation mechanisms [329], [374].

2.3.2. Cytoplasmic mRNA decay

Although specific insoluble RNA granules like P-bodies have initially been proposed as the cellular sites of cytoplasmic mRNA degradation, this process is generally considered to occur freely in the soluble cytoplasm. RNA granules play important regulatory roles that are closely linked to mRNA degradation. I here briefly discuss P-bodies and stress granules.

---

[23] Although I only discuss the degradation of coding RNAs here, decay in the nucleus is also part of important maturation processes that enable the functionalization of noncoding transcripts [329].

2.3.2.1.   P-bodies

P-bodies (PBs) are membraneless cytosolic messenger ribonucleoprotein (mRNP) assemblies that accumulate poly(A)-shortened mRNAs and proteins involved in translation repression and mRNA degradation [375], [376] (**Figure 38a**). Recent proteomic analyses of PBs revealed that they are more specifically composed of the RNA helicase DDX6 (Dhh1 in yeast), decapping factors (DCP1A/B, EDC3/4), as well as accessory proteins (such as LSM proteins), the CCR4-NOT complex, the exonuclease XRN1, specific RBPs and RNA-modifying enzymes [375]. PBs proteome is enriched in IDPs [377] (**Figure 38b**). They are formed through LLPS implicating complex intermolecular protein-protein, protein-RNA and RNA-RNA interactions [375] (**Figure 38c**). In particular, DDX6 appears to be a key factor in PB assembly [378].

Interestingly, PBs composition is well-conserved among eukaryotes (**Figure 38b**), suggesting that PBs play important functions, most likely in link with post-transcriptional regulation [376]. Historically, the presence of mRNA-decay intermediaries within PBs and the evidence that decapping and decay can occur in PBs led to the idea that they might represent mRNA decay facilities [379]–[381]. However, more recent highlights have somewhat challenged this view. First, PBs are dispensable for constitutive mRNA decay [382]. Second, normal mRNAs can be released from PBs to reenter translation [383]. Together with recent imaging and purification studies, these data support that PBs might rather be primarily mRNA storage depots [376]. Interestingly, transcriptomic analyses revealed that PBs contain a third of the coding transcriptome. Gene ontology analysis showed that PB-enriched mRNAs mainly encode regulators while PB-excluded mRNAs mainly encode housekeeping proteins, suggesting that PBs mediate the coordinated storage of specific mRNA regulons [376], [384]. To date, the precise functions of PBs remain an open question, largely due to the challenge of directly visualizing mRNA degradation in diffraction-limited structures within living cells, as well as the difficulty of biochemically purifying such labile liquid droplets from cells [375].

In mammalian cells, PBs are constitutively present, with ten or fewer per cell. They appear as droplets of ~0.5 µm in size [376], [384]. PBs are highly dynamic structures. They are known to disassemble and reassemble during cell cycle progression [385]. Moreover, cellular accumulation of poly(A)-shortened mRNAs due to mutation in downstream decay factors, such as decapping proteins or exonucleases, has been reported to trigger PBs assembly [386], [387]. In this context, PBs might function as 'waiting rooms' when mRNA-decay pathways are overloaded. By compartmentalizing mRNAs, PBs prevent mRNAs destined for degradation to be readenylated and to return to translation, thereby generating unwanted proteins [325]. Correspondingly, when mRNA-decay pathways can immediately degrade mRNAs, PBs appear to be dispensable – they decrease in size and number or disappear [386], [387]. Together, these data suggest that mRNA storage within PBs regulate the interplay between translation and mRNA decay [325].

a
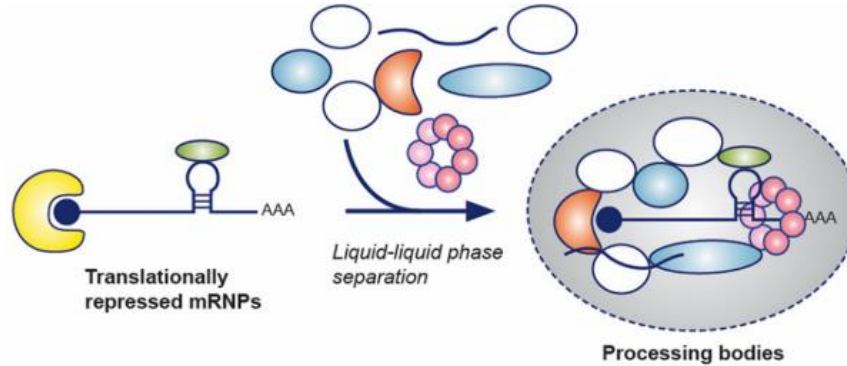
b
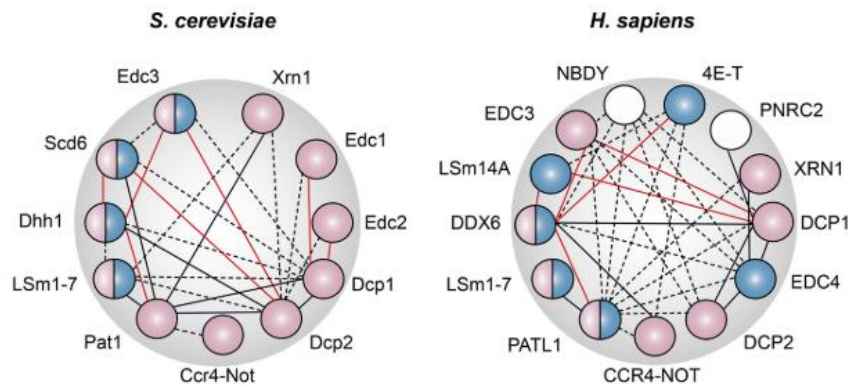
c
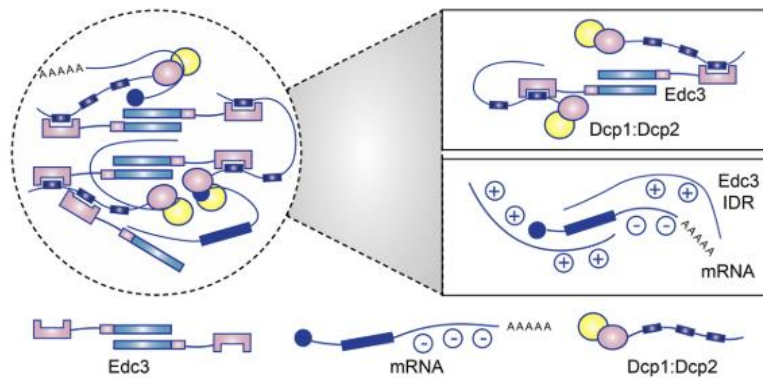
Figure 38. Overview of P-bodies. (**a**) P-bodies accumulate untranslating mRNPs and form via liquid-liquid phase separation. (**b**) P-bodies protein composition in yeasts and in humans. Components critical to assembly are colored in blue. Components that directly interact with RNA are colored in pink. Solid black lines indicate direct protein-protein interactions, and red lines indicate mutual exclusiveness. Dotted black lines indicate indirect or putative interactions. (**c**) Intermolecular interactions involved in P-bodies formation. Modified from [375].

2.3.2.2. Stress granules

SGs are membraneless mRNP assemblies that accumulate translationally-silenced mRNA and their associated translation initiation factors and RBPs [377], [388]. SGs proteome is composed of ~50% of RBPs [389]. Contrary to PBs that can form constitutively, SGs only occur under stress conditions such as oxidative stress, heat shock, ER stress, amino acid deprivation, *etc*. [388]. As for PBs, IDPs and LLPS processes appear to play an important driving role in their formation [388]. SGs are also highly dynamic structure that can undergo fusion, fission or movement [390]. After they formed from untranslating mRNPs, they can interact with PBs, exchange components with the soluble cytoplasm or be cleared by autophagy [388] (**Figure 39**). In cells, SGs mediate mRNP compartmentalization in order to regulate mRNA localization, translation and degradation. SGs formation is notably thought to represent an adaptive mechanism that help cells to survive and recover from harsh conditions [388]. Recent transcriptome analyses have provided mRNA snapshots of SGs, highlighting that individual mRNA species are differently targeted to SGs under stress conditions. Interestingly, transcript length and enrichment of some RNA elements have been linked to the specificity of SGs targeting [391]. Cytosolic biomolecular condensates like PBs and SGs represent an exciting area of research because their aberrant formation can cause neurodegenerative diseases and some cancers [388]. They have also been linked to chemoresistance [392].
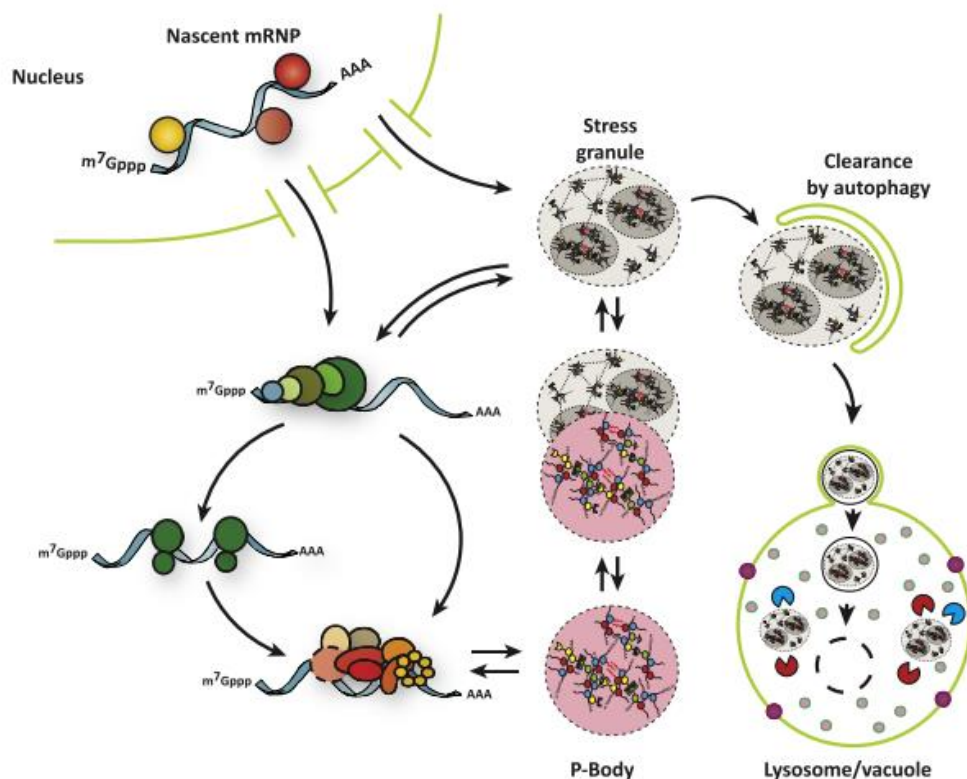
Figure 39. SGs are dynamic structures in the cell cytoplasm. See main text for details. Modified from [388].

2.4. Multilayered importance of RNA decay

Although RNA degradation has historically remained largely overlooked, it represents an essential aspect of cell molecular biology and a definitely worth-to-study area of research. Here, three layers of importance are discussed – in the context of normal cell physiology, diseases and RNA-based therapeutics development.

2.4.1.   Normal cell physiology

During the two last decades, modulation of mRNA stability has been evidenced to shape important physiological aspects of eukaryotic cell life, including cell-cycle progression [393], cell differentiation [394], [395], animal development [396], hematopoiesis [397], unfolded protein response [398], immunity [399], [400], and calcium signaling [401].

Typically, decay of cellular mRNAs can occur into three main contexts – mRNA half-lives can be modulated for the purpose of controlling gene expression quantity, gene expression quality and viral infection [402].

2.4.1.1.   Quantity control of gene expression

Gene expression is a complex process that is regulated at many levels [403] (**Figure 40**). At the level of the mRNA transcriptome, control of mRNA levels is a pivotal regulatory checkpoint [325], [326]. Since the mRNA transcriptome determines the proteome, maintaining proper mRNA levels firstly allows to avoid unphysiological surplus of proteins [404]. Additionally, it prevents deleterious mRNA surplus that may disrupts DNA replication by forming RNA-DNA hybrids and causes the sequestration of useful RBPs [327].
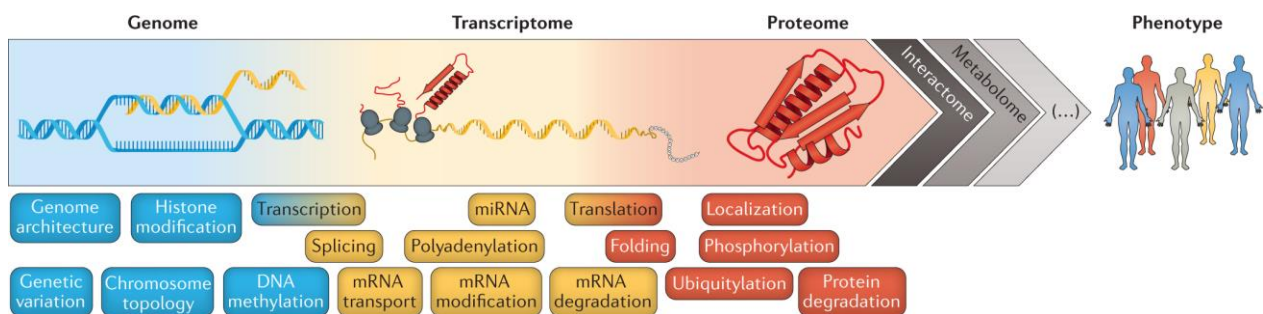
Figure 40. Multiple levels of gene expression regulation. See main text for details. From [403].

Control of cellular mRNA levels is a fundamental aspect of life. This is mainly achieved through a balance between mRNA synthesis and degradation. Historically, transcriptional regulation has been the focus of study. However, large-scale analyses have now revealed that mRNA degradation largely contributes in shaping mRNA transcriptome. In some responses, ~40-50% of changes in mRNA levels can be attributed to modulation of mRNA half-lives [325].

Importantly, the coordinated usage of mRNA synthesis and degradation has been argued to ease gene expression regulation in cells [405]. Figuratively, mRNA levels are somewhat like the speed of a car, transcription like the gas pedal and degradation like the brake [405]. If the driver wants to respect the law, relying solely on either the gas pedal or the brake will make the driving chaotic and uncomfortable. Instead, by using both pedals, the driver can more easily adapt its speed to fit outside circumstances. Similarly, by relying on both transcription and degradation, cells can more easily adapt mRNA levels to fit their needs.

2.4.1.2. Quality control of gene expression

Introducing errors is a frequent event during mRNA production that can occur at any steps. To preserve the integrity of the transcriptome, cells have therefore evolved complex RNA surveillance mechanisms to detect and eliminate aberrant transcripts [325], [326]. This surveillance occurs both in the nucleus and the cytoplasm. In the nucleus, it mainly relies on exonucleolytic decay by the RNA exosome complex [329] and deadenylation by the CCR4-NOT complex [360], [361] depending on the RNA substrate. Below, I also discuss three translation-dependent mRNA surveillance pathways that occur in the cell cytoplasm. They further exemplify the interplay that exists between mRNA translation and degradation.

a) Nonsense-mediated decay

Nonsense-mediated mRNA decay (NMD) is one of the best studied mechanism of mRNA quality control. This evolutionarily conserved mechanism detects and eliminates transcripts that contain premature termination codons (PTCs)[24] [325], [326], [406]. PTCs can have several origins, including mutations, frame-shifts, inefficient processing, leaky translation initiation and extended 3' UTRs [406]. If translated, PTCs-containing mRNAs can lead to the synthesis of unfunctional and/or dominant-negative proteins [406]. Generally, NMD discriminates mRNA targets by sensing the retention of the exon junction complex. A key NMD factor is the RNA-dependent helicase and ATPase UPF1. After a complex molecular cascade, NMD triggers mRNA degradation via the canonical mRNA decay pathway or via endonucleolytic decay. Of note, NMD has also been reported to target ~10% of normal mRNAs (*i.e.*, that lack any PTCs), and thus is also thought to participate in the quantity control of gene expression [406].

b) Non-stop decay

Non-stop decay (NSD) eliminates mRNAs lacking a stop codon, which can arise from premature polyadenylation or breakage. Without a stop codon, ribosomes proceed along the poly(A) tail. Therefore, NSD facilitates the recycling of ribosomes and associated factors [325].

---

[24] Interestingly, NMD is also known to modulate the stability of ~10% of normal cellular mRNAs, indicating that this surveillance mechanism also plays a role in gene expression control, with implications reported in development, differentiation and stress response [406].

c) No-go decay

No-go decay (NGD) eliminates mRNAs with stalled ribosomes, which can notably arise because of a strong secondary structure. NGD relies on endonucleolytic cleavage near the stall site which is followed by exonucleolytic decay of mRNA fragments by the RNA exosome and XRN1 [325].

2.4.1.3.   Antiviral defense

Lastly, by restricting viral infection, mRNA degradation is also part of innate immune system [407]. The implication of the exonucleolytic decay pathway via the exosome is largely documented [408]. It can act by directly targeting viral mRNAs for degradation or indirectly by limiting specific subsets of host mRNAs. In virus-infected cells, much more than a defense line, mRNA degradation is a battlefield. Indeed, by encoding specific factors like RNA methyltransferases [409], viruses can subvert host degradation machinery to evade innate immunity and/or favor their own replication [410]–[412].

2.4.2. Disease settings

Given the importance of mRNA degradation in normal cell physiology, its deregulation in diseases is not surprising. In cancer, defects in mRNA decay have long been associated with the aberrant regulation of the stability of proto-oncogene-encoding mRNAs, such as c-*fos* and c-*myc* [413]. Moreover, some of the regulators of mRNA stability like AREBPs, are long known as key oncogenic or tumor suppressor factors [414]. More recently, hijacking of canonical mRNA decay or NMD has also been described to shape cancer-specific programs like EMT and metastasis, with implications in the pathogenesis of several cancers; including B cell lymphoma [415], bladder cancer [416], [417], head and neck squamous cell carcinoma [418], lung cancer [419], clear cell renal cell carcinoma [420], multiple myeloma and plasma cell leukemia [421]. This can be mediated via mutations within genes encoding mRNA-decay machineries and regulators or within mRNA cis-acting elements. To date, the extent to which mRNA stability contributes to cancer cell transcriptome rewiring has, however, hardly been systematically characterized. Such studies should help in identifying cancer-associated mRNA stability drivers, and thereby novel actionable drugs targets [422]. Beyond cancer, mutations in genes encoding RNA exosome components or NMD factors have also been related to several intellectual disabilities [329], [406].

2.4.3. RNA-based therapeutics development

In cells, single-stranded RNA is an instable biomolecule compared to DNA. This is related to its chemistry and its high susceptibility to RNAse enzymes [423]. This feature is a major hurdle in the development of RNA-based therapeutics because therapeutic RNAs might potentially be immediately degraded after cellular delivery. By leveraging our comprehension of RNA stability, fundamental RNA biology has also helped in manipulating this type of therapeutics accordingly for therapeutic efficacy. This contributed to the emergence of mRNA vaccines, antisense oligonucleotides, aptamers, as well as siRNAs and miRNAs-based therapies [424]. Today, RNA

therapies constitute one of the hottest drug classes and should undoubtedly take further advantage of the future advancements in the field of RNA degradation.

2.5. Regulation of mRNA decay

As for transcription, mRNA decay is a process that is massively regulated. This regulation ensures that target mRNAs are accurately recognized in time and space [327]. It integrates intrinsic mRNA features (or cis-acting elements) and extrinsic operating factors (or trans-acting factors) and is governed by intracellular and/or extracellular stimuli [322], [326] (**Figure 41**).
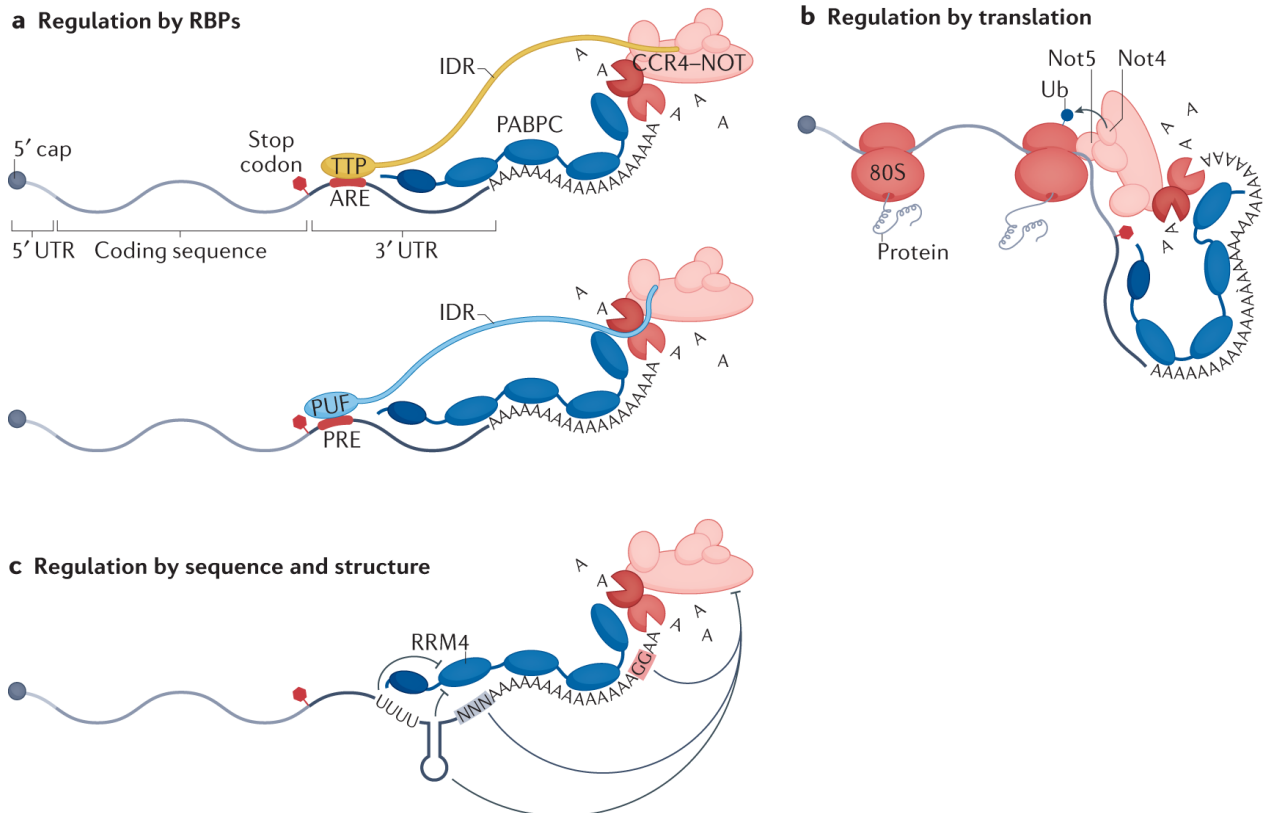
Figure 41. Overview of the regulation of mRNA decay. See main text for details. From [322].

2.5.1. Cis-acting elements

The 'degradation code' represents the full set of mRNA features (or cis-acting elements) that influence its stability. This comprises codon usage [425], [426], RNA-binding motifs and miRNA binding sites [322], [426], [427], GC content [428], [429], edited or modified nucleotides [430], [431], and RNA structures [426], [432]. A recent model suggests that cis-acting elements represent the most critical determinants of mRNA stability and, collectively, account for ~60% of the variation in mRNA half-lives [318]. Traditionally, these elements were thought to be mainly located in mRNA untranslated regions (UTRs) (**Figure 42**), and in particular, 3'UTRs for two main reasons. First, many motifs bound by regulatory RBPs or miRNAs were identified in this region [427], [433], [434]. Second, 3'UTRs provide a protective niche from traversing ribosomes to mRNP

protein complexes [318]. To date, however, the degradation code implicates all mRNA regions, giving a more prominent role than previously anticipated to the coding sequence (CDS). According to the current model, codon usage would actually explain most the variation in mRNA half-lives that is driven by mRNA sequence (55%) while 3'UTR motifs would only explain a small fraction of this variation (~5%) [322], [435].

Figure 42. Composition of a typical human protein-coding mRNA. 5'UTR and 3'UTR regions cover all the sequence upstream and downstream the coding sequence (CDS), respectively. Dashed border indicates that uORF might not be present. Modified from [436]. Created with BioRender.com.

2.5.1.1.   Codon optimality

Because of the degeneracy of the genetic code, multiple codons can encode the same amino acid. They are called 'synonymous codons'. Synonymous codons are differentially recognized by the ribosome in a way that is partly linked to the variability of transfer RNA (tRNA) intracellular concentrations. Whether decoding by the ribosome is fast or slow, codons are categorized as optimal or non-optimal, respectively. Along the mRNA CDS, codon optimality shapes the overall translation elongation rate [425]. Interestingly, recent genome-analysis have reported that ribosome dynamics is also closely associated with mRNA stability [322], [426]. Although the underlying principle is currently unclear, stable mRNAs tend to be enriched in optimal codons while unstable mRNAs tend to mainly contain non-optimal codons (**Figure 43**). Accordingly, swapping of non-optimal codons with synonymous optimal codons has been reported to increase mRNA stability, and inversely [435].
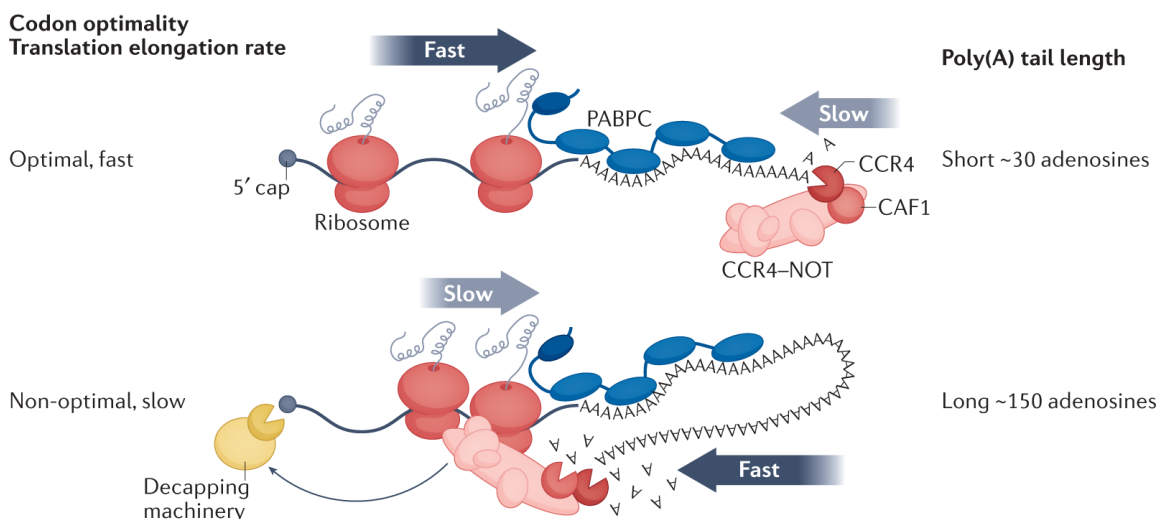
Figure 43. Influence of codon usage on translation elongation and deadenylation rates. See main text for details. From [322].

2.5.1.2.   RNA-binding motifs and miRNA binding sites

RNA-binding motifs are important determinants of mRNA stability [437]. Many have been identified in 3'UTR regions [433], [434]. They can serve as docking sites for RNA adapters (typically RBPs) that in turn regulate mRNA stability. AU-rich elements (AREs) are the best characterized class [433]. AREs are defined by the core AUUUA pentamer. The number and the type of combination of this pentamer delineates different families of AREs that can specifically affect mRNA stability [438]. AREs are found in the 3'UTR of many transcripts, such as those encoding cytokines, proto-oncogenes and TFs [433]. They are decoded by specific RBPs, called AU-rich binding proteins (AREBPs), that either promote or prevent mRNA decay. When mRNA decay is mediated via an ARE, it is commonly referred to as 'ARE-mediated mRNA decay' (AMD) [438]. Likewise, miRNA binding sites are well-known to govern mRNA stability. Many are found in 3'UTR regions. They are recognized via complementary pairing by small endogenous non-coding RNAs, also known as miRNAs [439]. When mRNA decay is mediated via a miRNA binding site, it is commonly referred to as 'miRNA-mediated mRNA decay'. ARE- and miRNA-mediated mRNA decay are further discussed later.

2.5.1.3.   GC content

GC content impacts mRNA stability via diverse mechanisms and has been suggested to play a central role in the coordination of mRNA decay and storage [428]. GC content influences codon usage [428], [429], targeting to PBs and the binding of trans-acting factors onto mRNAs because binding sites are biased in terms of GC content. Interestingly, GC-rich and AU-rich mRNA populations tend to have different post-transcriptional fates in the cytoplasm. GC-rich mRNAs appear to be excluded from PBs and to be degraded in a DDX6 and XRN1-dependent manner. By contrast, AU-rich mRNAs appear to be targeted to PBs where they undergo DDX6-dependent translation repression and their stability is regulated by PAT1B [428].

2.5.1.4.   Epitranscriptome

In analogy to the epigenome, the epitranscriptome designates the whole set of biochemical modifications found in RNA that do not involve, *per se*, the ribonucleotide sequence. It is dynamically remodeled via RNA editing and modification [324].

a) RNA editing

RNA editing is a molecular process during which discrete changes to specific bases are made within a RNA molecule after/during its synthesis by RNAPII. This may include the insertion, deletion, and base substitution of nucleotides [440]. Adenosine-to-inosine (A-to-I) editing is the most abundant type of RNA editing in mammals [441]. This process is catalyzed by a family of adenosine deaminases acting on RNA (ADAR) proteins, and occurs at thousands of loci [440], mainly co-transcriptionally [442]. Because edited mRNAs are differently recognized by RBPs and regulatory RNAs than their non-edited counterparts, RNA editing has been directly linked to

mRNA stability in many studies [430], [443]–[446]. RNA editing can also influence mRNA stability by altering RNA structure [447].

b) RNA modification

RNA modifications are well-known regulators of post-transcriptional mRNA fates [448], [449]. To date, >170 different modifications constitute the epitranscriptomic landscape [324]. Among them, several have been reported to modulate mRNA stability, including N6-methyladenosine (m6A), N6,2'-O-dimethyladenosine (m6Am), 8-oxo-7,8-dihydroguanosine (8-oxoG), pseudouridine (Ψ), 5-methylcytidine (m5C), and N4-acetylcytidine (ac4C) [431]. RNA modifications can serve as direct docking sites for specific trans-acting factors [450]. Moreover, they can stabilize or disrupt RNA structures and, in turn, dictate RNA-protein interactions [432], [451]. RNA modifications have important implications in normal cell physiology and in diseases, and notably cancer (reviewed in [452]–[455]).

In cells, the fate of modified mRNA transcripts is determined by the coordinated actions of the following three effector proteins: writers (RNA-modifying enzymes), readers (RBPs which specifically recognize the modified nucleotides) and erasers (proteins which remove specific chemical groups from the modified nucleotides) [450]. m6A is the most abundant and the best characterized modification. It is encoded co-transcriptionally on nascent transcripts by a methyltransferase complex, which mainly comprises methyltransferase-like protein 3 (METLL3), METTL14 and Wilms tumour 1-associated protein (WTAP) [450], [456]. When this modification is decoded by the YTH521-B homology (YTH) domain-containing proteins such as YTHDF2, it generally leads to rapid degradation of m6A-containing mRNAs via the canonical mRNA decay pathway or endoribonucleolytic cleavage [457]. By contrast, when this modification is decoded by FMRP, IG2BP or HuR, it generally leads to mRNA stabilization [458]. m6A modifications can also be removed by demethylase like α-ketoglutarate-dependent dioxygenase alkB homolog 5 protein (ALKBH5) and fat mass and obesity-associated protein (FTO) [450] (**Figure 44**).
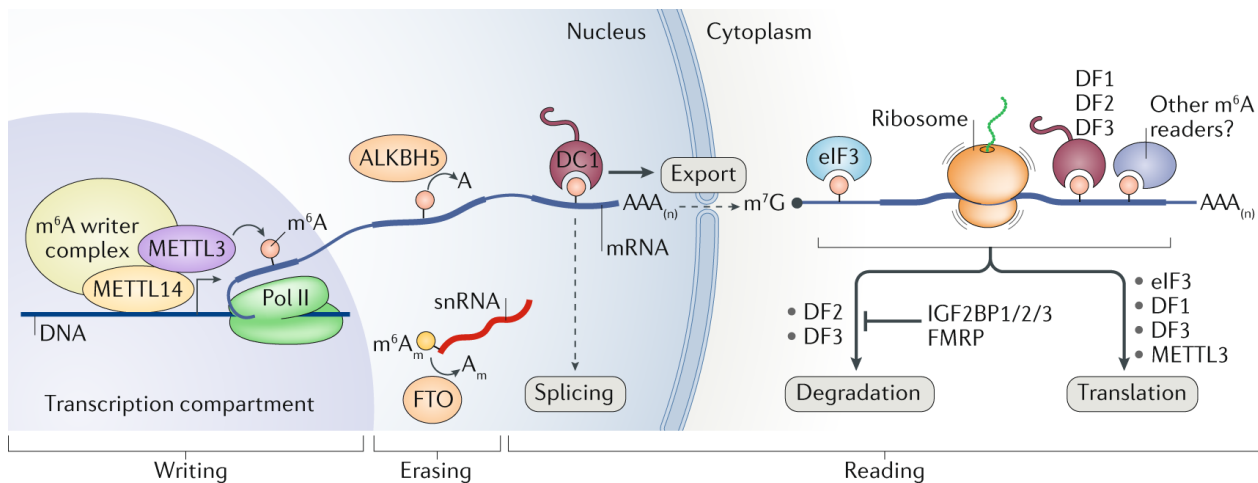
Figure 44. The m6A mRNA lifecycle. See main text for details. From [459].

2.5.1.5.   RNA structures

DNA universally folds into a double helix. By contrast, RNA can fold into diverse and complex structures via intramolecular interactions. RNA structural topography is an emerging and exciting field of research. It is highly dynamic and is regulated by many factors, such as temperature, RNA helicases, RBPs and RNA modifications (**Figure 45**). It ensures a myriad of functions and is an essential player of RNA biology. Typically, RNA structures can influence mRNA stability [432]. Stem-loop structures represent a well-known example. By their presence in 3'UTRs, they stabilize the non-polyadenylated mRNAs that encode replication-dependent histones [432]. In some context, they can also destabilize mRNAs and lead to Staufen-mediated mRNA decay (SMD), a pathway that is mechanistically linked to NMD [460]. Another, although less understood, example is provided by RNA G-quadruplex[25] that have been reported to promote mRNA decay [461], [462].
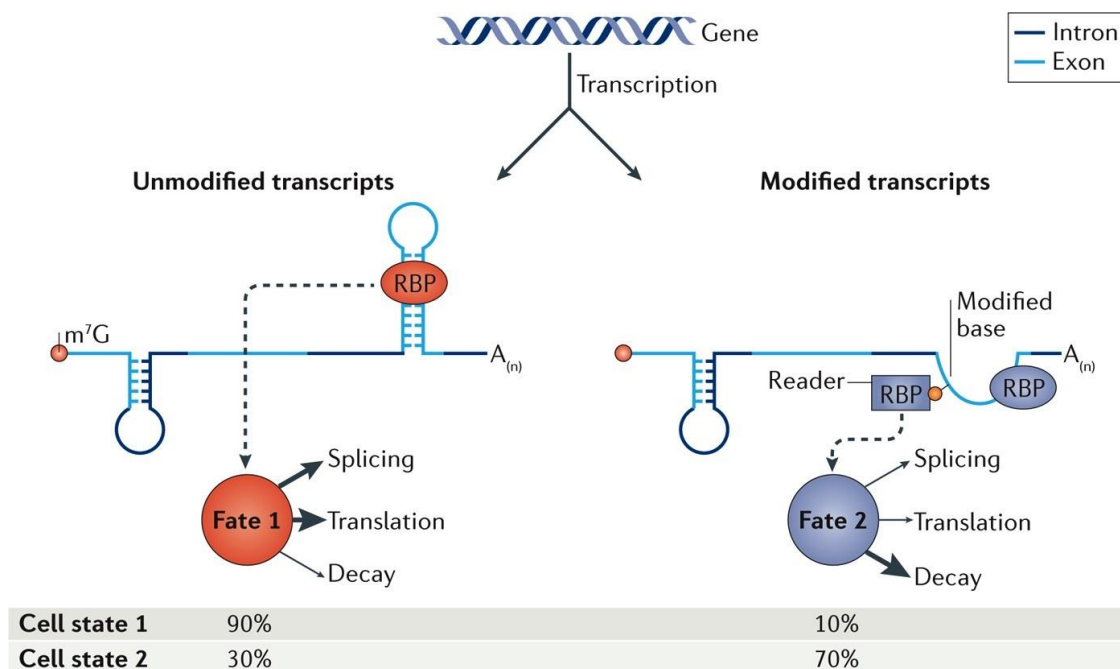
Figure 45. Interplay between RNA modifications and structures, and its influence on mRNA stability. See main text for details. Modified from [432].

2.5.2. Trans-acting factors

Trans-acting factors are sequence- or modification-specific factors that primarily modulate RNA stability via binding to mRNA cis-elements. They include two main classes: RBPs and ncRNAs. Here, I discuss how these factors regulate mRNA stability with a focus on a specific RBP named HuR.

---

[25] RNA G-quadruplex are four-stranded helical structure involving guanines

2.5.2.1.   RNA-binding proteins

RNA-binding proteins (RBPs) are key post-transcriptional regulators [463]. To date, >1000 RBPs have been identified in humans [229]. Among them, a vast array is capable of governing mRNA stability, the best-studied class being AU-rich binding proteins (AREBPs) [433].

a)   AU-rich binding proteins

AREBPs bind AREs and are either destabilizing or stabilizing RBPs whether they decrease or increase mRNA half-lives, respectively [433]. Typical examples of AREBPs are presented in **Table 2**. Destabilizing AREBPs (*e.g.*, TTP, AUF1, KSRP, BRF1, *etc.*) can serve as docking sites for decay machineries, such as the CCR4-NOT deadenylation complex. Interestingly, these interactions often involve IDRs [464] and are regulated by PTMs [326]. For example, phosphorylation of specific residues in TPP disrupts its binding to CCR4-NOT and prevents deadenylation [320]. By contrast, the mechanism of action of stabilizing AREBPs (*e.g.*, HuR, specific isoforms of AUF1, PTBP1, *etc.*) is more elusive. They might function simply by competing for the binding site of destabilizing AREBPs, or by retargeting mRNAs to insoluble RNA aggregates like PBs [465]. For example, HuR has been shown to compete with AUF1, KSRP and TTP [465], [466]. Of note, HuR has also been reported to attenuate miRNA-mediated repression by promoting the dissociation of the miRNA-induced silencing complex (miRISC) from mRNA [467], [468]. Alternatively, destabilizing AREBPs could also repress decay machineries via direct interactions [433]. Importantly, AREBPs, such as TIA1, TIAR and HuR, have also been linked to the regulation of translation [469], and might play a role in the coordination of translation and degradation. Below the case of HuR is further discussed.

Table 2. Well-known ARE-binding proteins and their function. From [326].

AREBPs (also known as)	Function	RNA-binding domains
TTP (ZFP36)	Destabilizing	CCCH zinc finger (x2)
BRF1 (ZFP36L1)	Destabilizing	CCCH zinc finger (x2)
BRF2 (ZFP36L2)	Destabilizing	CCCH zinc finger (x2)
AUF1 (hnRNPD, which includes 4 isoforms)	Most forms are destabilizing, some are stabilizing	RRM (x2)
KSRP	Destabilizing	K homology (x4)
HuR (ELAVL1, HuA)	Stabilizing	RRM (x3)

b) HuR

HuR is one of the best-characterized stabilizing AREBPs. This ubiquitous RBP is part of the embryonic lethal abnormal vision protein family (HuR is also known as ELAVL1[26], or HuA). Structurally, HuR is mainly composed of three RRMs and a nucleocytoplasmic shuttling sequence (HNS) (**Figure 46**) [470]. Recognition of ARE-containing mRNAs by HuR has been reported to involve all three RRMs [471]. HuR also has been reported to oligomerize and bind to target mRNA as an oligomer. Interestingly, HuR oligomerization is enhanced by PARylation, a PTM mainly catalyzed by PARP1 [468]. In physiologic condition, HuR is mainly found in the nucleus where it controls pre-mRNA splicing [466]. In stress conditions, HuR is redistributed via phosphorylation to the cytoplasm where it enhances mRNA stability and translation [469]. Interestingly, HuR has also been reported to decrease mRNA stability of two transcripts [472], [473], suggesting that HuR might act as both a stabilizing and destabilizing factor depending on the context.

HuR plays a role in many biological processes, including differentiation, DNA damage response, inflammation and immunity [470]. Interestingly, HuR silencing in MSCs has been reported to impair osteogenic differentiation. Mechanistically, this would rely on the negative regulation of the stability of mRNAs involved in extracellular matrix organization by HuR [474]. In addition, HuR has been implicated in the pathogenesis of several cancers [475], including for example osteosarcoma [476], breast [477], and brain cancers [478]. In this context, HuR has been described to promote cell survival, immune evasion, angiogenesis, invasion and metastasis [465] (**Figure 47**).

Crystal structure of RRM1 and RRM2 bound to mRNA (PDB 4ED5)
RRM1 and RRM2 are responsible for recognizing and binding ARE-containing mRNAs

Dynamic HuR nucleocytoplasmic shuttling
The localization of HuR is largely dependent on PTMs within the Hinge region

Crystal stucture of two RRM3 bound to mRNA (PDB 6GD2)
RRM3 binds long mRNA poly(A) tails
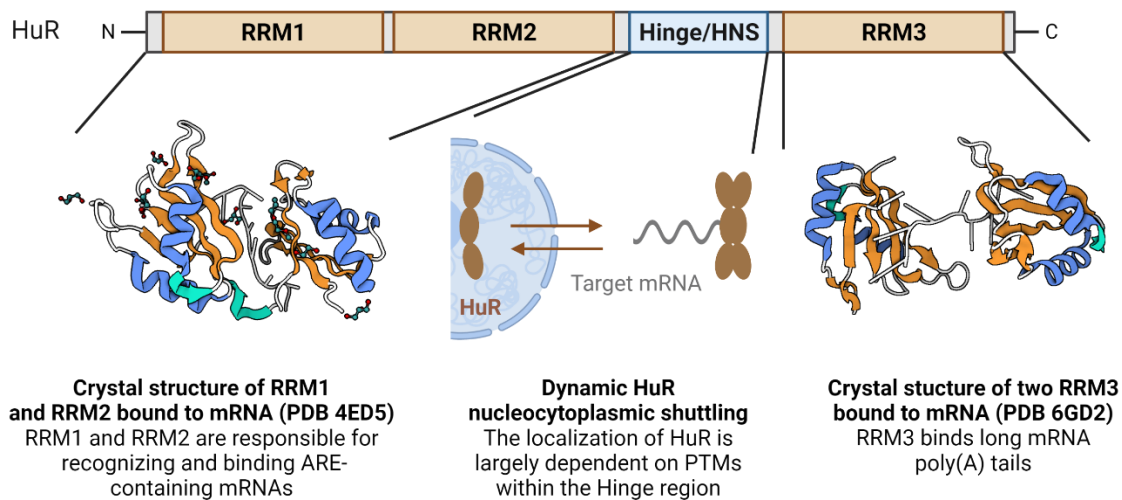
Figure 46. Structure and function of HuR. Modified from [470]. Created with BioRender.com.

---

[26] Or also embryonic lethal abnormal vision-like protein 1
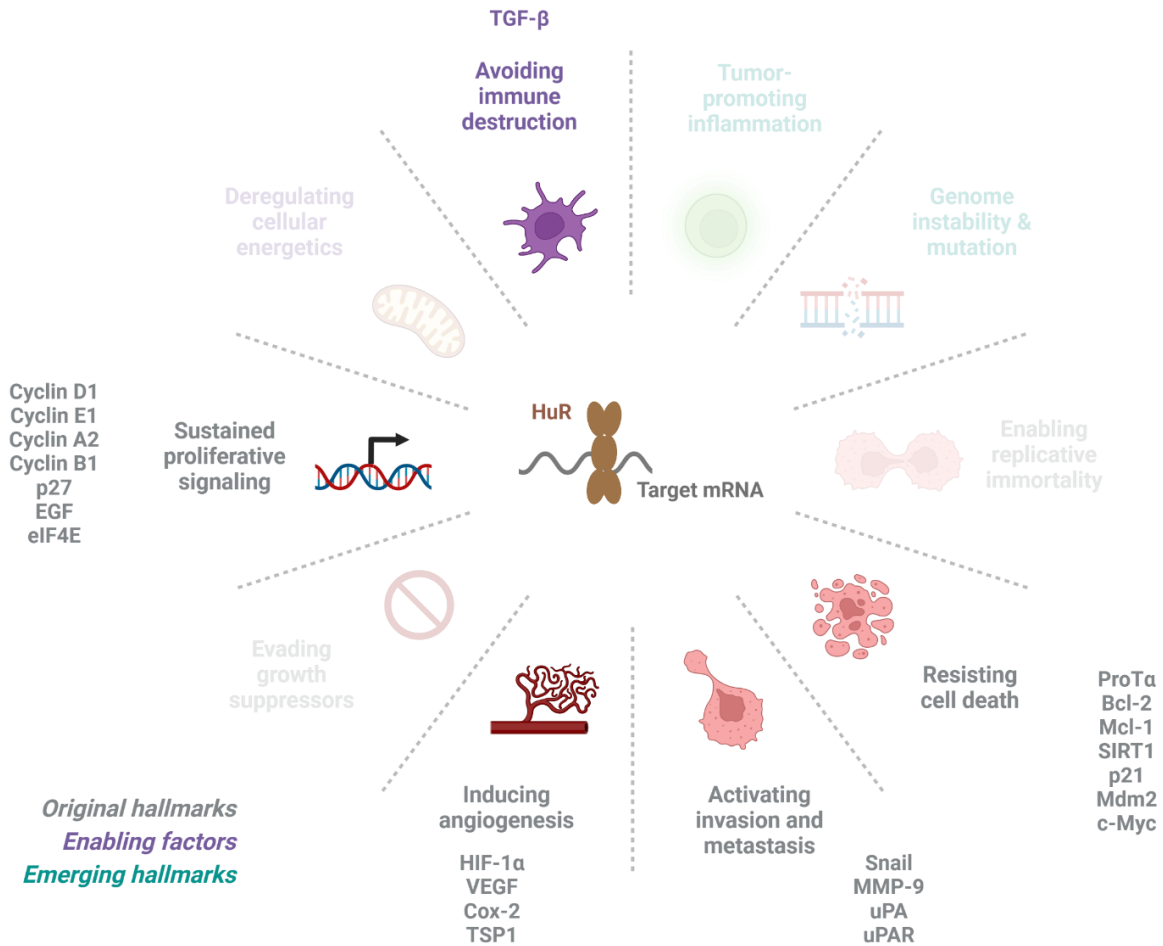
Figure 47. Post-transcriptional control of cancer hallmarks by HuR. Transparency indicates HuR-unrelated cancer hallmarks. Well-known gene targets of HuR are shown. Modified from [465]. Adapted from "Hallmarks of Cancer", by BioRender.com (2022). Retrieved from https://app.biorender.com/biorender-templates.

Clinically, HuR is generally considered to represent an attractive therapeutic target for cancer [465]. Several chemical inhibitors are commercially-available and have already been used in *in vivo* experiments. They can be categorized by their mechanisms of action [470], which include: interfering with HuR RNA-binding ability (*e.g.*, DHTS and CMLD-2) [479]–[481], preventing HuR homodimerization that is required to engage with mRNA (*e.g.*, MS-444) [482], [483], or preventing HuR nucleocytoplasmic shuttling (*e.g.*, MS-444, pyrvinium pamoate) [470].

2.5.2.2.   Non-coding RNAs

ncRNAs, such as miRNAs, can also influence mRNA stability. Unlike RBPs, which either promote or prevent mRNA degradation, miRNAs predominantly promote mRNA degradation. Typically, miRNAs associate with AGO and GW182 proteins to assemble the miRISC complex. This complex recognizes mRNA targets by base-pairing to partially complementary binding sites, which are often found in 3'UTR regions. It initiates mRNA decay by recruiting the cytoplasmic deadenylase

complexes PAN2-PAN3 and CCR4-NOT. Following deadenylation, mRNA targets are further degraded via 5'–3' exonucleolytic decay [439] (**Figure 48**). Although not discussed here, miRNAs can also inhibit translation [439].
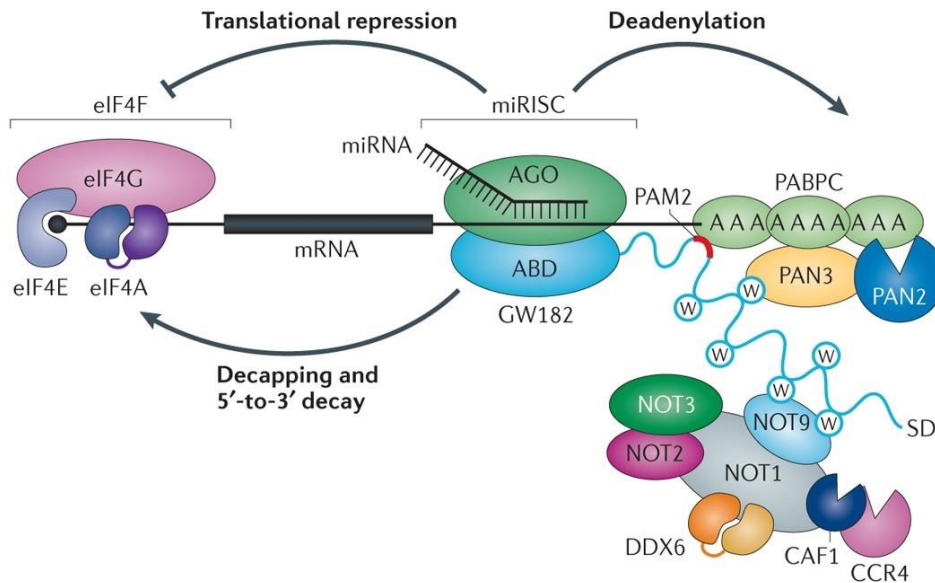
Figure 48. miRNA-mediated gene silencing. ABD = AGO-binding domain, SD = silencing domain. Modified from [439].

Long-noncoding RNAs (lncRNAs) have also been implicated in the regulation of mRNA degradation (**Figure 49**). They can work as molecular sponge for miRNAs or RBPs in order to reduce their availability, and indirectly modulate mRNA stability. They can also work directly by recruiting proteins to degrade mRNA [484]. For example, a specific group of lncRNAs has been linked to the activation of SMD [485].
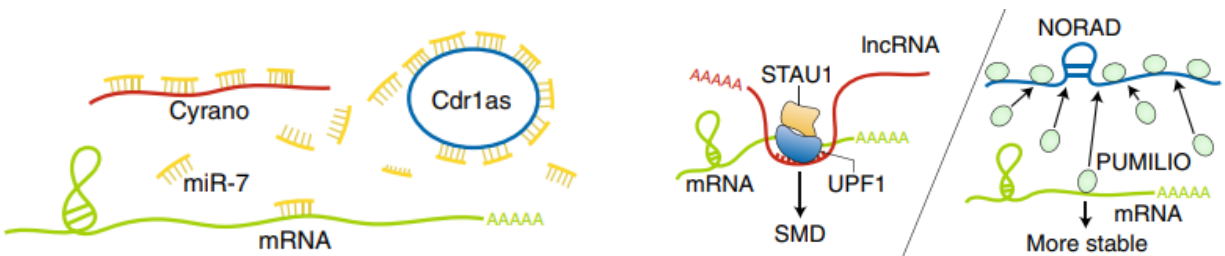
Figure 49. Roles of lncRNAs in the control of mRNA stability. See main text for details. Modified from [484].

2.5.3. Cellular stimuli

In eukaryotic cells, response to cellular stimuli via downstream signaling pathways provides an additional layer to the regulation of mRNA stability. Depending on the context, mRNA half-lives can be either lengthened or shortened [326]. Cellular stimuli can result in the nucleocytoplasmic partitioning or the retargeting to insoluble granules of decay machineries, trans-acting factors or specific mRNA populations [326], [329]. Additionally, it can lead to the modification of cis-acting elements or the addition of PTMs on regulatory RBPs in order to promote or prevent some RNA-protein or protein-protein interactions [326]. The outcome of several signaling pathways on AREBPs and ARE-containing mRNAs is illustrated in **Figure 50**.
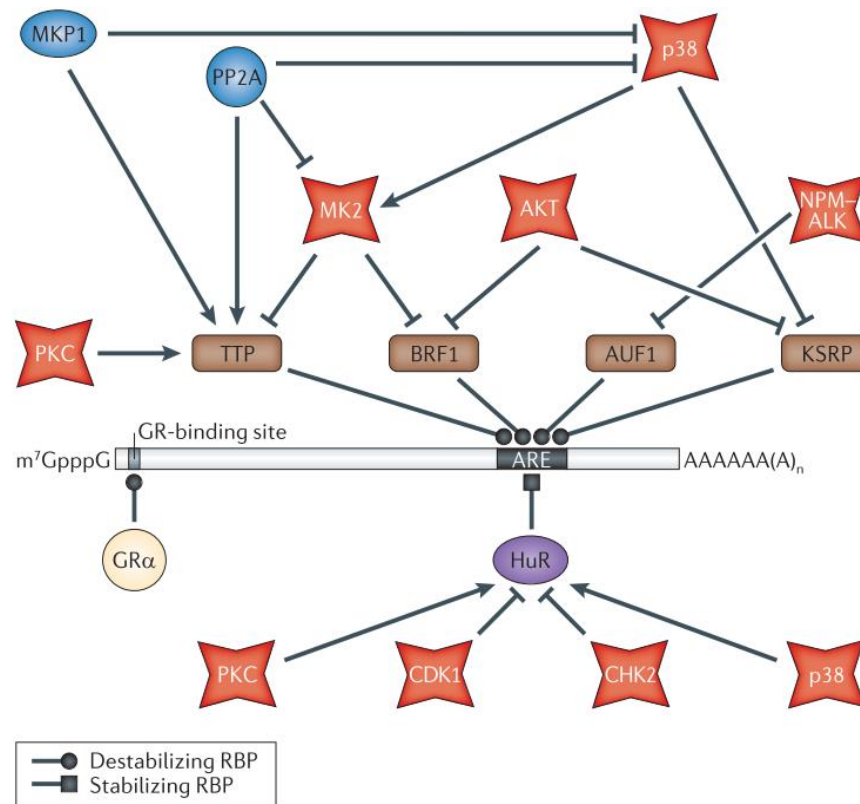
Figure 50. Cell signaling-dependent regulation of ARE- and GR-mediated mRNA decay. Destabilizing AREBPs are shown in the brown rectangles. HuR is shown in purple. Phosphatases and kinases are in blue and red, respectively. Modified from [326].

Cellular stimuli comprise intracellular and extracellular cues. Intracellular cues that occur in the context of mRNA surveillance after sensing of aberrant mRNAs are classical examples [325], [486]. Another example is provided by the IRE1-dependent decay (RIDD) pathway which promote degradation of selected mRNA transcripts via endonucleolytic cleavage during endoplasmic reticulum stress [326]. In addition, extracellular cues have also been described to regulate mRNA stability. For example, the glucocorticoid receptor, a TF of the nuclear receptor family, has been shown to bind to some mRNAs and activate decay upon sensing of glucocorticoids [326]. This pathway is also referred to as glucocorticoid-mediated mRNA decay (GMD) [487], [488].

2.6. Gene expression coupling

Gene expression is frequently viewed as a "linear assembly line" where the different steps are mechanistically and functionally disconnected from each other (**Figure 51a**). However, this represents a simplification of the underlying complex reality. Instead, gene expression might resemble a network of intertwined steps participating in a coordinated manner to its regulation (**Figure 51b**) [331], [489], [490]. Here, I discuss the concept, the functional relevance, and the identity of potential molecular effectors of 'gene expression coupling' with a focus on the control of mRNA synthesis and stability by canonical DNA-binding TFs.

a   **b**
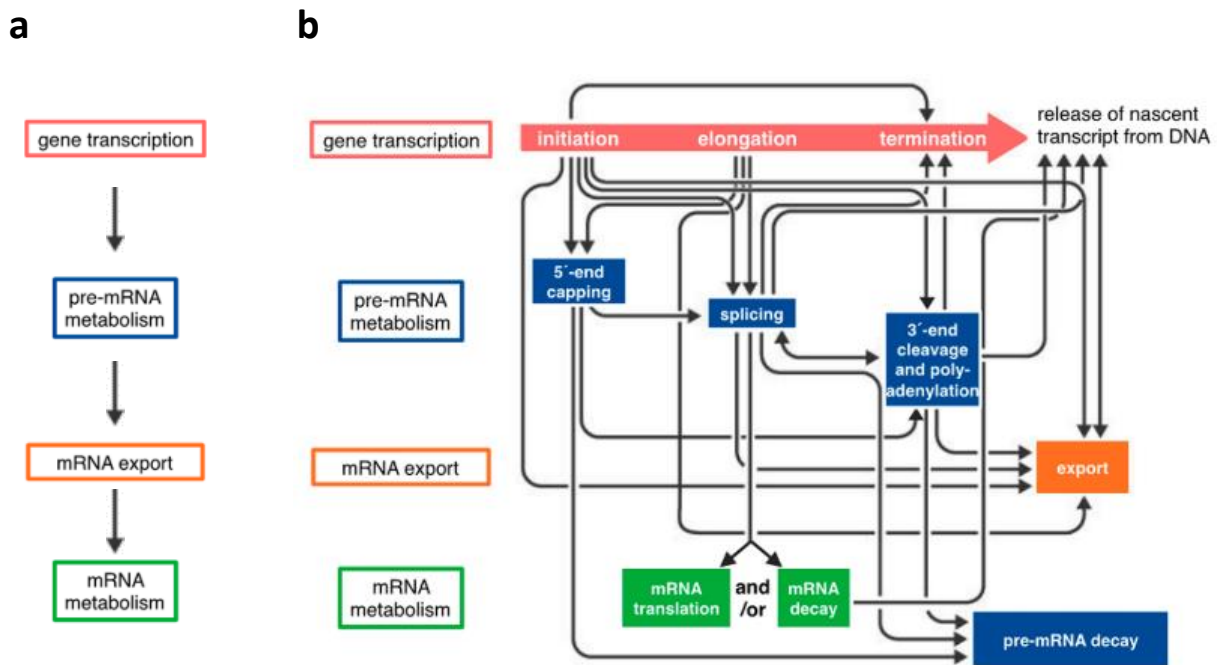
Figure 51. Models of gene expression. (**a**) Linear or uncoupled model. (**b**) Coupled model. Modified from [489].

2.6.1. Definition

In the literature, the concept of 'gene expression coupling' is not clearly defined. In general, two processes are considered to be coupled when "the properties of one process affect the outcome of the other" [491]. In this work, 'gene expression coupling' designates, more specifically, any situation in which identical mRNA transcripts are mechanistically controlled during the course of two (or more) different molecular processes by one (or more) common molecular effector(s). Hereafter, the molecular effector of the coupled processes is referred to as 'coupling factor'. Depending on the implicated cellular compartment(s), the types of nuclear, cytoplasmic and nucleocytoplasmic coupling are here further distinguished.

2.6.2. Nuclear and cytoplasmic coupling

Nuclear coupling involves molecular processes that are restricted to the cell nucleus. Coupling between transcription and alternative splicing (*i.e.*, the influence of transcription on splice site selection) is a well-described case of nuclear coupling. In the literature, two main explanatory models have been proposed: (i) the 'recruitment model' and (ii) the 'kinetic model'. In the first one, the recruitment of splicing factors onto the nascent transcript is determined by promoters and RNAPII CTD. In the second one, the 'window of opportunity' for a splicing event to occur is influenced by RNAPII elongation rate [319], [333], [491], [492]. Another example of nuclear coupling is the coupling between nuclear RNA decay and other nuclear processes. In particular, coupling between alternative splicing and non-sense mediated mRNA decay (also referred to as 'AS-NMD') is known to regulate the expression of many RBPs [493]. In addition, transcription can also be coupled with nuclear RNA decay.

Inversely, cytoplasmic coupling involves molecular processes that are restricted to the cell cytoplasm. Coupling between mRNA translation and cytoplasmic decay represents a typical case of cytoplasmic coupling. As discussed previously in part 2.5.1.1, it might be mediated by codon usage but the underlying mechanism remains unclear (see **Figure 43**) [322], [425], [494], [495].

2.6.3. Nucleocytoplasmic coupling

More surprisingly, nuclear processes can also be coupled to cytoplasmic processes, and *vice-versa*, leading to nucleocytoplasmic coupling. This type of coupling is less easy to anticipate because the nuclear envelope is often erroneously thought to act as a physical separation. Below two examples of nucleocytoplasmic coupling are briefly covered: coupling between either transcription or pre-mRNA processing, and cytoplasmic mRNA decay.

2.6.3.1.   Coupling transcription and cytoplasmic mRNA decay

Coupling between mRNA synthesis and cytoplasmic decay has first been evidenced in yeast, at both gene-specific and genomic scales [496]. Two modes have been described, including 'opposite coupling' and 'synergistic coupling' (**Figure 52**). Opposite coupling arises when mRNA synthesis is enhanced and mRNA stability is decreased, or *vice-versa* [497]. When transcription and degradation rates balance each other, mRNA steady-state levels remain unchanged, a phenomenon also known as 'transcript buffering'[27] [498]. Opposite coupling explains the peak-shaped behavior of some gene expression responses observed following an environmental stress or during cell cycle progression [497], [499]. Moreover, they enable a more rapid adaptation to

---

[27] Transcript buffering was first observed in yeast where steady-state mRNA levels appeared to be robust to the knockdown of components associated with the transcription or the degradation machineries. It indicates that defects in mRNA synthesis are rapidly balanced by adjustments in mRNA degradation and *vice-versa*. This mechanism was proposed to make total cellular mRNA levels highly robust to perturbations as it might occur during stress. In yeast, transcript buffering exists both at genomic and gene-specific scales. It has also been reported in mammals. Importantly, it suggests the existence of molecular effectors that are involved in both transcription and degradation processes [498].

new environmental conditions than would either mechanism acting alone [500]. They also bring gene expression robustness to environmental or genetic fluctuations. By contrast, synergistic coupling arises when mRNA synthesis and stability are together either enhanced or decreased. Suggested to be less frequent [501], this mode enables enduring gene expression responses. It has been observed notably during cell cycle progression for histone mRNAs [502], differentiation [503], DNA damage and osmotic stress [504]. Interestingly, the mode of coupling between mRNA synthesis and degradation appears to be condition-dependent [504], suggesting that subsets of mRNAs might potentially switch from one mode to another depending on the cellular context.
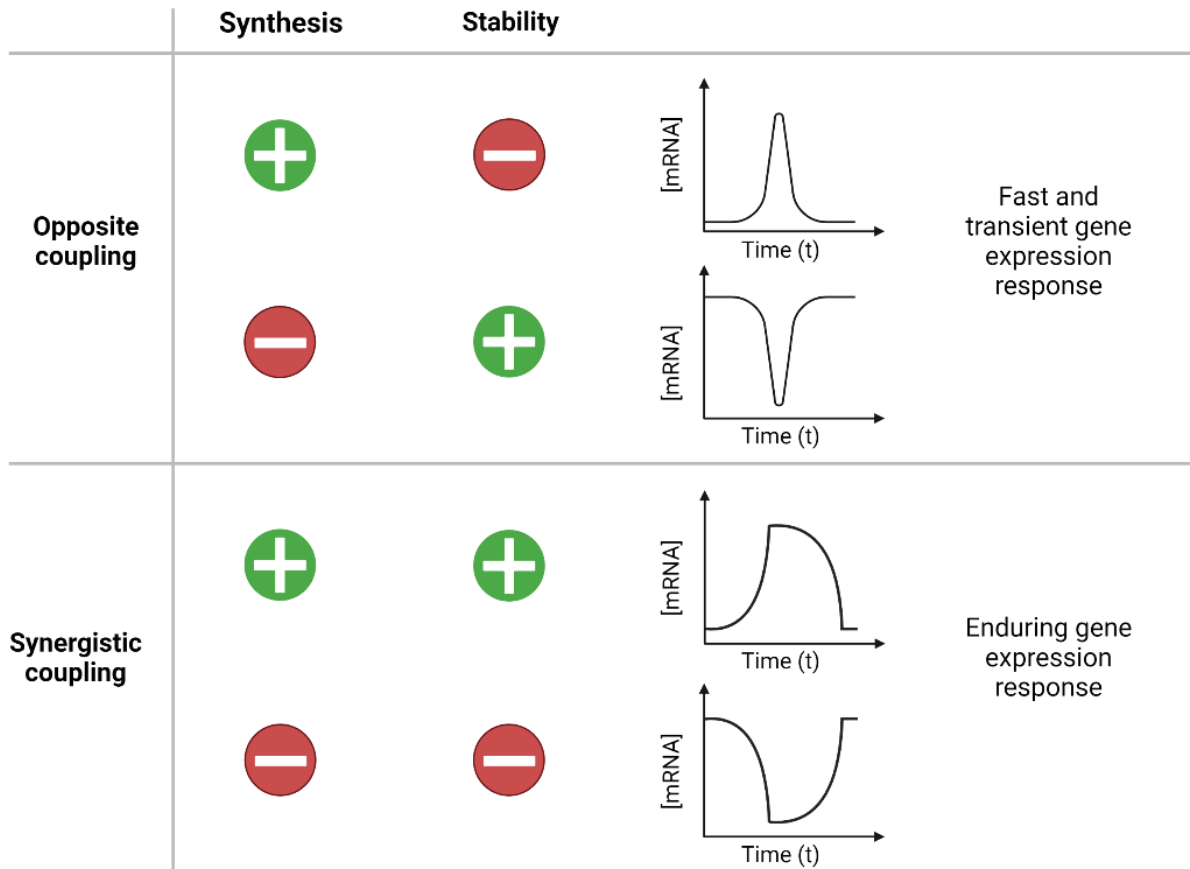
Figure 52. Modes of coupling between transcription and mRNA degradation. See main text for details. Created with BioRender.com.

2.6.3.2.   Coupling pre-mRNA processing and cytoplasmic mRNA decay

In higher eukaryotes, pre-mRNA processing has been reported to affect mRNA stability in the cytoplasm via alternative splicing, and alternative transcription start/termination [426], [505]. Of note, as most of the yeast genes are not spliced, coupling between mRNA splicing and cytoplasmic decay is less easy to anticipate with this model[28]. Alternative transcription start and termination are linked to the choice between alternative transcription start sites (TSS), and alternative polyadenylation (APA), respectively. Although these processes were also suggested to largely reflect molecular errors [506], they are traditionally thought to be part of adaptive mechanisms to diversify the cellular transcriptome. In particular, the alternative selection of TSS and APA leads to changes in 5' and 3' UTR lengths [426], [507]. Since these regions typically contain various cis-elements recognized by RBPs and regulatory RNAs, these nuclear processes can also affect mRNA stability in the cytoplasm [508], [509].

2.6.4. Functional relevance

There are many advantages of coupling the different steps of gene expression. Therefore, it is not surprising that cells evolved such mechanisms. As exemplified earlier, coupling transcription and mRNA degradation provides an elaborate and robust way to tune the celullar transcriptome and proteome because they facilitate the control of mRNA levels. Moreover, gene expression coupling has been proposed to facilitate evolution, mRNA surveillance and building of post-transcriptional regulons [510], [511].

2.6.5. Potential coupling factors

The identity of the molecular effectors that might coordinate gene expression is a major question in the field, especially in the case of nucleocytoplasmic coupling. Since the 2000's, several constituents of the transcription machinery (including RNAPII subunits, and well-described DNA-binding TFs) as well as promoters have been found to play non-canonical roles in post-transcriptional processes, including mRNA processing and, more strikingly, mRNA degradation. Likewise, post-transcriptional factors (including RBPs, and mRNA decay-associated machineries) have been found to play non-canonical roles in transcription or other processes, reinforcing the idea that gene expression is circular [512], [513]. In most cases, a remaining but crucial question is whether these findings might underline new examples of 'coupling', as defined earlier in part 2.6.1, or simply correspond to new examples of 'multitasking' (*i.e.*, the different molecular activities of a specific factor control distinct mRNA transcripts). Below I successively present several molecular factors that appear to link mRNA decay to other processes with a main focus on DNA-binding TFs.

---

[28] This model has thus the advantage of uncoupling mRNA degradation from pre-mRNA splicing.

2.6.5.1.   Transcription machinery and promoters

The roles of the transcription machinery and promoters are traditionnaly confined to the control of mRNA synthesis. As described here, a number of paradigm-shifting studies have interestingly linked them to other molecular processes throughout the eukaryotic cell.

a) Rpb4/7 imprinting

RNAPII is composed of several subunits, among which Rpb4/7. In yeast, these subunits have been reported to dissociate from RNAPII, bind nascent transcripts as they emerged from the exit channel and shuttle with them to the cytoplasm where they influence mRNA decay and translation [496], [514]–[516]. This process of co-transcriptional loading and chaperoning of nascent mRNAs to regulate their cytoplasmic fate was called 'mRNA imprinting'. Although Rpb4/7 imprinting seems to be conserved in yeast [501], it has not been reported in higher eukaryotes[29]. Moreover, this mechanism remains controversial in light of more recent studies [517], [518]. Nevertheless, co-transcriptional mRNA imprinting with other transcriptional regulators, decay factors or regulatory RBPs, and ncRNAs has also been reported [519]–[522]. This aspect is further discussed below.

b) Promoters

mRNA imprinting raised the exciting idea that a newly transcribed mRNA can be primed during transcription for future regulation in the cytoplasm [523]. The main issue, however, was the specificity of the putative mechanism. Remarkably, several studies have shown that mRNA degradation of many yeast genes is strikingly regulated in a promoter-dependent manner, suggesting that the specificity could come directly from cis-acting elements within gene promoters. Correspondingly, swapping promoters in yeast appeared to influence cytoplasmic mRNA stability, leading to promoter-mediated mRNA decay [497], [519]–[521], [524]. Although this mechanism was also suggested in humans [497], [499], [525]–[527], it has remained more elusive than in yeast.

c) DNA-binding transcription factors

TFs are traditionally defined as sequence-specific DNA-binding factors that regulate transcription (activation or repression) of a specific subset of genes [1] (see also the 'Preamble' section). Although they are increasingly recognized to also regulate post-transcriptional processes, most notably splicing, the model that prevails is that these non-canonical functions are related to indirect mechanisms. For examples, in the context of splicing, TFs may act via the modulation of either RNAPII elongation rate or the expression of direct splicing factors [489], [528], [529]. Nevertheless, more recently, this model has been challenged by a growing number of reports showing that *bona fide* TFs (such as ERG, Sp1, FOXA1, GATA4, GTF TFIID, but also EF) can also

---

[29] Interestingly, both EWSR1 and EF have been reported to interact with human Rpb7. The relevance of this interaction in the context of a functional coupling between transcription and mRNA degradation is however unclear [710].

control steps of pre-mRNA processing via direct mechanisms (*e.g.*, by binding to RNA and recruiting processing factors) [120], [209], [529]–[535]. Excitingly, the implication of TFs in splicing might represent a feature shared by several TF families [536]. Likewise, multiple TFs have now been reported to also directly impact more remote post-transcriptional processes, including mRNA decay [120], [487], [537]–[539] and translation [540], [541], in addition to their canonical function in transcription regulation. The implication of TFs in the control of mRNA decay is further discussed below.

As TFs are well-known to bind to gene promoters, they have historically been suggested to underline the phenomenon of promoter-mediated mRNA decay discovered in yeast (see 2.6.5.1a)). Based on a few emblematic examples, two models were proposed: (i) TFs are directly imprinted onto nascent mRNAs, or (ii) they regulate the imprinting of another protein without leaving the promoter region [497], [521], [524].

In human, the implication of TFs in the control of mRNA stability is more recent. In the literature, a dozen studies can be found on this topic, definitely confirming that this aspect is not a yeast-specific curiosity. An overview of several interesting and emblematic examples is shown in **Table 3**. Remarkably, TFs from several families appear to be implicated, suggesting that the control of mRNA stability by TFs might represent a widespread feature, as for their control of splicing. As summarized in **Table 3**, the biological context is diverse and mainly related to aspects of normal cell physiology, such as stem cell differentiation, adipogenesis, immunity, cell cycle progression, B lymphopoiesis and cortical neurogenesis. Also, the underlying mechanisms are various and more complex than anticipated from the studies in yeast. In particular, some TFs appear to increase mRNA stability (ZFP217, Sp1, WT1, YBX1, ARID5A, and E2F1), while others appear to rather decrease mRNA stability (SMAD2/3, GR, ERG, EBF1, KLF4, TP53, NRF2). Of note, the decrease of mRNA stability by a TF is hereafter also referred to as 'TF-mediated mRNA decay' (TFMD). More specifically, some TFs appear to control mRNA stability from the nucleus while others appear to shuttle to the cytoplasm to mediate their effects. Briefly, in the nucleus, they may act via less direct effects such as the regulation of mRNA processing (Sp1), or the deposition of regulatory modifications/trans-acting factors onto mRNAs (ZFP217, and SMAD2/3), sometimes through mechanisms that are reminiscent of mRNA imprinting. In the cytoplasm, they may act by directly recruiting degradation machineries onto specific mRNA subsets (GR, ERG, EBF1, and KLF4), or by masking regulatory cis-acting elements (WT1, YBX1, ARID5A, and TP53). Of note, in **Table 3**, the most emblematic examples of the implication of TFs in the control of mRNA decay are shown on a grey background. The last five examples (shown on a white background) may be regarded as less emblematic because either they are not (or not only) described as *bona fide* DNA-binding TFs (YBX1, and ARID5A), or the underlying mechanism remains unclear (TP53, NRF2, and E2F1).

Interestingly, some TFs appear to regulate common mRNAs via their dual function in transcription and the control of mRNA decay (SMAD2/3, ZFP217, Sp1, ERG, and EBF1) while others appear to mainly regulate distinct set of mRNAs (WT1). Consequently, the first category might represent new examples of coupling factors. Of note, for the other TFs, the question remains open as it is not directly addressed in the concerned studies.

In the laboratory of "Gene Expression and Cancer", we believe that TFs are today emerging as ideal moonlighting candidates (*i.e.*, molecular factors showing non-canonical functions), and thereby might represent master coordinators of the mRNA lifecycle from birth to death. Here are the main reasons. First, they are present from the beginning of gene expression, and are thus ideally positioned to early determine mRNA fates. Second, as described earlier, many post-transcriptional events occur co-transcriptionally and a number of TFs have already been evidenced to be directly involved in pre-mRNA processing steps, such as (alternative) splicing and APA [489], [530], [536]. Third, some TFs are known to shuttle between the nucleus and the cytoplasm [542], [543], suggesting that they might play a role in both cellular compartments. Fourth, TFs are known to be enriched with IDRs [544], [545], which make them susceptible to carry out multiple functions via binding to multiple protein partners [95]. Finally, although they lack any canonical RBD, TFs are increasingly reported to also bind to RNA either directly, presumably via their DBD or IDRs, or indirectly via binding to RBPs [120], [530], [546]. Altogether, these observations strongly suggest that the roles of TFs are not restricted to DNA-based processes.

Fundamentally, the moonlighting functions of TFs are challenging the molecular definition of a DNA-binding TF [120]. Functionally, they provide an additional layer of complexity to increase the efficiency, robustness, adaptability and precision of gene expression responses in cell [120]. In the future, it will be critical to determine whether TF-mediated control of mRNA stability represents a rare or rather general mechanism, and also contributes to disease development. This would be of paramount interest for clinical research given that TFs are both key drivers in diseases[30] [1], [269], [547] and complex therapeutic targets [268], [548].

---

[30] Among ~1,600 TFs estimated in the human genome [1], ~19% have been linked with diseases.

Table 3. Overview of human TFs involved in the control of mRNA stability. The effect on mRNA stability is shown: + = increased stability, − = decreased stability. Grey and white backgrounds indicate most and less emblematic cases, respectively. SMAD2/3 = SMAD family member 2/3, ZFP217 = zinc finger protein 217, Sp1 = specificity protein 1, GR = glucocorticoid receptor, GMD = glucocorticoid-mediated mRNA decay, ERG = ETS-related gene, EBF1 = early B-cell factor 2, KLF4 = Krüppel-like factor 4, SMD = Staufen-mediated mRNA decay, WT1 = Wilms' tumor 1, YBX1 = Y-box binding protein 1, ARID5A = AT-rich interactive domain 5A, TP53 = tumor protein 53, NRF2 = nuclear factor erythroid-2-related factor 2, E2F1 = E2F transcription factor 1, NA = not available, Ref. = reference.

Transcription factor	Family	Biological context	Mechanism	Effect on stability	Target mRNA transcripts	Date	Ref.
Control of mRNA stability from the nucleus							
SMAD2/3	SMAD	Stem cell pluripotency and differentiation	Direct recruitment of the m6A methylation complex upon TGFβ signaling	−	Pluripotency mRNAs such as *Nanog*	2018	[538]
ZFP217	C2H2 zinc Finger	Stem cell pluripotency and differentiation	Restriction of m6A deposition by sequestering METTL3 into an inactive complex	+	Yamanaka factors such as *Nanog*, *Sox2*, *Klf4* and *c-Myc*	2015	[549]
		Adipogenesis	Sequestration of the m6A reader YTHDF2 and activation of *FTO* gene transcription	+	*CCND1*	2019	[550]
Sp1	C2H2 zinc Finger	Breast cancer	Regulation of alternative polyadenylation	+	*YKT6, WDR7, PTPN21, ZNF184*	2022	[514]
Control of mRNA stability from the cytoplasm							
GR	Nuclear receptor	Chemotaxis of human monocytes	GMD via recruitment of PNRC2, UPF1 and DCP1A	−	*CCL2*	2015	[487]
		Immunity	GMD via recruitment of PNRC2, UPF1, YBX1 and HRSP12	−	Transcripts related to immune responses	2016	[488]
		Mechanotransduction	GMD via interaction with *LINC01569-YBX1* complex	−	*EGR1, CITED2, BMP7*	2021	[551]

Transcription factor	Family	Biological context	Mechanism	Effect on stability	Target mRNA transcripts	Date	Ref.
ERG	ETS	Cell cycle progression	Recruitment of the CCR4-NOT complex via CNOT2 and binding to mRNAs via RBPs such as RBPMS	−	186 mRNAs, among which 22 mitotic mRNAs like *AURKA/B*	2016	[120]
EBF1	EBF	B lymphopoiesis	Recruitment of the CCR4-NOT via CNOT3	−	Lineage-specific factors, such as *Heyl* and *Jag2*	2016	[537]
KLF4	C2H2 zinc finger	Cortical neurogenesis	SMD via interactions with STAU1, DDX5 and DDX17	−	*Dlx1/2* and *Tuj1*	2018	[539]
WT1	C2H2 zinc finger	Development	Binding to secondary structures in 3'UTRs	+	Developmental RNAs	2017	[543]
YBX1[31]	Y box	Pathogenesis of bladder cancer	Reading of m5C RNA modification and recruitment of HuR	+	Oncogenic mRNAs	2019	[417]
		Maternal-to-zygotic transition in zebrafish	Interaction with PABP	+	m^5C-modified maternal mRNAs	2019	[552]
	Y box	Mechanistic study in HeLa	Inhibition of decapping by binding to the mRNA cap	+	NA	2001	[553]
ARID5A[32]	ARID/BRIGHT	Immune regulation	Prevention of the binding of destabilizing RBPs	+	*IL-6, Stat3, Ox20, Tbx21, Cxcl1 and Cxcl5*	2020	[554]–[556]
TP53	TP53	Cancer cell lines	Binding to AREs, intrinsic exoribonuclease activity	−	*p53*	2020	[557]
NRF2	bZIP	Inflammation	Unclear	−	*TMEM173*	2018	[558]
E2F1	E2F	Wnt/beta-catenin signaling	Unclear	+	*Axin2*	2005	[559]

[31] YBX1 is described as both a DNA-binding TF and a multitasking RBP.
[32] ARID5A is not a *bona fide* DNA-binding TF but is rather described as both a transcriptional cofactor of TFs and a RBP. That said, ARID5A is able to bind to DNA.

2.6.5.2.   Post-transcriptional factors

Several post-transcriptional factors might also represent coupling factors between transcriptional and post-transcriptional processes, as well as between post-transcriptional processes. A few interesting examples are briefly discussed below. Unless otherwise clearly stated, they concern human cells.

a) RNA-binding proteins

A first example is provided by TARBP2, a nuclear RBP which has been shown to control the stability of its target transcripts by coordinating m6A modification, splicing and nuclear decay [560]. In addition, several RBPs largely described as splicing factors in the nucleus (*e.g.*, serine/arigine-rich proteins, FET-family proteins, RBPMS, and QKI) have been reported for their implication in post-splicing activities, including notably mRNA export, NMD, bulk mRNA decay and translation [75], [120], [561]–[565]. Also, several RBPs have been linked to transcription regulation by binding to chromatin [566], [567]. A last interesting case is the AREBP HuR, well-known for its role in mRNA stabilization, which has been described to also control pre-mRNA splicing of its target transcripts, suggesting that HuR couples pre-mRNA processing with cytoplasmic mRNA stability [568]. Except for TARBP2 and HuR, it remains unclear whether these RBPs are solely multitasking factors, or do represent real coupling factors.

b) Decay machineries

In yeast, several studies have reported that the decay factors Xrn1, Ccr4-not[33], Lsm-Pat1, and Dcp1/2 can bind to gene promoters and act as positive/negative transcriptional regulators [361], [512], [569]–[575]. In higher eukaryotes, CCR4-NOT has been linked to RNAPII-dependent transcription, splicing, mRNA transport and localization in addition to its well-described function in cytoplasmic mRNA decay, making a feedback loop that helps to maintain proper mRNA levels [361], [576]. Interestingly, Ccr4-Not also appears to couple translation and cytoplasmic mRNA decay in a manner that is dependent of codon optimality [350]. In addition, the CBCA components of the RNA exosome (see **Figure 37**) have been linked to transcription termination [577]. Together, these findings suggest that decay factors like CCR4-NOT might represent master coupling factors of eukaryotic gene expression [361].

---

[33] Molecular effectors that are capable of both stimulating or repressing mRNA synthesis and degradation, such as Rpb4/7, Ccr4-not and Xrn1, have sometimes been referred to as 'synthegradases' [711]. They are thought to be the molecular effectors of transcript buffering [498], [512].

3. Analysis of mRNA degradation

D etermining mRNA degradation rates is an important but not trivial task to fully portray gene expression dynamics in a given biological condition. Commonly, this is achieved indirectly by assessing steady-state mRNA levels, assuming that changes in mRNA abundance only reflect mRNA degradation. This represents however an oversimplification of the reality. In cells, mRNA levels are indeed determined by a complex interplay between transcription, processing and degradation, which may be fortuitously altered across experimental conditions. To address this issue, several experimental and computational methods have been developed to enable more direct measurements. In this chapter, after a mathematical description of mRNA dynamics, I will discuss these methods and highlight recent advancements.

3.1. Mathematical models of mRNA dynamics

In eukaryotic cells, total RNA levels (*i.e.*, pre-mRNA and mRNA levels) are defined from the complex interplay between mRNA synthesis, processing and degradation. In this model, pre-mRNAs are produced at a given synthesis rate and transformed into mRNAs at a given processing rate. mRNAs are finally destructed at a given decay rate (**Figure 53**).

Synthesis (k_1)   Processing (k_2)   Decay (k_3)

pre-mRNA (P)   mRNA (M)

Total RNA (T) = P + M
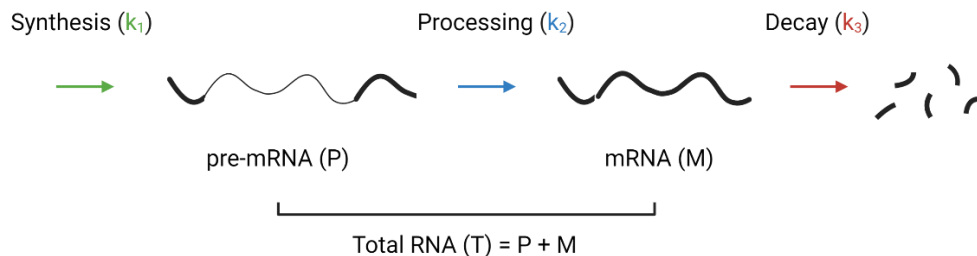
Figure 53. Schematic representation of the RNA lifecycle kinetics. See main text for details. Modified from [578]. Created with BioRender.com.

Typically, this model is described as a system of ordinary differential equations (ODEs) [579]. In time-course situations, the variations in pre-mRNAs and mRNAs abundance over time are given by:

$$\frac{dP}{dt} = k_1(t) - k_2(t).P \tag{3.1}$$

$$\frac{dM}{dt} = k_2(t).P - k_3(t).M \tag{3.2}$$

where P is the pre-mRNA abundance, M is the mRNA abundance, k_1 is the synthesis rate constant, k_2 is the processing rate constant, k_3 is the decay rate constant and t is the time. The minus symbol indicates that the specific RNA populations are being consumed. Importantly, pre-mRNA degradation is here neglected, which implies that the full population of pre-mRNAs is, sooner or later, processed into mRNAs. This represents obviously a simplification given that transcriptional

and processing machineries are susceptive to produce aberrant pre-mRNAs which are cleared by nuclear mRNA surveillance pathways.

At steady-state, the solutions of the ODEs system are:

$$\frac{dP}{dt} = 0 \quad \frac{dM}{dt} = 0 \tag{3.3}$$

$$P = \frac{k_1}{k_2} \quad M = \frac{k_2}{k_3} \quad \frac{P}{M} = \frac{k_3}{k_2} \tag{3.4}$$

These considerations mean that RNA dynamics, and in particular mRNA decay, can appropriately be derived from either M and k_1, or from P, M and k_2. Experimentally, P and T can be easily evaluated by qPCR using primers that match exon-intron junctions or exons, respectively. M can then be derived because M = T – P. Alternatively, P and T can be evaluated by northern blotting using adequate probes or by RNA-seq. By contrast, the assessment of the synthesis and processing rates is a complex task that has become feasible only recently owing to developments in deep-sequencing technologies. Therefore, measurement of mRNA decay rate after transcription inhibition has historically been used as a proxy to estimate RNA dynamics. Of note, assuming that pre-mRNAs are swiftly processed into mRNAs, P is negligible compared to T and M = ~T. In this context, mRNA decay rate is represented by the mRNA half-life (HL), defined as the time required to degrade 50% of the initial mRNA amount. To determine the mRNA HL, the decay rate constant needs first to be computed. This is usually achieved by modeling mRNA decay as first-order kinetics. Assuming that transcription inhibition is ideal, the previous system of ODEs is now described by the following equation:

$$\frac{dM}{dt} = -k_3(t).M \tag{3.5}$$

This relationship leads to the derivation of the equation:

$$\ln\left(\frac{M}{M_0}\right) = -k_3.t \tag{3.6}$$

which is equivalent to:

$$M = M_0.e^{-k_3 t} \tag{3.7}$$

where M_0 is the initial mRNA abundance, *i.e.*, before decay starts.

At half-life ($t_{1/2}$), M/M$_0$ = 1/2, which leads to the following equation:

$$ln\left(\frac{1}{2}\right) = -k_3.t_{1/2} \tag{3.8}$$

from where:

$$t_{1/2} = \frac{ln2}{k_3} \tag{3.9}$$

This means that the HL of an mRNA is inversely proportional to its decay rate constant.

In a typical time-course experiment, determining mRNA HL starts with the analysis of several RNA samples collected over time in order to monitor the decrease in mRNA abundance compared to an internal control (*e.g.*, spike-ins, stable housekeeping mRNAs). Next, normalized mRNA levels are plotted versus time in a convenient software (*e.g.*, GraphPad Prism) and data are fitted using a least-square nonlinear (first-order) regression. The decay rate constant is computed from the slope of a semilogarithmic plot of normalized mRNA levels as a function of time. Finally, the HL is obtained with equation (3.9).

In above equations, we implicitly assumed that the mRNA is completely degraded at infinite times, which is often not the case in biological systems. Instead, mRNA levels can reach a limit value (V) also known as 'plateau' at infinite times (**Figure 54**). In this situation, the equation (3.7) becomes:

$$M = (M_0 - V).e^{-k_3 t} + V \qquad\qquad (3.10)$$

If V = 0, this relationship gives back to the equation (3.7). Of note, the span is sometimes used to describe the difference between M_0 and V.
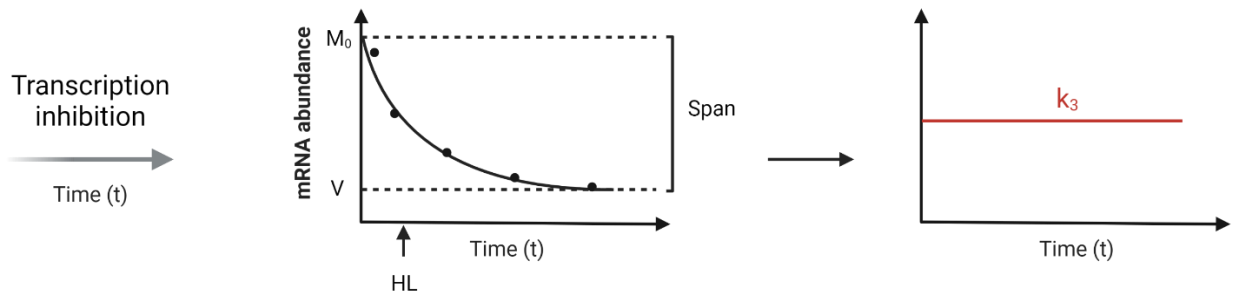
Figure 54. First-order mRNA decay kinetics. See main text for details. Modified from [578]. Created with BioRender.com.

For a given cell context, HL can substantially vary between individual mRNA transcripts owing to variabilities related to cis-acting elements, trans-acting factors and cellular cues. Recently, mRNA decay rates have been reported to span a 1,000-fold order of magnitude [580]. mRNA HL also appear to vary between species. In yeast, they can range from minutes to hours while, in humans, they can range from hours to days. This is partly linked to the cell doubling time. Typically, human mRNAs are considered to be stable when their HL >4 h and unstable when their HL <4 h [581].

3.2. Methods for measuring mRNA half-life

Over the years, several methods have been reported to monitor mRNA decay. They are presented below along with their main advantages and drawbacks. This includes classical time-course experiments, total RNA-seq, nascent RNA profiling, mRNA poly(A) tail sequencing and single-cell/molecule methods.

3.2.1. Classical time-course experiments

Classical time-course experiments are typically characterized by the collection of RNA samples at time intervals after an initial experimental manipulation (*e.g.*, transcription inhibition, RNA metabolic labeling). Following this, the levels of the mRNAs of interest are evaluated over time to calculate decay rates by assuming first-order kinetics. Generally, mRNA levels are monitored using either RT-qPCR, northern blotting or RNA-seq for transcriptome-wide analyses. A typical pipeline to analyze mRNA HL using RNA-seq is presented below.
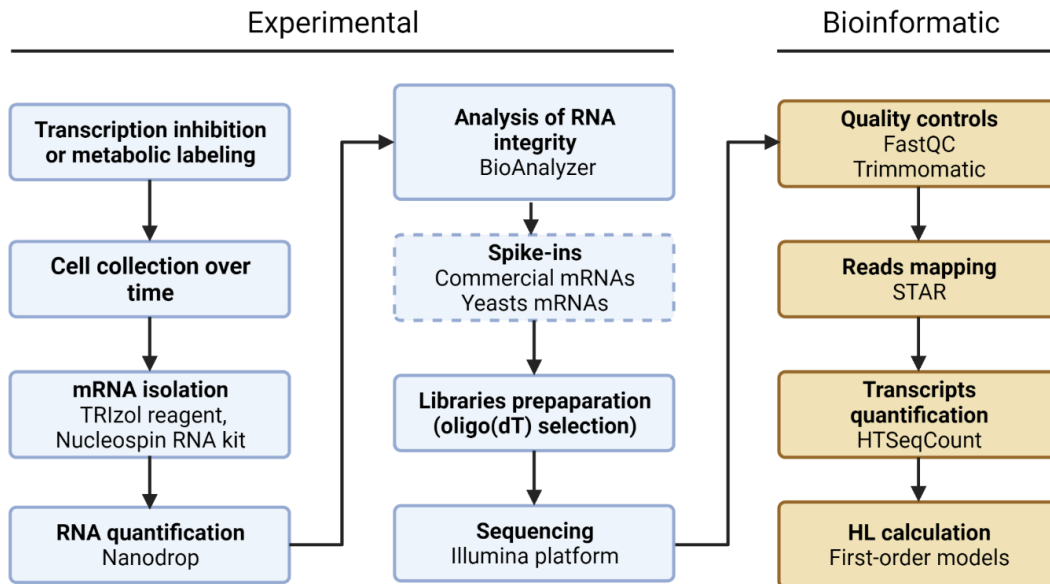
Figure 55. Typical RNA-seq-based pipeline to analyze mRNA HL. Dashed border indicates facultative step. Created with BioRender.com.

Depending on the initial experimental manipulation, three types of approaches can be further delineated, including general transcription inhibition, transcriptional pulsing and metabolic labeling.

3.2.1.1. General transcription inhibition

A first and straightforward approach to analyze mRNA decay rates relies on transcriptional blockage (also known as transcriptional shut-off) using chemical inhibitors, such as Actinomycin D (ActD) or α-amanitin. Among them, usage of ActD is common [120], [537]–[539], [582], [583]. It interferes with all RNA polymerases by intercalating into DNA. In a typical experimental set-up, cells are treated with 5-10 µg/ml of ActD before being collected at time intervals (maximum 24h) for mRNA extraction [584]–[586].

The main advantage of transcription inhibition is its ease of use and cost-effectiveness. Moreover, it is amenable to transcriptome-wide analysis [585]. Nevertheless, this approach suffers from several drawbacks. First, transcription inhibition represents a stress for cells which might

profoundly affect cell physiology. Sometimes, it leads to severe cytotoxicity, thereby limiting its application [584], [585]. Moreover, the above drugs have been shown to not completely block transcription, to alter the stability and the localization of many mRNAs [587]–[591] or to have pleiotropic effects (*e.g.*, ActD can also affects translation). Consequently, HL obtained with this method might diverge from unperturbed decay rates. Despite these caveats, transcription inhibition remains a widely-used approach [584], [585].

3.2.1.2.   Transcriptional pulsing

A second approach is transcriptional pulsing. It relies on the use of an inducible promoter to specifically promote transient transcription. Because transcription inhibitors are not required here, this ensures that mRNA decay is analyzed under physiologically unperturbed conditions. In a typical experiment set-up, an exogenous and inducible gene construction is primarily introduced into cells using transfection or transduction. Alternatively, a cell line can be engineered using gene-editing tools to replace the existing promoter of a specific endogenous gene by a designed inducible promoter. Next, a stimulus is provided to activate transcription, leading to a burst of mRNA synthesis. Within a narrow window of time, the stimulus is removed, leading to silencing of transcription [584]. Several systems have been described to offer a reliable and simple way to achieve a transient burst of transcription in mammalian cells. A well-known example is the Tet-On/Off regulatory promoter system [592].

The main advantage of transcriptional pulsing is that it circumvents the issues related to the use of transcriptional inhibitors [584]. However, it is not amenable to transcriptome-wide analysis [592] and priorily relies on the construction of a gene inducible cassette or an inducible cell line, which can represent time-consuming steps.

3.2.1.3.   RNA metabolic labeling

When analyzing mRNA stability via RNA metabolic labeling, a nucleoside analogue (often 4-thiouridine, 4SU) is added to cells and incorporated into newly transcribed mRNAs. Often, the incorporated analogue is chemically modified *in vitro* via biotinylation and labeled mRNAs are next selected by affinity purification using streptavidin beads. The labeled mRNAs are finally quantified by RT-qPCR or RNA-seq to estimate mRNA stability [592].

Metabolic labeling experiments can be broadly divided into three classes: pulse-chase, approach-to-equilibrium and other, more complex methods. Pulse-chase experiments are the most frequent. They are analogous to transcriptional pulsing in that following the pulse of the labeled nucleotide, the disappearance of the labeled RNA population is then monitored during the chase phase (**Figure 56**) [592]. Of note, RNA metabolic labeling is often involved in more sophisticated strategies, such as nascent RNA profiling (see later).

The main advantage of metabolic labeling is that it circumvents the issues related to the use of transcriptional inhibitors while being amenable to transcriptome-wide analysis. However, this

method has also its own caveats, such as bias in labeling efficiency across different RNA populations [592].
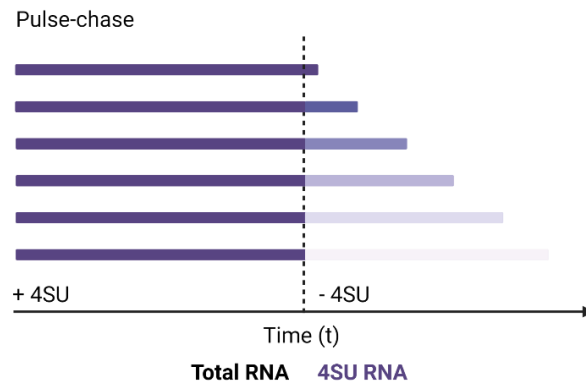
Figure 56. Typical pulse-chase metabolic labeling experiment. Modified from [585]. Created with BioRender.com.

3.2.2. Total RNA-seq

Capturing all three RNA kinetic rates based on pre-mRNA and mRNA expression at steady-states is not trivial, because three parameters are unknown and only two equations are available (see equations 3.4). A way to solve this is to either make assumptions about the RNA processing rates or to have time-course data [579]. Based on this, total RNA-seq-based approaches have been developed to infer mRNA decay rates.

Total RNA-seq experiments generate mainly exonic reads but also ~10% of intronic reads [593]. Intronic reads can serve to estimate intronic expression [594], which in turn is used as a proxy for synthesis rates. Then, mRNA decay rates can be derived from:

$$k_3 = \frac{k_1}{M} \tag{3.11}$$

In this context, RNA processing is assumed to be negligible or to occur at a constant rate. Several computational approaches have been reported, including for example exon-intron split analysis (EISA) [595], Rembrandts [596] and Snapshot-seq [597]. Alternatively, synthesis rates can be estimated from specific histone marks [598]. An approach based on time-course RNA-seq datasets has also been proposed [599].

Recently, a novel approach also based on time-course RNA-seq, namely INSPEcT-, has been developed. By contrast with other approaches, it enables the determination of all RNA kinetics rate by solving the system of ODEs at steady-state (see equations 3.4) [594], [600].

Because these approaches only need total RNA-seq data, they have the main advantage to be straightforward in their application. Moreover, they allow retrospective analysis of the numerous datasets archived in publicly-available repositories [585]. For example, INSPEcT- has been successfully used to retrospectively disentangle the transcriptional and post-transcriptional

influence of the MYC TF during B-cell activation [601]. Another important point is that executable codes have been released for several of these approaches. They are available as Bioconductor packages such as eisaR and INSPEcT. The main drawback of these methods is that, except for INSPEcT-, the contribution of RNA processing is not taken into account [579].

3.2.3.   Nascent RNA profiling

Nascent RNA profiling represents a recent advancement in the field of RNA dynamics. Compared to previous approaches, it provides a more direct measurement of RNA synthesis rates, thus facilitating the capture of processing and degradation rates. Multiple approaches have been described whether they rely on the isolation of chromatin-associated RNAs [602], the isolation of RNAPII-associated RNAs or metabolic labeling (**Figure 57**) [579].
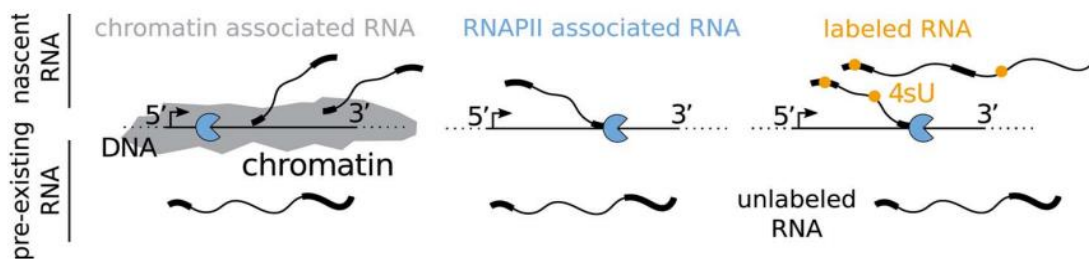
Figure 57. Three main classes of nascent RNA profiling. See main text for details. Modified from [578].

Global run-on sequencing (GRO-seq) and precision run-on sequencing (PRO-seq) are commonly-used methods that belong to the second class of nascent RNA profiling. When combined with total RNA-seq, they can be used to evaluate mRNA decay rates (reviewed in [603], [604]).

To profile nascent RNA via metabolic labeling, a number of computational tools have been reported. Although an in-depth description of these tools is beyond the scope of this work, an overview is available in **Table 4**. This table also gathers approaches that I discussed previously or will discuss later in this chapter. Interested readers can use it as a springboard for further information. Additional useful information can be found by referring to [540]. Complementing this, the experimental design, computational framework, output and corresponding computational tool for some of these approaches are presented in **Figure 58**. Of note, much more methods and tools are available in the literature. The ones described here only represent the tip of the iceberg. Importantly, all these methods and tools have obviously their own forces and limitations and might not apply to all context. Case-by-case analysis after referring to related articles is thus encouraged. The main advantage of all these methods is that they provide more accurate quantifications of RNA dynamics. However, this is at the cost of more elaborated and thus complex experimental and computational design.

Table 4. Overview of the methods currently available to evaluate transcriptome-wide mRNA decay rates. k_1 = synthesis rate constant, k_2 = processing rate constant, k_3 = decay rate constant. Modified from [578].

Experimental framework	Method	Info on k3	Limitations	Software	Ref.
Total RNA	Transcription inhibition	+	Disrupts normal cell physiology, neglects RNA processing, requires time-course data	-	[582]
	EISA	+	Neglects RNA processing	+	[595]
	Rembrandts	+	Assumes k2 is constant	+	[596]
	Snapshot-seq	+	Assumes k1 is ~constant	-	[597]
	Zeisel et al. (time-course)	+	Requires an independent characterization of k2	-	[599]
	Wang et al. (histone marks)	+	No info on k2	-	[598]
	INSPEcT- (time-course)	+	Requires time-course RNA-seq data	+	[594]
Nascent RNA	Chromatin-associated RNA	-	No info on k2 and k3 unless being combined with total RNA-seq	-	[602]
	GRO-seq	-		-	[603]
	PRO-seq	-		-	[604]
RNA metabolic labeling	DTA	+	No info on k2	+	[605]
	cDTA	+	No info on k2	+	[606]
	pulseR	+	No info on k2	+	[607]
	DRUID	+	No info on k1 and k2, laborious	+	[585]
	DRILL	+	Requires time-course RNA-seq data	+	[608]
	INSPEcT+	+	-	+	[609]
	Dyrec-seq	+	No info on k2, laborious	-	[610]

Experimental framework		Method	Info on k3	Limitations	Software	Ref.
		SLAM-DUNK	+	No info on k1 and k2	+	[611]
		GRAND-SLAM	+	No info on k1 and k2	+	[612]
Single-cell	Total RNA	RNA Velocity	~	No info on k3 at single-cell resolution, assumes k2 is constant	+	[613]
		scVelo	~	No info on k2 and k3 at single-cell resolution	+	[614]
	Metabolic labeling	NASC-seq	-	No info on k2 and k3	+	[615]
		Sci-fate	~	No info on k3 at single-cell resolution, no info on k2	+	[616]
		scSLAM-seq	-	No info on k2 and k3	-	[617]
		scEU-seq	~	No info on k1 and k3 at single-cell resolution, no info on k2	-	[618]
Single-molecule		nano-ID	+	No info on k2	+	[619]
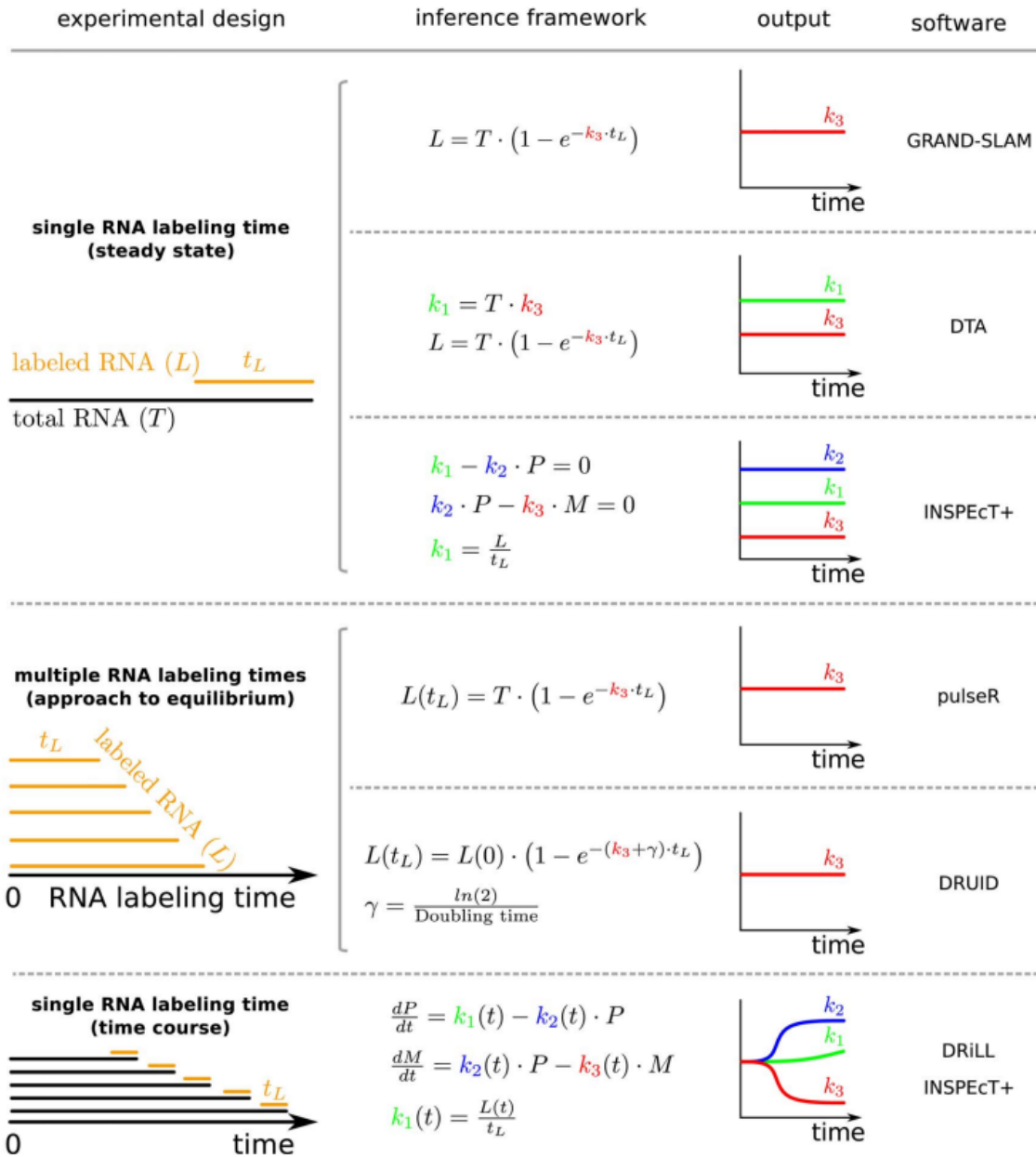
Figure 58. Summary of nascent RNA profiling methods. T = total RNA abundance, P = pre-mRNA abundance, M = mRNA abundance, k_1 = synthesis rate constant, k_2 = processing rate constant, k_3 = decay rate constant, L = amount of labeled RNA, t_L = time of labeling. Modified from [578].

3.2.4. Single-cell/molecule mRNA decay

In this era of single-cell transcriptomics, a number of experimental and computational approaches have unsurprisingly been developed to monitor mRNA decay at the single-cell level. This includes for example, RNA Velocity [613], [620], scVelo [614], NASC-seq [615], Sci-fate [616], scSLAM-seq [617], and scEU-seq [618]. Again, these methods allow to more accurately snapshot the biological complexity. However, they are less simple to implement and require a certain expertise.

Recent improvements also include single-molecule approaches. For example, nanopore sequencing-based isoform dynamics (nano-ID) has been developed to study the metabolism of RNA isoforms at the single-molecule level [619]. Another approach is 3'-RNA end accumulation during turnover (TREAT). It is based on imaging rather than sequencing. It allows to capture single-mRNA degradation dynamics in single fixed cells [621].

3.2.5. mRNA poly(A) tail sequencing

When using first-order models, mRNA degradation is implicitly depicted as a uniform process during which each individual mRNA is degraded at a constant rate over time. Although this appears to verify in prokaryotes, the reality is more complex in eukaryotes because mRNA decay generally occurs in a step-wise manner (**Figure 59**). As described previously, it is initiated by a deadenylation step during which the mRNA body remains intact. When the poly(A) tail reach a certain limit length, the mRNA is further degraded via exonucleolytic pathways. Because these two steps occur at their own rate[34], mRNA HL cannot appropriately be evaluated using merely first-order models.
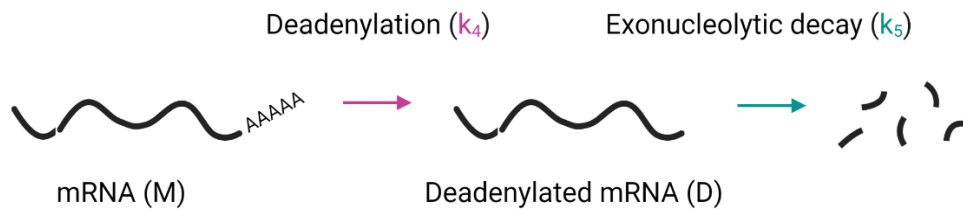
Figure 59. Step-wise mRNA decay in eukaryotic cells. See main text for details. Created with BioRender.com.

$$\frac{dD}{dt} = k_4(t).M - k_5(t).D \qquad (3.12)$$

This caveat fostered the emergence of novel methods to accurately monitor deadenylation rates. As mentioned in the previous chapter, mRNA decay rates are generally shaped by deadenylation rates. Interestingly, several advents into the sequencing of the mRNA poly(A) tail has recently evidenced that tail length is well correlated to mRNA levels and can be used to infer deadenylation dynamics [580]. Methods to measure poly(A) tail comprise either targeted methods [622], or transcriptome-wide methods, such as TAIL-seq [338], mTAIL-seq [623], FLAM-seq [339], and Nanopore sequencing-based approaches [624].

---

[34] mRNA body decay obeys first-order kinetics while deadenylation does not [584].

SECTION II   AIM

Gene fusions represent an important class of somatic alterations in cancer. In many cases, they encode pathognomonic fusion proteins with neomorphic properties and acting as potent oncogenic drivers. Typically, fusion proteins in cancers involve either kinases or TFs. In essence, oncogenic fusions are ideal drug targets which could make fusion-harboring cancers uniquely susceptive to precision oncology. However, contrary to fusion kinases, targeted therapy for fusion TFs remains actually highly challenging in practice. An important limiting factor is our partial understanding of the molecular mechanisms underlying the oncogenic activity of fusion TFs. Very interestingly, several non-fusion TFs have recently been reported to control mRNA decay via direct mechanisms (*e.g.*, by binding to mRNA and by recruiting decay factors) in human. Before starting this work, we hypothesized that the control of mRNA decay might also be a molecular feature of fusion TFs, which would thereby represent an important finding for three main reasons. First, this would enlarge the catalogue of TFs that can impact mRNA decay and would extend the contribution of these non-canonical functions to disease development. Second, by providing a more comprehensive portrait of the molecular functions of fusion TFs, this might potentially offer new promising options for targeted therapy of fusion TFs-driven cancers. Third, it would further evidence the importance of mRNA decay in oncogenesis, an aspect which, in contrast to transcription, has remained largely overlooked to date.

In this perspective, the general aim of this work was to study the contribution of mRNA decay to the oncogenic properties of FET::ETS fusion TFs, an important family of fusions acting as drivers in several sarcomas and leukemias. We reasoned that EwS might represent an attractive model for a proof-of-concept study. EwS is an aggressive childhood cancer driven by a fusion TF named EF that is emblematic of the other FET::ETS fusions. EF has, so far, mainly been studied for its aberrant role in transcription but a role in alternative splicing has also been reported, thus supporting the idea that post-transcriptional processes might also contribute to gene expression deregulation in EwS. Supporting this possibility, RBPs were found to be strongly enriched in a published interactome of EF. In addition, an important fraction of EF interactors (~10%) are known to regulate mRNA stability (**Figure 23**). On this basis, the first aim of this work was to examine whether EF was able to control mRNA stability at the transcriptome-wide level. To address this, we performed an ActD-based transcriptional shutoff experiment followed by RNA-seq in an EwS cell line in the presence/absence of EF. This experiment strengthened our assumption that EF might play a new function in mRNA decay. Next, we aimed at characterizing the molecular determinants of this new function, for instance by testing interactions between EF and decay machineries, by using mRNA tethering degradation assays and by performing motif enrichment analyses on the 3'UTR regions of EF decay targets. This work enabled us to design a decay mutant of EF. Finally, we pursued to assess the biological and clinical importance of our findings by comparing the oncogenic potential between EF and its decay mutant using several functional assays (*e.g.*, viability, spheroid growth and colony formation assays).

SECTION III   RESULTS

1. EF imposes an aberrant mRNA stability landscape in EwS

To interrogate a potential role for EF in the control of mRNA decay, we analyzed transcriptome-wide changes in RNA stability in EwS cells in the presence and absence of EF. To this aim, we used shA673-1c EwS cells, which contain a doxycycline-inducible shRNA targeting EF [236]. We prepared three independent series of RNA samples at 0, 1, 2 and 4h after transcription blockage with Actinomycin D (ActD) from cells treated or not with doxycycline (dox). We then assessed and compared the evolution of the steady-state levels of individual poly(A) RNAs over time by RNA-seq in EF-expressing and knocked-down (KD) cells (**Figure 60a**). EF knockdown was confirmed by i) western blotting analysis (**Figure 60b**), and ii) increased cell size following treatment with dox as previously described [236] (**Figure 60c**). Principal component analysis (PCA) of RNA-seq libraries showed the expected clustering among samples (**Figure 60d**).

Assuming first-order decay kinetics, we calculated half-lives (HLs) for 7,170 individual poly(A) RNA transcripts (including >99% of mRNAs, thus hereafter called "mRNAs") in dox-untreated (–dox) and dox-treated conditions (+dox). Next, we calculated a HL ratio for each transcript by dividing the HL in KD cells with that in EF-expressing cells and we associated a p-value to each HL ratio (see the 'Materials & Methods' section). Strikingly, we identified 772 individual mRNAs that were significantly stabilized ($\log_2$ HL ratio >0, p-value <0.05, two-sided Fischer's t-test) in the absence of EF, while only 26 were destabilized ($\log_2$ HL ratio <0, p-value <0.05, two-sided Fischer's t-test) (**Figure 61**). Gene ontology (GO) analysis of the 772 stabilized mRNAs after EF KD revealed enrichment in genes involved notably in pre-mRNA splicing, DNA damage response and cell division (**Figure 62**), supporting the idea that the remodeling of the mRNA stability landscape by EF might allow its control of functionally connected mRNA regulons. In contrast, no specific GO term was statistically enriched when analyzing mRNAs that were destabilized after EF knockdown.

To cross-validate these observations, we randomly selected a panel of 10 mRNA transcripts (hereafter called "decay targets panel") among the mRNA that were destabilized by EF (*i.e.*, mRNA whose stability was increased following EF KD) (**Figure 63a**). We then measured the HL of each of these mRNAs by RT-qPCR in two EwS cell lines (shA673-1c and shSK-E17T) before and after EF knockdown, as well as in bone-marrow derived human mesenchymal stem cells (hMSCs) before and after ectopic expression of EF. For each EwS cell line, we calculated the HL ratio as described above (HL in the EF KD cells/HL in the control EF-expressing cells). For MSCs, we computed the HL ratio by dividing the HL in the presence of EF by that in the absence of EF. Knockdown of EF in shA673-1c and shSK-E17T, and expression of EF in hMSCs were verified by western blotting analysis (**Figure 63b**) and shift in cell morphology as previously described [625] (**Figure 63c**). In agreement with our RNA-seq analysis, the mRNAs were all stabilized following EF KD in both EwS cell lines (**Figure 63d**). In contrast, these transcripts were all destabilized following expression of EF in MSCs. Altogether, these findings suggest that the control of mRNA stability might represent

a novel molecular function for the EwS TF EF. The observation that approximately 30 times more mRNA showed increased HL following EF KD pointed towards a mRNA destabilizing role for EF.

a
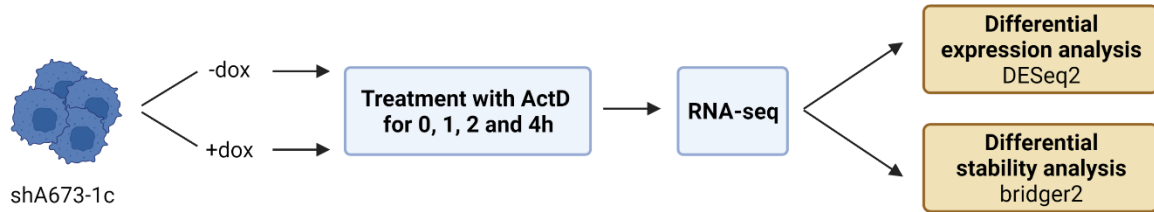
b
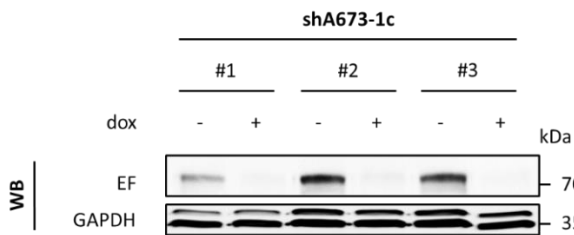
c
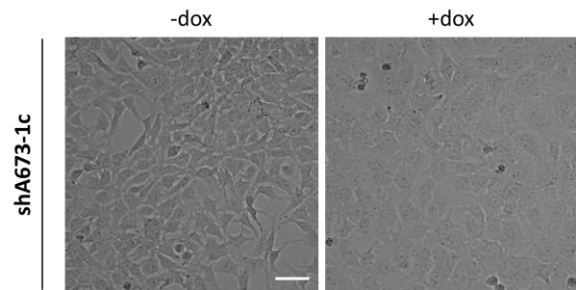
d
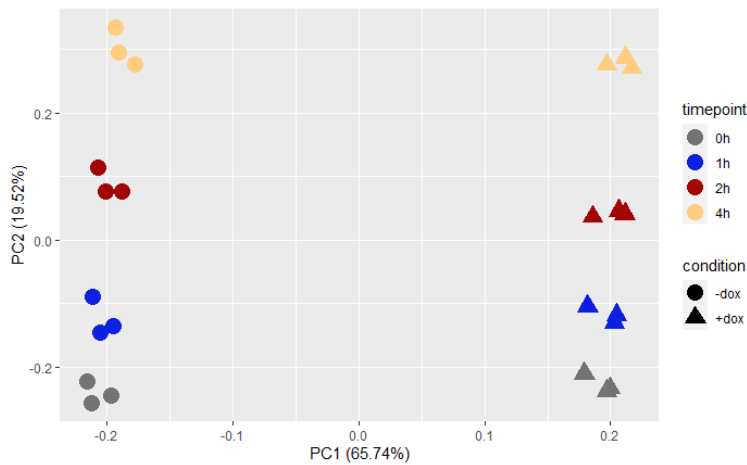
Figure 60. **Design and quality controls of the ActD RNA-seq experiments in shA673-1c -/+ dox cells.** (**a**) Overview of the experimental design for the analysis of abundance and stability changes upon EF knockdown in shA673-1c cells (n = 3 independent experiments). (**b**) Western blotting analysis of endogenous EF and GAPDH (loading control) in the three replicates used for the RNA-seq experiment. Samples are total cell lysates from shA673-1c -/+ dox cells. (**c**) Representative photographs (zoom 10x) of shA673-1c -/+ dox cells. Scale bar = 50 µm. (**d**) Principal component analysis (PCA) of RNA-seq libraries from shA673-1c -/+ dox cells (n = 3 independent experiments). Samples are segregated by condition and by time after treatment with ActD in principal component 1 (PC1) and 2 (PC2), respectively.
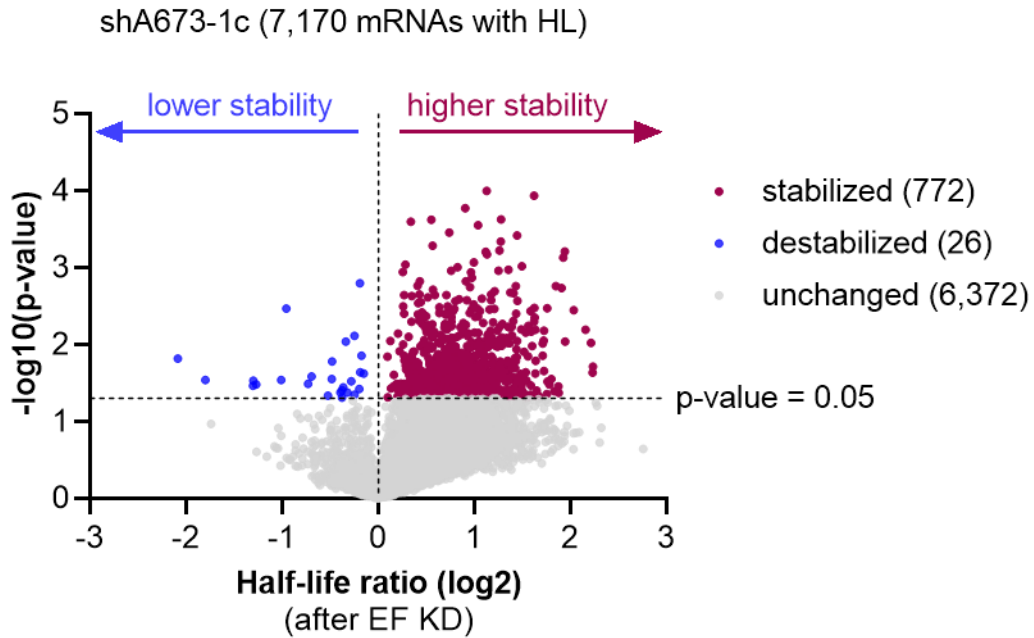
Figure 61. Transcriptome-wide changes in mRNA stability after EF knockdown. Volcano plot of significantly stabilized mRNA transcripts (red) and destabilized mRNA transcripts (blue) following EF knockdown (KD) in shA673-1c cells (n = 3 independent experiments, HL ratio >1, p-value <0.05). mRNAs whose stability was not significantly affected are in gray. mRNA numbers are indicated within brackets. Horizontal dotted line (in black) is drawn at p-value = 0.05. HL = half-life.
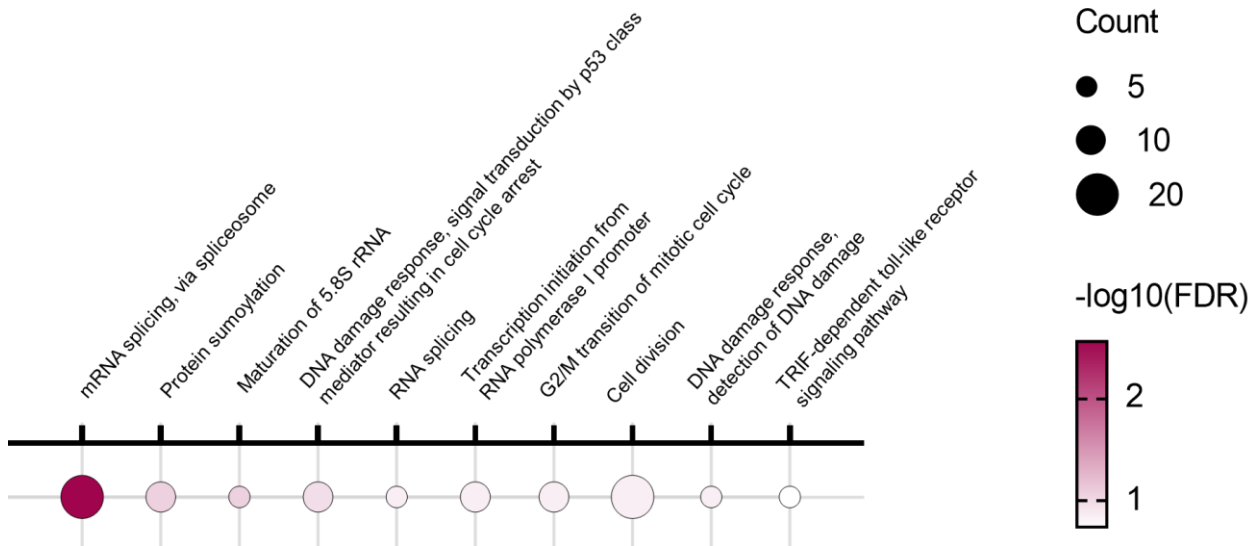
Figure 62. Gene ontology analysis of stabilized mRNAs after EF knockdown with DAVID. Enrichment of Gene Ontology (GO) Biological Process terms in genes with significantly increased stability upon EF knockdown in shA673-1c cells (FDR <0.2, gene count >5). GO terms are ranked by increasing order of FDR. Points are scaled by number of genes and are ranked according to colored p-values. Enrichment analysis was performed with DAVID and p-values were calculated using FDR correction.
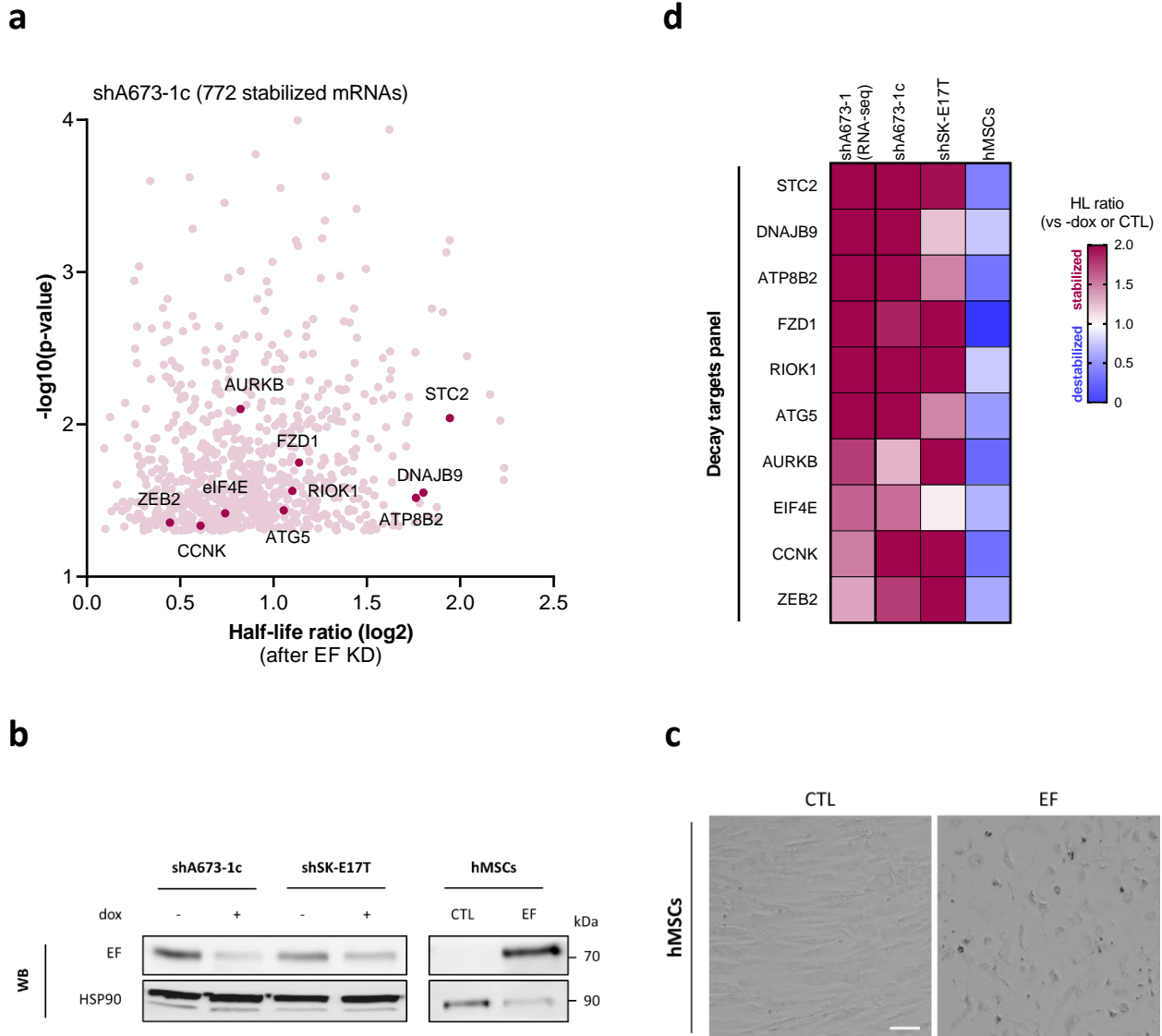
Figure 63. RT-qPCR stability analysis of the decay panel. (**a**) Log_2 half-life (HL) ratio of the selected EF decay targets (decay panel, black) among the stabilized mRNAs after EF knockdown in shA673-1c cells (grey). mRNA numbers are indicated within brackets. (**b**) Representative western blotting analysis of EF and HSP90 (loading control) in cells used for HL measurement by RT-qPCR analysis. Samples are total cell lysates from shA673-1c and shSK-E17T -/+ dox cells, and MSC CTL/EF cells. (**c**) Representative photographs (zoom 4x) of MSC CTL/EF cells. Scale bar = 50 μm. (**d**) Heatmap of half-life ratio detected by RNA-seq or by RT-qPCR after knockdown of EF in shA673-1c and shSK-E17T cells (+dox vs −dox); or expression of EF in MSC cells (EF vs CTL) for the mRNAs selected and indicated in (**a**). Results are shown as means (n = 3 and 4 independent experiments for RNA-seq and RT-qPCR, respectively). mRNAs are ranked by decreasing order of HL ratio as detected in the RNA-seq experiment.

Processing bodies (P-bodies, or PBs) are microscopic mRNA-protein complex (mRNP) aggregates that accumulate translationally repressed mRNAs and mRNA-decay associated factors such as decapping protein 1 A (DCP1A), enhancer of mRNA decapping 4 (EDC4) and subunits of the CCR4-NOT deadenylation complex [375]. Although the function of PBs remains debated, they are intimately linked to mRNA metabolism as recent evidence suggests that they contain mRNAs that are in equilibrium with polysomes and mRNA targeted for degradation [376]. For instance, blocking the 5'–3' mRNA degradation pathway leads to enlarged PBs [380], while treatment with translation inhibitors leads to their rapid disappearance [379]. To further support a role for EF in mRNA metabolism, we examined the formation of PBs in two EwS cell lines in the presence and absence of EF by staining for DCP1A and EDC4. Knockdown of EF correlated with a significant reduction in the number of PBs in EwS cells (**Figure 64**). In line with the idea that EF promotes mRNA degradation, this observation might indicate that a higher number of mRNA transcripts are targeted for degradation in the presence of EF.

a
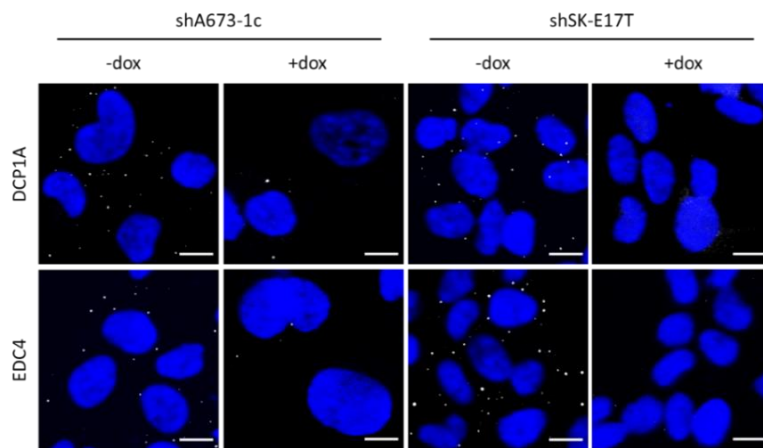
b
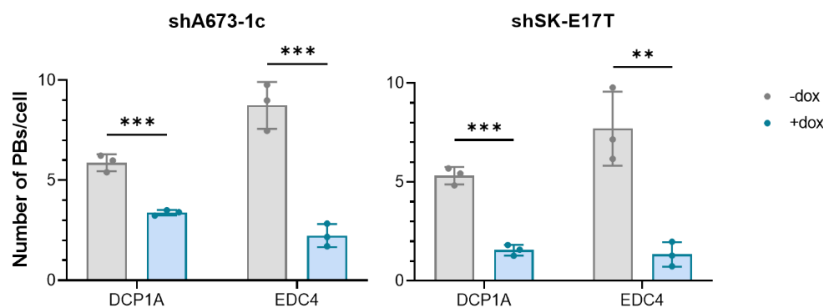
Figure 64. Analysis of P-bodies (PBs) upon EF knockdown in EwS cells. (**a**) Immunofluorescence of DCP1A and EDC4 (PBs markers, white) and DAPI (nuclear staining, blue) in shA673-1c and shSK-E17T -/+ dox cells. Scale bars = 10 μm. (**b**) Quantification of the number of PBs per cell from immunofluorescence described in **a**. Results are shown as mean ± SD (n = 3 independent experiments with >50 cells for each replicate). **p <0.01; ***p <0.001 compared to –dox by two-tailed unpaired Student's *t*-test.

EF is thought to act as an oncogenic TF that aberrantly controls the transcription of hundreds of genes contributing to EwS biology [155]. One possible explanation for the effects of EF on mRNA stability would be that EF regulates the expression of factors involved in mRNA degradation, although this would be difficult to reconcile with our observation that only specific mRNAs are stabilized by EF KD. To test this, we first identified genes whose expression levels are controlled by EF by performing a differential gene expression (DGE) analysis in shA673-1c -/+ dox (**Figure 60a**). We identified respectively 752 and 1,625 mRNAs that were significantly downregulated and upregulated after EF KD ($|log2FC| > 1$, padj <0.01, **Figure 65a**). As previously reported [155], downregulated genes (*i.e.*, genes that are activated by EF) were strongly enriched for GO terms related to cell division, cell proliferation and DNA replication while upregulated genes (*i.e.*, genes that are repressed by EF) were strongly enriched for GO terms linked to EMT-related processes, including cell adhesion, cell migration and differentiation (**Figure 65b-c**). In contrast, no GO term related to mRNA catabolism (*e.g.*, "regulation of mRNA stability", "mRNA catabolic process", "CCR4-NOT complex", "exosome (RNAse complex)", *etc.*) were significantly associated with the down- or upregulated genes.

Next, we compared the list of EF-regulated genes identified in our DGE analysis in shA673-1c -/+ dox (**Figure 65**) with a manually literature-curated list of 66 decay factors (decaysome, full list available in the 'Appendix' section). Out of this list, 61 were detected in our RNA-seq analysis, among which, only 7 exhibited significant changes following EF KD. More specifically, four factors were downregulated (*EXOSC5*, *MPP6*, *ZCCHC3* and *DCP2*) and three factors were upregulated (*ZFP36*, *ZFP36L1*, *ZFP36L2*) after EF KD (**Figure 66a**). All these modulated decay factors have a positive role in mRNA decay [326], [626]. Similarly, we compared the list of EF-regulated genes with a list of 371 high-confidence genes encoding PB constituents (PBome) collected from the RNP Granule Database [377]. Out of the 343 PB genes detected in the RNA-seq, only 16 genes were significantly upregulated after EF KD (**Figure 66b**). Importantly, the genetic perturbation of none of these 16 genes has been reported to affect PBs (http://rnagranuledb.lunenfeld.ca/). Additionally, we assessed the protein level of endogenous DCP1A and EDC4 in EF-depleted EwS cells and found that the protein levels of these two PBs markers are not affected by the presence of EF (**Figure 66c**). Taken together, these results suggest that the mRNA stabilization effects are very unlikely to be mediated by changes in the expression of decaysome or PBome factors. This conclusion led us to test the possibility that EF might play a direct role in the control of mRNA stability.

a
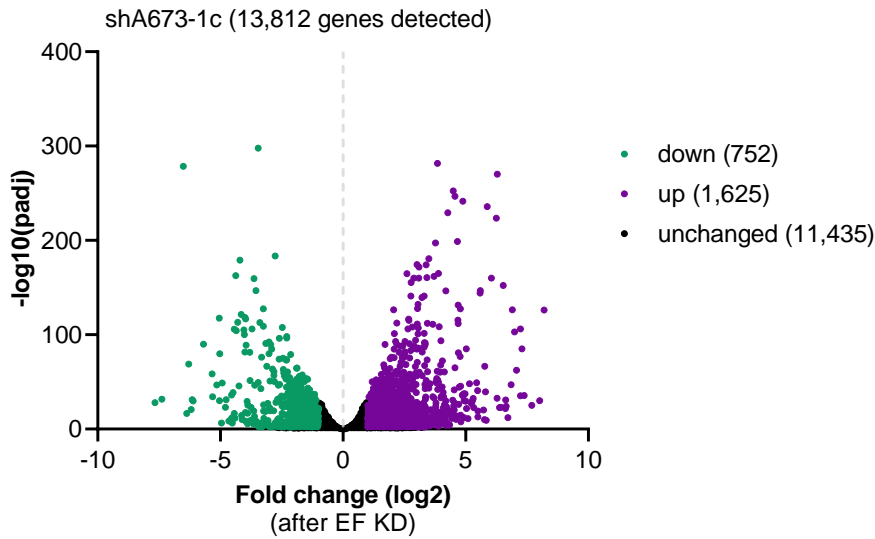
b
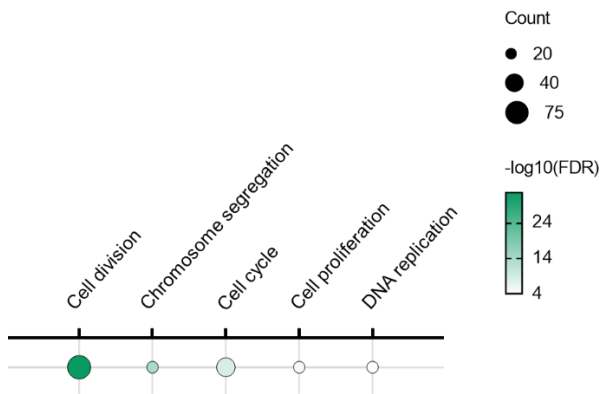
c
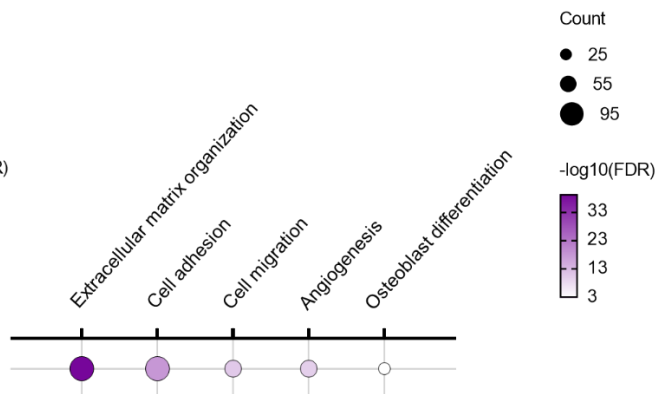
Figure 65. Differential gene expression analysis upon EF knockdown in shA673-1c cells. (**a**) Volcano plot of significantly downregulated genes (green) and upregulated genes (purple) upon EF knockdown (KD) in shA673-1c cells. Genes with unchanged expression are in black. Gene numbers are indicated within brackets. (**b-c**) Top-5 Gene Ontology (GO) Biological Process terms significantly enriched in genes downregulated (**b**) and upregulated (**c**) upon EF knockdown in shA673-1c cells (FDR <0.05). Points are scaled by number of genes and are ranked according to colored p-values. Enrichment analysis was performed with DAVID and p-values were calculated using FDR correction.

a
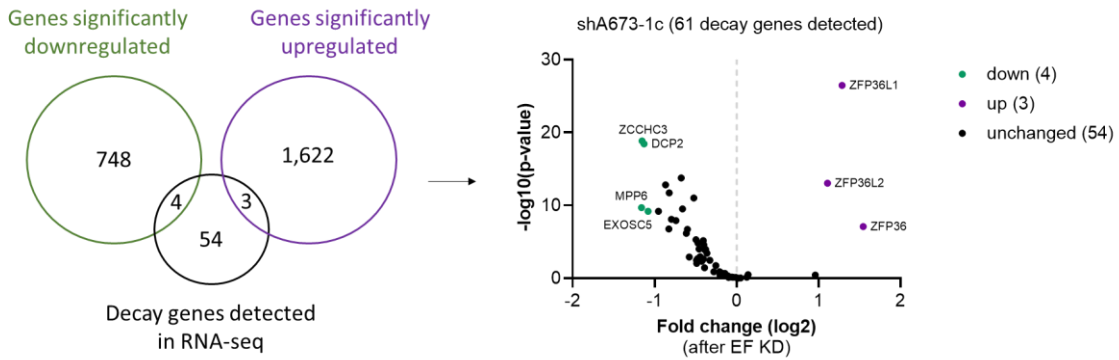
b
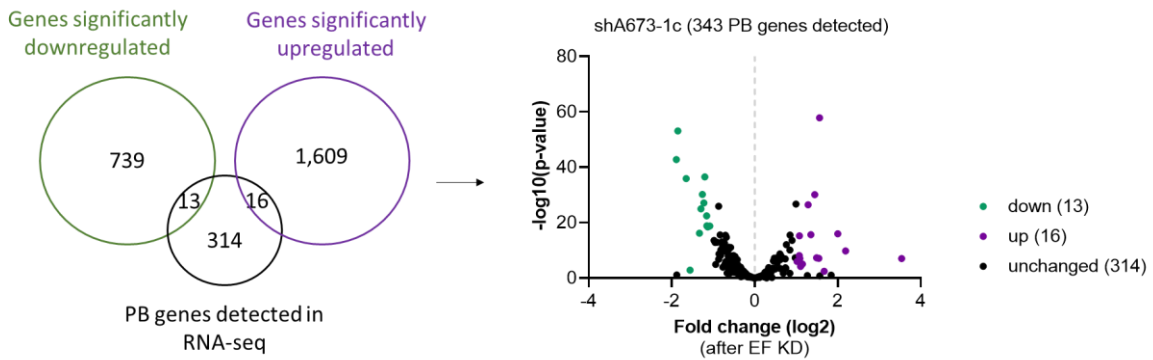
c
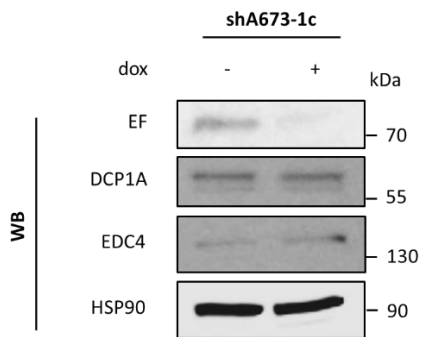
Figure 66. Comparison of the decaysome and the PBome with EF modulated targets. (**a**) Comparison of significantly downregulated genes and upregulated genes after EF knockdown (KD) in shA673-1c cells with genes encoding proteins involved in mRNA decay (decay genes) curated from literature (**b**) or with high-confidence genes encoding P-bodies proteins (PB genes) from the RNP Granule Database considering only tier 1. Log2FC of genes from the overlaps are shown on the right. Genes with padj <0.01 and |log2FC| >1) are colored. 61 out of the 66 initial decay genes and 343 out of the 371 initial PB genes were detected in the RNA-seq. (**c**) Western blotting analysis of endogenous EF, DCP1A, EDC4 and HSP90 (loading control). Samples are total cell lysates from shA673-1c -/+ dox cells.

2. EF associates with most of its decay targets and promotes decay of a tethered reporter mRNA

To investigate a more direct role of EF in mRNA degradation, we tested whether it had the ability to associate with its "decay targets", *i.e.*, the mRNAs that are destabilized in the presence of EF. To this aim, we performed RNA immunoprecipitation (RIP) experiments in shA673-1c cells. We immunoprecipitated EF with an anti-FLI1 antibody and assessed the presence of the representative mRNAs from the "decay targets panel" in the IP by RT-qPCR. Contrary to control mRNAs (*GAPDH*, *NDUFA12* and *RPL32*), we found that the majority of tested mRNAs (7 mRNAs out of 10) were significantly enriched in the EF IP, compared to control mRNAs (**Figure 67a**), indicating that EF is able to specifically associate with most its target mRNAs and that EF might destabilize its targets upon mRNA association.

a
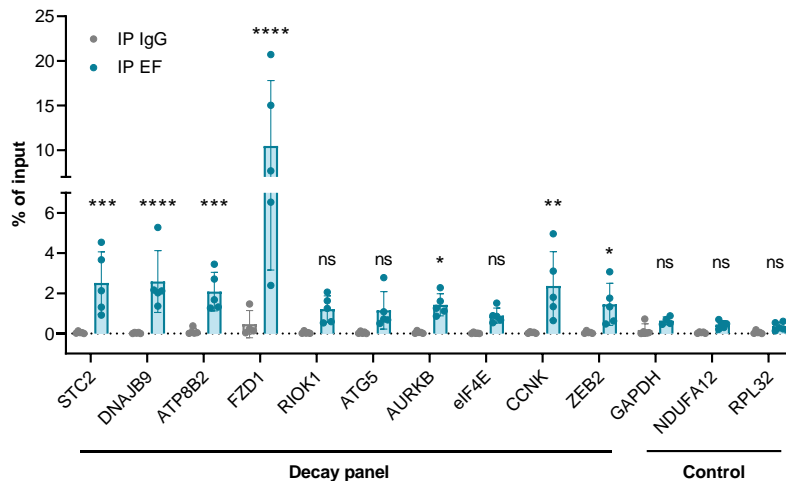
b
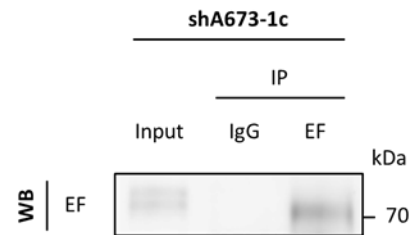
Figure 67. EF RNA IP experiment in shA673-1c cells. (**a**) Immunopurification of RNA-EF complexes and RT-qPCR for the decay panel and indicated control genes in shA673-1c cells (n = 5 independent experiments). Results are shown as means ± SD. *p <0.05; **p <0.01; ***p <0.001; ****p <0.0001 compared to mean % of input of control mRNAs by two-tailed unpaired Student's *t*-test. (**b**) Western blotting analysis of EF after RNA IP in shA673-1 cells.

To test this possibility, we used an mRNA stability tethering assay previously described in [627]. This assay uses a *Renilla* luciferase reporter mRNA carrying eight repeats of the binding sequence for the bacteriophage MS2 coat protein (MS2-CP) in its 3' untranslated region (UTR) (*R-Luc-8MS2*). This approach allows the specific recruitment of any protein of interest fused to the MS2-CP peptide onto the 3'UTR of the reporter transcript (**Figure 68a**). Using this assay, we tested EF as well as its N-terminal EWSR1-derived (EWS-Nter) and C-terminal FLI1-derived (FLI1-Cter) regions (**Figure 68b**). We transfected FLAG-tagged constructs encoding either MS2-CP alone (as control) or MS2-CP fused to full-length EF or to its Nter/Cter regions (EF-MS2-CP, Nter-MS2-CP and Cter-MS2-CP, respectively), together with the R-Luc-8MS2 reporter or with a control reporter lacking the MS2-binding sites (*R-Luc-0MS2*) in HeLa cells. Then, we assessed the stability of the *R-Luc-8MS2* and *R-Luc-0MS2* reporters by RT-qPCR under condition of transcription blockage with ActD. Interestingly, we found that the expression of EF-MS2-CP and Nter-MS2-CP but not Cter-MS2-CP decreased the stability of *R-Luc-8MS2* compared to control MS2-CP (**Figure 68c-d**). Importantly, the expression of these constructs had no effect on the stability of the non-tethered *R-Luc-0MS2*. These observations strongly support the idea that EF can promote mRNA destabilization via a mechanism that involves its association with the target mRNA and is mediated by its EWSR1-derived region.
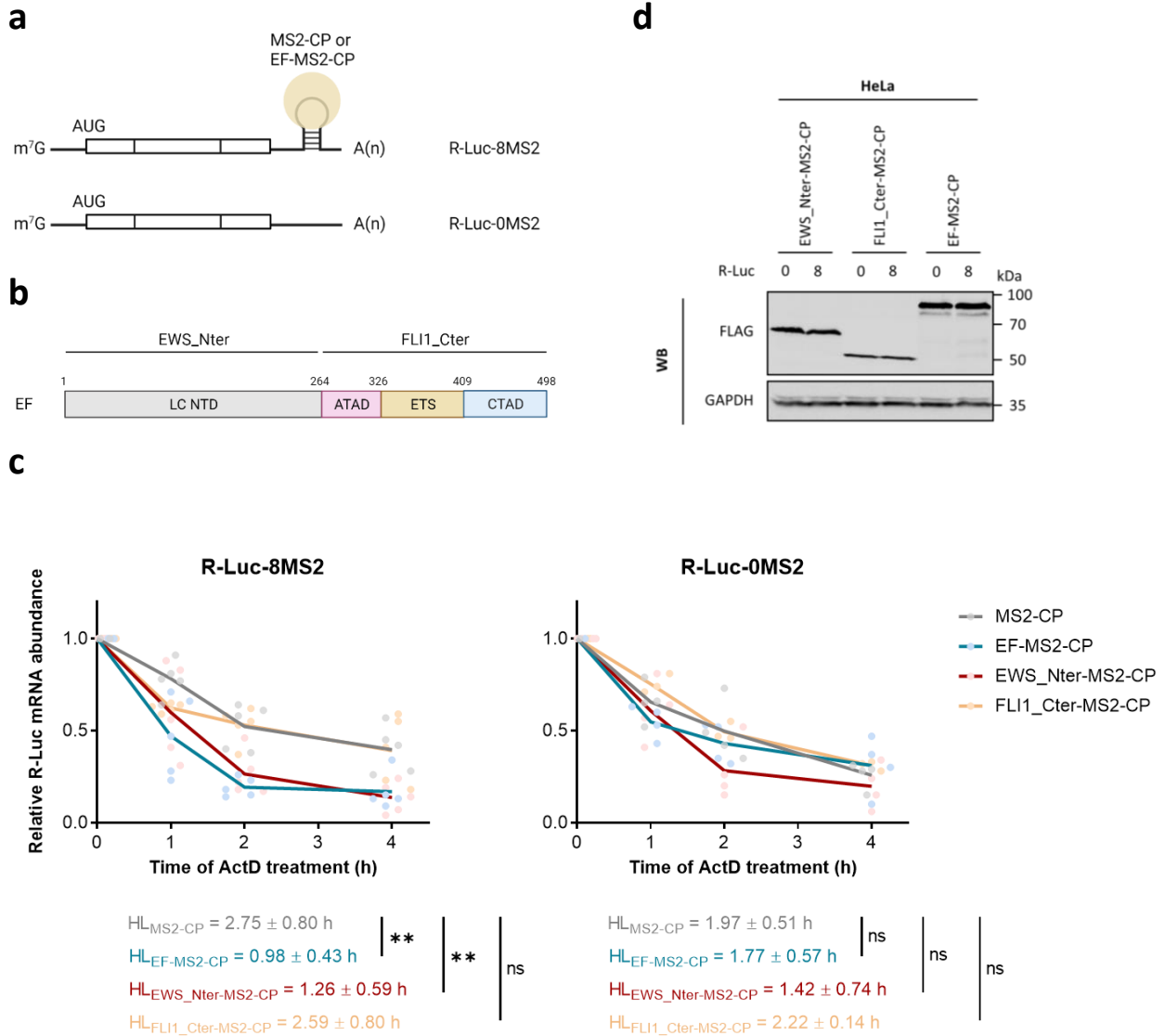
Figure 68. MS2-tethering degradation assay with EF and its Nter/Cter domains. (**a**) Schematic, representation of the *R-Luc-8MS2* and the *R-Luc-0MS2* mRNA reporters. (**b**) Schematic, domain structure of EF. Regions from respective EWSR1 and FLI1 parent proteins are indicated. (**c**) RT-qPCR stability analysis of the *R-Luc-8MS2* and the *R-Luc-0MS2* mRNA reporters. Samples are RNA from HeLa cells transfected with the indicated R-Luc reporters and MS2-CP-tagged constructs, and treated for 0, 1, 2, or 4h with ActD. Dots and lines indicate individual values and means, respectively (n = 5 and 4 independent experiments for *R-Luc-8MS2* and *R-Luc-0MS2*, respectively). **p <0.01; ns = not significant compared to MS2-CP by two-tailed unpaired Student's *t*-test. HL = half-life. (**d**) Western blotting analysis of the indicated MS2-tagged proteins with anti-FLAG antibody and GAPDH (loading control). Samples are total cell lysates from HeLa cells transfected with *R-Luc-0MS2* or *R-Luc-8MS2* and indicated MS2-tagged constructs.

3. EF interacts with the CCR4-NOT deadenylation machinery

In eukaryotic cells, deadenylation is often the first and rate-limiting step of mRNA decay [628], [629]. To further dissect the molecular mechanisms underlying the mRNA degradative activity of EF, we tested its interactions with subunits of the CCR4-NOT and PAN2-PAN3 complexes, the major deadenylation machineries in eukaryotes. For this, we used a previously described *Gaussian* luciferase (GLuc) protein complementation assay (gPCA) [630] (**Figure 69a**). We expressed independent GLucN1-tagged versions of various deadenylase complexes subunits together with GLucN2-tagged EF. As it is necessary and sufficient to promote mRNA degradation (see above), we also tested the Nter region of EF in parallel. For each protein pair, we computed a normalized luciferase ratio (NLR) as described in **Figure 69b**. Based on previous publications, gPCA interactions can be considered positive when NLR >3 [630].

a   **b**
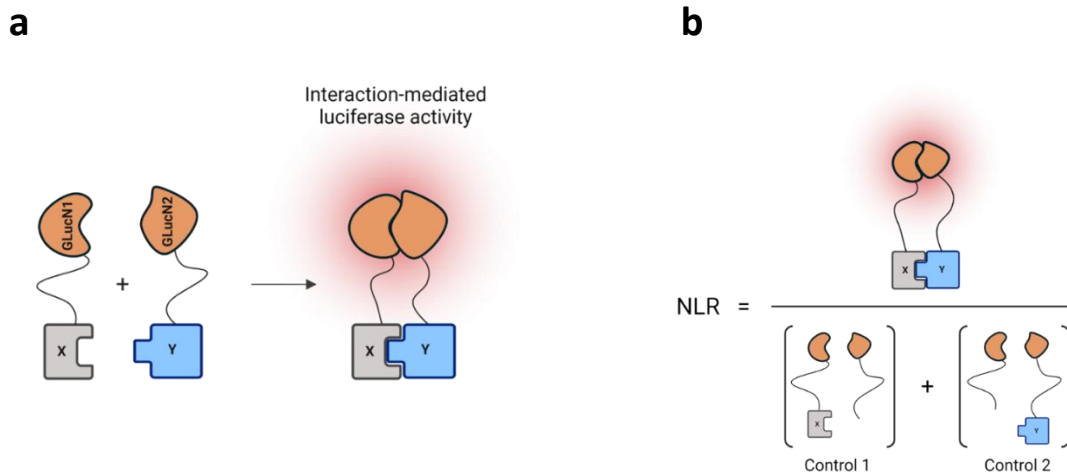
Figure 69. Gaussian luciferase protein complementation assay (gPCA). (**a**) Schematic of the Gaussian luciferase protein complementation assay (gPCA). X and Y are bait and prey proteins, and GLucN1 and GLucN2 are inactive fragments of the Gaussian luciferase. Modified from [630]. (**b**) Schematic of the normalized luminescence ratio (NLR) used in gPCA. The NLR for a given interacting protein pair X-Y corresponds to luminescence activity in cells expressing GLucN1-X and GLucN2-Y divided by the sum of the luminescence measured in control wells as indicated. Modified from [630].

Using this assay, we found a robust interaction between EF and the CNOT2 subunit of the CCR4-NOT complex (NLR ~10). (**Figure 70a**). Interestingly, this interaction was also detected with the EWSR1-derived Nter region of EF (NLR ~5). An interaction with PAN3 was also detected, although barely above the NLR cut-off (NLR = 3.3) and only observed for the Nter domain. The association between EF or its Nter region and CNOT2 was confirmed in a reverse tagging configuration (*i.e.*, GLucN2-CNOT2 and GLucN1-EF or GLucN1-EWS-Nter). Here, we also included the FLI1-derived Cter region of EF (GLucN1-FLI1-Cter). As expected, we found that EF and the Nter region were able to interact with CNOT2 (**Figure 71a-b**, NLR ~30 and 20, respectively), although a weak interaction was also detected for the Cter region (NLR = 3.6). Since gPCA has been reported to

106

preferentially detect direct interactions [630], these results indicate that the interaction with CNOT2 is likely to be direct.

a
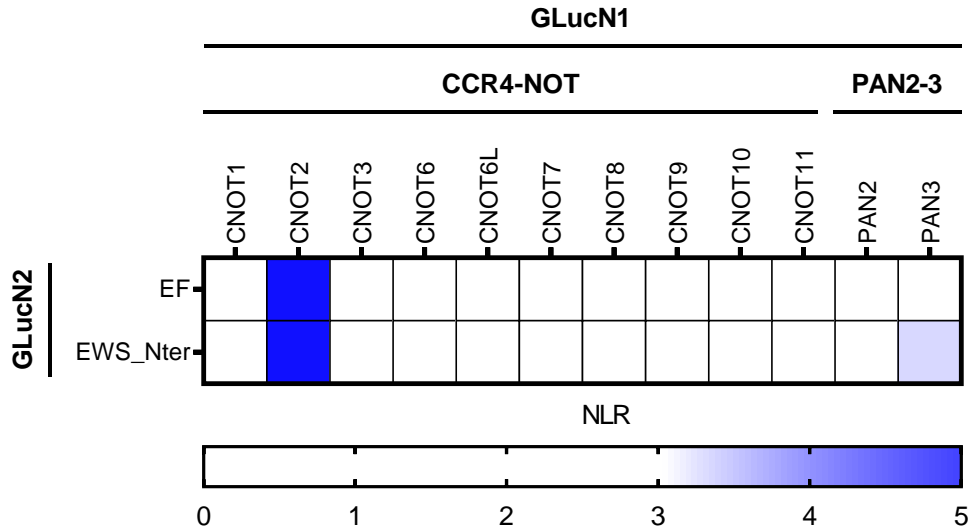
b
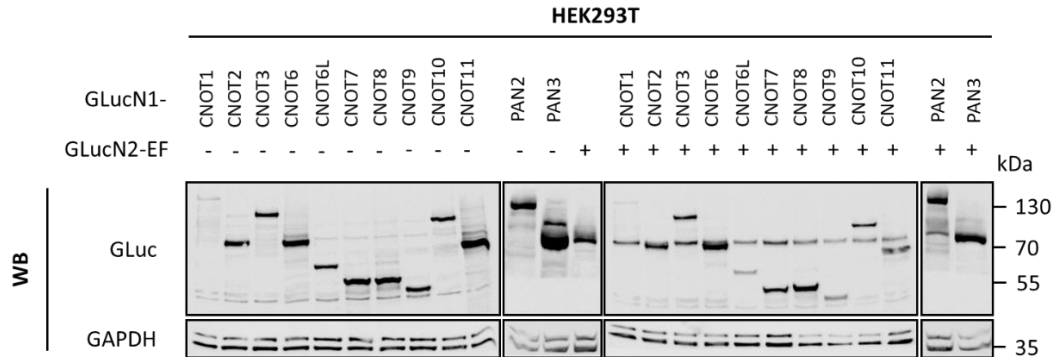
Figure 70. gPCA screening with subunits of the deadenylation complexes. (**a**) Heatmap showing mean NLR values for the indicated protein pairs (n = 3 independent experiments). The subunits of the CCR4-NOT and PAN2-PAN3 deadenylation complexes are tagged with GLucN1; and EF and EWS_Nter are tagged with GLucN2. (**b**) Representative western blotting analysis of the indicated GLucN1/2-tagged proteins and GAPDH (loading control). Samples are lysates from HEK293T cells used in (**a**).

a

b
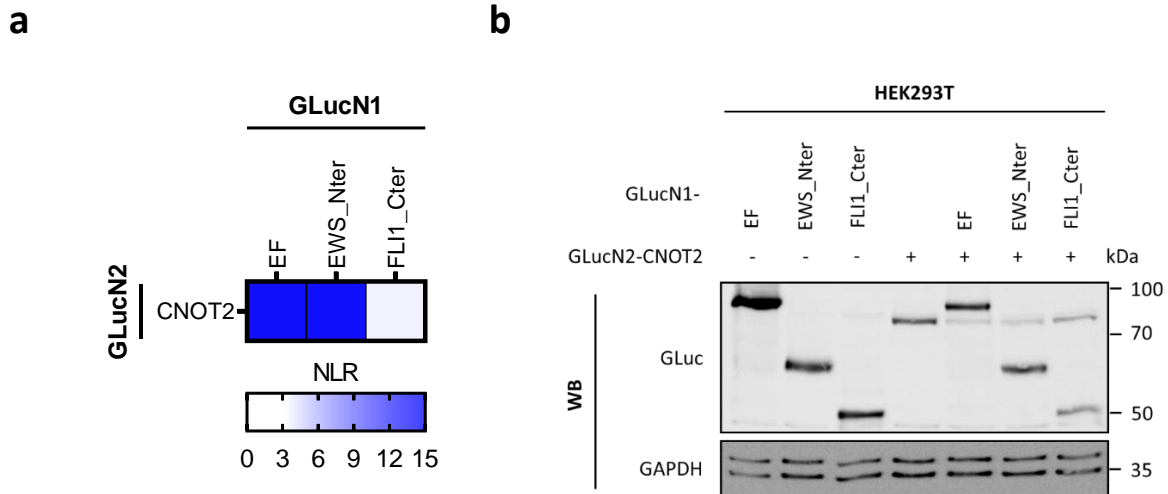
Figure 71. gPCA screening with Nter and Cter regions of EF. (**a**) Heatmap showing mean NLR values for the indicated protein pairs (n = 3 independent experiments). EF, EWS_Nter and FLI1_Cter are tagged with GLucN1; and CNOT2 is tagged with GLucN2. (**b**) Representative western blotting analysis of the indicated GLucN1/2-tagged proteins and GAPDH (loading control). Samples are lysates from HEK293T cells used for luminescence measurement.

The association between EF and CNOT2 was confirmed at the endogenous level in EwS cells by coimmunoprecipitation (**Figure 72a**). Interestingly, endogenous EF also copurified with CNOT1, the scaffold subunit of CCR4-NOT (**Figure 72b**), suggesting that EF could associate with the whole CCR4-NOT complex to achieve degradation of its target mRNA. To test this possibility, we first sought to verify that EF was able to associate with other subunits of the CCR4-NOT complex. By performing coimmunoprecipitations between FLAG-tagged EF and HA-tagged versions of the four catalytic subunits of CCR4-NOT, we found that CNOT6L and CNOT8 copurified with EF. In contrast, we detected no interaction with the CNOT6 or CNOT7 subunits, suggesting that EF specifically associates with the CNOT6L-CNOT8-containing species form of CCR4-NOT (**Figure 72c**). Importantly, the associations of EF with CNOT6L and CNOT8 were also confirmed at the endogenous level in EwS cells (**Figure 72d-e**). Together, these results suggest that via its direct association with CNOT2, EF might recruit a fully functional version of the CCR4-NOT deadenylation complex, containing CNOT6L and CNOT8 (**Figure 72f**).

a
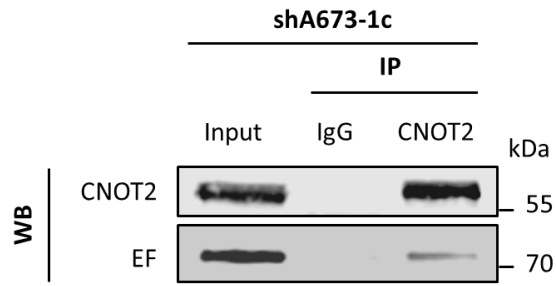
b
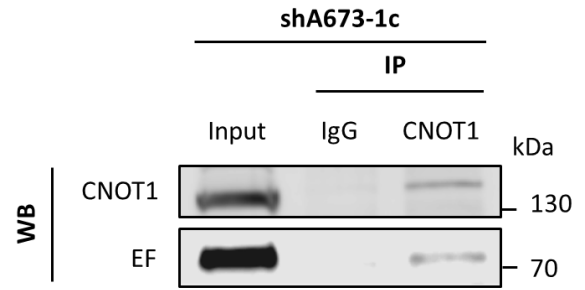
c
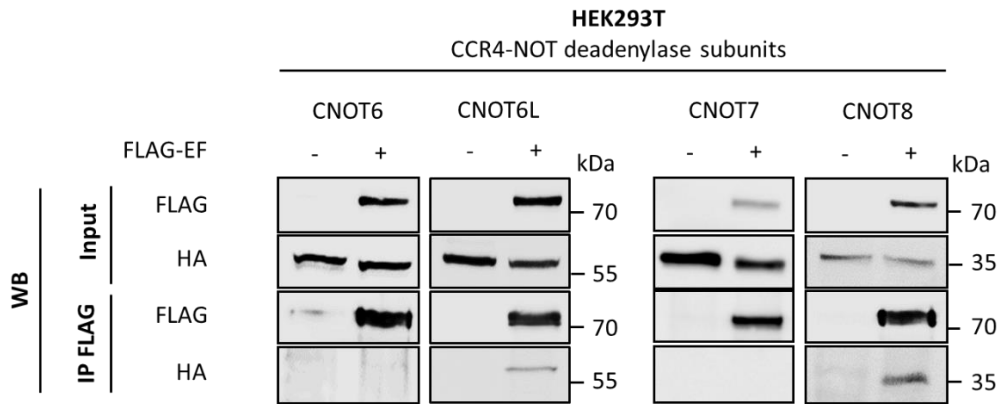
d
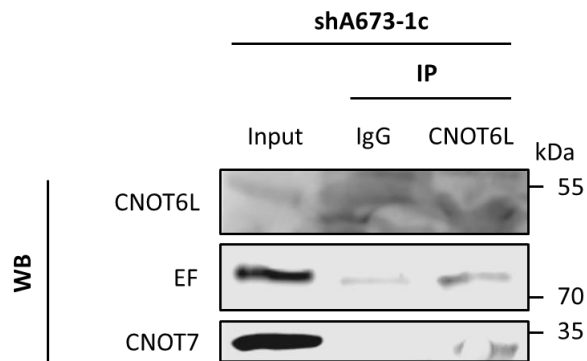
e
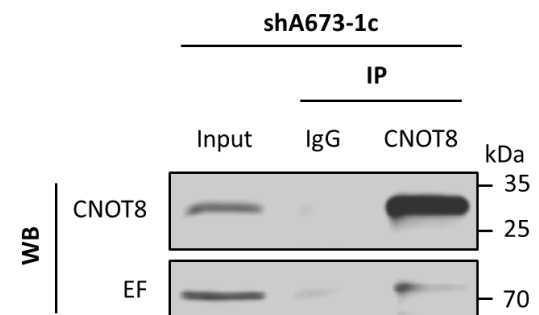
f
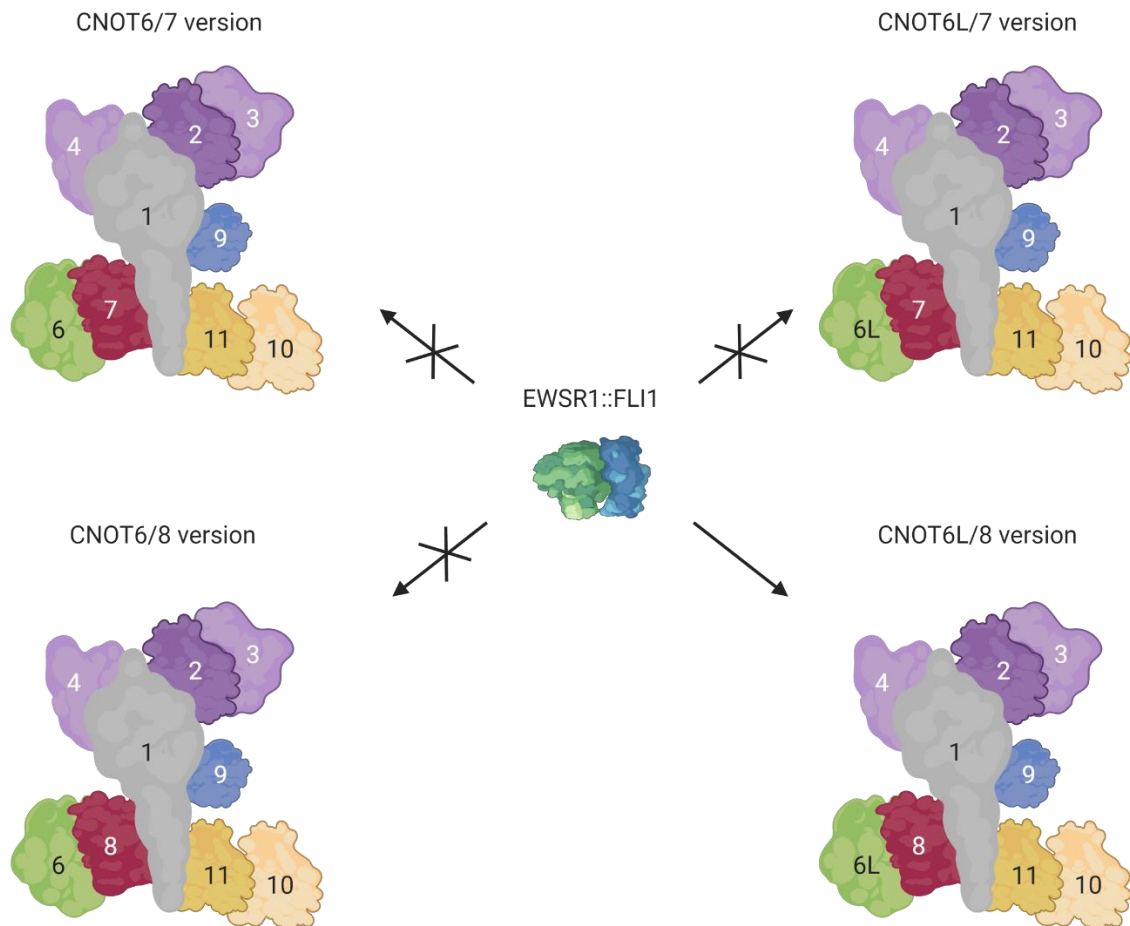
Figure 72. Coimmunoprecipitations experiments between EF and subunits of the CCR4-NOT complex. (**a**) Immunoprecipitation (IP) of endogenous CNOT2 and (**b**) CNOT1 from shA673-1c cell lysates followed by western blotting (WB) for the indicated proteins. (**c**) Immunoprecipitation (IP) of FLAG-tagged EF followed by anti-FLAG and anti-HA western blotting (WB). Samples are lysates from HEK293T cells transfected with HA-tagged indicated CCR4-NOT deadenylase subunits with either FLAG-EF or control FLAG empty-vector. (**d**) Immunoprecipitation (IP) of endogenous CNOT6L and (**e**) CNOT8 from shA673-1c cell lysates followed by western blotting (WB) for the indicated proteins. (**f**) EF associates only with the CNOT6L-CNOT8-containing version of CCR4-NOT. Numbers indicate CNOT subunits.

To better characterize the novel interaction between EF and the CCR4-NOT complex, we looked in which cellular compartment (cytoplasm or nucleus) this interaction takes place. To address this, we performed proximity-ligation assay (PLA) with FLAG-tagged EF and Myc-tagged CNOT2 in HeLa cells. Specific PLA signals, which are proxies for the EF/CNOT2 interaction were observed in both the nuclear and cytoplasmic compartments (**Figure 73**). So far, EF has been mainly described to be located in the nucleus, consistently with its canonical function as a TF. Because our PLA experiments suggest that at least a portion of EF might be present outside the nucleus, we performed immunostaining detection of EF in two EwS cell lines. We observed that, in addition to its mainly nuclear localization, EF also appeared as discrete cytoplasmic foci in both EwS cell

lines (**Figure 74a-b**). Because CNOT2 is a well-known constituent of PBs [375], we hypothesized that these EF-positive foci might be PBs. To test this, we performed co-immunostaining of EF and DCP1A or EDC4, two PBs markers. We found no colocalization of EF with the PB markers, indicating that cytoplasmic EF does not predominantly localize in PBs (**Figure 74c-d**). Alternatively, we repeated the PLA experiments in cells expressing EGFP-tagged DCP1A, allowing direct visualization of PBs. Again, we observed no PLA foci co-localizing with DCP1A, indicating that the cytoplasmic colocalization of EF with CNOT2 does not occur within PBs (not shown). Together, these results suggest that the decay function of EF might take place in both nuclear and cytoplasmic compartments but its precise subcellular localization remains undefined.
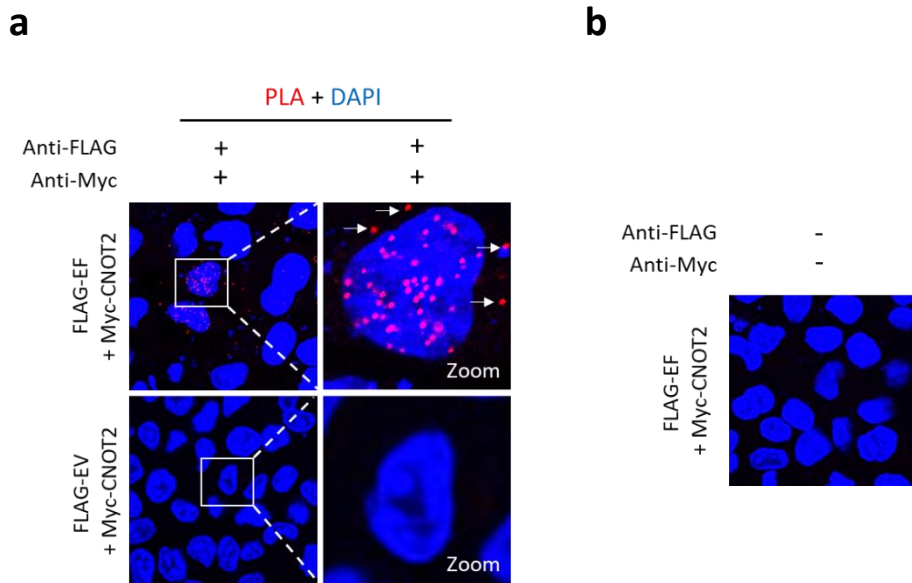
Figure 73. Proximity-ligation assay. (**a**) Representative images of FLAG-EF and Myc-CNOT2 interaction (in red) assessed by proximity ligation assay (PLA) in HeLa cells. Nuclei were counterstained in blue. Arrow indicates cytoplasmic red foci. EV = empty vector. (**b**) Control (no primary antibodies) for PLA.

a
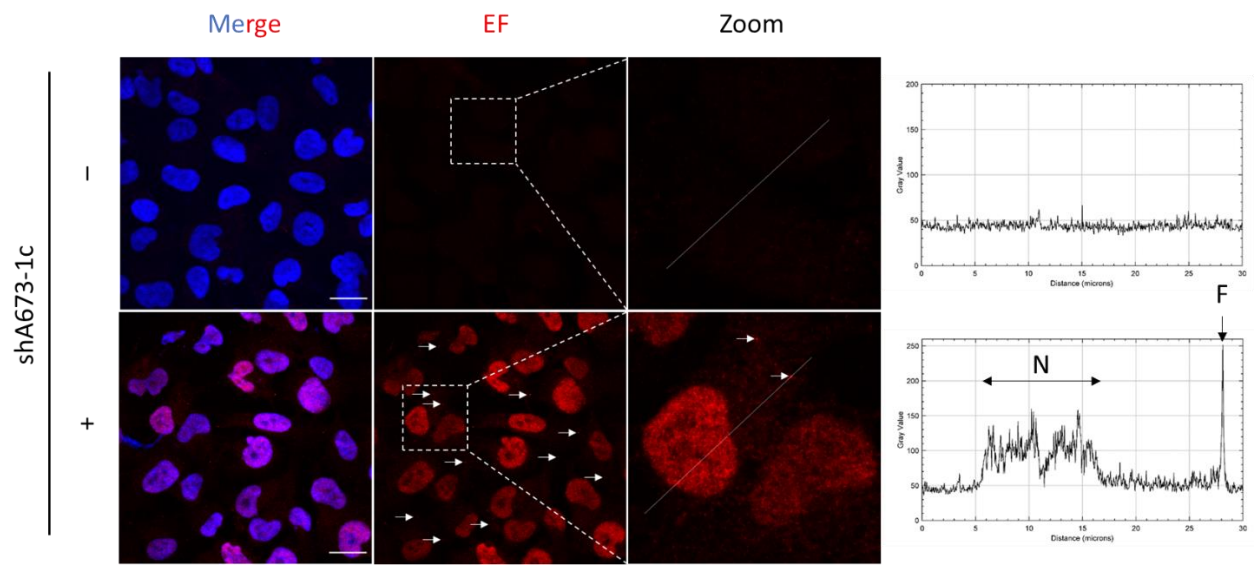
b
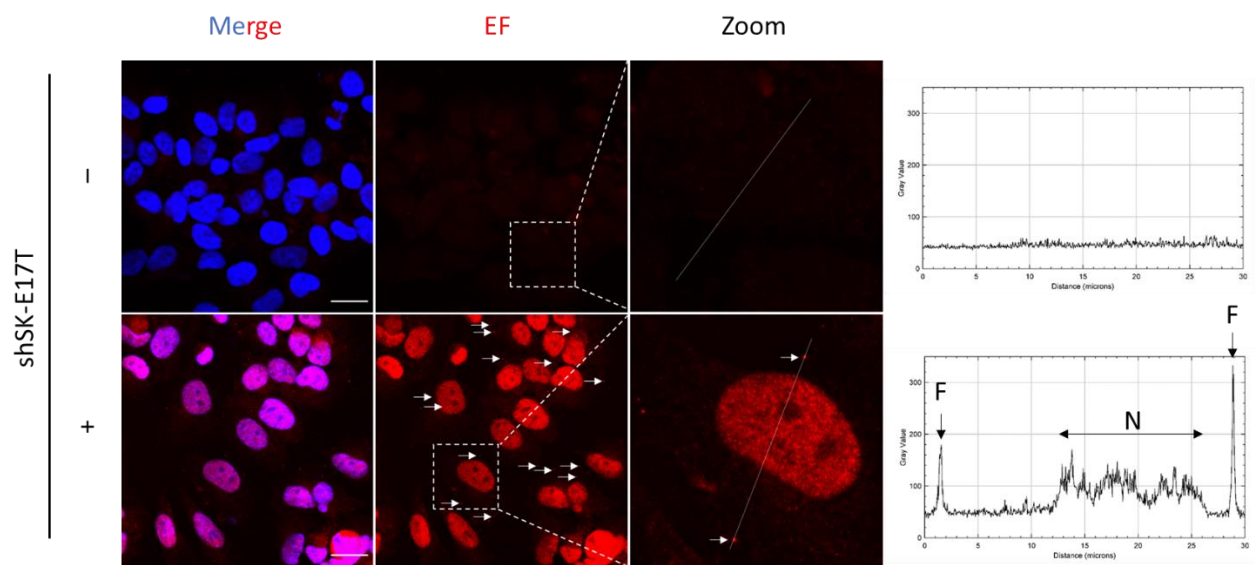
c
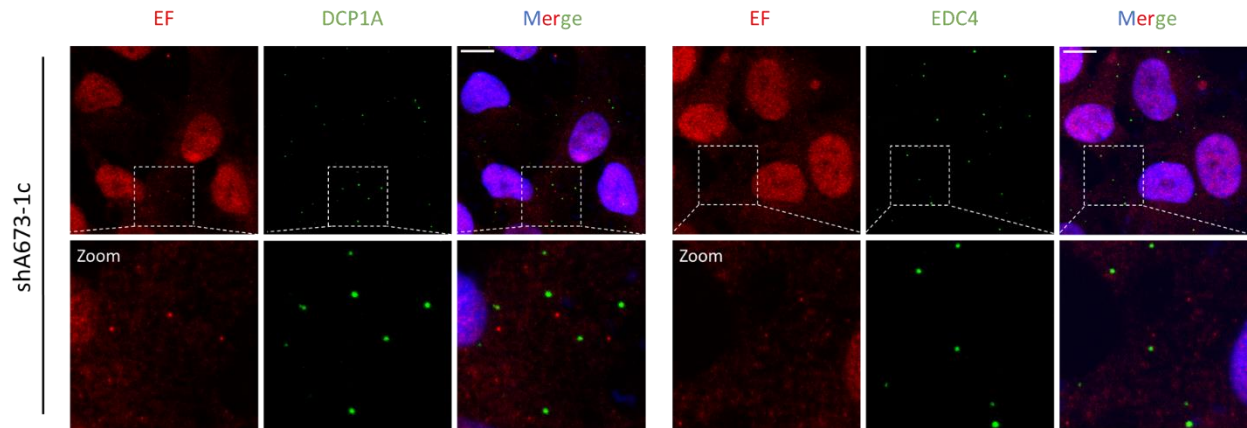
d
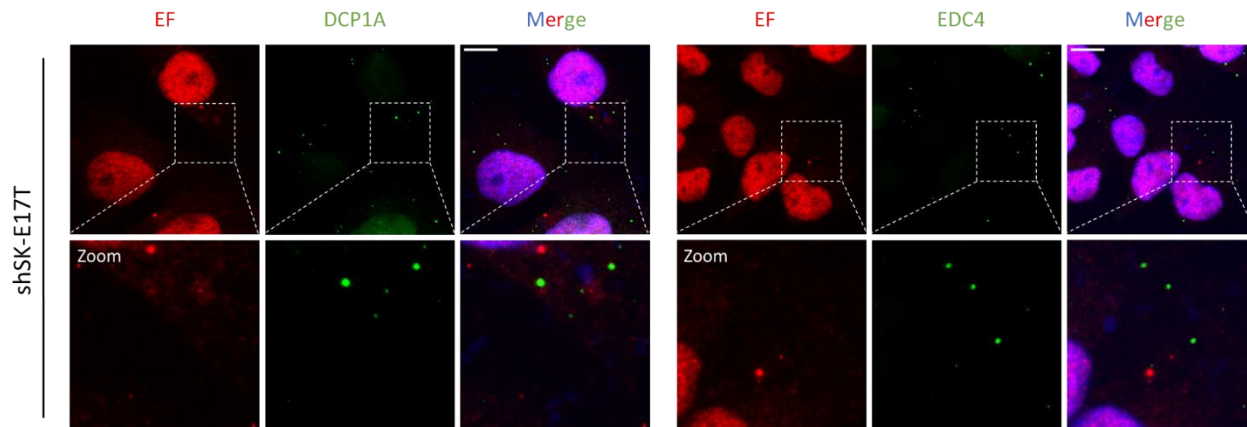
Figure 74. Subcellular localization of EF in two EwS cell lines. (**a**) Immunofluorescence of EF (red) and DAPI (nuclear staining, blue) in shA673-1c cells and (**b**) shSK-E17T cells incubated with (+) or without (-) primary anti-FLI1 antibody. Scale bar = 20 μm. Magnification of boxed regions and intensity plots (right) along respective sections (white lines) are shown. White arrows indicate intense cytoplasmic foci. N = nucleus; F = foci. (**c**) Immunofluorescence of EF (red), DCP1A (green, left), EDC4 (green, right) and DAPI (nuclear staining, blue) in shA673-1c cells and (**d**) shSK-E17T cells. Individual channels, merged channels with nuclear staining (in blue) and magnification of boxed regions are shown. Scale bar = 10 μm.

To further characterize the EF/CNOT2 interaction, we performed coimmunoprecipitations from cell lysates treated with RNAse A. RNAse A treatment did not affect the amount of CNOT2 co-purifying with EF (**Figure 75a**), indicating that RNA is dispensable for the formation of a stable EF-CNOT2 complex. Next, to map the region of CNOT2 involved in the interaction with EF, we undertook coimmunoprecipitation experiments between FLAG-tagged EF and a series of Myc-tagged deletion mutants of CNOT2 (**Figure 75b**). These experiments identified the NAR (Not1 anchor region) domain of CNOT2 as mediating the interaction with EF (**Figure 75c**).

a
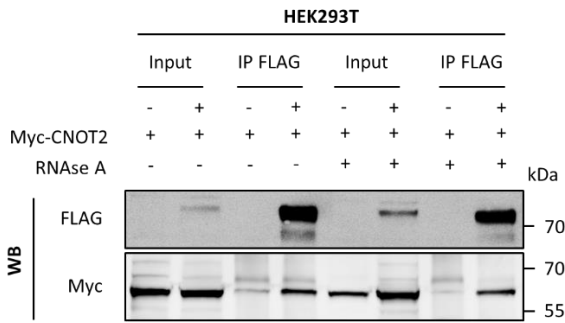
b
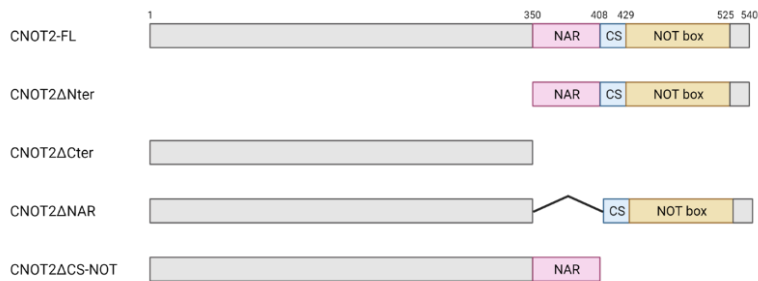
c
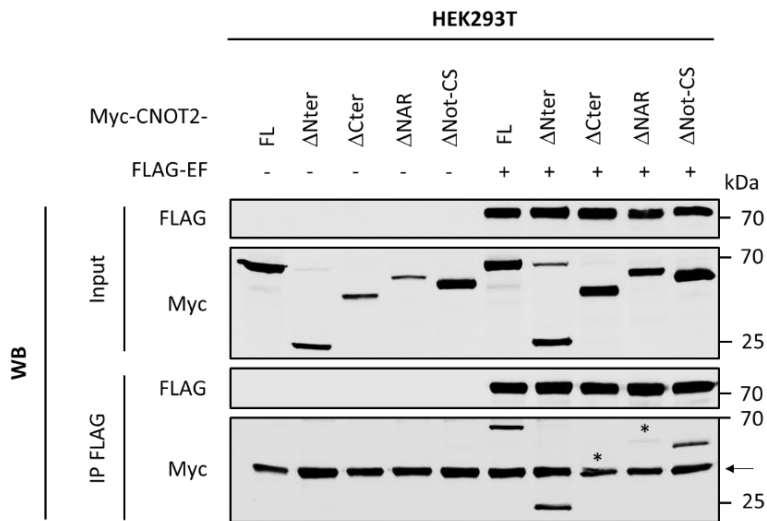
Figure 75. Other features of the EF/CNOT2 interaction. (**a**) Immunoprecipitation (IP) of FLAG-tagged EF followed by anti-FLAG and anti-Myc western blotting (WB). Samples are untreated or RNAse A-treated lysates from HEK293T cells transfected with Myc-CNOT2 alone or together with FLAG-EF. (**b**) Schematic, domain structure of CNOT2-deletion mutants. FL = full length, NAR = NOT1 anchor region, CS = connecting sequence. (**c**) Immunoprecipitation (IP) of FLAG-tagged EF followed by anti-FLAG and anti-HA western blotting (WB). Samples are lysates from HEK293T cells transfected with Myc-tagged CNOT2-deletion mutants alone or with FLAG-EF. Arrow indicates aspecific band; and asterisks indicate lost bands.

4. The decay activity of EF relies on its interaction with the CNOT2 subunit of the CCR4-NOT deadenylation complex

Based on our previous results, we hypothesized that CNOT2 might be critical for the decay activity of EF by allowing the recruitment of the full CCR4-NOT complex. To further test the importance of CNOT2 in our model, we repeated the MS2-tethering degradation assay with EF-MSP-CP in CNOT2-depleted HeLa cells. Interestingly, we found that siRNA-mediated depletion of CNOT2 abrogated the ability of EF to destabilize the *R-Luc-8MS2* reporter (**Figure 76a-b**). Moreover, we analyzed the stability of the representative EF decay targets in CNOT2-depleted shA673-1c EwS cells. Similarly to knocking down EF, depletion of CNOT2 led to the stabilization of the majority of the tested mRNAs (**Figure 76c-d**).

Because CNOT2 appears to mediate the association between EF and CCR4-NOT, we attempted to to build a mutant of EF for which the interaction with CNOT2 was compromised. To map more precisely the CNOT2-interaction domain on EF, we thus constructed deletion mutants of the Nter region of EF by removing successive 50 amino acids (aa) stretches from the 3' end (**Figure 77a**). Using gPCA, we tested interactions between the EF Nter deletion mutants and CNOT2, and found that most of the interaction was lost upon removal of the first 63 aa of EF N-terminus (NLR ~4). Correspondingly, the first 63 aa alone were able to recover an important fraction of the interaction (NLR >7, **Figure 77b-c**), thus suggesting the first 63 aa of EF are a major contributor in the interaction with CNOT2. When tested in the mRNA degradation tethering assay, the N-terminal region of EF lacking the first 63 aa (Δ63 EF Nter) did not promote the degradation of the *R-Luc-8MS2* reporter compared to control expression of MS2-CP (**Figure 78a-b**). Finally, removal of the 1-63 aa region abolished the ability of EF to promote degradation of its representative decay targets in hMSCs (**Figure 78b-c**). Altogether, these results point towards a model in which EF promotes the degradation of specific mRNA via its ability to associate with CNOT2.
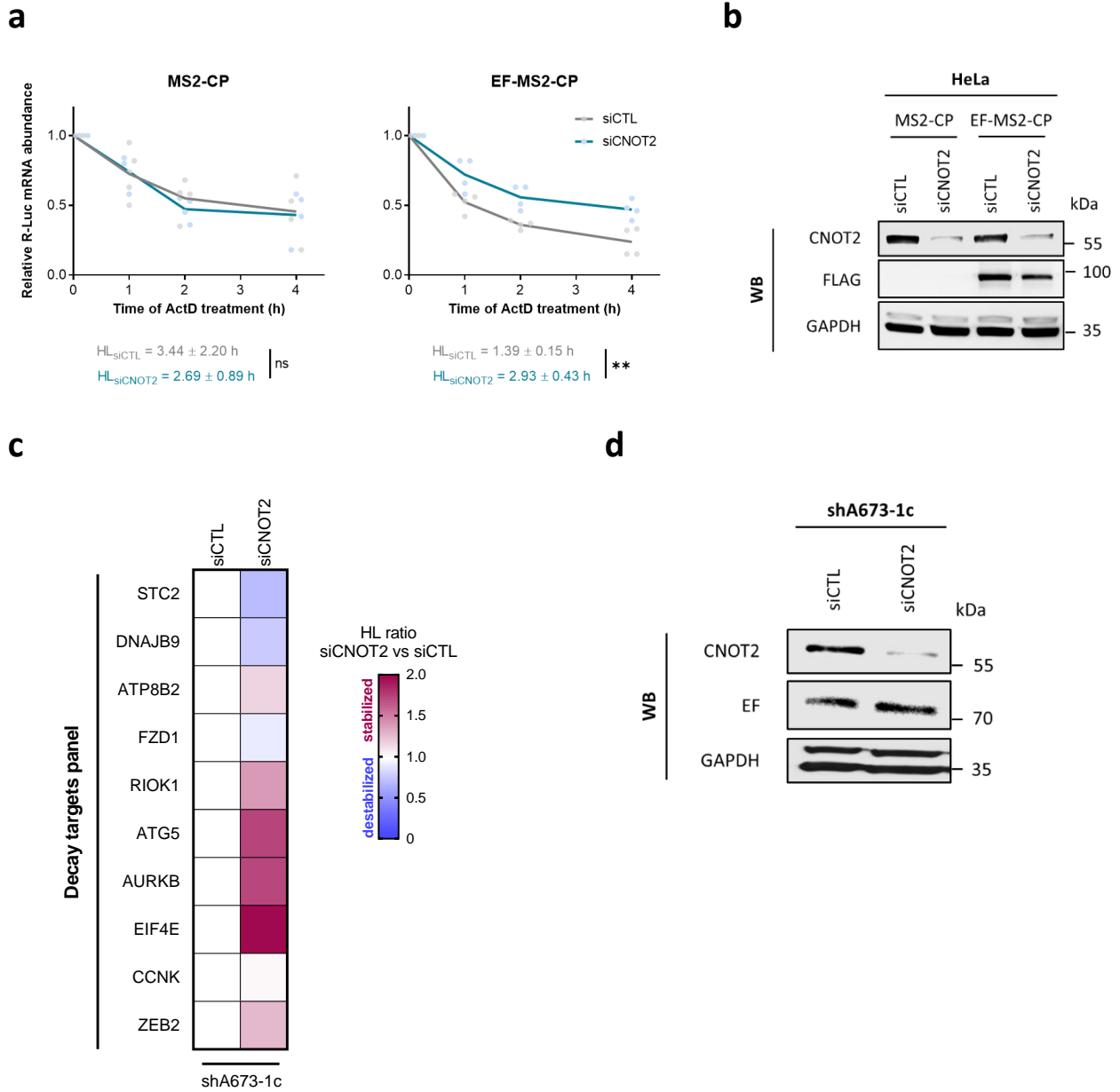
Figure 76. Decay activity of EF under CNOT2 depletion. (**a**) RT-qPCR analysis of the stability of the R-Luc-8MS2 mRNA reporter in HeLa -/+ siCNOT2 cells. Samples are RNA from siCTL/siCNOT2 HeLa cells transfected with the R-Luc-8MS2 reporter and MS2-CP or EF-MS2-CP and treated for 0, 1, 2, or 4 h with ActD. Dots and lines indicate individual values and means, respectively (n = 4 independent experiments). **p <0.01; ns = not significant compared to siCTL by two-tailed unpaired Student's *t*-test. HL = half-life. (**b**) Western blotting analysis of EF-MS2-CP (anti-FLAG antibody), CNOT2 and GAPDH (loading control). Samples are total cell lysates from HeLa cells before and after knockdown of CNOT2 and transfected with indicated MS2-tagged constructs. (**c**) Heatmap of half-life (HL) ratio detected by RT-qPCR before and after knockdown of CNOT2 in shA673-1c cells for the decay panel. Results are shown as means (n = 3-5 independent experiments). For each target, the HL ratio corresponds to the HL in siCTL condition divided by the HL in the siCNOT2 condition. (**d**) Western blotting analysis of CNOT2, EF and GAPDH (loading control). Samples are lysates from shA673-1c cells before and after knockdown of CNOT2.
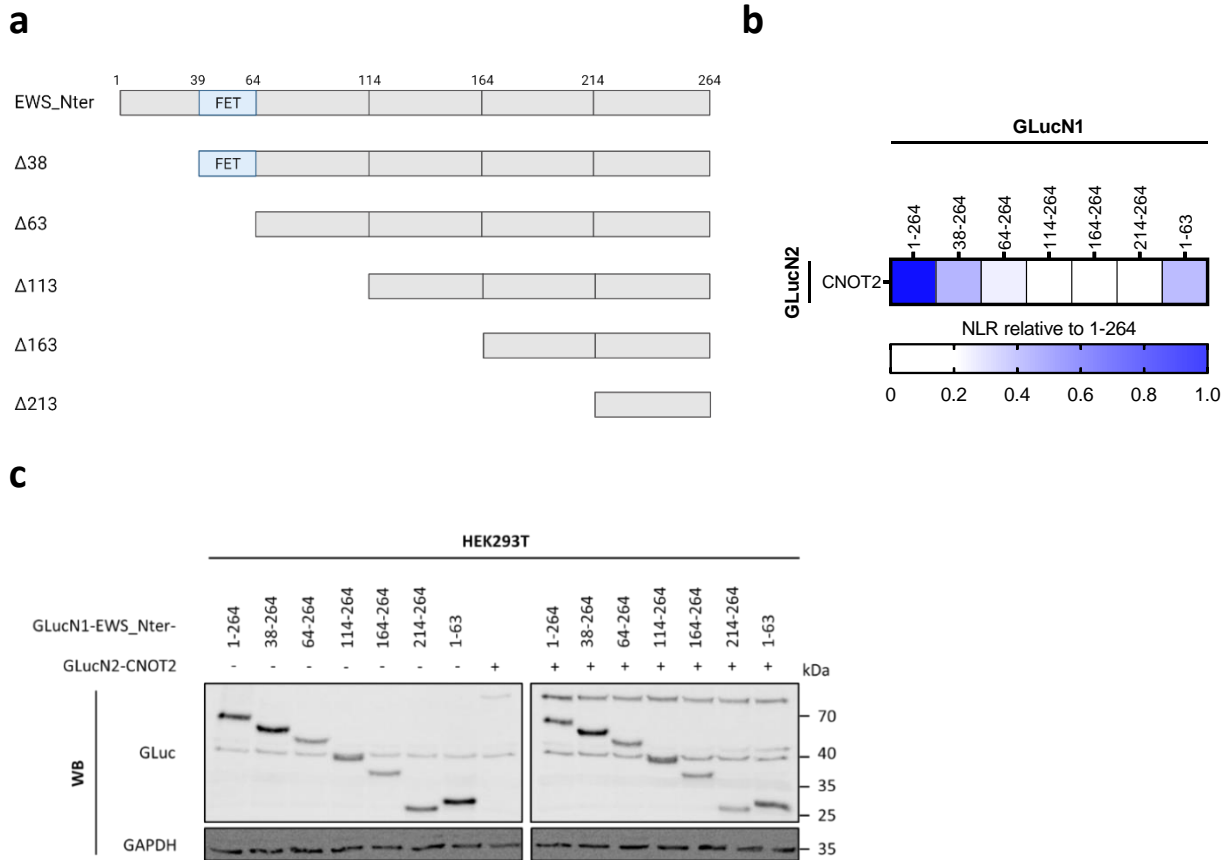
Figure 77. gPCA screening with the deletion mutants of EF Nter region. (**a**) Schematic, domain structure of EWS_Nter-deletion mutants. (**b**) Heatmap showing NLR values relative to 1-264 construct for the indicated protein pairs (n ≥ 2 independent experiments). EWS_Nter and deletion-mutants are tagged with GLucN1; and CNOT2 is tagged with GLucN2. (**c**) Representative western blotting analysis of the indicated GLucN1/2-tagged proteins and GAPDH (loading control). Samples are lysates from HEK293T cells used in (**b**).
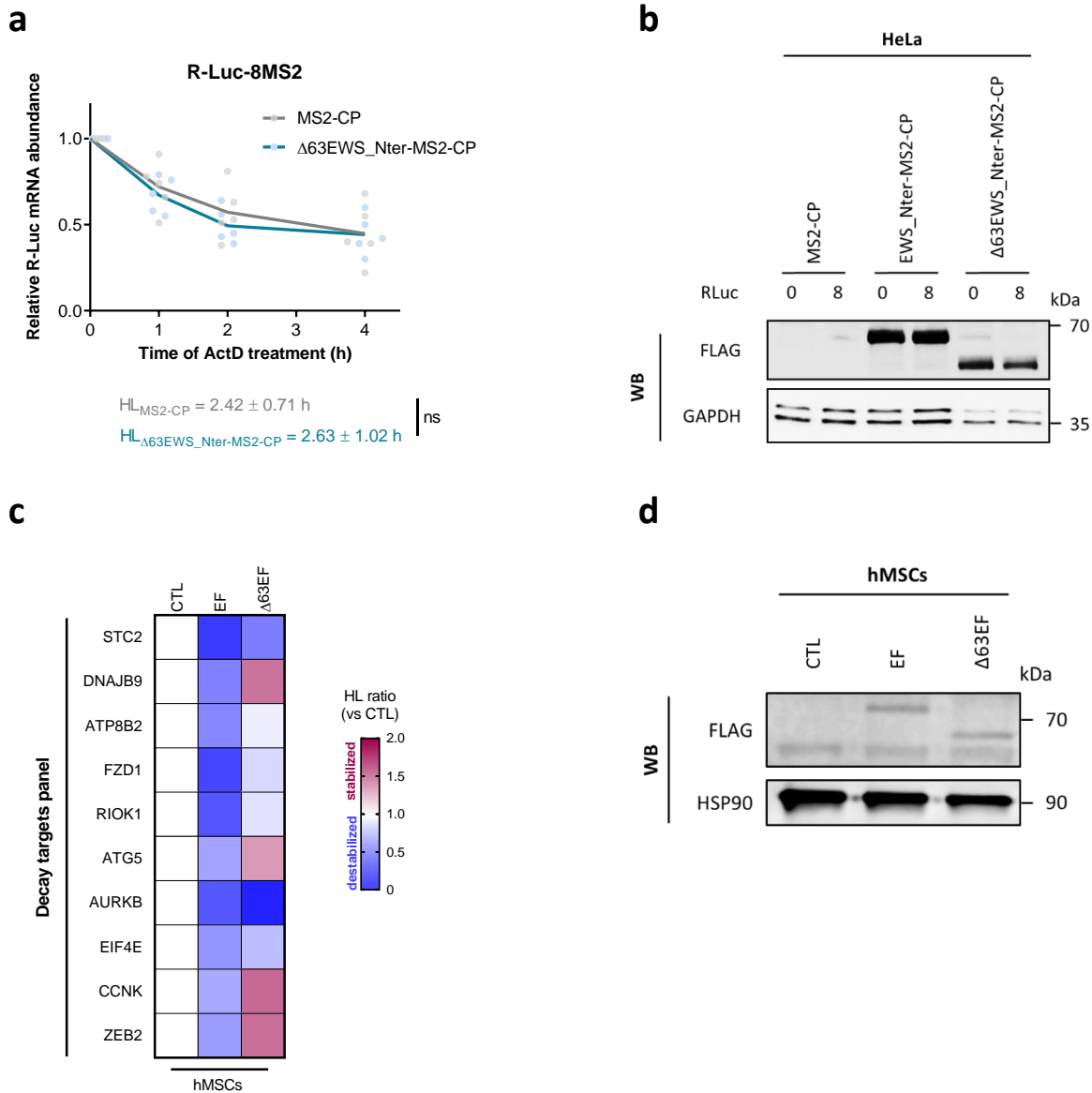
Figure 78. Decay activity of the Δ63 Nter mutant. (**a**) RT-qPCR analysis of the stability of the R-Luc-8MS2 mRNA reporter. Samples are RNA from HeLa cells transfected with the R-Luc-8MS2 reporter and either Δ63EWS_Nter-MS2-CP or MS2-CP, and treated for 0, 1, 2, or 4 h with ActD. Dots and lines indicate individual values and means, respectively (n = 5 independent experiments). ns = not significant compared to MS2-CP by two-tailed unpaired Student's *t*-test. HL = half-life. (**b**) Western blotting analysis of EWS_Nter-MS2-CP and Δ63_EWS_Nter-MS2-CP with anti-FLAG antibody and GAPDH (loading control). Samples are total cell lysates from HeLa cells transfected with R-Luc-0MS2 or R-Luc-8MS2 and indicated MS2-tagged constructs. (**c**) Heatmap of half-life (HL) ratio detected by RT-qPCR after expression of FLAG-tagged EF, Δ63EF or control FLAG empty vector (CTL) in MSC cells for the decay panel. Results are shown as means (n ≥ 2 independent experiments). For each target, the HL ratio corresponds to the HL in EF or Δ63EF condition divided by the HL in the CTL condition. (**d**) Western blotting analysis of FLAG- EF or Δ63EF and HSP90 (loading control). Samples are lysates from MSC cells expressing control FLAG empty vector (CTL) or indicated FLAG-tagged constructs.

Interestingly, we observed that the first 63 aa of EF corresponded to a local higher-order state in the otherwise highly disordered EF Nter region (**Figure 79a**). This region is also well-conserved among the three members of the FET family (**Figure 79b**), suggesting that the interaction with CNOT2 might be a conserved feature of the FET proteins.

a
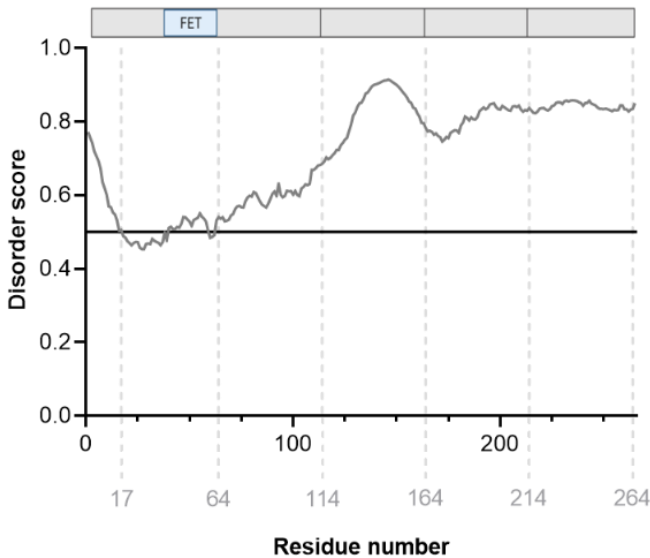
b
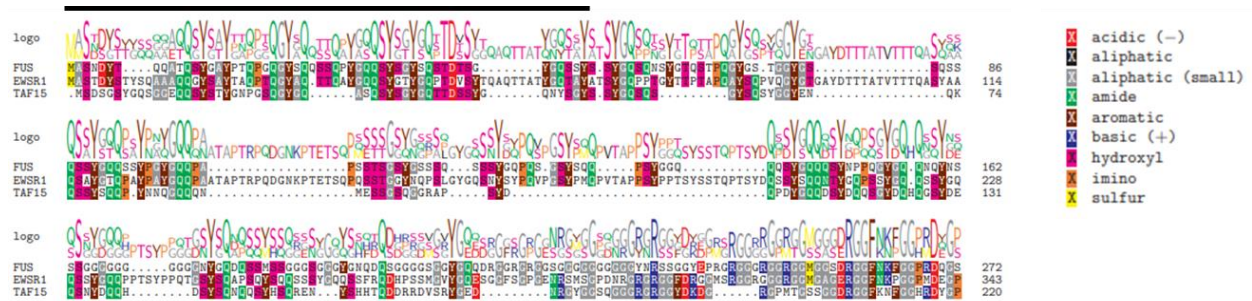
Figure 79. Features of the first 63 Nter amino acids of EF. (**a**) Disorder prediction along the EWS_Nter sequence. Results are shown as means from eight algorithms: IUPRED2, VL3, RONN, SPOT-Disorder, AUCPred, ESpritz, Metadisorder and POODLE. The threshold score for disorder is 0.5 (solid black line). (**b**) Sequence alignment of FUS, EWSR1 and TAF15 proteins. The first 63 amino acids are indicated (solid black line).

The EWSR1-derived region of EF is an intrinsically-disordered (ID) low-complexity (LC) region that contains 30 degenerate hexapeptides repeats (SYGQQS) with conserved tyrosines in second position. Replacing tyrosines by aliphatic amino acids like alanine or isoleucine in the first 17 of these repeats has been reported to abrogate the EF transcriptional activity [91]. By contrast, when tyrosines were replaced by phenylalanine, an aromatic amino acid, this activity was preserved; thus indicating that aromaticity might be important for the transcriptional activity of EF [91]. Here, we investigated whether tyrosines and aromaticity might also be important for the mRNA decay activity of EF. To this end, we first tested interactions between CNOT2 and three different tyrosine mutants of EF Nter region using gPCA (described in **Figure 80a**). We found that the SIGQQS and SAGQQS mutants were unable to interact with CNOT2. In contrast, a SFGQQS mutant retained strong association with CNOT2 (**Figure 80b**). The SIFGQQS mutant of the EF Nter region was also unable to destabilize the R-Luc-8MS2 reporter mRNA in the tethering assay, further supporting the idea that the mRNA degradative activity of EF relies on CNOT2 (**Figure 80c**). Interestingly, structural disorder prediction along the sequences of these three tyrosine mutants showed that the local higher-order state observed within the first 63 aa was lost when tyrosines are replaced by alanines or isoleucines but not phenylalanines (**Figure 81**).

a

b

c
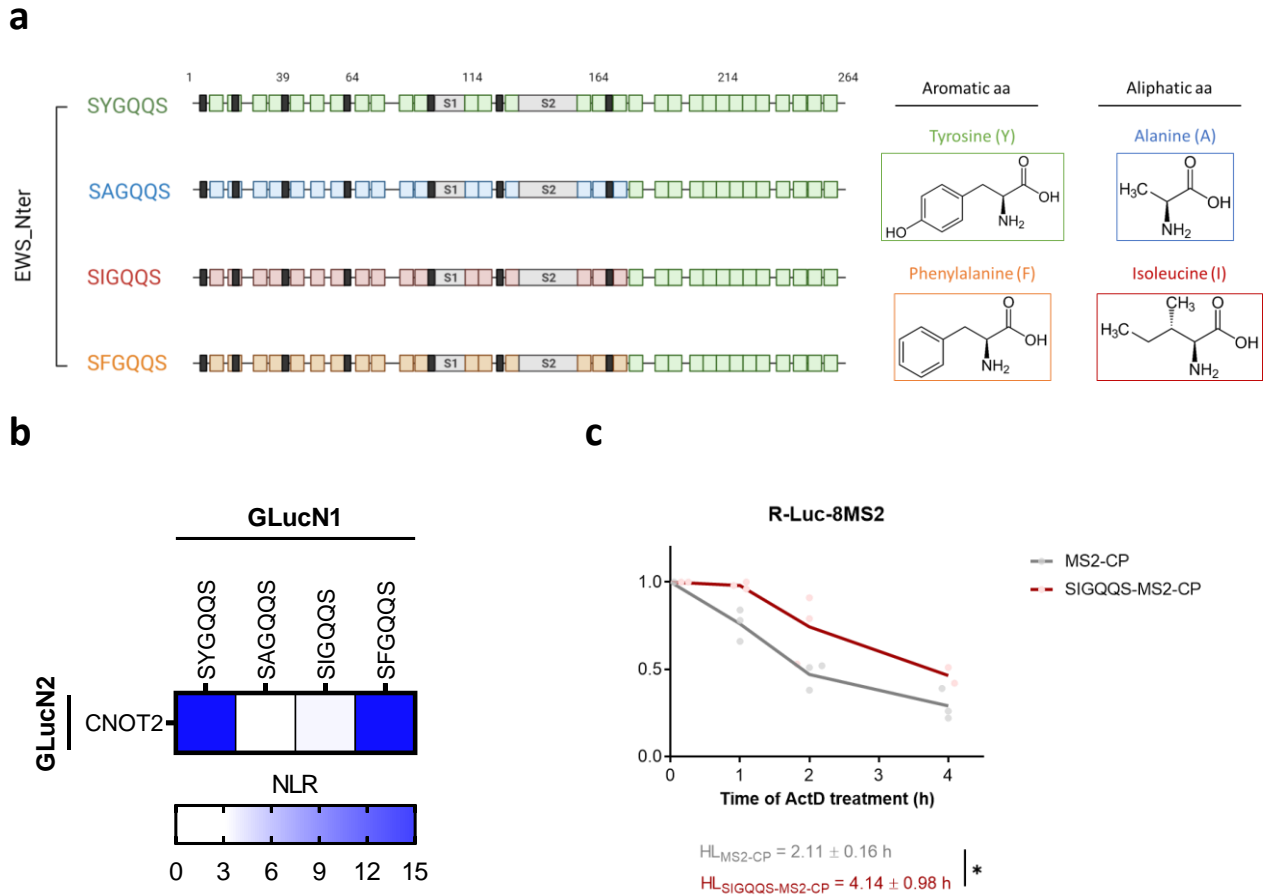
Figure 80. Features of the tyrosine mutants of EWS/EF Nter region. (a) Schematic, domain structure of tyrosine mutants of EWS_Nter region. Consensus sequence of degenerate hexapeptide repeats is shown and their localization is indicated by colored boxes. Tyrosines outside of DHRs are indicated by black boxes. Spacers between DHRs are generally of only a few residues except for S1 and S2 (shown in light grey). The chemical structure of tyrosine, alanine, isoleucine and phenylalanine amino acids (aa) is indicated on the right. (**b**) Heatmap showing mean NLR values for the indicated protein pairs (n = 3 independent experiments). EWS_Nter and tyrosine mutants are tagged with GLucN1; and CNOT2 is tagged with GLucN2. (**c**) RT-qPCR analysis of the stability of the R-Luc-8MS2 mRNA reporter. Samples are RNA from HeLa cells transfected with the R-Luc-8MS2 reporter and either SIGQQS-MS2-CP or MS2-CP, and treated for 0, 1, 2, or 4 h with ActD. Dots and lines indicate individual values and means, respectively (n = 3 independent experiments). *p <0.05 compared to MS2-CP by two-tailed unpaired Student's *t*-test. HL = half-life.
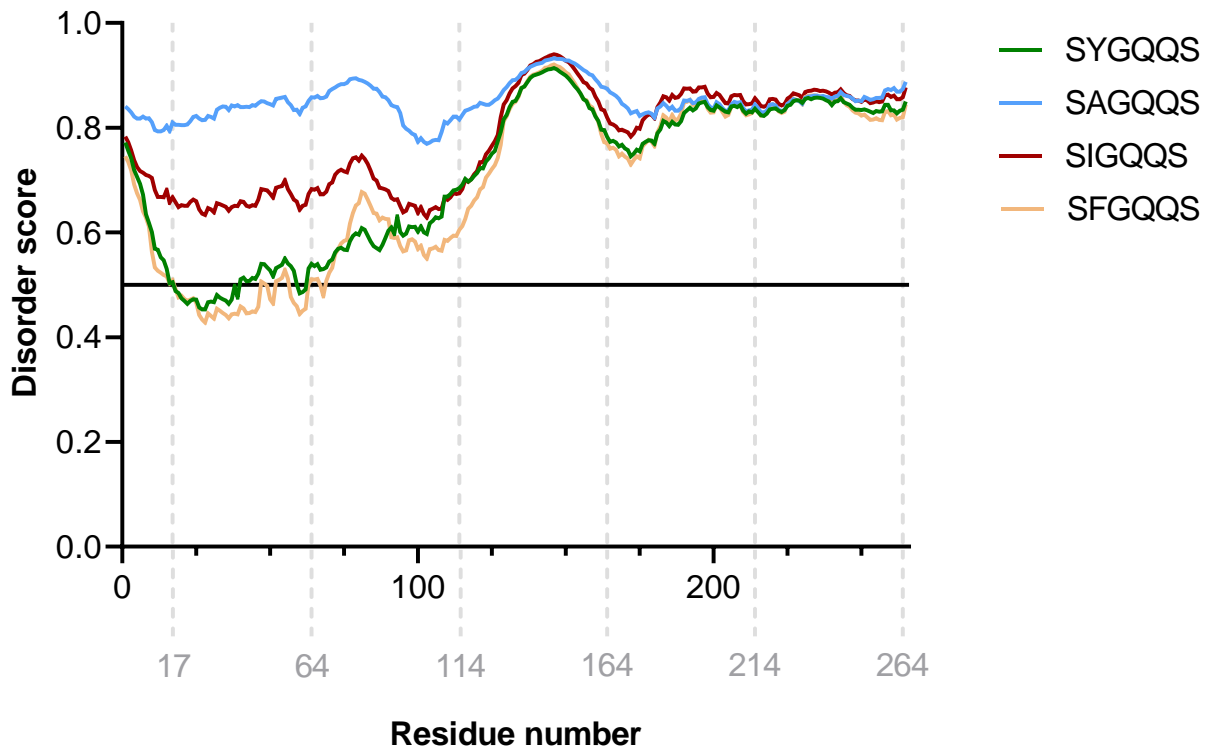
Figure 81. Disorder prediction along the EWS/EF_Nter sequence and three tyrosine mutants. Results are shown as means from eight algorithms: IUPRED2, VL3, RONN, SPOT-Disorder, AUCPred, ESpritz, Metadisorder and POODLE. The threshold score for disorder is 0.5 (solid horizontal black line).

5. The transcriptional, splicing and decay activities of EF are uncoupled

Given the well-described role of EF as a TF, we next investigated whether the transcriptional and decay activities of EF might be coupled. To address this issue, we first tested whether EF decay targets were transcribed from genes that are transcriptionally regulated by EF. To define the transcriptional target genes of EF, we used three different approaches criteria: we considered genes that i) were modulated after EF KD as identified in our DGE analysis (**Figure 82a**), ii) were bound by EF as determined by published ChIP-seq datasets [157], [243] (**Figure 82b**), or iii) genes whose expression was affected by EF KD that had a EF ChIP-seq peak (**Figure 82c**). For genes that were deregulated following KD of EF, we also distinguished between down- and up-regulated genes (**Figure 82d-e**). When generating lists of EF-bound genes based on ChIP-seq data from [243], we sub-categorized genes depending on peak location and considered EF ChIP-seq targets harboring a peak either within 2,000 kb upstream of the promoter (**Figure 82f-g**), or within the gene body (exons and introns) (**Figure 82h**). None of these datasets showed a significant overlap with EF mRNA decay targets, suggesting that the mRNA decay targets of EF are transcribed from genes that are not regulated nor bound by EF.

e

EF-repressed genes   EF decay targets

385 54 718

ns

f

% Feature

100
75
50
25
0

IP EF

- Exon
- TTS
- Promoter-TSS
- Intergenic
- Intron

g

EF-bound genes (promoter-TSS)   EF decay targets

847 107 665

ns

h

EF-bound genes (gene body)   EF decay targets

1,243 135 637

ns
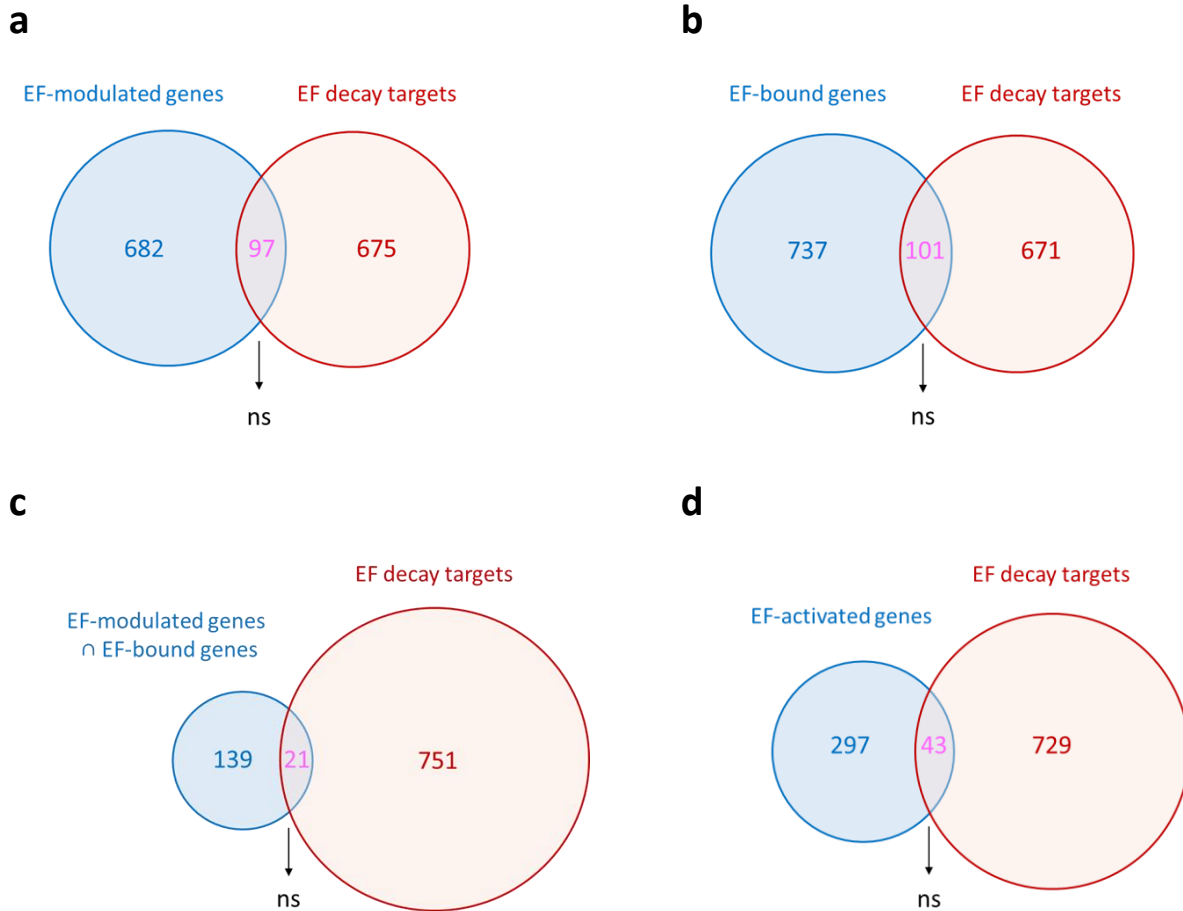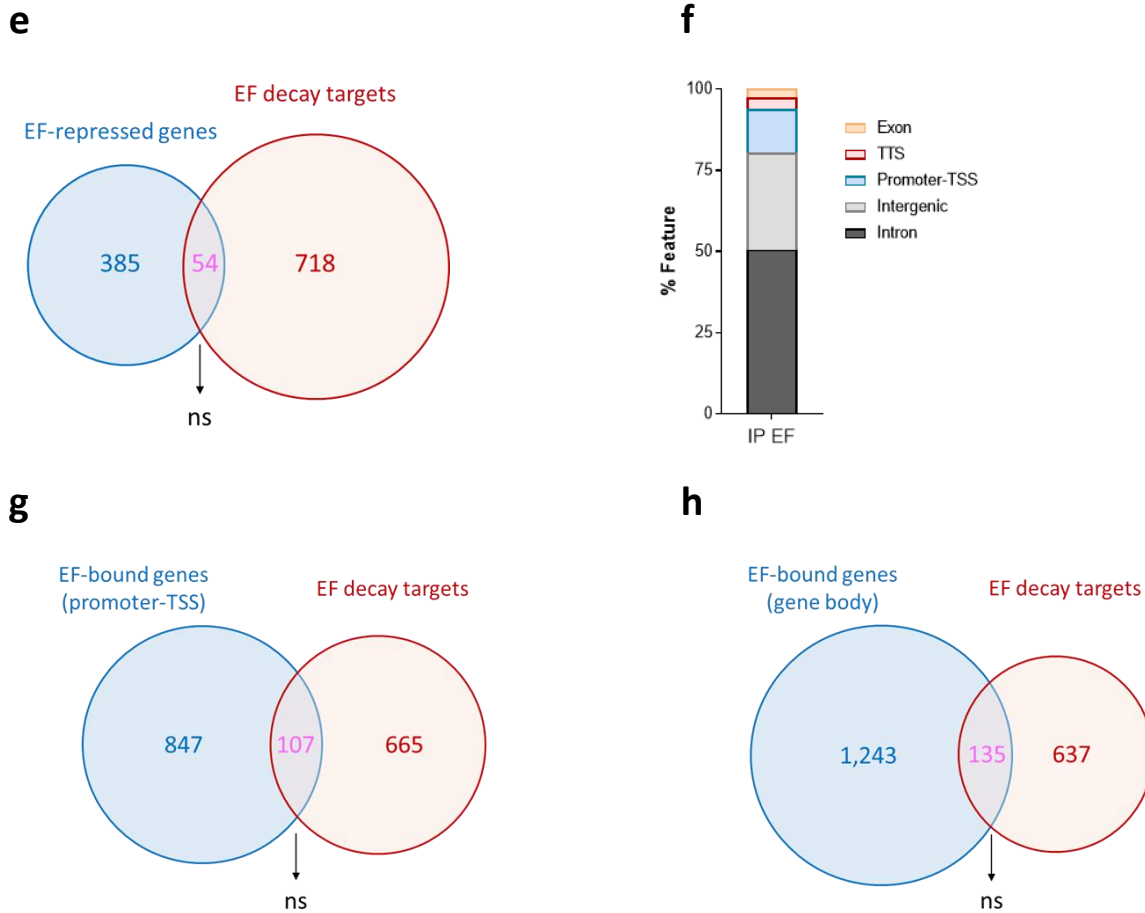
Figure 82. Comparison between EF transcriptional and mRNA decay targets. (**a**) Overlaps between either EF-modulated genes, EF-bound genes identified in [157] (**b**) or both modulated and bound genes (**c**) and decay targets identified in shA673-1c cells after EF knockdown. (**d**) Overlaps between either activated or (**e**) repressed genes and decay targets identified in shA673-1c cells after EF knockdown. (**f**) Peak location relative to annotation for EF ChIP-seq targets identified in [243]. (**g**) Overlaps between EF decay targets in shA673-1c cells after EF knockdown and EF-bound genes with a peak within 2000 kb upstream of the promoter or (**h**) within the gene body (exons + introns). For all comparisons, targets without detected half-life in shA673-1c cells were filtered out before testing overlap with EF decay targets. ns = not significant using Fisher's Exact Test.

To more directly test whether the mRNA decay function of EF might be linked to its transcriptional activity, we assessed the abilities of a transcriptional-defective mutant of EF (EFΔETS, harboring an 85 aa deletion within the ETS DNA-binding domain) to interact with CNOT2 and promote mRNA degradation of EF decay targets (**Figure 83a**). Compared to full-length EF, we found that the EFΔETS mutant, although transcriptionally inactive, retained full ability to interact with CNOT2 (**Figure 83b, c**). This was in sharp contrast to the EFYS37 mutant, which did not show any association with CNOT2 in the same assay, as expected (**Figure 80b**). Then, we expressed the FLAG-tagged version of the EFΔETS mutant in hMSCs and examined the change in HL of mRNAs from the panel of representative EF decay targets by RT-qPCR. As shown in **Figure 83**, the transcriptional mutant of EF promoted degradation of tested mRNAs, as efficiently as full-length EF (**Figure 83d, e**). Taken together, these results show that the ability to bind DNA is not involved in the mRNA decay activity of EF and that the transcriptional and decay functions of EF are independent.

Although our results suggest that EF controls different mRNA repertoires via its transcriptional and decay activities (see non-significant overlaps in **Figure 82**), it is possible that EF achieves control over the same biological functions through the concerted action of both activities. To test this, we compared the GO terms enriched in EF modulated genes (either downregulated or upregulated after EF KD) with the GO terms associated with EF mRNA decay targets. Interestingly, we found that GO terms related to cell cycle, cell division and cell proliferation were enriched both in the genes that are activated by EF and EF mRNA decay targets (**Figure 84a**). Similarly, we found that GO terms related to positive regulation of epithelial-to-mesenchymal transition and apoptotic processes were commonly enriched in EF-repressed genes and EF mRNA decay targets (**Figure 84b**). Together, this indicates that although the transcriptional and mRNA decay activities of EF target different genes, some of the resulting transcripts might encode functionally-related proteins.

In addition to transcription, EF has also been reported to play a role in mRNA alternative splicing [119], [203], [209], [213]. As for transcription, we therefore examined whether the mRNA splicing and decay functions of EF might be coupled. As for transcription, we found no significant overlap between the list of EF splicing targets identified in [119] and the list of its decay targets, identified here (**Figure 85a**). Interestingly, we found that GO terms related to cell cycle, which were already significantly over-represented both in EF transcriptional and decay targets (**Figure 84**) were also enriched in EF splicing targets (**Figure 85b**). This raises the intriguing possibility that EF might control specific biological pathways by the coordination of its transcriptional and post-transcriptional (*i.e.*, mRNA splicing and decay) activities.
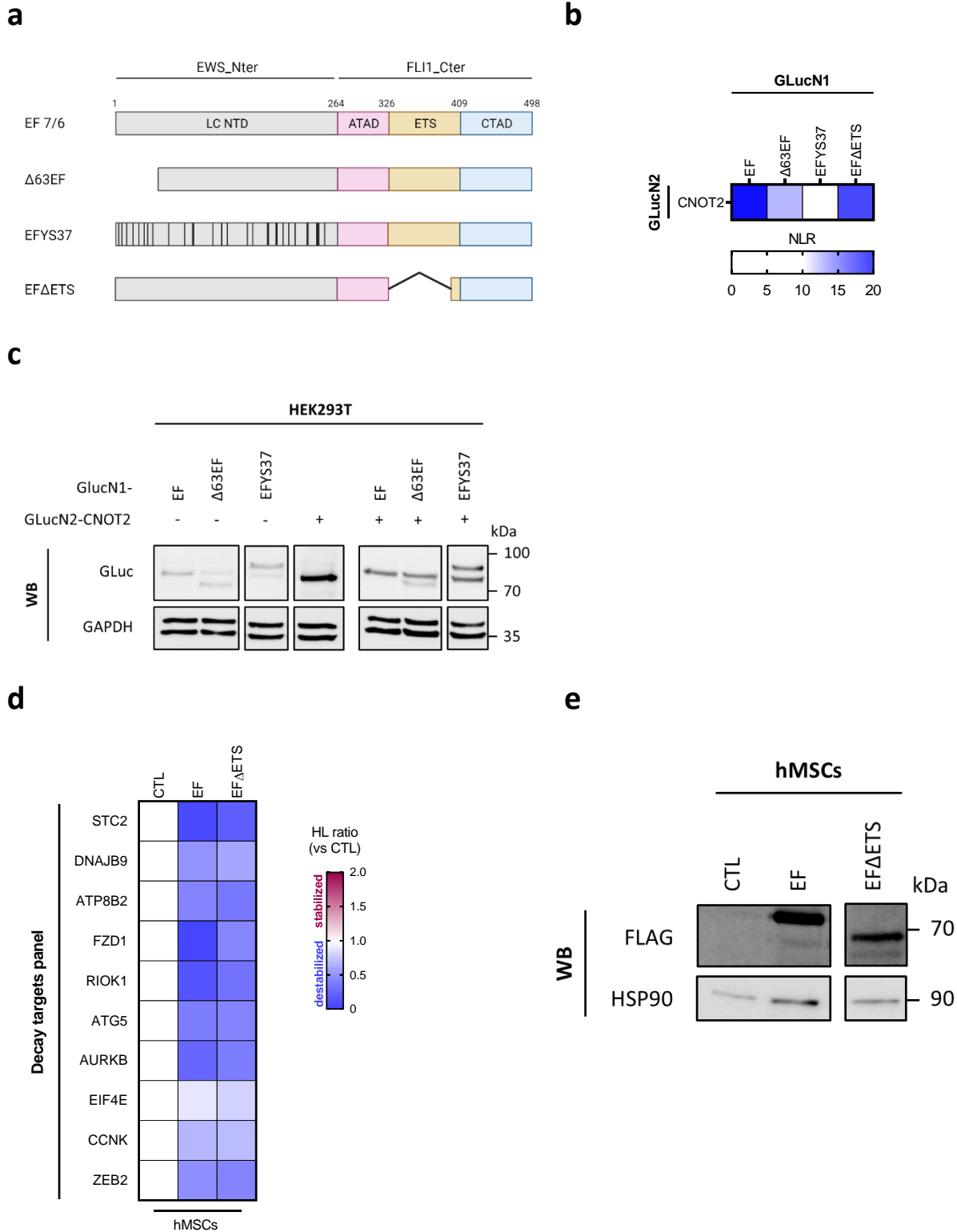
Figure 83. Decay activity of EFΔETS. (a) Schematic, domain structure of EF mutants (Δ63EF, EFYS37 and EFΔETS). Mutated tyrosine positions (black vertical bars) in EFYS37 do not reflect real positions. (**b**) Heatmap showing mean NLR values for the indicated protein pairs (n = 3 independent experiments). EF and EF mutants (Δ63EF, EFYS37 and EFΔETS) are tagged with GLucN1; and CNOT2 is tagged with GLucN2.

(**c**) Representative western blotting analysis of the indicated GLucN1/2-tagged proteins and GAPDH (loading control). Samples are lysates from HEK293T cells used for luminescence measurement. (**d**) Heatmap of half-life (HL) ratio detected by RT-qPCR after expression of FLAG-tagged EF, EFΔETS or control FLAG empty vector (CTL) in MSC cells for selected EF decay target genes (decay panel). Results are shown as means (n ≥ 2 independent experiments). For each gene, the HL ratio corresponds to the HL in EF or EFΔETS condition divided by the HL in the CTL condition. (**e**) Western blotting analysis of FLAG-EF or FLAG-EFΔETS and HSP90 (loading control). Samples are lysates from MSC cells expressing control FLAG empty vector (CTL) or indicated FLAG-tagged constructs.

a   **b**
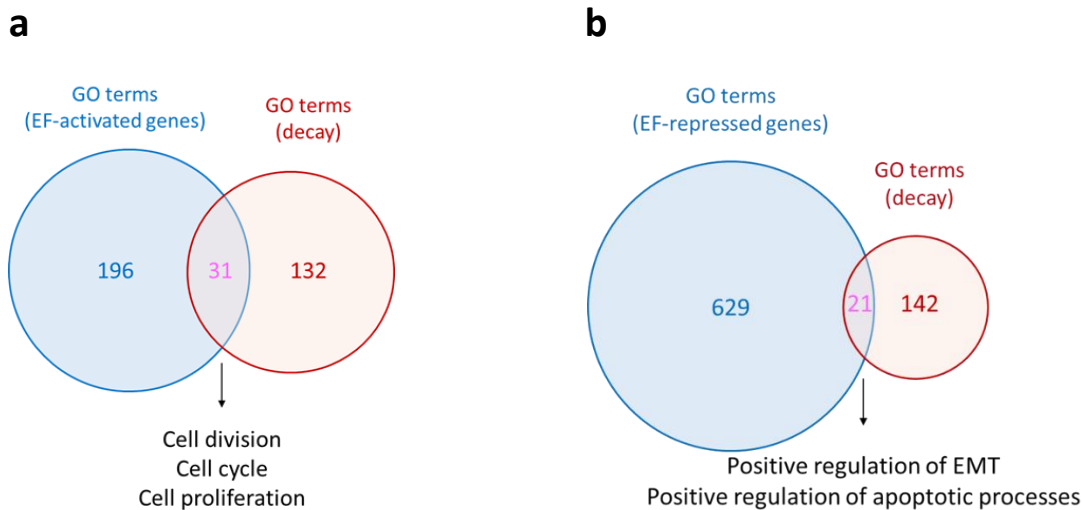
Figure 84. Functional coupling between the molecular roles of EF in transcription and decay. (**a**) Overlap of GO terms related to either EF downregulated genes (blue) or (**b**) EF upregulated genes (blue) and EF decay target genes (red).

a   **b**
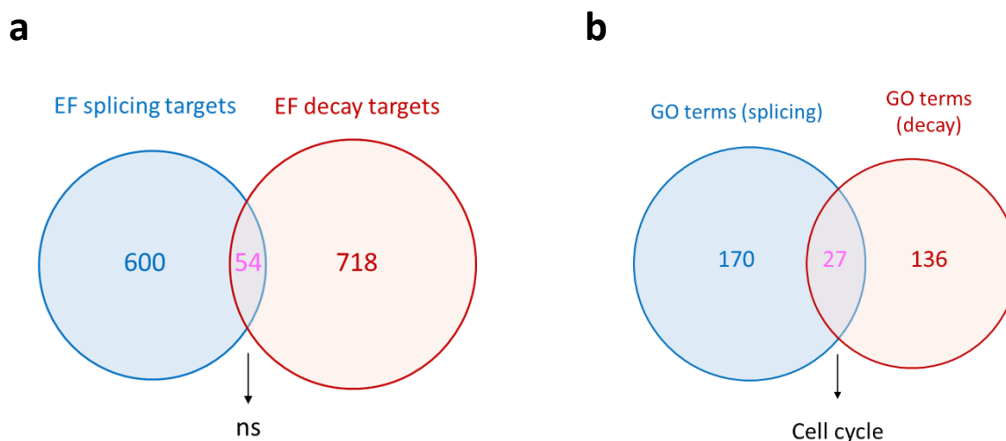
Figure 85. Comparison of the splicing and decay targets of EF. (**a**) Overlap between differentially stabilized genes and differentially spliced genes (identified in [119]) in shA673-1c cells after EF knockdown. ns = not significant using Fisher's Exact Test. EF splicing target genes without detected half-life in shA673-1c cells were filtered out before testing overlap with EF decay target genes. (**b**) Overlap of GO terms related to EF splicing target genes (blue) and EF decay target genes (red).

6. The decay mutant of EF is still active in transcription and splicing

To further disconnect the mRNA decay activity of EF from its previously described roles in transcription and mRNA splicing, we tested whether the mRNA decay mutant of EF (Δ63EF) was still functionally active as a transcription or splicing factor. To test the transcriptional activity of Δ63EF, we performed a reporter assay using a construct bearing a *Firefly* luciferase (*F-Luc*) gene expressed from a SV40 promoter harboring upstream 12x GGAA-repeats (**Figure 86a**). This reporter construct is specifically activated by EF, because of EF unique ability to bind to GGAA repeats [145], [158]. Although expressed at lower levels, the Δ63EF mRNA decay mutant behaved as a potent transcriptional activator in this assay and induced levels of *F-Luc* expression comparable to those induced by full-length EF, only slightly lower (**Figure 86b-c**). In contrast, negative controls, *i.e.*, the transcriptionally inactive FLAG-EFYS37 mutant [92], the DNA-binding deficient EFΔETS mutant or FLI1, had no effect, as expected. Transcriptional activity of EF has been directly linked to its phase transition properties, which are mediated by its EWSR1-derived N-terminal domain [92]. To evaluate the effect of deleting the first 63-aa of EF on its phase transition properties, we expressed FLAG-tagged versions of full-length EF, Δ63EF and EFYS37 in HeLa cells and performed a previously described biotinylated isoxazole (b-isox) precipitation assay [92]. EFYS37 is a tyrosine mutant of EF that lacks phase transition abilities [92]. b-isox-mediated precipitation of Δ63EF was comparable to that of full-length EF, while the EFYS37 mutant failed to precipitate, even in the presence of 100 µM of b-isox (**Figure 86d**). To confirm these results, we performed a previously described Number and Brightness (N&B) analysis [631] with cells expressing FLAG-tagged full-length EF or Δ63EF and found that EF and Δ63EF form aggregates with comparable stoichiometry of between 3 and 4 molecules (**Figure 86e**). Taken together, these results indicate that the transcriptional and phase transition properties of EF are not significantly affected in the Δ63EF mutant.

Next, we assessed the integrity of the newly described mRNA splicing function of EF in the Δ63 decay mutant. To this aim, we tested Δ63EF in a splicing reporter assay described in [119], [632]. In this assay, the Δ63EF mutant behaved similarly to full-length EF and induced inclusion of the reporter exon, albeit to a slightly smaller extent (**Figure 87**). Overall, we concluded that the molecular functions of EF in transcription, splicing and decay are disconnected and regulate different gene repertoires. Nevertheless, our analyses provide evidence that these molecular functions can control common biological functions such as cell cycle and cell proliferation.

a

SV40 promoter

Firefly luciferase

12xGGAA-repeats

d

b

e

c
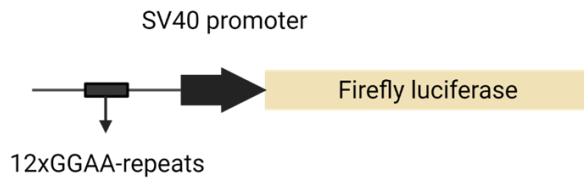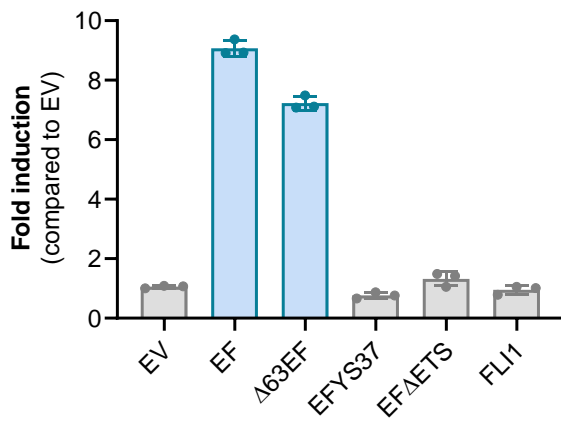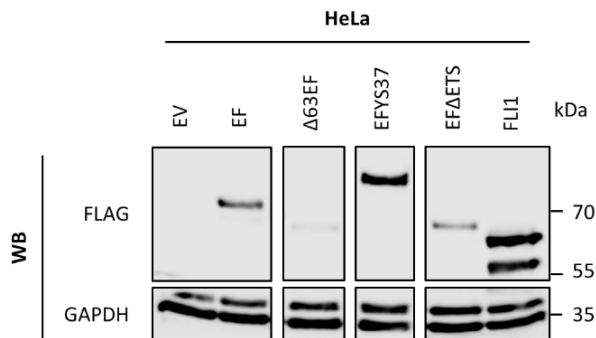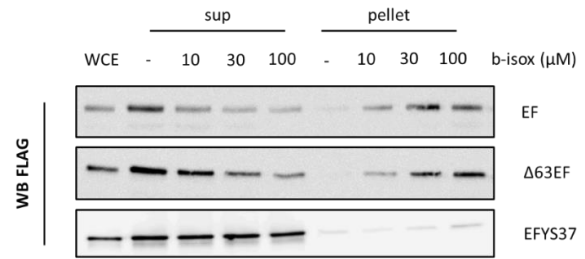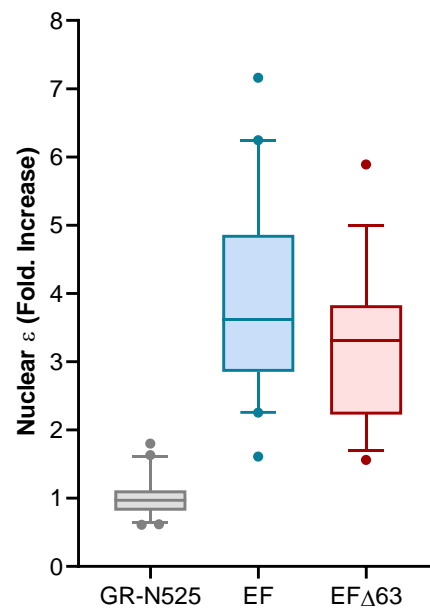
Figure 86. Transcriptional activity of the Δ63EF decay mutant. (**a**) Schematic, Firefly luciferase reporter harboring 12xGGAA-repeats upstream the SV40 promoter. (**b**) GGAA induction assay for the indicated FLAG-tagged constructs co-transfected into HeLa cells with a F-Luc reporter vector harboring 12x GGAA repeats and a R-Luc vector (internal control). Results are shown as means ± SD (n = 3 independent experiments). F-Luc activity was normalized to R-Luc activity. Fold induction are relative to normalized F-Luc activity for the control FLAG empty vector condition (EV). (**c**) Western blotting analysis of FLAG-tagged EF or indicated EF mutants, and GAPDH (loading control). Samples are lysates from HeLa cells used for GGAA induction assays. (**d**) Dose-dependent b-isox precipitation assay in HeLa cells transfected with FLAG-tagged EF or mutants (Δ63EF and EFYS37). WCE = whole cell extracts, sup = supernatant. (**e**) N&B analysis in U2OS cells transfected with EGFP-tagged indicated constructs (n = 2-4 independent experiments) or mGR-N525-EGFP (monomeric control). Y-axis shows the fold increase of the molecular brightness (ε) in the nucleus, relative to GR-N525. Centered lines show the medians, box limits indicate the 5th and 95th percentiles.
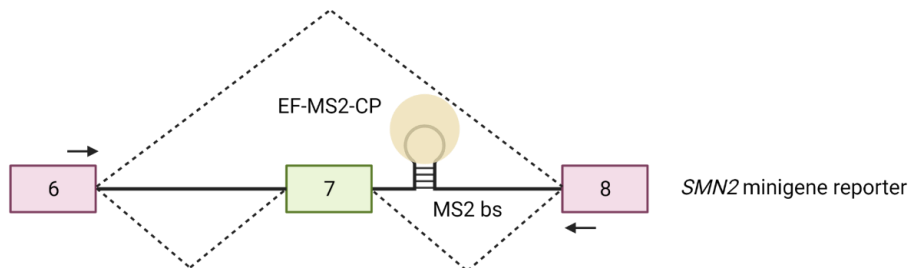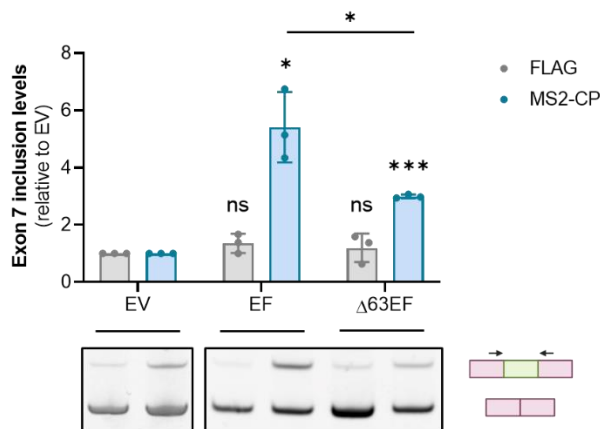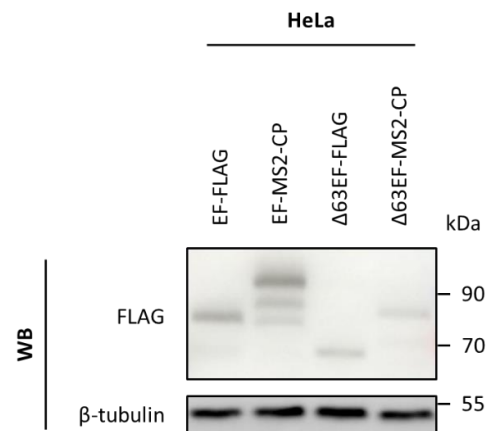
Figure 87. Splicing activity of the Δ63EF decay mutant. (**a**) Schematic, *SMN2* minigene reporter and MS2-CP-tagged EF. An MS2 binding site is inserted in the intron downstream from exon 7. The primers for qPCR are indicated by arrows. (**b**) qPCR analysis of *SMN2* minigene reporter exon 7 inclusion. Samples are RNA from HeLa cells transfected with the *SMN2* minigene reporter and either FLAG- or MS2-CP-tagged versions of EF and Δ63EF. Results are shown as means ± SD (n = 3 independent experiments) relative to control empty vector (EV). ***p <0.001; *p <0.05; ns = not significant by one-sample *t*-test, or two-tailed unpaired Student's *t*-test. (**c**) Representative western blotting analysis of the indicated FLAG/MS2-CP-tagged proteins and β-tubulin (loading control). Samples are lysates from HeLa cells used in (**b**).

7. EF is recruited to target mRNAs through its interaction with HuR

Our results so far point towards a model in which EF associates with specific mRNAs to promote their degradation via the recruitment of the CCR4-NOT complex. One critical question underlying this model is how EF might be recruited to its target mRNA transcripts in the absence of identifiable canonical RNA-binding domain. Because the 3'UTR region is a key determinant of mRNA stability [427], we reasoned that analyzing the features of the 3'UTR regions of EF mRNA decay targets might help in answering this question. To this aim, we retrieved the 3'UTR sequences (poly(A) tail not included) of mRNAs that are stabilized upon EF KD (called hereafter "target 3'UTRs"). As a control, we also retrieved the 3'UTR sequences of the mRNAs whose stability remained unchanged after EF KD (called hereafter "non-target 3'UTRs"). In total, we obtained 746 target 3'UTR sequences (746/772; ~97%) and 6,215 non-target 3'UTR sequences (6,215/6,372; ~98%).

Then, we searched for motifs of known RBP that might be enriched in target 3'UTRs using the MEME suite. Among the identified RBP motifs, were the motifs for HuR, PTBP1 and TIA1, which are AREBPs (**Figure 88a**). Interestingly, HuR stood out of this analysis as the RBP with the highest number of enriched motifs and as the RBP with the most statistically enriched motifs (**Figure 88b**). In agreement with this finding, a mass spectrometry-based study identified HuR among EF-interacting partners in EwS cells [209]. Of note, we also analyzed the length and GC content of 3'UTR sequences and found that on average, the 3'UTR of EF targets were significantly smaller and had a significantly lower GC content than non-target 3'UTRs (**Figure 88c-d**). GC content is an important feature of mRNA stability. For instance, low GC contents can result from overrepresentation of AU-rich motifs that are recognized by stabilizing or destabilizing ARE-binding proteins (AREBPs) [469], [633]. By performing an unbiased heptamer enrichment analysis, we found significant enrichment of AU-rich heptamers in the target 3'UTRs (**Figure 88e**), thus confirming our results from the MEME analysis. Altogether, these data suggest that EF might be recruited to its decay targets indirectly, through interactions with RBPs, including HuR.

To test this hypothesis, we compared the list of EF mRNA decay targets with a set of HuR binding targets identified from photoactivable ribonucleoside cross-linking and immunoprecipitation (PAR-CLIP)-seq study [568]. We found a significant overlap between EF decay targets and HuR targets (**Figure 89a**). GO analysis on the overlapping targets revealed a statistical enrichment for the GO terms related to cell division, transcription and cell cycle (**Figure 89b**). Interestingly, most (359/519; 69.2%) of the 519 overlapping mRNAs between EF decay targets and HuR binding targets appeared to have at least one HuR PAR-CLIP peak located in their 3'UTR (**Figure 90a**). The same holds true for the 10 representative EF decay targets, all of which were predicted to harbor at least one HuR binding site in their 3'UTR, using a bioinformatic prediction tools (**Figure 90b**). Association of HuR was verified for *EIF4E*, *ZEB2* and *ATP8B2* transcripts in EwS shA673-1c cells by RNA IP. Interestingly, these targets were similarly enriched in RNA-HuR IP whether EF was present (-dox) or absent (+dox) (**Figure 91**). This shows that the presence of EF does not influence HuR association with its target mRNAs.

a

b

Motif type	Motif	p-value
AU-rich	HuR RNCMPT00032	1.59e-52
	HuR RNCMPT00274	1.48e-43
	HuR RNCMPT00117	7.56e-20
	HuR RNCMPT00112	7.45e-17
	HuR RNCMPT00136	8.71e-10

c

d

e
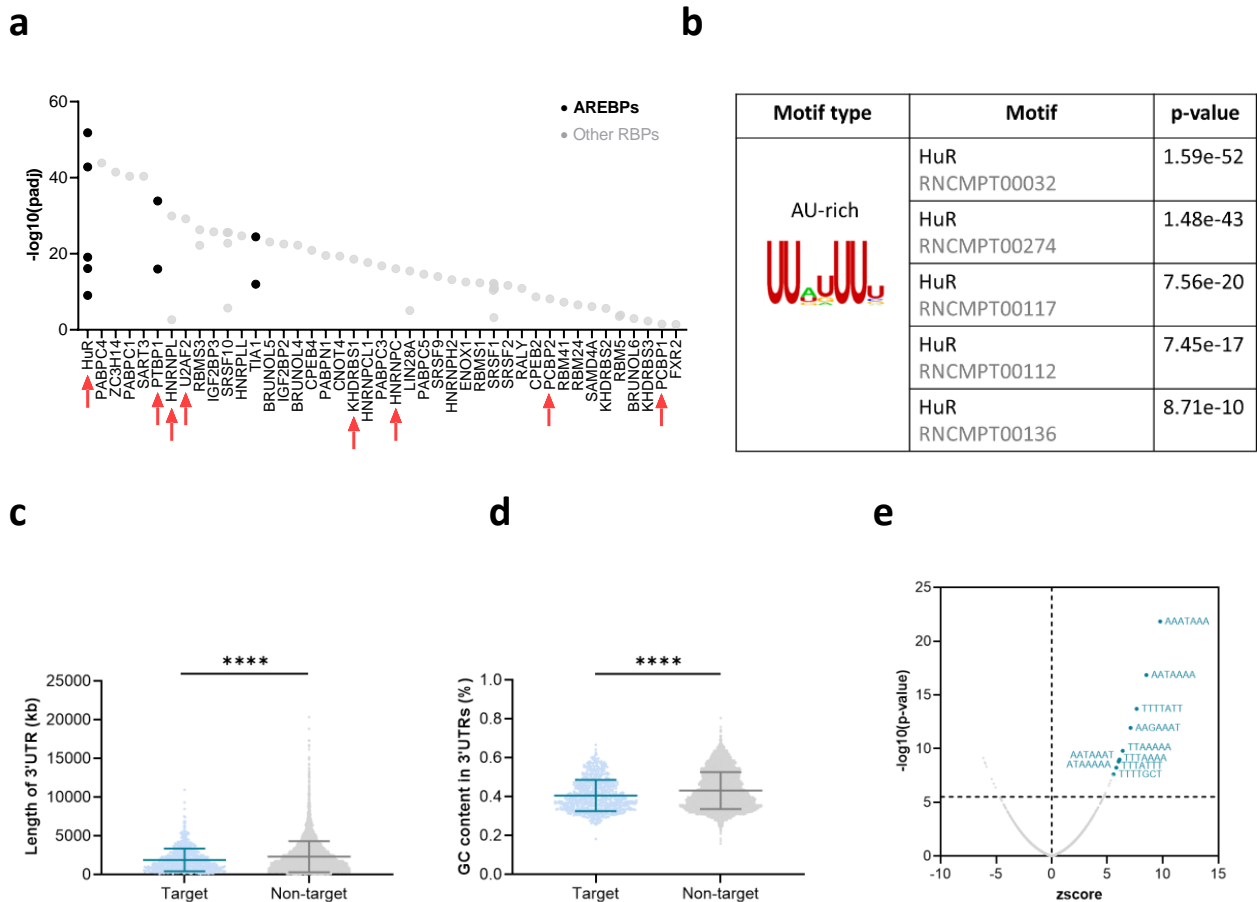
Figure 88. Features of the 3'UTR sequences of EF decay targets. (**a**) RNA-binding protein motif enrichment analysis of target 3'UTRs. 3'UTR sequences of EF decay targets were screened for RNA-binding motifs using AME from MEME suite. Enriched motif(s) of RBPs with an adjusted p-value (padj) <0.05 are shown. AU-rich RNA-binding proteins (AREBPs) are in black. Red arrows indicate RBPs identified in an interactome of EF [209]. (**b**) Table with enriched HuR motifs identified in AME analysis. (**c**) Comparison of 3'UTR length (kb) (**d**) and GC content (%) between target and non-target 3'UTRs. ****p <0.0001 compared to control by two-tailed unpaired Student's *t*-test with Welch's correction (**e**) Heptamer enrichment analysis of the EF decay targets detected in shA673-1c cells. Target and non-target 3'UTR sequences were screened for heptamers using regular expression in R. The 10-first most significantly enriched heptamers are indicated in blue. p-value threshold (black horizontal dotted line) was determined using bonferonni correction for multiple-testing.

a

b
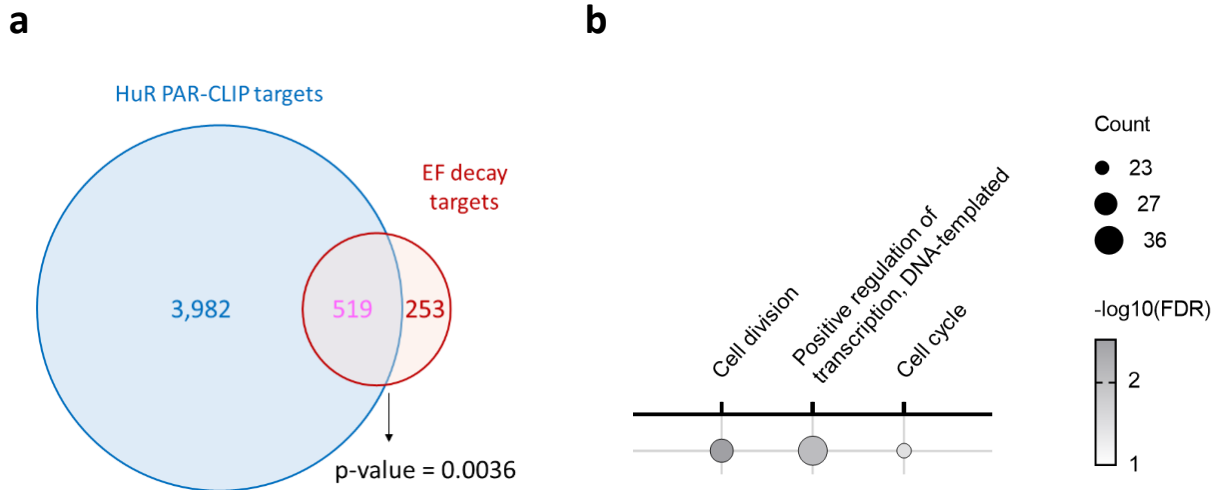
Figure 89. Comparison of EF mRNA decay targets with mRNA targets of HuR and GO analysis. (a) Overlap between EF mRNA decay targets and HuR binding targets identified in [568]. p-value was calculated using Fisher's Exact Test. mRNA targets without detected half-life in shA673-1c cells were filtered out before testing overlap with EF decay targets. **(b)** Enriched GO terms on the overlapping targets (FDR <0.1). Points are scaled by number of genes and ranked according to colored p-values. Enrichment analysis was performed with DAVID and p-values were calculated using FDR correction.

a

b
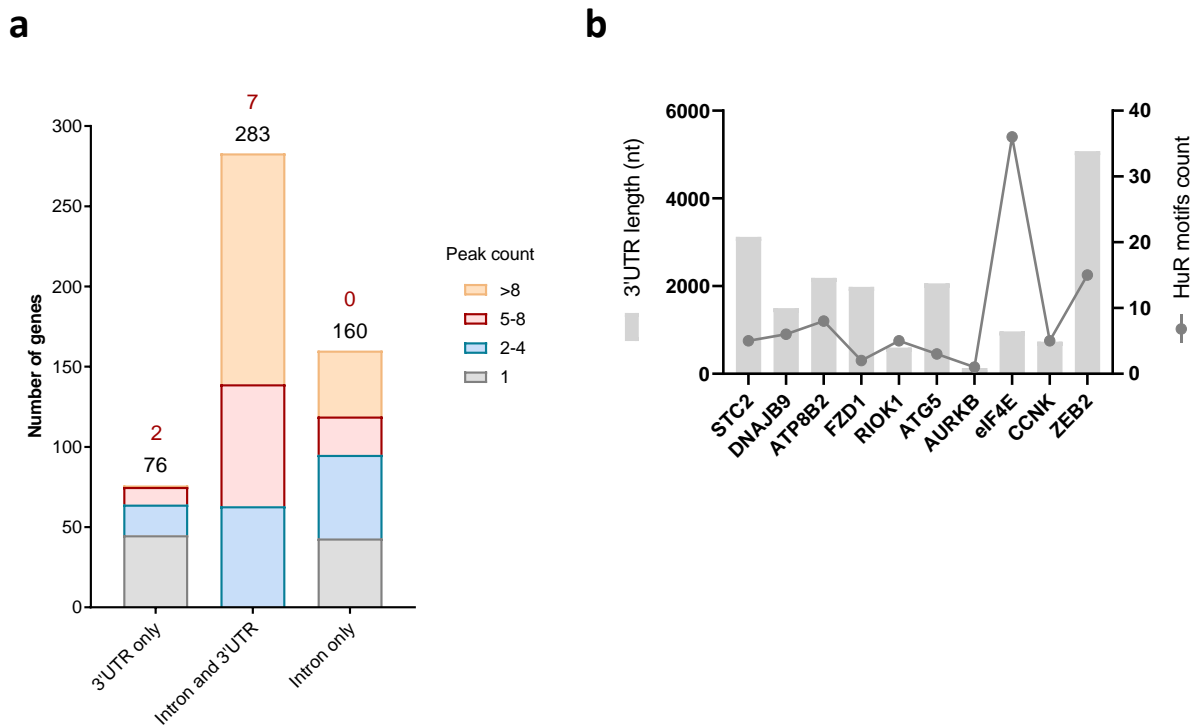
Figure 90. Features of EF decay targets. (a) Number of genes from overlap in **Figure 89a** classified relative to peak location and count. For each peak location, the total number of genes from overlapping targets and from the decay panel is indicated in black and in red, respectively. **(b)** Length and count of HuR binding motifs in the 3'UTRs of the representative set of EF decay targets. nt = nucleotide.

a
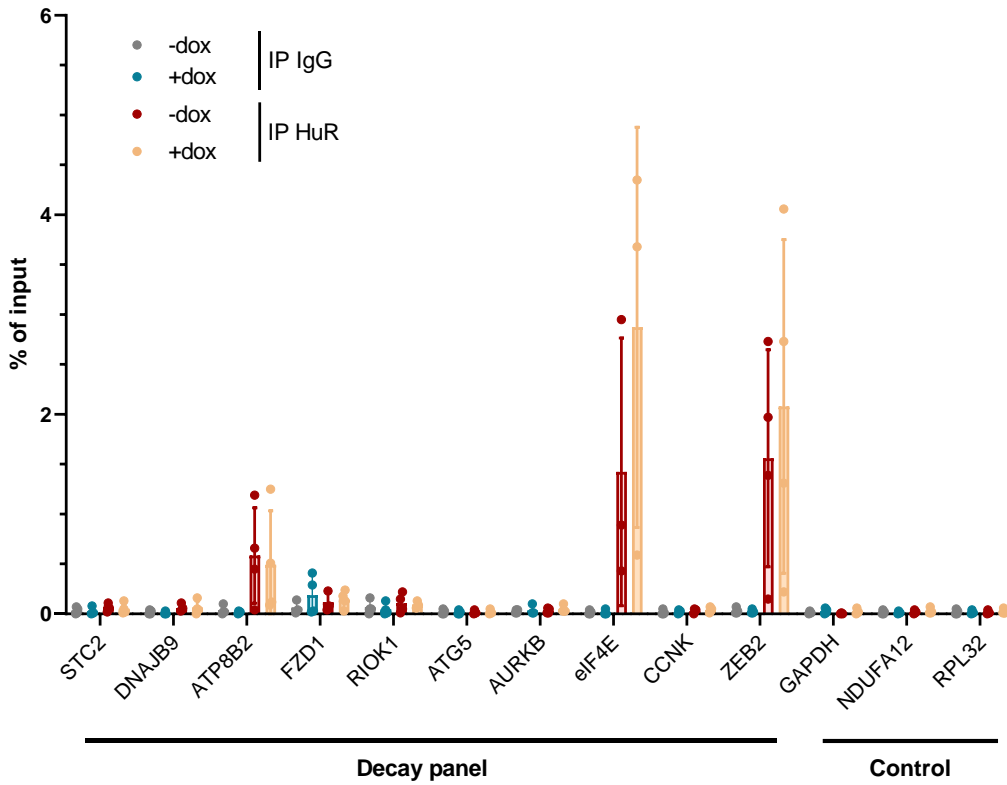
b
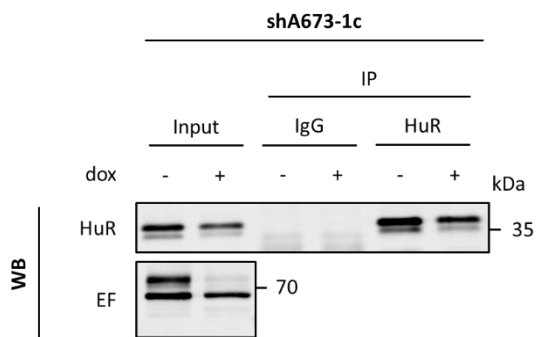
Figure 91. HuR RNA IP experiment in shA673-1c -/+ dox cells (**a**) Immunopurification of RNA-HuR complexes and RT-qPCR for the decay panel and indicated controls (n ≥ 3 independent experiments). Results are shown as means ± SD. (**b**) Immunoprecipitation (IP) of endogenous HuR in shA673-1c -/+ dox cells followed by western blotting analysis for the indicated proteins.

Then, we tested whether EF and HuR might associate in coimmunoprecipitation experiments and found that EF indeed copurified with endogenous HuR in EwS cells. In contrast, no association could be detected with TIA1 (**Figure 92a-b**). In a reverse approach, HuR copurified with EF (**Figure 92c**), supporting the idea that they might be part of the same complex. Then, we sought to identify the regions of HuR and EF involved in their interaction. Using different deletion mutants of EF and HuR, we located the interaction regions to the FLI1-derived CTAD domain on EF and the RRM3 domain on HuR (**Figure 93**). Both regions were necessary for the interaction to occur.

a

b

c
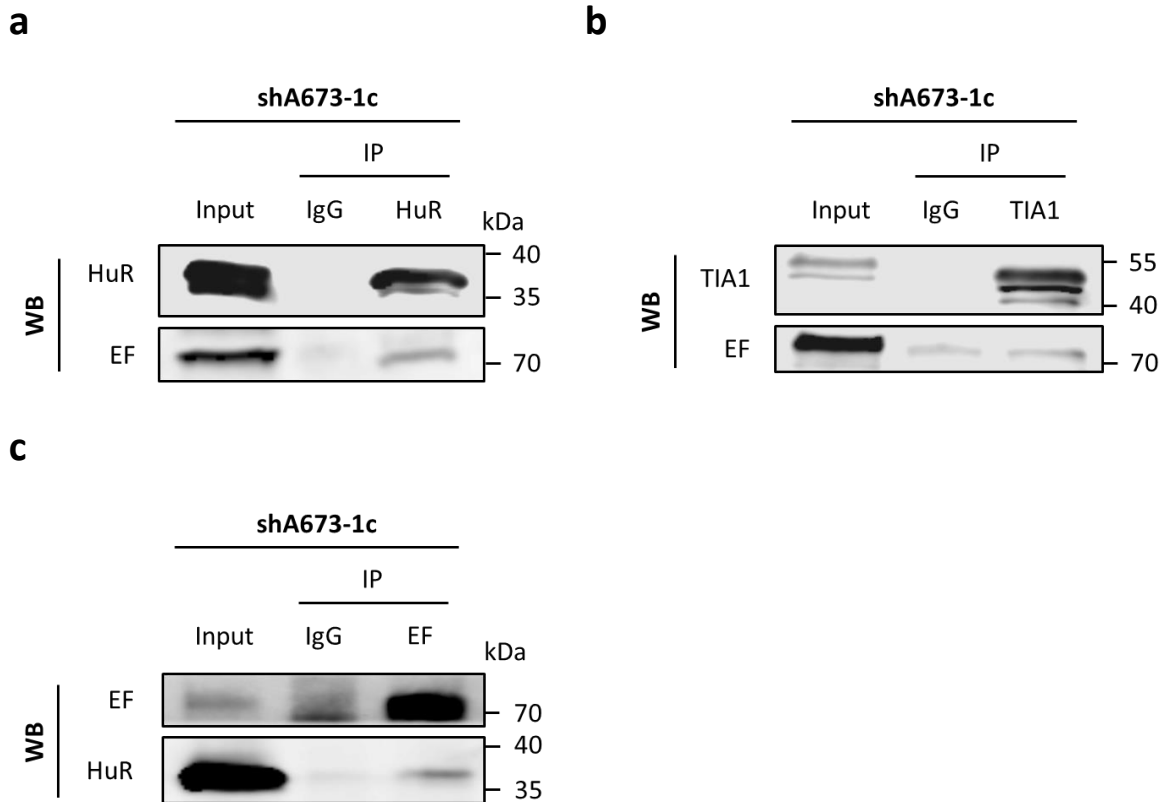
Figure 92. Coimmunoprecipitations between enriched AREBPs and EF. (**a**) Immunoprecipitation (IP) of endogenous HuR and (**b**) TIA1 with EF from shA673-1c cell lysates followed by western blotting (WB) for the indicated proteins. (**c**) Immunoprecipitation (IP) of endogenous EF with HuR from shA673-1c cell lysates followed by western blotting (WB) for the indicated proteins.
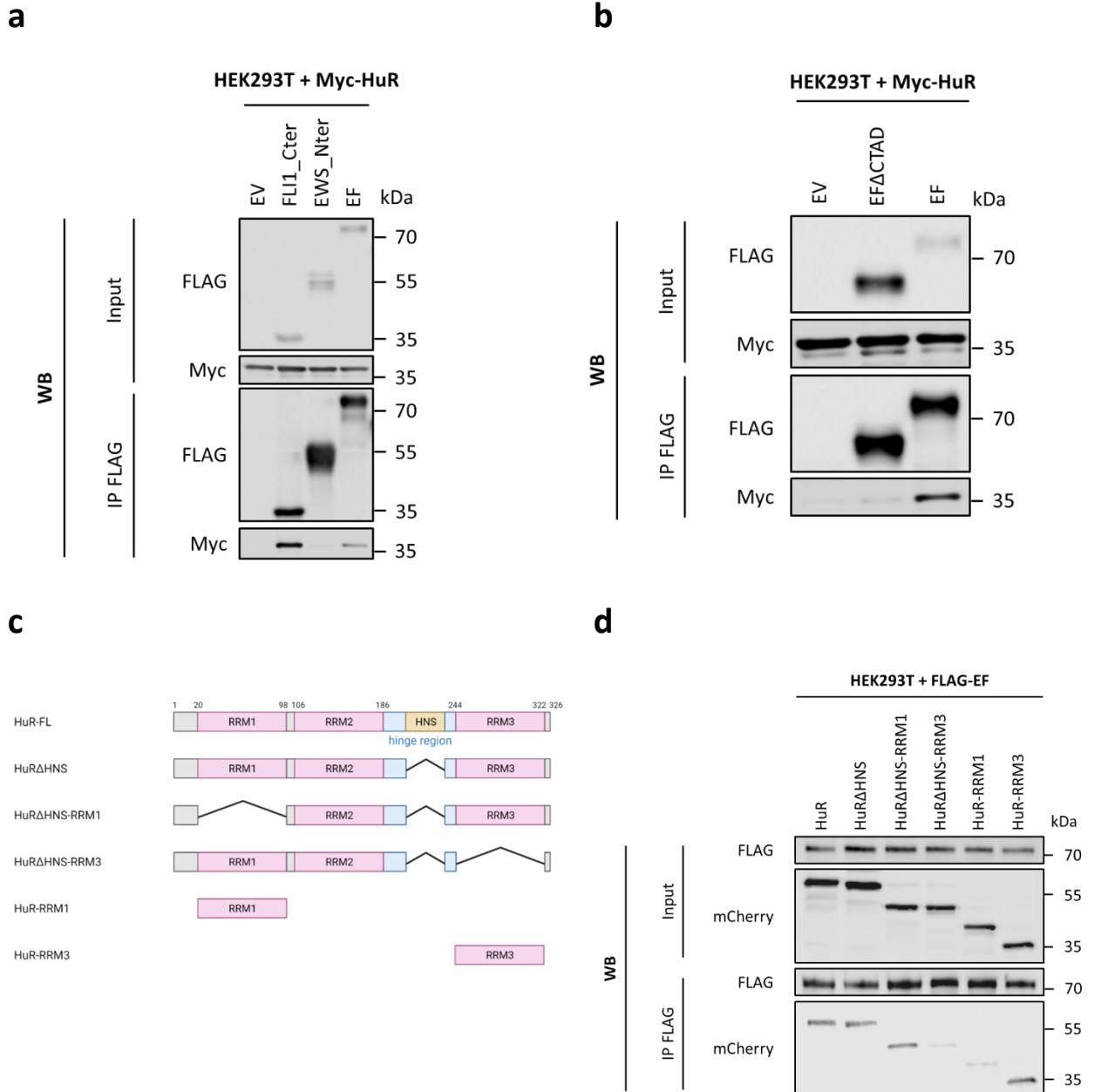
Figure 93. Mapping of the interaction between EF and HuR. (**a**) Immunoprecipitation (IP) of FLAG-tagged constructs followed by anti-FLAG and anti-Myc western blotting (WB). Samples are lysates from HEK293T cells transfected with FLAG-EF, FLAG-EWS_Nter, FLAG-FLI1_Cter, or control FLAG empty vector (EV); together with Myc-HuR. (**b**) Immunoprecipitation (IP) of FLAG-tagged EF or EFΔCTAD followed by anti-FLAG and anti-Myc western blotting (WB). Samples are lysates from HEK293T cells transfected with FLAG-EF, FLAG-EFΔCTAD, or control FLAG empty vector (EV); together with Myc-HuR. (**c**) Schematic, domain structure of HuR-deletion mutants. FL = full-length. (**d**) Immunoprecipitation (IP) of FLAG-tagged EF followed by anti-FLAG and anti-mCherry western blotting (WB). Samples are lysates from HEK293T cells transfected with the indicated mCherry-tagged HuR constructs and FLAG-EF.

Next, to further test the idea that EF is recruited to mRNAs via binding to HuR, we decided to assess the stability of the representative EF mRNA decay targets and the ability of EF to bind to these targets in EwS cells after treatment with dihydrotanshinone-I (DHTS), a chemical inhibitor of HuR known for interfering with its RNA-binding ability [479], [480] (see chemical structure in **Figure 96a**). To this aim, we preliminarily assessed the viability of shA673-1c cells after exposure to various concentrations of DHTS using a resazurin-based cell viability assay (not shown). Then, we treated EwS cells with sublethal doses of DHTS (10 μM for 1h) or vehicle (dimethylsulfoxide, DMSO) and assessed the stability of the representative EF mRNA decay targets by RT-qPCR. Similarly to knocking down EF or CNOT2, treatment with DHTS led to a significant stabilization of all EF decay targets (**Figure 96b**). Importantly, EF and HuR mRNA levels were not affected by DHTS (**Figure 96c**). Moreover, we found that DHTS treatment significantly compromised the ability of EF to associate with most of its decay targets (7 out of 10 targets, **Figure 95a**, control western blot in **Figure 95b**). Altogether, these results support that the RNA-binding ability of HuR is important for targeting the decay activity of EF.
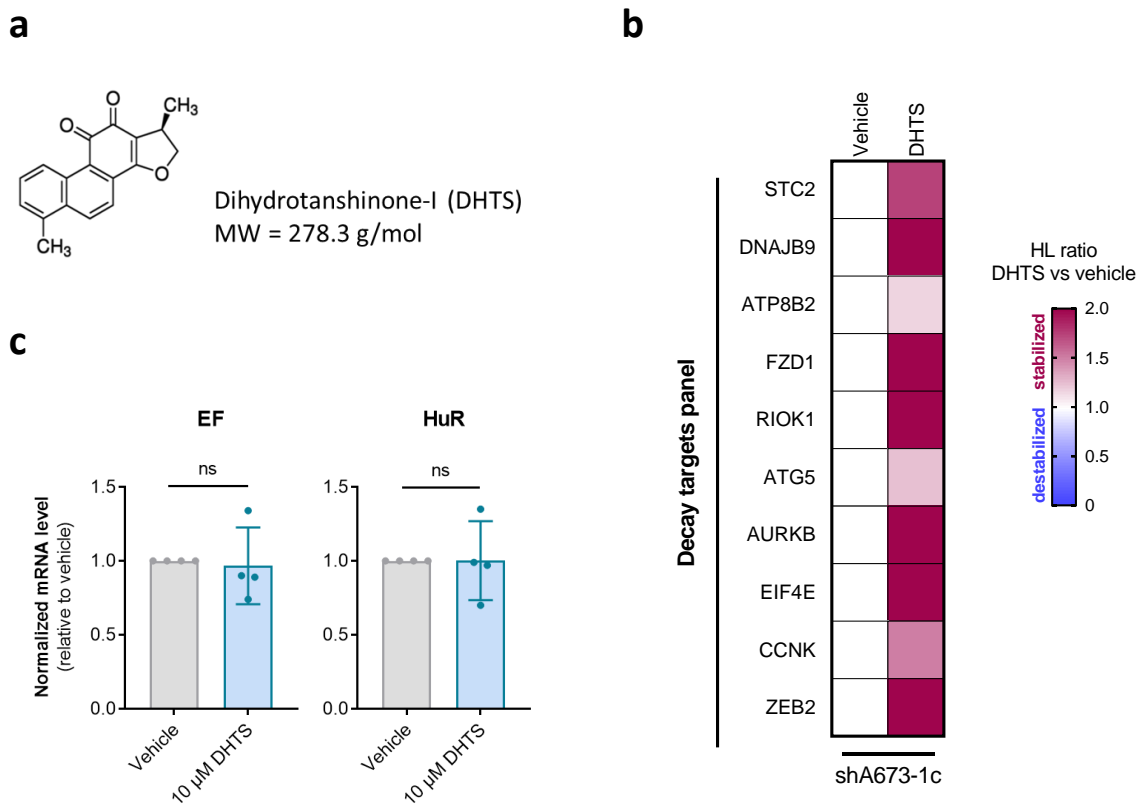
Figure 94. Stability of the decay panel after sublethal treatment with DHTS. (**a**) Chemical structure of DHTS. (**b**) Heatmap of half-life (HL) detected by RT-qPCR for selected EF decay target genes (decay panel) in shA673-1c cells treated with DMSO (vehicle) or with 10 μM DHTS for 1h. Results are shown as means (n = 4 independent experiments). (**c**) Normalized mRNA levels of EF and HuR assessed by in shA673-1c cells treated with 10 μM DHTS or vehicle. Results are shown as means ± SD (n = 4 independent experiments). mRNA levels are relative to vehicle condition. ns = not significant compared to vehicle condition by one-sample *t*-test.
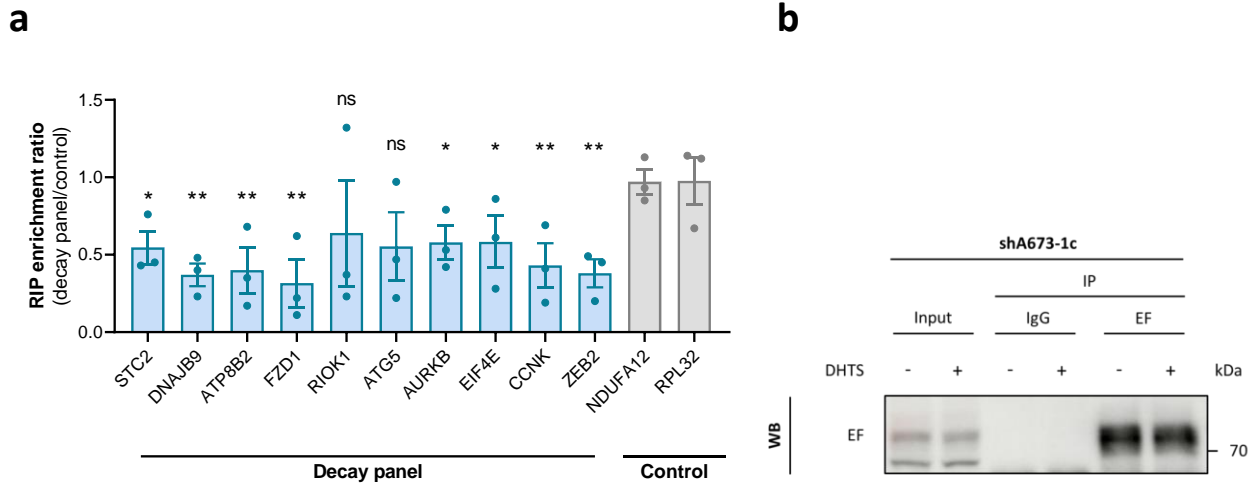
Figure 95. EF RNA IP experiment in shA673-1c cells treated with DHTS or vehicle. (**a**) Immunopurification of RNA-EF complexes and RT-qPCR for the decay panel and indicated control genes in shA673-1c cells treated with DMSO (vehicle) or with 10 µM DHTS for 1h (n = 3 independent experiments). For each mRNA, RIP enrichment is defined as the ratio between its % of input in the EF IP with DHTS and the one in the EF IP with vehicle. For each mRNA, RIP enrichment ratio is computed as the ratio between its RIP enrichment and the one of control mRNAs. Results are shown as means ± SD. *p <0.05; **p <0.01; ***p <0.001; ****p <0.0001; ns = not significant compared to mean RIP enrichment ratio of control mRNAs by two-tailed unpaired Student's *t*-test. (**b**) Western blotting analysis of EF after RNA IP in shA673-1 cells treated with vehicle (DMSO) or with 10 µM DHTS for 1h.

Based on our observations that EF associates with CCR4-NOT and HuR associates with EF, we hypothesized that EF might bring HuR and CCR4-NOT together in the same complex. To test this, we performed endogenous coimmunoprecipitations between CNOT2 and HuR in the presence or absence of EF in EwS cells. Strikingly, we found that HuR coimmunoprecipitated with CNOT2, only in the presence of EF (**Figure 96**).
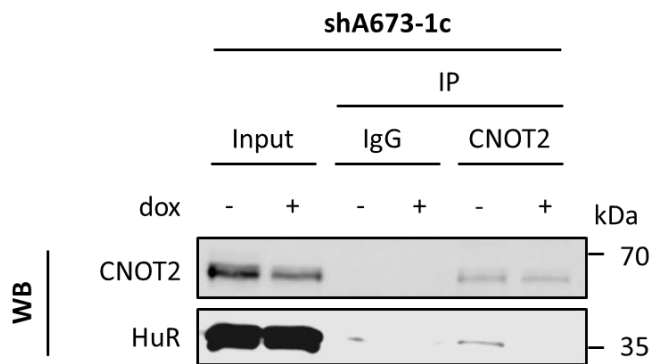
Figure 96. CNOT2/HuR association in the presence/absence of EF. Immunoprecipitation (IP) of endogenous CNOT2 followed by western blotting (WB) for the indicated proteins. Samples are total lysates from EwS shA673-1c -/+ dox cells.

8. EF antagonizes the mRNA protective function of HuR

HuR is a well-described cancer-associated RBP known to positively regulate mRNA stability by competing with TTP for AU-rich elements (AREs) [465], [568]. Because HuR normally acts as an mRNA stabilizing RBP, it was unexpected to find it associated with an mRNA destabilizing factor such as EF. To clarify this issue, we first investigated the effects of silencing HuR on the stability of the representative EF decay targets. In EwS cells, HuR KD strongly increased the stability of all tested EF targets, supporting the idea that in this cellular context, HuR behaves as an mRNA destabilizing factor. Remarkably, when repeating this analysis in EwS cells in which EF expression was prevented, we found that HuR KD had the opposite effect and decreased the stability of the EF decay targets (**Figure 97**). Importantly, we previously showed that the presence of EF does not influence HuR association with its target mRNAs (**Figure 91**).

To go further, we used a previously described HuR reporter assay [627]. This assay uses a *Renilla* luciferase reporter mRNA carrying eight AREs in its 3'UTR (*R-Luc-8AU*), allowing the specific recruitment of ectopically expressed HuR, and a control reporter lacking ARE (*R-Luc-0AU*) (**Figure 98a**). Stabilization of the reporter mRNA is then assessed by measuring luciferase expression and calculating a luciferase activity ratio between HuR-transfected and not transfected cells (luciferase activity in cells transfected with a HuR expression vector / luciferase activity in cells transfected with a control vector). An increase in the luciferase activity is thus a proxy for an increase in HuR mRNA stabilizing function. This assay was applied in shA673-1c EwS cells in the presence or absence of EF (-dox and +dox, respectively). shA673-1c cells were thus transfected either with mCherry-tagged HuR or a control mCherry empty vector together with *R-Luc*-8AU or *R-Luc-0AU* mRNA reporters and treated or not with dox, to KD EF expression. Consistent with our model, preventing expression of EF with dox increased the luciferase activity ratio for the *R-Luc-8AU* reporter, indicating that the presence of EF inhibits the mRNA protective effect of HuR (**Figure 98b-c**). As a control, EF KD had no effect on the luciferase activity ratio of the HuR-insensitive reporter (*R-Luc-0AU*). Interestingly, we also found that the knockdown of EF in shA673-1c cells, increased protein production of several targets of the decay panel (**Figure 98d**). Altogether, these observations support the idea that by associating with EF and the CCR4-NOT complex, HuR is turned into a destabilizing factor in EwS cells.
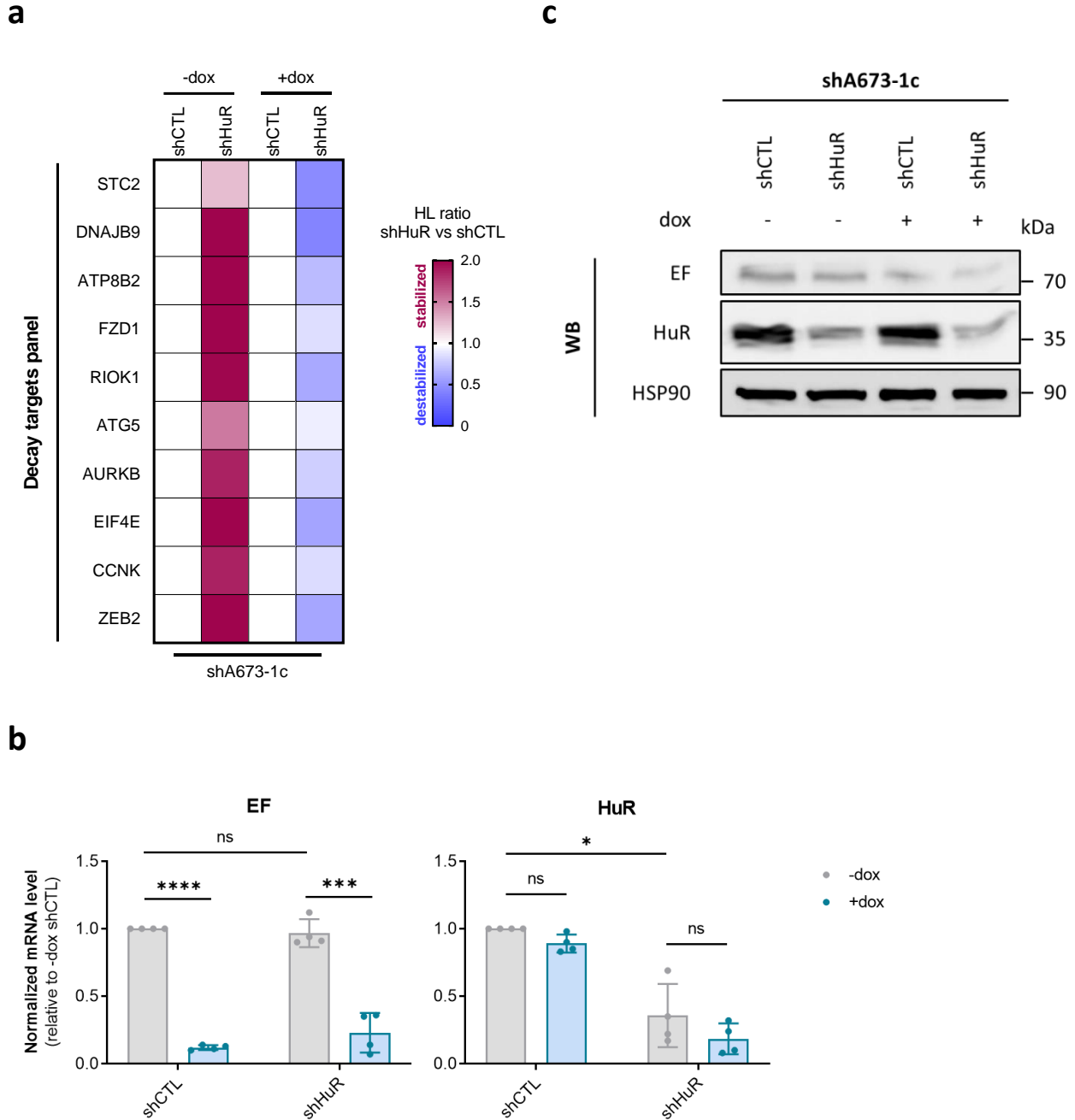
Figure 97. Stability of the decay panel after HuR silencing in shA673-1c -/+ dox cells. (a) Heatmap of half-life (HL) ratio detected by RT-qPCR for the decay panel. Results are shown as means (n = 3-4 independent experiments). For each target, the HL ratio corresponds to the HL in shHuR condition divided by the HL in the shCTL condition. **(b)** Normalized mRNA levels of EF and HuR assessed by RT-qPCR before and after knockdown of HuR in shA673-1c -/+ dox cells. Results are shown as means ± SD (n = 4 independent experiments). mRNA levels are relative to –dox shCTL condition. *p <0.05; ***p <0.001; ****p <0.0001; ns = not significant by one-sample *t*-test, or two-tailed unpaired Student's *t*-test. **(c)** Representative western blotting analysis of EF, HuR and HSP90 (loading control). Samples are lysates from shA673-1c -/+ dox cells before and after knockdown of HuR.
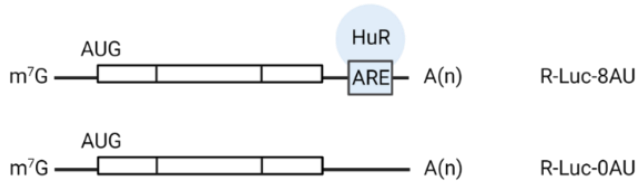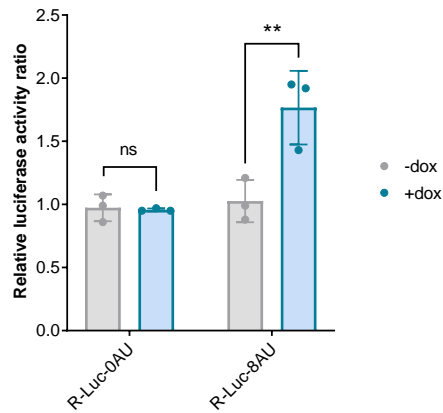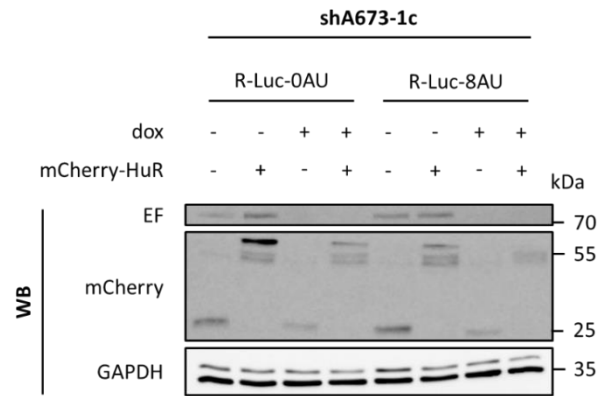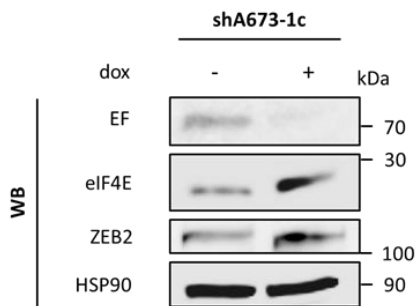
Figure 98. HuR reporter assay in shA673-1c -/+ dox cells. (**a**) Schematic representation of the *R-Luc-8AU* and the *R-Luc-0AU* mRNA reporters. (**b**) Luciferase ARE-reporter assay upon EF knockdown. Samples are lysates from cells transfected with the *R-Luc-8AU* or *R-Luc-0AU* reporters, and mCherry-HuR or control mCherry empty vector. Results are shown as means ± SD (n = 3 independent experiments). For each condition, luciferase activity with mCherry-HuR was normalized to luciferase activity with empty vector. For standardization, the *R-Luc-8AU* and *R-Luc-0AU* constructs express *Firefly* luciferase (*F-Luc*) and *Renilla* luciferase (*R-Luc*) from the same bidirectional promoter. **p <0.01; ns = not significant by two-tailed unpaired Student's *t*-test. (**c**) Western blotting analysis of mCherry-tagged HuR, endogenous EF and GAPDH (loading control). Samples are lysates from shA673-1c -/+ dox cells transfected with the *R-Luc-0AU* or *R-Luc-8AU* mRNA reporters, and mCherry-HuR or control mCherry empty vector. (**d**) Western blotting analysis of EF, eIF4E, ZEB2 and HSP90 (loading control). Samples are total lysates from shA673-1c -/+ dox cells.

9. The decay function of EF is oncogenic and unravels a new vulnerability towards HuR inhibition

Finally, we investigated whether the decay function of EF might open new therapeutic opportunities for EwS. To this aim, we analyzed the sensitivity of EwS and non-EwS cells after treatment with various concentrations of DHTS or vehicle (DMSO) for 24h. Strikingly, EwS cells were significantly more sensitive to DHTS than non-EwS cells, the only exception being HUVECs (**Figure 99a**), suggesting that the new function of EF in mRNA decay that we identified here might reveal a new vulnerability for EwS. Next, we tested whether this higher sensitivity was due to the presence of EF or to other alterations present in EwS cells. To this aim, we compared the sensitivity towards DHTS of EwS cells (shA673-1c, shSK-E17T and TC71) in the presence and absence of EF. As an alternative model, we also included hMSCs transduced with a EF-expressing or control vector. In each case, we found that the presence of EF conferred an increased sensitivity towards DHTS (**Figure 99b**). To verify that the higher sensitivity of EwS to HuR inhibition was linked to the mRNA decay function of EF, we used a previously described "knockdown/rescue system" [145]. Our goal was to replace full-length EF with a decay-defective mutant of EF (*i.e.*, Δ63EF decay mutant) and to assess the sensitivity of EwS cells towards DHTS. To this aim, we treated shA673-1c cells with dox to KD endogenous EF and expressed FLAG-tagged versions of full-length EF or of the Δ63EF decay mutant to comparable levels. Very interestingly, we found that cells rescued with the Δ63EF decay mutant were less sensitive to DHTS than cells rescued with full-length EF (**Figure 99c**). Together, these data indicate that the decay activity of EF might unravel an Ewing-sarcoma specific vulnerability to HuR chemical inhibition.
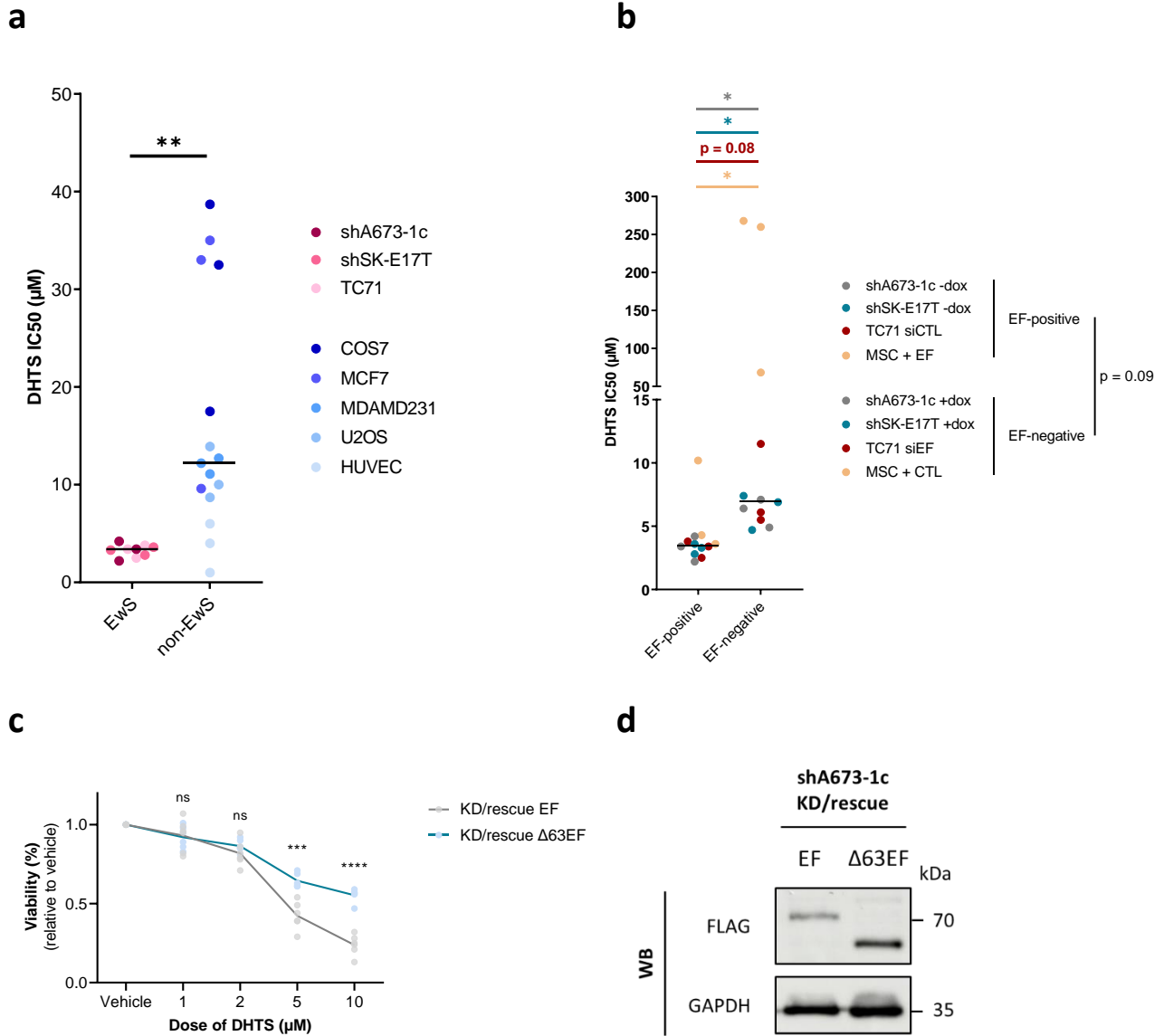
Figure 99. Resazurin viability assays with DHTS. (**a**) Resazurin-based cell viability assay of selected EwS and non-EwS cell lines 24h after DHTS addition. Dots indicate IC50 calculated based on a three-parameter log-logistic regression for 3 independent experiments. Median is shown (solid line). *p <0.05 using two-tailed unpaired Student's t test with Welch's correction. (**b**) Resazurin-based cell viability assay of EwS cell lines before and after EF knockdown, and MSC before and after EF expression 24h after DHTS addition. Dots indicate IC50 calculated based on a three-parameter log-logistic regression for 3 independent experiments. *p <0.05 by two-tailed unpaired Student's *t*-test. (**c**) Resazurin-based cell viability assay of shA673-1c KD cells expressing either FLAG-tagged EF or Δ63EF; 24h after DHTS addition. Dots and lines indicate individual values and means for 2 independent experiments (3 technical replicates each). ***p <0.001, ****p <0.0001, ns = not significant compared to vehicle by two-tailed unpaired Student's *t*-test. (**d**) Representative western blotting analysis of FLAG-tagged indicated constructs and GAPDH (loading control). Samples are cell lysates of shA673-1c KD/rescue EF/Δ63EF.

Importantly, using spheroid growth assays, we found that shA673-1c cells rescued with Δ63EF decay mutant produced significantly smaller spheroids that wild-type EF (**Figure 100**), thus suggesting that the novel molecular function of EF in mRNA decay might contribute oncogenic properties to the EF fusion protein. To further test this possibility, we investigated the effect of DHTS treatment on shA673-1c cells in spheroid growth and colony formation assays. We found that DHTS statistically decreased spheroid growth (**Figure 101a-b**) and the number of colonies (**Figure 101c-d**) in a dose-dependent manner. Interestingly, we also showed that DHTS treatment reduced the migration capacity of shA673-1c cells (**Figure 102**), thus suggesting that HuR inhibition might impede many malignant hallmarks in EwS.

a

b
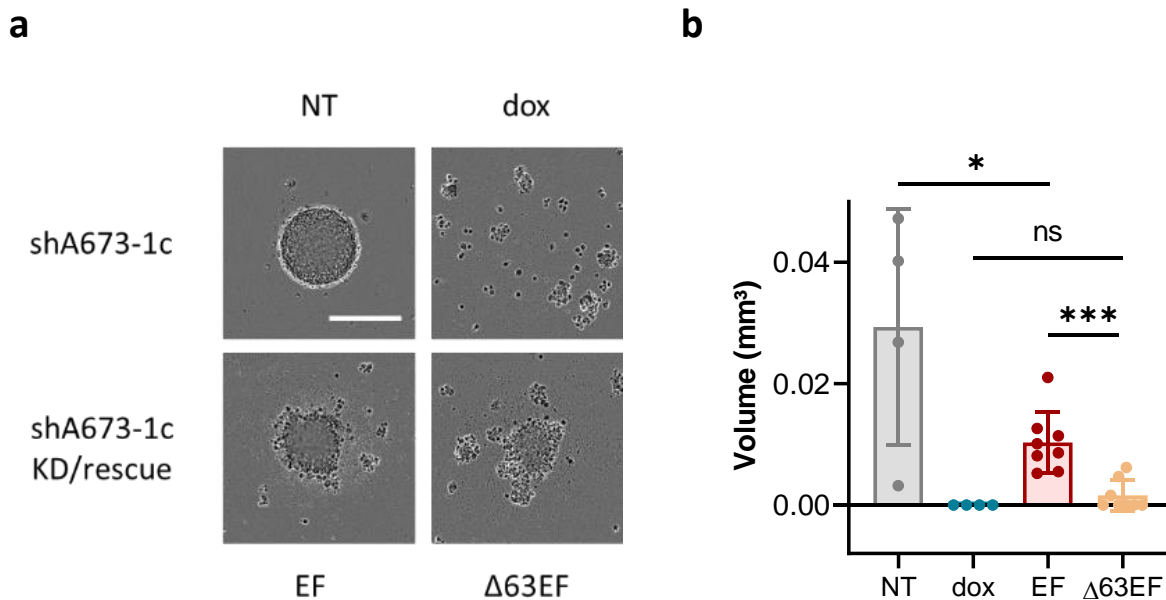
Figure 100. Spheroid growth assay with KD/rescue shA673-1c cells. (**a**) Representative spheroid assay picture after 96h for shA673-1c treated with dox or not (NT) and shA673-1c KD cells rescued with either FLAG-tagged EF or Δ63EF used in **Figure 99c-d**. Scale bar = 400 μm. (**b**) Quantification of spheroid volume. Results are shown as means ± SD (n = 4-8). *p <0.05, ***p <0.001, ns = not significant by two-tailed unpaired Student's *t*-test.
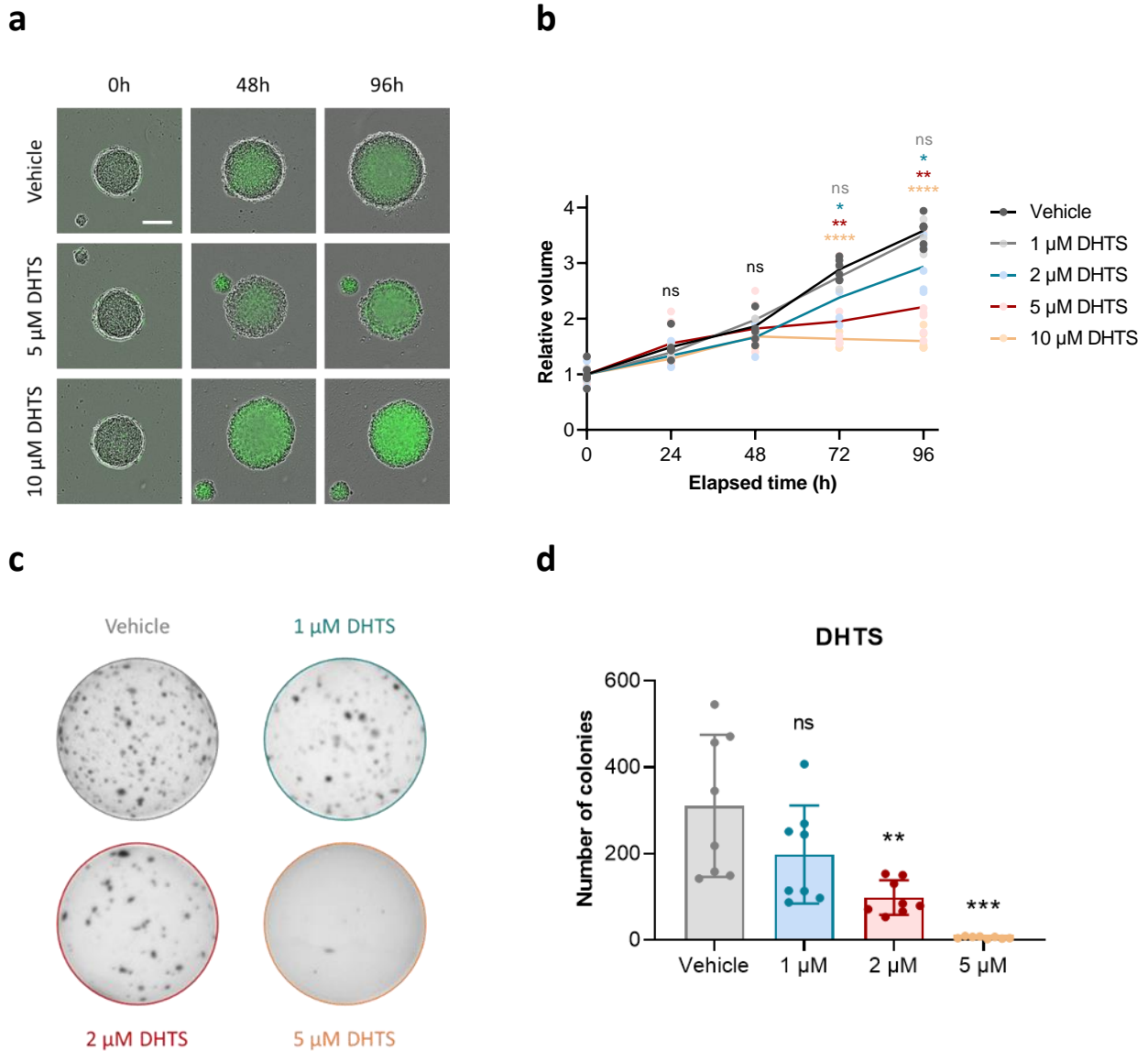
Figure 101. Spheroid growth and colony formation assays in shA673-1c cells treated with DHTS. (**a**) Representative spheroid assay picture at initial, 48h and 96h time points for shA673-1c cells treated as indicated and stained with SYTOX green. Scale bar = 200 μm. (**b**) Quantification of spheroid volume along the assay. For each treatment condition, volume is relative to initial time point. Dots and lines indicate individual values and means (n = 5-6). *p <0.05, **p <0.01, ****p <0.0001, ns = not significant compared to vehicle by two-tailed unpaired Student's *t*-test. (**c**) Representative soft agar assay for shA673-1c cells treated with DHTS as indicated. (**d**) Soft agar assay colony formation quantification. Data are shown as means ± SD (n = 3 independent experiments with 2 technical replicates each). **p <0.01, ***p <0.001, ns = not significant compared to vehicle by two-tailed unpaired Student's *t*-test.

a

b
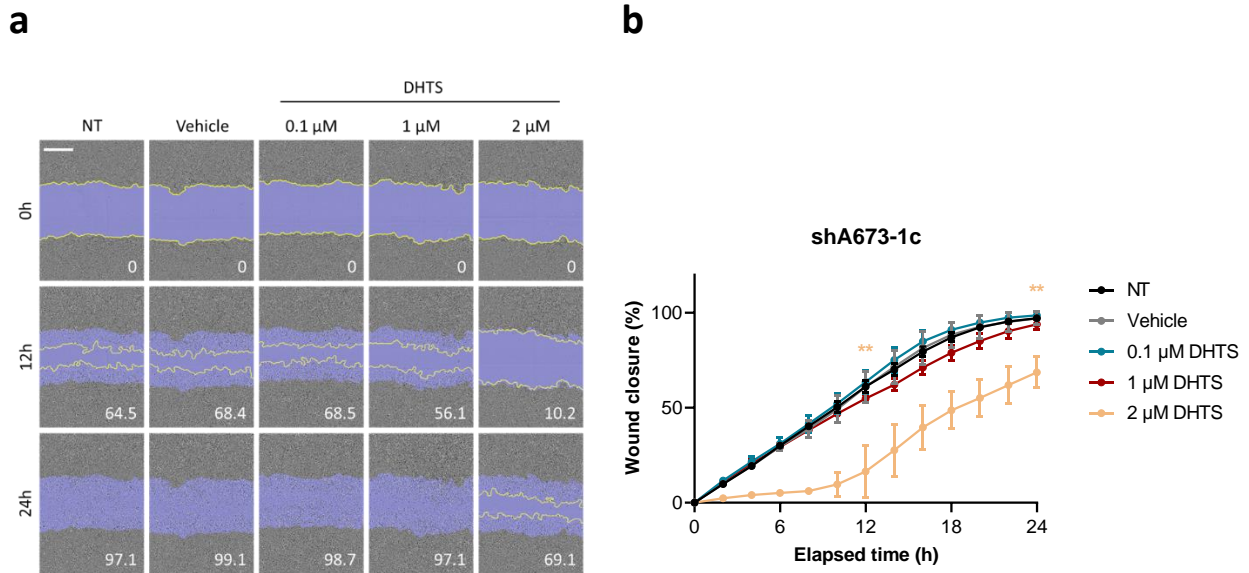
Figure 102. Wound healing assay in shA673-1c cells treated with DHTS. (**a**) Representative would healing assay picture at initial, 12h and 24h time points for shA673-1c cells treated as indicated. Computed migration front line (yellow), initial scratch wound (purple) and would closure (%, white) are shown. Scale bar = 400 μm. NT = not treated. (**b**) Quantification of wound closure along the assay. Results are shown as means ± SD (n = 3 independent experiments). Statistics at 12h and 24h time points are shown. **p <0.01 compared to vehicle by two-tailed unpaired Student's *t*-test. NT = not treated.

To further validate our results, we repeated several of the above-described assays using either shA673-1c cells after HuR silencing through lentiviral expression of shRNA, or another chemical inhibitor of HuR also known to interfere with its RNA-binding ability, namely CMLD-2 [470], [481]. Notably, we observed that HuR KD had similar effects as those observed with DHTS, decreasing spheroid growth (**Figure 103a-b**) and the number of colonies (**Figure 103c-d**). This suggests that our observations with DHTS are specific to HuR inhibition and not to side-effects. As for DHTS, we also showed that EwS cell lines are more sensitive to CMLD-2 when EF is present (**Figure 104a-b**). Moreover, we observed that treatment of shA673-1c cells with CMLD-2 decreased their number of colonies in colony formation assays (**Figure 104c-d**). Interestingly, we also found that shA673-1c seeded in medium with DHTS or CMLD-2 are unable to produce healthy spheroids (**Figure 105**). Taken together, these results evidence that the decay function of EF contributes oncogenic properties to the EF fusion protein in EwS and that its impairment through HuR inhibition might represent a novel therapeutic approach for this aggressive cancer.

a

b

c

d

e
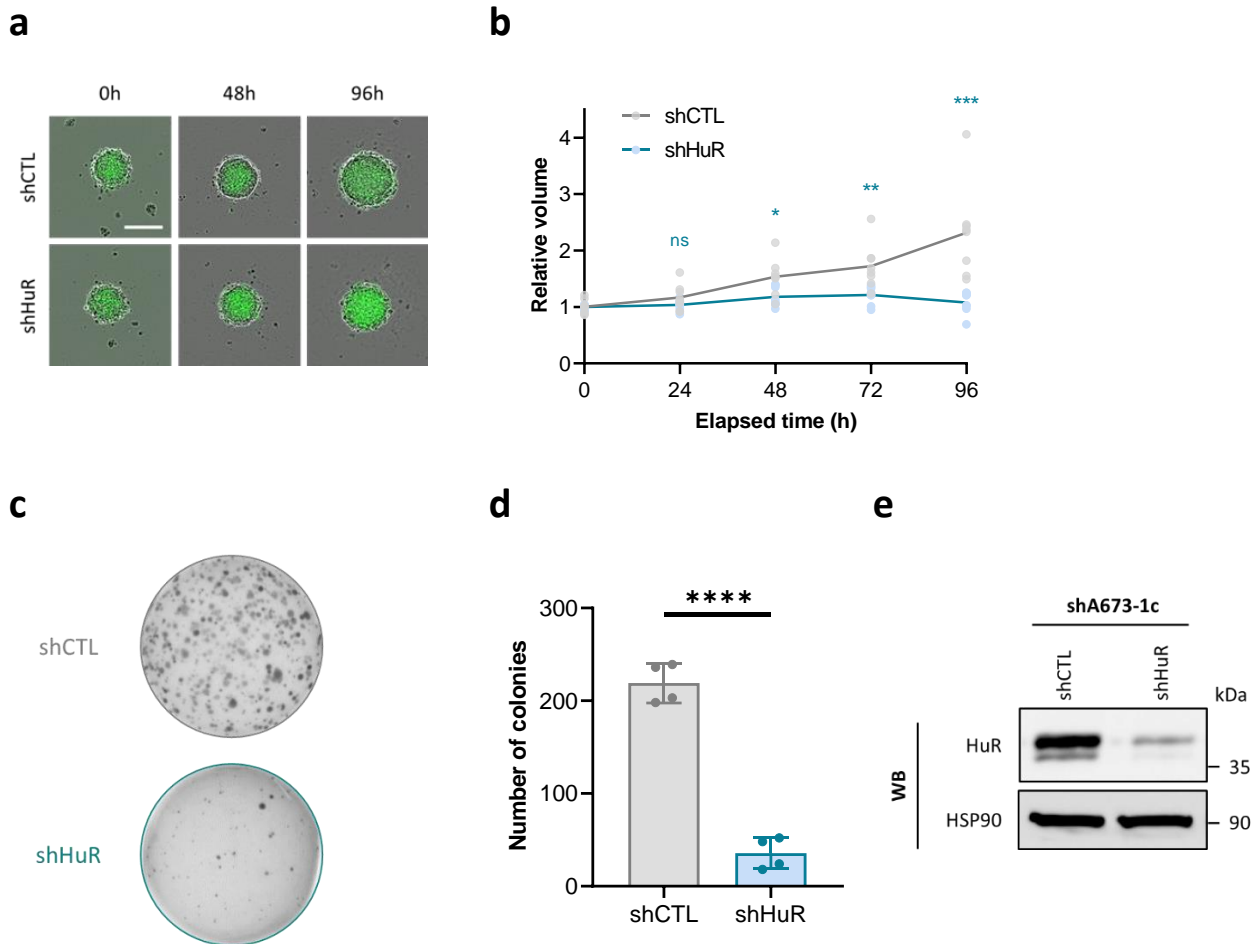
Figure 103. Spheroid growth and colony formation assays in shA673-1c cells after HuR silencing. (**a**) Representative spheroid assay picture at initial, 48h and 96h time points for shA673-1c shCTL/shHuR cells stained with SYTOX green. Scale bar = 200 μm. (**b**) Quantification of spheroid volume along the assay. For each condition, volume is relative to initial time point. Dots and lines indicate individual values and means (n = 8). *p <0.05, **p <0.01, ***p <0.001, ns = not significant compared to shCTL by two-tailed unpaired Student's *t*-test. (**c**) Representative soft agar assay for shA673-1c cells before and after knockdown of HuR. (**d**) Soft agar assay colony formation quantification. Data are shown as means ± SD (n = 4 independent experiments). ****p <0.0001 compared to vehicle by two-tailed unpaired Student's *t*-test. (**e**) Representative western blotting analysis of HuR and HSP90 (loading control). Samples are cell lysates of shA673-1c shCTL/shHuR.
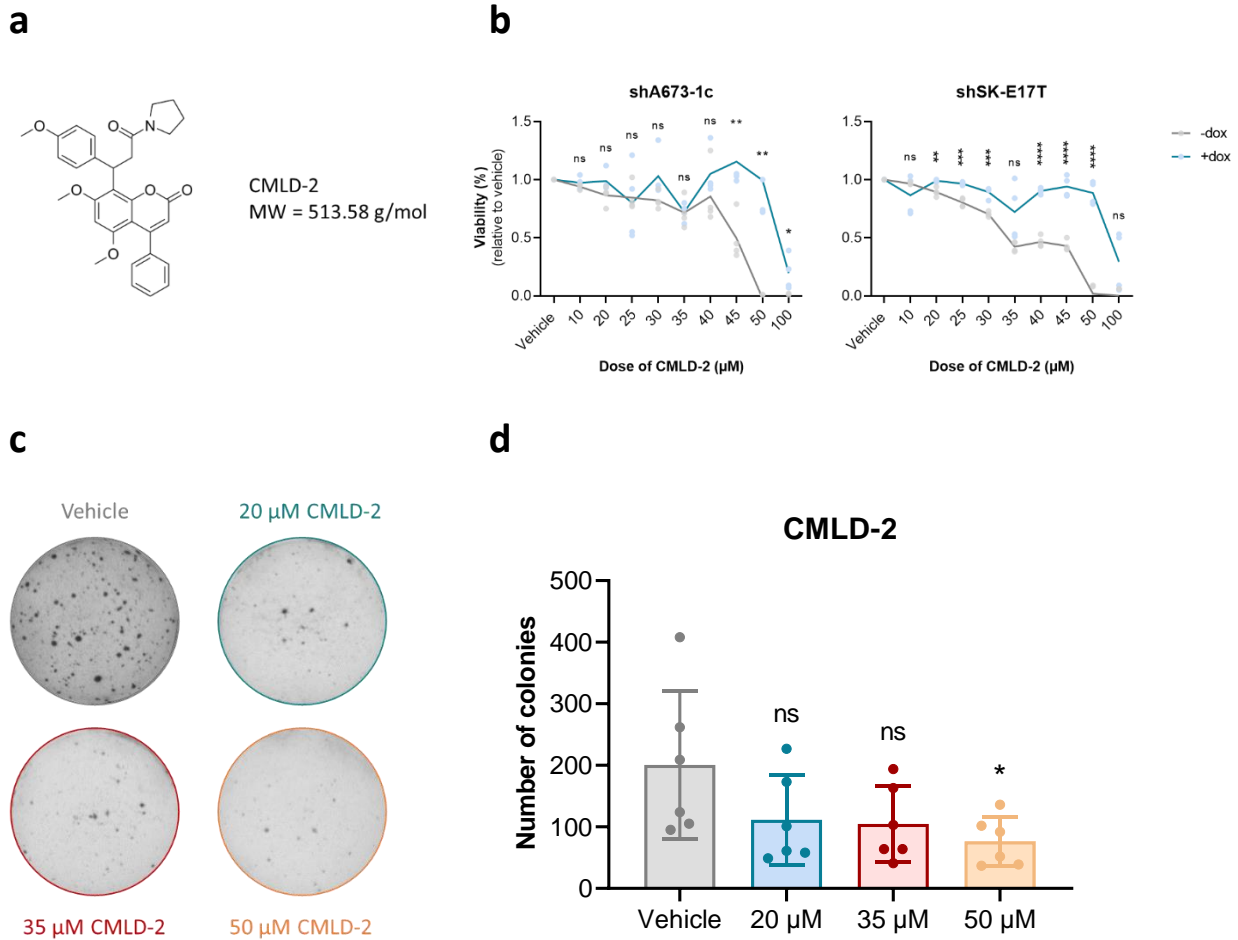
Figure 104. Viability and colony formation assays in EwS cells treated with CMLD-2. (**a**) Chemical structure of CMLD-2. (**b**) Resazurin-based cell viability assay of shA673-1c and shSK-E17T cells 24h after CMLD-2 addition. Dots and lines indicate individual values and means for 4 independent experiments (3 technical replicates each). ***p <0.001, ****p <0.0001, ns = not significant compared to vehicle by two-tailed unpaired Student's *t*-test. (**c**) Representative soft agar assay for shA673-1c cells treated with CMLD-2 as indicated. (**d**) Soft agar assay colony formation quantification. Data are shown as means ± SD (n = 3 independent experiments with 2 technical replicates each). **p <0.01, ***p <0.001, ns = not significant compared to vehicle by two-tailed unpaired Student's *t*-test.

a

b
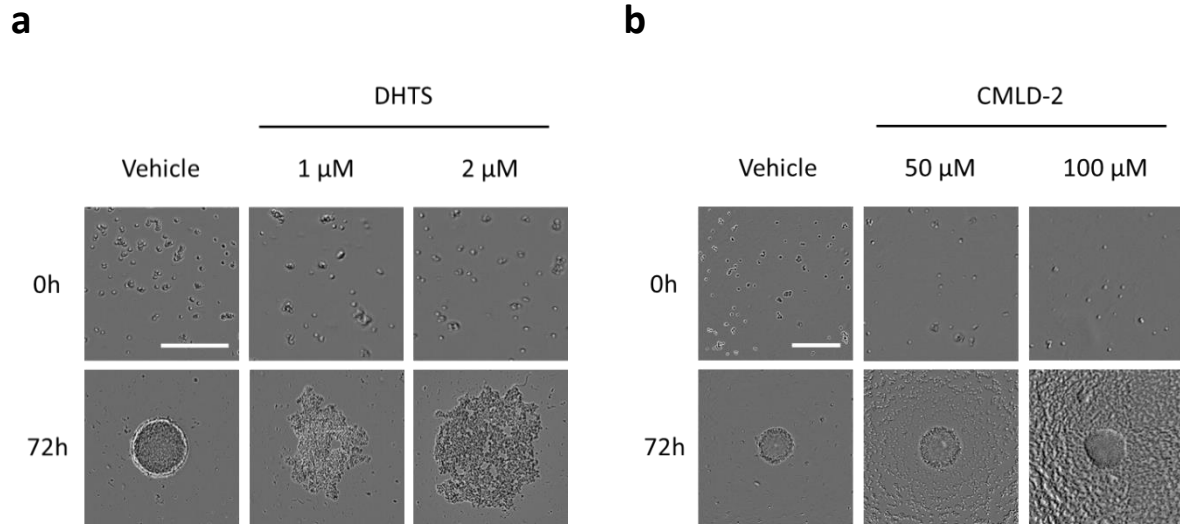
Figure 105. Spheroid formation assays in shA673-1c cells treated with DHTS or CMLD-2. (a) Representative spheroid assay picture at initial and 72h time points for shA673-1c cells treated with DHTS or (**b**) CMLD-2 directly after seeding. Scale bar = 400 μm.

Collectively, these results clearly establish a role for the aberrant TF EF in mRNA decay and reveal an important clinical context for this new function by showing that targeting EF-mediated mRNA degradation via inhibition of HuR is capable to impede the oncogenic potential of EF in EwS (**Figure 106**).

Figure 106. Model illustrating the new molecular function of EF in mRNA decay identified in this work. In addition to its roles in transcription and splicing, EF controls decay of mRNA transcripts related to cell cycle and cell progression via HuR and CNOT2. At some stage during or after transcription, EF is loaded onto specific transcripts via interaction of its FLI1-derived CTAD with HuR and presumably other RNA-binding proteins. At an undefined stage, EF aids in recruiting the CCR4-NOT deadenylation complex, via its capacity to interact with CNOT2 in its N-terminal EWSR1-derived region. The EF-HuR-CNOT2 mRNP complex initiates poly(A) tail shortening and ultimately leads to mRNA degradation. Together, the transcription, splicing and decay functions of EF orchestrate an EwS gene expression program that sustains oncogenic transformation/progression. Targeting of the decay function of EF shed light on a new vulnerability in EwS towards HuR inhibition with potential clinical application.

SECTION IV   COMPLEMENTARY RESULTS

The following results are not found in the 'Results' section. Although they are here simply listed with no more information than those provided by their caption, they will be useful to discuss and present future perspectives to this work where they are further described. They are gathered here in order to ease the reading of the next sections. To date, we do not plan to include most of these results in the publication that we are preparing for submission to 'Molecular Cell' journal.

a   **b**
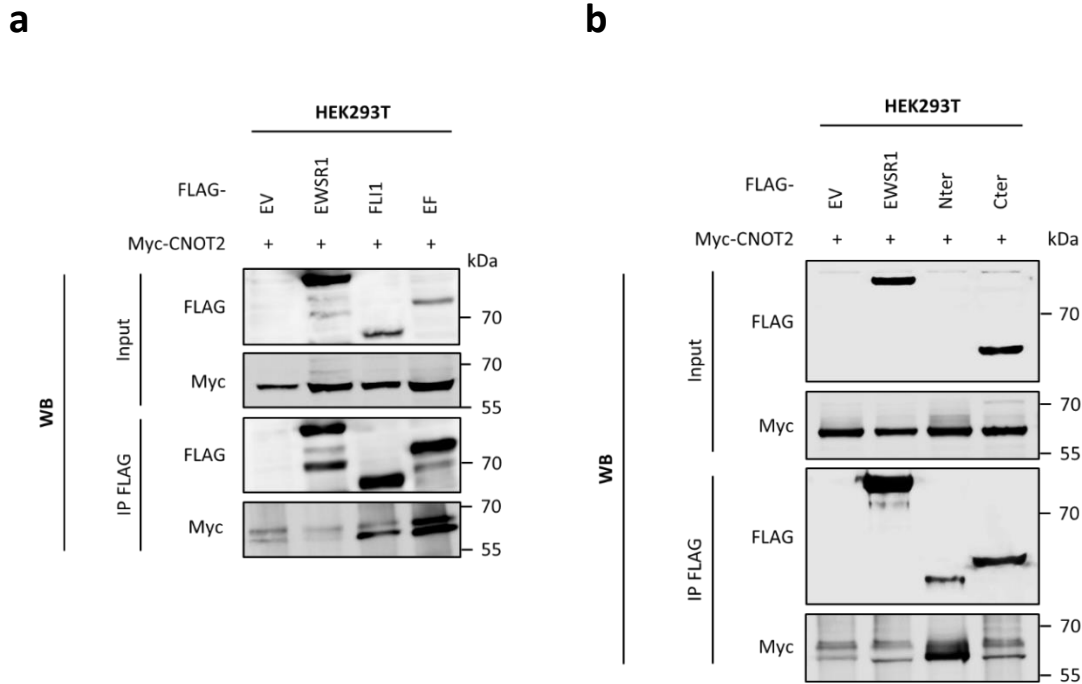
Figure 107. FLI1 but not EWSR1 associates with CNOT2. (**a**) Immunoprecipitation (IP) of indicated FLAG-tagged constructs followed by anti-FLAG and anti-Myc western blotting (WB). Samples are lysates from HEK293T cells transfected with Myc-tagged CNOT2 with either FLAG-EWSR1, FLAG-FLI1, FLAG-EF, or control FLAG empty-vector (EV). (**b**) Immunoprecipitation (IP) of indicated FLAG-tagged constructs followed by anti-FLAG and anti-Myc western blotting (WB). Samples are lysates from HEK293T cells transfected with Myc-tagged CNOT2 with either FLAG-EWSR1, FLAG-EWSR1_Nter, FLAG-EWSR1_Cter, or control FLAG empty-vector (EV).

a

$HL_{MS2-CP} = 2.62 \pm 0.92$ h

$HL_{EWSR1-MS2-CP} = 2.92 \pm 1.68$ h

$HL_{EWSR1\_Nter-MS2-CP} = 0.84 \pm 0.16$ h

$HL_{EWSR1\_Cter-MS2-CP} = 3.89 \pm 0.59$ h

$HL_{FLI1-MS2-CP} = 0.90 \pm 0.03$ h
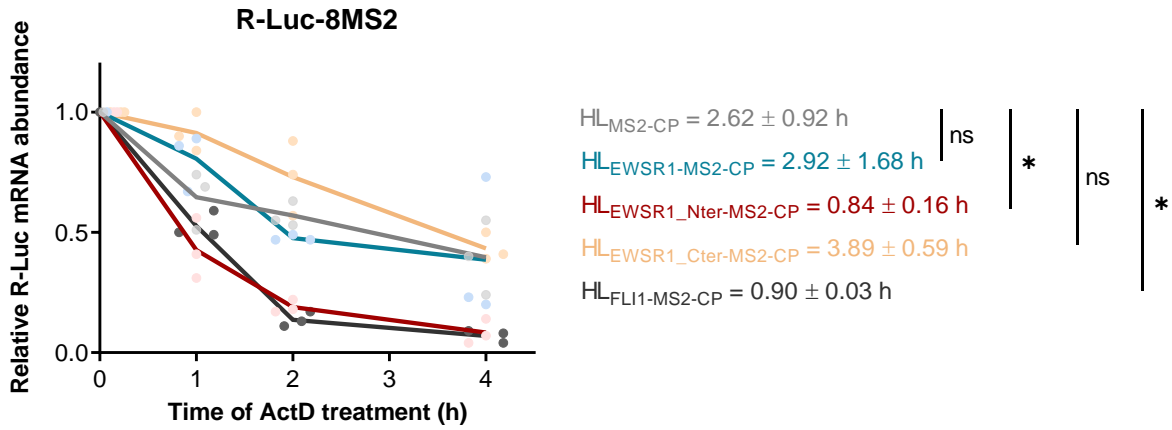
b
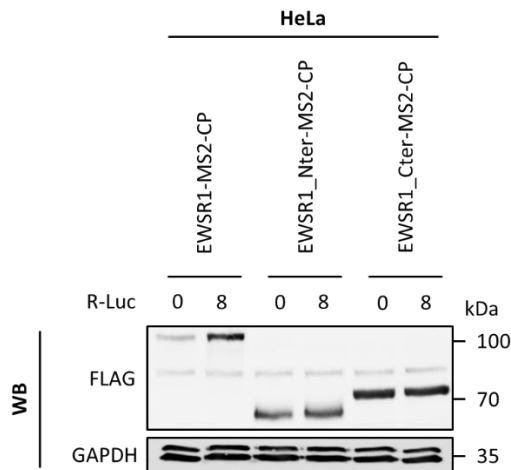
c
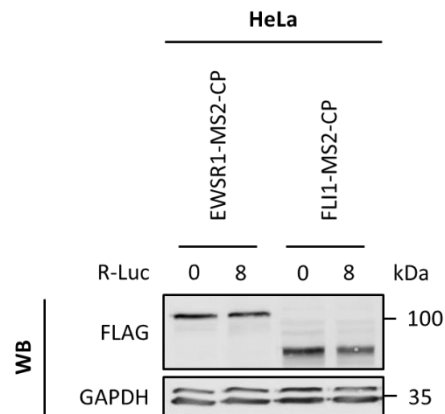
Figure 108. MS2-tethering degradation assay with EWSR1, EWSR1_Cter and FLI1. (a) RT-qPCR analysis of the stability of the *R-Luc-8MS2* mRNA reporter. Samples are RNA from HeLa cells transfected with *R-Luc-8MS2* and MS2-CP-tagged constructs, and treated for 0, 1, 2, or 4 h with ActD. Dots and lines indicate individual values and means, respectively (n = 3 independent experiments). *p <0.05; ns = not significant compared to MS2-CP by two-tailed unpaired Student's *t*-test. HL = half-life. (**b-c**) Western blotting analysis of the indicated MS2-tagged proteins with anti-FLAG antibody and GAPDH (loading control). Samples are total cell lysates from HeLa cells transfected with *R-Luc-0MS2* or *R-Luc-8MS2* and indicated MS2-tagged constructs.
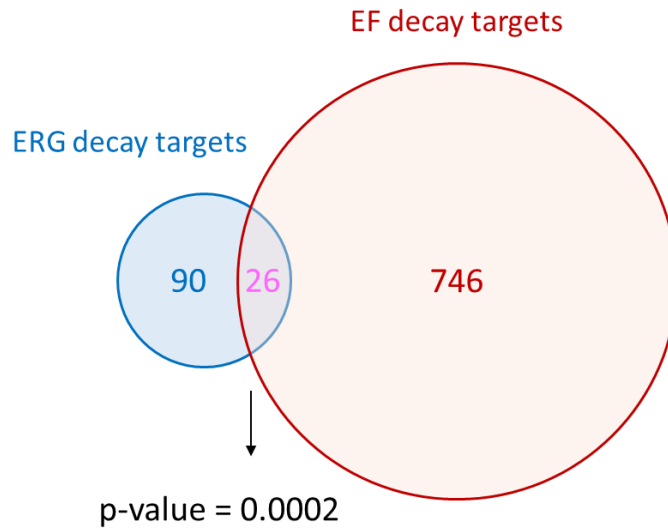
Figure 109. Comparison between EF and ERG decay targets. Overlap between decay targets identified in shA673-1c cells after EF knockdown and ERG decay targets identified in [120]. Targets without detected half-life in shA673-1c cells were filtered out before testing overlap with EF decay targets. p-value was calculated using Fisher's Exact Test.
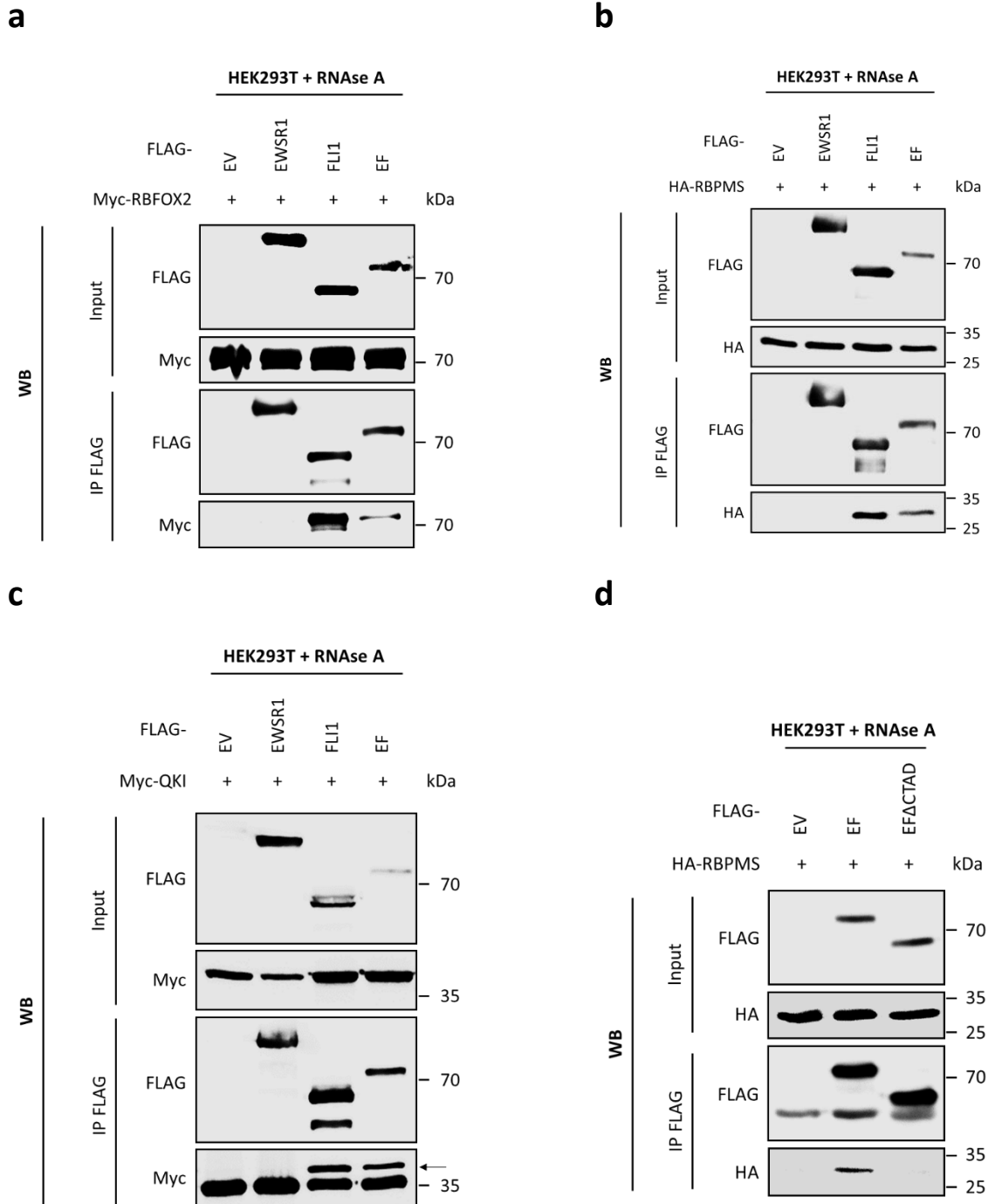
Figure 110. FLI1 and EF but not EWSR1 coimmunoprecipitate with RBFOX2, RBPMS and QKI. Immunoprecipitation (IP) of indicated FLAG-tagged constructs followed by anti-FLAG and anti-Myc/HA western blotting (WB). Samples are RNAse A-treated lysates from HEK293T cells transfected with Myc-tagged RBFOX2 (**a**), HA-tagged RBPMS (**b**) or Myc-tagged QKI (**c**), with either FLAG-EWSR1, FLAG-FLI1, FLAG-EF, or control FLAG empty-vector (EV). Arrow in panel c indicates QKI-related band. (**d**) Immunoprecipitation (IP) of indicated FLAG-tagged constructs followed by anti-FLAG and anti-HA western blotting (WB). Samples are RNAse A-treated lysates from HEK293T cells transfected with HA-tagged RBPMS with either FLAG-EF, FLAG-EFΔCTAD, or control FLAG empty-vector (EV).

a

b

c

d
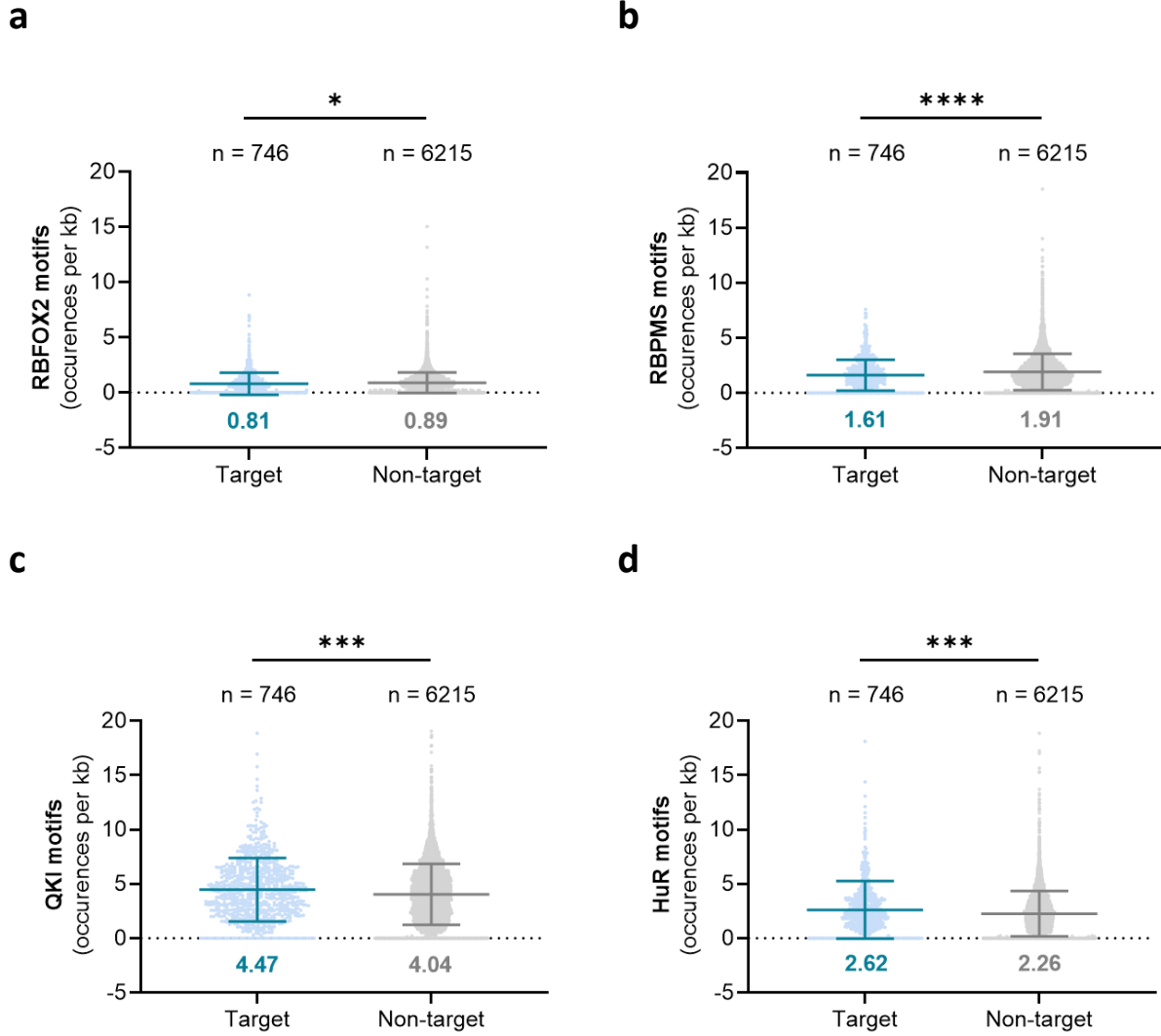
Figure 111. Analysis of RBFOX2, RBPMS, QKI and HuR motifs in EF target and non-target 3'UTR regions. (**a-d**) Number of occurrences per kb for the indicated RBPs. Results are shown as mean ± SD. Numbers written in bold are means. *p <0.05, **p <0.01, ***p < 0.001, ****p <0.0001 compared to control by two-tailed unpaired Student's *t*-test with Welch's correction.

a
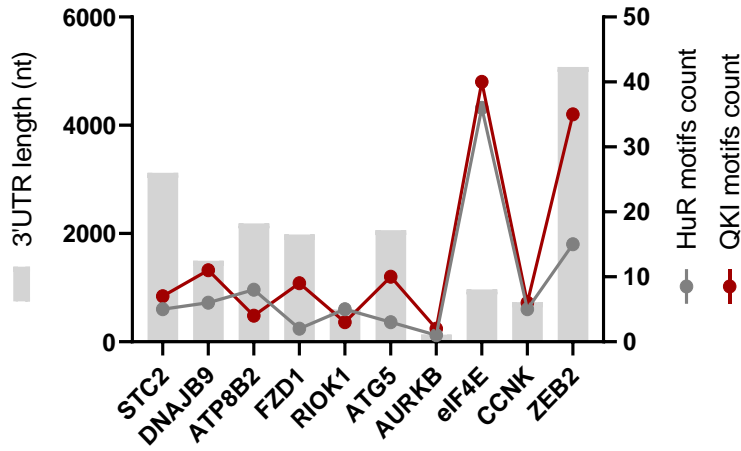
b
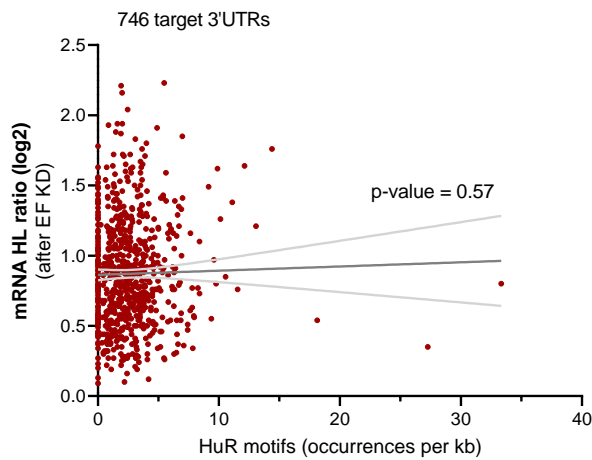
c
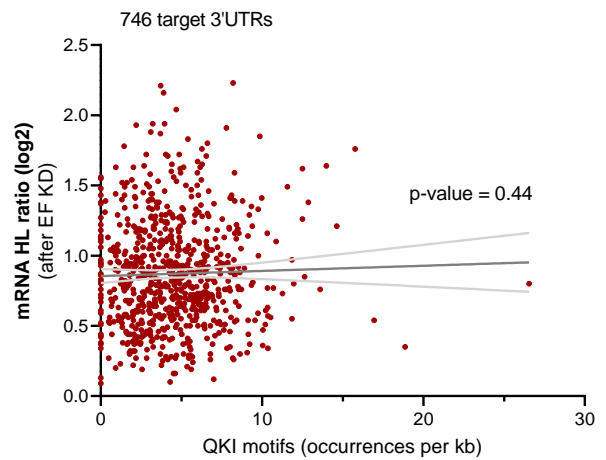
Figure 112. Occurrences of HuR and QKI binding motifs in EF target 3'UTRs. (**a**) Length and number of HuR and QKI binding motifs in the 3'UTRs of the representative set of EF decay targets. nt = nucleotide. (**b**) Correlation between the number of HuR or QKI (**c**) binding motifs in target 3'UTRs and their corresponding mRNA HL (log2). Linear regression line (dark grey) and 95%-confidence intervals (light grey) are shown.

a
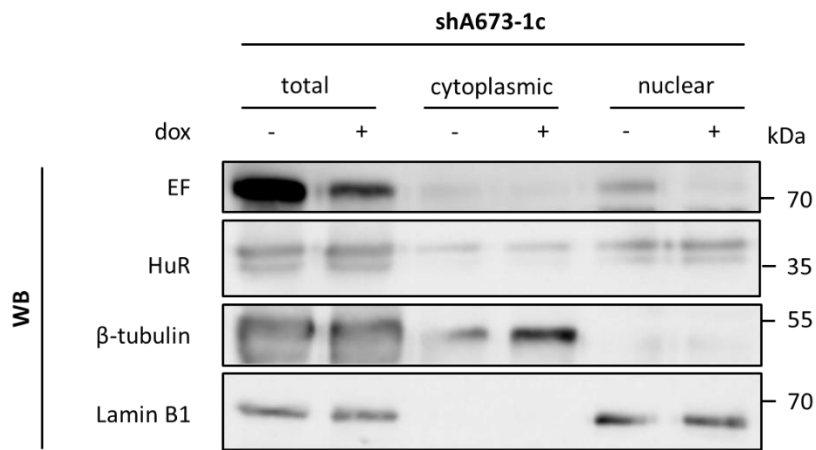
b
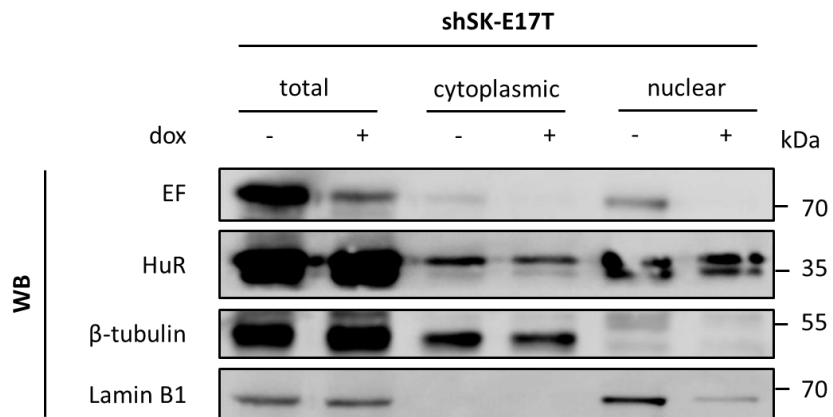
Figure 113. Nucleocytoplasmic fractionation experiments in EwS cells. (a) Western blotting analysis of EF and HuR in total, cytoplasmic and nuclear fractions from shA673-1c and shSK-E17T **(b)** -/+ dox cells. β-tubulin and lamin B1 were used as control for cytoplasmic and nuclear fraction purity, respectively.
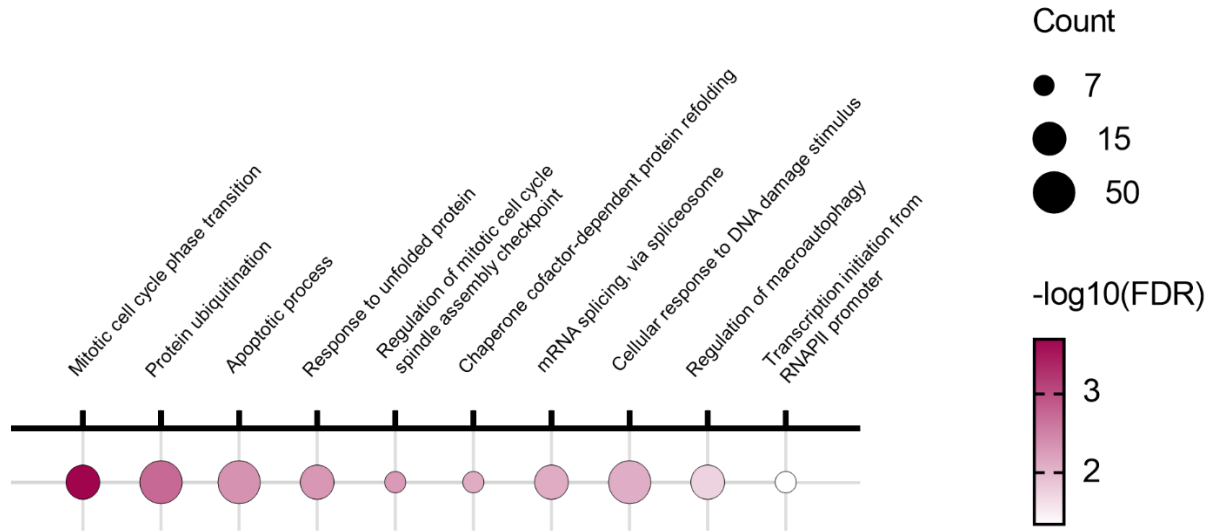
Figure 114. Gene ontology analysis of stabilized mRNAs after EF knockdown with PANTHER. Enrichment of Gene Ontology (GO) Biological Process terms in genes with significantly increased stability upon EF knockdown in shA673-1c cells (FDR <0.05). Points are scaled by number of genes and colored p-value. Enrichment analysis was performed with PANTHER and p-values were calculated using FDR correction.

a
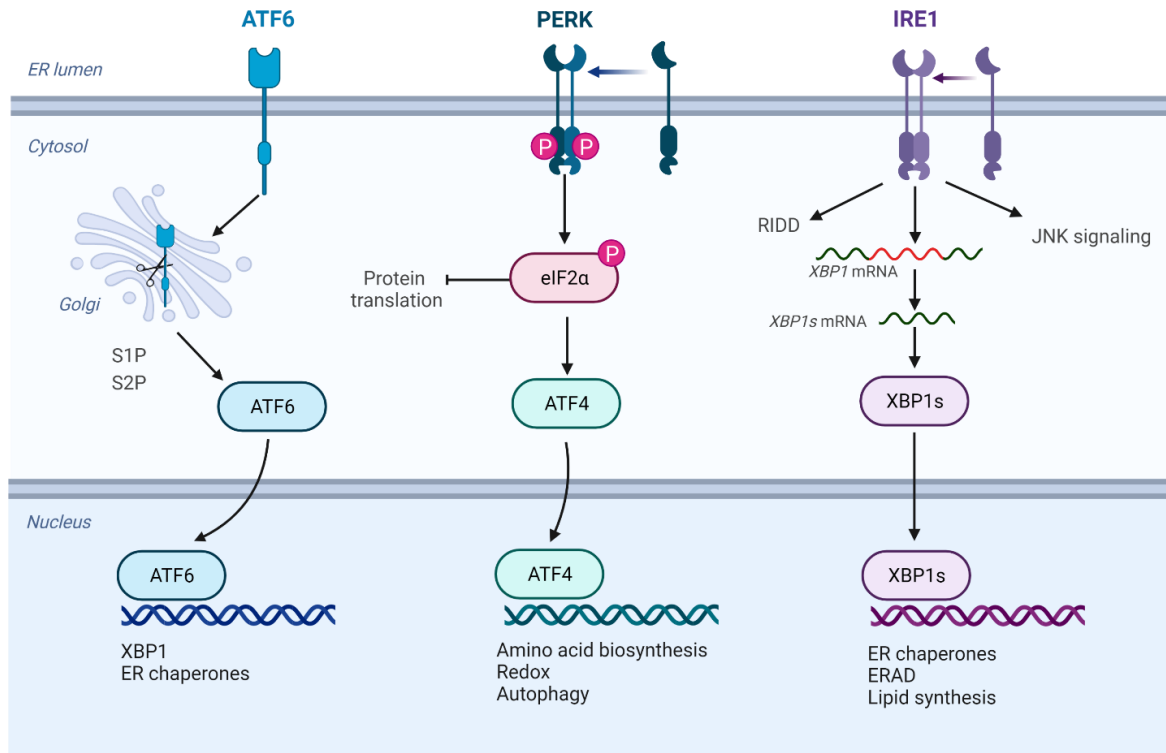
b
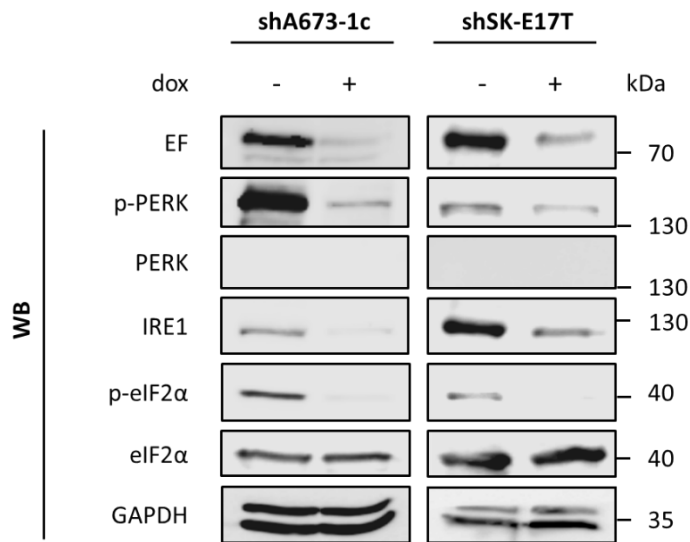
c
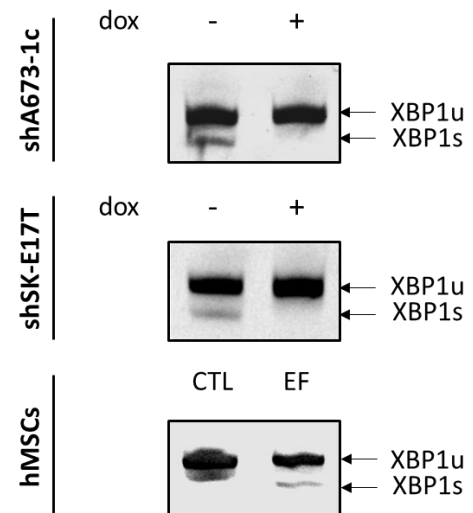
Figure 115. ER stress and UPR activation in EF-expressing cells. (**a**) UPR signaling pathways. Adapted from "UPR signaling (ATF6, PERK, IRE1)", by BioRender.com (2022). Retrieved from https://app.biorender.com/biorender-templates. (**b**) Western blotting analysis of EF, p-PERK, PERK, IRE1, p-eIF2α, eIF2α and GAPDH (loading control). Samples are total lysates from shA673-1c and shSK-E17T -/+ dox cells. (**c**) qPCR analysis of XBP1 splicing in the presence and absence of EF. XBP1u = XBP1 unspliced, XBP1s = XBP1 spliced.
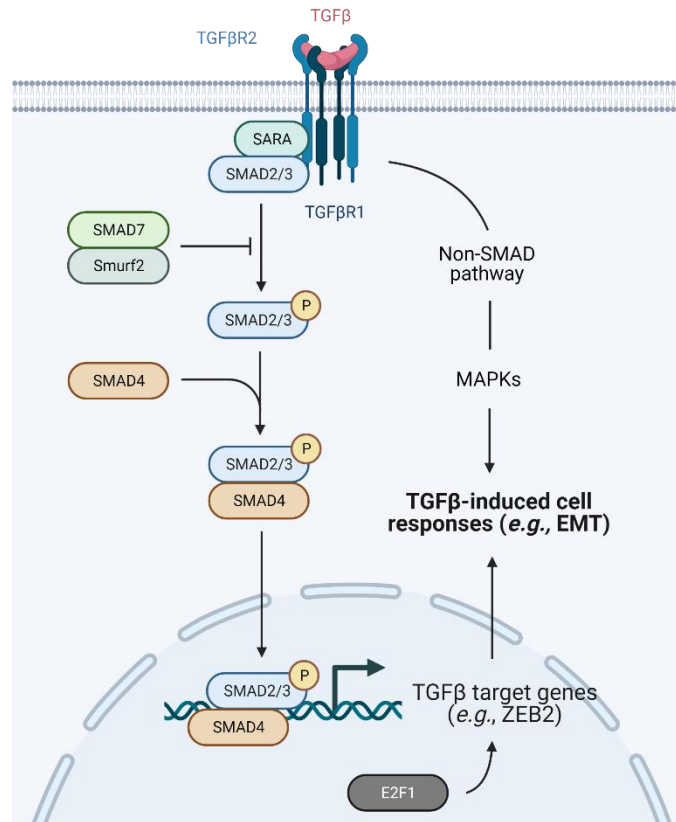
Figure 116. TGFβ signaling pathway. Following the binding of TGFβ to its receptor composed of TGFβR1 and TGFβR2, effectors transduce signals from the cell surface to the nucleus via either SMAD-dependent or SMAD-independent pathways. In the last case, MAPKs are implicated. Adapted from "TGF-Beta Signaling Pathway", by BioRender.com (2022). Retrieved from https://app.biorender.com/biorender-templates.
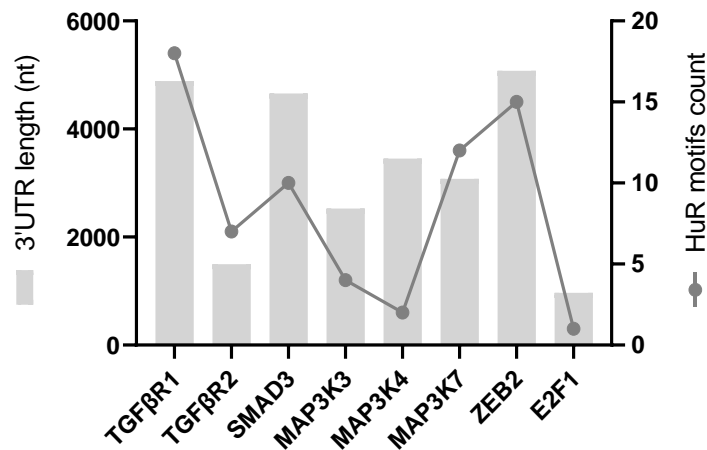
Figure 117. QKI binding sites in the 3'UTR region of EF decay targets related to TGFβ signaling. Length and count of HuR binding motifs are shown for each target 3'UTR. nt = nucleotide.
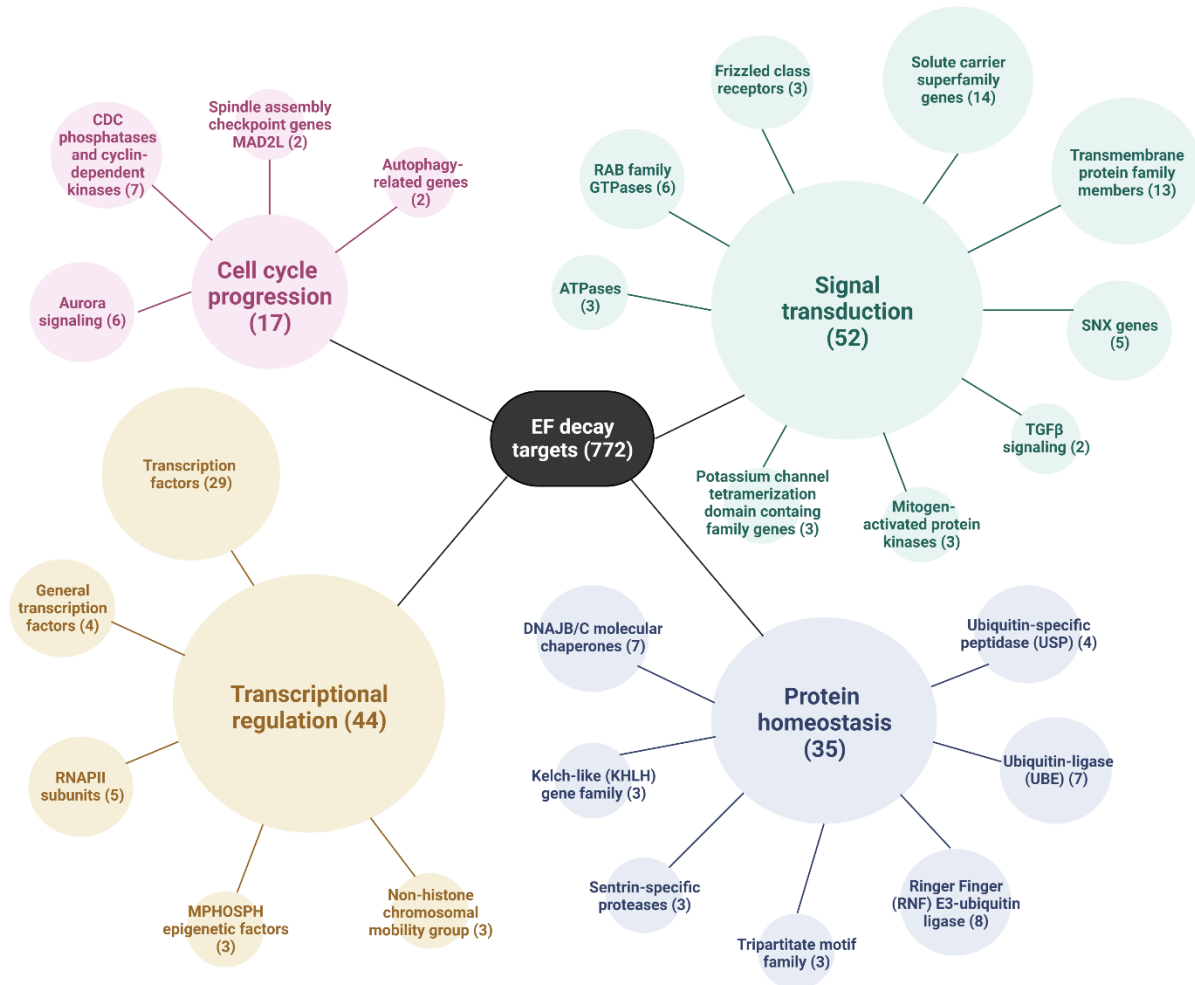
Figure 118. Main mRNA families identified by visual inspection of EF decay targets. Created with BioRender.com.

a

b
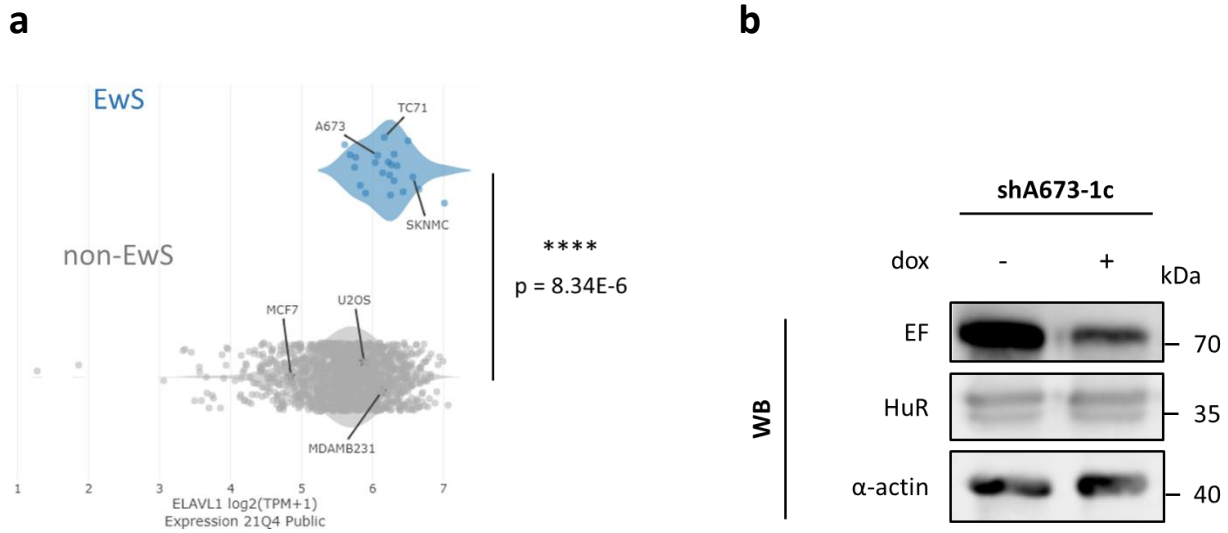
Figure 119. Expression levels of HuR in EwS and non-EwS cells. (**a**) Comparison of *HuR* (also known as ELAVL1) mRNA expression profile between EwS (blue) and non-EwS (gray) cell lines. The plot is generated based on DepMap Expression 21Q4 data. ****p <0.0001. (**b**) Western blotting analysis of EF, HuR and α-actin (loading control) in shA673-1c -/+ dox cells.

a

b
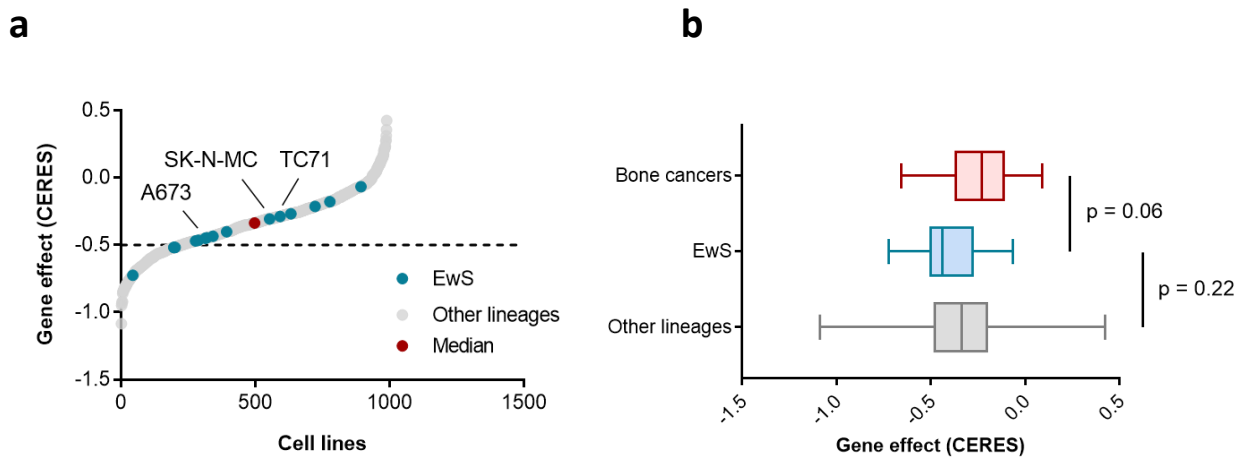
Figure 120. Effects of the loss of HuR on cell growth of human cancer cell lines. (**a**) Hockey plot depicting the distribution of HuR gene effect (CERES) scores across human cancer cell lines in CRISPR DepMap 22Q1 data. EwS cell lines are highlighted in blue. Median value is shown (red). (**b**) Comparison of gene effect (CERES) scores between Ewing sarcoma and either bone cancer or other lineages. p-values calculated using two-tailed unpaired Student's t test with Welch's correction are shown.

a
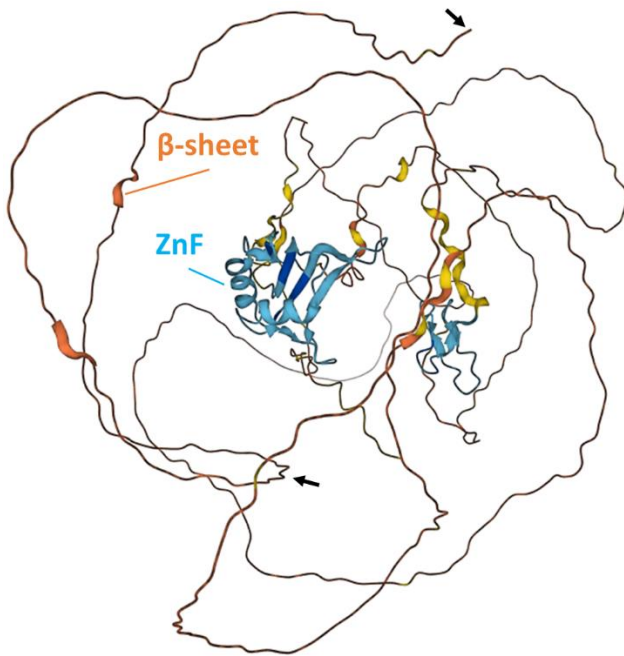
b
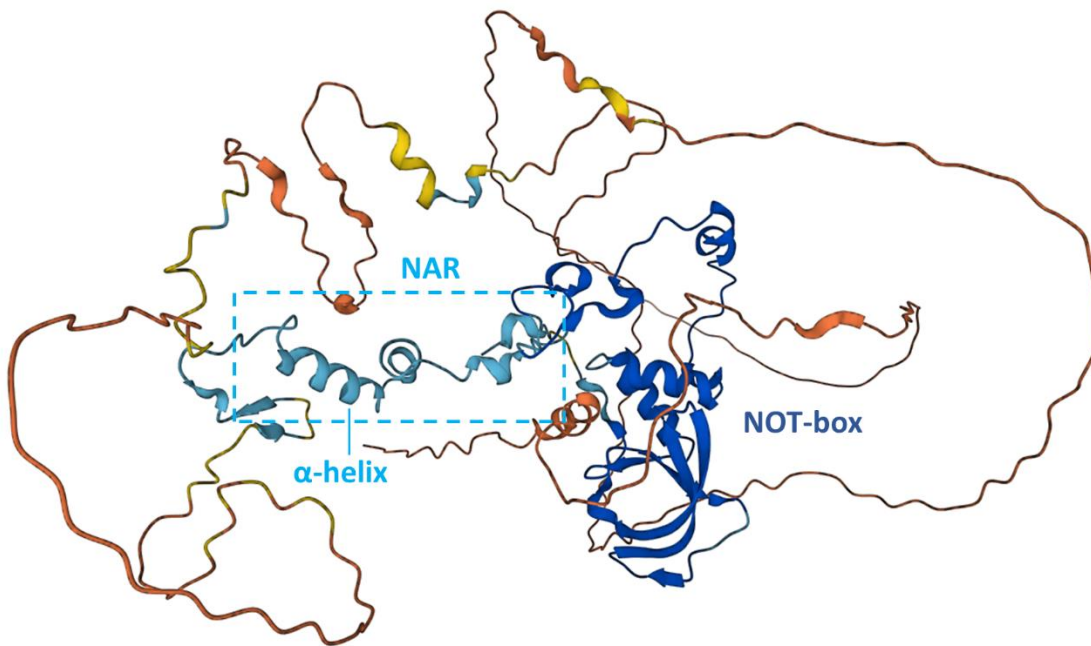
Figure 121. AlphaFold2 3D protein structure prediction of human EWSR1 and CNOT2. (**a**) Protein structure of EWSR1. The first 63 aa are delimited by the black arrows. ZnF = zinc finger. (**b**) Protein structure of CNOT2. The presence of an α-helix at the beginning of the NAR domain is shown.

a
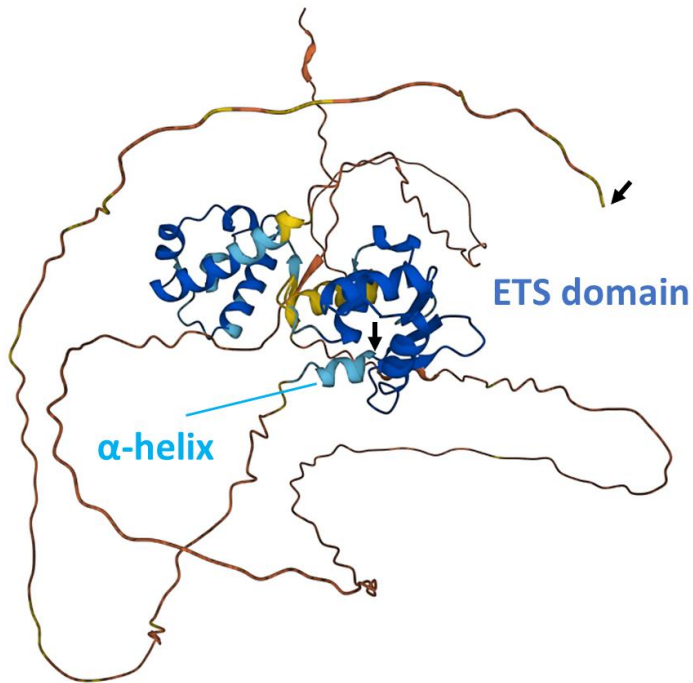
b
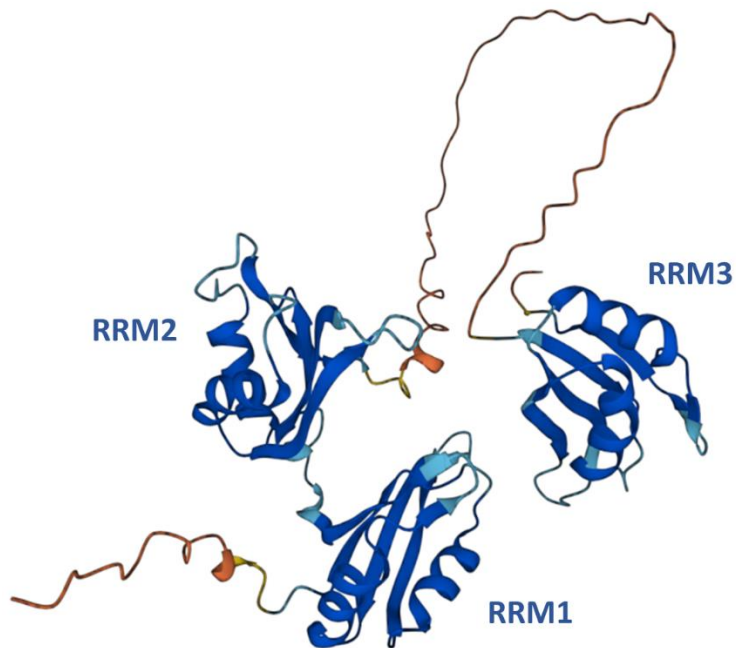
Figure 122. AlphaFold2 3D protein structure prediction of human FLI1 and HuR. (a) Protein structure of FLI1. The CTAD is delimited by the black arrows. The presence of an α-helix immediately downstream of the ETS domain is shown. (**b**) Protein structure of HuR. RRM = RNA-recognition motif.

a
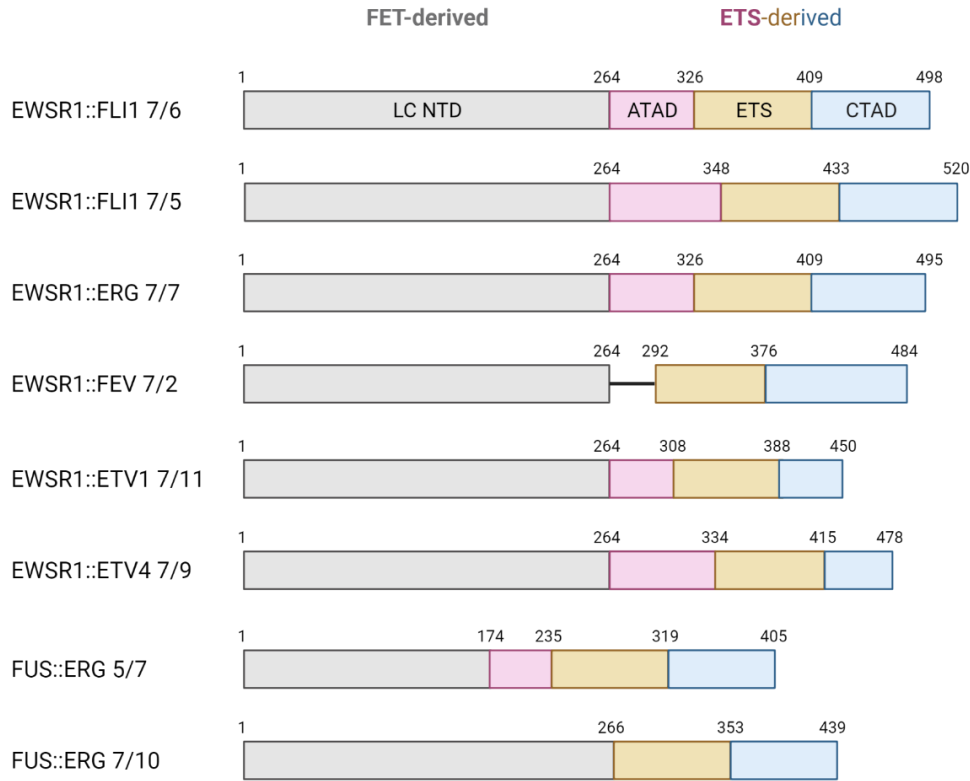
b
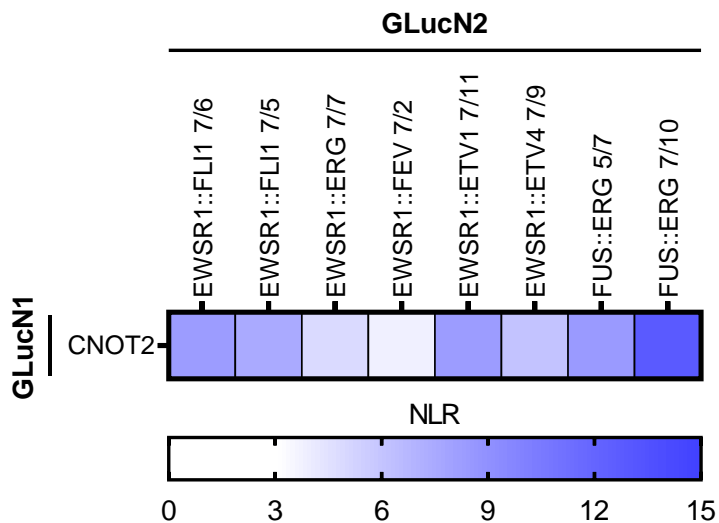
Figure 123. Other FET::ETS fusions also interact with CNOT2. (**a**) Schematic, domain structure of other FET::ETS fusions. Created with BioRender.com. (**b**) Heatmap showing mean NLR values for the indicated protein pairs (n = 2 independent experiments). CNOT2 is tagged with GLucN1; and FET::ETS fusions are tagged with GLucN2.

SECTION V DISCUSSION

To date, the fusion protein EF is described as an aberrant TF with roles mainly confined to the early steps of mRNA biogenesis. Although EF-mediated gene expression deregulation has also been proposed to also implicate late post-transcriptional processes [230], this aspect has remained elusive for many years. The recent realization that, in addition to transcription, EF can actively rewire the mRNA splicing landscape in EwS [119], [209], [213], [214] has prompted to further explore the contribution of more remote post-transcriptional processes, such as mRNA decay, to the establishment of oncogenic gene expression programs in EwS.

1. EF actively controls mRNA stability in Ewing sarcoma

In this work, we provide a substantial body of evidence that EF is a moonlighting fusion TF that imposes an aberrant mRNA stability landscape in EwS (**Figure 61**). Thereby, we demonstrate that EF does not only affect early co-/post-transcriptional processes but also late post-transcriptional processes. Importantly, we report that EF decreases mRNA stability via an active mechanism: EF recruits the CCR4-NOT decay machinery and is targeted to specific mRNA transcripts via binding to the RBP HuR. Although we also show that EF significantly modulates the expression of seven decay factors, several of our observations make very unlikely the possibility that EF impacts mRNA stability only via indirect mechanisms (such as EF function in transcription, deregulation of ncRNAs, aberrant rewiring of signaling pathways): (i) the four decay factors that are activated by EF (*EXOSC5*, *MPP6*, *ZCCHC3* and *DCP2*) and the three decay factors that are repressed by EF (*ZFP36*, *ZFP36L1*, *ZFP36L2*) are all known to encode proteins that negatively impact mRNA stability [326], [626] (**Figure 66a**), (ii) loss of EF leads to the destabilization of only a few mRNAs (26 mRNAs vs 772 stabilized mRNAs) (**Figure 61**), (iii) EF associates with most of its decay panel mRNA targets (**Figure 67**), (iv) EF binds to the CNOT2 subunit of the CCR4-NOT decay machinery (**Figure 70**) and associates with several of its catalytic subunits (**Figure 72**), and (v) the abilities to bind to CNOT2 and to trigger mRNA decay are not compromised by the removal of EF DBD (**Figure 83**). Therefore, our work adds a new member to the collection of TFs that can directly impact mRNA decay. Also, contrary to the majority of the other studies that are related to normal cell physiology (see **Table 3**), our work concerns a disease-defining TF. Therefore, our data indicate that TF-mediated mRNA decay (TFMD) might also contribute to disease development.

In addition, our work adds to a growing body of evidence showing that EF is a multitasking TF that governs multiple aspects of mRNA biology, including transcription, alternative splicing but also degradation. Based on transcriptome-wide comparisons between the transcriptional, splicing and decay targets of EF, we highlight that the different molecular activities of EF control different mRNA repertoires at the level of the transcriptome (**Figure 82**, **83**, **85**). This indicates that the majority of EF decay targets are transcribed from genes that are not regulated, not bound by EF, nor producing transcripts whose alternative splicing is regulated by EF. Further supporting this, we show that a mutant of EF that is unable to bind to DNA (*i.e.*, EFΔETS), is still able to destabilize

the mRNA targets of full-length EF (**Figure 83**). Likewise, we show that a decay mutant of EF (*i.e.*, Δ63EF) is still active in transcription and pre-mRNA splicing (**Figure 86-87**). Taken together, these findings indicate that the different molecular functions of EF are uncoupled (*i.e.*, mechanistically independent), although they appear to map to overlapping protein regions (see later). Based on these observations, our data tend to rule out the general idea that EF itself imprints its target transcripts during mRNA synthesis as previously suggested for ERG [120]. That said, this does not exclude that, in rare cases, EF might still be able to imprint some of its transcriptional targets (such as *AURKA*, *AURKB*, *etc*.) for later regulation. Altogether, our data indicate that, in general, EF does not act as a coupling factor of gene expression responses in EwS. Of note, the questions related to gene expression coupling are, in general, not directly addressed in the literature. Our approach encourages and provides a roadmap to tackle these critical questions.

2. EF and P-bodies assembly

We show that loss of EF decreases the number of PBs in two EwS cell lines (**Figure 64**). This observation might be linked to the decay activity of EF. Indeed, PBs are highly dynamic structures and cellular accumulation of poly(A)-shortened mRNAs is known to trigger PBs assembly [386], [387]. Also, PBs are known to mostly accumulate mRNAs with AU-rich 3'UTRs [634]. These findings are fully consistent with our results as we show that EF decay activity preferentially targets mRNA transcripts harboring AREs in their 3'UTR region for deadenylation (**Figure 88**). Therefore, our data points towards a model in which PBs assemble in the presence of EF as a result of EF-mediated mRNA degradation. Not mutually exclusive, we cannot exclude that EF might also play a direct role in P-bodies biogenesis.

3. EF controls mRNA stability via the CCR4-NOT complex

We show that EF is able to associate with the CCR4-NOT deadenylation complex (**Figure 72**). This result is consistent with the identification of CNOT1, the scaffold subunit of CCR4-NOT, among the EF interactors reported in [209] (**Figure 23d**). Interestingly, two other TFs involved in TFMD, namely ERG [120] and EBF1 [537], have also been shown to associate with the CCR4-NOT complex, suggesting that this might represent a recurrent theme in TFMD. Strikingly, for all three TFs, the recruitment of CCR4-NOT appears to be mediated via direct interactions with the NOT module (CNOT2-CNOT3). More specifically, ERG and EF appears to directly interact with CNOT2 while EBF1 appears to directly interact with CNOT3. Although the NOT module is known to serve as a binding platform for RBPs [364], these findings suggest that the NOT module might additionally serve as a binding platform for TFs.

In eukaryotic cells, CCR4-NOT exists under four different forms depending on which deadenylases are incorporated [361], [576]. Intriguingly, we show that EF appears to associate with a specific form of the complex containing the CNOT6L and CNOT8 deadenylase subunits (**Figure 72**). In contrast, no such preference has been reported for ERG and EBF1. The different forms of CCR4-NOT might target different mRNA repertoires for deadenylation. We believe that this specificity might be exploited by EF to target specific mRNA subsets, although this remains an open question in light of our current observations.

Furthermore, we show that EF interacts with CNOT2 mainly via its LC NTD derived from EWSR1 (**Figure 71**). Given that the full ATAD of FLI1 is also able to associate with CNOT2 [120], a small fraction of the EF/CNOT2 might also originate from the residual portion of the ATAD found in EF. Interestingly, the full LC NTD appears to contribute to the interaction with CNOT2 given that successive deletions in this domain progressively abrogate the EF/CNOT2 interaction. These observations are compatible with the "scratch model" that has been described for IDRs-mediated interactions in which strong interactions are mediated by multiple weak non-covalent bonds (*e.g.*, hydrogen bonds, π-π interactions and cations-π interactions) [635], [636]. In this context, deleting the first 63 aa was the best compromise we found to build a mutant of EF with impaired ability to recruit CNOT2 while preserving its transactivation and phase transition abilities.

Within the LC NTD, aromaticity represents a critical determinant of EF transcriptional and transforming activities [91], [92]. For instance, replacing tyrosines by aliphatic aa (such as serines) has been reported to abrogate EF phase transition properties and its ability to recruit the BAF complex [92]. Likewise, we find that aromaticity is essential for the EF/CNOT2 interaction. Interestingly, using disorder prediction tools, we further show that replacing 17 out of 30 DHR tyrosines by aliphatic aa globally increases structural disorder of the EF LC NTD and disruptes the EF/CNOT2 interaction. In contrast, when the same DHR tyrosines are replaced by phenylalanines (*i.e.*, another aromatic aa), structural disorder of EF LC NTD is not altered and the interaction with CNOT2 is conserved (**Figure 79-81**). Based on this, we can reasonably think that the structural

disorder landscape of EF LC NTD *per se* underlines the importance of aromaticity for EF PPIs both in transcription and mRNA degradation.

Next, we show using two alternative approaches that EF controls mRNA stability via its interaction with CNOT2 (and presumably via its association with CCR4-NOT) (**Figure 76**, **Figure 78**). An interesting question is whether this ability is a neomorphic property of EF or whether it is shared with parent proteins EWSR1 and FLI1. Preliminary results using coimmunoprecipitation experiments indicate that FLI1 but not EWSR1 is able to associate with CNOT2 (see the section 'Complementary Results', **Figure 107a**). For FLI1, this result is expected because ERG, which is highly homologous to FLI1, can also associate with CNOT2 [529]. In contrast, the inability of EWSR1 to associate with CNOT2 is more surprising at first sight. Indeed, the LC NTD which mediates the interaction between EF and CNOT2 is also present in wild-type EWSR1. Repeating coimmunoprecipitation experiments with FLAG-tagged constructs expressing full-length EWSR1, EWSR1 LC NTD (EWSR1_Nter) and EWSR1 CTD (EWSR1_Cter) revealed that the LC NTD is well-able to associate with CNOT2, although the CTD alone cannot (**Figure 107b**). Based on this, we hypothesize that in wild-type EWSR1, the inhibition of the LC NTD by the CTD (as described in the context of transcription regulation in [77]) might compromise the association with CNOT2. In EF, the inhibition by the CTD is lost via fusion, which enables the association with CNOT2. This feature further illustrates how domain reorganization via fusion can unlock the oncogenic potential of parent proteins. Of note, the inability of EWSR1 to associate with CNOT2 diverges from the observations about the BAF complex because both wild-type FET proteins and EF appear to associate with this complex [637].

Consistently with the results shown in **Figure 107**, we found that MS2-tagged FLI1 but not EWSR1 or its Cter region can decrease the stability of the *R-Luc-8MS2* reporter upon tethering (**Figure 108**). From our study on ERG [120], we expect that the ability of FLI1 to decrease mRNA stability arises from its association with CCR4-NOT via CNOT2 in its ATAD. These preliminary data might indicate that, from the point of view of EWSR1 but not FLI1, the control of mRNA stability represents a neomorphic property of EF that is revealed because the EWSR1 CTD is lost via fusion.

Although FLI1 and EF are both able to decrease the stability of a reporter mRNA upon tethering, these proteins might not necessarily be targeted to the same cellular mRNA transcripts. Because we do not have access to the endogenous decay targets of FLI1, we started testing the above possibility by comparing the decay targets of ERG identified in [120] with those of EF identified here. Interestingly, we found a significant overlap between these two datasets (**Figure 109**). Of note, gene ontology analysis on the overlapping targets revealed an enrichment for GO terms related to cell division and mitotic cell cycle (not shown). If these findings also verify for FLI1, they might reinforce the idea that the control of mRNA stability is a neomorphic property of EF only in the point of view of EWSR1.

4. EF controls mRNA stability via the AREBP HuR

Using RIP experiments in EwS cells, we show that EF is able to associate with most of its decay panel target mRNAs (**Figure 67**). Nevertheless, because EF lacks any identifiable RNA-binding domain, we expected that EF might not bind directly to its target mRNA transcripts. As ERG binds to RBPs via its CTAD [119], [120], we hypothesized this might occur via binding to RBPs given that EF CTAD is highly homologous to the one of ERG. Currently, our data indicate that EF might be targeted to its mRNAs by binding to HuR (**Figure 88-92**). In particular, we show that this might occur via the FLI1-derived CTAD (**Figure 93**). Interestingly, we also found that EF can associate with other RBPs, such as RBFOX2, RBPMS and QKI (**Figure 110a-c**), presumably via this region as formally shown for RBPMS (**Figure 110d**). Of note, HuR and QKI have also been identified in the interactome of EF [209]. The importance of the CTAD in EF function has hardly been investigated. Early studies in NIH3T3 cells (*i.e.*, non-EwS cells) revealed that this domain was necessary for full EF-mediated transformation and modulated EF transcriptional function [638]. More recently, these observations have been confirmed in EwS cells [145]. Altogether, our findings indicate that the CTAD might also serve as a binding platform for RBPs and might thus represent an important determinant of EF post-transcriptional functions.

Interestingly, in addition to pre-mRNA splicing, RBFOX2, RBPMS and QKI have been reported to influence mRNA stability [562]–[564], [639]–[641]. Therefore, we also investigated whether EF might control mRNA stability via these RBPs. To this aim, we analyzed whether their motifs were differently enriched in target vs. non-target 3'UTRs. RBFOX2 binds to UGCAUG motifs at various regulatory sites such as in pre-mRNA introns and mRNA 3'UTRs [639]. RBPMS binds to tandem CAC motifs separated by variable spacer length mainly in pre-mRNA introns, mRNA CDS and 3'UTRs [640], [642]. QKI binds to 5-nt YUAAY motifs (Y = a pyrimidine nucleobase). >90% of QKI targets contain at least one QKI motif. In ~50% of QKI targets, ~30-nt-long sites containing two or more YUAAY motifs separated by variable spacer length are found [643]. QKI recognition motifs have mainly been identified in pre-mRNA introns and mRNA 3'UTRs [644]. Because these motifs were not all included in the database used for the MEME analysis [645], we analyzed their occurrence in target and non-target 3'UTRs using an in-house R script (see the 'Materials & Methods' section). We used HuR motifs as a control. For QKI, we used the core YUAAY motif. Consistently with the MEME analysis, we found that HuR motifs were significantly enriched in target 3'UTRs. In addition, we found a similar enrichment for QKI motifs. In contrast, we found that target 3'UTRs surprisingly contained a lower number of RBFOX2 and RBPMS motifs (**Figure 111**). Importantly, as for HuR, all mRNA targets of the decay panel contained at least one QKI motif in their 3'UTR (**Figure 112a**). Together, these findings suggest that, in addition to HuR, EF might also be targeted to its decay targets via association with QKI. Of note, we found that neither the number of HuR nor QKI binding sites within target 3'UTRs was correlated with their corresponding mRNA HL ratio (**Figure 112b-c**). Subsequently, we decided to focus on HuR because its motifs were the first hits in the MEME analysis.

Strikingly, we report that loss of HuR does not abrogate the ability of EF to bind to its target mRNAs (not shown), contrary to the treatment with DHTS (**Figure 95**). To reconcile this result with our model, we assumed that, in the absence of HuR, EF is targeted to mRNAs via other RBPs, such as AREBPs or QKI. Supporting this, using resazurin viability assay, we found that HuR KD in shA673-1c cells affects more strongly unselected cells than their selected counterparts (not shown), reinforcing the idea that the function of HuR might be complemented after a specific time by one or several other RBPs. However, this also suggests that DHTS may not be specific to HuR but may also interfere with the RNA-binding ability of other AREBPs.

Next, we show that HuR KD led to the stabilization of the representative set of EF decay targets in EwS cells (**Figure 97a**). Very interestingly, we show that HuR actually acts as a stabilizing factor in the absence of EF and as a destabilizing factor in the presence of EF (**Figure 97**). Importantly, our results indicate that the presence of EF does not impair the ability of HuR to bind to its mRNA targets, ruling out the idea that EF might antagonize the mRNA protective function of HuR via titration from its target mRNAs (**Figure 91**). Instead, based on the ability of HuR to coimmunoprecipitate with CNOT2 only in the presence of EF (**Figure 96**), we propose that by interacting with both HuR and CCR4-NOT, EF associates its protein partners into the same mRNP complex. In turn, this reassociation causes HuR to switch from its canonical stabilizing function to a non-canonical destabilizing function. Although HuR has also been reported to destabilize two mRNA transcripts [472], [473], HuR is defined as a stabilizing factor. Our data thus reinforce the possibility that HuR might also act as a destabilizing factor into specific contexts. In light of this finding, it is tempting to speculate that other mRNA-decay associated RBPs might also have non-canonical stabilizing/destabilizing functions into specific contexts that remain to be defined. Of note, QKI has also been described as a stabilizing factor [562]–[564] and thus might also be switched into a destabilizing factor upon EF binding. More globally, these findings add on a number of evidence showing that PPI networks are dynamically remodeled via fusion [283].

Since TTP and HuR have opposite roles on mRNA stability [465], [568], it was intriguing to find that EF downregulates *TTP* mRNA transcript (also known as *ZFP36*) (**Figure 66a**). Although *TTP* is probably an indirect transcriptional target of EF (not found among EF-bound targets), this mechanism might foster the mRNA decay activity of EF by increasing the availability of AU-rich mRNA transcripts for targeting via HuR. Interestingly, such synergy has also been evidenced for another TF involved in the control of mRNA stability, namely ZFP217. Indeed, ZFP217 appears to both sequester the m6A reader protein YTHDF2 and to activate the demethylase FTO in 3T3L1 cells. The interaction with YTHDF2 is critical for allowing FTO to maintain its interaction with m6A sites on various mRNAs [550].

In the cell nucleus, HuR has been reported to regulate pre-mRNA splicing [568]. Although we focused our attention on mRNA decay, our results are compatible with the idea that EF and HuR might also collaborate in the context of pre-mRNA splicing. Supporting this, we found that the majority of the overlapping targets between EF decay targets and HuR PAR-CLIP targets contains HuR binding sites in both introns and 3'UTRs (**Figure 90a**).

5. Subcellular localization of EF-mediated mRNA decay

The subcellular localization of the here identified function of EF in mRNA decay remains an open question. On the one hand, our observations are compatible with a cytoplasmic localization. Indeed, although EF appears to be mainly localized in the cell nucleus which is consistent with its canonical role as a DNA-binding TF, we show that EF also appears as discrete cytoplasmic foci in two EwS cell lines (**Figure 74**). In addition, although we did not directly investigate this, we expect that EF/HuR interactions occur in the cytoplasm because HuR is known to regulate mRNA stability in this compartment. Interestingly, HuR is known to be relocated into the cell cytoplasm under stress conditions [646]. Because EF expression causes replication stress [312], we reasoned that HuR might be relocated to the cell cytoplasm in the presence of EF. However, in light of our current preliminary results using nucleocytoplasmic fractionation experiments (**Figure 113**), it remains unclear whether this might happen in EwS cells. If HuR is indeed relocated to the cell cytoplasm via EF, it might point towards a model in which stress-induced HuR relocalization to the cell cytoplasm is exploited by cytoplasmic EF molecules to target specific mRNA subsets for decay. Finally, using PLA, we show that the EF/CNOT2 interaction occurs in both the cell nucleus and cytoplasm (**Figure 73**). The interaction in the nucleus might take place in the context of transcription given than CCR4-NOT has also been described to play a role in this process [360], [361] while the interaction in the cytoplasm might take place in the context of cytoplasmic mRNA degradation.

On the other hand, the above considerations do not completely rule out a potential nuclear localization for EF-mediated mRNA decay. Indeed, there is no prior objection that HuR might control nuclear mRNA stability in addition to pre-mRNA splicing. Moreover, the nuclear EF/CNOT2 interactions might not necessarily or not only occur in the context of transcription.

6. Biological importance of EF-mediated mRNA decay

In normal cell, TFs and RBPs orchestrate transcriptional and post-transcriptional programs that together shape the transcriptome. In turn, the transcriptome shapes the composition of the proteome, which eventually governs cell identity and function. It is tempting to speculate that, likewise, the RBP-TF chimera EF reshapes the transcriptome of EwS cells via its different functions in transcription [92], pre-mRNA alternative splicing [119], [209], and mRNA decay (this work). In turn, this aberrant transcriptome reshapes the composition of the proteome, which eventually governs EwS biology (**Figure 124**). Supporting this model, we show that, although EF controls distinct mRNA transcripts via its transcriptional, splicing and decay activities (as discussed at the beginning of this section), it appears to control several sets of functionally-associated mRNAs and thus common biological processes, most notably cell cycle and cell proliferation (**Figure 84**, **Figure 85b**). Importantly, based on spheroid growth assays, we also show that abrogating the decay function alone is sufficient to impede EwS malignant hallmarks, thus indicating that EF-mediated mRNA decay is important for the oncogenic process in EwS (**Figure 100**).
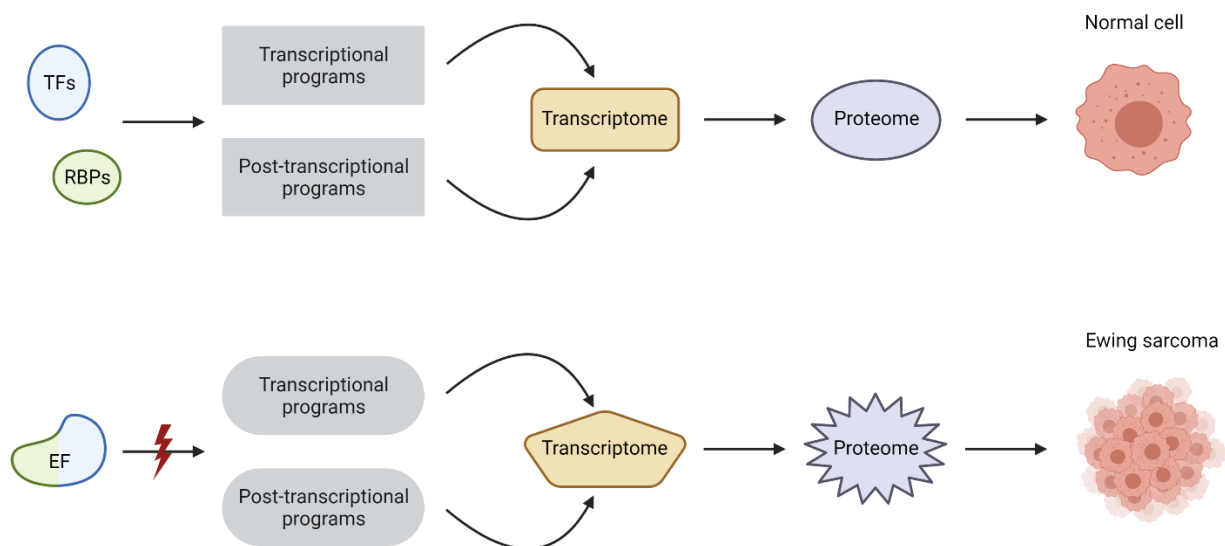
Figure 124. Outcome of the transcriptional and post-transcriptional programs in normal cell physiology and its EF-mediated deregulation in EwS. See main text for details. Created with BioRender.com.

Nevertheless, because HuR is known to favor cancer progression by enhancing the stability and translation of oncogenic mRNA transcripts, it sounds, at first sight, counterintuitive that EF-mediated mRNA decay of HuR mRNA targets might play a pro-oncogenic role in EwS. As further illustrated below, I believe that mRNA decay contributes to the oncogenic functions of EF by adding another layer of complexity to the regulation of gene expression. To explore how this complexity might materialize in EwS biology, I used two different approaches: (i) I performed gene ontology analyses of EF decay targets using DAVID and PANTHER tools, and (ii) I visually inspected the gene list of EF decay targets. Through this process, I have identified several biological contexts for which EwS can take advantage of the new molecular function of EF in mRNA decay. Using the

first approach, I found with DAVID tool that GO terms related to cell division, pre-mRNA splicing, response to DNA damage and transcription are enriched in EF decay targets (**Figure 62**). Importantly, similar results were obtained with PANTHER tool (**Figure 114**). Of note, two main differences can however be highlighted. First, GO analysis with PANTHER provided more significant results than with DAVID. Second, GO analysis with PANTHER revealed the statistical enrichment of other relevant GO terms, such as those related to apoptosis, response to unfolded protein and protein ubiquitination. Using the second approach, I found that mRNAs belonging to the same gene family were present in EF decay targets, suggesting that EF decay activity might contribute to the post-transcriptional control of mRNA families in EwS. Hereafter, I discuss the contribution of EF-mediated mRNA decay into four biological contexts, including cell cycle progression, response to unfolded protein, cell plasticity and post-transcriptional control of mRNA gene families.

6.1. Cell cycle progression

Aberrant cell cycle progression is a well-known hallmark in cancer. Generally, cancer-associated mutations ensure continuous rounds of division by preventing cell cycle exit [647]. In EwS, cell cycle control is aberrant [648]. Once again, this is orchestrated by the fusion protein EF which is known to modulate various cell cycle regulators, among which NR0B1 [160], Aurora kinases A and B [649], p21/CDKN1A [650], cyclin D [206], [651], cyclin E [652], p57/KIP2 [653], TGFβ- [142], IGF-[143], [654], and MAPK signaling [655]. Interestingly, we found that mRNAs encoding Aurora kinases A and B, cyclins, cyclin-dependent kinases, TGFβ receptors and MAPK proteins were also targeted for decay by EF. In particular, we found that well-known partners of Aurora kinases, such as AUNIP, FAM, HAUS8, WEE1 and MAD2L, were also present in the list of EF decay targets. Together, these observations indicate that, in addition to transcription, EF-mediated mRNA decay might contribute to aberrant cell cycle control in EwS. For instance, the decay activity of EF might specifically control Aurora signaling. Interestingly, EF is able to directly activate the transcription of Aurora kinases A and B [649]. Because EF also decreases the stability of their mRNAs, regulation of Aurora expression at the mRNA level belongs to the mode of opposite coupling. As described in 2.6.3.1, this mode enables fast and transient gene expression responses characterized by a peak-shaped profile (**Figure 52**). In yeast, periodic mRNA synthesis and decay have been reported to co-operate during cell cycle progression [393]. Interestingly, by combining fluorescence activated cell sorting (FACS) and single-cell RNA-sequencing (scRNA-seq), a very recent study has identified CNOT1, the scaffold subunit of CCR4-NOT, as an important factor for scheduled mRNA decay during the mitosis-to-G1 phase transition in human cells [656]. Based on these studies, EF-mediated mRNA decay of cell cycle regulators like Aurora kinases appears as a plausible mechanism allowing the timely progression through the different phases of the cell cycle in EwS, and thus participating in the high proliferative status of EF expressing cells.

6.2. Response to unfolded protein

GO analysis with PANTHER revealed that EF decay targets are enriched in transcripts related to the unfolded protein response (UPR). UPR is an adaptive cellular mechanism that evolved to cope with perturbed proteostasis (*i.e.*, control of protein homeostasis). In tumors, both intrinsic (*e.g.*, oncogenes activation, mutations, *etc*.) and extrinsic factors (*e.g.*, hypoxia, nutrient deprivation, acidosis, *etc*.) are well-known to cause endoplasmic reticulum (ER) stress due to the accumulation of misfolded proteins in the ER [657]. By restoring ER proteostasis, UPR activation, observed in several cancer models, is thought to contribute to malignant progression [658]. UPR is mediated by three main sensors found at the ER membrane, among which the activating transcription factor 6 (ATF6), the PKR-like ER kinase (PERK), and the inositol-requiring enzyme 1 (IRE1). Upon appropriate activation, UPR signaling regulates the activation of genes that ultimately lead to the clearance of misfolded proteins (**Figure 115a**). Importantly, unresolved proteostasis leads to cell apoptosis [657].

The finding that UPR-related mRNAs are enriched in EF decay targets has raised our interest for several reasons: (i) UPR signaling has been linked to the growth of solid tumors [657], [659], (ii) ATF4, a downstream TF of UPR signaling, has been reported as a direct transcriptional target that is activated by EF and regulated via post-transcriptional mechanisms [660], and (iii) NMD, a pathway of mRNA decay, has been described to shape UPR. Notably, NMD has been reported to delay UPR activation *in vitro* and *in vivo* and to schedule UPR termination [398]. Interestingly, preliminary results indicate that EwS cells undergo ER stress and UPR activation in a EF-dependent manner (**Figure 115b-c**). In total, 16 UPR-related transcripts were identified among the EF decay targets, such as *ATF6* (but not *ATF4*), *AMFR*, *ERO1A*, *HSPA8/9*, *HERPUD1*, *TOR1B*, and *DNAJB9*. Of note, the GO term related to UPR is also enriched in HuR PAR-CLIP targets (not shown). On this basis, I hypothesized that EF-mediated mRNA decay via HuR might also shape UPR in order to support Ewing sarcomagenesis.

6.3. Cell plasticity

EwS tumors display a phenotypic plasticity. This feature appears to be acquired through a process that resembles partial EMT [5]. EMT is initiated by signaling pathways that sense extracellular stimuli, among which transforming growth factor-β (TGFβ) family signaling plays a predominant role [233]. EMT is controlled by downstream TFs, including mainly SNAIL, TWIST and ZEB2 factors (**Figure 116**). Interestingly, we found many mRNAs encoding EMT-related proteins in EF decay targets, such as *TGFβR1/2* (TGFβ receptors 1 and 2), *SMAD3*, *MAPK3/4/7* (mitogen-activated protein kinases), *ZEB2* and *E2F1*. E2F1 is a TF that is related to EMT because it binds *ZEB2* gene promoter and control its transcription. Of note, although not significant, GO term related to TGFβ signaling went out with DAVID tool. Moreover, GO terms related to EMT and TGFβ signaling were significantly enriched in HuR PAR-CLIP targets (not shown). Supporting this, HuR binding sites in the 3'UTR region of all EMT mRNAs can be found (**Figure 117**). Notably, in ovarian cancer cells, HuR has been reported to bind to *ZEB2* 3'UTR [661].

Interestingly, *TGFβR2* is also a well-known direct repressed transcriptional target of EF. Because this gene appears to be both transcriptionally-repressed and destabilized at the mRNA level by EF, it represents a case of synergistic coupling (**Figure 52**). Together with the destabilization of *SMAD3* and *MAPK3/4/7*, it is tempting to speculate that EF-mediated mRNA decay might participate in switching off TGFβ signaling in EwS. Interestingly, *ZEB2 and E2F1* are transcriptional targets that are activated by EF. Because these genes appear to be both transcriptionally-activated and destabilized at the mRNA level by EF, it represents another case of opposite coupling (**Figure 52**). As covered previously, transcriptional antagonisms between EF and ZEB2 functions are one of the models that account for cell plasticity in EwS. In this perspective, the idea that *ZEB2* mRNA might be targeted by EF for decay while being activated at the level of transcription is an amazing finding. Indeed, the EF-mediated mRNA decay of *ZEB2* (as well as other EMT regulators) might add another layer of regulation to the EMT process in EwS. This hypothesis is further supported by the fact that EMT TFs are well-known to be finely regulated at all levels of gene expression [233]. Moreover, this might point towards a more integrated model of EwS cell plasticity in which post-transcriptional events mediated by EF, CCR4-NOT and HuR are implicated. Of note, interestingly, QKI has also been described to regulate the mesenchymal phenotype [662], [663]. Altogether, these data indicate that EF, via its transcriptional and post-transcriptional functions, might completely rewire TGFβ signaling control in EwS.

6.4. Post-transcriptional control of mRNA gene families

Interestingly, by visually exploring the list of EF decay targets, I identified the presence of several members belonging to specific mRNA families. These mRNA families were regrouped into four main functional categories, including cell cycle progression, signal transduction, transcriptional regulation and protein homeostasis (**Figure 118**). Of note, these categories account for ~20% of EF decay targets (148/772). This approach has yield similar findings than the one based on the use of GO tools. However, here, we also found that EF controls the stability of 29 TFs, including SMAD3, KLF11, 2 ETS factors (ETV5, ETV6), 2 E2F factors (E2F1 and E2F6), 5 ZBTB factors (Zinc Finger And BTB Domain Containing) and 18 ZnF factors (C2H2 Zinc Finger). These findings indicate that EF-mediated mRNA decay might also indirectly contribute to reshaping transcription in EwS by targeting transcripts encoding TFs for decay. In particular, this mechanism might participate in the repression of ETS factors, although this remains highly speculative at this stage.

7. Inhibition of EF-mediated mRNA decay and clinical relevance of DHTS in EwS

As many other TFs, the fusion protein EF is considered 'undruggable' because it lacks an enzymatic activity and contains IDRs. Based on our findings, we hypothesized that the new function in mRNA decay might unveil novel therapeutic opportunities for EwS. In this work, we show that EF-mediated mRNA decay is underlined by two important PPIs, involving the CCR4-NOT complex and the AREBP HuR. We reasoned that targeting HuR rather than CCR4-NOT represented the easiest and fastest approach to both address the significance of EF decay activity and further validate our model for several reasons. First, contrary to the CCR4-NOT complex, many chemical inhibitors of HuR are commercially-available and have already been used in *in vivo* experiments. Next, although using small molecule inhibitors of PPIs is clearly an attractive approach in our case, screening and validation methods are often time-consuming, especially when interactions involve IDRs. Third, because HuR controls many cancer hallmarks at the post-transcriptional level, this RBP is generally considered to represent an attractive therapeutic target for cancer [465] but its importance has hardly been investigated in EwS. Fourth, very recently, a computational analysis identified *HuR* mRNA transcript as an ideal target for Ewing sarcoma therapy [664]. Based on this, we envisioned to target the decay function of EF by inhibiting HuR through the use of either chemical compounds (DHTS and CMLD-2) or shRNA.

DHTS is a natural product found in the roots of *Salvia miltiorrhiza*, and well-known in traditional Chinese medicine practice. This compound has a low molecular weight and belongs to the bioactive family of diterpenic tanshinones. Tanshinones are anti-inflammatory agents that are notably used in the treatment of cardiovascular diseases [665]. In addition, tanshinones have been shown to display anti-cancer properties [666], [667]. In 2015, DHTS is identified via high-throughput screening of a library of anti-inflammatory agents as capable of interfering with the formation of the HuR:RNA complex [479]. The interaction between DHTS and HuR is mediated via residues within the RRM1 and RRM2 [479], [668]. By interfering with the mRNA binding properties of HuR, DHTS is believed to compromise its post-transcriptional functions in mRNA stabilization and translation. Interestingly, DHTS has not been associated with systemic toxicity *in vivo* [668].

First, we show that treatment with DHTS increases the stability of the representative set of EF decay targets (**Figure 94**), which further supports our model that EF-mediated mRNA decay depends on HuR. Although DHTS has been reported to paradoxically strengthen HuR affinity for target mRNAs with longer 3'UTR and higher density of AREs in HeLa cells [668], we found that *eIF4E* and *ZEB2* mRNAs, which fall into this category, were also effectively stabilized by DHTS. One possible explanation to this discrepancy might be related to cell type differences between HeLa and EwS cells.

Next, we evidence that EwS cells are more vulnerable to HuR inhibition than non-EwS cells (**Figure 99a**). Moreover, we report that loss of EF make EwS cells less sensitive to DHTS while ectopic expression of EF in hMSCs, otherwise highly resistant to DHTS, make them as sensitive as EwS cells (**Figure 99b**). Together, these results suggest a functional linkage between the vulnerability

to DHTS and the presence of EF. Importantly, because sensitivity to DHTS is modulated by HuR expression [479], we explored *HuR* mRNA expression levels in EwS and non-EwS cells using the Cancer Dependency Map (DepMap) public database [669]. At first sight, differences in sensitivity to DHTS between EwS and non-EwS cells appeared to be due to variations in *HuR* mRNA expression levels (**Figure 119a**). However, we found no variation in HuR expression at the protein level between EwS EF^high cells and EwS EF^low cells (**Figure 119b, Figure 113**). These observations suggest that variations in DHTS sensitivity, at least between EwS cell subpopulations, is not linked to HuR expression levels.

Based on the above findings, we hypothesized that the higher sensitivity to DHTS might be linked to the decay activity of EF. To test this possibility, we envisioned a KD/rescue experiment using shA673-1c EwS cells and FLAG-tagged constructs encoding either full-length EF or Δ63EF decay mutant. KD/rescue experiments are a very elegant approach to analyze mutants of EF in a relevant biological context (used for instance in [145]). In this work, the experimental design was however not optimal. Indeed, EwS cells used here are harboring a dox-inducible shRNA targeting the breakpoint region of EF. Therefore, upon induction, the shRNA was also able to target the ectopically-expressed constructs of EF. Although this aspect did not prevent the ectopic expression of our constructs, it would be better to repeat KD/rescue experiments in cells harboring a dox-inducible shRNA targeting the 3'UTR region of EF, thus unable to target FLAG-tagged constructs of EF which are lacking this region. It remains however to establish whether targeting the 3'UTR of endogenous EF will ensure a depletion as efficient as targeting the breakpoint region. Although a definitive demonstration is lacking here, our KD/rescue results tend, so far, to confirm the idea that EF-mediated mRNA decay confers a new vulnerability to HuR inhibition (**Figure 99c**) and contributes to the oncogenic process in EwS (**Figure 100**).

Furthermore, our results indicate that the RBP HuR might represent an attractive therapeutic target in EwS. HuR is well-known to control malignant hallmarks in various cancer settings. Recently, HuR has notably been reported to promote osteosarcoma, the most common type of bone cancer before EwS [476], [670]. Strikingly, the importance of HuR into EwS biology has hardly been investigated [664]. Here, we show that HuR inhibition compromises cell viability, anchorage-independent growth and cell migration of EwS cells (**Figure 99-102**). However, preliminary explorations using the Depmap database revealed that CRISPR/Cas9-based disruption of HuR did not affect the proliferation and/or viability of most EwS cell lines (**Figure 120a**). Again, one possible explanation is that, in the absence of HuR, another related AREBP can compensate its function. Very interestingly, we found that the essentiality of HuR for cell growth tends to be more pronounced in EwS as in other bone cancers (**Figure 120b**). Although still speculative at this stage, this might be functionally-linked to EF-mediated mRNA decay.

Although HuR chemical inhibition was the easiest and most straightforward approach to further validate our model, it remains to establish whether it is a viable therapeutic option in routine clinics for treatment of EwS. One important limitation is that DHTS is not effective against EwS EF^low cells, which are thought to mediate chemoresistance and relapse in EwS patients [671].

SECTION VI   PERSPECTIVES

In this section, several perspectives to the present work are covered. A first bunch of them aims at either consolidating the present findings by suggesting alternative experiments, or complementing them by addressing important open questions (see paragraph 1). Following this, another bunch of perspectives with a broader scope are proposed. These ones might provide guidelines for future research projects, a number of them being already ongoing in the host laboratory (see paragraphs 2 to 5).

1. Consolidatory/complementary experiments

1.1. KD/rescue experiments

As discussed in the previous section, a crucial perspective to this work is to repeat our KD/rescue experiments using a more optimal experimental design. Currently, we are designing new A673 cells that contain a dox-inducible shRNA targeting the 3'UTR region of EF. This should allow us to KD endogenous EF without affecting FLAG-tagged ectopically-expressed EF constructs. An important verification that was missing in our current experiments will be to assess the quality of endogenous EF KD after selection of rescued cell.

1.2. mRNA stability analysis

In this work, mRNA stability was investigated using time-course experiments after transcription blockage with ActD followed by RNA-seq or RT-qPCR. Although this remains a valid and common approach to analyze mRNA stability (used for instance in [120], [537]–[539], [582], [583]), ActD is known to disrupt normal cell physiology [586], [672]. Moreover, the contribution of pre-mRNA processing is neglected [578], [586], [672]. Together, these considerations imply that computed HL using ActD might not represent unperturbed degradation rates. Therefore, to reinforce our data, it might be relevant to repeat the transcriptome-wide analysis in shA673-1c using another approach. To this aim, many alternatives are available (reviewed in chapter 3). Currently, we are investigating the possibility to use a total RNA-seq-based approach using intronic expression as a proxy for the synthesis rate.

Importantly, we obtained consistent changes in mRNA stability for the representative set of EF decay targets panel between: (i) two different EwS cells lines after EF KD and, (ii) EwS cell lines after EF KD and hMSCs after EF ectopic expression (**Figure 63c**). Of note, unfortunately, we could not perform stability measurements in TC71 cells owing to their high sensitivity to ActD. This observation further advocates for the need of alternative approaches when the use of transcription blockage is not applicable. To more fully portray the aberrant mRNA stability landscape that is imposed by EF in EwS, it might be interesting to perform transcriptome-wide mRNA stability analyses in other EwS cells lines as well as in hMSCs.

Unexpectedly, we found that, for a representative set of EF decay targets, HuR acts as a destabilizing factor in the presence of EF and as a stabilizing factor in the absence of EF. To our knowledge, this is the first time that such an antagonism is reported. An important question is whether all endogenous mRNA targets of HuR are affected by this antagonism or not. If not, it might be interesting to analyze whether this is correlated to specific mRNA features (*e.g.*, specific RBP motifs, codon usage, *etc*.). To this aim, it would be necessary to perform transcriptome-wide mRNA stability analyses in shA673-1c -/+ dox shCTL/shHuR cells.

1.3. Recruitment of the CCR4-NOT complex

So far, our data point towards a model in which EF associates with CCR4-NOT via the CNOT2 subunit. To formally demonstrate this, we should test the ability of EF to coimmunoprecipitate with deadenylase subunits (CNOT6L and/or CNOT8) in the presence/absence of CNOT2. Although less direct, another approach is to analyze poly(A) tail length of a tethered mRNA or specific endogenous mRNA targets in the presence/absence of EF after resolution on a polyacrylamide gel as used in [350], [622].

1.4. A decay mutant of EF with compromised ability to recruit HuR

A major challenge of this work was to discriminate between EF transcriptional and decay activities. EF transcriptional activity is long known to depend on the LC NTD (transactivation), the ETS DBD (DNA-binding), and the CTAD (regulatory function) [109], [138], [638]. Using biochemical assays, we found that EF decay activity implicates the first 63 aa of the LC NTD and the CTAD. Based on this, two decay mutant of EF can be envisioned: Δ63EF and EFΔCTAD. Because the first 63 aa are only partially overlapping with EF transactivation function and because small fragments of the LC NTD fused to FLI1 are sufficient to recapitulate EF activity [92], we hypothesized that removing the first 63 aa was a more promising option than removing the full CTAD in order to disrupt EF decay activity without compromising EF transcriptional activity. Nevertheless, a more precise mapping of the EF/HuR interaction in order to restrict it to a subdomain or a few dominant aa might also offer the opportunity to build a second decay mutant of EF (further discussed later).

1.5. Importance of EF-mediated mRNA decay in EwS cell plasticity

Cell plasticity is a hot topic in the field of EwS because it is directly related to metastasis, the main cause of death in EwS patients. In the chapter 1 of the introduction, I mentionned that one of the model underlying EwS cell plasticity is related to a transcriptional antagonism between EF and ZEB2, a key TF in EMT regulation. In light of this, the role of EF in the control of *ZEB2* mRNA stability is an enthusiastic finding. To further explore this aspect, it might be interesting to identify the binding sites that are important for HuR binding. If dominant binding sites can be identified, a CRISPR-Cas9 EwS cell line harboring compromised HuR binding sites could be generated and used into different functional analysis (*e.g.*, spheroid migration assays, *etc*.)

1.6. Subcellular localization of EF-mediated mRNA decay

The subcellular localization of the EF decay activity remains an open question. Testing the colocalization of EF, CNOT2 and HuR using immunofluorescence-based approaches might help in addressing this question.

1.7. Other determinants of EF-mediated mRNA decay

Although the underlying mechanism remains unclear, the mRNA CDS is an important regulatory feature of mRNA stability [426], [673]. Because both CCR4-NOT and HuR have also been related to the interplay between translation and decay [646], [674], [675], it might be worth to explore codon usage and bias in target vs. non-target CDS.

2. In-depth characterization of the EF/CNOT2 and EF/HuR interactions

A more comprehensive characterization of the determinants of EF PPI network should undoubtedly inform both Ewing sarcomagenesis and therapeutics. In that context, an important perspective to this work is to map more precisely the interactions that we report with CNOT2 and HuR. So far, both the EF/CNOT2 and EF/HuR interactions have indeed been mapped to quite large protein regions. The EF/CNOT2 interaction was located within the first 63 aa of EF and the NAR domain of CNOT2 (59-aa long) while the EF/HuR interaction was located within the CTAD of EF (89-aa long) and the RRM3 domain of HuR (82-aa long). To move forward, we have retrieved AlphaFold2 3D protein structures of human EWSR1, CNOT2, FLI1 and HuR via the online portal at https://alphafold.com/ [676], [677]. Interestingly, we found that: (i) although the first 63 aa of EWSR1 are largely disordered, they contain a β-sheet secondary structure (**Figure 121a**), (ii) the NAR domain of CNOT2 contains an α-helix within its first half (**Figure 121b**), and (iii) the CTAD contains an α-helix immediately downstream of the ETS DBD while the remaining sequence is highly disordered (**Figure 121d**), which is in agreement with [145], [678]. Based on this, we asked whether the EF/CNOT2 and EF/HuR interactions might be mediated by these secondary structures. To address this question, we are now performing *in silico* analyses. Importantly, our preliminary results using docking and molecular dynamics analyses are, so far, confirming our biochemical data. In the future, these *in silico* investigations might also enable us to identify dominant amino acids and, in turn, the type of bonds involved in these PPIs (**Figure 125**). Because the LC NTD of EF is rich in tyrosines, we expect that the EF/CNOT2 interaction might at least partly be mediated via π-effects. Alternatively, nuclear magnetic resonance might represent a useful approach. In the long run, these data would allow us to build more constrained decay mutants of EF. Notably, it could potentially help in designing a mutant of EF in its CTAD that is unable to recruit HuR without affecting its transcriptional function. Moreover, these structural data should constitute an important basis to perform a virtual screening in order to identify small molecule inhibitors of the EF/CNOT2 and/or EF/HuR interaction(s). After their experimental validation, these iPPIs might represent an attractive drug class for the treatment of EwS.
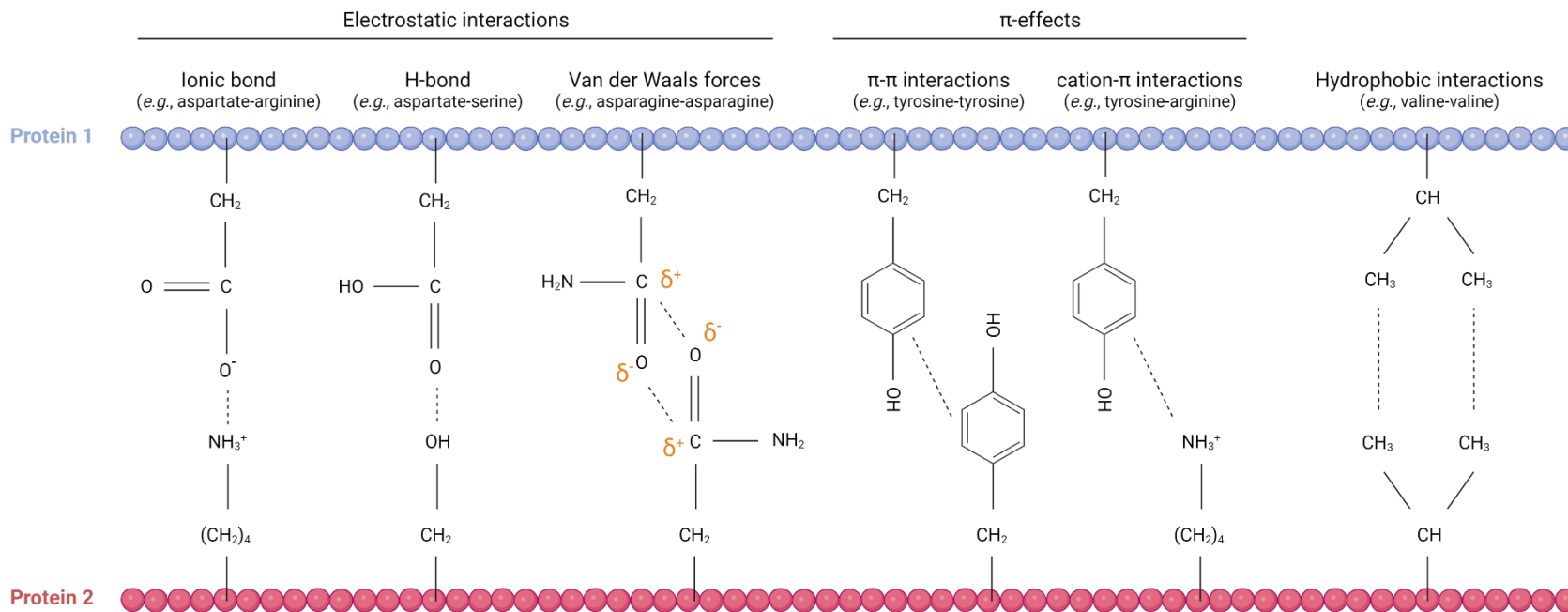
Figure 125. Main types of non-covalent bonds involved in protein-protein interactions. Created with BioRender.com.

3. Recycling oncogenic partnerships

EF-mediated mRNA decay is underlined by two important PPIs, involving the CCR4-NOT deadenylation complex and the AREBP HuR. Interestingly, both of these partners are involved in other molecular processes. CCR4-NOT is considered as a master regulator of gene expression and has notably been related to the control of transcription [360], [361]. In line with this, an interesting question is whether EF and CCR4-NOT might also collaborate in the context of transcription. As mentioned previously, the identification of EF/CNOT2 nuclear foci in our PLA experiment (**Figure 73**) is compatible with this possibility. In addition to the control of mRNA stability, HuR has been described to control pre-mRNA splicing [568]. Because EF is also involved in this process, the fate of the EF/HuR interaction on pre-mRNA splicing regulation is another interesting question. The same way of reasoning might also apply to QKI, which is largely known as a splicing factor. If EF and CCR4-NOT also collaborate in the context of transcription and if EF and HuR also collaborate in the context of splicing, these findings might point towards a model in which EF recycles its binding partners into different molecular contexts.

4. Fusion transcription factor-mediated mRNA decay

Given that the other FET::ETS fusions have a similar domain composition than EF, it is tempting to speculate that they might also promote mRNA degradation. Supporting this, we found that several other FET::ETS fusions are also able to interact with CNOT2 using a gPCA-based preliminary screening (**Figure 123**). Moreover, we found that FUS and TAF15 NTD are also able to recruit CNOT2 (not shown). Together, these data suggest than these fusions might also be able to associate with CCR4-NOT and trigger mRNA deadenylation.

As discussed in the previous section, our data are compatible with the possibility that the remaining Erg-derived ATAD also contributes to the EF/CNOT2 interaction. This contribution might be influenced by exon choices or breakpoint location, and thus vary between fusion variants as well as between FET::ETS fusions. For example, among EF variants, the contribution of the residual ATAD is expected to increase in EF 7/5, 10/5 and 9/4 compared to EF 7/6; and to decrease in EF 7/7, 9/7, 7/8 and 10/8 compared to EF 7/6 (**Figure 6**). Because there is no ATAD in EWSR1::FEV 7/2 and in FUS::ERG 7/10, the interaction with CNOT2 is expected to solely originate from the FET-derived region. In these two cases, CCR4-NOT might thus represent a neomorphic binding partner.

Next, because all FET::ETS fusions incorporate the CTAD, they are all expected to bind to RBPs, and possibly the same RBPs as for EF. Interestingly, HuR has also been reported in the interactome of ERG (BioGrid data based on [679]). Nevertheless, the ability to interact with HuR remains to be verified for each specific fusion. Indeed, the CTAD of FEV is more divergent than in ERG and FLI1, and interaction with HuR might not be preserved in this fusion. More importantly, the CTAD of ETV1/4 is significantly shorter than the one of FLI1 and does not share any substantial homology

with FLI1 CTAD [638]. Together, these observations indicate that sequence divergences might compromise the ability of some fusions to associate via their CTAD with RBPs such as HuR.

Another interesting question is whether TFMD is a widespread feature of fusion TFs beyond FET::ETS fusions. Although the question is completely open for non-FET::non-ETS fusions, it is reasonable to think that FET::non-ETS and non-FET::ETS fusions that incorporate a large fraction of the ATAD might also associate with CCR4-NOT. Similarly, non-FET::ETS fusions that also incorporate the CTAD might also be susceptive to bind to RBPs. These features alone should prompt to further investigate an implication into post-transcriptional processes.

5. Interactome of recurrent oncogenic fusion TFs

Interactomic data for fusion TFs are crucially lacking in the literature since fusion TF PPI network are only available for a few cases, such as EF (EwS) [209], FUS::DDIT3 (liposarcoma) [680], as well as NUP98::HOXA9 and SET::NUP214 (leukemia) [681]. This situation is very unfortunate given that the discovery of post-transcriptional functions for TFs frequently originated from these type of data in the past (*e.g.*, ERG, EBF1, SMAD2/3, KLF4, EF, etc.). In the future, the systematic investigation of the binding partners of pathognomonic and recurrent oncogenic fusion TFs might represent a highly useful resource. Notably, it should help in exploring whether other fusion TFs are also susceptive to be implicated in mRNA decay. Interestingly, by checking the binding partners of FUS::DDIT3 and NUP98::HOXA9, I respectively identified STAU1 and DCP1A. If these potential interactions were to be confirmed using biochemical assays, they might point towards an unsuspected function for FUS::DDIT3 in the control of SMD and for NUP98::HOXA9 in the control of decapping. Of note, although we focused our attention on the CCR4-NOT complex here, we do not exclude that EF might also interact with other decay machineries like the RNA exosome or decapping proteins as suggested by the interactome of EF identified in [209] (**Figure 23d**). Finally, if the work of mapping PPI for fusion TFs is undertaken, it would be ideal to also investigate, for each fusion protein, the binding partners of its parent proteins in order to identify neomorphic PPIs. To achieve this, protein complementation assays, such as gPCA or NanoLuc two-hybrid [682], might represent an attractive approach owing to their amenability to high-throughput screening. Otherwise, proximity-dependent biotinylation (BioID) and affinity purification mass spectrometry (AP-MS) represent well-described alternative methods [535].

SECTION VII   MATERIALS AND METHODS

1. Provenance of cell lines and cell culture conditions

HeLa, HEK293T, MCF7, MDA-MD-231 and U2OS cells were purchased from American Type Culture Collection (ATCC). HUVEC cells were purchased from Lonza. Ewing sarcoma cell lines shA673-1c and shSK-E17T were a generous gift from Dr. Olivier Delattre (Institut Curie, Paris). The TC71 Ewing sarcoma cell line was obtained from the German Collection of Microorganisms and Cell Cultures (DSMZ). Human bone marrow-derived mesenchymal stem cells (MSC) were kindly provided by Dr. Yves Beguin (CHU, Sart-Tilman). All cells were cultured in a 37°C 5% CO_2 humidified incubator with medium supplemented with 10% FBS (Gibco) and 1% Penn/Strep (Biowest). HeLa, HEK293T, MCF7, MDA-MD-231 and shSK-E17T were maintained in DMEM high glucose (Biowest), U2OS in McCoy's 5A Medium (Lonza), shA673-1c in DMEM high glucose with 20 µg/ml blasticidin and 200 µg/ml zeocyn (InvivoGen), TC71 in IMDM (Gibco), HUVEC in endothelial growth media-2 (EGM2, Lonza) without heparin and MSC in DMEM low glucose (Biowest) with 1% GlutaMax (Gibco). Primary cells with passages between 2 and 5 were used for all experiments. All cell lines were routinely checked for mycoplasma by MycoAlert™ Mycoplasma Detection Kit (Lonza).

2. Plasmids and cloning

Open reading frames (ORF) encoding human EWSR1 and FLI1 were obtained as pDONR223 from the human ORFeome v7.1 and v8.1 (The Center for Cancer Systems Biology, Dana-Farber Cancer Institute, CCSB-DFCI). The most frequent splicing variant of EF (*i.e.*, between exon 6 of EWSR1 and exon 7 of FLI1) was used in all experiments. EF 7/6 was generated from pDONR223-EWSR1 and pDONR223-FLI1 using PCR-fusion/Gateway cloning procedure as described in [683]. EFΔETS contains a deletion of 65 aa in its ETS domain and was previously described in [202]. It was generated from EF using PCR-fusion/Gateway cloning procedure. EFYS37 was synthesized by Integrated DNA Technologies (IDT) company. In this construct, all tyrosines (37 tyrosines) of the LC NTD are replaced by serines. SAGQQS, SIGQQS and SFGQQS tyrosine mutants of EWSR1 LC NTD were a generous gift from Dr. Kevin Lee [91]. In these constructs, 17 out of 30 tyrosines within DHRs are replaced by either alanine (A), isoleucine (I) or phenylalanines (F), respectively. EF7/6, EFΔETS, EFΔCTAD, Δ63EF, EWSR1_Nter, FLI1_Cter, EFYS37, SAGQQS, SIGQQS, SFGQQS and deletion mutants of EWSR1 LC NTD were inserted into pDONR223 by BP cloning (Gateway recombination technology, Invitrogen) with specific primers flanked at the 5'site by the following AttB1 and Attb2 Gateway sites: 5'-GGGGACAACTTTGTACAAAAAAGTTGGC(ATG)-3' (AttB1) and 5'-GGGGACAACTTTGTACAAGAAAGTTGA-3' (AttB2). All constructs include an ATG initiation codon and lack a STOP codon. Inserts from pDONR223 were subsequently transferred by LR cloning (Invitrogen) into different destination vectors: pDEST1899 (FLAG N-terminal tag), pCS3MTdest (Myc N-terminal tag, Addgene), pDEST475 (HA N-terminal tag, Invitrogen), pGLucN1 or pGLucN2 (Gaussian luciferase fragment 1 or 2 N-terminal tag) [630], and pDEST-EGFP (EGFP-N-terminal tag, Addgene). HA-tagged CNOT3, CNOT6 and CNOT7 were kindly provided by Elisa Izaurralde (European Molecular Biology Laboratory, Heidelberg, Germany). pCDNA3.1-mCherry empty

vector and pCDNA3.1-mCherry-HuR were kindly provided by Dr. Véronique Kruys (IBBM, ULB, Gosselies). For the tethering degradation assay (see below), pDEST1899 Flag-tagged ORFs were subcloned in the pN-MS2-CP (MS2 N-terminal tag, described in [684] following classical cloning procedure. For GGAA reporter assays, a pGL3-GGAA-Firefly reporter construct was first generated. Briefly, two single-stranded oligonucleotides encoding 12 GGAA repeats flanked by SacI and XhoI restriction sites (Thermo Fisher Scientific) were hybridized as followed. The oligonucleotides were mixed in equimolar amount, incubated for 5 min in boiling water and left for cooling down overnight. The resulting dimer was then cloned upstream the SV40 promoter of the pGL3-Firefly vector (Addgene) digested with SacI and XhoI restriction enzymes (Thermo Fisher Scientific).

Oligo-GGAA-F:

5'-CCGGAAGGAAGGAAGGAAGGAAGGAAGGAAGGAAGGAAGGAAGGAAGGAACC

Oligo-GGAA-R:

TCGAGGTTCCTTCCTTCCTTCCTTCCTTCCTTCCTTCCTTCCTTCCTTCCGGAGCT

For lentivirus-based transduction, a pLENTI-DEST vector was generated by transferring the insert from the pDEST1899 backbone vector to a pLENTI purchased from GenScript using XhoI restriction sites. All constructs were verified by Sanger sequencing at the GIGA-Genomics facility (University of Liege). All cloning and sequencing primers are listed in **Table S2**. Main plasmid maps are available in the 'Appendix' section.

3. Chemicals

For mRNA decay experiments, cells were treated with 5 µM ActD (Enzo Life Sciences) for up to 4 or 8h to block transcription. Inhibitors of HuR, dihydrotanshinone-I (DHTS) and CMLD-2, have been described elsewhere [479], [481], [668]. They were respectively purchased from Sigma-Aldrich and MedChemExpress, and were managed according to manufacturer's instructions. All chemicals used in this study were dissolved in DMSO (Carl Roth, A994.1).

4. Plasmid DNA and siRNA transfection

For the tethering degradation and GGAA induction assays, HeLa cells were transfected with polyethyleneimine (PEI) using 1:2 DNA/PEI ratio. For the Protein Complementation Assay and for coimmunoprecipitations, HEK293T cells were transfected with PEI or with a classical calcium phosphate procedure, respectively. For transient knockdown of CNOT2, siRNAs purchased from Eurogentec (Belgium) were used: siCNOT2, 5'-CAUCUGAGUACUUAACGAAtt-3'; and control siRNA (SR-CL000-005). siRNA and DNA-siRNA were transfected into HeLa or shA673-1c cells with JetPrime (Polyplus transfection) according to the manufacturer's instructions. Cells were processed at 24-48h or 72h after DNA or siRNA transfections, respectively.

5. Plasmid DNA and shRNA transduction

For stable ectopic (re)expression studies, FLAG-tagged constructs of EF or deletion mutants cloned into the XhoI sites of the pLENTI-DEST vector (described previously) were used. These constructs were delivered by lentivirus in MSC or shA673-1 cells after knockdown of endogenous EWSR1-FLI1. Lentivirus were prepared at the GIGA-Viral Vectors facility. Cells were transduced (MOI 100) with protamine sulfate. After 72h, cells were treated for 72h with 7 µg/ml blasticidin and then amplified for 2 weeks. Induction of EF breakpoint-specific shRNA in shA673-1c and shSK-E17T cells was performed by adding 1 µg/ml of doxycycline (dox) in the medium *ex-tempo*. shA673-1c and shSK-E17T cells were processed after 4 days or 7 days of dox treatment, respectively. For stable knockdown of HuR, shRNA constructs were prepared for lentivirus delivery and shA673-1c cells were transduced (MOI 20) as described above. Cells were subsequently processed or selected with 3 µg/ml puromycin for 72h. shRNA constructs were kindly provided by Dr. Véronique Kruys (ULB, IBBM, Gosselies): pLV-H1-EF1alpha-puro-shCTRL, 5'-GCAGTTATCTGGAAGATCAGGTTGGATCCAACCTGATCTTCCAGATAACTGC-3';   pLV-H1-EF1alpha-puro-shHuR2,   5'-AAAAGGGAATGGACCAAAGAGTTTCTTGGATCCAAGAAACTCTTTGGTCCATTCCC-3'. Proper expression of all coding plasmids and knockdown of target genes were verified by western blotting and/or qPCR as described below.

6. Western blotting

Cells were washed once with cold PBS, collected by trypsinization and centrifugation. The cell pellet was directly lysed in Laemmli buffer, ultrasonicated (when necessary), and boiled for 5 min at 100°C. Protein extracts were separated by sodium dodecyl sulfate-polyacrylamide gel (SDS-PAGE) electrophoresis and transferred onto nitrocellulose membrane. Membranes were blocked for 1h with 5% non-fat milk or 4% BSA and incubated overnight at 4°C with primary antibodies followed by HRP-conjugated secondary antibodies. Proteins were detected by chemiluminescence. Images were acquired with ImageQuant LAS 4000 device (GE Healthcare) and quantified using ImageJ. All primary antibodies are listed in **Table S1**.

7. RNA isolation and quantitative PCR

For expression studies and mRNA decay analyses, total RNA was isolated using the Nucleospin RNA kit (Macherey-Nagel). For RNA-immunoprecipitations, total RNA was extracted from inputs or beads with TRIzol Reagent (Thermo Fisher Scientific). Total RNA was then reverse-transcribed with random primers using the RevertAid H Minus First Strand cDNA Synthesis Kit (Thermo Fisher Scientific). cDNA was diluted between 10- and 300-fold depending on the abundance of targets, amplified and quantified in triplicate using FastStart SYBR Green Master mix (Roche) on a LightCycler 480 instrument (Roche). In expression studies, relative target mRNA levels were calculated with the ΔΔCt method with *GAPDH*, *NDUFA12* and *RPL32* as internal controls. For mRNA decay analyses, signals were normalized to the average levels of three highly stable mRNAs (*GAPDH*, *NDUFA12*, and *RPL32*) and HLs were calculated on the basis of first-order degradation

kinetics with GraphPad Prism 8. Primer specificities were evaluated *in silico* using a blast homology search and assessed post-amplification by examination of the melting curve. RT-qPCR primers are listed in **Table S3**.

8. Subcellular fractionation

Cells were washed once with cold PBS, collected by trypsinization and centrifugation. The cell pellet was resuspended in PBS supplemented with 0.1% NP-40 and 1X cOmplete protease inhibitor (Roche), incubated for 5 min on ice and centrifuged at 10,000 g for 10 min at 4°C. The supernatant was removed and used as the cytoplasmic fraction. The nuclei were washed twice with the lysis buffer and resuspended in Laemmli buffer. Total lysate was prepared by directly lysing pelleted cells in Laemmli buffer. Total, cytoplasmic and nuclear fractions were ultrasonicated and boiled for 5 min at 100°C before western blotting.

9. Transcriptome-wide mRNA decay, RNA-seq and analysis

Biological replicates of shA673-1c cells before (-dox) and after (+dox) knockdown of EF were seeded in 6-well plates and treated with 5 µM ActD for 0, 1, 2 and 4h. Total RNA was harvested and RNA quality was assessed by electrophoresis (BioAnalyzer). Libraries were prepared with the Illumina TruSeq stranded mRNA sample preparation kit (includes an oligo(dT) selection step) and single-end sequencing was performed with the Illumina NextSeq 500 instrument by the GIGA-Genomics facility (University of Liege). RNA-seq read quality was evaluated using FastQC. Sequence reads were aligned to the human genome hg19 (UCSC) using STAR [685]. Differential expression analysis was performed with DESeq2 [686] on read counts from STAR quant Mode. Genes were considered significantly up- or down-regulated if their base 2 logarithm fold change was >1 or <-1 and their adjusted p-value was <0.01. Differential stability analysis was performed on read counts from STAR quant Mode using R package bridger2 to compute mRNA HLs (https://CRAN.R-project.org/package=bridger2). Assuming first-order decay kinetics (see equation 1), mRNA HLs were calculated as the ratio between ln2 and the decay constant rate k (see equation 2).

$$M = M_0 . e^{-k.t} \tag{1}$$

where M_0 is the initial mRNA abundance, *i.e.*, before decay starts.

$$t_{1/2} = \frac{ln2}{k} \tag{2}$$

mRNAs with low expression levels (baseMean <100) were removed from this analysis. bridger2 outputs were used to compute HL ratio between –dox and +dox conditions. mRNAs were considered significantly stabilized or destabilized if their absolute HL ratio was >0 and their p-value <0.05 using two-sided Fischer's t-test. mRNAs with high HL in the –dox condition (>24h) were removed from the output results. All volcano plots and heatmaps presented in this study were generated using GraphPad Prism 8.

10. Luciferase reporter assays

Luciferase MS2-tethering degradation assays were performed in HeLa cells. Briefly, cells were transfected with control MS2-CP or various MS2-CP-tagged constructs, together with a bidirectional reporter encoding a control *Firefly* luciferase (F-Luc) and a targeted *Renilla* luciferase (R-Luc) carrying or lacking 8 repeats of the binding sequence for the MS2 coating peptide in its 3'UTR (R-Luc-8MS2 and R-Luc-0MS2, respectively) [627]. For each R-Luc construct, the net effect of an MS2-CP-tagged protein on the reporter stability over time was normalized to the first time point of the kinetic (*i.e.*, not treated with ActD). Luciferase ARE-tethering assays were performed in shA673-1c cells previously treated or not with dox. Briefly, cells were transfected with control pCDNA3.1-mCherry empty vector or pCDNA3.1-mCherry-HuR vector, together with a bidirectional reporter encoding a control *Firefly* luciferase (F-Luc) and a targeted *Renilla* luciferase carrying or lacking 8 repeats of AU-rich elements (AREs) in its 3'UTR (R-Luc-8AU and R-Luc-0AU, respectively). For GGAA reporter assays, HeLa cells were transfected with pGL3-GGAA-Firefly vector and various FLAG-tagged constructs, together with pRL-SV40 vector (Promega) to normalize for differences in cells count and transfection efficacy. For measuring luciferase activities in ARE-tethering and GGAA reporter assays, cell lysis and luciferase measurements were performed in triplicate on a TriStar² S LB 942 luminometer (Berthold) with twinlite *Firely* and *Renilla* Luciferase Reporter Gene Assay System (Perkin Elmer).

11. SMN2-MS2 minigene assay

SMN2-MS2 minigene assays were performed using HeLa cells co-transfected with either control empty vectors, or various FLAG- or MS2-CP-tagged constructs, together with SMN2-MS2 minigene previously described in [119], [632]. After 48h following transfection, cells were washed twice with PBS and harvested on ice. A third of the sample was subsequently subjected to western blotting analysis. Total RNA was isolated and reverse-transcribed from the remaining sample amount as described earlier in this section. Next, RT-PCR amplifications were performed using forward and reverse primers of SMN2-MS2 minigene located within exons 6 and 8, respectively (see **Table S3**). Then, PCR products were resolved by electrophoresis on a 12% polyacrylamide gel at 180V for 1h. Gels were incubated with GelStarTM fluorescent stain (Lonza) 1:10 000 in a Tris-Borate-EDTA buffer under gentle agitation for 25 min and washed twice with dH2O. Fluorescence was recorded using the Amarsham ImageQuant 800 (Cytiva) camera. Density analysis of the bands in the acquired images was performed using the ImageQuant TL software (v.7). Percentage spliced in (PSI) were computed based on the ratio between the densitometry values of the long isoform and all isoforms.

12. Protein complementation assay

ORFs encoding full-length EF, domains and deletion mutants were cloned in destination vectors containing GLucN1 and GLucN2 fragments of the *Gaussia princeps* luciferase. HEK293T cells were seeded in 24-well plates and transfected with 500 ng of the appropriate constructs (GLucN1 +

GLucN2), respectively. After 24h, cells were washed with PBS and lysed in 200 μL using the Renilla Luciferase Kit (Promega) according to manufacturer's instructions. 20 μL of lysates were then used to quantify luminescence in triplicate on a TriStar² S LB 942 luminometer (Berthold). The remaining volume of lysate was mixed with Laemmli buffer for SDS-PAGE analysis and western Blotting.

13. Immunofluorescence and confocal microscopy

HeLa, shA673-1c and shSK-E17T cells were seeded on coverslips in 24-well plates. Cells were washed with warm PBS and fixed in warm PBS with 4% paraformaldehyde (PAF) for 15 min. Cells were then washed in PBS, permeabilized in PBS with 0.5% Triton X-100 for 10 min and incubated in blocking solution (PBS with 0.025% Tween- 20 and 10% FBS) for 1h. The coverslips were then incubated overnight with primary antibodies and Alexa-conjugated secondary antibody for 1h in blocking solution. Nuclei were counterstained with DAPI (Life Technologies, 1:10,000 in PBS) for 10 min at room temperature in the dark and washed three times for 5 min each with PBS. The coverslips were mounted onto microscope slides with ProLong™ Diamond Antifade Mountant (Invitrogen). Images were obtained with a Zeiss HR LSM Airyscan 880 confocal microscope using a 40x or 63x oil immersion objective at GIGA-Imaging facility (University of Liege), visualized and analyzed with Fiji (ImageJ) software. PBs counting was performed on cells reconstituted in 3D with IMARIS v9.5.1 software. Surfaces were constructed from DCP1A and EDC4 labeling, considering fluorescence signals above a control threshold, and were filtered for a minimum volume of 0.01 μm³ or 0.1 μm³, respectively. PBs were counted with the appropriate IMARIS software function. Cell number was determined on the basis of the DAPI signal, and the mean number of PBs per cell was calculated as the ratio between the total number of PBs in a field and the total number of nuclei in the same field. All antibodies used in this study are listed in **Table S1**.

14. Number & Brightness (N&B) analysis

U2OS cells were transiently transfected with JetPrime for the indicated N-EGFP-tagged or mGR-N525-EGFP constructs, the latest being used as monomeric control. After 24h, images were taken using an LSM 780 laser scanning microscope (Carl Zeiss, Inc.) equipped with an environmental chamber. We used a 63× oil immersion objective (N.A. = 1.4). The excitation source was a multiline Ar laser tuned at 488 nm. Fluorescence was detected with a gallium arsenide phosphide (GaAsP) detector in photon-counting mode. N&B measurements were done as previously described [631]. Briefly, for each studied cell, a single-plane stack of 150 images (256 × 256 pixels) was taken in the conditions mentioned above, setting the pixel size to 80 nm and the pixel dwell time to 6.3 μs. In every case, we discarded the first 10 images of the sequence to reduce overall bleaching. The frame time under these conditions is 0.97s. Each stack was further analyzed using the N&B routine of the "GLOBALS for Images" program developed at the Laboratory for Fluorescence Dynamics (University of California, Irvine, CA). The experiments were independently repeated two to three times for each treatment/condition.

15. Coimmunoprecipitation

HEK293T cells coexpressing tagged interaction partners were lysed in IPLS (immunoprecipitation low salt; Tris-HCl, pH 7.5 50 mM, EDTA, pH 8, 0.5 mM, 0.5% NP-40, 10% glycerol, 120 mM NaCl) with 1x cOmplete Protease Inhibitor (Roche) and 1x Halt Phosphatase Inhibitors (Thermo Fisher Scientific). When necessary, cleared cell lysates were incubated at 37°C for 30 min with or without 10 µg/ml RNase A (Thermo Fisher Scientific). Supernatants were then incubated with anti-FLAG M2 agarose beads (Sigma-Aldrich) for 2h at 4°C. Beads were washed once with IPLS, twice with IPMS (immunoprecipitation medium salt, IPLS with 500 mM NaCl) and once with IPLS. Immunoprecipitates were finally boiled in 2x SDS loading buffer and subsequently analyzed by SDS-PAGE and western blotting. For endogenous coimmunoprecipitations, shA673-1c cell lysates were prepared with a modified IPLS-HEPES buffer (50 mM HEPES-NaOH, pH 7.4, instead of Tris buffer), precleared with Protein A/G magnetic beads (Millipore) for 1h at 4°C, and incubated overnight with 1 µg of relevant antibody or normal rabbit (Cell Signaling) or mouse (Santa Cruz) IgG. Then, samples were incubated with Protein A/G magnetic beads (Millipore) for 1h at 4°C. Beads were washed four times with IPLS-HEPES buffer. Immunoprecipitates were finally boiled in 2x SDS loading buffer and analyzed by SDS–PAGE and western blotting. All antibodies used in this study are listed in **Table S1**.

16. RNA-immunoprecipitation-qPCR analysis

Dynabeads Protein G magnetic beads (Invitrogen) were incubated with anti-FLI1 antibody (ab15289, Abcam), anti-HuR antibody (sc-5261, Santa Cruz), normal rabbit (Cell Signaling) or mouse IgG (Santa Cruz) at 4°C overnight with rotation. Cells were not subjected to crosslinking prior harvesting. Cells were washed twice with ice cold PBS and pelleted by centrifugation (4°C, 5 min, 1500 rpm). Cells were resuspended in 1 ml RIPA (50 mM Tris HCl, pH 8.0, 150 mM NaCl, 1.0% IGEPAL CA-630, 0.5% sodium deoxycholate, 0.1% SDS) with 1x cOmplete Protease Inhibitor (Roche) and lysed for 30 min at 4°C with rotation. Cell lysates were then sonicated on ice with a pulser mode (3x 30s with 30s break each) and cleared by centrifugation for 10 min at 4°C and at 10,000 x g. An aliquot was used for RNA input and was treated with proteinase K before RNA extraction. Proteins were quantified with Pierce BCA protein assay kit (Thermo Fisher Scientific). For immunoprecipitation, 400 µg of protein were incubated with antibody-loaded Dynabeads overnight at 4°C with rotation. Supernatant was removed and beads were washed 5 times with 1 ml RIPA buffer. RNA-protein complexes were then eluted by incubation with 100 µL of elution buffer (Tris–HCl pH 8 100 mM; Na2-EDTA 10 mM; 1% SDS in H_2O) for 3 min at 90°C. Proteins were digested with Proteinase K treatment and RNA from inputs or beads was extracted with TRIzol Reagent (Thermo Fisher Scientific) for RT-qPCR analysis. cDNA was diluted 10-fold. RIP enrichment was calculated as a percentage of input, unless otherwise clearly stated. The GAPDH, NDUFA12 and RPL32 mRNAs were used as controls. All primers used for RIP experiments are listed in **Table S3**.

17. RNA-binding motif enrichment analysis

3'UTR sequences of stabilized genes identified in the transcriptome-wide mRNA decay analysis were retrieved using biomaRt R package (10.18129/B9.bioc.biomaRt). The FASTA files generated were then interrogated for known RNA-binding motifs from the literature [645] using the AME software from MEME suite 5.0.2 with default settings [687]. Motifs with an adjusted p-value <0.05 were considered significant. Control sequences consisted of the 3'UTR region of genes with unchanged HL ratio before and after knockdown of EF. Alternatively, the built-in control provided by the MEME suite was also used.

18. Investigation of intrinsic disorder properties

Eight algorithms were used with default settings: IUPRED2 [688], VL3 [689], RONN [690], SPOT-Disorder [691], AUCPred [692], ESpritz [693], Metadisorder [694], and POODLE [695]. Results are shown as mean disorder scores from these algorithms.

19. Resazurin viability assay

Cells were seeded in triplicate at a density of 5,000-20,000 cells per well of a 96-well plate (Greiner). After 24h, cells were treated with varying doses of DHTS or CMDL-2 inhibitors (1% DMSO as control). After 24h, the medium was replaced by medium with 0.1% resazurin (Stemcell Technologies) and incubated at 37°C for 2-4h. Then, the medium was transferred to a reading plate (Corning, Costar black clear bottom). Finally, fluorescence was recorded at the excitation and emission wavelengths of 535/595 nm with a FiterMax F5 microplate reader (Molecular Devices). Measurements were normalized to control DMSO and the smallest dose, and IC50 were calculated based on a three-parameter log-logistic regression for 3 independent experiments.

20. Proliferation assay

Cells were seeded at a density of 5,000 cells per well in triplicate of a 96-well plate (Greiner). Cell growth was monitored and analyzed by time-lapse microscopy (IncuCyte S3, Essen Bioscience, Sartorius, 4x objective lens) every 2h for 72h.

21. Soft-agar colony formation assay

shA673-1c cells were resuspended in 0.3% of top agar and seeded in duplicate at a density of 8,000 cells per well of a 12-well plate with 0.6% bottom agar. The plate was left to solidify at room temperature for 30 min. If needed, cells were then treated with varying doses of DHTS and CMLD-2 inhibitors (1% DMSO as control). Plates were incubated in a cell culture incubator (37°C, 5% CO_2) for 3 weeks. Colonies were stained with crystal violet (0.1% crystal violet, 20% methanol, in dH_2O) for 30 min, washed four times with dH_2O, imaged with a Nikon D3200 and finally counted with ImageJ.

22. Wound healing migration assay

shA673-1c cells were seeded at a density of 20,000 cells per well in triplicate of a 96-well plate (Greiner). At cell confluence, scratch wounds were produced using a WoundMaker device (Essen Bioscience). Then, cell migration into the wound was monitored and analyzed by time-lapse microscopy (IncuCyte S3, Essen Bioscience, Sartorius, wound mode, 10x objective lens) every 2h for 24h.

23. Spheroid growth assay

Spheroids were formed in 96-well plates (Greiner, flat bottoms) previously coated with 1% agar prepared in dH_2O and sterilized by autoclaving. shA673-1c cells were seeded at a density of 5,000 cells per well in triplicate in DMEM supplemented with 2% FBS. If needed, cells were treated with varying doses of DHTS or CMLD-2 inhibitors (1% DMSO as control) with or without SYTOX Green (Thermo Fisher Scientific) directly after seeding or once spheroids were formed. Spheroid growth was monitored and analyzed by time-lapse microscopy (IncuCyte SX5, Essen Bioscience, Sartorius, spheroid mode, 4x objective lens) every 2h for 96h.

24. Statistics

Unless otherwise indicated, data are presented as mean ± SD, calculated for at least three independent experiments. Statistical tests were performed with GraphPad Prism 8 and are indicated in each figure legends. Significance in the overlap was determined with Fisher's Exact t-test using GeneOverlap R package. p-value thresholds are depicted as follows: *p <0.05; **p <0.01; ***p <0.001; ****p< 0.0001; ns, not significant.

25. Acknowledgements

26. Author contributions

I conceived and designed all the experiments with the help of my promoter. I performed all the experiments and analyzed all the data except rare cases, including the RIP experiments shown in **Figure 67**, **91**, **95** (performed by Jonathan Bruyr, technician in the host laboratory, and analyzed by J. Bruyr and I), the PLA experiment shown in **Figure 73** (performed and analyzed by Eric Hervouet and Paul Peixoto, RIGHT Institute, INSERM, University of Bourgogne Franche-Comté), the N&B analysis shown in **Figure 86e** (performed and analyzed by Gregory Fettweis at the time he was a postdoctoral fellow in the laboratory of "Receptor Biology and Gene Expression", National Institute of Health, Bethesda), the SMN2-MS2 minigene assays shown in **Figure 87** (performed by Eva Lucarelli during her Master 2 thesis under the supervision of Loïc Ongena, a doctoral fellow in the host laboratory, and analyzed by E. Lucarelli and I), as well as the structural disorder analyses shown in **Figure 79a**, **81** and two coimmunoprecipitation experiments shown in **Figure 93a-b** (performed by Loic Ongena at the time he was a Master 2 student under my supervision). I wrote alone the present thesis manuscript.

Table S1. Main reagents or resources used in this work with their source and identifier. NA = not available/applicable.

Reagent or resource	Source	Identifier
Antibodies		
Rabbit monoclonal anti-FLI1	Abcam	Cat#ab15289
Rabbit monoclonal anti-FLI1	Abcam	Cat#ab133485
Mouse monoclonal anti-DCP1A	Santa Cruz	sc-100706
Rabbit anti-EDC4	Cell Signaling	#2548
Rabbit monoclonal anti-CNOT2	Cell Signaling	#34214
Rabbit polyclonal anti-CNOT6L	Sigma-Aldrich	HPA042688
Rabbit polyclonal anti-CNOT8	Thermo Fisher Scientific	PA5-13451
Mouse monoclonal anti-HuR	Santa Cruz	sc-5261
Mouse monoclonal anti-GAPDH	Santa Cruz	sc-166545
Mouse monoclonal anti-HSP90	Santa Cruz	sc-13119
Mouse monoclonal anti-β-tubulin	Santa Cruz	sc-5274
Goat polyclonal anti-lamin B1	Santa Cruz	sc-6217
Mouse monoclonal anti-FLAG	Sigma-Aldrich	F3165
Mouse monoclonal anti-MYC	Santa Cruz	sc-40
Rat monoclonal anti-HA	Roche	ROAHAHA
Rabbit polyclonal anti-mCherry	Abcam	ab167453
Rabbit anti-Gaussian	BioLabs	E8023S
Mouse monoclonal anti-PERK	Santa Cruz	sc-377400
Mouse monoclonal anti-P-PERK	Santa Cruz	sc-7383
Rabbit polyclonal anti-IRE1	Abcam	ab37073

Reagent or resource	Source	Identifier
Rabbit polyclonal anti-EIF2α	Santa Cruz	sc-11386
Rabbit polyclonal anti-P-EIF2A	Cell Signaling	#9721
Normal mouse IgG	Santa Cruz	sc-2025
Normal rabbit IgG	Cell Signaling	#2729
Chemicals		
Doxycycline	Sigma-Aldrich	D3072
Actinomycin D	Enzo Life Sciences	BML-GR300-0005
Blasticidin	InvivoGen	ant-bl-1
Zeocyn	InvivoGen	ant-zn-1
Puromycin	InvivoGen	ant-pr-1
Spectinomycin	Sigma-Aldrich	S4014
Ampicillin	Sigma-Aldrich	A0166
Chloramphenicol	Sigma-Aldrich	C0378
DMSO	Carl Roth	A994.1
Dihydrotanshinone-I	Sigma-Aldrich	D0947
CMLD-2	MedChemExpress	HY-124828
Polyethyleneimine (PEI)	Sigma-Aldrich	NA
RNAseA	Thermo Fisher Scientific	Cat#EN0531
JetPrime	Polyplus	101000027
FastDigest XhoI (10 U/μL)	Thermo Fisher Scientific	FD0694
SacI (10 U/μL)	Thermo Fisher Scientific	ER1132
FastDigest PvuII	Thermo Fisher Scientific	FD0634
T4 DNA ligase	Thermo Fisher Scientific	EL0011

Reagent or resource	Source	Identifier
Resazurin	Stemcell Technologies	75005
cOmplete Protease Inhibitors	Roche	CO-RO
Halt Phosphatase Inhibitors	Thermo Fisher Scientific	78446
Anti-FLAG M2 agarose beads	Millipore	A2220
Pierce Protein A/G Magnetic beads	Thermo Fisher Scientific	11844554
Takyon™ No ROX SYBR 2X MasterMix blue dTTP	Eurogentec	UF-NSMT-B0701
Critical commercial assays		
TruSeq Stranded mRNA Sample Preparation	Illumina	20020595
twinlite Firely and Renilla Luciferase Reporter Gene Assay System	Perkin Elmer	6066709
NucleoSpin Plasmid EasyPure	Macherey-Nagel	740727.50
Nucleospin RNA kit	Macherey-Nagel	740955.50
Experimental model: cell lines and primary cells		
Human: HeLa	ATCC	CCL-2
Human: HEK293T	ATCC	CRL-3216
Human: U2OS	ATCC	HTB-96
Human: MDA-MD-231	ATCC	HTB-26
Human: MCF7	ATCC	HTB-22
Human: HUVEC	Lonza	C2519A
Human: shA673-1c	Dr. Olivier Delattre	NA
Human: shSK-E17T	Dr. Olivier Delattre	NA
Human: TC71	DSMZ	ACC 516
Human: MSCs	Dr. Yves Beguin	NA

Reagent or resource	Source	Identifier
Oligonucleotides		
See Table S2 for cloning and sequencing primers		
See Table S3 for PCR, RT-qPCR, and RIP-qPCR primers		
Plasmids		
Human ORFeome v7.1 and v8.1	The Center for Cancer Systems Biology (CCSB-DFCI)	http://horfdb.dfci.harvard.edu/
pDONR223	[120]	NA
pDEST1899	[120]	NA
pN-MS2-CP	[120]	NA
R-Luc-8MS2	[120]	NA
R-Luc-0MS2	[120]	NA
SMN2-MS2 minigene	[119], [632]	NA
pDEST475	[118]	NA
pCS3MTdest	[118]	NA
pGLucN1	[630]	NA
pGLucN2	[630]	NA
pDEST-N-EGFP	Addgene	122842
pLENTI-DEST	This work	NA
pGL3-promoter	Addgene	NA
pGL3-promoter 12xGGAA	This work	NA
pCDNA3.1-mCherry empty vector	Dr. Véronique Kruys	NA
pCDNA3.1-mCherry HuR and deletion mutants	Dr. Véronique Kruys	NA
R-Luc-8AU	Dr. Véronique Kruys	NA

Reagent or resource	Source	Identifier
R-Luc-0AU	Dr. Véronique Kruys	NA
Software, algorithms and web database		
BioRender	BioRender	https://biorender.com/
SnapGene Viewer 5.2.3	SnapGene software	https://www.snapgene.com/
GraphPad Prism 8/9	GraphPad Prism	https://www.graphpad.com/scientific-software/prism/
ImageJ/Fidji	[696]	https://imagej.nih.gov/ij/
STAR	[653]	NA
DESeq2	[686]	10.18129/B9.bioc.DESeq2
bridger2	CRAN	https://CRAN.R-project.org/package=bridger2
biomaRt	Bioconductor	10.18129/B9.bioc.biomaRt
GeneOverlap	Bioconductor	10.18129/B9.bioc.GeneOverlap
DAVID	[697]	https://david.ncifcrf.gov/home.jsp
PANTHER	[698]	http://geneontology.org/
AME	[687]	https://meme-suite.org/meme/
DepMap	[669]	https://depmap.org/portal/
IUPRED2	[688]	https://iupred2a.elte.hu/
VL3	[689]	
RONN	[690]	https://www.strubi.ox.ac.uk/RONN
SPOT-DISORDER	[691]	http://sparks-lab.org/server/spot-disorder/
AUCPred	[692]	
ESpritz	[693]	http://old.protein.bio.unipd.it/espritz/
Metadisorder	[694]	http://iimcb.genesilico.pl/metadisorder/
POODLE	[695]	http://mbs.cbrc.jp/poodle/poodle-l.html

Reagent or resource	Source	Identifier
RNP Granule Database	[377]	http://rnagranuledb.lunenfeld.ca/RNA/update_notice.php
AlphaFold2	[676], [677]	https://alphafold.com/

Table S2. Cloning and sequencing primers used in this work.

Target	Directionality	Sequence
Cloning		
EWSR1 1-264	Forward	GGGGACAACTTTGTACAAAAAAGTTGGCATGGCGTCCACGGATTACAG
	Reverse	GGGGACAACTTTGTACAAGAAAGTTGACTGCTGCCCGTAGCTGCTGC
EWSR1 1-63	Forward	GGGGACAACTTTGTACAAAAAAGTTGGCATGGCGTCCACGGATTACAG
	Reverse	GGGGACAACTTTGTACAAGAAAGTTGAGGTCTGCCCATAGGTTGC
EWSR1 64-264	Forward	GGGGACAACTTTGTACAAAAAAGTTGGCATGGCCTATGCAACTTCTTATGG
	Reverse	GGGGACAACTTTGTACAAGAAAGTTGACTGCTGCCCGTAGCTGCTGC
EWSR1 114-264	Forward	GGGGACAACTTTGTACAAAAAAGTTGGCATGCAGTCTGCATATGGCACTCAGC
	Reverse	GGGGACAACTTTGTACAAGAAAGTTGACTGCTGCCCGTAGCTGCTGC
EWSR1 164-264	Forward	GGGGACAACTTTGTACAAAAAAGTTGGCATGTATGGACAGAGTAACTACAG
	Reverse	GGGGACAACTTTGTACAAGAAAGTTGACTGCTGCCCGTAGCTGCTGC
EWSR1 214-264	Forward	GGGGACAACTTTGTACAAAAAAGTTGGCATGGGGCAACCGAGCAGCTATGG
	Reverse	GGGGACAACTTTGTACAAGAAAGTTGACTGCTGCCCGTAGCTGCTGC
Insert for cloning into pN-MS2 (from pDEST1899)	Forward	GCCCTCGAGGACTACAAAGACCATGACGGTGATTATAAA
	Reverse	GCGCTCGAGCGCTCTAGATCACACCACTTTGTACAAGAA
To build pLENTI-DEST (from pDEST1899)	Forward	CGGCTCGAGGCCACCATGGACTACAAAGACCATGACG
	Reverse	GGCCTCGAGCTATACCACTTTGTACAAGAAAGCTGAACG
Sequencing		

Target	Directionality	Sequence
pDONR223	Forward	TCCCAGTCACGACGTTGTAA
	Reverse	GTAATACGACTCACTATAGG
pDEST1899	Forward	GACGGTGATTATAAAGATCATGACATCG
	Reverse	GGAGTGGCAACTTCCAGGG
pN-MS2	Forward	CTAAAGTGGCAACCCAGACTGTTGG
	Reverse	GGAGGGGCAAACAACAGATGGC
pDEST475	Forward	CCGTATGATGTTCCTGATTATGCTAGC
	Reverse	GGAGTGGCAACTTCCAGGG
pGLucN1/2	Forward	CAGCTCTTAAGGCTAGAGTAC
	Reverse	CACTGCATTCTAGTTGTGGTTTGTCC
pDEST-N-EGFP	Forward	CATGGTCCTGCTGGAGTTCGTG
	Reverse	GCAACTAGAAGGCACAGTCGAGG
pLENTI-DEST	Forward	GACGGTGATTATAAAGATCATGACATCG
	Reverse	CTTCGGCCAGTAACGTTAGG

Table S3. PCR, RT-qPCR, and RIP-qPCR primers used in this work.

Target gene	Directionality	Sequence
PCR		
XBP1 u/s	Forward	CCTTGTAGTTGAGAACCAGG
	Reverse	GGGGCTTGGTATATATGTGG
RT-qPCR		
STC2	Forward	ATGCTACCTCAAGCACGACC
	Reverse	TCTGCTCACACTGAACCTGC
DNAJB9	Forward	CTGTATGCTGATTGGTAGAGTCAA
	Reverse	AGTAGACAAAGGCATCATTTCCAA
ATP8B2	Forward	GGGCTCTTCGACATGTTTC
	Reverse	GCCAACCCGCCGCATGCAGCG
FZD1	Forward	CCAAGAGAGGAGCCGAGA
	Reverse	CGGCACAAAGTTCCCAG
RIOK1	Forward	GGCTAAACACAGCAGAGATACC
	Reverse	AACTCCCGAGCCTTGGATTCT
ATG5	Forward	GAGATGTGTGGTTTGGACGA
	Reverse	ATTTCAGGGGTGTGCCTTCA
AURKB	Forward	ATCAGCTGCGCAGAGAGATCGAAA
	Reverse	CTGCTCGTCAAATGTGCAGCTCTT
EIF4E	Forward	ACAAGTCAGTCTGAAACCATCGAAC
	Reverse	CTTCATCCTCTTCGGCCACTCCTCC
CCNK	Forward	CAACGGTGGATGAGTGGTC
	Reverse	AGTTCTCCCCGACAGGTTAAG

Target gene	Directionality	Sequence
ZEB2	Forward	TCTCGCCCGAGTGAAGCCTT
	Reverse	GGGAGAATTGCTTGATGGAGC
GAPDH	Forward	TTGCCATCAATGACCCCTTCA
	Reverse	CGCCCCACTTGATTTTGGA
NDUFA12	Forward	ATGGCATCGTTGGCTTCAC
	Reverse	GCCAGTCACGTTGAATTTATGG
RPL32	Forward	CATCTCCTTCTCGGCATCA
	Reverse	AACCCTGTTGTCAATGCCTC
R-Luc	Forward	TCTTTTTCGCAACGGGTTT
	Reverse	GCCCAGTTTCTATTGGTCTCC
SMN2	Forward	TAATACGACTCACTATAGG
	Reverse	TAACGCTTCACATTCCAGATCTGTC
EF	Forward	AGTTACCCACCCCAAACTGG
	Reverse	CCAAGGGGAGGACTTTTGTT
HuR	Forward	AGGTGATCAAAGACGCCAAC
	Reverse	CTGGGGGTTTATGACCATTG
RIP-qPCR		
STC2	Forward	CCAAGCAAAAGGCTTCACGG
	Reverse	TCACGTGGTGCCAATTCTGA
DNAJB9	Forward	GTGACTTGCGTTGCAGAGTG
	Reverse	TCCTTTCTCAACCTTTCAGTAGCA
ATP8B2	Forward	GGGACCCACAGGGAGACTAT
	Reverse	GCTTCCCGGCATGGTACATT

Target gene	Directionality	Sequence
FZD1	Forward	TCAGCAGCACATTCTGAGGG
FZD1	Reverse	ATTTCAGGCGCTATCTCCCC
RIOK1	Forward	TCCTCAGTTCCTTTTCTCGCC
RIOK1	Reverse	CTTCACAGACAGTGCCACGA
ATG5	Forward	GTTTTGGGCCATCAATCGGAA
ATG5	Reverse	TCTCCTAGTGTGTGCAACTGT
AURKB	Forward	CGGGTGCGTGTGTTTGTATG
AURKB	Reverse	ACAAAGGAGGAGGTAGAAAACAG
EIF4E	Forward	TGTGGCGCTGTTGTTAATGT
EIF4E	Reverse	ATTGCTTGACGCAGTCTCCT
CCNK	Forward	TGAAGTGGGTAAGCAGCAGG
CCNK	Reverse	AGGTGTGAGGACCACTCTGA
ZEB2	Forward	CTGAACACCCCTGCCCATTT
ZEB2	Reverse	TCAGGCCTAAGCTTACAGTGTC
GAPDH	Forward	TTGCCATCAATGACCCCTTCA
GAPDH	Reverse	CGCCCCACTTGATTTTGGA

SECTION VIII REFERENCES

[1]   S. A. Lambert *et al.*, "The Human Transcription Factors.", *Cell*, vol. 172, no. 4, pp. 650–665, Feb. 2018.

[2]   "The classic. Diffuse endothelioma of bone. By James Ewing. 1921.", *Clin. Orthop. Relat. Res.*, no. 185, pp. 2–5, May 1984.

[3]   H. F. Jürgens, "Ewing's sarcoma and peripheral primitive neuroectodermal tumor.", *Curr. Opin. Oncol.*, vol. 6, no. 4, pp. 391–396, Jul. 1994.

[4]   L. A. Doyle, "Sarcoma classification: an update based on the 2013 World Health Organization Classification of Tumors of Soft Tissue and Bone.", *Cancer*, vol. 120, no. 12, pp. 1763–1774, Jun. 2014.

[5]   T. G. P. Grünewald *et al.*, "Ewing sarcoma.", *Nat. Rev. Dis. Prim.*, vol. 4, no. 1, p. 5, Dec. 2018.

[6]   M. Gambarotti *et al.*, "CIC-DUX4 fusion-positive round-cell sarcomas of soft tissue and bone: a single-institution morphological and molecular analysis of seven cases.", *Histopathology*, vol. 69, no. 4, pp. 624–634, Oct. 2016.

[7]   C. R. Antonescu *et al.*, "Sarcomas With CIC-rearrangements Are a Distinct Pathologic Entity With Aggressive Outcome: A Clinicopathologic and Molecular Study of 115 Cases.", *Am. J. Surg. Pathol.*, vol. 41, no. 7, pp. 941–949, Jul. 2017.

[8]   Y.-C. Kao *et al.*, "BCOR-CCNB3 Fusion Positive Sarcomas: A Clinicopathologic and Molecular Analysis of 36 Cases With Comparison to Morphologic Spectrum and Clinical Behavior of Other Round Cell Sarcomas.", *Am. J. Surg. Pathol.*, vol. 42, no. 5, pp. 604–615, May 2018.

[9]   K. Szuhai, M. Ijszenga, D. de Jong, A. Karseladze, H. J. Tanke, and P. C. W. Hogendoorn, "The NFATc2 gene is involved in a novel cloned translocation in a Ewing sarcoma variant that couples its function in immunology to oncology.", *Clin. cancer Res. an Off. J. Am. Assoc. Cancer Res.*, vol. 15, no. 7, pp. 2259–2268, Apr. 2009.

[10]   F. Cidre-Aranaz *et al.*, "Small round cell sarcomas.", *Nat. Rev. Dis. Prim.*, vol. 8, no. 1, p. 66, Oct. 2022.

[11]   M. Sbaraglia, E. Bellan, and A. P. Dei Tos, "The 2020 WHO Classification of Soft Tissue Tumours: news and perspectives.", *Pathologica*, vol. 113, no. 2, pp. 70–84, Apr. 2021.

[12]   C. A. Stiller *et al.*, "Descriptive epidemiology of sarcomas in Europe: report from the RARECARE project.", *Eur. J. Cancer*, vol. 49, no. 3, pp. 684–695, Feb. 2013.

[13]   M. Bernstein *et al.*, "Ewing's sarcoma family of tumors: current management.", *Oncologist*, vol. 11, no. 5, pp. 503–519, May 2006.

[14]   N. Riggi, M. L. Suvà, and I. Stamenkovic, "Ewing's Sarcoma.", *N. Engl. J. Med.*, vol. 384, no. 2, pp. 154–164, Jan. 2021.

[15]   I. M. Ambros, P. F. Ambros, S. Strehl, H. Kovar, H. Gadner, and M. Salzer-Kuntschik, "MIC2 is a specific marker for Ewing's sarcoma and peripheral primitive neuroectodermal tumors. Evidence for a common histogenesis of Ewing's sarcoma and peripheral primitive neuroectodermal tumors from MIC2 expression and specific chromosome aberration.", *Cancer*, vol. 67, no. 7, pp. 1886–1893,

Apr. 1991.

[16]   G. Prakash, P. Ganesan, A. Ahuja, and S. Bakhshi, "MIC-2 positive granulocytic sarcoma of ulna mimicking Ewing sarcoma.", *Pediatric blood & cancer*, vol. 51, no. 6. United States, pp. 836–837, Dec-2008.

[17]   M. U. Jawad, M. C. Cheung, E. S. Min, M. M. Schneiderbauer, L. G. Koniaris, and S. P. Scully, "Ewing sarcoma demonstrates racial disparities in incidence-related and sex-related differences in outcome: an analysis of 1631 cases from the SEER database, 1973-2005.", *Cancer*, vol. 115, no. 15, pp. 3526–3536, Aug. 2009.

[18]   P. C. Valery, W. McWhirter, A. Sleigh, G. Williams, and C. Bain, "Farm exposures, parental occupation, and risk of Ewing's sarcoma in Australia: a national case-control study.", *Cancer Causes Control*, vol. 13, no. 3, pp. 263–270, Apr. 2002.

[19]   M. J. Joyce, D. C. Harmon, H. J. Mankin, H. D. Suit, A. L. Schiller, and J. T. Truman, "Ewing's sarcoma in female siblings. A clinical report and review of the literature.", *Cancer*, vol. 53, no. 9, pp. 1959–1962, May 1984.

[20]   S. Postel-Vinay *et al.*, "Common variants near TARDBP and EGR2 are associated with susceptibility to Ewing sarcoma.", *Nat. Genet.*, vol. 44, no. 3, pp. 323–327, Feb. 2012.

[21]   M. J. Monument *et al.*, "Clinical and biochemical function of polymorphic NR0B1 GGAA-microsatellites in Ewing sarcoma: a report from the Children's Oncology Group.", *PLoS One*, vol. 9, no. 8, p. e104378, 2014.

[22]   M. Martinelli *et al.*, "CD99 polymorphisms significantly influence the probability to develop Ewing sarcoma in earlier age and patient disease progression.", *Oncotarget*, vol. 7, no. 47, pp. 77958–77967, Nov. 2016.

[23]   B. Widhe and T. Widhe, "Initial symptoms and clinical features in osteosarcoma and Ewing sarcoma.", *J. Bone Joint Surg. Am.*, vol. 82, no. 5, pp. 667–674, May 2000.

[24]   L. Alonso, V. Navarro-Perez, A. Sanchez-Muñoz, and E. Alba, "Time to diagnosis of ewing tumors in children and adolescents is not associated with metastasis or survival.", *Journal of clinical oncology : official journal of the American Society of Clinical Oncology*, vol. 32, no. 35. United States, p. 4020, Dec-2014.

[25]   F. Cidre-Aranaz and T. G. Grünewald, "Ewing Sarcoma. Methods and Protocols.", in *Methods in Molecular Biology*, New York, NY: Springer US, 2021, p. 333.

[26]   M. Krumbholz *et al.*, "Genomic EWSR1 Fusion Sequence as Highly Sensitive and Dynamic Plasma Tumor Marker in Ewing Sarcoma.", *Clin. cancer Res. an Off. J. Am. Assoc. Cancer Res.*, vol. 22, no. 17, pp. 4356–4365, Sep. 2016.

[27]   T. G. Grünewald *et al.*, "Sarcoma treatment in the era of molecular medicine.", *EMBO Mol. Med.*, vol. 12, no. 11, p. e11131, Nov. 2020.

[28]   S. G. Dubois, C. L. Epling, J. Teague, K. K. Matthay, and E. Sinclair, "Flow cytometric detection of Ewing sarcoma cells in peripheral blood and bone marrow.", *Pediatr. Blood Cancer*, vol. 54, no. 1, pp. 13–18, Jan. 2010.

[29]   C. Koelsche *et al.*, "Sarcoma classification by DNA methylation profiling.", *Nat. Commun.*, vol. 12, no. 1, p. 498, Jan. 2021.

[30]   C. Koelsche *et al.*, "Array-based DNA-methylation profiling in sarcomas with small blue round cell histology provides valuable diagnostic information.", *Mod. Pathol. an Off. J. United States Can. Acad. Pathol. Inc*, vol. 31, no. 8, pp. 1246–1256, Aug. 2018.

[31]   S. P. Wu *et al.*, "DNA Methylation-Based Classifier for Accurate Molecular Diagnosis of Bone Sarcomas.", *JCO Precis. Oncol.*, vol. 2017, 2017.

[32]   D. Priya, R. V Kumar, L. Appaji, B. S. Aruna Kumari, M. Padma, and P. Kumari, "Histological diversity and clinical characteristics of Ewing sarcoma family of tumors in children: A series from a tertiary care center in South India.", *Indian J. Cancer*, vol. 52, no. 3, pp. 331–335, 2015.

[33]   A. S. Pappo and U. Dirksen, "Rhabdomyosarcoma, Ewing Sarcoma, and Other Round Cell Sarcomas.", *J. Clin. Oncol. Off. J. Am. Soc. Clin. Oncol.*, vol. 36, no. 2, pp. 168–179, Jan. 2018.

[34]   H. L. Spraker *et al.*, "The clone wars - revenge of the metastatic rogue state: the sarcoma paradigm.", *Front. Oncol.*, vol. 2, p. 2, 2012.

[35]   S. Takenaka *et al.*, "Treatment outcomes of Japanese patients with Ewing sarcoma: differences between skeletal and extraskeletal Ewing sarcoma.", *Jpn. J. Clin. Oncol.*, vol. 46, no. 6, pp. 522–528, Jun. 2016.

[36]   N. Gaspar *et al.*, "Ewing Sarcoma: Current Management and Future Approaches Through Collaboration.", *J. Clin. Oncol. Off. J. Am. Soc. Clin. Oncol.*, vol. 33, no. 27, pp. 3036–3046, Sep. 2015.

[37]   N. J. Balamuth and R. B. Womer, "Ewing's sarcoma.", *Lancet. Oncol.*, vol. 11, no. 2, pp. 184–192, Feb. 2010.

[38]   V. Damerell, M. S. Pepper, and S. Prince, "Molecular mechanisms underpinning sarcomas and implications for current and future therapy.", *Signal Transduct. Target. Ther.*, vol. 6, no. 1, p. 246, Jun. 2021.

[39]   A. D. Waldman, J. M. Fritz, and M. J. Lenardo, "A guide to cancer immunotherapy: from T cell basic science to clinical practice.", *Nat. Rev. Immunol.*, vol. 20, no. 11, pp. 651–668, Nov. 2020.

[40]   C. Spurny *et al.*, "Programmed cell death ligand 1 (PD-L1) expression is not a predominant feature in Ewing sarcomas.", *Pediatr. Blood Cancer*, vol. 65, no. 1, Jan. 2018.

[41]   I. Machado, J. A. López-Guerrero, K. Scotlandi, P. Picci, and A. Llombart-Bosch, "Immunohistochemical analysis and prognostic significance of PD-L1, PD-1, and CD8+ tumor-infiltrating lymphocytes in Ewing's sarcoma family of tumors (ESFT).", *Virchows Arch.*, vol. 472, no. 5, pp. 815–824, May 2018.

[42]   S. de Groot, B. Röttgering, H. Gelderblom, H. Pijl, K. Szuhai, and J. R. Kroep, "Unraveling the Resistance of IGF-Pathway Inhibition in Ewing Sarcoma.", *Cancers (Basel).*, vol. 12, no. 12, Nov. 2020.

[43]   E. Morales, M. Olson, F. Iglesias, T. Luetkens, and D. Atanackovic, "Targeting the tumor microenvironment of Ewing sarcoma.", *Immunotherapy*, vol. 13, no. 17, pp. 1439–1451, Dec. 2021.

[44]   E. Morales, M. Olson, F. Iglesias, S. Dahiya, T. Luetkens, and D. Atanackovic, "Role of immunotherapy in Ewing sarcoma.", *J. Immunother. cancer*, vol. 8, no. 2, Dec. 2020.

[45]   H. Yu, Y. Ge, L. Guo, and L. Huang, "Potential approaches to the treatment of Ewing's sarcoma.",

Oncotarget, vol. 8, no. 3, pp. 5523–5539, Jan. 2017.

[46] C. H. Evans *et al.*, "EWS-FLI-1-targeted cytotoxic T-cell killing of multiple tumor types belonging to the Ewing sarcoma family of tumors.", *Clin. cancer Res. an Off. J. Am. Assoc. Cancer Res.*, vol. 18, no. 19, pp. 5341–5351, Oct. 2012.

[47] T.-C. Chang *et al.*, "The neoepitope landscape in pediatric cancers.", *Genome Med.*, vol. 9, no. 1, p. 78, Aug. 2017.

[48] W. Yang *et al.*, "Immunogenic neoantigens derived from gene fusions stimulate T cell responses.", *Nat. Med.*, vol. 25, no. 5, pp. 767–775, May 2019.

[49] C. C. Smith, S. R. Selitsky, S. Chai, P. M. Armistead, B. G. Vincent, and J. S. Serody, "Alternative tumour-specific antigens.", *Nat. Rev. Cancer*, vol. 19, no. 8, pp. 465–478, Aug. 2019.

[50] E. C. Toomey, J. D. Schiffman, and S. L. Lessnick, "Recent advances in the molecular pathogenesis of Ewing's sarcoma.", *Oncogene*, vol. 29, no. 32, pp. 4504–4516, Aug. 2010.

[51] H. Kovar, "Context matters: The hen or egg problem in Ewing's sarcoma.", *Semin. Cancer Biol.*, vol. 15, no. 3, pp. 189–196, Jun. 2005.

[52] E. R. Lawlor and P. H. Sorensen, "Twenty Years on: What Do We Really Know about Ewing Sarcoma and What Is the Path Forward?.", *Crit. Rev. Oncog.*, vol. 20, no. 3–4, pp. 155–171, 2015.

[53] H. Kovar, "Downstream EWS/FLI1 - upstream Ewing's sarcoma.", *Genome Med.*, vol. 2, no. 1, p. 8, Jan. 2010.

[54] M. A. Teitell, A. D. Thompson, P. H. Sorensen, H. Shimada, T. J. Triche, and C. T. Denny, "EWS/ETS fusion genes induce epithelial and neuroectodermal differentiation in NIH 3T3 fibroblasts.", *Lab. Invest.*, vol. 79, no. 12, pp. 1535–1543, Dec. 1999.

[55] S. Hu-Lieskovan, J. Zhang, L. Wu, H. Shimada, D. E. Schofield, and T. J. Triche, "EWS-FLI1 fusion protein up-regulates critical genes in neural crest development and is responsible for the observed phenotype of Ewing's family of tumors.", *Cancer Res.*, vol. 65, no. 11, pp. 4633–4644, Jun. 2005.

[56] R. Rodriguez, R. Rubio, and P. Menendez, "Modeling sarcomagenesis using multipotent mesenchymal stem cells.", *Cell Res.*, vol. 22, no. 1, pp. 62–77, Jan. 2012.

[57] Y. Castillero-Trejo, S. Eliazer, L. Xiang, J. A. Richardson, and R. L. J. Ilaria, "Expression of the EWS/FLI-1 oncogene in murine primary bone-derived cells Results in EWS/FLI-1-dependent, ewing sarcoma-like tumors.", *Cancer Res.*, vol. 65, no. 19, pp. 8698–8705, Oct. 2005.

[58] N. Riggi *et al.*, "Development of Ewing's sarcoma from primary bone marrow-derived mesenchymal progenitor cells.", *Cancer Res.*, vol. 65, no. 24, pp. 11459–11468, Dec. 2005.

[59] E. C. Torchia, S. Jaishankar, and S. J. Baker, "Ewing tumor fusion proteins block the differentiation of pluripotent marrow stromal cells.", *Cancer Res.*, vol. 63, no. 13, pp. 3464–3468, Jul. 2003.

[60] F. Tirode, K. Laud-Duval, A. Prieur, B. Delorme, P. Charbord, and O. Delattre, "Mesenchymal stem cell features of Ewing tumors.", *Cancer Cell*, vol. 11, no. 5, pp. 421–429, May 2007.

[61] F. Mertens, B. Johansson, T. Fioretos, and F. Mitelman, "The emerging complexity of gene fusions in cancer.", *Nat. Rev. Cancer*, vol. 15, no. 6, pp. 371–381, Jun. 2015.

[62] C. Turc-Carel *et al.*, "Chromosomes in Ewing's sarcoma. I. An evaluation of 85 cases of remarkable

consistency of t(11;22)(q24;q12).", *Cancer Genet. Cytogenet.*, vol. 32, no. 2, pp. 229–238, Jun. 1988.

[63]   O. Delattre *et al.*, "Gene fusion with an ETS DNA-binding domain caused by chromosome translocation in human tumours.", *Nature*, vol. 359, no. 6391, pp. 162–165, Sep. 1992.

[64]   N. D. Anderson *et al.*, "Rearrangement bursts generate canonical gene fusions in bone and soft tissue tumors.", *Science*, vol. 361, no. 6405, Aug. 2018.

[65]   J. Zucman *et al.*, "Combinatorial generation of variable fusion proteins in the Ewing family of tumours.", *EMBO J.*, vol. 12, no. 12, pp. 4481–4487, Dec. 1993.

[66]   P. H. Sorensen, S. L. Lessnick, D. Lopez-Terrada, X. F. Liu, T. J. Triche, and C. T. Denny, "A second Ewing's sarcoma translocation, t(21;22), fuses the EWS gene to another ETS-family transcription factor, ERG.", *Nat. Genet.*, vol. 6, no. 2, pp. 146–151, Feb. 1994.

[67]   M. Peter *et al.*, "A new member of the ETS family fused to EWS in Ewing tumors.", *Oncogene*, vol. 14, no. 10, pp. 1159–1164, Mar. 1997.

[68]   I. S. Jeon *et al.*, "A variant Ewing's sarcoma translocation (7;22) fuses the EWS gene to the ETS gene ETV1.", *Oncogene*, vol. 10, no. 6, pp. 1229–1234, Mar. 1995.

[69]   D. C. Shing *et al.*, "FUS/ERG gene fusions in Ewing's tumors.", *Cancer Res.*, vol. 63, no. 15, pp. 4568–4576, Aug. 2003.

[70]   Y. Kaneko *et al.*, "Fusion of an ETS-family gene, EIAF, to EWS by t(17;22)(q12;q12) chromosome translocation in an undifferentiated sarcoma of infancy.", *Genes. Chromosomes Cancer*, vol. 15, no. 2, pp. 115–121, Feb. 1996.

[71]   F. Urano, A. Umezawa, W. Hong, H. Kikuchi, and J. Hata, "A novel chimera gene between EWS and E1A-F, encoding the adenovirus E1A enhancer-binding protein, in extraosseous Ewing's sarcoma.", *Biochem. Biophys. Res. Commun.*, vol. 219, no. 2, pp. 608–612, Feb. 1996.

[72]   T. L. Ng *et al.*, "Ewing sarcoma with novel translocation t(2;16) producing an in-frame fusion of FUS and FEV.", *J. Mol. Diagn.*, vol. 9, no. 4, pp. 459–463, Sep. 2007.

[73]   A. D. Thompson, M. A. Teitell, A. Arvand, and C. T. Denny, "Divergent Ewing's sarcoma EWS/ETS fusions confer a common tumorigenic phenotype on NIH3T3 cells.", *Oncogene*, vol. 18, no. 40, pp. 5506–5513, Sep. 1999.

[74]   C. Picard *et al.*, "Identification of a novel translocation producing an in-frame fusion of TAF15 and ETV4 in a case of extraosseous Ewing sarcoma revealed in the prenatal period.", *Virchows Arch.*, May 2022.

[75]   J. C. Schwartz, T. R. Cech, and R. R. Parker, "Biochemical Properties and Biological Functions of FET Proteins.", *Annu. Rev. Biochem.*, vol. 84, pp. 355–379, 2015.

[76]   H. Kovar, "Dr. Jekyll and Mr. Hyde: The Two Faces of the FUS/EWS/TAF15 Protein Family.", *Sarcoma*, vol. 2011, p. 837474, 2011.

[77]   D. Alex and K. A. W. Lee, "RGG-boxes of the EWS oncoprotein repress a range of transcriptional activation domains.", *Nucleic Acids Res.*, vol. 33, no. 4, pp. 1323–1331, 2005.

[78]   M. P. Paronetto, B. Miñana, and J. Valcárcel, "The Ewing Sarcoma Protein Regulates DNA Damage-Induced Alternative Splicing.", *Mol. Cell*, vol. 43, no. 3, pp. 353–368, 2011.

[79]   M. P. Paronetto *et al.*, "Regulation of FAS exon definition and apoptosis by the Ewing sarcoma protein.", *Cell Rep.*, vol. 7, no. 4, pp. 1211–1226, May 2014.

[80]   H. Ouyang *et al.*, "The RNA binding protein EWS is broadly involved in the regulation of pri-miRNA processing in mammalian cells.", *Nucleic Acids Res.*, 2017.

[81]   T. Zhang *et al.*, "FUS Regulates Activity of MicroRNA-Mediated Gene Silencing.", *Mol. Cell*, vol. 69, no. 5, pp. 787-801.e8, Mar. 2018.

[82]   J. I. Hoell *et al.*, "RNA targets of wild-type and mutant FET family proteins.", *Nat. Struct. Mol. Biol.*, vol. 18, no. 12, pp. 1428–1431, Nov. 2011.

[83]   M. Sévigny, I. B. Julien, J. P. Venkatasubramani, J. B. Hui, P. A. Dutchak, and C. F. Sephton, "FUS contributes to mTOR-dependent inhibition of translation.", *J. Biol. Chem.*, 2020.

[84]   T. Udagawa *et al.*, "FUS regulates AMPA receptor function and FTLD/ALS-associated behaviour via GluA1 mRNA stabilization.", *Nat. Commun.*, vol. 6, p. 7098, May 2015.

[85]   C. J. Oldfield and A. K. Dunker, "Intrinsically disordered proteins and intrinsically disordered protein regions.", *Annu. Rev. Biochem.*, vol. 83, pp. 553–584, 2014.

[86]   R. Van Der Lee *et al.*, "Classification of intrinsically disordered regions and proteins.", *Chem. Rev.*, vol. 114, no. 13, pp. 6589–6631, 2014.

[87]   S. Calabretta and S. Richard, "Emerging Roles of Disordered Sequences in RNA-Binding Proteins.", *Trends Biochem. Sci.*, vol. 40, no. 11, pp. 662–672, Nov. 2015.

[88]   V. Vacic *et al.*, "Characterization of molecular recognition features, MoRFs, and their binding partners.", *J. Proteome Res.*, vol. 6, no. 6, pp. 2351–2366, Jun. 2007.

[89]   R. J. Weatheritt, K. Luck, E. Petsalaki, N. E. Davey, and T. J. Gibson, "The identification of short linear motif-mediated interfaces within the human interactome.", *Bioinformatics*, vol. 28, no. 7, pp. 976–982, Apr. 2012.

[90]   M. Kato *et al.*, "Cell-free formation of RNA granules: low complexity sequence domains form dynamic fibers within hydrogels.", *Cell*, vol. 149, no. 4, pp. 753–767, May 2012.

[91]   K. P. Ng, G. Potikyan, R. O. V Savene, C. T. Denny, V. N. Uversky, and K. A. W. Lee, "Multiple aromatic side chains within a disordered structure are critical for transcription and transforming activity of EWS family oncoproteins.", *Proc. Natl. Acad. Sci. U. S. A.*, vol. 104, no. 2, pp. 479–484, Jan. 2007.

[92]   G. Boulay *et al.*, "Cancer-Specific Retargeting of BAF Complexes by a Prion-like Domain.", *Cell*, vol. 171, no. 1, pp. 163-178.e19, Sep. 2017.

[93]   M. Lindén *et al.*, "FET family fusion oncoproteins target the SWI/SNF chromatin remodeling complex.", *EMBO Rep.*, vol. 20, no. 5, May 2019.

[94]   J. Habchi, P. Tompa, S. Longhi, and V. N. Uversky, "Introducing protein intrinsic disorder.", *Chem. Rev.*, vol. 114, no. 13, pp. 6561–6588, Jul. 2014.

[95]   A. K. Dunker, M. S. Cortese, P. Romero, L. M. Iakoucheva, and V. N. Uversky, "Flexible nets. The roles of intrinsic disorder in protein interaction networks.", *FEBS J.*, vol. 272, no. 20, pp. 5129–5148, Oct. 2005.

[96]   J. Wang *et al.*, "A Molecular Grammar Governing the Driving Forces for Phase Separation of Prion-

like RNA Binding Proteins.", *Cell*, vol. 174, no. 3, pp. 688-699.e16, Jul. 2018.

[97] A. C. Murthy *et al.*, "Molecular interactions contributing to FUS SYGQ LC-RGG phase separation and co-partitioning with RNA polymerase II heptads.", *Nat. Struct. Mol. Biol.*, vol. 28, no. 11, pp. 923–935, Nov. 2021.

[98] Z. Monahan *et al.*, "Phosphorylation of the FUS low-complexity domain disrupts phase separation, aggregation, and toxicity.", *EMBO J.*, vol. 36, no. 20, pp. 2951–2967, Oct. 2017.

[99] M. L. Nosella *et al.*, "O-Linked- N-Acetylglucosaminylation of the RNA-Binding Protein EWS N-Terminal Low Complexity Region Reduces Phase Separation and Enhances Condensate Dynamics.", *J. Am. Chem. Soc.*, vol. 143, no. 30, pp. 11520–11534, 2021.

[100] M. Hofweber *et al.*, "Phase Separation of FUS Is Suppressed by Its Nuclear Import Receptor and Arginine Methylation.", *Cell*, vol. 173, no. 3, pp. 706-719.e13, Apr. 2018.

[101] S. Qamar *et al.*, "FUS Phase Separation Is Modulated by a Molecular Chaperone and Methylation of Arginine Cation-π Interactions.", *Cell*, 2018.

[102] C. Tanikawa *et al.*, "Citrullination of RGG Motifs in FET Proteins by PAD4 Regulates Protein Aggregation and ALS Susceptibility.", *Cell Rep.*, vol. 22, no. 6, pp. 1473–1483, Feb. 2018.

[103] J. C. Schwartz, C. C. Ebmeier, E. R. Podell, J. Heimiller, D. J. Taatjes, and T. R. Cech, "FUS binds the CTD of RNA polymerase II and regulates its phosphorylation at Ser2.", *Genes Dev.*, vol. 26, no. 24, pp. 2690–2695, Dec. 2012.

[104] E. Guccione and S. Richard, "The regulation, functions and clinical relevance of arginine methylation.", *Nat. Rev. Mol. Cell Biol.*, vol. 20, no. 10, pp. 642–657, 2019.

[105] M. P. Paronetto, "Ewing sarcoma protein: a key player in human cancer.", *Int. J. Cell Biol.*, vol. 2013, p. 642853, 2013.

[106] D. Nishiyama *et al.*, "EWSR1 overexpression is a pro-oncogenic event in multiple myeloma.", *Int. J. Hematol.*, vol. 113, no. 3, pp. 381–394, Mar. 2021.

[107] A. Y. Tan and J. L. Manley, "The TET family of proteins: functions and roles in disease.", *J. Mol. Cell Biol.*, vol. 1, no. 2, pp. 82–92, Dec. 2009.

[108] J. A. Perry, B. K. A. Seong, and K. Stegmaier, "Biology and therapy of dominant fusion oncoproteins involving transcription factor and chromatin regulators in sarcomas.", *Annu. Rev. Cancer Biol.*, vol. 3, no. 1, pp. 299–321, 2019.

[109] W. A. May *et al.*, "The Ewing's sarcoma EWS/FLI-1 fusion gene encodes a more potent transcriptional activator and is a more powerful transforming gene than FLI-1.", *Mol. Cell. Biol.*, vol. 13, no. 12, pp. 7393–7398, Dec. 1993.

[110] G. L. Brien, K. Stegmaier, and S. A. Armstrong, "Targeting chromatin complexes in fusion protein-driven malignancies.", *Nat. Rev. Cancer*, vol. 19, no. 5, pp. 255–269, 2019.

[111] F. Svetoni, P. Frisone, and M. P. Paronetto, "Role of FET proteins in neurodegenerative disorders.", *RNA Biol.*, vol. 13, no. 11, pp. 1089–1102, Nov. 2016.

[112] M. Kamelgarn, J. Chen, L. Kuang, H. Jin, E. J. Kasarskis, and H. Zhu, "ALS mutations of FUS suppress protein translation and disrupt the regulation of nonsense-mediated decay.", *Proc. Natl. Acad. Sci.*

U. S. A., vol. 115, no. 51, pp. E11904–E11913, Dec. 2018.

[113] O. Saulnier, "Deciphering the splicing landscape of Ewing sarcoma.", Paris Diderot VII, Sorbonne Paris Cité, 2018.

[114] P. C. Hollenhorst, L. P. McIntosh, and B. J. Graves, "Genomic and biochemical insights into the specificity of ETS transcription factors.", *Annu. Rev. Biochem.*, vol. 80, pp. 437–471, 2011.

[115] A. D. Sharrocks, "The ETS-domain transcription factor family.", *Nat. Rev. Mol. Cell Biol.*, vol. 2, no. 11, pp. 827–837, Nov. 2001.

[116] T. Oikawa and T. Yamada, "Molecular biology of the Ets family of transcription factors.", *Gene*, vol. 303, pp. 11–34, Jan. 2003.

[117] G. H. Wei *et al.*, "Genome-wide analysis of ETS-family DNA-binding in vitro and in vivo.", *EMBO J.*, vol. 29, no. 13, pp. 2147–2160, Jul. 2010.

[118] X. Rambout, "Construction of an interactomic map of Ets factors and identification of new functions in mRNA processing.", Gembloux Agro-Bio Tech, 2013.

[119] O. Saulnier *et al.*, "ERG transcription factors have a splicing regulatory function involving RBFOX2 that is altered in the EWS-FLI1 oncogenic fusion.", *Nucleic Acids Res.*, vol. 49, no. 9, pp. 5038–5056, May 2021.

[120] X. Rambout *et al.*, "The transcription factor ERG recruits CCR4-NOT to control mRNA decay and mitotic progression.", *Nat. Struct. Mol. Biol.*, vol. 23, no. 7, pp. 663–672, Jul. 2016.

[121] L. W. Donaldson, J. M. Petersen, B. J. Graves, and L. P. McIntosh, "Solution structure of the ETS domain from murine Ets-1: a winged helix-turn-helix DNA binding motif.", *EMBO J.*, vol. 15, no. 1, pp. 125–134, Jan. 1996.

[122] L. W. Donaldson, J. M. Petersen, B. J. Graves, and L. P. McIntosh, "Secondary structure of the ETS domain places murine Ets-1 in the superfamily of winged helix-turn-helix DNA-binding proteins.", *Biochemistry*, vol. 33, no. 46, pp. 13509–13516, Nov. 1994.

[123] H. Liang *et al.*, "Solution structure of the ets domain of Fli-1 when bound to DNA.", *Nat. Struct. Biol.*, vol. 1, no. 12, pp. 871–875, Dec. 1994.

[124] G. M. Sizemore, J. R. Pitarresi, S. Balakrishnan, and M. C. Ostrowski, "The ETS family of oncogenic transcription factors in solid tumours.", *Nat. Rev. Cancer*, 2017.

[125] E. A. Fry, A. Mallakin, and K. Inoue, "Translocations involving ETS family proteins in human cancer.", *Integr. cancer Sci. Ther.*, vol. 5, no. 4, Aug. 2018.

[126] N. V. Dharia *et al.*, "A first-generation pediatric cancer dependency map.", *Nat. Genet.*, vol. 53, no. 4, pp. 529–538, 2021.

[127] F. Tirode *et al.*, "Genomic landscape of Ewing sarcoma defines an aggressive subtype with co-association of STAG2 and TP53 mutations.", *Cancer Discov.*, vol. 4, no. 11, pp. 1342–1353, Nov. 2014.

[128] A. S. Brohl *et al.*, "The genomic landscape of the Ewing Sarcoma family of tumors reveals recurrent STAG2 mutation.", *PLoS Genet.*, vol. 10, no. 7, p. e1004475, Jul. 2014.

[129] B. D. Crompton *et al.*, "The genomic landscape of pediatric Ewing sarcoma.", *Cancer Discov.*, vol. 4,

no. 11, pp. 1326–1341, Nov. 2014.

[130] D. A. Solomon *et al.*, "Mutational inactivation of STAG2 causes aneuploidy in human cancer.", *Science*, vol. 333, no. 6045, pp. 1039–1043, Aug. 2011.

[131] A. S. Brohl *et al.*, "Frequent inactivating germline mutations in DNA repair genes in patients with Ewing sarcoma.", *Genet. Med. Off. J. Am. Coll. Med. Genet.*, vol. 19, no. 8, pp. 955–958, Aug. 2017.

[132] M. J. Machiela *et al.*, "Genome-wide association study identifies multiple new loci associated with Ewing sarcoma susceptibility.", *Nat. Commun.*, vol. 9, no. 1, p. 3184, Aug. 2018.

[133] F. Mugneret, S. Lizard, A. Aurias, and C. Turc-Carel, "Chromosomes in Ewing's sarcoma. II. Nonrandom additional changes, trisomy 8 and der(16)t(1;16).", *Cancer Genet. Cytogenet.*, vol. 32, no. 2, pp. 239–245, Jun. 1988.

[134] C. M. Hattinger *et al.*, "Prognostic impact of chromosomal aberrations in Ewing tumours.", *Br. J. Cancer*, vol. 86, no. 11, pp. 1763–1769, Jun. 2002.

[135] P. Roberts *et al.*, "Ploidy and karyotype complexity are powerful prognostic indicators in the Ewing's sarcoma family of tumors: a study by the United Kingdom Cancer Cytogenetics and the Children's Cancer and Leukaemia Group.", *Genes. Chromosomes Cancer*, vol. 47, no. 3, pp. 207–220, Mar. 2008.

[136] K. Tanaka, T. Iwakuma, K. Harimaya, H. Sato, and Y. Iwamoto, "EWS-Fli1 antisense oligodeoxynucleotide inhibits proliferation of human Ewing's sarcoma and primitive neuroectodermal tumor cells.", *J. Clin. Invest.*, vol. 99, no. 2, pp. 239–247, Jan. 1997.

[137] G. Stoll *et al.*, "Systems biology of Ewing sarcoma: A network model of EWS-FLI1 effect on proliferation and apoptosis.", *Nucleic Acids Res.*, 2013.

[138] R. A. Bailly *et al.*, "DNA-binding and transcriptional activation properties of the EWS-FLI-1 fusion protein resulting from the t(11;22) translocation in Ewing sarcoma.", *Mol. Cell. Biol.*, vol. 14, no. 5, pp. 3230–3241, May 1994.

[139] T. Ohno, V. N. Rao, and E. S. Reddy, "EWS/Fli-1 chimeric protein is a transcriptional activator.", *Cancer Res.*, vol. 53, no. 24, pp. 5859–5863, Dec. 1993.

[140] W. A. May *et al.*, "Ewing sarcoma 11;22 translocation produces a chimeric transcription factor that requires the DNA-binding domain encoded by FLI1 for transformation.", *Proc. Natl. Acad. Sci. U. S. A.*, vol. 90, no. 12, pp. 5752–5756, 1993.

[141] S. L. Lessnick, B. S. Braun, C. T. Denny, and W. A. May, "Multiple domains mediate transformation by the Ewing's sarcoma EWS/FLI-1 fusion gene.", *Oncogene*, 1995.

[142] K. B. Hahm *et al.*, "Repression of the gene encoding the TGF-beta type II receptor is a major target of the EWS-FLI1 oncoprotein.", *Nat. Genet.*, vol. 23, no. 2, pp. 222–227, Oct. 1999.

[143] A. Prieur, F. Tirode, P. Cohen, and O. Delattre, "EWS/FLI-1 silencing and gene profiling of Ewing cells reveal downstream oncogenic pathways and a crucial role for repression of insulin-like growth factor binding protein 3.", *Mol. Cell. Biol.*, vol. 24, no. 16, pp. 7275–7283, Aug. 2004.

[144] A. Arvand, S. M. Welford, M. A. Teitell, and C. T. Denny, "The COOH-terminal domain of FLI-1 is necessary for full tumorigenesis and transcriptional modulation by EWS/FLI-1.", *Cancer Res.*, vol. 61, no. 13, pp. 5311–5317, Jul. 2001.

[145] M. A. Boone *et al.*, "The FLI portion of EWS/FLI contributes a transcriptional regulatory function that is distinct and separable from its DNA-binding function in Ewing sarcoma.", *Oncogene*, vol. 40, no. 29, pp. 4759–4769, Jul. 2021.

[146] B. S. Braun, R. Frieden, S. L. Lessnick, W. A. May, and C. T. Denny, "Identification of target genes for the Ewing's sarcoma EWS/FLI fusion protein by representational difference analysis.", *Mol. Cell. Biol.*, vol. 15, no. 8, pp. 4623–4630, Aug. 1995.

[147] A. D. Thompson *et al.*, "EAT-2 is a novel SH2 domain containing protein that is up regulated by Ewing's sarcoma EWS/FL11 fusion gene.", *Oncogene*, 1996.

[148] W. A. May, A. Arvand, A. D. Thompson, B. S. Braun, M. Wright, and C. T. Denny, "EWS/FLI1-induced manic fringe renders NIH 3T3 cells tumorigenic.", *Nat. Genet.*, vol. 17, no. 4, pp. 495–497, Dec. 1997.

[149] A. Arvand, H. Bastians, S. M. Welford, A. D. Thompson, J. V Ruderman, and C. T. Denny, "EWS/FLI1 up regulates mE2-C, a cyclin-selective ubiquitin conjugating enzyme involved in cyclin B destruction.", *Oncogene*, vol. 17, no. 16, pp. 2039–2045, Oct. 1998.

[150] N. Riggi *et al.*, "EWS-FLI-1 expression triggers a Ewing's sarcoma initiation program in primary human mesenchymal stem cells.", *Cancer Res.*, vol. 68, no. 7, pp. 2176–2185, Apr. 2008.

[151] L. Cironi *et al.*, "IGF1 is a common target gene of Ewing's sarcoma fusion proteins in mesenchymal progenitor cells.", *PLoS One*, vol. 3, no. 7, p. e2634, Jul. 2008.

[152] R. Smith *et al.*, "Expression profiling of EWS/FLI identifies NKX2.2 as a critical target gene in Ewing's sarcoma.", *Cancer Cell*, vol. 9, no. 5, pp. 405–416, May 2006.

[153] O. M. Tirado *et al.*, "Caveolin-1 (CAV1) is a target of EWS/FLI-1 and a key determinant of the oncogenic phenotype and tumorigenicity of Ewing's sarcoma cells.", *Cancer Res.*, vol. 66, no. 20, pp. 9937–9947, Oct. 2006.

[154] M. Kinsey, R. Smith, and S. L. Lessnick, "NR0B1 is required for the oncogenic phenotype mediated by EWS/FLI in Ewing's sarcoma.", *Mol. Cancer Res.*, vol. 4, no. 11, pp. 851–859, Nov. 2006.

[155] M. Kauer *et al.*, "A molecular function map of Ewing's sarcoma.", *PLoS One*, vol. 4, no. 4, p. e5415, 2009.

[156] N. Guillon, F. Tirode, V. Boeva, A. Zynovyev, E. Barillot, and O. Delattre, "The oncogenic EWS-FLI1 protein binds in vivo GGAA microsatellite sequences with potential transcriptional activation function.", *PLoS One*, vol. 4, no. 3, p. e4932, 2009.

[157] N. Riggi *et al.*, "EWS-FLI1 utilizes divergent chromatin remodeling mechanisms to directly activate or repress enhancer elements in Ewing sarcoma.", *Cancer Cell*, vol. 26, no. 5, pp. 668–681, Nov. 2014.

[158] K. Gangwal *et al.*, "Microsatellites as EWS/FLI response elements in Ewing's sarcoma.", *Proc. Natl. Acad. Sci. U. S. A.*, vol. 105, no. 29, pp. 10149–10154, Jul. 2008.

[159] K. Gangwal, D. Close, C. A. Enriquez, C. P. Hill, and S. L. Lessnick, "Emergent Properties of EWS/FLI Regulation via GGAA Microsatellites in Ewing's Sarcoma.", *Genes Cancer*, vol. 1, no. 2, pp. 177–187, Feb. 2010.

[160] E. García-Aragoncillo *et al.*, "DAX1, a direct target of EWS/FLI1 oncoprotein, is a principal regulator

of cell-cycle progression in Ewing's tumor cells.", *Oncogene*, vol. 27, no. 46, pp. 6034–6043, Oct. 2008.

[161] A. Marchetto *et al.*, "Oncogenic hijacking of a developmental transcription factor evokes vulnerability toward oxidative stress in Ewing sarcoma.", *Nat. Commun.*, vol. 11, no. 1, p. 2423, May 2020.

[162] K. M. Johnson *et al.*, "Role for the EWS domain of EWS/FLI in binding GGAA-microsatellites required for Ewing sarcoma anchorage independent growth.", *Proc. Natl. Acad. Sci. U. S. A.*, vol. 114, no. 37, pp. 9870–9875, Sep. 2017.

[163] V. Boeva *et al.*, "De novo motif identification improves the accuracy of predicting transcription factor binding sites in ChIP-Seq data analysis.", *Nucleic Acids Res.*, vol. 38, no. 11, p. e126, Jun. 2010.

[164] K. Gangwal and S. L. Lessnick, "Microsatellites are EWS/FLI response elements: genomic 'junk' is EWS/FLI's treasure.", *Cell Cycle*, vol. 7, no. 20, pp. 3127–3132, Oct. 2008.

[165] L. A. Owen and S. L. Lessnick, "Identification of target genes in their native cellular context: An analysis of EWS/FLI in Ewing's sarcoma.", *Cell Cycle*, 2006.

[166] C. L. Braunreiter, J. D. Hancock, C. M. Coffin, K. M. Boucher, and S. L. Lessnick, "Expression of EWS-ETS fusions in NIH3T3 cells reveals significant differences to Ewing's sarcoma.", *Cell Cycle*, vol. 5, no. 23, pp. 2753–2759, Dec. 2006.

[167] R. Beck *et al.*, "EWS/FLI-responsive GGAA microsatellites exhibit polymorphic differences between European and African populations.", *Cancer Genet.*, vol. 205, no. 6, pp. 304–312, 2012.

[168] T. G. P. Grünewald *et al.*, "Chimeric EWSR1-FLI1 regulates the Ewing sarcoma susceptibility gene EGR2 via a GGAA microsatellite.", *Nat. Genet.*, vol. 47, no. 9, pp. 1073–1078, Sep. 2015.

[169] J. Musa *et al.*, "Cooperation of cancer drivers with regulatory germline variants shapes clinical outcomes.", *Nat. Commun.*, vol. 10, no. 1, p. 4128, Sep. 2019.

[170] R. Schwentner *et al.*, "EWS-FLI1 employs an E2F switch to drive target gene expression.", *Nucleic Acids Res.*, vol. 43, no. 5, pp. 2780–2789, Mar. 2015.

[171] S. Niedan *et al.*, "Suppression of FOXO1 is responsible for a growth regulatory repressive transcriptional sub-signature of EWS-FLI1 in Ewing sarcoma.", *Oncogene*, vol. 33, no. 30, pp. 3927–3938, Jul. 2014.

[172] L. A. Owen, A. A. Kowalewski, and S. L. Lessnick, "EWS/FLI mediates transcriptional repression via NKX2.2 during oncogenic transformation in Ewing's sarcoma.", *PLoS One*, vol. 3, no. 4, p. e1965, Apr. 2008.

[173] J. Fadul, R. Bell, L. M. Hoffman, M. C. Beckerle, M. E. Engel, and S. L. Lessnick, "EWS/FLI utilizes NKX2-2 to repress mesenchymal features of Ewing sarcoma.", *Genes Cancer*, vol. 6, no. 3–4, pp. 129–143, Mar. 2015.

[174] L. García-García *et al.*, "The Transcription Factor FEZF1, a Direct Target of EWSR1-FLI1 in Ewing Sarcoma Cells, Regulates the Expression of Neural-Specific Genes.", *Cancers (Basel).*, vol. 13, no. 22, Nov. 2021.

[175] A. M. Katschnig *et al.*, "EWS-FLI1 perturbs MRTFB/YAP-1/TEAD target gene regulation inhibiting cytoskeletal autoregulatory feedback in Ewing sarcoma.", *Oncogene*, vol. 36, no. 43, pp. 5995–

6005, Oct. 2017.

[176] B. A. Nacev *et al.*, "The epigenomics of sarcoma.", *Nat. Rev. Cancer*, vol. 20, no. 10, pp. 608–623, Oct. 2020.

[177] N. C. Gomez, A. J. Hepperla, R. Dumitru, J. M. Simon, F. Fang, and I. J. Davis, "Widespread Chromatin Accessibility at Repetitive Elements Links Stem Cells with Human Cancer.", *Cell Rep.*, vol. 17, no. 6, pp. 1607–1620, Nov. 2016.

[178] E. M. Tomazou *et al.*, "Epigenome mapping reveals distinct modes of gene regulation and widespread enhancer reprogramming by the oncogenic fusion protein EWS-FLI1.", *Cell Rep.*, vol. 10, no. 7, pp. 1082–1095, Feb. 2015.

[179] N. C. Sheffield *et al.*, "DNA methylation heterogeneity defines a disease spectrum in Ewing sarcoma.", *Nat. Med.*, vol. 23, no. 3, pp. 386–395, Mar. 2017.

[180] J. Shorter, "Prion-like Domains Program Ewing's Sarcoma.", *Cell*, vol. 171, no. 1, pp. 30–31, Sep. 2017.

[181] S. Sankar *et al.*, "Mechanism and relevance of EWS/FLI-mediated transcriptional repression in Ewing sarcoma.", *Oncogene*, vol. 32, no. 42, pp. 5089–5100, Oct. 2013.

[182] R. B. Davis, T. Kaur, M. M. Moosa, and P. R. Banerjee, "FUS oncofusion protein condensates recruit mSWI/SNF chromatin remodeler via heterotypic interactions between prion-like domains.", *Protein Sci.*, vol. 30, no. 7, pp. 1454–1466, 2021.

[183] H. J. Zullow *et al.*, "The FUS::DDIT3 fusion oncoprotein inhibits BAF complex targeting and activity in myxoid liposarcoma.", *Mol. Cell*, vol. 82, no. 9, pp. 1737-1750.e8, May 2022.

[184] B. E. Gryder *et al.*, "PAX3-FOXO1 establishes myogenic super enhancers and confers BET bromodomain vulnerability.", *Cancer Discov.*, vol. 7, no. 8, pp. 884–899, 2017.

[185] B. D. Sunkel *et al.*, "Evidence of pioneer factor activity of an oncogenic fusion transcription factor.", *iScience*, vol. 24, no. 8, p. 102867, Aug. 2021.

[186] M. J. McBride *et al.*, "The SS18-SSX Fusion Oncoprotein Hijacks BAF Complex Targeting and Function to Drive Synovial Sarcoma.", *Cancer Cell*, vol. 33, no. 6, pp. 1128-1141.e7, Jun. 2018.

[187] C. Kadoch and G. R. Crabtree, "Reversible disruption of mSWI/SNF (BAF) complexes by the SS18-SSX oncogenic fusion in synovial sarcoma.", *Cell*, vol. 153, no. 1, pp. 71–85, Mar. 2013.

[188] J. Li *et al.*, "A Role for SMARCB1 in Synovial Sarcomagenesis Reveals That SS18-SSX Induces Canonical BAF Destruction.", *Cancer Discov.*, vol. 11, no. 10, pp. 2620–2637, Oct. 2021.

[189] G. H. S. Richter *et al.*, "EZH2 is a mediator of EWS/FLI1 driven tumor growth and metastasis blocking endothelial and neuro-ectodermal differentiation.", *Proc. Natl. Acad. Sci. U. S. A.*, vol. 106, no. 13, pp. 5324–5329, Mar. 2009.

[190] X. Shi *et al.*, "EWS-FLI1 regulates and cooperates with core regulatory circuitry in Ewing sarcoma.", *Nucleic Acids Res.*, vol. 48, no. 20, pp. 11434–11451, Nov. 2020.

[191] O. Schmidt *et al.*, "Class I histone deacetylases (HDAC) critically contribute to Ewing sarcoma pathogenesis.", *J. Exp. Clin. Cancer Res.*, vol. 40, no. 1, p. 322, Oct. 2021.

[192] H. Zheng and W. Xie, "The role of 3D genome organization in development and cell

differentiation.", *Nat. Rev. Mol. Cell Biol.*, vol. 20, no. 9, pp. 535–550, Sep. 2019.

[193]   I. Jerkovic´ and G. Cavalli, "Understanding 3D genome organization by multidisciplinary methods.", *Nat. Rev. Mol. Cell Biol.*, vol. 22, no. 8, pp. 511–528, 2021.

[194]   I. A. Showpnil *et al.*, "EWS/FLI mediated reprogramming of 3D chromatin promotes an altered transcriptional state in Ewing sarcoma.", *bioRxiv*, p. 2021.09.30.462658, Jan. 2021.

[195]   E. Möller *et al.*, "EWSR1-ATF1 dependent 3D connectivity regulates oncogenic and differentiation programs in Clear Cell Sarcoma.", *Nat. Commun.*, vol. 13, no. 1, p. 2267, Apr. 2022.

[196]   J. H. Ahn *et al.*, "Phase separation drives aberrant chromatin looping and cancer development.", *Nature*, vol. 595, no. 7868, pp. 591–595, Jul. 2021.

[197]   S. Terlecki-Zaniewicz *et al.*, "Biomolecular condensation of NUP98 fusion proteins drives leukemogenic gene expression.", *Nat. Struct. Mol. Biol.*, vol. 28, no. 2, pp. 190–201, Feb. 2021.

[198]   B. Chandra *et al.*, "Phase Separation Mediates NUP98 Fusion Oncoprotein Leukemic Transformation.", *Cancer Discov.*, vol. 12, no. 4, pp. 1152–1169, Apr. 2022.

[199]   S. Mehta and J. Zhang, "Liquid-liquid phase separation drives cellular function and dysfunction in cancer.", *Nat. Rev. Cancer*, vol. 22, no. 4, pp. 239–252, Apr. 2022.

[200]   B. Carter and K. Zhao, "The epigenetic basis of cellular heterogeneity.", *Nat. Rev. Genet.*, vol. 22, no. 4, pp. 235–250, Apr. 2021.

[201]   S. Jaishankar, J. Zhang, M. F. Roussel, and S. J. Baker, "Transforming activity of EWS/FLI is not strictly dependent upon DNA-binding activity.", *Oncogene*, vol. 18, no. 40, pp. 5592–5597, Sep. 1999.

[202]   S. M. Welford, S. P. Hebert, B. Deneen, A. Arvand, and C. T. Denny, "DNA binding domain-independent pathways are involved in EWS/FLI1-mediated oncogenesis.", *J. Biol. Chem.*, vol. 276, no. 45, pp. 41977–41984, Nov. 2001.

[203]   L. L. Knoop and S. J. Baker, "EWS/FLI alters 5'-splice site selection.", *J. Biol. Chem.*, vol. 276, no. 25, pp. 22317–22322, Jun. 2001.

[204]   H. A. Chansky, M. Hu, D. D. Hickstein, and L. Yang, "Oncogenic TLS/ERG and EWS/Fli-1 fusion proteins inhibit RNA splicing mediated by YB-1 protein.", *Cancer Res.*, 2001.

[205]   L. Yang, H. A. Chansky, and D. D. Hickstein, "EWS.Fli-1 fusion protein interacts with hyperphosphorylated RNA polymerase II and interferes with serine-arginine protein-mediated RNA splicing.", *J. Biol. Chem.*, vol. 275, no. 48, pp. 37612–37618, Dec. 2000.

[206]   G. Sanchez *et al.*, "Alteration of cyclin D1 transcript elongation by a mutated transcription factor up-regulates the oncogenic D1b splice isoform in cancer.", *Proc. Natl. Acad. Sci. U. S. A.*, vol. 105, no. 16, pp. 6004–6009, Apr. 2008.

[207]   G. Sanchez, O. Delattre, D. Auboeuf, and M. Dutertre, "Coupled alteration of transcription and splicing by a single oncogene: boosting the effect on cyclin D1 activity.", *Cell Cycle*, vol. 7, no. 15, pp. 2299–2305, Aug. 2008.

[208]   H. V. Erkizan *et al.*, "RNA helicase A activity is inhibited by oncogenic transcription factor EWS-FLI1.", *Nucleic Acids Res.*, vol. 43, no. 2, pp. 1069–1080, Jan. 2015.

[209]   S. P. Selvanathan *et al.*, "Oncogenic fusion protein EWS-FLI1 is a network hub that regulates

alternative splicing.", *Proc. Natl. Acad. Sci. U. S. A.*, vol. 112, no. 11, pp. E1307-16, Mar. 2015.

[210] H. V Erkizan *et al.*, "A small molecule blocking oncogenic protein EWS-FLI1 interaction with RNA helicase A inhibits growth of Ewing's sarcoma.", *Nat. Med.*, vol. 15, no. 7, pp. 750–756, Jul. 2009.

[211] J. M. Povedano *et al.*, "TK216 targets microtubules in Ewing sarcoma cells.", *Cell Chem. Biol.*, vol. 29, no. 8, pp. 1325-1332.e4, Aug. 2022.

[212] J. H. Park *et al.*, "A multifunctional protein, EWS, is essential for early brown fat lineage determination.", *Dev. Cell*, vol. 26, no. 4, pp. 393–404, Aug. 2013.

[213] S. P. Selvanathan *et al.*, "EWS-FLI1 modulated alternative splicing of ARID1A reveals novel oncogenic function through the BAF complex.", *Nucleic Acids Res.*, vol. 47, no. 18, pp. 9619–9636, Oct. 2019.

[214] G. T. Graham *et al.*, "Comprehensive profiling of mRNA splicing indicates that GC content signals altered cassette exon inclusion in Ewing sarcoma.", *NAR cancer*, vol. 4, no. 1, p. zcab052, Mar. 2022.

[215] M. Esteller, "Non-coding RNAs in human disease.", *Nat. Rev. Genet.*, vol. 12, no. 12, pp. 861–874, Nov. 2011.

[216] E. Lekka and J. Hall, "Noncoding RNAs in disease.", *FEBS Lett.*, vol. 592, no. 17, pp. 2884–2900, Sep. 2018.

[217] J. Ban *et al.*, "Hsa-mir-145 is the top EWS-FLI1-repressed microRNA involved in a positive feedback loop in Ewing's sarcoma.", *Oncogene*, vol. 30, no. 18, pp. 2173–2180, May 2011.

[218] E. L. McKinsey *et al.*, "A novel oncogenic mechanism in Ewing sarcoma involving IGF pathway targeting by EWS/Fli1-regulated microRNAs.", *Oncogene*, vol. 30, no. 49, pp. 4910–4920, Dec. 2011.

[219] G.-A. Franzetti, K. Laud-Duval, D. Bellanger, M.-H. Stern, X. Sastre-Garau, and O. Delattre, "MiR-30a-5p connects EWS-FLI1 and CD99, two major therapeutic targets in Ewing tumor.", *Oncogene*, vol. 32, no. 33, pp. 3915–3921, Aug. 2013.

[220] A. Parafioriti *et al.*, "Ewing's sarcoma: An analysis of miRNA expression profiles and target genes in paraffin-embedded primary tumor tissue.", *Int. J. Mol. Sci.*, vol. 17, no. 5, 2016.

[221] L. Martignetti *et al.*, "Antagonism pattern detection between microRNA and target expression in Ewing's sarcoma.", *PLoS One*, vol. 7, no. 7, 2012.

[222] A. De Feo *et al.*, "miR-214-3p Is Commonly Downregulated by EWS-FLI1 and by CD99 and Its Restoration Limits Ewing Sarcoma Aggressiveness.", *Cancers (Basel).*, vol. 14, no. 7, Mar. 2022.

[223] G. M. Roberto *et al.*, "MiR-708-5p is inversely associated with EWS/FLI1 Ewing sarcoma but does not represent a prognostic predictor.", *Cancer Genet.*, vol. 230, pp. 21–27, Jan. 2019.

[224] Q. Lu, M. Lu, D. Li, and S. Zhang, "MicroRNA-34b promotes proliferation, migration and invasion of Ewing's sarcoma cells by downregulating Notch1.", *Mol. Med. Rep.*, vol. 18, no. 4, pp. 3577–3588, Oct. 2018.

[225] M. Marques Howarth *et al.*, "Long noncoding RNA EWSAT1-mediated gene repression facilitates Ewing sarcoma oncogenesis.", *J. Clin. Invest.*, vol. 124, no. 12, pp. 5275–5290, Dec. 2014.

[226] L. Ma *et al.*, "LncRNA SOX2 overlapping transcript acts as a miRNA sponge to promote the

proliferation and invasion of Ewing's sarcoma.", *Am. J. Transl. Res.*, vol. 11, no. 6, pp. 3841–3849, 2019.

[227] H. Li, F. Huang, X.-Q. Liu, H.-C. Liu, M. Dai, and J. Zeng, "LncRNA TUG1 promotes Ewing's sarcoma cell proliferation, migration, and invasion via the miR-199a-3p-MSI2 signaling pathway.", *Neoplasma*, vol. 68, no. 3, pp. 590–601, May 2021.

[228] J. Xiong *et al.*, "LncRNA FOXP4-AS1 Promotes Progression of Ewing Sarcoma and Is Associated With Immune Infiltrates.", *Front. Oncol.*, vol. 11, p. 718876, 2021.

[229] M. W. Hentze, A. Castello, T. Schwarzl, and T. Preiss, "A brave new world of RNA-binding proteins.", *Nat. Rev. Mol. Cell Biol.*, vol. 19, no. 5, pp. 327–341, May 2018.

[230] K. A. France, J. L. Anderson, A. Park, and C. T. Denny, "Oncogenic fusion protein EWS/FLI1 down-regulates gene expression by both transcriptional and posttranscriptional mechanisms.", *J. Biol. Chem.*, vol. 286, no. 26, pp. 22750–22757, Jul. 2011.

[231] D. Hanahan, "Hallmarks of Cancer: New Dimensions.", *Cancer Discov.*, vol. 12, no. 1, pp. 31–46, Jan. 2022.

[232] I. Pastushenko and C. Blanpain, "EMT Transition States during Tumor Progression and Metastasis.", *Trends Cell Biol.*, vol. 29, no. 3, pp. 212–226, Mar. 2019.

[233] A. Dongre and R. A. Weinberg, "New insights into the mechanisms of epithelial-mesenchymal transition and implications for cancer.", *Nat. Rev. Mol. Cell Biol.*, vol. 20, no. 2, pp. 69–84, Feb. 2019.

[234] S. Brabletz, H. Schuhwerk, T. Brabletz, and M. P. Stemmler, "Dynamic EMT: a multi-tool for tumor progression.", *EMBO J.*, vol. 40, no. 18, p. e108647, Sep. 2021.

[235] G. Sannino, A. Marchetto, T. Kirchner, and T. G. P. Grünewald, "Epithelial-to-Mesenchymal and Mesenchymal-to-Epithelial Transition in Mesenchymal Tumors: A Paradox in Sarcomas?.", *Cancer Res.*, vol. 77, no. 17, pp. 4556–4561, Sep. 2017.

[236] G.-A. Franzetti *et al.*, "Cell-to-cell heterogeneity of EWSR1-FLI1 activity determines proliferation/migration choices in Ewing sarcoma cells.", *Oncogene*, vol. 36, no. 25, pp. 3505–3514, Jun. 2017.

[237] M.-M. Aynaud *et al.*, "Transcriptional Programs Define Intratumoral Heterogeneity of Ewing Sarcoma at Single-Cell Resolution.", *Cell Rep.*, vol. 30, no. 6, pp. 1767-1779.e6, Feb. 2020.

[238] A. Chaturvedi, L. M. Hoffman, A. L. Welm, S. L. Lessnick, and M. C. Beckerle, "The EWS/FLI Oncogene Drives Changes in Cellular Morphology, Adhesion, and Migration in Ewing Sarcoma.", *Genes Cancer*, vol. 3, no. 2, pp. 102–116, Feb. 2012.

[239] D. N. T. Aryee *et al.*, "Hypoxia modulates EWS-FLI1 transcriptional signature and enhances the malignant properties of Ewing's sarcoma cells in vitro.", *Cancer Res.*, vol. 70, no. 10, pp. 4015–4023, May 2010.

[240] E. T. Wiles, R. Bell, D. Thomas, M. Beckerle, and S. L. Lessnick, "ZEB2 Represses the Epithelial Phenotype and Facilitates Metastasis in Ewing Sarcoma.", *Genes Cancer*, vol. 4, no. 11–12, pp. 486–500, Nov. 2013.

[241] T. S. McCann *et al.*, "KDM5A and PHF2 positively control expression of pro-metastatic genes

repressed by EWS/Fli1, and promote growth and metastatic properties in Ewing sarcoma.", *Oncotarget*, vol. 11, no. 43, pp. 3818–3831, Oct. 2020.

[242] A. A. Apfelbaum *et al.*, "EWS-FLI1 and HOXD13 control tumor cell plasticity in Ewing sarcoma.", *Clin. cancer Res. an Off. J. Am. Assoc. Cancer Res.*, Jun. 2022.

[243] D. Surdez *et al.*, "STAG2 mutations alter CTCF-anchored loop extrusion, reduce cis-regulatory interactions and EWSR1-FLI1 activity in Ewing sarcoma.", *Cancer Cell*, vol. 39, no. 6, pp. 810-826.e9, Jun. 2021.

[244] B. Adane *et al.*, "STAG2 loss rewires oncogenic and developmental programs to promote metastasis in Ewing sarcoma.", *Cancer Cell*, vol. 39, no. 6, pp. 827-844.e10, Jun. 2021.

[245] H.-F. Zhang *et al.*, "Proteomic Screens for Suppressors of Anoikis Identify IL1RAP as a Promising Surface Target in Ewing Sarcoma.", *Cancer Discov.*, vol. 11, no. 11, pp. 2884–2903, Nov. 2021.

[246] A. Mendoza-Naranjo *et al.*, "ERBB4 confers metastatic capacity in Ewing sarcoma.", *EMBO Mol. Med.*, vol. 5, no. 7, pp. 1087–1102, Jul. 2013.

[247] T. G. P. Grunewald *et al.*, "The Zyxin-related protein thyroid receptor interacting protein 6 (TRIP6) is overexpressed in Ewing's sarcoma and promotes migration, invasion and cell growth.", *Biol. cell*, vol. 105, no. 11, pp. 535–547, Nov. 2013.

[248] F. B. Markey, B. Romero, V. Parashar, and M. Batish, "Identification of a New Transcriptional Co-Regulator of STEAP1 in Ewing's Sarcoma.", *Cells*, vol. 10, no. 6, May 2021.

[249] T. G. P. Grunewald *et al.*, "STEAP1 is associated with the invasive and oxidative stress phenotype of Ewing tumors.", *Mol. Cancer Res.*, vol. 10, no. 1, pp. 52–65, Jan. 2012.

[250] K. Hauer *et al.*, "DKK2 mediates osteolysis, invasiveness, and metastatic spread in Ewing sarcoma.", *Cancer Res.*, vol. 73, no. 2, pp. 967–977, Jan. 2013.

[251] G. H. S. Richter *et al.*, "G-Protein coupled receptor 64 promotes invasiveness and metastasis in Ewing sarcomas through PGF and MMP1.", *J. Pathol.*, vol. 230, no. 1, pp. 70–81, May 2013.

[252] L. Lagares-Tena *et al.*, "Caveolin-1 promotes Ewing sarcoma metastasis regulating MMP-9 expression through MAPK/ERK pathway.", *Oncotarget*, vol. 7, no. 35, pp. 56889–56903, Aug. 2016.

[253] F. Cidre-Aranaz *et al.*, "Integrative gene network and functional analyses identify a prognostically relevant key regulator of metastasis in Ewing sarcoma.", *Molecular cancer*, vol. 21, no. 1. p. 1, Jan-2022.

[254] J. Ban *et al.*, "EWS-FLI1 suppresses NOTCH-activated p53 in Ewing's sarcoma.", *Cancer Res.*, vol. 68, no. 17, pp. 7100–7109, Sep. 2008.

[255] J. Ban *et al.*, "Suppression of deacetylase SIRT1 mediates tumor-suppressive NOTCH response and offers a novel treatment option in metastatic Ewing sarcoma.", *Cancer Res.*, vol. 74, no. 22, pp. 6578–6588, 2014.

[256] F. Cidre-Aranaz *et al.*, "EWS-FLI1-mediated suppression of the RAS-antagonist Sprouty 1 (SPRY1) confers aggressiveness to Ewing sarcoma.", *Oncogene*, vol. 36, no. 6, pp. 766–776, 2017.

[257] S.-H. Hong *et al.*, "High neuropeptide Y release associates with Ewing sarcoma bone dissemination - in vivo model of site-specific metastases.", *Oncotarget*, vol. 6, no. 9, pp. 7151–7165, Mar. 2015.

[258] A. M. El-Naggar *et al.*, "Translational Activation of HIF1α by YB-1 Promotes Sarcoma Metastasis.", *Cancer Cell*, vol. 27, no. 5, pp. 682–697, May 2015.

[259] K. M. Bailey, M. Airik, M. A. Krook, E. A. Pedersen, and E. R. Lawlor, "Micro-Environmental Stress Induces Src-Dependent Activation of Invadopodia and Cell Migration in Ewing Sarcoma.", *Neoplasia*, vol. 18, no. 8, pp. 480–488, Aug. 2016.

[260] M. A. Krook, L. A. Nicholls, C. A. Scannell, R. Chugh, D. G. Thomas, and E. R. Lawlor, "Stress-induced CXCR4 promotes migration and invasion of Ewing sarcoma.", *Mol. Cancer Res.*, vol. 12, no. 6, pp. 953–964, Jun. 2014.

[261] M. Ehnman, W. Chaabane, F. Haglund, and P. Tsagkozis, "The Tumor Microenvironment of Pediatric Sarcoma: Mesenchymal Mechanisms Regulating Cell Migration and Metastasis.", *Curr. Oncol. Rep.*, vol. 21, no. 10, p. 90, Aug. 2019.

[262] S. Kamura *et al.*, "Basic fibroblast growth factor in the bone microenvironment enhances cell motility and invasion of Ewing's sarcoma family of tumours by activating the FGFR1-PI3K-Rac1 pathway.", *Br. J. Cancer*, vol. 103, no. 3, pp. 370–381, Jul. 2010.

[263] A. Lissat *et al.*, "IL6 secreted by Ewing sarcoma tumor microenvironment confers anti-apoptotic and cell-disseminating paracrine responses in Ewing sarcoma cells.", *BMC Cancer*, vol. 15, p. 552, Jul. 2015.

[264] J. P. Koivunen *et al.*, "EML4-ALK fusion gene and efficacy of an ALK kinase inhibitor in lung cancer.", *Clin. cancer Res. an Off. J. Am. Assoc. Cancer Res.*, vol. 14, no. 13, pp. 4275–4283, Jul. 2008.

[265] A. Y. Li *et al.*, "RET fusions in solid tumors.", *Cancer Treat. Rev.*, vol. 81, p. 101911, Dec. 2019.

[266] E. Cocco, M. Scaltriti, and A. Drilon, "NTRK fusion-positive cancers and TRK inhibitor therapy.", *Nat. Rev. Clin. Oncol.*, vol. 15, no. 12, pp. 731–747, Dec. 2018.

[267] R. Roskoski, "Properties of FDA-approved small molecule protein kinase inhibitors: A 2022 update.", *Pharmacol. Res.*, vol. 175, no. December 2021, p. 106037, 2022.

[268] J. H. Bushweller, "Targeting transcription factors in cancer - from undruggable to reality.", *Nat. Rev. Cancer*, vol. 19, no. 11, pp. 611–624, Nov. 2019.

[269] J. E. Bradner, D. Hnisz, and R. A. Young, "Transcriptional Addiction in Cancer.", *Cell*, vol. 168, no. 4, pp. 629–643, 2017.

[270] M. M. L. Knott, T. L. B. Hölting, S. Ohmura, T. Kirchner, F. Cidre-Aranaz, and T. G. P. Grünewald, "Targeting the undruggable: exploiting neomorphic features of fusion oncoproteins in childhood sarcomas for innovative therapies.", *Cancer Metastasis Rev.*, vol. 38, no. 4, pp. 625–642, Dec. 2019.

[271] S. Sengupta and R. E. George, "Super-Enhancer-Driven Transcriptional Dependencies in Cancer.", *Trends in cancer*, vol. 3, no. 4, pp. 269–281, Apr. 2017.

[272] D. L. Casey, T.-Y. Lin, and N.-K. V Cheung, "Exploiting Signaling Pathways and Immune Targets Beyond the Standard of Care for Ewing Sarcoma.", *Front. Oncol.*, vol. 9, p. 537, 2019.

[273] D. Fayzullina *et al.*, "Novel Targeted Therapeutic Strategies for Ewing Sarcoma.", *Cancers (Basel).*, vol. 14, no. 8, Apr. 2022.

[274] S. T. Cervera *et al.*, "Therapeutic Potential of EWSR1-FLI1 Inactivation by CRISPR/Cas9 in Ewing

Sarcoma.", *Cancers (Basel).*, vol. 13, no. 15, Jul. 2021.

[275] S. A. Mitra, N. Ravinder, V. Magnon, J. Nagy, and T. J. Triche, "Abstract 4499: Genomic editing of EWS-FLI1 and its targets, and its therapeutic potential in treatment of Ewing sarcoma.", *Cancer Res.*, vol. 79, no. 13_Supplement, p. 4499, Jul. 2019.

[276] C. Jacques *et al.*, "Targeting the epigenetic readers in Ewing sarcoma inhibits the oncogenic transcription factor EWS/Fli1.", *Oncotarget*, vol. 7, no. 17, pp. 24125–24140, Apr. 2016.

[277] G. Boulay *et al.*, "Epigenome editing of microsatellite repeats defines tumor-specific enhancer functions and dependencies.", *Genes Dev.*, vol. 32, no. 15–16, pp. 1008–1019, Aug. 2018.

[278] T. L. B. Hölting *et al.*, "Neomorphic DNA-binding enables tumor-specific therapeutic gene expression in fusion-addicted childhood sarcoma.", *bioRxiv*, p. 2022.01.05.475061, Jan. 2022.

[279] H. A. Chansky *et al.*, "Targeting of EWS/FLI-1 by RNA interference attenuates the tumor phenotype of Ewing's sarcoma cells in vitro.", *J. Orthop. Res. Off. Publ. Orthop. Res. Soc.*, vol. 22, no. 4, pp. 910–917, Jul. 2004.

[280] C. Neckles *et al.*, "HNRNPH1-dependent splicing of a fusion oncogene reveals a targetable RNA G-quadruplex interaction.", *RNA*, vol. 25, no. 12, pp. 1731–1750, Dec. 2019.

[281] C. Neckles, S. Sundara Rajan, and N. J. Caplen, "Fusion transcripts: Unexploited vulnerabilities in cancer?.", *Wiley Interdiscip. Rev. RNA*, vol. 11, no. 1, p. e1562, Jan. 2020.

[282] T. Vo *et al.*, "HNRNPH1 destabilizes the G-quadruplex structures formed by G-rich RNA sequences that regulate the alternative splicing of an oncogenic fusion transcript.", *Nucleic Acids Res.*, vol. 50, no. 11, pp. 6474–6496, Jun. 2022.

[283] N. S. Latysheva *et al.*, "Molecular Principles of Gene Fusion Mediated Rewiring of Protein Interaction Networks in Cancer.", *Mol. Cell*, vol. 63, no. 4, pp. 579–592, Aug. 2016.

[284] A. Ghidini, A. Cléry, F. Halloy, F. H. T. Allain, and J. Hall, "RNA-PROTACs: Degraders of RNA-Binding Proteins.", *Angew. Chem. Int. Ed. Engl.*, vol. 60, no. 6, pp. 3163–3169, Feb. 2021.

[285] K. T. G. Samarasinghe *et al.*, "Targeted degradation of transcription factors by TRAFTACs: TRAnscription Factor TArgeting Chimeras.", *Cell Chem. Biol.*, vol. 28, no. 5, pp. 648-661.e5, May 2021.

[286] M. Schneider *et al.*, "The PROTACtable genome.", *Nat. Rev. Drug Discov.*, vol. 20, no. 10, pp. 789–797, Oct. 2021.

[287] B. K. A. Seong *et al.*, "TRIM8 modulates the EWS/FLI oncoprotein to promote survival in Ewing sarcoma.", *Cancer Cell*, pp. 1262–1278, 2021.

[288] S. Ramazi and J. Zahiri, "Posttranslational modifications in proteins: resources, tools and prediction methods.", *Database (Oxford).*, vol. 2021, Apr. 2021.

[289] R. J. Olsen and S. H. Hinrichs, "Phosphorylation of the EWS IQ domain regulates transcriptional activity of the EWS/ATF1 and EWS/FLI1 fusion proteins.", *Oncogene*, vol. 20, no. 14, pp. 1756–1764, Mar. 2001.

[290] R. Bachmaier *et al.*, "O-GlcNAcylation is involved in the transcriptional activity of EWS-FLI1 in Ewing's sarcoma.", *Oncogene*, vol. 28, no. 9, pp. 1280–1284, Mar. 2009.

[291]   M. E. Gierisch *et al.*, "USP19 deubiquitinates EWS-FLI1 to regulate Ewing sarcoma growth.", *Sci. Rep.*, vol. 9, no. 1, p. 951, Jan. 2019.

[292]   M. L. Harlow *et al.*, "Lurbinectedin Inactivates the Ewing Sarcoma Oncoprotein EWS-FLI1 by Redistributing It within the Nucleus.", *Cancer Res.*, vol. 76, no. 22, pp. 6657–6668, Nov. 2016.

[293]   M. L. Harlow *et al.*, "Trabectedin Inhibits EWS-FLI1 and Evicts SWI/SNF from Chromatin in a Schedule-dependent Manner.", *Clin. cancer Res. an Off. J. Am. Assoc. Cancer Res.*, vol. 25, no. 11, pp. 3417–3429, Jun. 2019.

[294]   H. Hegyi, L. Buday, and P. Tompa, "Intrinsic structural disorder confers cellular viability on oncogenic fusion proteins.", *PLoS Comput. Biol.*, vol. 5, no. 10, Oct. 2009.

[295]   N. S. Latysheva and M. M. Babu, "Molecular Signatures of Fusion Proteins in Cancer.", *ACS Pharmacol. Transl. Sci.*, vol. 2, no. 2, pp. 122–133, Apr. 2019.

[296]   R. J. Wheeler, "Therapeutics-how to treat phase separation-associated diseases.", *Emerg. Top. life Sci.*, vol. 4, no. 3, pp. 307–318, Dec. 2020.

[297]   F. de Nigris, C. Ruosi, and C. Napoli, "Clinical efficiency of epigenetic drugs therapy in bone malignancies.", *Bone*, vol. 143, p. 115605, Feb. 2021.

[298]   E. R. Theisen, K. I. Pishas, R. S. Saund, and S. L. Lessnick, "Therapeutic opportunities in Ewing sarcoma: EWS-FLI inhibition via LSD1 targeting.", *Oncotarget*, vol. 7, no. 14, pp. 17616–17630, Apr. 2016.

[299]   A. B. Iniguez *et al.*, "EWS/FLI Confers Tumor Cell Synthetic Lethality to CDK12 Inhibition in Ewing Sarcoma.", *Cancer Cell*, vol. 33, no. 2, pp. 202-216.e6, 2018.

[300]   T. Balestra *et al.*, "Targeting CD99 Compromises the Oncogenic Effects of the Chimera EWS-FLI1 by Inducing Reexpression of Zyxin and Inhibition of GLI1 Activity.", *Mol. Cancer Ther.*, vol. 21, no. 1, pp. 58–69, Jan. 2022.

[301]   P. van der Lelij *et al.*, "Synthetic lethality between the cohesin subunits STAG1 and STAG2 in diverse cancer contexts.", *Elife*, vol. 6, Jul. 2017.

[302]   D. Yee *et al.*, "Insulin-like growth factor I expression by tumors of neuroectodermal origin with the t(11;22) chromosomal translocation. A potential autocrine growth factor.", *J. Clin. Invest.*, vol. 86, no. 6, pp. 1806–1814, Dec. 1990.

[303]   K. Scotlandi *et al.*, "Blockage of insulin-like growth factor-I receptor inhibits the growth of Ewing's sarcoma in athymic mice.", *Cancer Res.*, vol. 58, no. 18, pp. 4127–4131, Sep. 1998.

[304]   A. S. Martins *et al.*, "Insulin-like growth factor I receptor pathway inhibition by ADW742, alone or in combination with imatinib, doxorubicin, or vincristine, is a novel therapeutic approach in Ewing tumor.", *Clin. cancer Res. an Off. J. Am. Assoc. Cancer Res.*, vol. 12, no. 11 Pt 1, pp. 3532–3540, Jun. 2006.

[305]   L. M. Guenther *et al.*, "A Combination CDK4/6 and IGF1R Inhibitor Strategy for Ewing Sarcoma.", *Clin. cancer Res. an Off. J. Am. Assoc. Cancer Res.*, vol. 25, no. 4, pp. 1343–1357, Feb. 2019.

[306]   K. Baird *et al.*, "Gene expression profiling of human sarcomas: insights into sarcoma biology.", *Cancer Res.*, vol. 65, no. 20, pp. 9226–9235, Oct. 2005.

[307] E. Beauchamp *et al.*, "GLI1 is a direct transcriptional target of EWS-FLI1 oncoprotein.", *J. Biol. Chem.*, vol. 284, no. 14, pp. 9074–9082, Apr. 2009.

[308] F. Cidre-Aranaz and J. Alonso, "EWS/FLI1 Target Genes and Therapeutic Opportunities in Ewing Sarcoma.", *Front. Oncol.*, vol. 5, p. 162, 2015.

[309] A. G. Hawkins *et al.*, "Wnt/β-catenin-activated Ewing sarcoma cells promote the angiogenic switch.", *JCI insight*, vol. 5, no. 13, Jul. 2020.

[310] M. Hayashi *et al.*, "Inhibition of porcupine prolongs metastasis free survival in a mouse xenograft model of Ewing sarcoma.", *Oncotarget*, vol. 8, no. 45, pp. 78265–78276, Oct. 2017.

[311] A. Marnef and G. Legube, "R-loops as Janus-faced modulators of DNA repair.", *Nat. Cell Biol.*, vol. 23, no. 4, pp. 305–313, Apr. 2021.

[312] A. Gorthi *et al.*, "EWS-FLI1 increases transcription to cause R-loops and block BRCA1 repair in Ewing sarcoma.", *Nature*, vol. 555, no. 7696, pp. 387–391, Mar. 2018.

[313] X. A. Su *et al.*, "RAD21 is a driver of chromosome 8 gain in Ewing sarcoma to mitigate replication stress.", *Genes Dev.*, vol. 35, no. 7–8, pp. 556–572, Apr. 2021.

[314] S. Kailayangiri *et al.*, "EZH2 Inhibition in Ewing Sarcoma Upregulates G D2 Expression for Targeting with Gene-Modified T Cells.", *Mol. Ther.*, vol. 27, no. 5, pp. 933–946, 2019.

[315] J. Li *et al.*, "Therapeutic targeting of the PLK1-PRC1-axis triggers cell death in genomically silent childhood cancer.", *Nat. Commun.*, vol. 12, no. 1, p. 5356, Sep. 2021.

[316] Bruce Alberts, Alexander Johnson, Julian Lewis, Martin Raff, K. Roberts, and P. Walter, *Molecular biology of the cell*, 4h ed. New York, NY: Garland Science Inc, 2002.

[317] P. Cramer, "Organization and regulation of gene transcription.", *Nature*, vol. 573, no. 7772, pp. 45–54, Sep. 2019.

[318] N. Al-Husini, S. Medler, and A. Ansari, "Crosstalk of promoter and terminator during RNA polymerase II transcription cycle.", *Biochim. Biophys. acta. Gene Regul. Mech.*, vol. 1863, no. 12, p. 194657, Dec. 2020.

[319] D. L. Bentley, "Coupling mRNA processing with transcription in time and space.", *Nature reviews. Genetics*, vol. 15, no. 3. pp. 163–175, Mar-2014.

[320] A. Ghosh and C. D. Lima, "Enzymology of RNA cap synthesis.", *Wiley Interdiscip. Rev. RNA*, vol. 1, no. 1, pp. 152–172, 2010.

[321] Y. Shi, "Mechanistic insights into precursor messenger RNA splicing by the spliceosome.", *Nat. Rev. Mol. Cell Biol.*, vol. 18, no. 11, pp. 655–670, Nov. 2017.

[322] L. A. Passmore and J. Coller, "Roles of mRNA poly(A) tails in regulation of eukaryotic gene expression.", *Nat. Rev. Mol. Cell Biol.*, vol. 23, no. 2, pp. 93–106, Feb. 2022.

[323] F. E. Baralle and J. Giudice, "Alternative splicing as a regulator of development and tissue identity.", *Nat. Rev. Mol. Cell Biol.*, vol. 18, no. 7, pp. 437–451, Jul. 2017.

[324] D. Wiener and S. Schwartz, "The epitranscriptome beyond m(6)A.", *Nat. Rev. Genet.*, vol. 22, no. 2, pp. 119–131, Feb. 2021.

[325] N. L. Garneau, J. Wilusz, and C. J. Wilusz, "The highways and byways of mRNA decay.", *Nat. Rev. Mol. Cell Biol.*, vol. 8, no. 2, pp. 113–126, Feb. 2007.

[326] D. R. Schoenberg and L. E. Maquat, "Regulation of cytoplasmic mRNA decay.", *Nat. Rev. Genet.*, vol. 13, no. 4, pp. 246–259, Mar. 2012.

[327] J. Houseley and D. Tollervey, "The many pathways of RNA degradation.", *Cell*, vol. 136, no. 4, pp. 763–776, Feb. 2009.

[328] E. Wahle and G. S. Winkler, "RNA decay machines: deadenylation by the Ccr4-not and Pan2-Pan3 complexes.", *Biochim. Biophys. Acta*, vol. 1829, no. 6–7, pp. 561–570, 2013.

[329] M. Schmid and T. H. Jensen, "Controlling nuclear RNA levels.", *Nat. Rev. Genet.*, vol. 19, no. 8, pp. 518–529, Aug. 2018.

[330] V. Balagopal and R. Parker, "Polysomes, P bodies and stress granules: states and fates of eukaryotic mRNAs.", *Curr. Opin. Cell Biol.*, vol. 21, no. 3, pp. 403–408, Jun. 2009.

[331] T. Maniatis and R. Reed, "An extensive network of coupling among gene expression machines.", *Nature*, vol. 416, no. 6880, pp. 499–506, Apr. 2002.

[332] G. Orphanides and D. Reinberg, "A unified theory of gene expression.", *Cell*. 2002.

[333] O. Dahan, H. Gingold, and Y. Pilpel, "Regulatory mechanisms and networks couple the different phases of gene expression.", *Trends Genet.*, vol. 27, no. 8, pp. 316–322, Aug. 2011.

[334] A. C. Goldstrohm and M. Wickens, "Multifunctional deadenylase complexes diversify mRNA control.", *Nature reviews. Molecular cell biology*, vol. 9, no. 4. England, pp. 337–344, Apr-2008.

[335] A. L. Nicholson and A. E. Pasquinelli, "Tales of Detailed Poly(A) Tails.", *Trends Cell Biol.*, vol. 29, no. 3, pp. 191–200, Mar. 2019.

[336] R. W. P. Smith, T. K. P. Blee, and N. K. Gray, "Poly(A)-binding proteins are required for diverse biological processes in metazoans.", *Biochem. Soc. Trans.*, vol. 42, no. 4, pp. 1229–1237, Aug. 2014.

[337] S. A. Lima *et al.*, "Short poly(A) tails are a conserved feature of highly expressed genes.", *Nat. Struct. Mol. Biol.*, vol. 24, no. 12, pp. 1057–1063, Dec. 2017.

[338] H. Chang, J. Lim, M. Ha, and V. N. Kim, "TAIL-seq: genome-wide determination of poly(A) tail length and 3' end modifications.", *Mol. Cell*, vol. 53, no. 6, pp. 1044–1052, Mar. 2014.

[339] I. Legnini, J. Alles, N. Karaiskos, S. Ayoub, and N. Rajewsky, "FLAM-seq: full-length mRNA sequencing reveals principles of poly(A) tail length control.", *Nat. Methods*, vol. 16, no. 9, pp. 879–886, Sep. 2019.

[340] J. Lim *et al.*, "Mixed tailing by TENT4A and TENT4B shields mRNA from rapid deadenylation.", *Science*, vol. 361, no. 6403, pp. 701–704, Aug. 2018.

[341] D. Kim *et al.*, "Viral hijacking of the TENT4-ZCCHC14 complex protects viral RNAs via mixed tailing.", *Nat. Struct. Mol. Biol.*, vol. 27, no. 6, pp. 581–588, Jun. 2020.

[342] B. W. Baer and R. D. Kornberg, "The protein responsible for the repeating structure of cytoplasmic poly(A)-ribonucleoprotein.", *J. Cell Biol.*, vol. 96, no. 3, pp. 717–721, Mar. 1983.

[343] C. G. Burd, E. L. Matunis, and G. Dreyfuss, "The multiple RNA-binding domains of the mRNA poly(A)-

binding protein have different RNA-binding activities.", *Mol. Cell. Biol.*, vol. 11, no. 7, pp. 3419–3424, Jul. 1991.

[344] I. B. Schäfer *et al.*, "Molecular Basis for poly(A) RNP Architecture and Recognition by the Pan2-Pan3 Deadenylase.", *Cell*, vol. 177, no. 6, pp. 1619-1631.e21, May 2019.

[345] J. Xie, G. Kozlov, and K. Gehring, "The 'tale' of poly(A) binding protein: the MLLE domain and PAM2-containing proteins.", *Biochim. Biophys. Acta*, vol. 1839, no. 11, pp. 1062–1068, Nov. 2014.

[346] U. Nudel, H. Soreq, and U. Z. Littauer, "Globin mRNA species containing poly(A) segments of different lengths. Their functional stability in Xenopus oocytes.", *Eur. J. Biochem.*, vol. 64, no. 1, pp. 115–121, Apr. 1976.

[347] J. F. Mercer and S. A. Wake, "An analysis of the rate of metallothionein mRNA poly(A)-shortening using RNA blot hybridization.", *Nucleic Acids Res.*, vol. 13, no. 22, pp. 7929–7943, Nov. 1985.

[348] T. Wilson and R. Treisman, "Removal of poly(A) and consequent degradation of c-fos mRNA facilitated by 3' AU-rich sequences.", *Nature*, vol. 336, no. 6197, pp. 396–399, Nov. 1988.

[349] P. Bernstein, S. W. Peltz, and J. Ross, "The poly(A)-poly(A)-binding protein complex is a major determinant of mRNA stability in vitro.", *Mol. Cell. Biol.*, vol. 9, no. 2, pp. 659–670, Feb. 1989.

[350] M. W. Webster *et al.*, "mRNA Deadenylation Is Coupled to Translation Rates by the Differential Activities of Ccr4-Not Nucleases.", *Mol. Cell*, 2018.

[351] S. Z. J. Tarun and A. B. Sachs, "Association of the yeast poly(A) tail binding protein with translation initiation factor eIF-4G.", *EMBO J.*, vol. 15, no. 24, pp. 7168–7177, Dec. 1996.

[352] A. Jacobson and S. W. Peltz, "Interrelationships of the pathways of mRNA decay and translation in eukaryotic cells.", *Annu. Rev. Biochem.*, vol. 65, pp. 693–739, 1996.

[353] J. Wolf *et al.*, "Structural basis for Pan3 binding to Pan2 and its function in mRNA recruitment and deadenylation.", *EMBO J.*, vol. 33, no. 14, pp. 1514–1526, Jul. 2014.

[354] S. Jonas *et al.*, "An asymmetric PAN3 dimer recruits a single PAN2 exonuclease to mediate mRNA deadenylation and decay.", *Nat. Struct. Mol. Biol.*, vol. 21, no. 7, pp. 599–608, Jul. 2014.

[355] I. B. Schäfer, M. Rode, F. Bonneau, S. Schüssler, and E. Conti, "The structure of the Pan2-Pan3 core complex reveals cross-talk between deadenylase and pseudokinase.", *Nat. Struct. Mol. Biol.*, vol. 21, no. 7, pp. 591–598, Jul. 2014.

[356] N. Siddiqui, D. A. Mangus, T.-C. Chang, J.-M. Palermino, A.-B. Shyu, and K. Gehring, "Poly(A) nuclease interacts with the C-terminal domain of polyadenylate-binding protein domain from poly(A)-binding protein.", *J. Biol. Chem.*, vol. 282, no. 34, pp. 25067–25075, Aug. 2007.

[357] R. Boeck, S. J. Tarun, M. Rieger, J. A. Deardorff, S. Müller-Auer, and A. B. Sachs, "The yeast Pan2 protein is required for poly(A)-binding protein-stimulated   poly(A)-nuclease activity.", *J. Biol. Chem.*, vol. 271, no. 1, pp. 432–438, Jan. 1996.

[358] C. E. Brown, S. Z. J. Tarun, R. Boeck, and A. B. Sachs, "PAN3 encodes a subunit of the Pab1p-dependent poly(A) nuclease in Saccharomyces cerevisiae.", *Mol. Cell. Biol.*, vol. 16, no. 10, pp. 5744–5753, Oct. 1996.

[359] H. Yi, J. Park, M. Ha, J. Lim, H. Chang, and V. N. Kim, "PABP Cooperates with the CCR4-NOT Complex

to Promote mRNA Deadenylation and Block Precocious Decay.", *Mol. Cell*, 2018.

[360] N. Chalabi Hagkarim and R. J. Grand, "The Regulatory Properties of the Ccr4-Not Complex.", *Cells*, vol. 9, no. 11, Oct. 2020.

[361] M. A. Collart, "The Ccr4-Not complex is a key regulator of eukaryotic gene expression.", *Wiley Interdiscip. Rev. RNA*, vol. 7, no. 4, pp. 438–454, Jul. 2016.

[362] N. C. Lau *et al.*, "Human Ccr4-Not complexes contain variable deadenylase subunits.", *Biochem. J.*, vol. 422, no. 3, pp. 443–453, Sep. 2009.

[363] M. A. Collart and O. O. Panasenko, *The ccr4-not complex: Architecture and structural insights*, vol. 83. 2017.

[364] T. Raisch, C.-T. Chang, Y. Levdansky, S. Muthukumar, S. Raunser, and E. Valkov, "Reconstitution of recombinant human CCR4-NOT reveals molecular insights into regulated deadenylation.", *Nat. Commun.*, vol. 10, no. 1, p. 3173, Jul. 2019.

[365] L. Maillet, C. Tu, Y. K. Hong, E. O. Shuster, and M. A. Collart, "The essential function of Not1 lies within the Ccr4-Not complex.", *J. Mol. Biol.*, vol. 303, no. 2, pp. 131–143, Oct. 2000.

[366] A. Boland *et al.*, "Structure and assembly of the NOT module of the human CCR4-NOT complex.", *Nat. Struct. Mol. Biol.*, vol. 20, no. 11, pp. 1289–1297, Nov. 2013.

[367] N. Alhusaini and J. Coller, "The deadenylase components Not2p, Not3p, and Not5p promote mRNA decapping.", *RNA*, vol. 22, no. 5, pp. 709–721, May 2016.

[368] O. O. Panasenko, "The role of the E3 ligase Not4 in cotranslational quality control.", *Front. Genet.*, vol. 5, p. 141, 2014.

[369] K. Ito, T. Inoue, K. Yokoyama, M. Morita, T. Suzuki, and T. Yamamoto, "CNOT2 depletion disrupts and inhibits the CCR4-NOT deadenylase complex and induces apoptotic cell death.", *Genes Cells*, vol. 16, no. 4, pp. 368–379, Apr. 2011.

[370] S. Bresson and D. Tollervey, "Tailing Off: PABP and CNOT Generate Cycles of mRNA Deadenylation.", *Mol. Cell*, vol. 70, no. 6, pp. 987–988, Jun. 2018.

[371] C.-Y. Lee and G. Seydoux, "Dynamics of mRNA entry into stress granules.", *Nat. Cell Biol.*, vol. 21, no. 2, pp. 116–117, Feb. 2019.

[372] S. Jonas and E. Izaurralde, "The role of disordered protein regions in the assembly of decapping complexes and RNP granules.", *Genes Dev.*, vol. 27, no. 24, pp. 2628–2641, Dec. 2013.

[373] C. Kilchert, S. Wittmann, and L. Vasiljeva, "The regulation and functions of the nuclear RNA exosome complex.", *Nat. Rev. Mol. Cell Biol.*, vol. 17, no. 4, pp. 227–239, Apr. 2016.

[374] A. Tudek, M. Schmid, and T. H. Jensen, "Escaping nuclear decay: the significance of mRNA export for gene expression.", *Curr. Genet.*, vol. 65, no. 2, pp. 473–476, Apr. 2019.

[375] Y. Luo, Z. Na, and S. A. Slavoff, "P-Bodies: Composition, Properties, and Functions.", *Biochemistry*, vol. 57, no. 17, pp. 2424–2431, May 2018.

[376] N. Standart and D. Weil, "P-Bodies: Cytosolic Droplets for Coordinated mRNA Storage.", *Trends Genet.*, vol. 34, no. 8, pp. 612–626, Aug. 2018.

[377] J.-Y. Youn *et al.*, "Properties of Stress Granule and P-Body Proteomes.", *Mol. Cell*, vol. 76, no. 2, pp. 286–294, Oct. 2019.

[378] N. Minshall, M. Kress, D. Weil, and N. Standart, "Role of p54 RNA helicase activity and its C-terminal domain in translational repression, P-body localization and assembly.", *Mol. Biol. Cell*, vol. 20, no. 9, pp. 2464–2472, May 2009.

[379] N. Cougot, S. Babajko, and B. Séraphin, "Cytoplasmic foci are sites of mRNA decay in human cells.", *J. Cell Biol.*, vol. 165, no. 1, pp. 31–40, Apr. 2004.

[380] U. Sheth and R. Parker, "Decapping and decay of messenger RNA occur in cytoplasmic processing bodies.", *Science*, vol. 300, no. 5620, pp. 805–808, May 2003.

[381] A. Aizer *et al.*, "Quantifying mRNA targeting to P-bodies in living human cells reveals their dual role in mRNA decay and storage.", *J. Cell Sci.*, vol. 127, no. Pt 20, pp. 4443–4456, Oct. 2014.

[382] A. Eulalio, I. Behm-Ansmant, D. Schweizer, and E. Izaurralde, "P-body formation is a consequence, not the cause, of RNA-mediated gene silencing.", *Mol. Cell. Biol.*, vol. 27, no. 11, pp. 3970–3981, Jun. 2007.

[383] M. Brengues, D. Teixeira, and R. Parker, "Movement of eukaryotic mRNAs between polysomes and cytoplasmic processing bodies.", *Science*, vol. 310, no. 5747, pp. 486–489, Oct. 2005.

[384] A. Hubstenberger *et al.*, "P-Body Purification Reveals the Condensation of Repressed mRNA Regulons.", *Mol. Cell*, vol. 68, no. 1, pp. 144-157.e5, Oct. 2017.

[385] Z. Yang *et al.*, "GW182 is critical for the stability of GW bodies expressed during the cell cycle and cell proliferation.", *J. Cell Sci.*, vol. 117, no. Pt 23, pp. 5567–5578, Nov. 2004.

[386] D. Zheng, N. Ezzeddine, C.-Y. A. Chen, W. Zhu, X. He, and A.-B. Shyu, "Deadenylation is prerequisite for P-body formation and mRNA decay in mammalian cells.", *J. Cell Biol.*, vol. 182, no. 1, pp. 89–101, Jul. 2008.

[387] T. M. Franks and J. Lykke-Andersen, "The control of mRNA decapping and P-body formation.", *Mol. Cell*, vol. 32, no. 5, pp. 605–615, Dec. 2008.

[388] D. S. W. Protter and R. Parker, "Principles and Properties of Stress Granules.", *Trends Cell Biol.*, vol. 26, no. 9, pp. 668–679, Sep. 2016.

[389] S. Jain, J. R. Wheeler, R. W. Walters, A. Agrawal, A. Barsic, and R. Parker, "ATPase-Modulated Stress Granules Contain a Diverse Proteome and Substructure.", *Cell*, vol. 164, no. 3, pp. 487–498, Jan. 2016.

[390] N. Kedersha *et al.*, "Stress granules and processing bodies are dynamically linked sites of mRNP remodeling.", *J. Cell Biol.*, vol. 169, no. 6, pp. 871–884, Jun. 2005.

[391] S. Namkoong, A. Ho, Y. M. Woo, H. Kwak, and J. H. Lee, "Systematic Characterization of Stress-Induced RNA Granulation.", *Mol. Cell*, vol. 70, no. 1, pp. 175-187.e8, Apr. 2018.

[392] Y. Zhan *et al.*, "Understanding the roles of stress granule during chemotherapy for patients with malignant tumors.", *Am. J. Cancer Res.*, vol. 10, no. 8, pp. 2226–2241, 2020.

[393] P. Eser *et al.*, "Periodic mRNA synthesis and degradation co-operate during cell cycle gene expression.", *Mol. Syst. Biol.*, vol. 10, no. 1, p. 717, 2014.

[394] C.-H. Lou, E. Y. Shum, and M. F. Wilkinson, "RNA degradation drives stem cell differentiation.", *EMBO J.*, vol. 34, no. 12, pp. 1606–1608, Jun. 2015.

[395] I. Fraga De Andrade, C. Mehta, and E. H. Bresnick, "Post-transcriptional control of cellular differentiation by the RNA exosome complex.", *Nucleic Acids Res.*, vol. 48, no. 21, pp. 11913–11928, 2021.

[396] C. R. Alonso, "A complex 'mRNA degradation code' controls gene expression during animal development.", *Trends Genet.*, vol. 28, no. 2, pp. 78–88, Feb. 2012.

[397] R. A. Steinman, "mRNA stability control: A clandestine force in normal and malignant hematopoiesis.", *Leukemia*, vol. 21, no. 6. Nature Publishing Group, pp. 1158–1171, 2007.

[398] R. Karam, C.-H. Lou, H. Kroeger, L. Huang, J. H. Lin, and M. F. Wilkinson, "The unfolded protein response is shaped by the NMD pathway.", *EMBO Rep.*, vol. 16, no. 5, pp. 599–609, May 2015.

[399] S. Akira and K. Maeda, "Control of RNA Stability in Immunity.", *Annu. Rev. Immunol.*, vol. 39, pp. 481–509, Apr. 2021.

[400] T. Akiyama, T. Suzuki, and T. Yamamoto, "RNA decay machinery safeguards immune cell development and immunological responses.", *Trends Immunol.*, vol. 42, no. 5, pp. 447–460, 2021.

[401] C. M. Misquitta, T. Chen, and A. K. Grover, "Control of protein expression through mRNA stability in calcium signalling.", *Cell Calcium*, vol. 40, no. 4, pp. 329–346, Oct. 2006.

[402] R. Parker and H. Song, "The enzymes and control of eukaryotic mRNA turnover.", *Nat. Struct. Mol. Biol.*, vol. 11, no. 2, pp. 121–127, Feb. 2004.

[403] C. Buccitelli and M. Selbach, "mRNAs, proteins and the emerging principles of gene expression control.", *Nat. Rev. Genet.*, vol. 21, no. 10, pp. 630–644, 2020.

[404] C. J. Wilusz, M. Wormington, and S. W. Peltz, "The cap-to-tail guide to mRNA turnover.", *Nat. Rev. Mol. Cell Biol.*, vol. 2, no. 4, pp. 237–246, Apr. 2001.

[405] O. Shalem, B. Groisman, M. Choder, O. Dahan, and Y. Pilpel, "Transcriptome kinetics is governed by a genome-wide coupling of mRNA production and degradation: A role for RNA pol II.", *PLoS Genet.*, vol. 7, no. 9, 2011.

[406] T. Kurosaki, M. W. Popp, and L. E. Maquat, "Quality and quantity control of gene expression by nonsense-mediated mRNA decay.", *Nat. Rev. Mol. Cell Biol.*, vol. 20, no. 7, pp. 406–420, Jul. 2019.

[407] J. M. Molleston and S. Cherry, "Attacked from All Sides: RNA Decay in Antiviral Defense.", *Viruses*, vol. 9, no. 1, Jan. 2017.

[408] J. M. Molleston *et al.*, "A conserved virus-induced cytoplasmic TRAMP-like complex recruits the exosome to target viral RNA for degradation.", *Genes Dev.*, vol. 30, no. 14, pp. 1658–1670, Jul. 2016.

[409] R. Nencka *et al.*, "Coronaviral RNA-methyltransferases: function, structure and inhibition.", *Nucleic Acids Res.*, vol. 50, no. 2, pp. 635–650, Jan. 2022.

[410] E. Abernathy and B. Glaunsinger, "Emerging roles for RNA degradation in viral replication and antiviral defense.", *Virology*, vol. 479–480, pp. 600–608, May 2015.

[411] W. Rodriguez, D. Macveigh-Fierro, J. Miles, and M. Muller, "Fated for decay: RNA elements targeted

by viral endonucleases.", *Semin. Cell Dev. Biol.*, vol. 111, pp. 119–125, Mar. 2021.

[412] L. Gaucherand and M. M. Gaglia, "The Role of Viral RNA Degrading Factors in Shutoff of Host Gene Expression.", *Annu. Rev. Virol.*, Jun. 2022.

[413] S. C. Schiavi, J. G. Belasco, and M. E. Greenberg, "Regulation of proto-oncogene mRNA stability.", *Biochim. Biophys. Acta*, vol. 1114, no. 2–3, pp. 95–106, Dec. 1992.

[414] D. Benjamin and C. Moroni, "mRNA stability and cancer: an emerging link?.", *Expert Opin. Biol. Ther.*, vol. 7, no. 10, pp. 1515–1529, Oct. 2007.

[415] A. Kishor, Z. Ge, and J. R. Hogg, "hnRNP L-dependent protection of normal mRNAs from NMD subverts quality control in B cell lymphoma.", *EMBO J.*, vol. 38, no. 3, Feb. 2019.

[416] F. Li *et al.*, "HnRNP-F regulates EMT in bladder cancer by mediating the stabilization of Snail1 mRNA by binding to its 3' UTR.", *EBioMedicine*, vol. 45, pp. 208–219, Jul. 2019.

[417] X. Chen *et al.*, "5-methylcytosine promotes pathogenesis of bladder cancer through stabilizing mRNAs.", *Nat. Cell Biol.*, vol. 21, no. 8, pp. 978–990, Aug. 2019.

[418] S. Soni, M. K. Saroch, B. Chander, N. V. Tirpude, and Y. S. Padwad, "MAPKAPK2 plays a crucial role in the progression of head and neck squamous cell carcinoma by regulating transcript stability.", *J. Exp. Clin. Cancer Res.*, vol. 38, no. 1, p. 175, Apr. 2019.

[419] X. Wang *et al.*, "UDP-glucose accelerates SNAI1 mRNA decay and impairs lung cancer metastasis.", *Nature*, vol. 571, no. 7763, pp. 127–131, Jul. 2019.

[420] Q. Lv, F. Dong, Y. Zhou, Z. Cai, and G. Wang, "RNA-binding protein SORBS2 suppresses clear cell renal cell carcinoma metastasis by enhancing MTUS1 mRNA stability.", *Cell Death Dis.*, vol. 11, no. 12, p. 1056, Dec. 2020.

[421] S. R. Robinson, A. W. Oliver, T. J. Chevassut, and S. F. Newbury, "The 3' to 5' Exoribonuclease DIS3: From Structure and Mechanisms to Biological Functions and Role in Human Disease.", *Biomolecules*, vol. 5, no. 3, pp. 1515–1539, Jul. 2015.

[422] G. Perron *et al.*, "Pan-cancer analysis of mRNA stability for decoding tumour post-transcriptional programs.", *Commun. Biol.*, vol. 5, no. 1, p. 851, Aug. 2022.

[423] S. Pascolo, "Synthetic Messenger RNA-Based Vaccines: from Scorn to Hype.", *Viruses*, vol. 13, no. 2, Feb. 2021.

[424] T. R. Damase, R. Sukhovershin, C. Boada, F. Taraballi, R. I. Pettigrew, and J. P. Cooke, "The Limitless Future of RNA Therapeutics.", *Front. Bioeng. Biotechnol.*, vol. 9, p. 628137, 2021.

[425] G. Hanson and J. Coller, "Translation and Protein Quality Control: Codon optimality, bias and usage in translation and mRNA decay.", *Nat. Rev. Mol. Cell Biol.*, vol. 19, no. 1, pp. 20–30, 2018.

[426] C.-Y. A. Chen and A.-B. Shyu, "Emerging Themes in Regulation of Global mRNA Turnover in cis.", *Trends Biochem. Sci.*, vol. 42, no. 1, pp. 16–27, Jan. 2017.

[427] V. K. Mayya and T. F. Duchaine, "Ciphers and Executioners: How 3'-Untranslated Regions Determine the Fate of Messenger RNAs.", *Front. Genet.*, vol. 10, p. 6, 2019.

[428] M. Courel *et al.*, "GC content shapes mRNA storage and decay in human cells.", *Elife*, vol. 8, Dec. 2019.

[429] S. L. Gillen, C. Giacomelli, K. Hodge, S. Zanivan, M. Bushell, and A. Wilczynska, "Differential regulation of mRNA fate by the human Ccr4-Not complex is driven by coding sequence composition and mRNA localization.", *Genome Biol.*, vol. 22, no. 1, p. 284, Oct. 2021.

[430] A. Anantharaman *et al.*, "ADAR2 regulates RNA stability by modifying access of decay-promoting RNA-binding proteins.", *Nucleic Acids Res.*, vol. 45, no. 7, pp. 4189–4201, Apr. 2017.

[431] S. H. Boo and Y. K. Kim, "The emerging role of RNA modifications in the regulation of mRNA stability.", *Exp. Mol. Med.*, vol. 52, no. 3, pp. 400–408, Mar. 2020.

[432] C. J. T. Lewis, T. Pan, and A. Kalsotra, "RNA modifications and structures cooperate to guide RNA-protein interactions.", *Nat. Rev. Mol. Cell Biol.*, vol. 18, no. 3, pp. 202–210, Mar. 2017.

[433] C. Mayr, "Evolution and Biological Roles of Alternative 3'UTRs.", *Trends Cell Biol.*, 2016.

[434] P. Oikonomou, H. Goodarzi, and S. Tavazoie, "Systematic identification of regulatory elements in conserved 3' UTRs of human transcripts.", *Cell Rep.*, vol. 7, no. 1, pp. 281–292, Apr. 2014.

[435] V. Presnyak *et al.*, "Codon optimality is a major determinant of mRNA stability.", *Cell*, vol. 160, no. 6, pp. 1111–1124, 2015.

[436] F. Gebauer and M. W. Hentze, "Molecular mechanisms of translational control.", *Nat. Rev. Mol. Cell Biol.*, vol. 5, no. 10, pp. 827–835, Oct. 2004.

[437] C. Mayr, "Regulation by 3'-Untranslated Regions.", *Annu. Rev. Genet.*, vol. 51, pp. 171–194, Nov. 2017.

[438] K. S. A. Khabar, "Hallmarks of cancer and AU-rich elements.", *Wiley Interdiscip. Rev. RNA*, vol. 8, no. 1, pp. 1–25, 2017.

[439] S. Jonas and E. Izaurralde, "Towards a molecular understanding of microRNA-mediated gene silencing.", *Nat. Rev. Genet.*, vol. 16, no. 7, pp. 421–433, Jul. 2015.

[440] K. Nishikura, "A-to-I editing of coding and non-coding RNAs by ADARs.", *Nat. Rev. Mol. Cell Biol.*, vol. 17, no. 2, pp. 83–96, Feb. 2016.

[441] B. L. Bass, "RNA editing by adenosine deaminases that act on RNA.", *Annu. Rev. Biochem.*, vol. 71, pp. 817–846, 2002.

[442] V. Blanc and N. O. Davidson, "APOBEC-1-mediated RNA editing.", *Wiley Interdiscip. Rev. Syst. Biol. Med.*, vol. 2, no. 5, pp. 594–602, 2010.

[443] G. M. Borchert *et al.*, "Adenosine deamination in human transcripts generates novel microRNA binding sites.", *Hum. Mol. Genet.*, vol. 18, no. 24, pp. 4801–4807, Dec. 2009.

[444] Y. Morita, T. Shibutani, N. Nakanishi, K. Nishikura, S. Iwai, and I. Kuraoka, "Human endonuclease V is a ribonuclease specific for inosine-containing RNA.", *Nat. Commun.*, vol. 4, p. 2273, 2013.

[445] K. Stellos *et al.*, "Adenosine-to-inosine RNA editing controls cathepsin S expression in atherosclerosis by enabling HuR-mediated post-transcriptional regulation.", *Nat. Med.*, vol. 22, no. 10, pp. 1140–1150, Oct. 2016.

[446] M. Sakurai *et al.*, "ADAR1 controls apoptosis of stressed cells by inhibiting Staufen1-mediated mRNA decay.", *Nat. Struct. Mol. Biol.*, vol. 24, no. 6, pp. 534–543, Jun. 2017.

[447] A. Brümmer, Y. Yang, T. W. Chan, and X. Xiao, "Structure-mediated modulation of mRNA abundance by A-to-I editing.", *Nat. Commun.*, vol. 8, no. 1, pp. 1–13, Dec. 2017.

[448] S. Nachtergaele and C. He, "Chemical Modifications in the Life of an mRNA Transcript.", *Annu. Rev. Genet.*, vol. 52, no. 1, pp. 349–372, Nov. 2018.

[449] B. S. Zhao, I. A. Roundtree, and C. He, "Post-transcriptional gene regulation by mRNA modifications.", *Nat. Rev. Mol. Cell Biol.*, vol. 18, no. 1, pp. 31–42, Jan. 2017.

[450] S. Zaccara, R. J. Ries, and S. R. Jaffrey, "Reading, writing and erasing mRNA methylation.", *Nat. Rev. Mol. Cell Biol.*, vol. 20, no. 10, pp. 608–624, Oct. 2019.

[451] N. Liu, K. I. Zhou, M. Parisien, Q. Dai, L. Diatchenko, and T. Pan, "N6-methyladenosine alters RNA structure to regulate binding of a low-complexity protein.", *Nucleic Acids Res.*, vol. 45, no. 10, pp. 6051–6063, Jun. 2017.

[452] V. Haran and N. Lenka, "Deciphering the Epitranscriptomic Signatures in Cell Fate Determination and Development.", *Stem cell Rev. reports*, vol. 15, no. 4, pp. 474–496, Aug. 2019.

[453] H. Huang, H. Weng, and J. Chen, "m(6)A Modification in Coding and Non-coding RNAs: Roles and Therapeutic Implications in Cancer.", *Cancer Cell*, vol. 37, no. 3, pp. 270–288, Mar. 2020.

[454] S. Delaunay and M. Frye, "RNA modifications regulating cell fate in cancer.", *Nat. Cell Biol.*, vol. 21, no. 5, pp. 552–559, May 2019.

[455] P. Nombela, B. Miguel-López, and S. Blanco, "The role of m(6)A, m(5)C and Ψ RNA modifications in cancer: Novel therapeutic opportunities.", *Mol. Cancer*, vol. 20, no. 1, p. 18, Jan. 2021.

[456] D. Garcias Morales and J. L. Reyes, "A birds'-eye view of the activity and specificity of the mRNA m(6) A methyltransferase complex.", *Wiley Interdiscip. Rev. RNA*, vol. 12, no. 1, p. e1618, Jan. 2021.

[457] H. Du *et al.*, "YTHDF2 destabilizes m6A-containing RNA through direct recruitment of the CCR4-NOT deadenylase complex.", *Nat. Commun.*, vol. 7, 2016.

[458] H. Huang *et al.*, "Recognition of RNA N(6)-methyladenosine by IGF2BP proteins enhances mRNA stability and translation.", *Nat. Cell Biol.*, vol. 20, no. 3, pp. 285–295, Mar. 2018.

[459] S. Zaccara, R. J. Ries, and S. R. Jaffrey, "Reading, writing and erasing mRNA methylation.", *Nat. Rev. Mol. Cell Biol.*, vol. 20, no. 10, pp. 608–624, Oct. 2019.

[460] E. Park and L. E. Maquat, "Staufen-mediated mRNA decay.", *Wiley Interdiscip. Rev. RNA*, vol. 4, no. 4, pp. 423–435, 2013.

[461] J.-D. Beaudoin and J.-P. Perreault, "Exploring mRNA 3'-UTR G-quadruplexes: evidence of roles in both alternative polyadenylation and mRNA shortening.", *Nucleic Acids Res.*, vol. 41, no. 11, pp. 5898–5911, Jun. 2013.

[462] L. Dumas, P. Herviou, E. Dassi, A. Cammas, and S. Millevoi, "G-Quadruplexes in RNA Biology: Recent Advances and Future Directions.", *Trends Biochem. Sci.*, vol. 46, no. 4, pp. 270–283, Apr. 2021.

[463] N. H. Gehring, E. Wahle, and U. Fischer, "Deciphering the mRNP Code: RNA-Bound Determinants of Post-Transcriptional Gene Regulation.", *Trends Biochem. Sci.*, vol. 42, no. 5, pp. 369–382, May 2017.

[464] M. W. Webster, J. A. W. Stowell, and L. A. Passmore, "The mechanism of Ccr4-Not recruitment to

specific mRNAs involves sequence-selective tethering by RNA-binding proteins.", *bioRxiv*, p. 478008, Jan. 2018.

[465] K. Abdelmohsen and M. Gorospe, "Posttranscriptional regulation of cancer traits by HuR.", *Wiley Interdiscip. Rev. RNA*, vol. 1, no. 2, pp. 214–229, 2010.

[466] N. Mukherjee *et al.*, "Integrative Regulatory Mapping Indicates that the RNA-Binding Protein HuR Couples Pre-mRNA Processing and mRNA Stability.", *Mol. Cell*, 2011.

[467] P. Kundu, M. R. Fabian, N. Sonenberg, S. N. Bhattacharyya, and W. Filipowicz, "HuR protein attenuates miRNA-mediated repression by promoting miRISC dissociation from the target RNA.", *Nucleic Acids Res.*, vol. 40, no. 11, pp. 5088–5100, Jun. 2012.

[468] Y. Ke *et al.*, "Poly(ADP-ribosyl)ation enhances HuR oligomerization and contributes to pro-inflammatory gene mRNA stabilization.", *Cell. Mol. Life Sci.*, vol. 78, no. 4, pp. 1817–1835, Feb. 2021.

[469] H. Otsuka, A. Fukao, Y. Funakami, K. E. Duncan, and T. Fujiwara, "Emerging Evidence of Translational Control by AU-Rich Element-Binding Proteins.", *Front. Genet.*, vol. 10, p. 332, 2019.

[470] C. W. Schultz, R. Preet, T. Dhir, D. A. Dixon, and J. R. Brody, "Understanding and targeting the disease-related RNA binding protein human antigen R (HuR).", *Wiley Interdiscip. Rev. RNA*, vol. 11, no. 3, p. e1581, May 2020.

[471] M. Pabis *et al.*, "HuR biological function involves RRM3-mediated dimerization and RNA binding by all three RRMs.", *Nucleic Acids Res.*, vol. 47, no. 2, pp. 1011–1029, Jan. 2019.

[472] N. Chang *et al.*, "HuR uses AUF1 as a cofactor to promote p16INK4 mRNA decay.", *Mol. Cell. Biol.*, vol. 30, no. 15, pp. 3875–3886, Aug. 2010.

[473] A. Cammas *et al.*, "Destabilization of nucleophosmin mRNA by the HuR/KSRP complex is required for muscle fibre formation.", *Nat. Commun.*, vol. 5, p. 4190, Jun. 2014.

[474] S. K. Kota, Z. W. Lim, and S. B. Kota, "Elavl1 Impacts Osteogenic Differentiation and mRNA Levels of Genes Involved in ECM Organization.", *Front. cell Dev. Biol.*, vol. 9, p. 606971, 2021.

[475] E. Hitti *et al.*, "Systematic analysis of AU-Rich element expression in cancer reveals common functional clusters regulated by key RNA-Binding proteins.", *Cancer Res.*, vol. 76, no. 14, pp. 4068–4080, 2016.

[476] Y. Liu *et al.*, "Silencing of HuR Inhibits Osteosarcoma Cell Epithelial-Mesenchymal Transition via AGO2 in Association With Long Non-Coding RNA XIST.", *Front. Oncol.*, vol. 11, p. 601982, 2021.

[477] M. Heinonen *et al.*, "Cytoplasmic HuR expression is a prognostic factor in invasive ductal breast carcinoma.", *Cancer Res.*, vol. 65, no. 6, pp. 2157–2161, Mar. 2005.

[478] N. Filippova *et al.*, "Hu antigen R (HuR) multimerization contributes to glioma disease progression.", *J. Biol. Chem.*, vol. 292, no. 41, pp. 16999–17010, Oct. 2017.

[479] V. G. D'Agostino *et al.*, "Dihydrotanshinone-I interferes with the RNA-binding activity of HuR affecting its post-transcriptional function.", *Sci. Rep.*, vol. 5, no. October, pp. 1–15, 2015.

[480] P. Lal *et al.*, "Regulation of HuR structure and function by dihydrotanshinone-I.", *Nucleic Acids Res.*, vol. 45, no. 16, pp. 9514–9527, Sep. 2017.

[481]   L. Allegri *et al.*, "The HuR CMLD-2 inhibitor exhibits antitumor effects via MAD2 downregulation in thyroid cancer cells.", *Sci. Rep.*, vol. 9, no. 1, p. 7374, May 2019.

[482]   M. Pabis *et al.*, "HuR biological function involves RRM3-mediated dimerization and RNA binding by all three RRMs.", *Nucleic Acids Res.*, 2019.

[483]   N. Filippova *et al.*, "Targeting the HuR oncogenic role with a new class of cytoplasmic dimerization inhibitors.", *Cancer Res.*, vol. 81, no. 8, pp. 2220–2233, 2021.

[484]   R.-W. Yao, Y. Wang, and L.-L. Chen, "Cellular functions of long noncoding RNAs.", *Nat. Cell Biol.*, vol. 21, no. 5, pp. 542–551, May 2019.

[485]   C. Gong and L. E. Maquat, "lncRNAs transactivate STAU1-mediated mRNA decay by duplexing with 3' UTRs via Alu elements.", *Nature*, vol. 470, no. 7333, pp. 284–288, Feb. 2011.

[486]   S. L. Wolin and L. E. Maquat, "Cellular RNA surveillance in health and disease.", *Science*, vol. 366, no. 6467, pp. 822–827, Nov. 2019.

[487]   H. Cho *et al.*, "Glucocorticoid receptor interacts with PNRC2 in a ligand-dependent manner to recruit UPF1 for rapid mRNA degradation.", *Proc. Natl. Acad. Sci. U. S. A.*, vol. 112, no. 13, pp. E1540-9, Mar. 2015.

[488]   O. H. Park, J. Park, M. Yu, H.-T. An, J. Ko, and Y. K. Kim, "Identification and molecular characterization of cellular factors required for glucocorticoid receptor-mediated mRNA decay.", *Genes Dev.*, vol. 30, no. 18, pp. 2093–2105, Sep. 2016.

[489]   X. Rambout, F. Dequiedt, and L. E. Maquat, "Beyond Transcription: Roles of Transcription Factors in Pre-mRNA Splicing.", *Chem. Rev.*, vol. 118, no. 8, pp. 4339–4364, Apr. 2018.

[490]   S. Komili and P. A. Silver, "Coupling and coordination in gene expression processes: a systems biology view.", *Nat. Rev. Genet.*, vol. 9, no. 1, pp. 38–48, Jan. 2008.

[491]   I. E. Schor, L. I. Gómez Acuña, and A. R. Kornblihtt, "Coupling between transcription and alternative splicing.", *Cancer Treat. Res.*, vol. 158, pp. 1–24, 2013.

[492]   S. Naftelberg, I. E. Schor, G. Ast, and A. R. Kornblihtt, "Regulation of alternative splicing through coupling with transcription and chromatin structure.", *Annu. Rev. Biochem.*, vol. 84, pp. 165–198, 2015.

[493]   S. Zheng, "Alternative splicing and nonsense-mediated mRNA decay enforce neural specific gene expression.", *Int. J. Dev. Neurosci. Off. J. Int. Soc. Dev. Neurosci.*, vol. 55, pp. 102–108, Dec. 2016.

[494]   A. C. Tuck *et al.*, "Mammalian RNA Decay Pathways Are Highly Specialized and Widely Linked to Translation.", *Mol. Cell*, vol. 77, no. 6, pp. 1222-1236.e13, Mar. 2020.

[495]   A. A. Bicknell and E. P. Ricci, "When mRNA translation meets decay.", *Biochem. Soc. Trans.*, vol. 45, no. 2, pp. 339–351, Apr. 2017.

[496]   V. Goler-Baron, M. Selitrennik, O. Barkai, G. Haimovich, R. Lotan, and M. Choder, "Transcription in the nucleus and mRNA decay in the cytoplasm are coupled processes.", *Genes Dev.*, vol. 22, no. 15, pp. 2022–2027, Aug. 2008.

[497]   M. Dori-Bachash, O. Shalem, Y. S. Manor, Y. Pilpel, and I. Tirosh, "Widespread promoter-mediated coordination of transcription and mRNA degradation.", *Genome Biol.*, vol. 13, no. 12, p. R114, Dec.

2012.

[498] H. T. M. Timmers and L. Tora, "Transcript Buffering: A Balancing Act between mRNA Synthesis and mRNA Degradation.", *Mol. Cell*, vol. 72, no. 1, pp. 10–17, Oct. 2018.

[499] M. Rabani *et al.*, "Metabolic labeling of RNA uncovers principles of RNA production and degradation dynamics in mammalian cells.", *Nat. Biotechnol.*, 2011.

[500] K. A. Braun and E. T. Young, "Coupling mRNA synthesis and decay.", *Mol. Cell. Biol.*, vol. 34, no. 22, pp. 4078–4087, Nov. 2014.

[501] M. Dori-Bachash, E. Shema, and I. Tirosh, "Coupled evolution of transcription and mRNA degradation.", *PLoS Biol.*, vol. 9, no. 7, p. e1001106, Jul. 2011.

[502] W. F. Marzluff, E. J. Wagner, and R. J. Duronio, "Metabolism and regulation of canonical histone mRNAs: life without a poly(A) tail.", *Nat. Rev. Genet.*, vol. 9, no. 11, pp. 843–854, Nov. 2008.

[503] M. J. Amorim, C. Cotobal, C. Duncan, and J. Mata, "Global coordination of transcriptional control and mRNA decay during cellular differentiation.", *Mol. Syst. Biol.*, vol. 6, p. 380, Jun. 2010.

[504] O. Shalem *et al.*, "Transient transcriptional responses to stress are generated by opposing effects of mRNA production and degradation.", *Mol. Syst. Biol.*, vol. 4, p. 223, 2008.

[505] V. N. Kim and G. Dreyfuss, "Nuclear mRNA binding proteins couple pre-mRNA splicing and post-splicing events.", *Mol. Cells*, vol. 12, no. 1, pp. 1–10, Aug. 2001.

[506] C. Xu, J.-K. Park, and J. Zhang, "Evidence that alternative transcriptional initiation is largely nonadaptive.", *PLoS Biol.*, vol. 17, no. 3, p. e3000197, Mar. 2019.

[507] P. Carninci *et al.*, "Genome-wide analysis of mammalian promoter architecture and evolution.", *Nat. Genet.*, vol. 38, no. 6, pp. 626–635, Jun. 2006.

[508] C. S. Lutz and A. Moreira, "Alternative mRNA polyadenylation in eukaryotes: an effective regulator of gene expression.", *Wiley Interdiscip. Rev. RNA*, vol. 2, no. 1, pp. 23–31, 2011.

[509] A. J. Gruber and M. Zavolan, "Alternative cleavage and polyadenylation in health and disease.", *Nat. Rev. Genet.*, vol. 20, no. 10, pp. 599–614, Oct. 2019.

[510] G. Haimovich, M. Choder, R. H. Singer, and T. Trcek, "The fate of the messenger is pre-determined: a new model for regulation of gene expression.", *Biochim. Biophys. Acta*, vol. 1829, no. 6–7, pp. 643–653, 2013.

[511] J. D. Keene, "RNA regulons: coordination of post-transcriptional events.", *Nat. Rev. Genet.*, vol. 8, no. 7, pp. 533–543, Jul. 2007.

[512] G. Haimovich *et al.*, "Gene expression is circular: factors for mRNA degradation also foster mRNA synthesis.", *Cell*, vol. 153, no. 5, pp. 1000–1011, May 2013.

[513] M. A. Collart and J. C. Reese, "Gene expression as a circular process: cross-talk between transcription and mRNA degradation in eukaryotes; International University of Andalusia (UNIA) Baeza, Spain.", *RNA biology*, vol. 11, no. 4. pp. 320–323, 2014.

[514] R. Lotan, V. G. Bar-On, L. Harel-Sharvit, L. Duek, D. Melamed, and M. Choder, "The RNA polymerase II subunit Rpb4p mediates decay of a specific class of mRNAs.", *Genes Dev.*, vol. 19, no. 24, pp. 3004–3016, Dec. 2005.

[515] R. Lotan, V. Goler-Baron, L. Duek, G. Haimovich, and M. Choder, "The Rpb7p subunit of yeast RNA polymerase II plays roles in the two major cytoplasmic mRNA decay mechanisms.", *J. Cell Biol.*, vol. 178, no. 7, pp. 1133–1143, Sep. 2007.

[516] L. Harel-Sharvit, N. Eldad, G. Haimovich, O. Barkai, L. Duek, and M. Choder, "RNA polymerase II subunits link transcription and mRNA decay to translation.", *Cell*, vol. 143, no. 4, pp. 552–563, Nov. 2010.

[517] D. Schulz, N. Pirkl, E. Lehmann, and P. Cramer, "Rpb4 subunit functions mainly in mRNA synthesis by RNA polymerase II.", *J. Biol. Chem.*, vol. 289, no. 25, pp. 17446–17452, Jun. 2014.

[518] L. Duek, O. Barkai, R. Elran, I. Adawi, and M. Choder, "Dissociation of Rpb4 from RNA polymerase II is important for yeast functionality.", *PLoS One*, vol. 13, no. 10, p. e0206161, 2018.

[519] A. Bregman, M. Avraham-Kelbert, O. Barkai, L. Duek, A. Guterman, and M. Choder, "Promoter elements regulate cytoplasmic mRNA decay.", *Cell*, vol. 147, no. 7, pp. 1473–1483, Dec. 2011.

[520] T. Trcek, D. R. Larson, A. Moldón, C. C. Query, and R. H. Singer, "Single-molecule mRNA decay measurements reveal promoter- regulated mRNA stability in yeast.", *Cell*, vol. 147, no. 7, pp. 1484–1497, Dec. 2011.

[521] M. Catala and S. Abou Elela, "Promoter-dependent nuclear RNA degradation ensures cell cycle-specific gene expression.", *Commun. Biol.*, vol. 2, p. 211, 2019.

[522] A. I. Garrido-Godino *et al.*, "Rpb4 and Puf3 imprint and post-transcriptionally control the stability of a common set of mRNAs in yeast.", *RNA Biol.*, vol. 18, no. 8, pp. 1206–1220, Aug. 2021.

[523] I. Tirosh, "Transcriptional priming of cytoplasmic post-transcriptional regulation.", *Transcription*, vol. 2, no. 6, pp. 258–262, 2011.

[524] R. Visintin and A. Amon, "Regulation of the mitotic exit protein kinases Cdc15 and Dbf2.", *Mol. Biol. Cell*, vol. 12, no. 10, pp. 2961–2974, Oct. 2001.

[525] J. Enssle, W. Kugler, M. W. Hentze, and A. E. Kulozik, "Determination of mRNA fate by different RNA polymerase II promoters.", *Proc. Natl. Acad. Sci. U. S. A.*, vol. 90, no. 21, pp. 10091–10095, Nov. 1993.

[526] K. Helenius, Y. Yang, T. V. Tselykh, H. K. J. Pessa, M. J. Frilander, and T. P. Mäkelä, "Requirement of TFIIH kinase subunit Mat1 for RNA Pol II C-terminal domain Ser5 phosphorylation, transcription and mRNA turnover.", *Nucleic Acids Res.*, 2011.

[527] R. Elkon, E. Zlotorynski, K. I. Zeller, and R. Agami, "Major role for mRNA stability in shaping the kinetics of gene induction.", *BMC Genomics*, vol. 11, p. 259, Apr. 2010.

[528] U. Braunschweig, S. Gueroussov, A. M. Plocik, B. R. Graveley, and B. J. Blencowe, "Dynamic integration of splicing within gene regulatory pathways.", *Cell*, vol. 152, no. 6, pp. 1252–1269, Mar. 2013.

[529] H. Han *et al.*, "Multilayered Control of Alternative Splicing Regulatory Networks by Transcription Factors.", *Mol. Cell*, 2017.

[530] J. Song *et al.*, "Regulation of alternative polyadenylation by the C2H2-zinc-finger protein Sp1.", *Mol. Cell*, vol. 82, no. 17, pp. 3135-3150.e9, Sep. 2022.

[531] L. Zhu *et al.*, "Transcription Factor GATA4 Regulates Cell Type-Specific Splicing Through Direct Interaction With RNA in Human Induced Pluripotent Stem Cell-Derived Cardiac Progenitors.", *Circulation*, vol. 146, no. 10, pp. 770–787, Sep. 2022.

[532] M. Del Giudice *et al.*, "FOXA1 regulates alternative splicing in prostate cancer.", *Cell Rep.*, vol. 40, no. 13, p. 111404, Sep. 2022.

[533] J. C. Dantonel, K. G. Murthy, J. L. Manley, and L. Tora, "Transcription factor TFIID recruits factor CPSF for formation of 3' end of mRNA.", *Nature*, vol. 389, no. 6649, pp. 399–402, Sep. 1997.

[534] P. Boumpas, S. Merabet, and J. Carnesecchi, "Integrating transcription and splicing into cell fate: Transcription factors on the block.", *Wiley Interdiscip. Rev. RNA*, p. e1752, Jul. 2022.

[535] H. Göös *et al.*, "Human transcription factor protein interaction networks.", *Nat. Commun.*, vol. 13, no. 1, p. 766, Feb. 2022.

[536] H. Han *et al.*, "Multilayered Control of Alternative Splicing Regulatory Networks by Transcription Factors.", *Mol. Cell*, vol. 65, no. 3, pp. 539-553.e7, Feb. 2017.

[537] C.-Y. Yang *et al.*, "Interaction of CCR4-NOT with EBF1 regulates gene-specific transcription and mRNA stability in B lymphopoiesis.", *Genes Dev.*, vol. 30, no. 20, pp. 2310–2324, Oct. 2016.

[538] A. Bertero *et al.*, "The SMAD2/3 interactome reveals that TGFβ controls m(6)A mRNA methylation in pluripotency.", *Nature*, vol. 555, no. 7695, pp. 256–259, Mar. 2018.

[539] B.-S. Moon, J. Bai, M. Cai, C. Liu, J. Shi, and W. Lu, "Kruppel-like factor 4-dependent Staufen1-mediated mRNA decay regulates cortical neurogenesis.", *Nat. Commun.*, vol. 9, no. 1, p. 401, Jan. 2018.

[540] A. C. Panda *et al.*, "Novel RNA-binding activity of MYF5 enhances Ccnd1/Cyclin D1 mRNA translation during myogenesis.", *Nucleic Acids Res.*, vol. 44, no. 5, pp. 2393–2408, Mar. 2016.

[541] S. J. Miller, T. Suthiphongchai, G. P. Zambetti, and M. E. Ewen, "p53 binds selectively to the 5' untranslated region of cdk4, an RNA element necessary and sufficient for transforming growth factor beta- and p53-mediated translational inhibition of cdk4.", *Mol. Cell. Biol.*, vol. 20, no. 22, pp. 8420–8431, Nov. 2000.

[542] P. Cartwright and K. Helin, "Nucleocytoplasmic shuttling of transcription factors.", *Cell. Mol. Life Sci.*, vol. 57, no. 8–9, pp. 1193–1206, Aug. 2000.

[543] R. Bharathavikru *et al.*, "Transcription factor Wilms' tumor 1 regulates developmental RNAs through 3' UTR interaction.", *Genes Dev.*, vol. 31, no. 4, pp. 347–352, Feb. 2017.

[544] S. Brodsky *et al.*, "Intrinsically Disordered Regions Direct Transcription Factor In Vivo Binding Specificity.", *Mol. Cell*, vol. 79, no. 3, pp. 459-471.e4, Aug. 2020.

[545] J. J. Ferrie, J. P. Karr, R. Tjian, and X. Darzacq, "'Structure'-function relationships in eukaryotic transcription factors: The role of intrinsically disordered regions in gene regulation.", *Mol. Cell*, Oct. 2022.

[546] O. Oksuz *et al.*, "Transcription factors interact with RNA to regulate genes.", *bioRxiv*, p. 2022.09.27.509776, Jan. 2022.

[547] J. E. Bradner, D. Hnisz, and R. A. Young, "Transcriptional Addiction in Cancer.", *Cell*, vol. 168, no. 4,

pp. 629–643, Feb. 2017.

[548] M. J. Henley and A. N. Koehler, "Advances in targeting 'undruggable' transcription factors with small molecules.", *Nat. Rev. Drug Discov.*, vol. 20, no. 9, pp. 669–688, 2021.

[549] F. Aguilo *et al.*, "Coordination of m6A mRNA Methylation and Gene Transcription by ZFP217 Regulates Pluripotency and Reprogramming.", *Cell Stem Cell*, vol. 17, no. 6, pp. 689–704, 2015.

[550] T. Song *et al.*, "Zfp217 mediates m6A mRNA methylation to orchestrate transcriptional and post-transcriptional regulation to promote adipogenic differentiation.", *Nucleic Acids Res.*, vol. 47, no. 12, pp. 6130–6144, 2019.

[551] H. Zhu *et al.*, "Glucocorticoid counteracts cellular mechanoresponses by LINC01569-dependent glucocorticoid receptor-mediated mRNA decay.", *Sci. Adv.*, vol. 7, no. 9, Feb. 2021.

[552] Y. Yang *et al.*, "RNA 5-Methylcytosine Facilitates the Maternal-to-Zygotic Transition by Preventing Maternal mRNA Decay.", *Mol. Cell*, vol. 75, no. 6, pp. 1188-1202.e11, Sep. 2019.

[553] V. Evdokimova *et al.*, "The major mRNA-associated protein YB-1 is a potent 5' cap-dependent mRNA stabilizer.", *EMBO J.*, vol. 20, no. 19, pp. 5491–5502, Oct. 2001.

[554] K. K. Nyati, M. M.-U. Zaman, P. Sharma, and T. Kishimoto, "Arid5a, an RNA-Binding Protein in Immune Regulation: RNA Stability, Inflammation, and Autoimmunity.", *Trends Immunol.*, vol. 41, no. 3, pp. 255–268, Mar. 2020.

[555] K. Masuda *et al.*, "Arid5a controls IL-6 mRNA stability, which contributes to elevation of IL-6 level in vivo.", *Proc. Natl. Acad. Sci. U. S. A.*, vol. 110, no. 23, pp. 9409–9414, Jun. 2013.

[556] K. Masuda *et al.*, "Arid5a regulates naive CD4+ T cell fate through selective stabilization of Stat3 mRNA.", *J. Exp. Med.*, vol. 213, no. 4, pp. 605–619, Apr. 2016.

[557] S. Derech-Haim, Y. Friedman, A. Hizi, and M. Bakhanashvili, "p53 regulates its own expression by an intrinsic exoribonuclease activity through AU-rich elements.", *J. Mol. Med.*, 2020.

[558] D. Olagnier *et al.*, "Nrf2 negatively regulates STING indicating a link between antiviral sensing and metabolic reprogramming.", *Nat. Commun.*, vol. 9, no. 1, 2018.

[559] T. A. Hughes and H. J. M. Brady, "E2F1 up-regulates the expression of the tumour suppressor axin2 both by activation of transcription and by mRNA stabilisation.", *Biochem. Biophys. Res. Commun.*, vol. 329, no. 4, pp. 1267–1274, Apr. 2005.

[560] L. Fish *et al.*, "Nuclear TARBP2 Drives Oncogenic Dysregulation of RNA Splicing and Decay.", *Mol. Cell*, vol. 75, no. 5, pp. 967-981.e9, Sep. 2019.

[561] J. C. Long and J. F. Caceres, "The SR protein family of splicing factors: master regulators of gene expression.", *Biochem. J.*, vol. 417, no. 1, pp. 15–27, Jan. 2009.

[562] Z. Li, Y. Zhang, D. Li, and Y. Feng, "Destabilization and mislocalization of myelin basic protein mRNAs in quaking dysmyelination lacking the QKI RNA-binding proteins.", *J. Neurosci. Off. J. Soc. Neurosci.*, vol. 20, no. 13, pp. 4944–4953, Jul. 2000.

[563] R.-L. Zhang *et al.*, "RNA-binding protein QKI-5 inhibits the proliferation of clear cell renal cell carcinoma via post-transcriptional stabilization of RASA1 mRNA.", *Cell Cycle*, vol. 15, no. 22, pp. 3094–3104, Nov. 2016.

[564] D. Larocque, A. Galarneau, H.-N. Liu, M. Scott, G. Almazan, and S. Richard, "Protection of p27(Kip1) mRNA by quaking RNA binding proteins promotes oligodendrocyte differentiation.", *Nat. Neurosci.*, vol. 8, no. 1, pp. 27–33, Jan. 2005.

[565] X.-Y. Zhong, P. Wang, J. Han, M. G. Rosenfeld, and X.-D. Fu, "SR proteins in vertical integration of gene expression from transcription to RNA processing to translation.", *Mol. Cell*, vol. 35, no. 1, pp. 1–10, Jul. 2009.

[566] R. Xiao *et al.*, "Pervasive Chromatin-RNA Binding Protein Interactions Enable RNA-Based Regulation of Transcription.", *Cell*, vol. 178, no. 1, pp. 107-121.e18, Jun. 2019.

[567] E. L. Van Nostrand *et al.*, "A large-scale binding and functional map of human RNA-binding proteins.", *Nature*, vol. 583, no. 7818, pp. 711–719, Jul. 2020.

[568] N. Mukherjee *et al.*, "Integrative regulatory mapping indicates that the RNA-binding protein HuR couples pre-mRNA processing and mRNA stability.", *Mol. Cell*, vol. 43, no. 3, pp. 327–339, Aug. 2011.

[569] D. A. Medina, A. Jordán-Pla, G. Millán-Zambrano, S. Chávez, M. Choder, and J. E. Pérez-Ortín, "Cytoplasmic 5'-3' exonuclease Xrn1p is also a genome-wide transcription factor in yeast.", *Front. Genet.*, vol. 5, p. 1, 2014.

[570] J. A. Kruk, A. Dutta, J. Fu, D. S. Gilmour, and J. C. Reese, "The multifunctional Ccr4-Not complex directly promotes transcription elongation.", *Genes Dev.*, vol. 25, no. 6, pp. 581–593, Mar. 2011.

[571] M. Sun *et al.*, "Global analysis of eukaryotic mRNA degradation reveals Xrn1-dependent buffering of transcript levels.", *Mol. Cell*, vol. 52, no. 1, pp. 52–62, Oct. 2013.

[572] V. Begley *et al.*, "The mRNA degradation factor Xrn1 regulates transcription elongation in parallel to Ccr4.", *Nucleic Acids Res.*, vol. 47, no. 18, pp. 9524–9541, Oct. 2019.

[573] M. A. Collart and K. Struhl, "NOT1(CDC39), NOT2(CDC36), NOT3, and NOT4 encode a global-negative regulator of transcription that differentially affects TATA-element utilization.", *Genes Dev.*, vol. 8, no. 5, pp. 525–537, Mar. 1994.

[574] U. Oberholzer and M. A. Collart, "In vitro transcription of a TATA-less promoter: negative regulation by the Not1 protein.", *Biol. Chem.*, vol. 380, no. 12, pp. 1365–1370, Dec. 1999.

[575] J. Fischer, Y. S. Song, N. Yosef, J. di Iulio, L. S. Churchman, and M. Choder, "The yeast exoribonuclease Xrn1 and associated factors modulate RNA polymerase II processivity in 5' and 3' gene regions.", *J. Biol. Chem.*, vol. 295, no. 33, pp. 11435–11454, Aug. 2020.

[576] N.-C. Lau *et al.*, "Human Ccr4-Not complexes contain variable deadenylase subunits.", *Biochem. J.*, vol. 422, no. 3, pp. 443–453, Aug. 2009.

[577] C. Iasillo *et al.*, "ARS2 is a general suppressor of pervasive transcription.", *Nucleic Acids Res.*, vol. 45, no. 17, pp. 10229–10241, Sep. 2017.

[578] M. Furlan, S. de Pretis, and M. Pelizzola, "Dynamics of transcriptional and post-transcriptional regulation.", *Brief. Bioinform.*, vol. 22, no. 4, Jul. 2021.

[579] M. Furlan, S. De Pretis, and M. Pelizzola, "Dynamics of transcriptional and post-transcriptional regulation.", *Brief. Bioinform.*, vol. 22, no. 4, pp. 1–13, 2021.

[580] T. J. Eisen *et al.*, "The Dynamics of Cytoplasmic mRNA Metabolism.", *Mol. Cell*, vol. 77, no. 4, pp. 786-799.e10, 2020.

[581] H. Tani *et al.*, "Genome-wide determination of RNA stability reveals hundreds of short-lived noncoding transcripts in mammals.", *Genome Res.*, vol. 22, no. 5, pp. 947–956, May 2012.

[582] H. Chen, K. Shiroguchi, H. Ge, and X. S. Xie, "Genome-wide study of mRNA degradation and transcript elongation in Escherichia coli.", *Mol. Syst. Biol.*, vol. 11, no. 1, p. 781, Jan. 2015.

[583] T. Kurosaki *et al.*, "Loss of the fragile X syndrome protein FMRP results in misregulation of nonsense-mediated mRNA decay.", *Nat. Cell Biol.*, vol. 23, no. 1, pp. 40–48, 2021.

[584] C. Y. A. Chen, N. Ezzeddine, and A. Bin Shyu, "Messenger RNA Half-Life Measurements in Mammalian Cells.", *Methods Enzymol.*, vol. 448, no. 08, pp. 335–357, 2008.

[585] A. Lugowski, B. Nicholson, and O. S. Rissland, "Determining mRNA half-lives on a transcriptome-wide scale.", *Methods*, vol. 137, pp. 90–98, Mar. 2018.

[586] W. S. Lai, R. M. Arvola, A. C. Goldstrohm, and P. J. Blackshear, "Inhibiting transcription in cultured metazoan cells with actinomycin D to monitor mRNA turnover.", *Methods*, vol. 155, pp. 77–87, Feb. 2019.

[587] C. Y. Chen and A. B. Shyu, "AU-rich elements: characterization and importance in mRNA degradation.", *Trends Biochem. Sci.*, vol. 20, no. 11, pp. 465–470, Nov. 1995.

[588] S. Harrold, C. Genovese, B. Kobrin, S. L. Morrison, and C. Milcarek, "A comparison of apparent mRNA half-life using kinetic labeling techniques vs decay following administration of transcriptional inhibitors.", *Anal. Biochem.*, vol. 198, no. 1, pp. 19–29, Oct. 1991.

[589] C. Seiser, M. Posch, N. Thompson, and L. C. Kühn, "Effect of transcription inhibitors on the iron-dependent degradation of transferrin receptor mRNA.", *J. Biol. Chem.*, vol. 270, no. 49, pp. 29400–29406, Dec. 1995.

[590] A. B. Shyu, M. E. Greenberg, and J. G. Belasco, "The c-fos transcript is targeted for rapid decay by two distinct mRNA degradation pathways.", *Genes Dev.*, vol. 3, no. 1, pp. 60–72, Jan. 1989.

[591] C. Speth and I. Oberbäumer, "Expression of basement membrane proteins: evidence for complex post-transcriptional control mechanisms.", *Exp. Cell Res.*, vol. 204, no. 2, pp. 302–310, Feb. 1993.

[592] A. T. Das, L. Tenenbaum, and B. Berkhout, "Tet-On Systems For Doxycycline-inducible Gene Expression.", *Curr. Gene Ther.*, vol. 16, no. 3, pp. 156–167, 2016.

[593] X. Adiconis *et al.*, "Comparative analysis of RNA sequencing methods for degraded or low-input samples.", *Nat. Methods*, vol. 10, no. 7, pp. 623–629, Jul. 2013.

[594] M. Furlan *et al.*, "Genome-wide dynamics of RNA synthesis, processing, and degradation without RNA metabolic labeling.", *Genome Res.*, vol. 30, no. 10, pp. 1492–1507, Oct. 2020.

[595] D. Gaidatzis, L. Burger, M. Florescu, and M. B. Stadler, "Analysis of intronic and exonic reads in RNA-seq data characterizes transcriptional and post-transcriptional regulation.", *Nat. Biotechnol.*, vol. 33, no. 7, pp. 722–729, Jul. 2015.

[596] R. Alkallas, L. Fish, H. Goodarzi, and H. S. Najafabadi, "Inference of RNA decay rate from transcriptional profiling highlights the regulatory programs of Alzheimer's disease.", *Nat.*

Commun., vol. 8, no. 1, p. 909, Oct. 2017.

[597] J. M. Gray *et al.*, "SnapShot-Seq: a method for extracting genome-wide, in vivo mRNA dynamics from a single total RNA sample.", *PLoS One*, vol. 9, no. 2, p. e89673, 2014.

[598] C. Wang *et al.*, "Computational inference of mRNA stability from histone modification and transcriptome profiles.", *Nucleic Acids Res.*, vol. 40, no. 14, pp. 6414–6423, Aug. 2012.

[599] A. Zeisel *et al.*, "Coupled pre-mRNA and mRNA dynamics unveil operational strategies underlying transcriptional responses to stimuli.", *Mol. Syst. Biol.*, vol. 7, p. 529, Sep. 2011.

[600] S. de Pretis, M. Furlan, and M. Pelizzola, "INSPEcT-GUI Reveals the Impact of the Kinetic Rates of RNA Synthesis, Processing, and Degradation, on Premature and Mature RNA Species.", *Front. Genet.*, vol. 11, p. 759, 2020.

[601] A. Tesi *et al.*, "An early Myc-dependent transcriptional program orchestrates cell growth during B-cell activation.", *EMBO Rep.*, vol. 20, no. 9, p. e47987, Sep. 2019.

[602] E. M. Wissink, A. Vihervaara, N. D. Tippens, and J. T. Lis, "Nascent RNA analyses: tracking transcription and its regulation.", *Nat. Rev. Genet.*, vol. 20, no. 12, pp. 705–723, Dec. 2019.

[603] R. Lopes, R. Agami, and G. Korkmaz, "GRO-seq, A Tool for Identification of Transcripts Regulating Gene Expression.", *Methods Mol. Biol.*, vol. 1543, pp. 45–55, 2017.

[604] A. Blumberg *et al.*, "Characterizing RNA stability genome-wide through combined analysis of PRO-seq and RNA-seq data.", *BMC Biol.*, vol. 19, no. 1, p. 30, Feb. 2021.

[605] B. Schwalb *et al.*, "Measurement of genome-wide RNA synthesis and decay rates with Dynamic Transcriptome Analysis (DTA).", *Bioinformatics*, vol. 28, no. 6, pp. 884–885, Mar. 2012.

[606] M. Sun *et al.*, "Comparative dynamic transcriptome analysis (cDTA) reveals mutual feedback between mRNA synthesis and degradation.", *Genome Res.*, vol. 22, no. 7, pp. 1350–1359, Jul. 2012.

[607] A. Uvarovskii and C. Dieterich, "pulseR: Versatile computational analysis of RNA turnover from metabolic labeling experiments.", *Bioinformatics*, vol. 33, no. 20, pp. 3305–3307, Oct. 2017.

[608] M. Rabani *et al.*, "High-resolution sequencing and modeling identifies distinct dynamic RNA regulatory strategies.", *Cell*, vol. 159, no. 7, pp. 1698–1710, Dec. 2014.

[609] S. de Pretis *et al.*, "INSPEcT: a computational tool to infer mRNA synthesis, processing and degradation dynamics from RNA- and 4sU-seq time course experiments.", *Bioinformatics*, vol. 31, no. 17, pp. 2829–2835, Sep. 2015.

[610] K. Kawata *et al.*, "Metabolic labeling of RNA using multiple ribonucleoside analogs enables the simultaneous evaluation of RNA synthesis and degradation rates.", *Genome Res.*, vol. 30, no. 10, pp. 1481–1491, 2020.

[611] T. Neumann *et al.*, "Quantification of experimentally induced nucleotide conversions in high-throughput sequencing datasets.", *BMC Bioinformatics*, vol. 20, no. 1, p. 258, May 2019.

[612] C. Jürges, L. Dölken, and F. Erhard, "Dissecting newly transcribed and old RNA using GRAND-SLAM.", *Bioinformatics*, vol. 34, no. 13, pp. i218–i226, Jul. 2018.

[613] G. La Manno *et al.*, "RNA velocity of single cells.", *Nature*, vol. 560, no. 7719, pp. 494–498, Aug. 2018.

[614] V. Bergen, M. Lange, S. Peidli, F. A. Wolf, and F. J. Theis, "Generalizing RNA velocity to transient cell states through dynamical modeling.", *Nat. Biotechnol.*, vol. 38, no. 12, pp. 1408–1414, Dec. 2020.

[615] G.-J. Hendriks *et al.*, "NASC-seq monitors RNA synthesis in single cells.", *Nat. Commun.*, vol. 10, no. 1, p. 3138, Jul. 2019.

[616] J. Cao, W. Zhou, F. Steemers, C. Trapnell, and J. Shendure, "Sci-fate characterizes the dynamics of gene expression in single cells.", *Nat. Biotechnol.*, vol. 38, no. 8, pp. 980–988, Aug. 2020.

[617] F. Erhard *et al.*, "scSLAM-seq reveals core features of transcription dynamics in single cells.", *Nature*, vol. 571, no. 7765, pp. 419–423, Jul. 2019.

[618] N. Battich *et al.*, "Sequencing metabolically labeled transcripts in single cells reveals mRNA turnover strategies.", *Science*, vol. 367, no. 6482, pp. 1151–1156, Mar. 2020.

[619] K. C. Maier, S. Gressel, P. Cramer, and B. Schwalb, "Native molecule sequencing by nano-ID reveals synthesis and stability of RNA isoforms.", *Genome Res.*, vol. 30, no. 9, pp. 1332–1344, Sep. 2020.

[620] A. Riba *et al.*, "Cell cycle gene regulation dynamics revealed by RNA velocity and deep-learning.", *Nat. Commun.*, vol. 13, no. 1, p. 2865, May 2022.

[621] I. Horvathova *et al.*, "The Dynamics of mRNA Turnover Revealed by Single-Molecule Imaging in Single Cells.", *Mol. Cell*, vol. 68, no. 3, pp. 615-625.e9, Nov. 2017.

[622] M. W. Webster, J. A. W. Stowell, T. T. L. Tang, and L. A. Passmore, "Analysis of mRNA deadenylation by multi-protein complexes.", *Methods*, vol. 126, pp. 95–104, Aug. 2017.

[623] J. Lim, M. Lee, A. Son, H. Chang, and V. N. Kim, "mTAIL-seq reveals dynamic poly(A) tail regulation in oocyte-to-embryo development.", *Genes Dev.*, vol. 30, no. 14, pp. 1671–1682, Jul. 2016.

[624] R. E. Workman *et al.*, "Nanopore native RNA sequencing of a human poly(A) transcriptome.", *Nat. Methods*, vol. 16, no. 12, pp. 1297–1305, Dec. 2019.

[625] P. P. Lin, Y. Wang, and G. Lozano, "Mesenchymal Stem Cells and the Origin of Ewing's Sarcoma.", *Sarcoma*, vol. 2011, 2011.

[626] J. Houseley and D. Tollervey, "The Many Pathways of RNA Degradation.", *Cell*, vol. 136, no. 4, pp. 763–776, Feb. 2009.

[627] C. Barreau, T. Watrin, H. Beverley Osborne, and L. Paillard, "Protein expression is increased by a class III AU-rich element and tethered CUG-BP1.", *Biochem. Biophys. Res. Commun.*, vol. 347, no. 3, pp. 723–730, Sep. 2006.

[628] Y.-B. Yan, "Deadenylation: enzymes, regulation, and functional implications.", *Wiley Interdiscip. Rev. RNA*, vol. 5, no. 3, pp. 421–443, 2014.

[629] C.-Y. A. Chen and A.-B. Shyu, "Mechanisms of deadenylation-dependent decay.", *Wiley Interdiscip. Rev. RNA*, vol. 2, no. 2, pp. 167–183, 2011.

[630] P. Cassonnet *et al.*, "Benchmarking a luciferase complementation assay for detecting protein complexes.", *Nature methods*, vol. 8, no. 12. United States, pp. 990–992, Nov-2011.

[631] M. A. Digman, R. Dalal, A. F. Horwitz, and E. Gratton, "Mapping the number of molecules and brightness in the laser scanning microscope.", *Biophys. J.*, vol. 94, no. 6, pp. 2320–2332, Mar. 2008.

[632] S. Sun, Z. Zhang, O. Fregoso, and A. R. Krainer, "Mechanisms of activation and repression by the alternative splicing factors RBFOX1/2.", *RNA*, vol. 18, no. 2, pp. 274–283, Feb. 2012.

[633] C. Mayr, "Evolution and Biological Roles of Alternative 3'UTRs.", *Trends Cell Biol.*, vol. 26, no. 3, pp. 227–237, Mar. 2016.

[634] M. Courel *et al.*, "GC content shapes mRNA storage and decay in human cells.", *Elife*, 2019.

[635] V. N. Uversky and A. K. Dunker, "Understanding protein non-folding.", *Biochim. Biophys. Acta*, vol. 1804, no. 6, pp. 1231–1264, Jun. 2010.

[636] A. Mohan *et al.*, "Analysis of molecular recognition features (MoRFs).", *J. Mol. Biol.*, vol. 362, no. 5, pp. 1043–1059, Oct. 2006.

[637] M. Lindén *et al.*, "FET family fusion oncoproteins target the SWI/SNF chromatin remodeling complex.", *EMBO Rep.*, vol. 20, no. 5, May 2019.

[638] A. Arvand *et al.*, "The COOH-terminal domain of FLI-1 is necessary for full tumorigenesis and transcriptional modulation by EWS/FLI-1.", *Cancer Res.*, 2001.

[639] J. G. Conboy, "Developmental regulation of RNA processing by Rbfox proteins.", *Wiley Interdiscip. Rev. RNA*, vol. 8, no. 2, Mar. 2017.

[640] M. Teplova, T. A. Farazi, T. Tuschl, and D. J. Patel, "Structural basis underlying CAC RNA recognition by the RRM domain of dimeric RNA-binding protein RBPMS.", *Q. Rev. Biophys.*, vol. 49, p. e1, Jan. 2016.

[641] C. A. Chénard and S. Richard, "New implications for the QUAKING RNA binding protein in human disease.", *J. Neurosci. Res.*, vol. 86, no. 2, pp. 233–242, Feb. 2008.

[642] T. A. Farazi *et al.*, "Identification of the RNA recognition element of the RBPMS family of RNA-binding proteins and their transcriptome-wide mRNA targets.", *RNA*, vol. 20, no. 7, pp. 1090–1102, Jul. 2014.

[643] M. Teplova, M. Hafner, D. Teplov, K. Essig, T. Tuschl, and D. J. Patel, "Structure-function studies of STAR family Quaking proteins bound to their in vivo RNA target sites.", *Genes Dev.*, vol. 27, no. 8, pp. 928–940, Apr. 2013.

[644] M. Hafner *et al.*, "Transcriptome-wide Identification of RNA-Binding Protein and MicroRNA Target Sites by PAR-CLIP.", *Cell*, vol. 141, no. 1, pp. 129–141, 2010.

[645] D. Ray *et al.*, "A compendium of RNA-binding motifs for decoding gene regulation.", *Nature*, vol. 499, no. 7457, pp. 172–177, Jul. 2013.

[646] C. W. Schultz, R. Preet, T. Dhir, D. A. Dixon, and J. R. Brody, "Understanding and targeting the disease-related RNA binding protein human antigen R (HuR).", *Wiley Interdiscip. Rev. RNA*, 2020.

[647] H. K. Matthews, C. Bertoli, and R. A. M. de Bruin, "Cell cycle control in cancer.", *Nat. Rev. Mol. Cell Biol.*, vol. 23, no. 1, pp. 74–88, Jan. 2022.

[648] G. Stoll *et al.*, "Systems biology of Ewing sarcoma: a network model of EWS-FLI1 effect on proliferation and apoptosis.", *Nucleic Acids Res.*, vol. 41, no. 19, pp. 8853–8871, Oct. 2013.

[649] K. Wakahara *et al.*, "EWS-Fli1 up-regulates expression of the Aurora A and Aurora B kinases.", *Mol. Cancer Res.*, vol. 6, no. 12, pp. 1937–1945, Dec. 2008.

[650] F. Nakatani *et al.*, "Identification of p21WAF1/CIP1 as a direct target of EWS-Fli1 oncogenic fusion protein.", *J. Biol. Chem.*, vol. 278, no. 17, pp. 15105–15115, Apr. 2003.

[651] M. Fukuma, H. Okita, J.-I. Hata, and A. Umezawa, "Upregulation of Id2, an oncogenic helix-loop-helix protein, is mediated by the chimeric EWS/ets protein in Ewing sarcoma.", *Oncogene*, vol. 22, no. 1, pp. 1–9, Jan. 2003.

[652] X. Li *et al.*, "Transactivation of cyclin E gene by EWS-Fli1 and antitumor effects of cyclin dependent kinase inhibitor on Ewing's family tumor cells.", *Int. J. cancer*, vol. 116, no. 3, pp. 385–394, Sep. 2005.

[653] L. Dauphinot *et al.*, "Analysis of the expression of cell cycle regulators in Ewing cell lines: EWS-FLI-1 modulates p57KIP2and c-Myc expression.", *Oncogene*, vol. 20, no. 25, pp. 3258–3265, May 2001.

[654] K. Scotlandi *et al.*, "Insulin-like growth factor I receptor-mediated circuit in Ewing's sarcoma/peripheral neuroectodermal tumor: a possible therapeutic target.", *Cancer Res.*, vol. 56, no. 20, pp. 4570–4574, Oct. 1996.

[655] S. Benini *et al.*, "Contribution of MEK/MAPK and PI3-K signaling pathway to the malignant behavior of Ewing's sarcoma cells: therapeutic prospects.", *Int. J. cancer*, vol. 108, no. 3, pp. 358–366, Jan. 2004.

[656] L. Krenning, S. Sonneveld, and M. Tanenbaum, "Time-resolved single-cell sequencing identifies multiple waves of mRNA decay during the mitosis-to-G1 phase transition.", *Elife*, vol. 11, Feb. 2022.

[657] H. Urra, E. Dufey, T. Avril, E. Chevet, and C. Hetz, "Endoplasmic Reticulum Stress and the Hallmarks of Cancer.", *Trends in cancer*, vol. 2, no. 5, pp. 252–262, May 2016.

[658] H. J. Clarke, J. E. Chambers, E. Liniker, and S. J. Marciniak, "Endoplasmic reticulum stress in malignancy.", *Cancer Cell*, vol. 25, no. 5, pp. 563–573, May 2014.

[659] C. Hetz, K. Zhang, and R. J. Kaufman, "Mechanisms, regulation and functions of the unfolded protein response.", *Nat. Rev. Mol. Cell Biol.*, vol. 21, no. 8, pp. 421–438, 2020.

[660] J. A. Jiménez *et al.*, "EWS-FLI1 and Menin Converge to Regulate ATF4 Activity in Ewing Sarcoma.", *Mol. Cancer Res.*, vol. 19, no. 7, pp. 1182–1195, Jul. 2021.

[661] S. Prislei *et al.*, "Role and prognostic significance of the epithelial-mesenchymal transition factor ZEB2 in ovarian cancer.", *Oncotarget*, 2015.

[662] H. Zhang *et al.*, "QKI-6 Suppresses Cell Proliferation, Migration, and EMT in Non-Small Cell Lung Cancer.", *Front. Oncol.*, vol. 12, p. 897553, 2022.

[663] S. Wang *et al.*, "Quaking 5 suppresses TGF-β-induced EMT and cell invasion in lung adenocarcinoma.", *EMBO Rep.*, vol. 22, no. 6, p. e52079, Jun. 2021.

[664] D. T. Weaver *et al.*, "Network potential identifies therapeutic miRNA cocktails in Ewing sarcoma.", *PLoS Comput. Biol.*, vol. 17, no. 10, p. e1008755, Oct. 2021.

[665] X. Wang, S. L. Morris-Natschke, and K.-H. Lee, "New developments in the chemistry and biology of the bioactive constituents of Tanshen.", *Med. Res. Rev.*, vol. 27, no. 1, pp. 133–148, Jan. 2007.

[666] C.-Y. Lee *et al.*, "Anticancer effects of tanshinone I in human non-small cell lung cancer.", *Mol. Cancer Ther.*, vol. 7, no. 11, pp. 3527–3538, Nov. 2008.

[667] C. Lin, L. Wang, H. Wang, L. Yang, H. Guo, and X. Wang, "Tanshinone IIA inhibits breast cancer stem cells growth in vitro and in vivo through attenuation of IL-6/STAT3/NF-kB signaling pathways.", *J. Cell. Biochem.*, vol. 114, no. 9, pp. 2061–2070, Sep. 2013.

[668] P. Lal *et al.*, "Regulation of HuR structure and function by dihydrotanshinone-I.", *Nucleic Acids Res.*, vol. 45, no. 16, pp. 9514–9527, 2017.

[669] A. Tsherniak *et al.*, "Defining a Cancer Dependency Map.", *Cell*, vol. 170, no. 3, pp. 564-576.e16, Jul. 2017.

[670] W. Pan *et al.*, "RNA binding protein HuR promotes osteosarcoma cell progression via suppressing the miR-142-3p/HMGA1 axis.", *Oncol. Lett.*, vol. 16, no. 2, pp. 1475–1482, Aug. 2018.

[671] S. Grissenberger *et al.*, "Automated compound testing in zebrafish xenografts identifies combined MCL-1 and BCL-XL inhibition to be effective against Ewing sarcoma.", *bioRxiv*, p. 2021.06.17.448794, Jan. 2021.

[672] A. Lugowski, B. Nicholson, and O. S. Rissland, "Determining mRNA half-lives on a transcriptome-wide scale.", *Methods*, vol. 137, pp. 90–98, Mar. 2018.

[673] G. Hanson and J. Coller, "Codon optimality, bias and usage in translation and mRNA decay.", *Nat. Rev. Mol. Cell Biol.*, vol. 19, no. 1, pp. 20–30, Jan. 2018.

[674] R. Buschauer *et al.*, "The Ccr4-Not complex monitors the translating ribosome for codon optimality.", *Science*, vol. 368, no. 6488, Apr. 2020.

[675] Z. Villanyi and M. A. Collart, "Ccr4-Not is at the core of the eukaryotic gene expression circuitry.", *Biochem. Soc. Trans.*, vol. 43, no. 6, pp. 1253–1258, Dec. 2015.

[676] M. Varadi *et al.*, "AlphaFold Protein Structure Database: massively expanding the structural coverage of protein-sequence space with high-accuracy models.", *Nucleic Acids Res.*, vol. 50, no. D1, pp. D439–D444, Jan. 2022.

[677] J. Jumper *et al.*, "Highly accurate protein structure prediction with AlphaFold.", *Nature*, vol. 596, no. 7873, pp. 583–589, Aug. 2021.

[678] C. Hou and O. V Tsodikov, "Structural Basis for Dimerization and DNA Binding of Transcription Factor FLI1.", *Biochemistry*, vol. 54, no. 50, pp. 7365–7374, Dec. 2015.

[679] S. Wang *et al.*, "Ablation of the oncogenic transcription factor ERG by deubiquitinase inhibition in prostate cancer.", *Proc. Natl. Acad. Sci. U. S. A.*, vol. 111, no. 11, pp. 4251–4256, Mar. 2014.

[680] J. S. E. Yu, S. Colborne, C. S. Hughes, G. B. Morin, and T. O. Nielsen, "The FUS-DDIT3 Interactome in Myxoid Liposarcoma.", *Neoplasia*, vol. 21, no. 8, pp. 740–751, Aug. 2019.

[681] A. Mendes, R. Jühlen, S. Bousbata, and B. Fahrenkrog, "Disclosing the Interactome of Leukemogenic NUP98-HOXA9 and SET-NUP214 Fusion Proteins Using a Proteomic Approach.", *Cells*, vol. 9, no. 7, Jul. 2020.

[682] S. G. Choi *et al.*, "Maximizing binary interactome mapping with a minimal number of assays.", *Nat. Commun.*, vol. 10, no. 1, p. 3907, Aug. 2019.

[683] I. I. Atanassov, I. I. Atanassov, J. P. Etchells, and S. R. Turner, "A simple, flexible and efficient PCR-fusion/Gateway cloning procedure for gene fusion, site-directed mutagenesis, short sequence

insertion and domain deletions and swaps.", *Plant Methods*, vol. 5, p. 14, Oct. 2009.

[684] J. Lykke-Andersen, M. D. Shu, and J. A. Steitz, "Human Upf proteins target an mRNA for nonsense-mediated decay when bound downstream of a termination codon.", *Cell*, vol. 103, no. 7, pp. 1121–1131, Dec. 2000.

[685] A. Dobin *et al.*, "STAR: ultrafast universal RNA-seq aligner.", *Bioinformatics*, vol. 29, no. 1, pp. 15–21, Jan. 2013.

[686] M. I. Love, W. Huber, and S. Anders, "Moderated estimation of fold change and dispersion for RNA-seq data with DESeq2.", *Genome Biol.*, vol. 15, no. 12, p. 550, 2014.

[687] R. C. McLeay and T. L. Bailey, "Motif Enrichment Analysis: a unified framework and an evaluation on ChIP data.", *BMC Bioinformatics*, vol. 11, p. 165, Apr. 2010.

[688] B. Mészáros, G. Erdos, and Z. Dosztányi, "IUPred2A: context-dependent prediction of protein disorder as a function of redox state and protein binding.", *Nucleic Acids Res.*, vol. 46, no. W1, pp. W329–W337, Jul. 2018.

[689] Z. Obradovic, K. Peng, S. Vucetic, P. Radivojac, C. J. Brown, and A. K. Dunker, "Predicting intrinsic disorder from amino acid sequence.", *Proteins*, vol. 53 Suppl 6, pp. 566–572, 2003.

[690] Z. R. Yang, R. Thomson, P. McNeil, and R. M. Esnouf, "RONN: the bio-basis function neural network technique applied to the detection of natively disordered regions in proteins.", *Bioinformatics*, vol. 21, no. 16, pp. 3369–3376, Aug. 2005.

[691] J. Hanson, Y. Yang, K. Paliwal, and Y. Zhou, "Improving protein disorder prediction by deep bidirectional long short-term memory recurrent neural networks.", *Bioinformatics*, vol. 33, no. 5, pp. 685–692, Mar. 2017.

[692] S. Wang, J. Ma, and J. Xu, "AUCpreD: proteome-level protein disorder prediction by AUC-maximized deep convolutional neural fields.", *Bioinformatics*, vol. 32, no. 17, pp. i672–i679, Sep. 2016.

[693] I. Walsh, A. J. M. Martin, T. Di Domenico, and S. C. E. Tosatto, "ESpritz: accurate and fast prediction of protein disorder.", *Bioinformatics*, vol. 28, no. 4, pp. 503–509, Feb. 2012.

[694] L. P. Kozlowski and J. M. Bujnicki, "MetaDisorder: a meta-server for the prediction of intrinsic disorder in proteins.", *BMC Bioinformatics*, vol. 13, p. 111, May 2012.

[695] S. Hirose, K. Shimizu, S. Kanai, Y. Kuroda, and T. Noguchi, "POODLE-L: a two-level SVM prediction system for reliably predicting long disordered regions.", *Bioinformatics*, vol. 23, no. 16, pp. 2046–2053, Aug. 2007.

[696] C. A. Schneider, W. S. Rasband, and K. W. Eliceiri, "NIH Image to ImageJ: 25 years of image analysis.", *Nat. Methods*, vol. 9, no. 7, pp. 671–675, Jul. 2012.

[697] D. W. Huang, B. T. Sherman, and R. A. Lempicki, "Systematic and integrative analysis of large gene lists using DAVID bioinformatics resources.", *Nat. Protoc.*, 2009.

[698] P. D. Thomas *et al.*, "PANTHER: a browsable database of gene products organized by biological function, using curated protein family and subfamily classification.", *Nucleic Acids Res.*, vol. 31, no. 1, pp. 334–341, Jan. 2003.

[699] E. A. Bruford *et al.*, "HUGO Gene Nomenclature Committee (HGNC) recommendations for the

designation of gene fusions.", *Leukemia*, vol. 35, no. 11, pp. 3040–3043, Nov. 2021.

[700] A. F. Harrison and J. Shorter, "RNA-binding proteins with prion-like domains in health and disease.", *Biochem. J.*, vol. 474, no. 8, pp. 1417–1438, Apr. 2017.

[701] W.-J. Huang, W.-W. Chen, and X. Zhang, "Prions mediated neurodegenerative disorders.", *Eur. Rev. Med. Pharmacol. Sci.*, vol. 19, no. 21, pp. 4028–4034, Nov. 2015.

[702] D. J. Elzi, M. Song, P. J. Houghton, Y. Chen, and Y. Shiio, "The role of FLI-1-EWS, a fusion gene reciprocal to EWS-FLI-1, in Ewing sarcoma.", *Genes Cancer*, vol. 6, no. 11–12, pp. 452–461, Nov. 2015.

[703] M. A. Dawson and T. Kouzarides, "Cancer epigenetics: from mechanism to therapy.", *Cell*, vol. 150, no. 1, pp. 12–27, Jul. 2012.

[704] A. Panigrahi and B. W. O'Malley, "Mechanisms of enhancer action: the known and the unknown.", *Genome Biol.*, vol. 22, no. 1, p. 108, Apr. 2021.

[705] W. A. Whyte *et al.*, "Master transcription factors and mediator establish super-enhancers at key cell identity genes.", *Cell*, vol. 153, no. 2, pp. 307–319, 2013.

[706] R. Khoogar *et al.*, "Single-cell RNA profiling identifies diverse cellular responses to EWSR1/FLI1 downregulation in Ewing sarcoma cells.", *Cell. Oncol. (Dordr).*, vol. 45, no. 1, pp. 19–40, Feb. 2022.

[707] F. Mitelman, B. Johansson, and F. Mertens, "The impact of translocations and gene fusions on cancer causation.", *Nat. Rev. Cancer*, vol. 7, no. 4, pp. 233–245, Apr. 2007.

[708] F. Mertens, C. R. Antonescu, and F. Mitelman, "Gene fusions in soft tissue tumors: Recurrent and overlapping pathogenetic themes.", *Genes. Chromosomes Cancer*, vol. 55, no. 4, pp. 291–310, Apr. 2016.

[709] Z.-H. Chen *et al.*, "Targeting genomic rearrangements in tumor cells through Cas9-mediated insertion of a suicide gene.", *Nat. Biotechnol.*, vol. 35, no. 6, pp. 543–550, Jun. 2017.

[710] R. Petermann, B. M. Mossier, D. N. Aryee, V. Khazak, E. A. Golemis, and H. Kovar, "Oncogenic EWS-Fli1 interacts with hsRPB7, a subunit of human RNA polymerase II.", *Oncogene*, vol. 17, no. 5, pp. 603–610, Aug. 1998.

[711] N. Dahan and M. Choder, "The eukaryotic transcriptional machinery regulates mRNA translation and decay in the cytoplasm.", *Biochim. Biophys. Acta*, vol. 1829, no. 1, pp. 169–173, Jan. 2013.

SECTION IX   PUBLICATIONS

Sorting and packaging of RNA into extracellular vesicles shape intracellular transcript levels (BMC Biology, 2022)

Tina O'Grady, Makon-Sébastien Njock, Michelle Lion, Jonathan Bruyr, Emeline Mariavelle, **Bartimée Galvan**, Amandine Boeckx, Ingrid Struman and Franck Dequiedt

Background: Extracellular vesicles (EVs) are released by nearly every cell type and have attracted much attention for their ability to transfer protein and diverse RNA species from donor to recipient cells. Much attention has been given so far to the features of EV short RNAs such as miRNAs. However, while the presence of mRNA and long noncoding RNA (lncRNA) transcripts in EVs has also been reported by multiple different groups, the properties and function of these longer transcripts have been less thoroughly explored than EV miRNA. Additionally, the impact of EV export on the transcriptome of exporting cells has remained almost completely unexamined. Here, we globally investigate mRNA and lncRNA transcripts in endothelial EVs in multiple different conditions.

Results: In basal conditions, long RNA transcripts enriched in EVs have longer than average half-lives and distinctive stability-related sequence and structure characteristics including shorter transcript length, higher exon density, and fewer 3' UTR A/U-rich elements. EV-enriched long RNA transcripts are also enriched in HNRNPA2B1 binding motifs and are impacted by HNRNPA2B1 depletion, implicating this RNA-binding protein in the sorting of long RNA to EVs. After signaling-dependent modification of the cellular transcriptome, we observed that, unexpectedly, the rate of EV enrichment relative to cells was altered for many mRNA and lncRNA transcripts. This change in EV enrichment was negatively correlated with intracellular abundance, with transcripts whose export to EVs increased showing decreased abundance in cells and vice versa. Correspondingly, after treatment with inhibitors of EV secretion, levels of mRNA and lncRNA transcripts that are normally highly exported to EVs increased in cells, indicating a measurable impact of EV export on the long RNA transcriptome of the exporting cells. Compounds with different mechanisms of inhibition of EV secretion affected the cellular transcriptome differently, suggesting the existence of multiple EV subtypes with different long RNA profiles.

Conclusions: We present evidence for an impact of EV physiology on the characteristics of EV-producing cell transcriptomes. Our work suggests a new paradigm in which the sorting and packaging of transcripts into EVs participate, together with transcription and RNA decay, in controlling RNA homeostasis and shape the cellular long RNA abundance profile.

The HTLV-1 viral oncoproteins Tax and HBZ reprogram the cellular mRNA splicing landscape (PLOS PATHOGENS, 2021)

Charlotte Vandermeulen, Tina O'Grady, Jerome Wayet, **Bartimée Galvan**, Sibusiso Maseko, Majid Cherkaoui, Alice Desbuleux, Georges Coppin, Julien Olivet, Lamya Ben Ameur, Keisuke Kataoka, Seishi Ogawa, Olivier Hermine, Ambroise Marcais, Marc Thiry, Franck Mortreux, Michael A. Calderwood, Johan Van Weyenbergh, Jean-Marie Peloponese,Benoit Charloteaux, Anne Van den Broeke, David E. Hill, Marc Vidal, Franck Dequiedt, Jean-Claude Twizere

Viral infections are known to hijack the transcription and translation of the host cell. However, the extent to which viral proteins coordinate these perturbations remains unclear. Here we used a model system, the human T-cell leukemia virus type 1 (HTLV-1), and systematically analyzed the transcriptome and interactome of key effectors oncoviral proteins Tax and HBZ. We showed that Tax and HBZ target distinct but also common transcription factors. Unexpectedly, we also uncovered a large set of interactions with RNA-binding proteins, including the U2 auxiliary factor large subunit (U2AF2), a key cellular regulator of pre-mRNA splicing. We discovered that Tax and HBZ perturb the splicing landscape by altering cassette exons in opposing manners, with Tax inducing exon inclusion while HBZ induces exon exclusion. Among Tax- and HBZ-dependent splicing changes, we identify events that are also altered in Adult T cell leukemia/lymphoma (ATLL) samples from two independent patient cohorts, and in well-known cancer census genes. Our interactome mapping approach, applicable to other viral oncogenes, has identified spliceosome perturbation as a novel mechanism coordinated by Tax and HBZ to reprogram the transcriptome.

ERG transcription factors have a splicing regulatory function involving RBFOX2 that is altered in the EWS-FLI1 oncogenic fusion (Nucleic Acids Research, 2021)

Olivier Saulnier, Katia Guedri-Idjouadiene, Marie-Ming Aynaud, Alina Chakraborty, Jonathan Bruyr, Joséphine Pineau, Tina O'Grady, Olivier Mirabeau, Sandrine Grossetête, **Bartimée Galvan**, Margaux Claes, Zahra Al Oula Hassoun, Benjamin Sadacca, Karine Laud, Sakina Zaïdi, Didier Surdez, Sylvain Baulande, Xavier Rambout, Franck Tirode, Martin Dutertre, Olivier Delattre, and Franck Dequiedt

ERG family proteins (ERG, FLI1 and FEV) are a subfamily of ETS transcription factors with key roles in physiology and development. In Ewing sarcoma, the oncogenic fusion protein EWS-FLI1 regulates both transcription and alternative splicing of pre-messenger RNAs. However, whether wild-type ERG family proteins might regulate splicing is unknown. Here, we show that wild-type ERG proteins associate with spliceosomal components, are found on nascent RNAs, and induce alternative splicing when recruited onto a reporter minigene. Transcriptomic analysis revealed that ERG and FLI1 regulate large numbers of alternative spliced exons (ASEs) enriched with RBFOX2 motifs and co-regulated by this splicing factor. ERG and FLI1 are associated with RBFOX2 via their conserved carboxy-terminal domain, which is present in EWS-FLI1. Accordingly, EWS-FLI1 is also associated with RBFOX2 and regulates ASEs enriched in RBFOX2 motifs. However, in contrast to wild-type ERG and FLI1, EWS-FLI1 often antagonizes RBFOX2 effects on exon inclusion. In particular, EWS-FLI1 reduces RBFOX2 binding to the ADD3 pre-mRNA, thus increasing its long isoform, which represses the mesenchymal phenotype of Ewing sarcoma cells. Our findings reveal a RBFOX2-mediated splicing regulatory function of wild-type ERG family proteins, that is altered in EWS-FLI1 and contributes to the Ewing sarcoma cell phenotype.

SECTION X   APPENDIX

1. Annotated protein sequence of EF 7/6 (also known as type I splicing variant)

MASTDYSTYSQAAAQQGYSAYTAQPTQGYAQTTQAYGQQSYGTYGQPTDVSYTQAQTTATYGQTAYATSYG
QPPTGYTTPTAPQAYSQPVQGYGTGAYDTTTATVTTTQASYAAQSAYGTQPAYPAYGQQPAATAPTRPQDG
NKPTETSQPQSSTGGYNQPSLGYGQSNYSYPQVPGSYPMQPVTAPPSYPPTSYSSTQPTSYDQSSYSQQNT
YGQPSSYGQQSSYGQQSSYGQQPPTSYPPQTGSYSQAPSQYSQQSSSYGQQ
NPSYDSVRRGAWGNNMNSGLNKSPPLGGAQTISKNTEQRPQPDPYQILGPTSSRLANPGSG*QIQLWQFLLE*
*LLSDSANASCITWEGTNGEFKMTDPDEVARRWGERKSKPNMNYDKLSRALRYYYD*KNIMTKVHGKRYAYKF
DFHGIAQALQPHPTESSMYKYPSDISYMPSYHAHQQKVNFVPPHPSSMPVTSSSFFGAASQYWTSPTGGIY
PNPNVPRHPNTHVPSHLGSYY

EWSR1-derived region (aa 1-264)

FLI1-derived region (aa 265-498)

ETS DNA-binding domain (aa 326-409)

Removed in EFΔETS (aa 326-390)

CTAD (aa 410-498)

Removed in EFΔCTAD

2. Annotated protein sequence of EWSR1 LC NTD

MASTDYSTYSQAAAQQGYSAYTAQPTQGYAQTTQAYGQQSYGTYGQPTDVSYTQAQTTATYGQTAYATSY
GQPPTGYTTPTAPQAYSQPVQGYGTGAY**DTTTATVTTTQA**SYAAQSAYGTQPAYPAYGQQP**AATAPTRPQ**
DGNKPTETSQPQSSTGGYNQPSLGYGQSNYSYPQVPGSYPMQPVTAPPSYPPTSYSSTQPTSYDQSSYSQ
QNTYGQPSSYGQQSSYGQQSSYGQQPPTSYPPQTGSYSQAPSQYSQQSSSYGQQSFRQDHPSSMGVYGQ
ESGGFSG

Degenerate hexapeptide repeats (DHRs)

Conserved tyrosines within DHRs (n = 30)

Tyrosines outside DHRs (n = 7)

Glutamine

Spacers

Black horizontal line indicates FET motif (aa 39-64).

Arrow indicates breakpoint relative to EF 7/6 (at aa = 264).

3. Annotated protein sequence of CNOT2

MVRTDGHTLSEKRNYQVTNSMFGASRKKFVEGVDSDYHDENMYYSQSSMFPHRSEKDMLASPSTSGQLSQF
GASLYGQQSALGLPMRGMSNNTPQLNRSLSQGTQLPSHVTPTTGVPTMSLHTPPSPSRGILPMNPRNMMNH
SQVGQGIGIPSRTNSMSSSGLGSPNRSSPSIICMPKQQPSRQPFTVNSMSGFGMNRNQAFGMNNSLSSNIF
NGTDGSENVTGLDLSDFPALADRNRREGSGNPTPLINPLAGRAPYVGMVTKPANEQSQDFSIHNEDFPALP
GSSYKDPTSSNDDSKSNLNTSGKTTSSTDGPKFPGDKSSTTQNNNQQKKGIQVLPDGRVTNIPQGM**VTDQF
GM**<mark>**IGLLTFIRAAET**</mark>**DPGMVHLALGSDLTTLGLNLNSPENLYPKFASPWASSPCR**PQDIDFHVPSEYLTNIH
IRDKLAAIKLGRYGEDLLFYLYYMNGGDVLQLLAAVELFNRDWRYHKEERVWITRAPGMEPTMKTNTYERG
TYYFFDCLNWRKVAKEFHLEYDKLEERPHLPSTFNYNPAQQAF

NAR domain (aa 351-409)

<mark>**Helix (aa 357-369)**</mark>

<mark>**Transactivation domain (aa 359-367)**</mark>
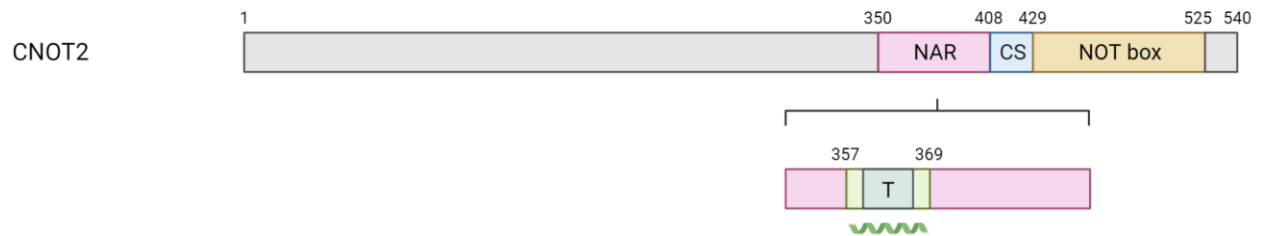

Figure 126. Schematic, domain structure of the CNOT2 subunit of the CCR4-NOT complex. T = transactivation domain. Created with BioRender.com.

4. Annotated protein sequence of HuR

MSNGYEDHMAEDCRGDIGRTNLIVNYLPQNMTQDELRSLFSSIGEVESAKLIRDKVAGHSLGYGFVNYVTA
KDAERAINTLNGLRLQSKTIKVSYARPSSEVIKDANLYISGLPRTMTQKDVEDMFSRFGRIINSRVLVDQT
TGLSRGVAFIRFDKRSEAEEAITSFNGHKPPGSSEPITVKFAANPNQNKNVALLSQLYHSPARRFGGPVHH
QAQRFRFSPMGVDHMSGLSGVNVPGNASSG**WCIFIYNLGQDADEGILWQMFGPFGAVTNVKVIRDFNTNKC
KGFGFVTMTNYEEAAMAIASLNGYRLGDKILQVSFKTNKSHK**

RRM3 (aa 244-326)

5. Decaysome gene list

Table S4. Manually literature-curated gene list of decay factors (decaysome). Gene symbol, NCBI Gene ID and full name are provided for each decay factor.

| Gene symbol	NCBI Gene ID	Full name
APPBP2	10513	amyloid beta precursor protein binding protein 2
BRF1	2972	butyrate response factor 1
BRF2	55290	butyrate response factor 2
C1D	10438	C1D nuclear receptor corepressor
CELF1	10658	CUGBP Elav-like family member 1
CNOT1	23019	CCR4-NOT transcription complex subunit 1
CNOT2	4848	CCR4-NOT transcription complex subunit 2
CNOT3	4849	CCR4-NOT transcription complex subunit 3
CNOT6	57472	CCR4-NOT transcription complex subunit 6
CNOT6L	246175	CCR4-NOT transcription complex subunit 6L
CNOT7	29883	CCR4-NOT transcription complex subunit 7
CNOT8	9337	CCR4-NOT transcription complex subunit 8
CNOT9	9125	CCR4-NOT transcription complex subunit 9
CNOT10	25904	CCR4-NOT transcription complex subunit 10
CNOT11	55571	CCR4-NOT transcription complex subunit 11
DCP1A	55802	decapping mRNA 1A
DCP1B	196513	decapping mRNA 1B
DCP2	167227	decapping mRNA 2
DIS3	22894	DIS3 homolog, exosome endoribonuclease and 3'-5' exoribonuclease
DIS3L	115752	DIS3 like exosome 3'-5' exoribonuclease

Gene symbol	NCBI Gene ID	Full name
EXOSC1	51013	exosome component 1
EXOSC2	23404	exosome component 2
EXOSC3	51010	exosome component 3
EXOSC4	54512	exosome component 4
EXOSC5	56915	exosome component 5
EXOSC6	118460	exosome component 6
EXOSC7	23016	exosome component 7
EXOSC8	11340	exosome component 8
EXOSC9	5393	exosome component 9
hNRNPD	3184	heterogeneous nuclear ribonucleoprotein D
IRE1	2081	inositol-requiring enzyme 1
KHSRP	8570	KH-type splicing regulatory protein
LSM1	27257	LSM1 homolog, mRNA degradation associated
LSM2	57819	LSM2 homolog, U6 small nuclear RNA and mRNA degradation associated
LSM3	27258	LSM3 homolog, U6 small nuclear RNA and mRNA degradation associated
LSM4	25804	LSM4 homolog, U6 small nuclear RNA and mRNA degradation associated
LSM5	23658	LSM5 homolog, U6 small nuclear RNA and mRNA degradation associated
LSM6	11157	LSM6 homolog, U6 small nuclear RNA and mRNA degradation associated
LSM7	51690	LSM7 homolog, U6 small nuclear RNA and mRNA degradation associated
MPP6	51678	MAGUK p55 subfamily member 6
NUDT16	131870	nudix hydrolase 16
PAN2	9924	poly(A) specific ribonuclease subunit PAN2
PAN3	255967	poly(A) specific ribonuclease subunit PAN3

Gene symbol	NCBI Gene ID	Full name
PAPD5	64282	PAP associated domain containing 5
PAPD7	11044	PAP associated domain containing 7
PARN	5073	poly(A)-specific ribonuclease
PUM2	23369	pumilio RNA binding family member 2
PUM3	9933	pumilio RNA binding family member 3
SKIC2	6499	SKI2 subunit of superkiller complex
SKIV2L2	23517	Superkiller viralicidic activity 2-like 2
SMG1	23049	SMG1 nonsense mediated mRNA decay associated PI3K related kinase
SMG5	23381	SMG5 nonsense mediated mRNA decay factor
SMG6	23293	SMG6 nonsense mediated mRNA decay factor
SMG7	9887	SMG7 nonsense mediated mRNA decay factor
STAU1	6780	staufen double-stranded RNA binding protein 1
SUPV3L1	6832	Suv3 like RNA helicase
UPF1	5976	UPF1 RNA helicase and ATPase
UPF2	26019	UPF2 regulator of nonsense mediated mRNA decay
UPF3B	65109	UPF3B regulator of nonsense mediated mRNA decay
XRN1	54464	5'-3' exoribonuclease 1
XRN2	22803	5'-3' exoribonuclease 2
ZC3H12A	80149	zinc finger CCCH-type containing 12A
ZCCHC3	85364	zinc finger CCHC-type containing 3
ZFP36	7538	ZFP36 ring finger protein
ZFP36L1	677	ZFP36 ring finger protein like 1
ZFP36L2	678	ZFP36 ring finger protein like 2

6. Supplementary methods
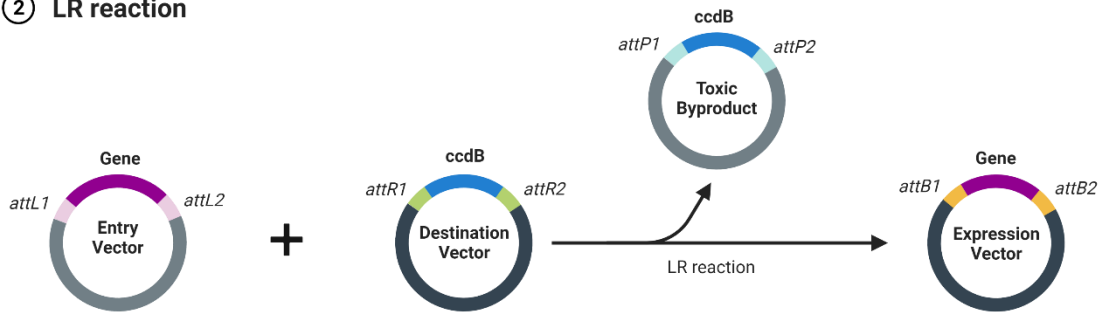
6.1. Gateway reactions
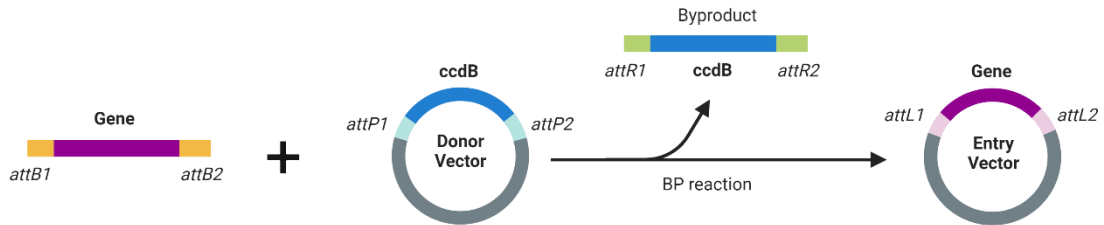
Figure 127. Gateway cloning procedure. ccdB gene codes for a toxic protein that acts as a DNA gyrase poison. Adapted from "Gateway Cloning", by BioRender.com (2022). Retrieved from https://app.biorender.com/biorender-templates.
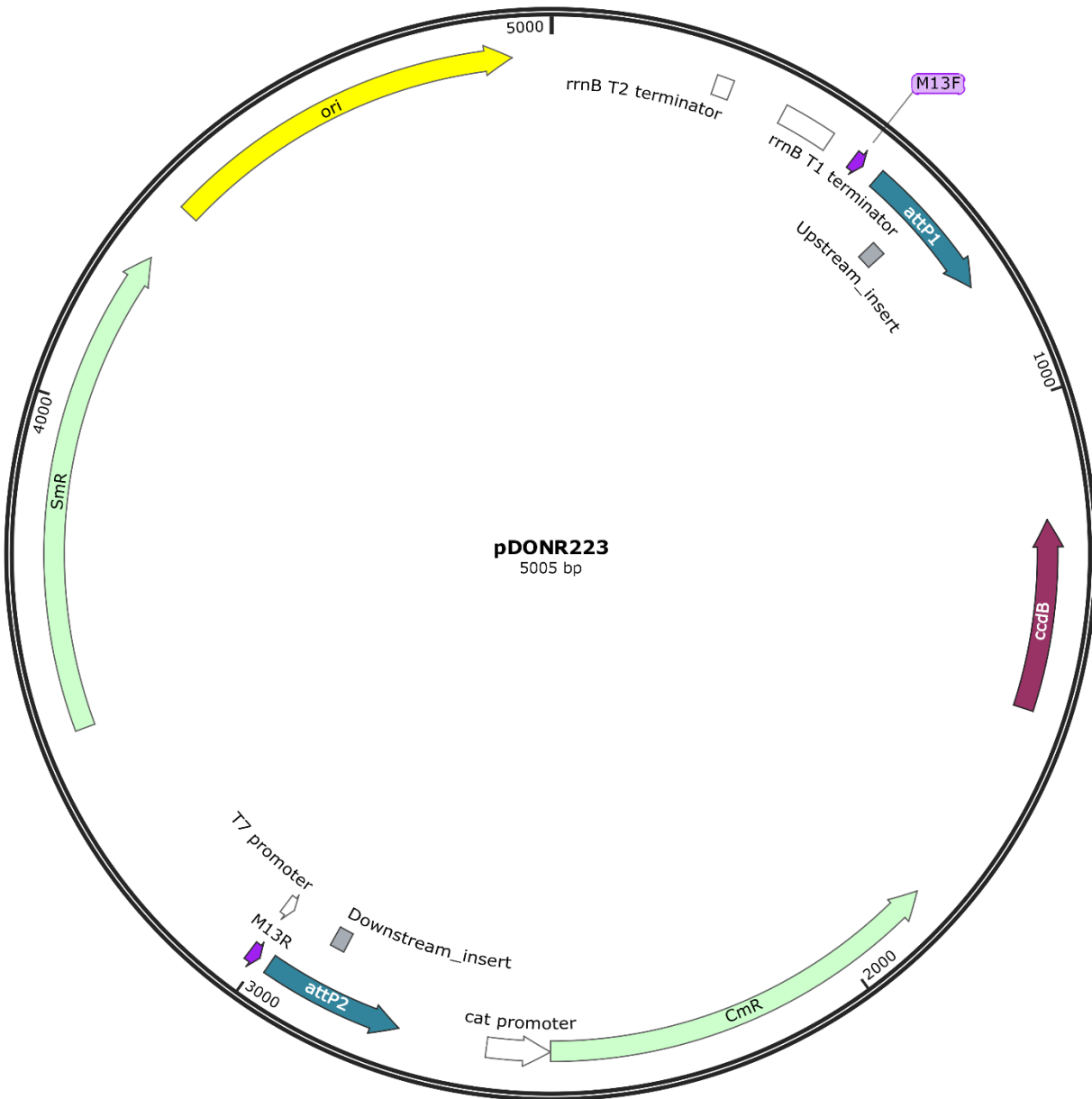
6.2. Plasmid maps

Figure 128. Annotated plasmid map of the pDONR223 vector. attP1 and attP2 are Gateway sites for BP cloning. ccdB gene codes for a toxic protein that acts as a DNA gyrase poison. SmR = spectinomycin resistance gene. CmR = chloramphenicol resistance gene. ori = bacterial origin of replication. M13F and M13R indicate sequencing primer sites. Created with SnapGene.
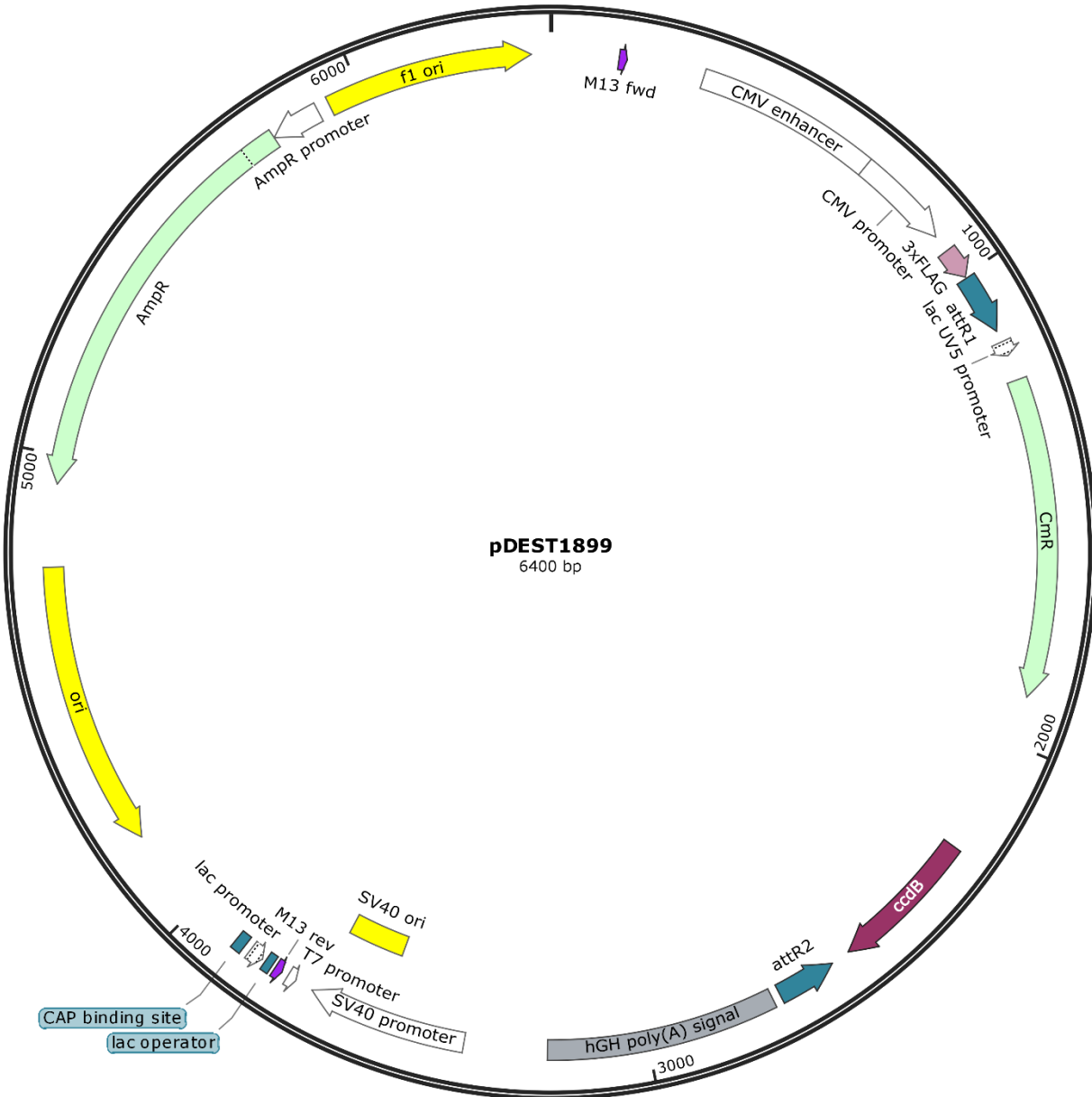
Figure 129. Annotated plasmid map of the pDEST1899 vector. 3xFLAG tag is indicated. attR1 and attR2 are Gateway sites for LR cloning. ccdB gene codes for a toxic protein that acts as a DNA gyrase poison. AmpR = ampicillin resistance gene. CmR = chloramphenicol resistance gene. ori = bacterial origin of replication. Created with SnapGene.
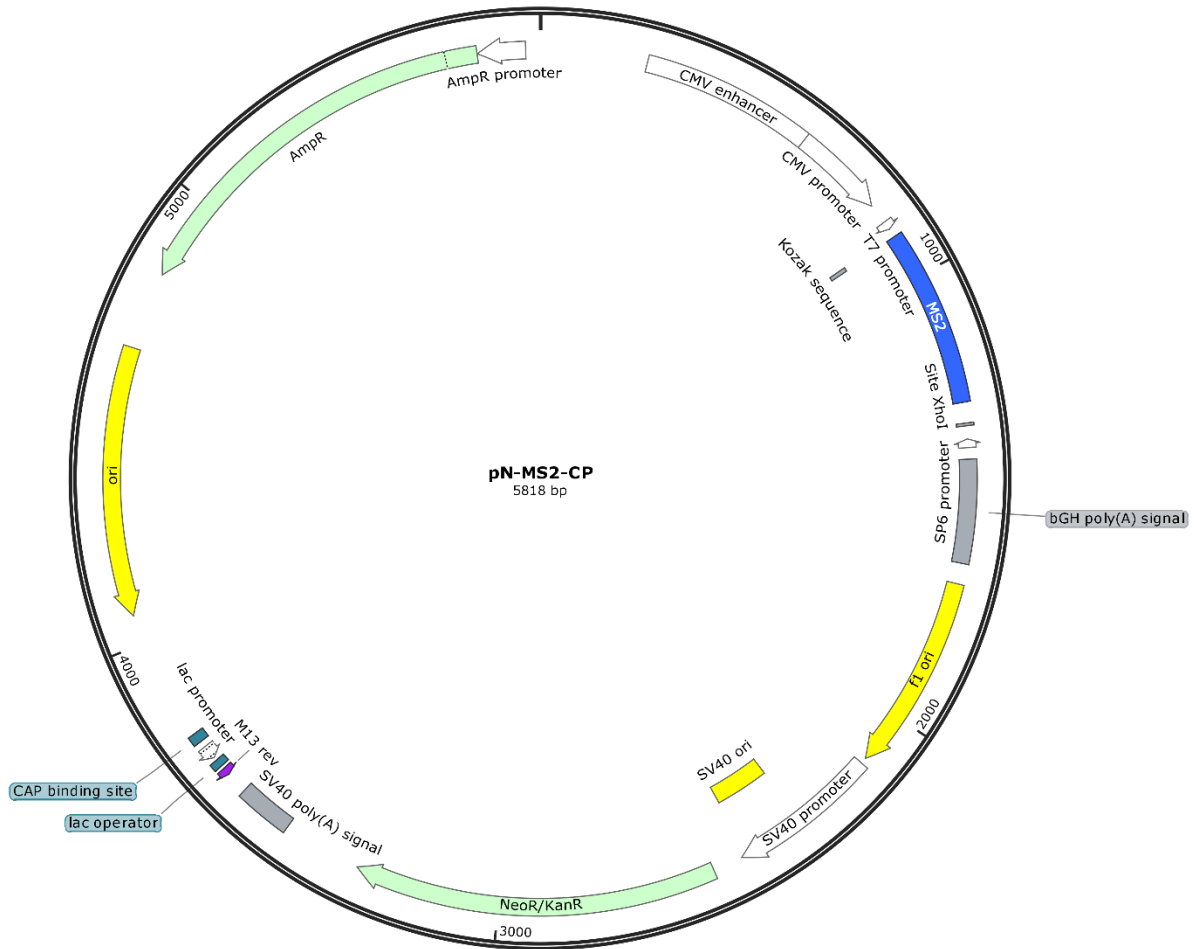
Figure 130. Annotated plasmid map of the pN-MS2-CP vector. AmpR = ampicillin resistance gene. NeoR/KanR = neomycin/kanamycin resistance gene. ori = bacterial origin of replication. Cloning into this vector is performed after XhoI digestion. Created with SnapGene.
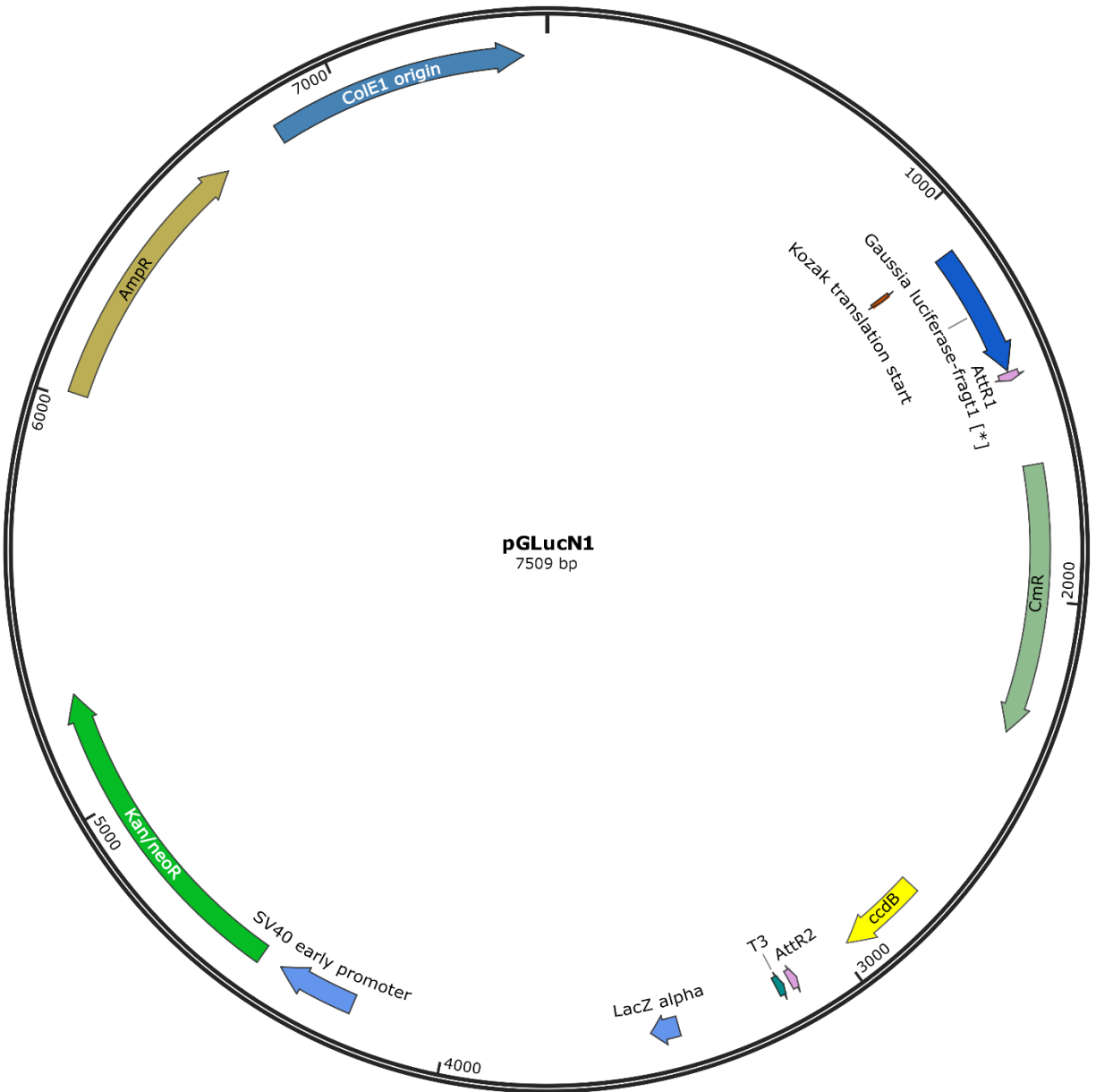
Figure 131. Annotated plasmid map of the pGLucN1 vector encoding the N-terminal moiety of the Gaussian luciferase. The vector encoding the C-terminal moiety of the Gaussian luciferase (pGLucN2) is identical. attR1 and attR2 are Gateway sites for LR cloning. ccdB gene codes for a toxic protein that acts as a DNA gyrase poison. AmpR = ampicillin resistance gene. CmR = chloramphenicol resistance gene. Kan/neoR = kanamycin/neomycin resistance gene. ori = bacterial origin of replication. Created with SnapGene.
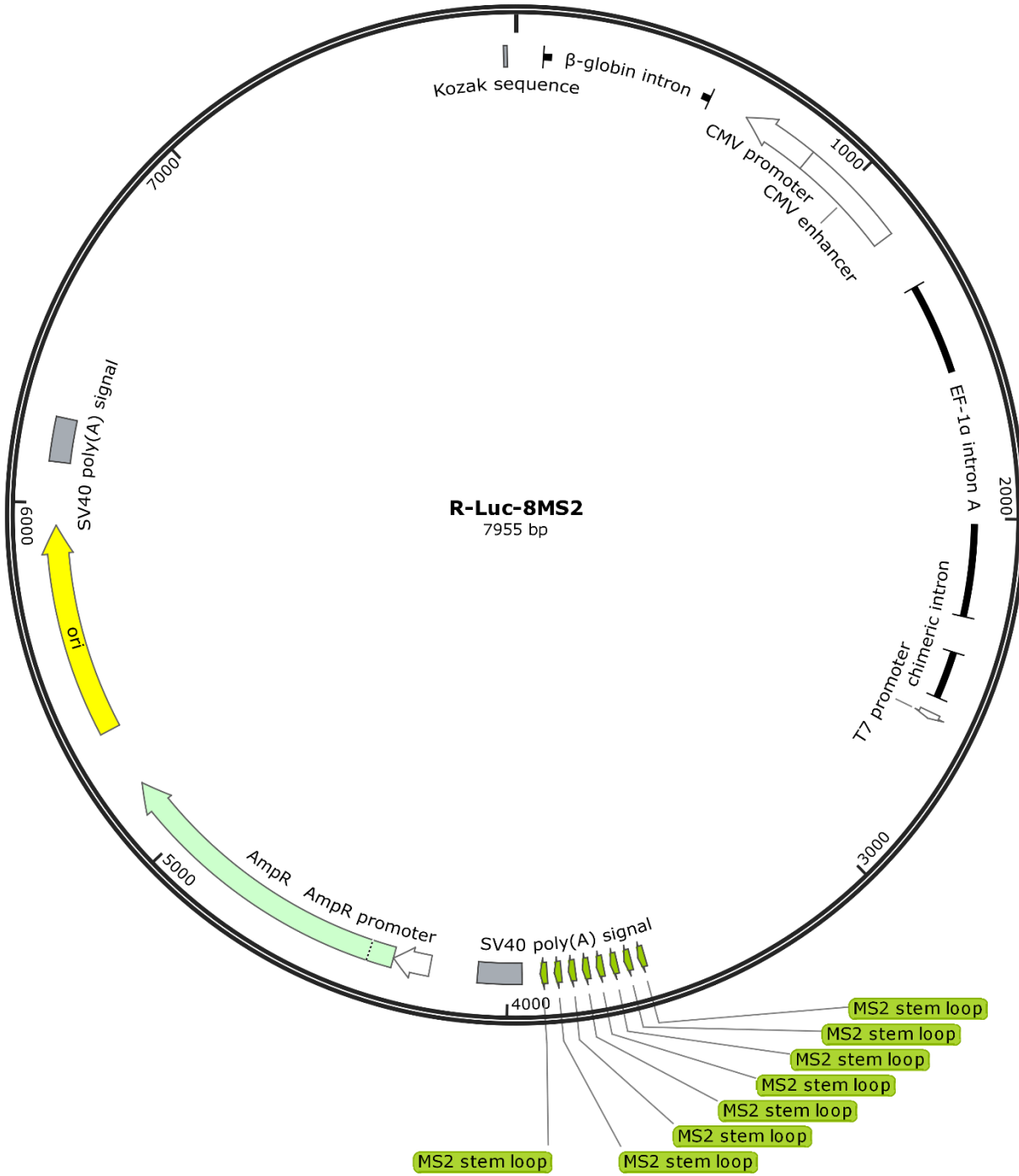
Figure 132. Annotated plasmid map of the R-Luc-8MS2 vector. *Renilla* and *Firefly* luciferases are encoded from a CMV (cytomegalo virus) bidirectional promoter. AmpR = ampicillin resistance gene. ori = bacterial origin of replication. MS2 stem loops are indicated. The vector without the MS2 stem loops has a similar organization. Created with SnapGene.
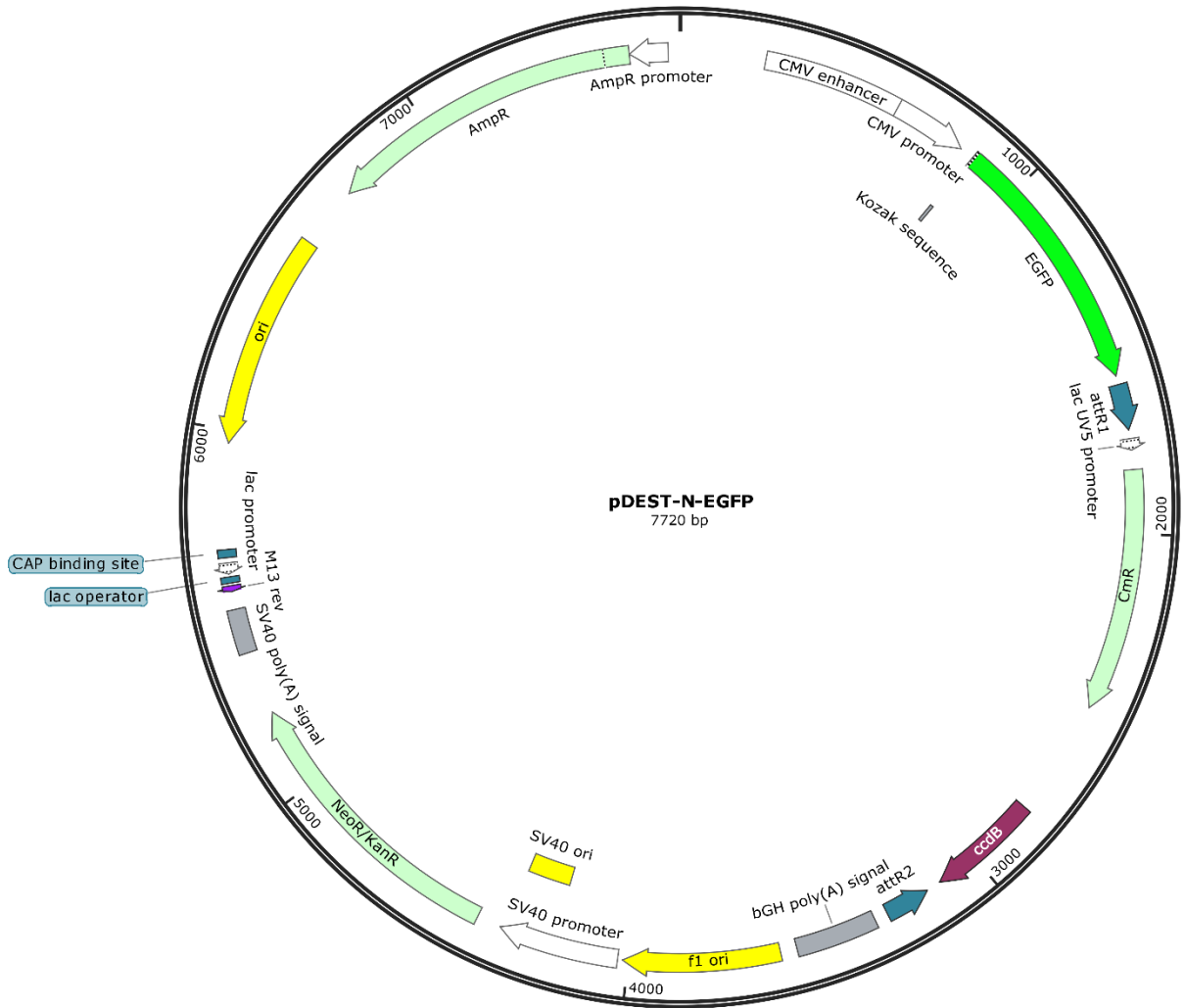
Figure 133. Annotated plasmid map of the pLENTI-DEST. SFFV = spleen focus-forming virus (promoter). IRES = Internal ribosome entry site. attR1 and attR2 are Gateway sites for LR cloning. ccdB gene codes for a toxic protein that acts as a DNA gyrase poison. AmpR = ampicillin resistance gene. ori = bacterial origin of replication. Created with SnapGene.

Figure 134. Annotated plasmid map of the pDEST-N-EGFP vector encoding the N-terminal moiety of the EGFP. EGFP = enhanced green fluoresecent protein. attR1 and attR2 are Gateway sites for LR cloning. ccdB gene codes for a toxic protein that acts as a DNA gyrase poison. AmpR = ampicillin resistance gene. CmR = chloramphenicol resistance gene. NeoR/KanR = kanamycin/neomycin resistance gene. ori = bacterial origin of replication. Created with SnapGene.